

**FREE VIBRATION ANALYSIS OF  
ANISOTROPIC LAMINATED COMPOSITE SHELLS OF REVOLUTION**

**A THESIS SUBMITTED TO  
THE GRADUATE SCHOOL OF NATURAL AND APPLIED SCIENCES  
OF  
MIDDLE EAST TECHNICAL UNIVERSITY**

**BY**

**ERDEM YAVUZBALKAN**

**IN PARTIAL FULFILLMENT OF THE REQUIREMENTS  
FOR  
THE DEGREE OF MASTER OF SCIENCE  
IN  
AEROSPACE ENGINEERING**

**AUGUST 2005**

Approval of the Graduate School of Natural and Applied Sciences.

\_\_\_\_\_  
Prof. Dr. Canan ÖZGEN  
Director

I certify that this thesis satisfies all the requirements as a thesis for the degree of Master of Science.

\_\_\_\_\_  
Prof. Dr. Nafiz ALEMDAROĞLU  
Head of the Department

This is to certify that we have read this thesis and that in our opinion it is fully adequate, in scope and quality, as a thesis for the degree of Master of Science.

\_\_\_\_\_  
Assoc. Prof. Dr. Altan KAYRAN  
Supervisor

Examining Committee Members

Prof. Dr. Yavuz YAMAN (METU, AEE)

\_\_\_\_\_

Assoc. Prof. Dr. Altan KAYRAN (METU, AEE)

\_\_\_\_\_

Assoc. Prof. Dr. Ata MUĞAN (Istanbul Technical Univ., ME)

\_\_\_\_\_

Assoc. Prof. Dr. Ozan TEKİNALP (METU, AEE)

\_\_\_\_\_

Dr. Volkan NALBANTOĞLU (ASELSAN)

\_\_\_\_\_

**I hereby declare that all information in this document has been obtained and presented in accordance with academic rules and ethical conduct. I also declare that, as required by these rules and conduct, I have fully cited and referenced all material and results that are not original to this work.**

Name, Last name: Erdem YAVUZBALKAN

Signature :

## **ABSTRACT**

### **FREE VIBRATION ANALYSIS OF ANISOTROPIC LAMINATED COMPOSITE SHELLS OF REVOLUTION**

Yavuzbalkan, Erdem

M.S., Department of Aerospace Engineering

Supervisor: Assoc. Prof. Dr. Altan Kayran

August 2005, 288 pages

In this thesis, the free vibration analysis of anisotropic laminated composite shells of revolution (ALCSOR) is studied. The governing equations are kinematic, constitutive, and motion equations. Geometrically linear strain-displacement equations of Reissner-Naghdi shell theory in combination with first-order shear deformation theory in which transverse shear and rotatory inertia effects are taken into consideration. The constitutive relations are for macroscopically ALCSOR in which statically equivalent force and moment resultants, instead of internal stresses for a single layer, are introduced. Equations of motion for the free vibration problem are obtained by the Hamilton's principle. The derived governing equations for the free vibration analysis of ALCSOR are initially formulated into a system of partial differential equations in terms of fundamental variables. Then, those partial differential equations are reduced to a system of first order ordinary differential equations by applying finite exponential Fourier Transform method resulting in a two point boundary value problem. It has been demonstrated that the application of the finite exponential Fourier transform made it possible to solve the governing equations, comprising the full anisotropic form of the constitutive equations, which was otherwise impossible to solve with the classical Fourier decomposition method. First, the boundary value problem formulated is reduced to a series of initial value problems, then the multisegment numerical integration is used in combination with the frequency trial method in order to find the critical modes within a given range of natural frequencies.

A computer code DALSOR is written for the solution of the natural frequencies and mode shapes of macroscopically ALCSOR. DALSOR is applicable to any general boundary condition at both ends of the shell, and allows for variation of all elastic and geometric properties in the meridional direction.

Numerical results are presented, and mainly discussions on the method of solution and the effect of macroscopic anisotropy on modal characteristics, mainly natural frequencies, are made. Various case studies are performed primarily on cylindrical shells in order to investigate the effects of mainly fiber orientation angle, stacking sequence, arbitrary boundary conditions at the edges of the shell, thickness-to-radius ratio on the modal characteristics, mainly natural frequencies. Application of the method of solution has also been demonstrated for a truncated composite spherical shell.

**Keywords:** free vibrations, composite shells, anisotropy, shells of revolution, finite exponential Fourier transform, frequency trial method

## ÖZ

# ANİZOTROPİK KATMANLI KOMPOZİT EKSENEL SİMETRİK KABUKLARIN SERBEST TİTREŞİM ANALİZİ

Yavuzbalkan, Erdem

Yüksek Lisans, Havacılık ve Uzay Mühendisliği Bölümü

Tez Yöneticisi: Doç. Dr. Altan Kayran

Ağustos 2005, 288 sayfa

Bu tezde, Makroskopik Anizotropik Katmanlı Kompozit Eksenel Simetrik Kabukların (MAKKESK) serbest titreşim analizleri çalışılmıştır. Ana denklemler kinematik, konstitütif ve hareket denklemleridir. Kinematik denklemler Reissner-Naghdi kabuk teorisinin geometrik lineer genlemeler değiştirme denklemlerinin enine kesme ve dönel atalet etkilerini de barındıran birinci derece kayma – deformasyon teorisi ile birlikte kullanılmasından oluşmaktadır. Konstitütif denklemlerde MAKKESK'nin tek katman için içsel gerilmelerin yerine statik eşdeğer yük ve moment sonuçları kullanılmıştır. Hareket denklemleri ise serbest titreşim problemi için Hamilton prensibi kullanılarak elde edilmiştir. MAKKESK'nin serbest titreşim analizi için türetilen ana denklemler temel değerlerle formüle edilmiş kısmi diferansiyel denklem sistemine dönüştürülmüştür. Sonra bu denklemleri iki noktalı sınır değer problemi olacak şekilde sonlu Üstel Fourier Dönüşüm Metodu (ÜFDM) uygulanarak birinci dereceden adi diferansiyel denklemlere dönüştürülmüştür. Gösterilmiştir ki ÜFDM'nin uygulanması, tam anizotropik şeklindeki konstitütif denklemlerinin klasik Fourier Ayırıştırma metodu kullanılarak olanaksız görülen çözümünü olası kılmıştır. Sınır değer problemi öncelikle bir grup başlangıç değer problemine dönüştürülmüştür. Bunun ardından verilen doğal frekans aralığındaki kritik modlar frekans deneme metodu ile bütünlük çok parçalı sayısal integrasyon kullanılarak bulunmuştur. MAKKESK'nin doğal frekans ve mod şekillerinin çözümü için

DALSOR isimli bir bilgisayar kodu yazılmıştır. DALSOR her türlü sınır koşulları ve kabuğun eksenine boyunca elastik ve geometrik özellik değişimleri için uygulanabilir.

Sayısal sonuçlar sunulmuş ve çözüm metodu ve modal karakteristikler, daha çok doğal frekanslar, üzerindeki makroskopik anizotropi etkisi tartışılmıştır. Silindirik kabuklar üzerinde, ana olarak, fiber oryantasyon açısı, istif sırası, kabuğun her iki ucundaki keyfi sınır koşulları, modal karakteristeki kalınlık yarıçap oranının etkisini inceleyen bir çok durum çalışması gerçekleştirilmiştir. Çözüm metodunun kesik kompozit küresel kabuk üzerine uygulanması da ayrıca gösterilmiştir.

**Anahtar kelimeler:** Serbest titreşim, kompozit kabuklar, anizotropi, aksiyel simetrik kabuklar, sonlu üstel Fourier dönüşümü, frekans deneme metodu

*To my parents  
and  
To all people who believe in  
honor, respect and loyalty*

## ACKNOWLEDGEMENTS

I would like to express my gratitude to all those who gave me the possibility to complete this thesis. As a start, I am deeply grateful to my supervisor *Assoc. Prof Dr. Altan Kayran* whose help, stimulating suggestions and encouragement helped me in all the time of research for and writing of this thesis.

I am deeply grateful to my very dear parents, especially my mother, for supporting me and for showing me love, patience and prayers to carry on my work successfully and complete my higher education.

I owe special thanks to my very dear friends Arzu Taşçı, Yavuz Güleç and Celal Soyarslan for all their help, support and valuable hints that helped me much in accomplishing this work. I also want to thank all my friends at the department; Utku Dinçer, Tahir Turgut, and Özhan Turgut for their interests and help.

# TABLE OF CONTENTS

Plagiarism .....	iii
Abstract .....	iv
Öz .....	vi
Dedication .....	viii
Acknowledgements .....	ix
Table of Contents .....	x
List of Tables .....	xiii
List of Figures .....	xvii
List of Symbols .....	xxiv
<b>CHAPTERS</b>	
1.INTRODUCTION.....	1
1.1 Background .....	1
1.2 Literature Survey .....	9
1.3 Present Research .....	16
1.3.1 Motivation .....	16
1.3.2 Objective and Scope.....	17
1.3.3 Overview of the Thesis .....	19
2. MATHEMATICAL MODELING .....	21
2.1 Introduction .....	21
2.2 Reference Surface of Shell .....	21
2.3 Differential Geometry .....	22
2.3.1 Space Curves .....	22
2.3.1.1 Unit Tangent Vector.....	23
2.3.1.2 Osculating Plane, Principal Normal .....	24
2.3.1.3 Curvature .....	24
2.3.2 Surfaces .....	26
2.3.2.1 Parametric Curves of a Surface; First Fundamental Form	26
2.3.2.2 Normal to a Surface.....	27
2.3.2.3 Second Fundamental Form .....	28
2.3.2.4 Principal Curvatures .....	31
2.3.2.5 Derivatives of Unit Vectors along Parametric Lines .....	32
2.3.2.6 Fundamental Theorem of the Theory of Surfaces .....	36
2.4 Classification of Shell Surfaces .....	37

2.4.1	Shells of Revolution .....	39
2.5	Theory of Laminated Composite Elastic Shells for Dynamic Analysis	45
2.5.1	The Coordinate System and Differential Element of a Single-Layer Doubly Curved Thin Shell and Its Surface Related Features .....	52
2.5.2	Kinematic Relations of a Laminated Composite Doubly Curved Shell .....	63
2.5.3	Constitutive Relations of an Anisotropic Laminated Composite Doubly Curved Shell .....	67
2.5.4	Equations of Motion of an Anisotropic Laminated Composite Doubly Curved Shell .....	80
2.6	Governing Equations for Free Vibration Analysis of Anisotropic Laminated Composite Shells of Revolution .....	86
3	METHOD OF SOLUTION .....	90
3.1	Introduction .....	90
3.2	Overview of the Methods of Solution for Free Vibration of Homogeneous or Laminated Shells of Revolution .....	90
3.3	Formulation of the System of First Order Ordinary Differential Equations .....	93
3.3.1	System of Partial Differential Equations .....	94
3.3.2	System of First Order Ordinary Differential Equations .....	99
3.4	Nondimensionalization of the System of First Order Ordinary Differential Equations .....	103
3.5	Numerical Solution for the Two Point Boundary Value Problems .....	104
3.5.1	Reduction to Initial Value Problems .....	107
3.5.2	Method of Solution for a One Segment Shell .....	109
3.5.3	Extension to Present Method of Solution to a Multisegment Shell .....	111
3.6	Frequency Trial Method .....	114
3.7	Description and Flow-Chart of the Developed Code, DALSOR .....	119
4	NUMERICAL RESULTS AND DISCUSSIONS .....	122
4.1	Introduction .....	122
4.2	Laminated Composite Circular Cylindrical Shell .....	123
4.3	Verification of the DALSOR .....	125
4.3.1	Verification of the Present Method of Solution .....	125
4.4	Case Studies .....	128
4.4.1	Case Study on the Effect of Fiber Orientation Angle .....	128
4.4.2	Case Study on Stacking Sequence .....	144
4.4.3	Case Study on Boundary Condition .....	152
4.4.4	Case Study on Thickness-to-Radius Ratio .....	157
4.4.5	Case Study on Effect of Coupling Terms .....	171

4.4.6	Case Study on the Existence of Coupling Terms .....	179
4.5	Laminated Composite Spherical Shell .....	184
5.	CONCLUSIONS AND RECOMMENDATIONS .....	188
	Recommendations for Future Work .....	192
	References .....	194
APPENDICES		
A.	VARIATIONAL COMPUTATION OF THE STRAIN ENERGY ( $\delta U$ ) .....	200
B.	SYMBOLIC COMPUTATION OF EQUATION (3.14) .....	208
C.	COEFFICIENTS OF THE SYSTEM OF PARTIAL DIFFERENTIAL EQUATIONS DERIVED IN SECTION 3.3.1 .....	211
D.	METHOD OF FINITE EXPONENTIAL FOURIER TRANSFORM .....	228
E.	APPLICATION OF METHOD OF FINITE FOURIER TRANSFORM TO THE SYSTEM OF DIFFERENTIAL EQUATIONS DERIVED IN SECTION 3.2.1 .....	230
F.	THE ELEMENTS OF COEFFICIENT MATRIX K .....	257
G.	DEMONSTRATION OF THE RELATION BETWEEN THE DETERMINANT OF THE CHARACTERISTIC EQUATION DETERMINED BY THE TRADITIONAL FOURIER DECOMPOSITION METHOD AND THE ONE BY THE FINITE EXPONENTIAL FOURIER TRANSFORM METHOD .....	264
H.	MODE SHAPES OF SYMMETRIC, ANTISYMMETRIC and UNSYMMETRIC LAYUPS for N=0, 1, and 2 CASES .....	280

## LIST OF TABLES

Table 1.1	Advantages and disadvantages of composite materials over metals .....	2
Table 1.2	Computational modeling approaches for two-dimensional approximation theories used for layered composite shells .....	13
Table 3.1	Trial natural frequencies and their computed determinants in order to find first natural frequency of the example problem with traditional Fourier Decomposition procedure .....	116
Table 3.2	Trial natural frequencies and their computed determinants in order to find first natural frequency of the example problem with method of Finite Exponential Fourier Transform .....	118
Table 4.1	Geometrical and material properties of the single layer, simply supported circular cylindrical shell used in comparison study of the method of solution	126
Table 4.2	Natural Frequencies (rad/sec) calculated with DALSOR as the present method of solution and calculated with the exact solution in [13] and the relative % differences between them for $m=1-3$ and $n=0-10$ .....	127
Table 4.3	Geometrical, material properties, and laminate properties of the simply supported laminated composite circular cylindrical shell used for the case study on the fiber orientation angle .....	128
Table 4.4	Natural Frequencies (rad/sec) when the fiber orientation angle changing from 0 to 90 with the increment of 10 degrees for $n=0$ , and $m=1,2$ , and 3 .....	131
Table 4.5	Natural Frequencies (rad/sec) when the fiber orientation angle changing from 0 to 90 with the increment of 10 degrees for $n=1$ , and $m=1,2$ , and 3 .....	132
Table 4.6	Natural Frequencies (rad/sec) when the fiber orientation angle changing from 0 to 90 with the increment of 10 degrees for $n=2$ , and $m=1,2$ , and 3 .....	132
Table 4.7	Natural Frequencies (rad/sec) when the fiber orientation angle changing from 0 to 90 with the increment of 10 degrees for $n=3$ , and $m=1,2$ , and 3 .....	132
Table 4.8	Natural Frequencies (rad/sec) when the fiber orientation angle changing from 0 to 90 with the increment of 10 degrees for $n=4$ , and $m=1,2$ , and 3 .....	132

Table 4.9	Natural Frequencies (rad/sec) when the fiber orientation angle changing from 0 to 90 with the increment of 10 degrees for n=5, and m=1,2, and 3 .....	133
Table 4.10	Natural Frequencies (rad/sec) when the fiber orientation angle changing from 0 to 90 with the increment of 10 degrees for n=6, and m=1,2, and 3 .....	133
Table 4.11	Natural Frequencies (rad/sec) when the fiber orientation angle changing from 0 to 90 with the increment of 10 degrees for n=7, and m=1,2, and 3 .....	133
Table 4.12	Natural Frequencies (rad/sec) when the fiber orientation angle changing from 0 to 90 with the increment of 10 degrees for n=8, and m=1,2, and 3 .....	133
Table 4.13	Natural Frequencies (rad/sec) when the fiber orientation angle changing from 0 to 90 with the increment of 10 degrees for n=9, and m=1,2, and 3 .....	134
Table 4.14	Natural Frequencies (rad/sec) when the fiber orientation angle changing from 0 to 90 with the increment of 10 degrees for n=10, and m=1,2, and 3 .....	134
Table 4.15	Six symmetric layups used in the case study on the stacking sequence .....	144
Table 4.16	Geometrical, material properties, and laminate properties of the clamped-clamped laminated composite circular cylindrical shell used for the case study on stacking sequence .....	145
Table 4.17	Natural frequencies (rad/sec) for n 0 to 9 for the layup 1 in Table 4.15 for CC (h/R=0.01) .....	147
Table 4.18	Natural frequencies (rad/sec) for n 0 to 9 for the layup 2 in Table 4.15 for CC (h/R=0.01).....	147
Table 4.19	Natural frequencies (rad/sec) for n 0 to 9 for the layup 3 in Table 4.15 for CC (h/R=0.01) .....	148
Table 4.20	Natural frequencies (rad/sec) for n 0 to 9 for the layup 4 in Table 4.15 for CC (h/R=0.01) .....	148
Table 4.21	Natural frequencies (rad/sec) for n 0 to 9 for the layup 5 in Table 4.15 for CC (h/R=0.01) .....	148
Table 4.22	Natural frequencies (rad/sec) for n 0 to 9 for the layup 6 in Table 4.15 for CC (h/R=0.01) .....	148
Table 4.23	Natural frequencies (rad/sec) for n 0 to 9 for the layup 1 in Table 4.15 for CF (h/R=0.01) .....	152
Table 4.24	Natural frequencies (rad/sec) for n 0 to 9 for the layup 2 in Table 4.15 for CF (h/R=0.01) .....	152
Table 4.25	Natural frequencies (rad/sec) for n 0 to 9 for the layup 3 in Table 4.15 for CF (h/R=0.01) .....	153
Table 4.26	Natural frequencies (rad/sec) for n 0 to 9 for the layup 4 in Table 4.15 for CF (h/R=0.01) .....	153
Table 4.27	Natural frequencies (rad/sec) for n 0 to 9 for the layup 5 in Table 4.15 for CF (h/R=0.01) .....	153

Table 4.28	Natural frequencies (rad/sec) for n 0 to 9 for the layup 6 in Table 4.15 for CF (h/R=0.01) .....	153
Table 4.29	Natural frequencies (rad/sec) for n 0 to 9 for the layup 1 in Table 4.15 for CC (h/R=0.1) .....	161
Table 4.30	Natural frequencies (rad/sec) for n 0 to 9 for the layup 2 in Table 4.15 for CC (h/R=0.1) .....	161
Table 4.31	Natural frequencies (rad/sec) for n 0 to 9 for the layup 3 in Table 4.15 for CC (h/R=0.1) .....	161
Table 4.32	Natural frequencies (rad/sec) for n 0 to 9 for the layup 4 in Table 4.15 for CC (h/R=0.1) .....	161
Table 4.33	Natural frequencies (rad/sec) for n 0 to 9 for the layup 5 in Table 4.15 for CC (h/R=0.1) .....	162
Table 4.34	Natural frequencies (rad/sec) for n 0 to 9 for the layup 6 in Table 4.15 for CC (h/R=0.1) .....	162
Table 4.35	Natural frequencies (rad/sec) for n 0 to 9 for the layup 1 in Table 4.15 for CF (h/R=0.1) .....	164
Table 4.36	Natural frequencies (rad/sec) for n 0 to 9 for the layup 2 in Table 4.15 for CF (h/R=0.1) .....	164
Table 4.37	Natural frequencies (rad/sec) for n 0 to 9 for the layup 3 in Table 4.15 for CF (h/R=0.1) .....	164
Table 4.38	Natural frequencies (rad/sec) for n 0 to 9 for the layup 4 in Table 4.15 for CF (h/R=0.1) .....	164
Table 4.39	Natural frequencies (rad/sec) for n 0 to 9 for the layup 5 in Table 4.15 for CF (h/R=0.1) .....	165
Table 4.40	Natural frequencies (rad/sec) for n 0 to 9 for the layup 6 in Table 4.15 for CF (h/R=0.1) .....	165
Table 4.41	Three different layups used in the case study on effect of coupling terms .....	171
Table 4.42	Geometrical, material properties, and laminate properties of the simply supported laminated composite circular cylindrical shell used for the case study on type of lamination scheme .....	172
Table 4.43	Natural frequencies (rad/sec) of circular cylindrical shell with symmetric layup $[0/30/90/60]_s$ .....	174
Table 4.44	Natural frequencies (rad/sec) of circular cylindrical shell with antisymmetric layup $[0/30/90/60/-60/-90/-30/0]$ .....	174
Table 4.45	Natural frequencies (rad/sec) of circular cylindrical shell with unsymmetric layup $[0/30/90/60/0/30/90/60]$ .....	175

Table 4.46	Dominant mode shapes for three layups for n=0, and n=1.....	178
Table 4.47	Natural frequencies (rad/sec) of circular cylindrical shell with unsymmetric layup $[0/30/90/60/0/30/90/60]$ with all coupling terms omitted .....	181
Table 4.48	Comparison of the natural frequencies (rad/sec) between antisymmetric layup case and unsymmetric layup with coupling terms omitted for n=0,1, and 2.....	184
Table 4.49	Geometrical, material properties, and laminate properties of the clamped-free laminated composite spherical shell .....	185
Table 4.50	Natural Frequencies for the laminated composite spherical shell (n=1) .....	185

## LIST OF FIGURES

Figure 1.1	Specific strength and specific stiffness of advanced composite materials [1] .....	3
Figure 1.2	A unidirectional fiber-reinforced lamina with the principal material directions (1, 2, and 3) and the global or lamina coordinates (x, y, and z) [3] .....	7
Figure 1.3	Deformation of isotropic, orthotropic and anisotropic rectangular block under uniaxial tensile and pure shear loading [1] .....	8
Figure 2.1	The position vector of a space curve .....	22
Figure 2.2	Tangent vector description .....	24
Figure 2.3	Parametric curves of a surface and differential change of a position vector on the surface .....	27
Figure 2.4	Some examples for surfaces of revolution (a) Circular Cylinder, (b) Cone, (c) Elliptic dome, (d) Hyperboloid of revolution, (e) Toroid .....	38
Figure 2.5	Some examples for Surfaces of translation (a) Elliptic paraboloid, (b) Hyperbolic paraboloid, (c) Hyper and its straight-line generators .....	39
Figure 2.6	Ruled Surfaces (a) Hyperboloid of revolution of one sheet, (b) Conoid ....	39
Figure 2.7	Geometry and coordinate system of shells of revolution .....	41
Figure 2.8	Differential element and coordinate system of a doubly curved thin shell [12] .....	53
Figure 2.9	(a) Specially Orthotropic Lamina, (b) Generally Orthotropic Lamina .....	70
Figure 2.10	Internal Stresses on a Doubly Curved Shell Element .....	73
Figure 2.11	Force resultants in the shell coordinates .....	75
Figure 2.12	Moment resultants in the shell coordinates .....	75
Figure 2.13	N-layered laminate of a doubly curved shell element .....	76
Figure 3.1	Division of meridional length of the shell of revolution into segments ....	112
Figure 3.2	The subparts of the second part of Frequency Trial Method .....	115
Figure 3.3	Finding first natural frequency of the example problem with (a) Traditional Fourier decomposition method, and (b) Method of finite exponential Fourier transform .....	117

Figure 3.4	Flow-chart of Laminate and Natural Frequency Programs of the developed Fortran code DALSOR .....	120
Figure 3.5	Flow-chart of Mode Shape Program of the developed Fortran code DALSOR .....	121
Figure 4.1	General Configuration and Coordinate System of Laminated Composite Circular Cylindrical Shell and its Laminate .....	124
Figure 4.2	Circumferential Nodal Patterns and Axial Nodal Patterns for a Simply Supported Circular Cylindrical Shell without axial constraint [78] .....	125
Figure 4.3	The comparison of natural frequencies calculated by the exact method of solution [13] with those calculated by the present method of solution from $n=0$ to $n=10$ for $m=1, 2,$ and $3$ .....	127
Figure 4.4	Effect of the fiber orientation angle on the elements of stretching stiffness matrix .....	130
Figure 4.5	Effect of the fiber orientation angle on the elements of transverse shear stiffness matrix .....	130
Figure 4.6	Effect of the fiber orientation angle on the elements of flexural stiffness matrix .....	131
Figure 4.7	Natural Frequency versus circumferential wave number changing from 0 to 10 for fiber orientation angle of $0^\circ$ to $90^\circ$ with the increment of 10 degrees when $m=1$ .....	135
Figure 4.8	Natural Frequency versus circumferential wave number changing from 0 to 10 for fiber orientation angle of $0^\circ$ to $90^\circ$ with the increment of 10 degrees when $m=2$ .....	135
Figure 4.9	Natural Frequency versus circumferential wave number changing from 0 to 10 for fiber orientation angle of $0^\circ$ to $90^\circ$ with the increment of 10 degrees when $m=3$ .....	136
Figure 4.10	Variation in strain energy in a particular cylindrical shell with increasing number of circumferential modes [79] .....	136
Figure 4.11	Natural Frequency versus fiber orientation angle for the first lowest fundamental mode ( $m=1$ ) .....	137
Figure 4.12	Natural Frequency versus fiber orientation angle for the second lowest fundamental mode ( $m=2$ ) .....	137
Figure 4.13	Natural Frequency versus fiber orientation angle for the third lowest fundamental mode ( $m=3$ ) .....	138
Figure 4.14	Mode shapes for the first fundamental transverse mode when $\alpha$ changes from $0^\circ$ to $90^\circ$ with the increment of $10^\circ$ ( $n=1$ ) .....	140-141

Figure 4.15	Mode shapes for the first fundamental transverse mode when $\alpha$ changes from $0^\circ$ to $90^\circ$ with the increment of $10^\circ$ ( $n=2$ ) .....	141-142
Figure 4.16	Mode shapes for the first fundamental transverse mode when $\alpha$ changes from $0^\circ$ to $90^\circ$ with the increment of $10^\circ$ ( $n=3$ ) .....	142-143
Figure 4.17	Effect of the stacking sequence on the elements of stretching stiffness matrix ( $h/R=0.01$ ) .....	146
Figure 4.18	Effect of the stacking sequence on the elements of transverse shear stiffness matrix ( $h/R=0.01$ ) .....	146
Figure 4.19	Effect of the stacking sequence on the elements of flexural stiffness matrix ( $h/R=0.01$ ) .....	147
Figure 4.20	Natural frequencies versus circumferential wave numbers for all stacking sequence for clamped-clamped (CC) boundary condition ( $m=1$ and $h/R=0.01$ ) .....	150
Figure 4.21	Natural frequencies versus circumferential wave numbers for all stacking sequence for clamped-clamped (CC) boundary condition ( $m=2$ and $h/R=0.01$ ) .....	151
Figure 4.22	Natural frequencies versus circumferential wave numbers for all stacking sequence for clamped-clamped (CC) boundary condition ( $m=3$ and $h/R=0.01$ ) .....	151
Figure 4.23	Natural frequencies versus circumferential wave numbers for all stacking sequence for clamped-free (CF) boundary condition ( $m=1$ and $h/R=0.01$ ) .....	154
Figure 4.24	Natural frequencies versus circumferential wave numbers for all stacking sequence for clamped-free (CF) boundary condition ( $m=2$ and $h/R=0.01$ ) .....	155
Figure 4.25	Natural frequencies versus circumferential wave numbers for all stacking sequence for clamped-free (CF) boundary condition ( $m=3$ and $h/R=0.01$ ) .....	155
Figure 4.26	Comparison of the natural frequencies of the laminated composite circular cylindrical shell having CC boundary conditions with the ones having CF boundary conditions ( $m=1$ and $h/R=0.01$ ) .....	156
Figure 4.27	Comparison of the natural frequencies of the laminated composite circular cylindrical shell having CC boundary conditions with the ones having CF boundary conditions ( $m=2$ and $h/R=0.01$ ) .....	156
Figure 4.28	Comparison of the natural frequencies of the laminated composite circular cylindrical shell having CC boundary conditions with the ones having CF boundary conditions ( $m=3$ and $h/R=0.01$ ) .....	157
Figure 4.29	Effect of the stacking sequence on the elements of stretching stiffness matrix ( $h/R=0.1$ ) .....	158
Figure 4.30	Effect of the stacking sequence on the elements of transverse shear stiffness matrix ( $h/R=0.1$ ) .....	158

Figure 4.31	Effect of the stacking sequence on the elements of flexural stiffness matrix ( $h/R=0.1$ ) .....	159
Figure 4.32	Natural frequencies versus circumferential wave numbers for all stacking sequence for clamped-clamped (CC) boundary condition ( $m=1$ and $h/R=0.1$ ) .....	162
Figure 4.33	Natural frequencies versus circumferential wave numbers for all stacking sequence for clamped-clamped (CC) boundary condition ( $m=2$ and $h/R=0.1$ ) .....	163
Figure 4.34	Natural frequencies versus circumferential wave numbers for all stacking sequence for clamped-clamped (CC) boundary condition ( $m=3$ and $h/R=0.1$ ).....	163
Figure 4.35	Natural frequencies versus circumferential wave numbers for all stacking sequence for clamped-free (CF) boundary condition ( $m=1$ and $h/R=0.1$ ) ..	165
Figure 4.36	Natural frequencies versus circumferential wave numbers for all stacking sequence for clamped-free (CF) boundary condition ( $m=2$ and $h/R=0.1$ ) ..	166
Figure 4.37	Natural frequencies versus circumferential wave numbers for all stacking sequence for clamped-free (CF) boundary condition ( $m=3$ and $h/R=0.1$ ) ..	166
Figure 4.38	Comparison of the natural frequencies of the laminated composite circular cylindrical shell having CC boundary conditions with the ones having CF boundary conditions ( $m=1$ and $h/R=0.1$ ) .....	167
Figure 4.39	Comparison of the natural frequencies of the laminated composite circular cylindrical shell having CC boundary conditions with the ones having CF boundary conditions ( $m=2$ and $h/R=0.1$ ) .....	167
Figure 4.40	Comparison of the natural frequencies of the laminated composite circular cylindrical shell having CC boundary conditions with the ones having CF boundary conditions ( $m=3$ and $h/R=0.1$ ) .....	168
Figure 4.41	Comparison of the natural frequencies of the thick and thin shell configurations for clamped-clamped (CC) boundary condition ( $m=1$ ) .....	168
Figure 4.42	Comparison of the natural frequencies of the thick and thin shell configurations for clamped-clamped (CC) boundary condition ( $m=2$ ) .....	169
Figure 4.43	Comparison of the natural frequencies of the thick and thin shell configurations for clamped-clamped (CC) boundary condition ( $m=3$ ) .....	169
Figure 4.44	Comparison of the natural frequencies of the thick and thin shell configurations for clamped-free (CF) boundary condition ( $m=1$ ) .....	170
Figure 4.45	Comparison of the natural frequencies of the thick and thin shell configurations for clamped-free (CF) boundary condition ( $m=2$ ) .....	170
Figure 4.46	Comparison of the natural frequencies of the thick and thin shell configurations for clamped-free (CF) boundary condition ( $m=3$ ) .....	171

Figure 4.47	Effect of the stacking sequence on the elements of stretching stiffness matrix for three different layups in the case study on effect of coupling terms .....	172
Figure 4.48	Effect of the stacking sequence on the elements of transverse shear stiffness matrix for three different layups in the case study on effect of coupling terms .....	173
Figure 4.49	Effect of the stacking sequence on the elements of stretching-flexural coupling stiffness matrix for three different layups in the case study on effect of coupling terms .....	173
Figure 4.50	Effect of the stacking sequence on the elements of flexural stiffness matrix for three different layups in the case study on effect of coupling terms .....	174
Figure 4.51	Effect of coupling terms on the natural frequencies of the simply supported laminated composite circular cylindrical shell (m=1) .....	175
Figure 4.52	Effect of coupling terms on the natural frequencies of the simply supported laminated composite circular cylindrical shell (m=2) .....	176
Figure 4.53	Effect of coupling terms on the natural frequencies of the simply supported laminated composite circular cylindrical shell (m=3) .....	176
Figure 4.54	Elements of stretching stiffness matrix for the layups used in the case study on the existence of coupling terms .....	179
Figure 4.55	Elements of transverse shear stiffness matrix for the layups used in the case study on the existence of coupling terms .....	180
Figure 4.56	Elements of stretching-flexural coupling stiffness matrix for the layups used in the case study on the existence of coupling terms .....	180
Figure 4.57	Elements of flexural stiffness matrix for the layups used in the case study on the existence of coupling terms .....	181
Figure 4.58	Effect of the coupling terms on the natural frequencies over n range of 0-9 (m=1) .....	182
Figure 4.59	Effect of the coupling terms on the natural frequencies over n range of 0-9 (m=2) .....	182
Figure 4.60	Effect of the coupling terms on the natural frequencies over n range of 0-9 (m=3) .....	183
Figure 4.61	The side and perspective views of the laminated composite spherical shell .....	186
Figure 4.62	Dominant mode shapes (transverse displacement) of the corresponding natural frequencies given in Table 4.50 for (a) m=1, (b) m=2, and (c) m=3 .....	186

Figure 5.1	Cross-sections of the circular cylindrical shells with (a) a single stiffener, (b) two stiffeners or, (c) multi-stiffeners .....	193
Figure H.1	Mode Shapes in displacements of (a) $w$ (b) $u_\phi$ (c) $u_\theta$ for (n=0) and (m=1); (d) $w$ (e) $u_\phi$ (f) $u_\theta$ for (n=0) and (m=2); and (g) $w$ (h) $u_\phi$ (i) $u_\theta$ for (n=0) and (m=3) for symmetric layup .....	280
Figure H.2	Mode Shapes in displacements of (a) $w$ (b) $u_\phi$ (c) $u_\theta$ for (n=1) and (m=1); (d) $w$ (e) $u_\phi$ (f) $u_\theta$ for (n=1) and (m=2); and (g) $w$ (h) $u_\phi$ (i) $u_\theta$ for (n=1) and (m=3) for symmetric layup .....	281
Figure H.3	Mode Shapes in displacements of (a) $w$ (b) $u_\phi$ (c) $u_\theta$ for (n=2) and (m=1); (d) $w$ (e) $u_\phi$ (f) $u_\theta$ for (n=2) and (m=2); and (g) $w$ (h) $u_\phi$ (i) $u_\theta$ for (n=2) and (m=3) for symmetric layup .....	282
Figure H.4	Mode Shapes in displacements of (a) $w$ (b) $u_\phi$ (c) $u_\theta$ for (n=0) and (m=1); (d) $w$ (e) $u_\phi$ (f) $u_\theta$ for (n=0) and (m=2); and (g) $w$ (h) $u_\phi$ (i) $u_\theta$ for (n=0) and (m=3) for antisymmetric layup .....	283
Figure H.5	Mode Shapes in displacements of (a) $w$ (b) $u_\phi$ (c) $u_\theta$ for (n=1) and (m=1); (d) $w$ (e) $u_\phi$ (f) $u_\theta$ for (n=1) and (m=2); and (g) $w$ (h) $u_\phi$ (i) $u_\theta$ for (n=1) and (m=3) for antisymmetric layup .....	284
Figure H.6	Mode Shapes in displacements of (a) $w$ (b) $u_\phi$ (c) $u_\theta$ for (n=2) and (m=1); (d) $w$ (e) $u_\phi$ (f) $u_\theta$ for (n=2) and (m=2); and (g) $w$ (h) $u_\phi$ (i) $u_\theta$ for (n=2) and (m=3) for antisymmetric layup .....	285
Figure H.7	Mode Shapes in displacements of (a) $w$ (b) $u_\phi$ (c) $u_\theta$ for (n=0) and (m=1); (d) $w$ (e) $u_\phi$ (f) $u_\theta$ for (n=0) and (m=2); and (g) $w$ (h) $u_\phi$ (i) $u_\theta$ for (n=0) and (m=3) for unsymmetric layup .....	286
Figure H.8	Mode Shapes in displacements of (a) $w$ (b) $u_\phi$ (c) $u_\theta$ for (n=1) and (m=1); (d) $w$ (e) $u_\phi$ (f) $u_\theta$ for (n=1) and (m=2); and (g) $w$ (h) $u_\phi$ (i) $u_\theta$ for (n=1) and (m=3) for unsymmetric layup .....	287

Figure H.9	Mode Shapes in displacements of (a) $w$ (b) $u_\phi$ (c) $u_\theta$ for (n=2) and (m=1); (d) $w$ (e) $u_\phi$ (f) $u_\theta$ for (n=2) and (m=2); and (g) $w$ (h) $u_\phi$ (i) $u_\theta$ for (n=2) and (m=3) for unsymmetric layup .....	288
------------	---	-----

## LIST OF SYMBOLS

1, 2, 3	: Principal material coordinates
$A$	: An $m \times m$ coefficient matrix.
$A_1, A_2$	: Lamé parameters for a shell.
$A_\phi, A_\theta$	: Lamé parameters for a shell of revolution.
$A_{ij}$	: Extensional stiffness matrix which relates the in-plane stress resultants to the reference surface strains where (i,j=1,2,6).
$A_{12}$	: Extension-extension coupling happens when a normal force resultant $N_{\xi_1}$ causes elongation in the $\xi_2$ direction $\mathcal{E}_{\xi_2}^0$ , and a normal force resultant $N_{\xi_2}$ causes elongation in the $\xi_1$ direction $\mathcal{E}_{\xi_1}^0$ .
$A_{16}$	: Extension-shear couplings take place when in-plane normal force resultant $N_{\xi_1}$ causes shear deformation $\gamma_{\xi_1 \xi_2}^0$ , and a shear (or twist) force resultant $N_{\xi_1 \xi_2}$ causes elongations in the $\xi_1$ direction.
$A_{26}$	: Extension-shear couplings take place when in-plane normal force resultant $N_{\xi_2}$ causes shear deformation $\gamma_{\xi_1 \xi_2}^0$ , and a shear (or twist) force resultant $N_{\xi_1 \xi_2}$ causes elongations in the $\xi_2$ direction.
$As_{45}$	: Transverse shear coupling between the shear strain in the $\phi - \zeta$ plane and shear strain in the $\theta - \zeta$ plane.
$As_{ij}$	: transverse shear stiffness matrix which relates the transverse shear resultants to transverse shear strains where (i,j=4,5).
$B_{ij}$	: Bending-stretching coupling matrix which relates the in-plane stress resultants and bending and twisting moment resultants to curvature and twist changes of the reference surface where (i,j=1,2,6).

$B_{16}$	: Extension-twist and bending-shear coupling exists when in-plane normal force resultant $N_{\xi_1}$ causes twist $\kappa_{\xi_1 \xi_2}$ , and bending moment resultant $M_{\xi_1}$ results in in-plane shear deformation $\gamma_{\xi_1 \xi_2}^0$ .
$B_{26}$	: Extension-twist and bending-shear coupling exists when in-plane normal force resultant $N_{\xi_2}$ causes twist $\kappa_{\xi_1 \xi_2}$ , and bending moment resultant $M_{\xi_2}$ results in in-plane shear deformation $\gamma_{\xi_1 \xi_2}^0$ .
$C_M$	: The characteristic matrix in order to calculate the natural frequencies obtained after the application of boundary conditions with the multisegment numerical integration method in combination with the frequency trial method.
$C_{ijkl}$	: Stiffness tensor or the material coefficients.
$D_{ij}$	: Bending stiffness matrix which relates the bending and twisting moments to curvature and twist changes of the reference surface where (i,j=1,2,6).
$D_{16}$	: Bending-twist coupling takes place when bending moment resultant $M_{\xi_1}$ causes the twist of the laminate $\kappa_{\xi_1 \xi_2}$ , and a twist moment resultant $M_{\xi_1 \xi_2}$ causes curvatures in the $\xi_1 - \zeta$ plane, namely $\kappa_{\xi_1}$ .
$D_{26}$	: Bending-twist coupling takes place when bending moment resultants $M_{\xi_2}$ causes the twist of the laminate $\kappa_{\xi_1 \xi_2}$ , and a twist moment resultant $M_{\xi_1 \xi_2}$ causes curvatures in the $\xi_2 - \zeta$ plane, namely $\kappa_{\xi_2}$ .
$\vec{e}_1, \vec{e}_2, \vec{e}_3$	: The unit normal vectors of the rectangular coordinate system.
$E_1$	: The Young's modulus in the 1-direction.
$E_2$	: The Young's modulus in the 2-direction.
$E_3$	: The Young's modulus in the 3-direction.
$G_{23}$	: The Shear Modulus in the 2-3 direction.
$G_{13}$	: The Shear Modulus in the 1-3 direction.
$G_{12}$	: The Shear Modulus in the 1-2 direction.

$E, F, G$	: First fundamental magnitudes of the surface $S$ denoted by the vector $\vec{r}(\alpha_1, \alpha_2)$ .
$g_{i(or j)}$	: Geometrical scale factor quantities.
$h$	: Total thickness of the laminate of the shell.
$i$	: Imaginary quantity where it equals to $\sqrt{-1}$ .
$k$	: The curvature.
$\vec{k}$	: The curvature vector which expresses the rate of change of the tangent vector as a point moves along a curve.
$K_n$	: The normal curvature.
$K_1, K_2$	: The principal curvatures of the lines in the family of $\alpha_1$ and $\alpha_2$ curves.
$K$	: The kinetic energy of the elastic body; namely, the elastic shell.
$K(\phi)$	: The 20x20 coefficient matrix whose elements are given in Appendix F.
$L, M, N$	: Second fundamental magnitudes of the surface $S$ denoted by the vector $\vec{r}(\alpha_1, \alpha_2)$ .
$m$	: The number of half waves in the axial direction of the shell.
$n$	: The wave number in the circumferential direction of the shell.
$\vec{n}$	: The normal unit vector passing through an arbitrary point on a surface of a doubly curved shell.
$\vec{N}$	: A unit normal vector in the direction of the principal normal to the curve at a point.
$M_{\xi_1}$	: The bending moment resultant per unit length having unit surface normal in $\xi_1$ -direction.
$M_{\xi_2}$	: The bending moment resultant per unit length having unit surface normal in $\xi_2$ -direction.
$M_{\xi_1\xi_2}$	: The twisting moment resultant per unit length having unit surface normal in $\xi_1$ -direction.
$M_{\xi_2\xi_1}$	: The twisting moment resultant per unit length having unit surface normal in $\xi_2$ -direction.
$M_\phi, M_{\phi\theta}$	: Normal and twisting moment resultants in the fundamental variables.

$N_{\xi_1}$	: The in-plane normal force resultant per unit length having unit surface normal in $\xi_1$ -direction.
$N_{\xi_2}$	: The in-plane normal force resultant per unit length having unit surface normal in $\xi_2$ -direction.
$N_{\xi_1\xi_2}$	: The in-plane shear force resultant per unit length having unit surface normal in $\xi_1$ -direction.
$N_{\xi_2\xi_1}$	: The in-plane shear force resultant per unit length having unit surface normal in $\xi_2$ -direction.
$N_\phi, N_{\phi\theta}$	: Normal and shear force resultants in the fundamental variables.
$P$	: Strain energy density function.
$Q_{ij}$	: The reduced stiffnesses.
$\bar{Q}_{ij}$	: The transformed reduced stiffnesses.
$Q_{\xi_1}$	: The shear force resultant per unit length acting on the face perpendicular to the $\xi_1$ coordinate and is parallel to $\zeta$ -direction.
$Q_{\xi_2}$	: The shear force resultant per unit length acting on the face perpendicular to the $\xi_2$ coordinate and is parallel to $\zeta$ -direction.
$Q_\phi$	: Transverse force resultant in the fundamental variables.
$\vec{r}(\phi, \theta)$	: The position vector of the point P on the reference surface of the shells of revolution.
$R$	: The mean radius of the laminated composite circular cylindrical shell.
$R (= k^{-1})$	: The radius of curvature.
$R_1, R_2$	: The principal radii of curvatures in the curvilinear coordinate system.
$R_0$	: The radius of the parallel at position $x_3$ shown in Figure 2.7.
$S$	: Any surface in the rectangular coordinate system $(x_1, x_2, x_3)$ .
$t$	: time.
$\vec{t}$	: A unit tangent vector.
$T$	: Period $\left( = \frac{2\pi}{\omega} \right)$ .

$T(\phi)$	: The transfer matrix of the shell, and it depends only on the geometric and material properties of the shell given by the coefficient matrix $K(\phi)$ .
$T^j(\phi)$	: The 10x10 partitioned matrix of $T(\phi)$ .
$T_i(\phi)$	: The transfer matrix of a segment $i$ .
$\vec{T}_1$	: The tangent unit vector passing through an arbitrary point on a surface of a doubly curved shell along $\xi_1$ coordinate.
$\vec{T}_2$	: The tangent unit vector passing through an arbitrary point on a surface of a doubly curved shell along $\xi_2$ coordinate.
$T_1, T_2$	: Transformation matrices obtained from the direction cosines.
$u^0, v^0, w^0$	: The displacements of a point on the reference surface of the shell in $\xi_1, \xi_2, \zeta$ coordinates, respectively.
$w^0, u_\phi^0, u_\theta^0$	: Displacements in the fundamental variables.
$\vec{U}, \vec{V}, \vec{W}$	: The displacement vectors along the $\xi_1, \xi_2, \zeta$ coordinates, respectively.
$U$	: The strain energy of the shell.
$U_{ABR}$	: The energy input to the shell due to the applied boundary resultant.
$U_{DL}$	: The energy input due to the distributed loading applied on the surface of the shell.
$x_1, x_2, x_3$	: The orthogonal rectangular coordinate system.
$y(\phi)$	: An (m,1) column matrix which contains m unknown dependent variables.
$\alpha$	: The fiber orientation angle.
$\alpha_1, \alpha_2, \zeta$	: The orthogonal curvilinear coordinate system.
$\beta_1$	: The rotation of a transverse normal about the $\xi_2$ -curvilinear coordinate.
$\beta_2$	: The rotation of a transverse normal about the $\xi_1$ -curvilinear coordinate.
$\beta_\phi, \beta_\theta$	: Rotations in the fundamental variables.
$\gamma_{12}$	: the inplane shearing strain.
$\gamma_{1\zeta}$	: The transverse shear strain whose normal is in 1-direction.

$\gamma_{2\zeta}$	: The transverse shear strain whose normal is in 2-direction.
$\gamma_i^0$	: Shearing strains of the reference surface of the shell (i=1-2).
$\epsilon_{kl}$	: The infinitesimal strain components (k, l=1-3).
$\epsilon_1$	: The inplane normal strain component in 1-direction.
$\epsilon_2$	: The inplane normal strain component in 2-direction.
$\epsilon_i^0$	: Normal strains of the reference surface of the shell (i=1-2).
$\zeta$	: The thickness coordinate of a shell of revolution.
$\eta_i$	: The transverse shear strains of the reference surface of the shell (i=1-2).
$\theta$	: The tangential coordinate of a shell of revolution.
$\kappa_i$	: The curvature changes of the reference surface of the shell (i=1-2).
$\nu_{ij}$	: Poisson's ratio.
$\xi_1, \xi_2, \zeta$	: The orthogonal curvilinear coordinate system of a doubly curved shell.
$\Pi$	: The total potential energy of the shell.
$\rho$	: The overall density of the composite laminate of the shell.
$\sigma_{ij}$	: The Cauchy stress components (i,j=1-3).
$\tau_i$	: The twist changes of the reference surface of the shell (i=1-2).
$\phi$	: The meridional coordinate of a shell of revolution.
$\phi, \theta, \zeta$	: The orthogonal curvilinear coordinate system of the reference surface of a shell of revolution.
$\psi$	: The column vector of fundamental variables.
$\bar{\psi}$	: The column vector of nondimensional fundamental variables.
$\omega_m$	: The natural frequency corresponding to the m <sup>th</sup> mode. In short, it is denoted as $\omega$ .
$\Omega$	: Dimensional natural frequency.
$\bar{\Omega}$	: Nondimensional natural frequency ( $= \omega h \sqrt{\rho/E_1}$ ).

# CHAPTER 1

## INTRODUCTION

### 1.1 BACKGROUND

Composites are defined as materials which are combinations of two or more materials such as reinforcing elements, fillers, and composite matrix binder. Those materials differ in form or composition on a macroscale. The entities of the components in the composites do not change. Also, components of the composites can be physically identified and exhibit an interface between one another. Reinforcing material and matrix material are general two materials in the formation of composites. The task of the reinforcing material is to be the reinforcing or load-carrying agent. The reinforcing materials, which are typically strong and stiff, are mostly existed in the form of fibers or filaments. A filament, which is the smallest unit of a fibrous material, is usually of extreme length and very small diameter, usually less than 25  $\mu\text{m}$ . A fiber is a general term for the filament with a finite length that is at least 100 times its diameter, which typically corresponds to 0.10 to 0.13 mm. Fibers can be continuous or specific short lengths (discontinuous). Common metals like aluminum, copper, iron, nickel, steel, and titanium, and organic materials like glass, carbon, boron, and graphite materials are used as the fiber materials. The function of the matrix is to support and protect the fibers and to provide a means of distributing load among and transmitting load between the fibers. The matrix can be organic, ceramic, or metallic. There are three commonly accepted types of composite materials:

1. Fibrous composites which consist of fibers in a matrix.
2. Laminated composites which consist of layers of various materials.
3. Particulate composites which are composed of particles in a matrix.

Many composite structures used in aeronautical and astronautical, civil, maritime, nuclear, automotive, petroleum and petrochemical engineering are made of laminated fiber-reinforced composites. The laminated fiber-reinforced composites consist of layers of fibers embedded into the matrix. Each layer is called a lamina or ply. The lamina is the fundamental building block of laminated fiber-reinforced composite materials. The layers of fiber-reinforced material are built up with the fiber directions of each layer typically oriented in different directions to give different

strengths and stiffnesses in the various directions. Thus, the strengths and stiffnesses of the laminated fiber-reinforced composite can be tailored to the specific design requirements of the structural element being built [1,2]. The laminated fiber-reinforced composite materials are also called advanced composite materials.

Composite materials have better engineering properties than the conventional engineering materials, for instance, metals. The advantages and disadvantages of composite materials over metals are listed in the Table 1.1.

**Table 1.1** Advantages and disadvantages of composite materials over metals [3]

<b>Advantages of Composite Materials over Metals</b>
<ul style="list-style-type: none"> <li>• Light weight</li> <li>• Resistance to corrosion</li> <li>• High resistance to fatigue damage</li> <li>• Reduced machining</li> <li>• Tapered sections and compound contours easily accomplished</li> <li>• Can orientate fibers in direction of strength/stiffness needed</li> <li>• Reduced number of assemblies and reduced fastener count when cocure and co-consolidation is used</li> <li>• Absorb radar microwaves (stealth capability)</li> <li>• Thermal expansion close to zero reduces thermal problems in outer space applications</li> </ul>
<b>Disadvantages of Composite Materials over Metals</b>
<ul style="list-style-type: none"> <li>• Material is expensive</li> <li>• Lack of established design allowables</li> <li>• Corrosion coupling can result from improper coupling with metals, especially when carbon or graphite is used (sealing is essential)</li> <li>• Degradation of structural properties under temperature extremes and wet conditions</li> <li>• Poor energy absorption and impact damage</li> <li>• Expensive and complicated inspection methods</li> <li>• Reliable detection of substandard bonds is difficult</li> <li>• Defects can be known to exist but precise location can not be determined</li> <li>• Requirement of intensive labor in manufacturing</li> <li>• Higher production and prototype tooling costs</li> </ul>

Additionally, a representation of the strength-to-density and stiffness-to-density of many materials such as advanced composite materials and metals is shown in Figure 1.1. It is seen from Figure 1.1 that fibers alone are stiffer and stronger than when embedded in a matrix. Also, unidirectional configurations are stiffer and stronger than biaxially isotropic configurations. As seen from Figure 1.1, the highest stiffness and strength per unit weight can be obtained with boron fibers. When a unidirectional boron fibers embedded in an epoxy as a lamina, a significant decrease take place in the the relative strength of boron. whereas there is a quite little decrease in the relative stiffness of boron. A biaxially isotropic configured boron/epoxy is still stiffer than steel or titanium, although they both have same relative strength. High strength graphite fibers and composites behave similarly as boron/epoxy. However, the relative strengths of high modulus graphite fibers are generally lower than the materials depicted in Figure 1.1 although the stiffnesses of high modulus graphite fibers are biggest in all configurations among the other materials. The relative strength of a unidirectional S glass fiber embedded in an epoxy matrix is 2½ times greater than the relative strengths of steel or titanium. However, S glass/epoxy is less stiffer than steel or titanium. In Figure 1.1, the relative stiffness of beryllium is six times greater than the relative stiffness of steel, titanium or aluminum. Some of general characteristics of beryllium wires in a matrix behave similarly as other composites depicted in Figure 1.1 [1].

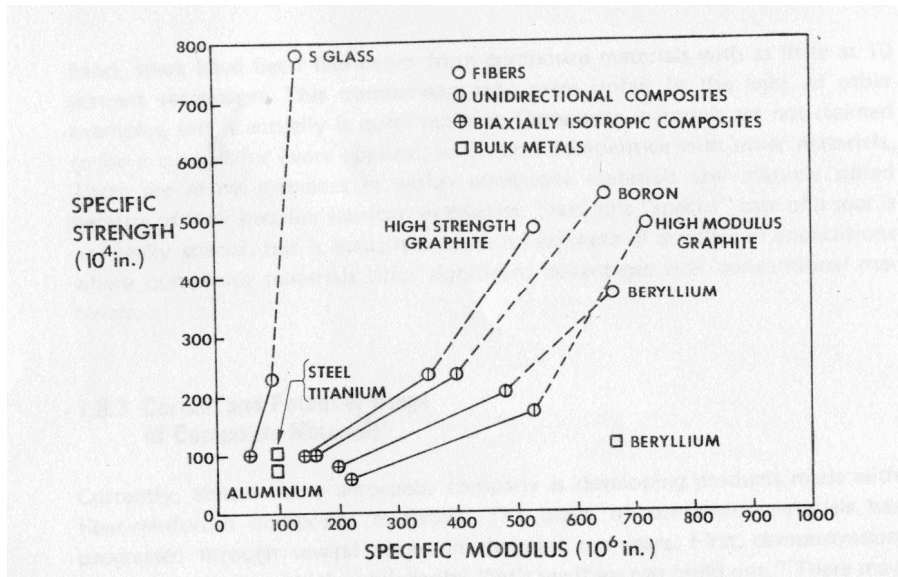


**Figure 1.1** Specific strength and specific stiffness of advanced composite materials [1]

Advanced composite materials or fiber-reinforced composite materials are ideal for structural applications where high strength-to-weight and stiffness-to-weight ratios are required. Since aircraft

and spacecraft are typical weight-sensitive structures, advanced composite materials are essentially suitable and effective for aircraft and spacecraft structures. Actually, the need for reduced weight and increased performance properties in the structural applications of aircraft and spacecraft have led to the development and usage of advanced composite materials.

“The most commonly used advanced composite fibers are carbon and graphite, Kevlar and boron. Among these fibers, carbon fiber is the most versatile of the advanced reinforcements and the most widely used by the aeronautical and space structural applications. On the other hand, matrix materials used in advanced composites to interconnect the fibrous reinforcements are as varied as the reinforcements. Resins or plastic materials, metals, and even ceramic materials are used as matrices. Today, epoxy resin is the primary thermoset composite matrix for airframe and aerospace applications. In all thermoset materials, the matrix is cured by means of time, temperature, and pressure into a dense, low-void-content structure in which the reinforcement is aligned in the direction of anticipated loads. Thermoset matrices are dominated because they allow ready impregnation of fibers, their malleability permits manufacture of complex forms, and they provide a means of achieving high-strength, high-stiffness crosslinked networks in a cured part. In addition to thermosets, thermoplastics are rapidly taking place as the matrix materials. The advantages of thermoplastics over thermoset matrix composites include high service temperature, shorter fabrication cycle, no refrigeration required for storage, increased toughness, low moisture sensitivity, and no need for chemical cure” [3].

“Although man-made composites have existed for thousands of years, the high technology of composites has evolved in the aeronautics industry only in the last thirty years. Filament-wound pressure vessels using glass fibers were the first strength critical application for composites. World War II has been started the development of advanced composite materials due to the need for materials with improved structural properties. Before the emerge of advanced composite materials, aluminum and aluminum alloys, which provide high strength and fairly high stiffness at low weight, have provided good performance and have been the main materials used in aeronautical structures over the years. However, both corrosion and fatigue in aluminum alloys have produced problems. To eliminate corrosion and crack formation in high-performance structures was the initial motive to develop and use the advanced composite materials. Fiberglass-reinforced plastics had been used successfully in filament-wound rocket motors and in various other structural applications such as the pressure vessels. Then, with the salient developments and programs since 1950s, advanced composite materials have become an increasingly attractive alternative to metals, especially aluminum alloys, for many airframe structural applications due to strong, durable, damage tolerant, and less weight characteristics and adequate satisfaction of design and certification requirements. Composite materials can also provide significant cost reductions because they readily adapt to innovative manufacturing techniques” [2].

There have been four stages for the application of advanced composites to military and civil airframe structures. The first stage is the building of *demonstration pieces*. The philosophy of the first stage is “let’s see if we can build one”. The built pieces in the first stage have never been any intention to put the part on an aircraft and flight-test it. The second stage was the *replacement pieces*. The objective of the second stage was to flight-test a part that was designed to replace a metal part on an existing aircraft. The third stage was the actual *production pieces*. By the third stage, various parts of the aircraft were designed from the beginning and fabricated using fiber-reinforced composite materials. The final stage was the *all-composite aircraft* [1]. Serious development work with advanced composite materials started in the middle of 1960s with the boron fibers embedded in an epoxy resin matrix. After development of boron filaments, US Air Force has started to fund programs for usage of advanced composites in the aeronautical structures in the beginning of 1970s. These programs have resulted in the design, production, test, and development of primary and secondary aeronautical structures and aeronautical structural components made of advanced composites. The structures were fuselage sections, flight control surfaces and empennage parts. The General Dynamics F-111 horizontal stabilizer was the first flight-worthy composite component. It is made of boron/epoxy like its fuselage section. Moreover, graphite/epoxy fuselage component for Northrop F-5 made by General Dynamics, and horizontal stabilizer of F-14 made of boron/epoxy, and carbon/epoxy horizontal stabilizer, vertical stabilizer, leading edge, and rudder in the empennage of F-16, the X-29A having a forward swept composite, carbon/epoxy wing box, forward fuselage, horizontal stabilizer, elevators, rudder, other control surfaces, wing skins and over-wing fairings of U.S. Navy’s AV-8B, and carbon/epoxy wing skins, the horizontal and vertical tail boxes, the wing and tail control surfaces, the speed brake, the leading edge extension, and various doors of F-18 could be given some examples for first, second and third stages. Subsequently, three programs which were the graphite/epoxy replacement of A-6 wing box, the Navy’s V-22 tilt rotor aircraft, and the U.S. Advanced Tactical Fighter F-22, have aimed to employ considerable amount of advanced composites. Apart from military advanced composite applications, NASA started Aircraft Energy Efficiency (ACEE) programs in 1975 for the design, manufacturing, and testing of composites. The ACEE programs greatly expanded the scope of commercial transport composite applications including three secondary and three primary aeronautical structures. The secondary aeronautical structures of ACEE programs were inboard aileron of Lockheed L-1011 (sandwich construction), elevator of Boeing 727 (sandwich construction), and rudder of McDonnell-Douglas DC-10 (all-graphite/epoxy structural box). The primary aeronautical structures of ACEE programs were vertical fin box of Lockheed L-1011, horizontal stabilizer box of Boeing 737 (graphite/epoxy), and vertical fin box of McDonnell-Douglas DC-10 (sandwich construction). The experience gained from the ACEE programs has resulted in increased composite usage on the next generation of commercial transports, such as the flight control surfaces and components of empennage of the Boeing B747, B757, B767, and B777. In 1985, Airbus became the first airframe manufacturer to use composite materials for series production of primary structures when it began to assemble the A310 with fins built of carbon/epoxy. The all-composite fin box of the Airbus A310-300 is an impressive structure in its simplicity in terms of only 95 parts

compared with 2076 parts in the previous aluminum box structure, insuring a reduction of assembly costs. As a result, aircraft manufacturers became more comfortable with the composite materials and more efficient construction techniques were developed; the increased demand led to lower costs of composite materials. Since the beginning of the 1980's, an all- or mostly-composite airframe has almost become a must in the developing and manufacturing of business aircraft as well as general aviation aircraft. Design approaches which differ from those of most commercial transport airframes and used to reduce cost and structural weight. These innovative designs and manufacturing techniques are pioneers in composite airframe structure development. P-180 Avanti, which had all-composite tail, utilized composites on the nose cone, forward wing (canard), nacelles, wing trailing edge, empennage, and control surfaces. The examples for all-composite utility aircraft can be given as the Lear Fan 2100, the Starship, the AvTek 400, and the Voyager. The Lear Fan 2100 is the first all-composite airframe aircraft in which graphite/epoxy and Kevlar/epoxy composite materials were used. Titanium was used for all major fittings attached to graphite/epoxy structures to avoid galvanic corrosion [3,5]. In 1986, the Voyager [7], which was large span (36.09 m), high aspect ratio, long range all-composite aircraft, flined around the world in nine days. The Voyager was an aircraft with structural weight/gross weight fraction of only 9%; significantly lower than any existing man-rated aircraft. This flying-around-the-world record was developed by the Global Flyer [7] which was built of graphite/epoxy. The nonstop and unrefueled flight of Global Flyer around world was performed only in 67 hours in 2005. Recently, the world's first twin-deck super-jumbo airliner, Airbus A380 has got 25% of its airframe structures built of advanced composites. Also, space tourisms will be performed by spacecrafts built of advanced composites within 10 years. The successful flight of Space Ship One [7] made us think in this respect.

It is seen that using advanced composites has become an inevitable and standard task in the design and construction of the airframe structures of military and civil aeronautical and space vehicles. "The advanced composites should be treated totally different than metallic materials from the view point of design and analysis. Many structural metallic materials generally have homogeneous and isotropic properties. This implies that the mechanical, thermal, and environmental (like moisture) properties of the material are equal in all directions and at all locations. In contrast to a metallic material, a unidirectionally fiber-reinforced laminated composite material behaves like a homogeneous anisotropic material. On the account of the fact that the unidirectional fiber-reinforced lamina has inherent anisotropy, the corresponding properties exhibit different properties along different axes. For instance, a unidirectional fiber-reinforced lamina will be very strong along the fiber direction and weak in the transverse direction which is perpendicular to the fiber direction. Also, in order to compute mechanical behavior under loading two elastic constants should be known in the stiffness matrix for isotropic materials. Conversely, four and six elastic constants should be known for orthotropic and anisotropic materials, respectively in the stiffness matrix" [3].

“A typical unidirectional fiber-reinforced lamina, which is shown in Figure 1.2, is orthotropic in nature, having three mutually perpendicular planes of elastic symmetry. Two of the elastic symmetry planes are parallel and transverse to the fiber direction, and the third is perpendicular to the plane of the lamina or parallel to the thickness direction. The principal material 1 and global lamina coordinate  $x$  are taken to be parallel to the fiber, the 2-axis and  $y$ -axis transverse to the fiber direction in the plane of the lamina, and the 3-axis and  $z$ -axis are perpendicular to the lamina” [3].

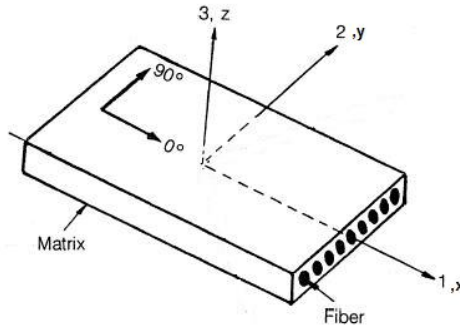


**Figure 1.2** A unidirectional fiber-reinforced lamina with the principal material directions (1, 2, and 3) and the global or lamina coordinates ( $x$ ,  $y$ , and  $z$ ) [3].

Simple tension and shear tests are quite enough to understand to have indications for the qualitative understanding of the anisotropic behavior of a material. The outcomes of these tests are shown in Figure 1.3. Application of a normal stress to a rectangular block of isotropic or orthotropic material leads to only extension in the direction of the applied stress and contraction perpendicular to it, whereas an anisotropic material experiences extension in the direction of the applied normal stress, contraction perpendicular to it, as well as shearing strain. Conversely, shearing strains as well as normal strains caused by the application of a shear stress to an anisotropic material. Normal stress applied to an orthotropic material at an angle to its principal material directions causes it to behave like an anisotropic materials. This occurs because of the coupling between the two loading modes and the two deformation modes. Furthermore, when there is an angle between the global coordinates and the principal material coordinates in the lamina, some coupling terms between extension, shear, bending and twisting do exist in the stress-strain relations causing to an anisotropic behavior of the lamina [1]. This situation is comprehensively discussed with the derivation of the governing equations of the present research given in Chapter 2.

The aeronautical structures are considered to be thin-walled structures. The basic elements of the thin-walled structures are beams, plates, and shells. Beams, plates and shells are known as continuous systems of structural mechanics. Generally, the aeronautical structures are combinations of various shapes of thin shell structures.

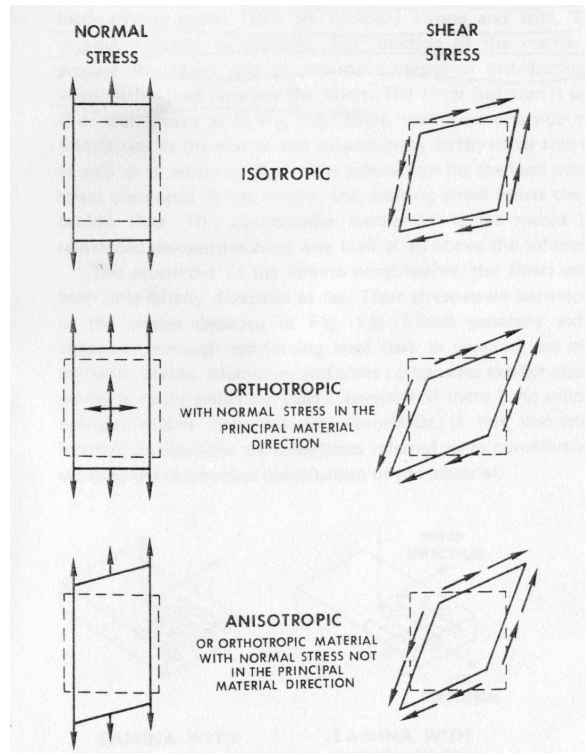


**Figure 1.3** Deformation of isotropic, orthotropic and anisotropic rectangular block under uniaxial tensile and pure shear loading [1].

“A shell is a three-dimensional body which is bound by two closely spaced curved surfaces. In case of a thin shell, the distance between the surfaces is small in comparison with the other dimensions. The locus of points which lies midway between these surfaces is called the middle surface of the shell. A shell has three fundamental identifying features: its reference surface, its thickness, and its edges. Of these, the reference surface is the most significant because it defines the shape of the shell, and the behavior of the shell is governed by the behavior of its reference surface” [71].

“Time-dependent vibratory motions are set up in a shell whenever it is disturbed from a position of stable equilibrium. If these motions occur in the absence of external loads, they are

classified as free vibrations. If these motions are set up by time-dependent external loads, they are referred to as forced vibrations. A shell, since it is an example of an elastic continuous body, is composed of an infinite number of mass particles. As a consequence, when it is set into motion it possesses an infinite number of degrees of freedom. Its response to a disturbance may thus be analyzed into an infinite number of periodic motions which are referred to as its normal modes of free vibration. Each of these normal modes has an associated natural frequency of free vibration” [71].

In the current thesis, we would like to address the dynamic analysis issue of the thin shell structures made of advanced composites. The foundations and scientific works about the free vibrations of anisotropic laminated composite shells of revolution will be reviewed in the following section.

## 1.2 LITERATURE SURVEY

Historical development of vibration analysis of continuous structural elements is explained in the first chapter of Soedel [8]. The analytical methods for the vibration of continuous systems like beams and plates can be studied in Meirovitch [9].

Leissa [11] reviewed the shell vibration research up to 1973. It included about 1000 papers on the shell vibration. The vast majority of papers dealing with shell vibrations have focused on homogeneous isotropic shells with few papers regarding composite shells (less than 20 out of 1000). All of the shell theories in the Leissa’s monograph was classical shell theories based on the first accurate thin shell theory of Love [10]. In this theory, Love introduced his first approximation for bending analysis of shells. This approximation defined a linear analysis of thin shells, in which various assumptions were introduced. These assumptions are known to be the Love-Kirchhoff assumptions which are: (1) the shell is thin; (2) the displacements and rotations are small; (3) transverse normal stresses are negligible; and (4) normals to the shell reference surface before deformation remain normal after deformation. These assumptions led to thin shell theory which was an extension to Kirchhoff plate theory. In fact, three-dimensional phenomena of vibration analysis is reduced to two-dimensional approximated theory by Love-Kirchhoff’s thin elastic shell theory. In deriving the equilibrium equations, statically equivalent forces and moments acting on the reference surfaces can be defined by integrating stresses through the thickness. In this way, the three-dimensional shell behavior can be fully described using a two-dimensional approximation.

Since the first approximation of Love-Kirchhoff thin shell theory, other classical shell theories were developed. The reason why many classical shell theories based on more or less on Love-Kirchhoff first approximation for thin shell theory have been developed was that there was an inconsistency in the original version of Love-Kirchhoff thin shell theory since all strains did not vanish for rigid-body motion. The classical shell theories differed with some terms in the derivations.

Review of different classical shell theories was presented in the Leissa's monograph [11] and the books by Kraus [12] and Soedel [13]. Chapter 8 of Kraus's book gave a very comprehensive description of the shell vibration topic along with methods of solution and example solutions of cylindrical and spherical shells. On the other hand, Soedel's book was entirely devoted to vibrations of shells and plates, and it was an excellent reference for the introduction to the free vibration and dynamic analysis of shell and plate type structures. These different classical shell theories were derived from the original version of Love-Kirchhoff thin shell theory. Also, Bushnell [16] discussed the equations governing stress, stability, and vibration analyses for unstiffened and stiffened elastic shells of revolution using classical shell theories.

There are many theories for layered anisotropic shells in the literature. Many of these theories were developed for thin shells and are based on the Kirchhoff-Love first approximation. The first analysis which incorporated the bending-stretching coupling was done by Ambartsumyan [17]. The bending-stretching coupling takes place when the layers are arranged unsymmetrically around the reference surface of the shell. He assumed that the individual orthotropic layers were oriented such that the principal axes of material symmetry coincided with the principal coordinates of the shell reference surface. When the material symmetry axes do not coincide with the principal coordinates of the shell reference surface, the shell is said to be anisotropic. This induces coupling between the membrane and in-plane shear effects and between bending and twisting effects.

In the classical shell theories, the shell is assumed to be so thin that all transverse deformation effects, transverse stresses and strains can be neglected. However, these transverse effects become more significant as the shell becomes thicker relative to its in-plane dimensions and radius of curvature. There is a gross error in predicting the natural frequencies without considering the transverse shear deformation effects. The experimental observations revealed that classical plate theory neglecting transverse shear strains leads to underestimates of deflections and overpredictions of natural frequencies and buckling loads. In addition, the transverse shear deformation should be included in the computational modeling for shells built of advanced anisotropic laminated composite materials such as graphite/epoxy and boron/epoxy, where the ratio of elastic moduli to shear moduli are very high. The effective flexural stiffness of anisotropic laminated shells is reduced with the transverse shear strains. Koiter [18] pointed out that meaningful refinement of Love-Kirchhoff first approximation for thin elastic shell can be made by taking the effects of transverse shear and normal stresses into consideration. The inclusion of shear deformation was made for beams by Timoshenko [19] and expanded for plates by Reissner [20] and Mindlin [21]. Mindlin also included the rotary inertia terms in the free vibration analysis in the plates. The refined shell theories which account for shear deformation and rotary inertia effects are known to be thick shell theories or shear deformation shell theories. A first-order shear deformation shell theory (FOSDST) is the simplest of the shear deformation shell theories in which there is a uniform distribution of transverse shear strains through the thickness. Dong and Tso [22] were the first to carry out a first-order shear deformation shell

theory. They retained one or two terms in the Taylor's series for transverse and tangential displacement components, respectively. They constructed a laminated orthotropic shell theory including the effects of transverse shear deformation through the thickness.

“In laminated composite plates and shells using FOSDST, the transverse shear stresses vary through layer thickness and do not satisfy the transverse shear boundary conditions on the top and bottom surfaces of the plate or shell because of the assumption of a constant shear angle through the thickness. This discrepancy is often corrected in computing the transverse shear force resultants by considering shear correction factor. This factor is computed such that the strain energy due to transverse shear stresses equals the strain energy due to the true transverse stresses predicted by the three-dimensional elasticity theory. This factor depends, in general, on the lamination parameters such as number of layers, stacking sequence, degree of orthotropy and fiber orientation in each individual layer in the laminate” [39]. The shear correction factor is studied in [23,24, and 25] comprehensively.

Whitney and Sun [26,27] developed a shear deformation theory for laminated anisotropic cylindrical shells which includes both transverse shear deformation and transverse normal strain as well as expansional strains. The theory is based on a displacement field in which the displacements in the surface of the shell are expanded as linear functions of the thickness coordinate and the transverse displacement is expanded as a quadratic function of the thickness coordinate. There are other higher order shear deformation shell theories such as Reddy and Liu [28], Bhimaraddi [29], Librescu [30] and Librescu and Khedir [31] based on nonlinear (or piecewise linear) variation of displacements and/or stresses through the shell thickness other than the Whitney and Sun's shell theory. Noor and Burton [32] made a review of the different approaches for computational models used for multilayered composite shells. They focused on different approaches for developing two-dimensional shear deformation theories; classification of two-dimensional theories based on introducing plausible displacement, strain and/or stress assumptions in the thickness direction; first-order shear deformation theories based on linear displacement assumptions in the thickness coordinate; and efficient computational strategies for anisotropic composite shells. In addition, Noor, Burton and Peters [33] conducted numerical studies to show the effects of variation in the lamination and geometric parameters of simply supported composite cylinders on the accuracy of the static and vibrational responses predicted by eight different modeling approaches based on two-dimensional shear deformation theories. Computational modeling approaches for two-dimensional approximation theories used for layered composite shells are given in Table 1.2. Furthermore, Noor and Burton also carried out [34,35] the similar studies done for same shell structures [32,33] for multilayered anisotropic plates.

There has been some attempts to make a unique and generalized laminated shell theory by combining the classical shell theories with the shear deformation shell theories. Touratier [36] presented a generalization of geometrically linear shear deformation theories for small elastic strains

for multilayered axisymmetric shells of general shape without any assumption other than neglecting the transverse normal strain. The shear is taken into account by using a function which is introduced in the assumed kinematics. All equations with the shear function in the kinematics are directly applicable to: Kirchhoff-Love, first-order shear deformation, third-order shear deformation theories, and the proposed generalized shear deformation theory by using certain sine shear function. Therefore, no shear correction factors are needed with the proposed generalization of shear deformation theories. Furthermore, Soldatos and Timarci [37] achieved a theoretical unification of most of the variationally consistent classical and shear deformable cylindrical shell theories by introducing certain general shear deformation shape functions into the shell displacement approximation involving five unknown displacement components. The choice of such a shear deformation shape function is not unique and is based on the satisfaction of certain mechanical, material and/or geometrical constraints of the problem considered, and in general, characterizes the degree of sophistication or even the degree of accuracy of the resulting shell theory. The general shear deformation shape functions are not introduced before or during the variational formulation of the theory, and this procedure leads to leaving open possibilities for a multiple, a-posteriori specification of such a shear deformation shape function.

Toorani and Lakis [39] gave the general equations of anisotropic plates and shells including transverse shear deformations, rotatory inertia and initial curvature effects. They also reviewed the literature with respect to three topics: the discussion of both linear and nonlinear theories on the analysis of plate and shell structures; the study of the effect of shear deformation on both the static and dynamic behavior of plates and shells; especially those made of advanced composite (or anisotropic) materials; and the discussion of the effects of structure-fluid interaction on the vibrations of plates and shells giving special attention to cylindrical shells immersed in or filled with a liquid or subjected to a flowing fluid.

Noor [41] discussed a number of aspects of the mechanics of anisotropic plates and shells. He covered the topics including computational models of anisotropic plates and shells, consequences of anisotropy on deformation couplings, symmetry types, stress concentrations and edge effects, and importance of transverse shear deformation, recent applications and recent advances in the modeling and analysis of anisotropic plates and shells, and new research directions.

Qatu has investigated recent research advances in the dynamic behavior of shells between 1989 and 2000 for laminated composite shells [42] and for isotropic shells [43]. In his papers, he listed more than 350 papers for laminated composite shells and 600 papers for isotropic shells on the dynamic behavior of shells, heavily emphasized the free vibration problem. He studied the dynamic behavior of shells according to shell theories, shell geometries, experimental investigations, analytical and numerical methods, comparisons among various theories, and complicating effects. Recently, he has given the governing equations, the methods of solution about the vibrations of laminated shells and plates in different configurations in his book [44].

**Table 1.2** Computational modeling approaches for two-dimensional approximation theories used for layered composite shells [28]

Model number	Description	Through-the-thickness displacement assumptions	Constraint conditions on stresses	Total number of displacement parameters
1, 1A	First-order shear deformation theory	<ul style="list-style-type: none"> <li>• linear <math>u, v</math></li> <li>• constant <math>w</math></li> </ul>	$\sigma_r = 0$	5
2	First-order theory with transverse normal stresses and strains included	<ul style="list-style-type: none"> <li>• linear <math>u, v,</math> and <math>w</math></li> </ul>	none	6
3	Lo-Christensen-Wu type theory	<ul style="list-style-type: none"> <li>• cubic <math>u, v</math></li> <li>• quadratic <math>w</math></li> </ul>	none	11
4	Higher-order shear deformation theory	<ul style="list-style-type: none"> <li>• quintic <math>u, v,</math> and <math>w</math></li> </ul>	none	18
5	Simplified higher-order theory	<ul style="list-style-type: none"> <li>• cubic <math>u, v</math></li> <li>• constant <math>w</math></li> </ul>	$\sigma_r = 0$ throughout and $\sigma_{rx}$ and $\sigma_{r\theta} = 0$ at top and bottom surfaces	5
6	Discrete-layer theory (based on purely kinematic hypotheses)	<ul style="list-style-type: none"> <li>• Piecewise linear <math>u, v</math></li> <li>• Constant <math>w</math> (through-the-thickness)</li> </ul>	$\sigma_r = 0$ throughout	$2 \times NL + 3$ ( $NL$ : number of layers)
7	Simplified discrete-layer theory	<ul style="list-style-type: none"> <li>• Piecewise linear <math>u, v</math></li> <li>• Constant <math>w</math> (through-the-thickness)</li> </ul>	<ul style="list-style-type: none"> <li>• <math>\sigma_r = 0</math></li> <li>• Continuity of <math>\sigma_{rx}</math> and <math>\sigma_{r\theta}</math> at layer interfaces</li> </ul>	5
8, 8A	Predictor-corrector procedures	Predictor Phase <ul style="list-style-type: none"> <li>• Linear <math>u, v</math></li> <li>• constant <math>w</math></li> </ul> Corrector Phase See the note 1	Predictor Phase $\sigma_r = 0$ Corrector Phase None	5

(1) In model 8, the corrector phase is based on adjusting the transverse shear stiffnesses, and in model 8A it is based on correcting the thickness distribution of the in-plane and transverse displacement components.

Cohen [45] developed an integrated computer program entitled Field Analysis of Shells of Revolution (FASOR) in order to analyze prebuckling, buckling, initial postbuckling and vibrations under axisymmetric static loads as well as linear response and bifurcation under asymmetric static loads. He also extended the capability of FASOR to solve the problems of general anisotropy and transverse shear deformations of stiffened laminated shells. The response modes of each of the problems of nonlinear prebuckling, buckling, initial postbuckling and vibration under axisymmetric static loads and linear prebuckling and (bifurcation) buckling under asymmetric static loads were calculated by reducing to the solution of a sequence of even-ordered linear Hermitian self-adjoint boundary-value problems in ordinary differential equations. Then, each of these problems was solved by the field method in which the boundary-value problem is converted into two numerically stable initial-value problems which in turn were solved by a standard forward integration scheme (Runge-Kutta) with self-regulating step size.

Padovan [49] developed a quasi-analytical finite element procedure which can analyze the static and dynamic problems for axisymmetric fully anisotropic shells and three-dimensional solids using complex series representations. The solution procedure presented by Padovan was for the problems of axisymmetric shells or three-dimensional solids with arbitrary laminate construction with locally mechanically anisotropic lamina composed of composite materials, meridional and radial variations in material properties, arbitrary boundary and initial conditions. In addition, static as well as transient problems were solved. Padovan and Lestingi [50] also developed a complex multi-segment numerical integration procedure in combination with a complex series representation in order to make static analysis of mechanically and thermally loaded branched laminated anisotropic shells of revolution with arbitrary meridional variations in thickness and material properties.

Tan [51] presented an efficient substructuring analysis method for predicting the natural frequencies of shells of revolution in arbitrary shape of meridian, general type of material property and any kind of boundary condition using the first-order shear deformation theory as well as the classical thin shell theory. The method effectively used the symmetry property of a shell of revolution. In this respect, the shell of revolution was discretized by the meridians of circumferentially, and general spline functions and Lagrangian polynomials were used to represent the displacement variations along the meridian and in the circumferential direction in an element, respectively. The Sturm sequence method in conjunction with the massive substructuring technique was used so as to find the natural frequencies of a shell of revolution.

Ganesan and Sivadas [52] presented the free vibration analysis of circular cylindrical and circular conical composite shells (angle wound) using Love-Kirchhoff first approximation for thin elastic shells and moderately thick shell with shear deformation and rotatory inertia. In the solution, the semi-analytical finite element method was used. In the meridional direction, the thin shells, and moderately thick shells were discretized with a two-noded axisymmetric finite element with 16

degrees of freedom per element, and a higher-order semi-analytical finite element with three nodes and 30 degrees of freedom per element respectively. The circumferential variation was presented in terms of a double Fourier series in order to incorporate the effect of coupling due to anisotropic properties.

Heylinger and Jilani [56] used the Ritz method for the problem of free vibrations of laminated anisotropic composite shells with various end conditions. The natural frequencies were evaluated for a number of geometric and material combinations using a combination of power and Fourier series as the approximating functions for three displacement components. No assumptions were required regarding the type of motion because of the usage of the full equations in the formulation. The transverse shear strains, deformation of the normals, and all inertial terms were included in the formulation. The form of the approximating function assumed the continuity of the displacement components and their derivatives through the thickness of the shell.

Noor Ahmed K., and Peters Jeanne M. [58] presented an efficient computational procedure for the free vibration analysis of laminated anisotropic shells of revolution, and for assessing the sensitivity of their response to anisotropic material coefficients. The analytical formulation was based on a form of the Sanders-Budiansky shell theory including the effects of both the transverse shear deformation and the laminated anisotropic material response. The fundamental unknowns in the computational procedure were the eight stress resultants, the eight strain components, and the five generalized displacements of the shell. Each of the shell variables were expressed in terms of trigonometric functions in the circumferential coordinate and a three-field mixed finite element model was used for the discretization in the meridional direction. The three key elements of the procedure were: (a) use of three-field mixed finite element models in the meridional direction with discontinuous stress resultants and strain components at the element interfaces, thereby allowing the elimination of the stress resultants and strain components on the element level; (b) operator splitting, or decomposition of the material stiffness matrix of the shell into the sum of an orthotropic and anisotropic parts, thereby uncoupling the governing finite element equations corresponding to the symmetric and antisymmetric vibrations of each Fourier harmonic; and (c) application of a reduction method through the successive use of the finite element method and the classical Bubnov-Galerkin technique.

The three-dimensional elasticity theory solution for free vibrations of anisotropic laminated composite shells of revolution is always sought to check the accuracy of the natural frequencies calculated by the two-dimensional shell theories. Noor and Peters [60] developed an efficient computational procedure for stress, free vibration, and buckling analyses of multilayered composite cylinders with a large number of layers. The analytical formulation was based on the linear three-dimensional elasticity theory, including the effects of the orthotropic material response of the individual layers. The fundamental unknowns consisted of the six stress components and three

displacement components of the cylinder. Each of the stress and displacement components was expanded in a double Fourier series in the circumferential and longitudinal directions, and a two-field mixed finite element model was used for the discretization in the thickness. The basic idea of the proposed procedure was to approximate the stress, vibration, and buckling responses of the cylinder associated with a certain range of Fourier harmonics in the circumferential and longitudinal directions by a linear combination of global approximation vectors generated for a particular pair of Fourier harmonics within that range. The three key elements of the procedure were: (1) Two-field mixed finite element models in the thickness direction, with the stress components allowed to be discontinuous at element interfaces; (2) operator splitting or additive decomposition of the different arrays in the governing finite element equations to delineate the effects of the different Fourier harmonics in the longitudinal and circumferential directions; and (3) a reduction method or successive application of the finite element method and the classical Rayleigh-Ritz technique. Soldatos [62] reviewed the literature on three-dimensional dynamic analyses of circular cylinders and cylindrical shells.

## **1.3 PRESENT RESEARCH**

### **1.3.1 MOTIVATION**

The use of anisotropic laminated composite shells as structural elements in many engineering applications of aeronautical, maritime, civil, space, automotive, and nuclear engineering has been increased tremendously and significantly in the last four decades. By virtue of their high strength-to-weight and stiffness-to-weight ratios compared to metallic materials, the advanced composite materials are preferred in the design and manufacture of anisotropic laminated composite shells. As a result of the increase in their use, the static and dynamic behavior of the anisotropic laminated composite shells under divergent loading must be clearly understood so that they can be used safely.

The main interest of this study is the dynamic behavior of anisotropic laminated composite shells used in airframe and space structures. Generally speaking, a knowledge of the free-vibration characteristics of shells is important both to our general understanding of the fundamentals of the behavior of a shell and to the industrial application of shell structures. The structural design of a typical shell type structure requires that the response of the shell to various mission-dictated excitations be accurately predicted so that the integrity of the shell structure can be assessed. To this end, a thorough understanding of the natural modes of the shell is extremely helpful, if not essential.

Actually, the mechanical and material properties of anisotropic laminated composite shells are different from isotropic shells, a consistent computational model is required in the structural analysis and design. The computational models are divided into two: exact or three-dimensional models and two-dimensional or approximated models. The use of three-dimensional and quasi-three-dimensional models for predicting the response characteristics of anisotropic laminated composite

shells is computationally expensive, and not feasible for practical structures in engineering. “The two-dimensional shear-deformable models can give fairly accurate predictions for the gross response characteristics (such as free vibration frequencies, buckling loads) of laminated composite shells; however, they are not adequate for the accurate prediction of the transverse stresses and deformations” [32].

Shells of revolution, in particular circular cylindrical shell, made of composite material find widespread applications in various industries including the aerospace industry. Some common examples are pressure vessels used for various purposes of storing high pressurized gases. Filament winding is one manufacturing method used to produce cylindrical shells for this purpose. With this manufacturing technique, one can produce cylinders composed of multilayers with each layer at a pre-specified orientation. In addition to filament winding method, normal wet lay-up, vacuum bagging, vacuum infusion methods are some of the other manufacturing techniques with which one can produce laminated shells with each layer being at any arbitrary fiber orientation by using unidirectional fiber rolls.

Besides pressure vessels, cylindrical shells also find application in external stores integrated to airframe structures such as aircraft and helicopter. These structures can serve for the purpose of carrying various equipment ranging from electronic devices to fuel. When combined with the primary structure of the vehicle to which it is installed, the dynamic characteristic of the store itself becomes very important. Structural integrity of the store is not the only concern that one has to tackle but also possible interference of the external store and primary structure dynamic characteristics can give rise to serious dynamic instability problems ranging from limit cycle oscillations to flutter. One can actually increase the examples for the use of thin shells of revolution in aerospace structures. However, in all the applications an accurate estimate of the dynamic characteristics of the composite shells of revolution is quite important.

Fiber orientation is one critical parameter which only affect the stiffness coefficients but also cause for deformation coupling between different modes of deformation. The effect of anisotropy on the dynamic characteristics of shells of revolution has not received the attention it deserves simply because of the complexity of the resulting equations for a general shell of revolution. In this thesis one of the aims is to characterize the effect of anisotropy on the dynamic characteristics of shells of revolution and understand the dynamics of thin-walled shells of revolution better.

### **1.3.2 OBJECTIVE AND SCOPE**

The objective of the present thesis is to determine free vibration characteristics such as natural frequencies and associated mode shapes of anisotropic laminated composite shells of revolution. To achieve this objective, a computer code DALSOR (Dynamic Analysis of Anisotropic

Laminated Shells of Revolution) is developed in Fortran 77. A flow-diagram and a brief explanation of the developed code DALSOR are given in Chapter 3. The theory used in DALSOR is the first-order shear deformation theory. The governing equations of an anisotropic laminated composite shell of revolution are derived and the process is given in the Chapter 2. The developed code DALSOR has the following main capabilities:

- Inclusion of the transverse shear deformation effects to the geometrical linear Reissner-Naghdi thin shell theory equations (First-Order Shear Deformation Theory).
- Determination of natural frequencies and displacement, rotation, force and moment resultant mode shapes along the meridional direction of any laminated composite shell of revolution.
- Analysis with general boundary conditions at the ends (initial end point and final end point) of the shells of revolution (including any linear combination of displacements).
- Any general type of shell of revolution (circular cylindrical, truncated conical, paraboloid shells, etc.).
- Full anisotropic constitutive equations.
- Framework for continuous variation of material and geometric properties in the meridional direction of the shell.
- Framework for discrete variation of material and geometric properties in the meridional direction of the shell.

Most of the previous work listed in the Literature Survey section either lack the comprehensive treatment of the effect of anisotropy on the dynamic characteristics of shells or lack a general methodology for the solution for general shells of revolution and concentrate on simple shell geometries such as cylindrical or conical shells where the meridional curvature vanishes and general equations of motion simplify significantly.

In case of shells of revolution, which have complete circumferential properties, an alternate method based on multisegment numerical integration procedure is available in addition to the finite element/finite difference techniques. For such geometries the multisegment numerical integration technique has demonstrated advantages over both of these methods. Of utmost importance is the uniform convergence property of the multisegment numerical integration technique.

The present work has its foundations on the general method of multisegment numerical integration for the solution of static and dynamic analysis of shells of revolution developed brilliantly by Kalnins [66,67]. Kalnins in his papers [66] and [67] demonstrated the application of multisegment numerical integration method for the solution of static and dynamic problems of shells of revolution using classical shell equations and for isotropic materials.

Kayran in his works [72] and [73] extended the applicability of the multisegment numerical integration method for the solution of free vibration problems of general shells of revolution using classical shell theory equations and including first-order shear deformation theory and for orthotropic cross-ply laminates in which most of the coupling terms vanish.

The present work extends the work of Kalnins and Kayran by incorporating full anisotropic nature of constitutive equations in which all coupling terms are included. It has already been demonstrated that when all the coupling terms are included in the constitutive equations, the application of the traditional Fourier decomposition to the fundamental shell variables does not lead to elimination of the circumferential coordinate; hence, preventing the generation of ordinary differential equations.

In the present work, the well-known Reissner-Naghdi thin shell theory equations are used and full anisotropic constitutive relations are utilized. It has been shown that through the use of Finite Exponential Fourier Transform Method one can actually double the size of fundamental system of equations but completely get rid of the circumferential coordinate; and thus end up with ordinary differential equations to which multisegment integration method can be applied.

In this thesis, the traditional frequency trial method developed by Kalnins is carried out in a modified way to the equations of free vibrations of full anisotropic laminated composite shells of revolution and it has been shown that one can actually determine the natural frequency of the full anisotropic laminated composite shells of revolution through the use of modified frequency trial method.

### **1.3.3 OVERVIEW OF THE THESIS**

The remaining chapters of this thesis are organized as follows:

Chapter 2 presents the mathematical modeling for free vibration analysis of anisotropic laminated composite shells of revolution. In this respect, the governing equations of free vibration analysis of anisotropic laminated composite shells of revolution are derived.

Chapter 3 explains the reduction of the governing equations into a system of ordinary differential equations involving a two-point boundary value problem through the use of Finite Exponential Fourier Transform Method. Chapter 3 also gives the conversion of the two-point boundary value problem into a series of initial value problems and explains the use of modified frequency trial method for the determination of natural frequencies and mode shapes of full anisotropic laminated composite shells of revolution. Chapter 3 concludes with the brief description and flow-diagram of the developed code DALSOR.

Chapter 4 starts with one case study in order to show the reliability of the DALSOR. Then, various numerical results are obtained so as to investigate the effects of the variation of the geometrical, material and lamination properties to the free vibration characteristics. The numerical results for the specified different case studies are given in tabular and graphical forms. Additionally, the discussions about the numerical results are made.

Finally, conclusions are summarized and recommendations for future work are discussed in Chapter 5.

## **CHAPTER 2**

### **MATHEMATICAL MODELING**

#### **2.1 INTRODUCTION**

In this chapter, the mathematical modeling for the free vibration analysis of macroscopically anisotropic laminated shells of revolution is presented. The relationships governing the behavior of thin elastic shells are based on the study of the deformations of its reference surface. Thus, it is appropriate to have an understanding of the basic principles of the differential geometry for the deformation analysis of reference surface before embarking upon the derivation of the theory of thin elastic shells. After studying the basic principles of the differential geometry, the properties of surfaces of revolution is given to define shells of revolution. Then, basic considerations of the Reissner-Naghdi shell theory for the present study are expressed. Within the framework of the Reissner-Naghdi shell theory, the kinematic relations such as displacement functions and strain-displacement equations are defined with respect to the reference surface of the thin doubly curved elastic shells using First Order Shear Deformation Theory (FOSDT). Next, constitutive equations are derived valid for anisotropic laminated composite doubly curved shells. By using Hamilton's principle, the dynamic equations of motion are obtained for this study. Finally, the field equations of anisotropic laminated composite doubly curved shells are transformed to those of anisotropic laminated composite shells of revolution

#### **2.2 REFERENCE SURFACE OF SHELL**

This study is concerned with thin elastic shells. A thin shell is a three-dimensional elastic body which is bounded by two closely spaced curved surfaces. In case of a thin shell, the distance between the surfaces is small in comparison with the other two dimensions. The locus of points which lies midway between these surfaces is called the middle or reference surface of the shell.

A shell has three fundamental identifying features: its reference surface, its thickness, and its edges. Of these, the reference surface is the most significant because it defines the shape of the shell, and the behavior of the shell is governed by the behaviour of its reference surface. Therefore , it may

be worthwhile to discuss the differential geometry or the theory of surfaces so as to analyze the deformation of the reference surface. This is done in the following section.

## 2.3 DIFFERENTIAL GEOMETRY

This section consists of two parts: the theory of space curves and the theory of surface. All materials of section 2.3, which are the basics of the differential geometry in order to describe the deformation of the reference surface of the shell, are taken from Kraus [12].

### 2.3.1 SPACE CURVES

“A three-dimensional curve in a rectangular coordinate system  $(x_1, x_2, x_3)$  can be represented by the locus of the end point of the position vector (Figure 2.1):

$$\vec{x} = x_1(t)\vec{e}_1 + x_2(t)\vec{e}_2 + x_3(t)\vec{e}_3 \quad (2.1)$$

for all values of the parameter  $t$  that lie in the interval  $t_1 \leq t \leq t_2$ . If we require that the  $x_i$  ( $i=1,2,3$ ) be single-valued functions of the parameter  $t$ , then we shall insure that a given value of  $t$  defines only one point on the space curve. In Equation 2.1,  $\vec{e}_1, \vec{e}_2, \vec{e}_3$  are the unit normal vectors of the rectangular coordinate system.

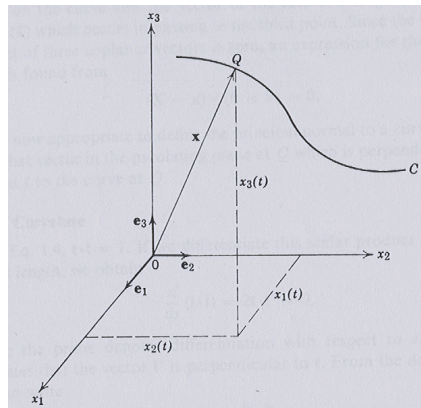


**Figure 2.1** The position vector of a space curve [12].

### 2.3.1.1 UNIT TANGENT VECTOR

Let us call  $s$  the variable of arc length along the space curve defined by Equation 2.1 and take the derivative of the position vector  $\vec{x}$  with respect to  $s$ ,

$$\frac{d\vec{x}}{ds} = \frac{dx_1}{ds} \vec{e}_1 + \frac{dx_2}{ds} \vec{e}_2 + \frac{dx_3}{ds} \vec{e}_3 \quad (2.2)$$

Now if we form the scalar product of the foregoing derivative with itself, we obtain

$$\frac{d\vec{x}}{ds} \cdot \frac{d\vec{x}}{ds} = \left( \frac{dx_1}{ds} \right)^2 + \left( \frac{dx_2}{ds} \right)^2 + \left( \frac{dx_3}{ds} \right)^2 \quad (2.3)$$

From the differential calculus, we know that

$$(ds)^2 = (dx_1)^2 + (dx_2)^2 + (dx_3)^2 \quad (2.4)$$

hence

$$\frac{d\vec{x}}{ds} \cdot \frac{d\vec{x}}{ds} = 1 \quad (2.5)$$

This tells us that  $d\vec{x}/ds$  is a unit vector. Its geometrical interpretation is depicted in the Figure 2.2. The vector  $\Delta\vec{x}$  joins two consecutive points  $Q$  and  $Q'$  on a curve  $C$ . Thus, the vector  $\Delta\vec{x}/\Delta s$  has the same dimension as  $\Delta\vec{x}$  and, as  $\Delta s$  approaches zero,  $\Delta\vec{x}/\Delta s$  becomes the vector tangent to the curve  $C$  at the point  $Q$ . We call the vector

$$\vec{t} = \frac{d\vec{x}}{ds} = \lim_{\Delta s \rightarrow 0} \frac{\Delta\vec{x}}{\Delta s} \quad (2.6)$$

the unit tangent vector. We note further that

$$\dot{\vec{x}} = \frac{d\vec{x}}{dt} = \frac{d\vec{x}}{ds} \frac{ds}{dt} \quad (2.7)$$

is also a tangent vector but it is not necessarily of unit length.

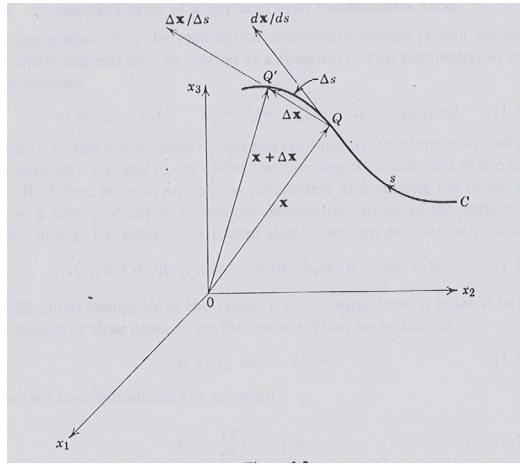


Figure 2.2 Tangent vector description [12].

### 2.3.1.2 OSCULATING PLANE, PRINCIPAL NORMAL

In the preceding section, the tangent to a curve at a point  $Q$  was found to be the limiting position of the line connecting the points  $Q$  and  $Q'$  as  $Q'$  approaches  $Q$ . Thus, it could be stated that the tangent to a curve passes through two consecutive points on the curve. As a next step, it is natural to consider the limiting position of a plane passing through three consecutive points of a curve as two of the points approach the third. Such a plane is called the osculating plane. It can be found by specifying that the vector  $(\vec{X} - \vec{x})$  from a general point  $X$  in the osculating plane to a general point  $x$  on the curve must lie in the same plane as the tangent vector  $\dot{\vec{x}}$  joining two points on the curve and the rate of change in the tangent vector  $(\ddot{\vec{x}})$  which occurs in passing to the third point. Since the triple scalar product of three coplanar vectors is zero, an expression for the osculating plane is found from

$$(\vec{X} - \vec{x}) \cdot (\dot{\vec{x}} \times \ddot{\vec{x}}) = 0 \quad (2.8)$$

It is now appropriate to define the principal normal to a curve at a point  $Q$  as that vector in the osculating plane  $Q$  which is perpendicular to the tangent  $\vec{t}$  to the curve at  $Q$ .

### 2.3.1.3 CURVATURE

By Equation (2.5),  $\vec{t} \cdot \vec{t} = 1$ . If we differentiate this scalar product with respect to arc length, we obtain

$$\frac{d}{ds}(\vec{t} \cdot \vec{t}) = 2\vec{t} \cdot \vec{t}' = 0 \quad (2.9)$$

where the prime denotes differentiation with respect to  $s$ . This result indicates that the vector  $\vec{t}'$  is perpendicular to  $\vec{t}$ . From the definition of  $\vec{t}$ , we can write

$$\vec{t} = \frac{d\vec{x}}{ds} = \frac{d\vec{x}}{dt} \frac{dt}{ds} = \dot{\vec{x}} \dot{t}', \quad (2.10)$$

and upon differentiation with respect to the arc length  $s$  the result is

$$\vec{t}' = \dot{\vec{x}} \ddot{t}' + \ddot{\vec{x}} (\dot{t}')^2 \quad (2.11)$$

This indicates that the vector  $\vec{t}'$  lies in the plane of the vectors  $\dot{\vec{x}}$  and  $\ddot{\vec{x}}$  (that is, in the osculating plane). Since  $\vec{t}'$  has also been shown to be perpendicular to the tangent  $\vec{t}$ , we conclude that  $\vec{t}'$  is parallel to the principal normal and is, therefore, proportional to it as follows:

$$\vec{t}' = \vec{k} = k\vec{N} \quad (2.12)$$

where  $\vec{N}$  is a unit normal vector in the direction of the principal normal to the curve at a point. The vector  $\vec{k}$  is called the curvature vector and expresses the rate of change of the tangent vector as a point moves along the curve. The proportionality factor  $k$  is called the curvature, and its reciprocal ( $R = k^{-1}$ ) is the radius of curvature. It is the radius of the osculating circle that passes through three consecutive points of the curve. Although the sense of  $\vec{t}'$  is determined solely by the curve, the sense of the principal normal  $\vec{N}$  is arbitrary. The sign of the factor  $k$ , therefore, depends on the sense of  $\vec{N}$ . To maintain consistency in our development, we shall assume that the normal vector  $\vec{N}$  points away from the center of curvature. Thus, Equation (2.12) tells us that when the sense of  $\vec{N}$  and  $k$  are the same,  $k > 0$ , and when the sense of  $\vec{N}$  is opposite to that of  $k$ , we have  $k < 0$ .

## 2.3.2 SURFACES

### 2.3.2.1 PARAMETRIC CURVES OF A SURFACE; FIRST FUNDAMENTAL FORM

Every surface  $S$  in the rectangular coordinate system may be written as a function of two parameters  $\alpha_1$  and  $\alpha_2$  as follows:

$$x_1 = f_1(\alpha_1, \alpha_2), \quad x_2 = f_2(\alpha_1, \alpha_2), \quad x_3 = f_3(\alpha_1, \alpha_2) \quad (2.13)$$

where  $f_1, f_2$  and  $f_3$  are single-valued and continuous functions of  $\alpha_1$  and  $\alpha_2$ . The parameters  $\alpha_1$  and  $\alpha_2$  are called the curvilinear coordinates of the surface. By fixing, in turn, one of the parameters and varying the other, we obtain a family of curves called the parametric curves of the surface as shown in Figure 2.3. Equation (2.13) can also be written as a vector equation

$$\vec{r}(\alpha_1, \alpha_2) = f_1(\alpha_1, \alpha_2)\vec{e}_1 + f_2(\alpha_1, \alpha_2)\vec{e}_2 + f_3(\alpha_1, \alpha_2)\vec{e}_3 \quad (2.14)$$

A differential change  $d\vec{r}$  in the vector  $\vec{r}$  as we move from a point  $P$  to an infinitesimally close point  $P'$  on the surface  $S$  can be written as

$$d\vec{r} = \vec{r}_{,1}d\alpha_1 + \vec{r}_{,2}d\alpha_2 \quad (2.15)$$

where we have introduced the notation

$$\vec{r}_{,i} = \frac{\partial \vec{r}}{\partial \alpha_i}, \quad i = 1, 2 \quad (2.16)$$

for partial derivatives of vectors. The square of the magnitude of the differential change vector  $d\vec{r}$  is obtained by taking the scalar product of  $d\vec{r}$  with itself. Thus

$$(ds)^2 = d\vec{r} \cdot d\vec{r} = E(d\alpha_1)^2 + 2F(d\alpha_1 d\alpha_2) + G(d\alpha_2)^2 \quad (2.17)$$

where

$$E = \vec{r}_{,1} \cdot \vec{r}_{,1}, \quad F = \vec{r}_{,1} \cdot \vec{r}_{,2}, \quad G = \vec{r}_{,2} \cdot \vec{r}_{,2}, \quad (2.18)$$

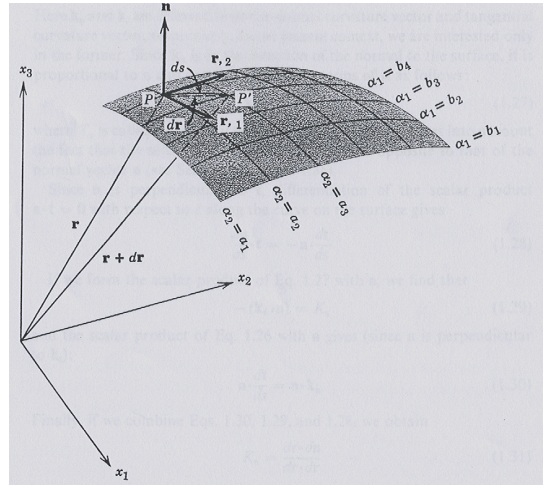


**Figure 2.3** Parametric curves of a surface and differential change of a position vector on the surface [12].

Equation (2.17) is known as the first fundamental form of the surface  $S$  defined by the vector  $\vec{r}(\alpha_1, \alpha_2)$ ;  $E, F$ , and  $G$  are called the first fundamental magnitudes. Along the parametric curves themselves, the differential length of arc takes the simplified forms

$$\begin{aligned} ds_1 &= \sqrt{E}d\alpha_1 && \text{along a curve of constant } \alpha_2 \\ ds_2 &= \sqrt{G}d\alpha_2 && \text{along a curve of constant } \alpha_1 \end{aligned} \quad (2.19)$$

We notice here that since  $\vec{r}_{,1}$  and  $\vec{r}_{,2}$  are tangent to curves of constant  $\alpha_2$  and  $\alpha_1$ , respectively, the quantity  $F$  will be zero if the parametric curves form an orthogonal net. In such cases, it is customary to write the first fundamental form as

$$(ds)^2 = A_1^2(d\alpha_1)^2 + A_2^2(d\alpha_2)^2 \quad (2.20)$$

where

$$A_1 = \sqrt{E}, \quad A_2 = \sqrt{G}, \quad \text{and} \quad F = 0 \quad (2.21)$$

### 2.3.2.2 NORMAL TO A SURFACE

At every point  $P$  of a surface there exists a unit normal vector  $\vec{n}(\alpha_1, \alpha_2)$  which is perpendicular to  $\vec{r}_{,1}$  and  $\vec{r}_{,2}$  and hence to the plane at  $P$  that contains these vectors (the tangent plane

at  $P$ ). The unit normal vector is thus parallel to the cross product of  $\vec{r}_1$  and  $\vec{r}_2$ . Since a unit vector is a vector divided by its magnitude, an expression for  $\vec{n}(\alpha_1, \alpha_2)$  is given as

$$\vec{n}(\alpha_1, \alpha_2) = (\vec{r}_1 \times \vec{r}_2) / |\vec{r}_1 \times \vec{r}_2| \quad (2.22)$$

From vector algebra, we have

$$|\vec{r}_1 \times \vec{r}_2| = |\vec{r}_1| |\vec{r}_2| \sin \theta \quad (2.23)$$

and

$$\vec{r}_1 \cdot \vec{r}_2 = |\vec{r}_1| |\vec{r}_2| \cos \theta \quad (2.24)$$

where  $\theta$  is the angle between the vectors  $\vec{r}_1$  and  $\vec{r}_2$ . Thus, from Equation (2.18), we obtain

$$\cos \theta = F / \sqrt{EG} \quad (2.25)$$

and, therefore,

$$\sin \theta = \sqrt{(EG - F^2) / EG} \quad (2.26)$$

The final expression for the unit normal vector is

$$\vec{n}(\alpha_1, \alpha_2) = \left( \frac{\vec{r}_1 \times \vec{r}_2}{H} \right), \quad H = \sqrt{EG - F^2} \quad (2.27)$$

provided that  $H$  does not vanish. We should point out here that the principal normal  $\vec{N}$  of a curve on a surface need not be normal to the surface (that is, generally  $\vec{N} \cdot \vec{n} \neq 1$ ).

Like the principal normal of a curve, the sense of the normal to a surface is arbitrary. Therefore, we should adopt the convention that the parametric curves should always be arranged in such a manner that the normal  $\vec{n}$  points from the concave side to the convex side of the surface.

### 2.3.2.3 SECOND FUNDAMENTAL FORM

In our previous discussion, we have described the curvature vector  $\vec{k}$  of a space curve. We shall now consider a curve on a surface and use the properties of the curvature vector to derive an

important feature of surfaces called the second fundamental form. Let us resolve the curvature vector  $\vec{k}$  of the curve into its components normal and tangential to the surface. Thus

$$\vec{k} = \frac{d\vec{t}}{ds} = \vec{k}_n + \vec{k}_t \quad (2.28)$$

Here  $\vec{k}_n$  and  $\vec{k}_t$  are referred to as the normal curvature vector and tangential curvature vector, respectively. In our analysis, we are only interested in the former one. Since  $\vec{k}_n$  is in the direction of the normal to the surface, it is proportional to  $\vec{n}$  and can be expressed in terms of it as follows:

$$\vec{k}_n = -K_n \vec{n} \quad (2.29)$$

where  $K_n$  is called the normal curvature. The minus sign takes into account the fact that the sense of the curvature vector  $\vec{k}$  is opposite to that of the normal vector  $\vec{n}$ .

Since  $\vec{n}$  is perpendicular to  $\vec{t}$ , differentiation of the scalar product  $\vec{n} \cdot \vec{t} = 0$  with respect to  $s$  along the curve on the surface gives

$$\frac{d\vec{n}}{ds} \cdot \vec{t} = -\vec{n} \cdot \frac{d\vec{t}}{ds} \quad (2.30)$$

If we form the scalar product of Equation (2.29) with  $\vec{n}$ , we find that

$$-(\vec{k}_n \cdot \vec{n}) = K_n \quad (2.31)$$

and the scalar product of Equation (2.28) with  $\vec{n}$  gives (since  $\vec{n}$  is perpendicular to  $\vec{k}_t$ ):

$$\vec{n} \cdot (d\vec{t}/ds) = \vec{n} \cdot \vec{k}_n \quad (2.32)$$

Finally, if we combine Equations (2.32), (2.31), and (2.30), we obtain

$$K_n = (d\vec{r} \cdot d\vec{n}) / (d\vec{r} \cdot d\vec{r}) \quad (2.33)$$

where we have used  $(ds)^2 = d\vec{r} \cdot d\vec{r}$ . Now, if we notice that

$$d\vec{n} = \vec{n}_{,1}d\alpha_1 + \vec{n}_{,2}d\alpha_2, \quad d\vec{r} = \vec{r}_{,1}d\alpha_1 + \vec{r}_{,2}d\alpha_2 \quad (2.34)$$

and if we substitute the foregoing expressions into Equation (2.33), we obtain

$$K_n = \frac{II}{I} = \frac{L(d\alpha_1)^2 + 2Md\alpha_1d\alpha_2 + N(d\alpha_2)^2}{E(d\alpha_1)^2 + 2Fd\alpha_1d\alpha_2 + G(d\alpha_2)^2} \quad (2.35)$$

where the following new quantities, which are called fundamental magnitudes, have been defined:

$$L = \vec{r}_{,1} \cdot \vec{n}_{,1}, \quad 2M = (\vec{r}_{,1} \cdot \vec{n}_{,2} + \vec{r}_{,2} \cdot \vec{n}_{,1}), \quad N = \vec{r}_{,2} \cdot \vec{n}_{,2} \quad (2.36)$$

By differentiation of the expressions  $\vec{r}_{,1} \cdot \vec{n} = 0$ , and  $\vec{r}_{,2} \cdot \vec{n} = 0$ , we obtain the alternative expressions:

$$L = -\vec{r}_{,11} \cdot \vec{n}, \quad M = -\vec{r}_{,12} \cdot \vec{n}, \quad N = -\vec{r}_{,22} \cdot \vec{n} \quad (2.37)$$

where we have used the following notation

$$\vec{r}_{,ij} = \frac{\partial^2 \vec{r}}{\partial \alpha_i \partial \alpha_j}, \quad i, j = 1, 2 \quad (2.38)$$

We have also assumed, in the derivation of the alternate expression for  $M$  that  $\vec{r}$  has continuous second derivatives. This will insure that  $\vec{r}_{,12} = \vec{r}_{,21}$

In the expression (2.35) for the normal curvature, we notice that the denominator ( $I$ ) is the first fundamental form which is derived previously. The numerator ( $II$ ) is referred to as the second fundamental form. Since  $E, F, G, L, M, N$  can all be expressed as functions of  $\alpha_1$  and  $\alpha_2$ . They are constants at a given point, it is seen upon consideration of Eq.(2.35) that the normal curvature depends only on the direction  $d\alpha_1/d\alpha_2$ . It can thus be stated that all curves through a point on a surface which are tangent to the same direction have the same normal curvature.

### 2.3.2.4 PRINCIPAL CURVATURES

It is interesting at this point to seek those directions  $d\alpha_2/d\alpha_1$  for which the normal curvature  $K_n$  has a maximum or a minimum. If, from now on, we drop the subscript  $n$ , and if we define the direction to be  $\lambda = d\alpha_2/d\alpha_1$ , the expression for the normal curvature becomes

$$K(\lambda) = \frac{L + 2M\lambda + N\lambda^2}{E + 2F\lambda + G\lambda^2} \quad (2.39)$$

The normal curvature attains an extremum in a particular direction  $\lambda$  if  $dK/d\lambda = 0$ , or

$$(E + 2F\lambda + G\lambda^2)(M + N\lambda) - (L + 2M\lambda + N\lambda^2)(F + G\lambda) = 0 \quad (2.40)$$

By noting also that

$$E + 2F\lambda + G\lambda^2 = (E + F\lambda) + \lambda(F + G\lambda) \quad (2.41)$$

$$L + 2M\lambda + N\lambda^2 = (L + M\lambda) + \lambda(M + N\lambda)$$

we find that

$$(E + F\lambda)(M + N\lambda) = (F + G\lambda)(L + M\lambda) \quad (2.42)$$

The extremum curvature is now found by substituting Equation (2.40) into Equation (2.39) and then making use of Equation (2.42). This procedure gives

$$K = \frac{M + N\lambda}{F + G\lambda} = \frac{L + M\lambda}{E + F\lambda} \quad (2.43)$$

An equation for determining the direction  $\lambda$  corresponding to the extremum curvatures is found by expanding Equation (2.42), with the result that

$$(MG - NF)\lambda^2 + (LG - NE)\lambda + (LF - ME) = 0 \quad (2.44)$$

This quadratic equation yields two roots,  $\lambda_1$  and  $\lambda_2$ , corresponding to two directions,  $(d\alpha_2/d\alpha_1)_1$  and  $(d\alpha_2/d\alpha_1)_2$ , of extremum curvature. One of these solutions is the maximum

curvature while the other is the minimum curvature.  $K_1$  and  $K_2$ , corresponding to  $\lambda_1$  and  $\lambda_2$ , are called the principal curvatures, and  $R_1 = K_1^{-1}$  and  $R_2 = K_2^{-1}$  are the principal radii of curvature. The directions of principal curvature are orthogonal. Proof of this orthogonality is given in detail in the section 1.3d of [12]. Integration of Equation (2.44) gives us the lines of curvature on the surface. These form an orthogonal family of curves on the surface.

Now let us examine the situation in which the lines of curvature are taken as the parametric lines (curves) of the surface. In this case, Equation (2.44) must be satisfied by  $d\alpha_1/d\alpha_2 = 0$  and  $d\alpha_2/d\alpha_1 = 0$ . For this to be possible, we must have

$$LF - ME = 0 \text{ and } MG - NF = 0 \quad (2.45)$$

Since we have postulated the parametric lines are to be the lines of curvature and since the latter is known to be orthogonal,  $F = 0$ . It can be shown that  $EG - F^2 > 0$ , so that for  $F = 0$ , neither  $E$  nor  $G$  can be zero. Thus, we are led to the conclusion, from Equation (2.45), that  $M = 0$  and, therefore, the conditions under which the parametric lines are also lines of curvature are

$$F = M = 0 \quad (2.46)$$

When the parametric curves are the lines of curvature, we can find their curvatures by setting  $F=M=0$  in Equation (2.35), then letting  $d\alpha_1 = 0$  and  $d\alpha_2 = 0$ , in turn, to give

$$K_1 = \frac{1}{R_1} = \frac{L}{E}, \quad K_2 = \frac{1}{R_2} = \frac{N}{G} \quad (2.47)$$

The development of the theory of thin elastic shells is considerably clarified if the lines of curvature of the reference surface are used as the parametric lines. Thus, we shall assume that Equation (2.46) is satisfied our subsequent work.

### 2.3.2.5 DERIVATIVES OF UNIT VECTORS ALONG PARAMETRIC LINES

In our development of the fundamental theorem of the theory of surfaces, it will be necessary to have on hand some expressions for the derivatives of unit vector along the parametric lines. With this in mind, let us, therefore, consider a triplet of mutually orthogonal unit vectors  $(\vec{t}_1, \vec{t}_2, \vec{n})$  that are oriented at a given point on a surface so as to be tangent to the  $\alpha_1$  and  $\alpha_2$  directions and normal to the surface, respectively. As the triplet of unit vectors is moved over the surface, the magnitudes of the

vectors will remain constant at unity and their directions will remain mutually orthogonal. However, the orientation of the triplet will vary and, as a result, special attention must be given to the derivatives of the unit vectors. To begin, we notice that a unit vector can be defined to be any vector divided by its magnitude. Thus

$$\begin{aligned}\vec{t}_1 &= \vec{r}_{,1}/|\vec{r}_{,1}| = \vec{r}_{,1}/A_1 \\ \vec{t}_2 &= \vec{r}_{,2}/|\vec{r}_{,2}| = \vec{r}_{,2}/A_2 \\ \vec{n} &= (\vec{t}_1 \times \vec{t}_2) = (\vec{r}_{,1} \times \vec{r}_{,2})/(A_1 A_2)\end{aligned}\tag{2.48}$$

where we have adopted the notation introduced by Equation (2.20) for orthogonal systems of parametric lines. Since derivatives  $\vec{n}_{,1}$  and  $\vec{n}_{,2}$  are perpendicular to  $\vec{n}$ , they lie in the plane formed by  $\vec{t}_1$  and  $\vec{t}_2$  and each can be decomposed into its components along  $\vec{t}_1$  and  $\vec{t}_2$ . For example,

$$\vec{n}_{,1} = a\vec{t}_1 + b\vec{t}_2\tag{2.49}$$

where  $a$  and  $b$  are unknowns which represent the projections of  $\vec{n}_{,1}$  on  $\vec{t}_1$  and  $\vec{t}_2$ , respectively. To determine  $a$  and  $b$ , we form the following scalar products:

$$\begin{aligned}\vec{t}_1 \cdot \vec{n}_{,1} &= \frac{\vec{r}_{,1} \cdot \vec{n}_{,1}}{A_1} = \frac{L}{A_1} = a(\vec{t}_1 \cdot \vec{t}_1) + b(\vec{t}_1 \cdot \vec{t}_2) \\ \vec{t}_2 \cdot \vec{n}_{,1} &= \frac{\vec{r}_{,2} \cdot \vec{n}_{,1}}{A_2} = \frac{M}{A_2} = a(\vec{t}_2 \cdot \vec{t}_1) + b(\vec{t}_2 \cdot \vec{t}_2)\end{aligned}\tag{2.50}$$

On account of our restriction to orthogonal systems,  $M = 0 = \vec{t}_1 \cdot \vec{t}_2$  and, therefore,

$$a = \frac{L}{A_1}, \quad b = 0\tag{2.51}$$

An expression for  $\vec{n}_{,1}$  is then,

$$\vec{n}_{,1} = \frac{L}{A_1} \vec{t}_1\tag{2.52}$$

and since, by Equation (2.47)

$$K_1 = \frac{1}{R_1} = \frac{L}{A_1^2} \quad (2.53)$$

we obtain as the final result

$$\vec{n}_{,1} = \frac{A_1}{R_1} \vec{t}_1 \quad (2.54)$$

In a similar fashion, it follows that

$$\vec{n}_{,2} = \frac{A_2}{R_2} \vec{t}_2 \quad (2.55)$$

To find the derivatives of  $\vec{t}_1$  and  $\vec{t}_2$  along the parametric lines we proceed as we did for the case of the derivatives of  $\vec{n}$ . The manipulations are slightly more involved in this case and are facilitated by noting, first, that for functions with continuous second derivatives  $\vec{r}_{,12} = \vec{r}_{,21}$ . This permits us to write, taking into account Equations (2.48),

$$(A_1 \vec{t}_1)_{,2} = (A_2 \vec{t}_2)_{,1} \quad (2.56)$$

or

$$\vec{t}_{2,1} = \frac{1}{A_2} [A_1 \vec{t}_{1,2} + \vec{t}_1 A_{1,2} - \vec{t}_2 A_{2,1}] \quad (2.57)$$

To find  $\vec{t}_{1,1}$ , for example, we observe that this derivative will be perpendicular to  $\vec{t}_1$  and will thus lie in the plane formed by  $\vec{t}_2$  and  $\vec{n}$ . We may, hence, express  $\vec{t}_{1,1}$  in terms of  $\vec{t}_2$  and  $\vec{n}$  as

$$\vec{t}_{1,1} = c \vec{n} + d \vec{t}_2 \quad (2.57)$$

where  $c$  and  $d$  are the unknown projections of  $\vec{t}_{1,1}$  on  $\vec{t}_2$  and  $\vec{n}$ . To determine  $c$  and  $d$  we form the scalar products

$$\vec{n} \cdot \vec{t}_{1,1} = c (\vec{n} \cdot \vec{n}) + d (\vec{n} \cdot \vec{t}_2) = c \quad (2.58)$$

$$\vec{t}_2 \cdot \vec{t}_{1,1} = c(\vec{t}_2 \cdot \vec{n}) + d(\vec{t}_2 \cdot \vec{t}_2) = d$$

We now proceed by noting that, since  $(\vec{t}_1 \cdot \vec{n}) = 0$ ,

$$(\vec{t} \cdot \vec{n})_{,1} = \vec{t}_1 \cdot \vec{n}_{,1} + \vec{n} \cdot \vec{t}_{1,1} = 0 \quad (2.59)$$

and therefore,

$$c = \vec{n} \cdot \vec{t}_{1,1} = -\vec{t}_1 \cdot \vec{n}_{,1} = -\frac{A_1}{R_1} \quad (2.60)$$

where we have employed Equation (2.54). In the same way,

$$d = \vec{t}_2 \cdot \vec{t}_{1,1} = -\vec{t}_1 \cdot \vec{t}_{2,1} \quad (2.61)$$

and becomes, upon use of Equation (2.56),

$$d = -\frac{\vec{t}_1}{A_2} \cdot [A_1 \vec{t}_{1,2} + \vec{t}_1 A_{1,2} - \vec{t}_2 A_{2,1}] \quad (2.62)$$

Since  $\vec{t}_{1,2}$  is perpendicular to  $\vec{t}_1$ , the above expression simplifies to

$$d = -\frac{1}{A_2} A_{1,2} \quad (2.63)$$

The final result for  $\vec{t}_{1,1}$  is

$$\vec{t}_{1,1} = -\frac{A_1}{R_1} \vec{n} - \frac{1}{A_2} \frac{\partial A_1}{\partial \alpha_2} \vec{t}_2 \quad (2.64)$$

By proceeding in an analogous manner, we can show that the remaining derivatives are given by

$$\begin{aligned} \vec{t}_{1,2} &= \frac{1}{A_1} \frac{\partial A_2}{\partial \alpha_1} \vec{t}_2 \\ \vec{t}_{2,1} &= \frac{1}{A_2} \frac{\partial A_1}{\partial \alpha_2} \vec{t}_1 \end{aligned} \quad (2.65)$$

$$\vec{t}_{2,2} = -\frac{A_2}{R_2} \vec{n} - \frac{1}{A_1} \frac{\partial A_2}{\partial \alpha_1} \vec{t}_1$$

### 2.3.2.6 FUNDAMENTAL THEOREM OF THE THEORY OF SURFACES

We shall now derive three differential equations (known as the Gauss-Codazzi conditions) that relate the quantities  $A_1$ ,  $A_2$ ,  $R_1$ , and  $R_2$  of a given surface. These equations, as part of the fundamental theory of surfaces, are used to ascertain whether an arbitrary choice of these four parameters will define a valid surface. These relationships are found from the equality of the mixed second derivatives of the unit vectors, a result which presumes that these vectors have continuous second derivatives. For example, if we start with

$$\vec{n}_{,12} = \vec{n}_{,21} \quad (2.66)$$

we notice, upon use of expressions for the derivatives of  $\vec{n}$  along the parametric lines derived in the previous section, that

$$\left( \frac{A_1}{R_1} \vec{t}_1 \right)_{,2} - \left( \frac{A_2}{R_2} \vec{t}_2 \right)_{,1} = 0 \quad (2.67)$$

If we carry out the differentiations indicated in the foregoing and make use of the expressions for the derivatives of  $\vec{t}_1$  and  $\vec{t}_2$ , we obtain

$$\vec{t}_1 \left[ \frac{-1}{R_2} A_{1,2} + \left( \frac{A_1}{R_1} \right)_{,2} \right] + \vec{t}_2 \left[ \frac{1}{R_1} A_{2,1} - \left( \frac{A_2}{R_2} \right)_{,1} \right] = 0 \quad (2.68)$$

This vector equation will be true only if the square brackets vanish; hence we obtain

$$\frac{1}{R_2} A_{1,2} = \left( \frac{A_1}{R_1} \right)_{,2}, \quad \frac{1}{R_1} A_{2,1} = \left( \frac{A_2}{R_2} \right)_{,1} \quad (2.69)$$

These are known as the Codazzi conditions. If we proceed in a similar fashion from the equation

$$\vec{t}_{1,12} = \vec{t}_{1,21} \quad (2.70)$$

We obtain two more relations of which only the following is new:

$$\left( \frac{1}{A_1} A_{2,1} \right)_{,1} + \left( \frac{1}{A_2} A_{1,2} \right) = -\frac{A_1 A_2}{R_1 R_2} \quad (2.71)$$

This is known as the Gauss condition. The fact that four quantities can be related by no more than three homogeneous equations, if they are to possess nontrivial solutions, leads us to the conclusion that no new information will be obtained from a consideration of the remaining equality

$$\vec{t}_{2,12} = \vec{t}_{2,21} \quad (2.72)$$

We now indicate, in a formal manner, the role of the Gauss-Codazzi conditions by stating the fundamental theorem of the theory of surfaces:

If  $E, G, L,$  and  $N$  are given as functions of the real curvilinear coordinates  $\alpha_1$  and  $\alpha_2$  and are sufficiently differentiable and satisfy the Gauss-Codazzi conditions while  $E > 0$  and  $G > 0$ , then there exists a real surface which has its first and second fundamental forms

$$I = E (d\alpha_1)^2 + G (d\alpha_2)^2, \quad II = L (d\alpha_1)^2 + N (d\alpha_2)^2$$

This surface is uniquely determined except for its position in space.

As a consequence of the fundamental theorem, we might refer to the Gauss-Codazzi conditions as the compatibility conditions of the theory of surfaces. It should be noticed that, as stated above, the theorem is already restricted to the surfaces whose lines of curvature are also its parametric lines (since  $F=M=0$ ). The extension to more general parametric lines can be made but requires more general forms of the Gauss-Codazzi conditions than we have derived here”.

## 2.4 CLASSIFICATION OF SHELL SURFACES

There are three types of shell surfaces such as surfaces of revolution, surfaces of translation, and ruled surfaces.

“Surfaces of revolution are generated by revolving a plane curve, called the meridian, about an axis not necessarily intersecting the meridian”[15]. Some examples for surfaces of revolution are given in the Figure 2.4. In Figure 2.4, the radius of curvatures are denoted as  $r_i$   $i=1, 2$ .

“A surface of translation is defined as the surface generated by keeping a plane curve parallel to its initial plane as we move it along another plane curve”[15]. Figure 2.5 shows the surfaces of translation.

“Ruled surfaces are obtained by the translation of straight lines over two end curves”[15]. They are depicted in the Figure 2.6.

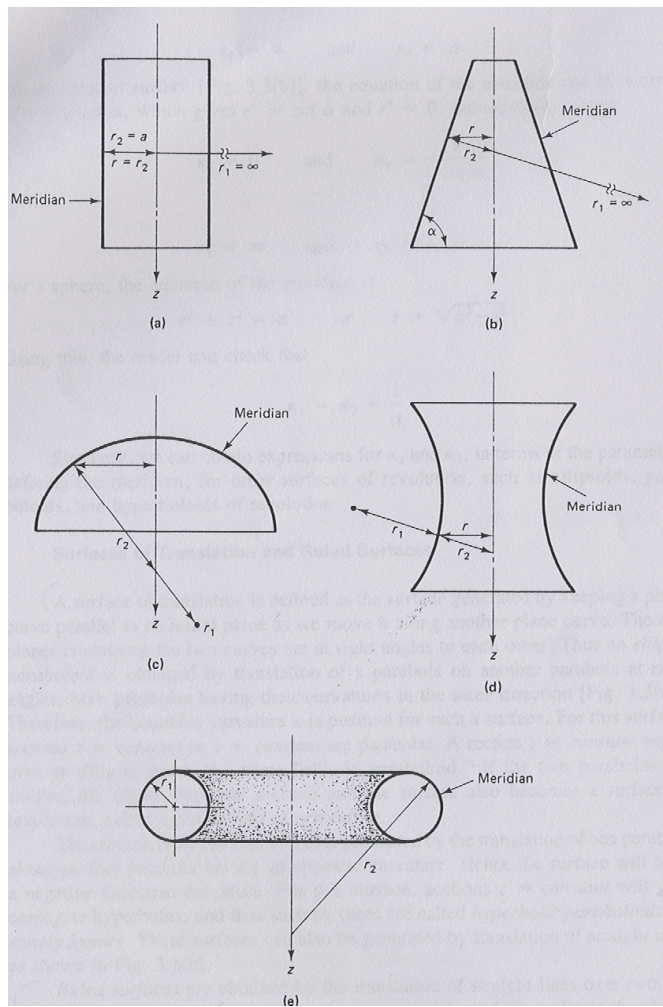


**Figure 2.4** Some examples for surfaces of revolution

(a) Circular Cylinder, (b) Cone, (c) Elliptic dome, (d) Hyperboloid of revolution, (e) Toroid [15].

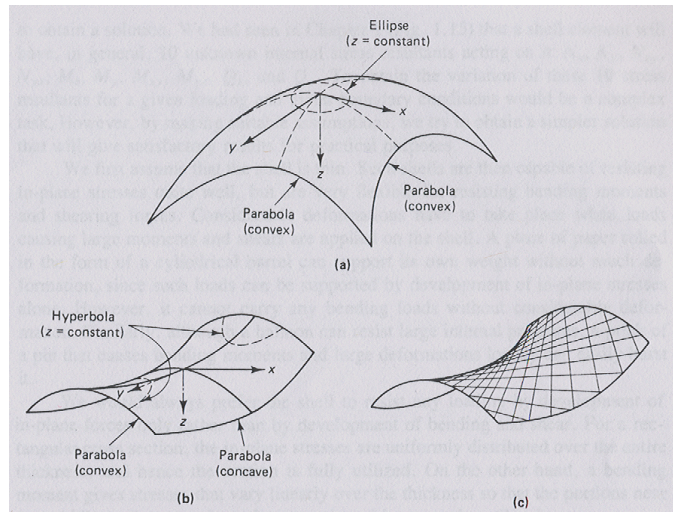


**Figure 2.5** Some examples for Surfaces of translation

(a) Elliptic paraboloid, (b) Hyperbolic paraboloid, (c) Hyper and its straight-line generators [15].

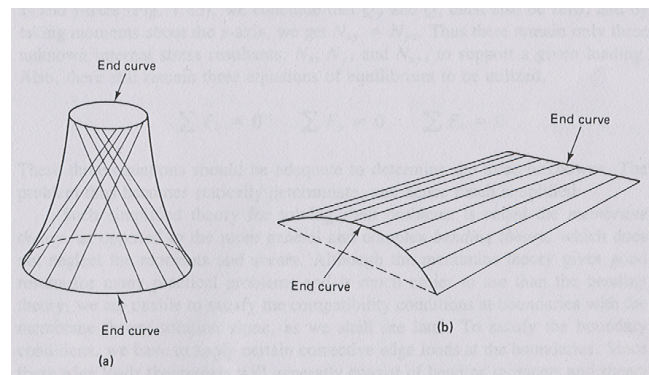


**Figure 2.6** Ruled Surfaces (a) Hyperboloid of revolution of one sheet, (b) Conoid [15].

Since the main concern of this study is the shells of revolution, the surface of revolution is studied comprehensively in the next section.

### 2.4.1 SHELLS OF REVOLUTION

Shells whose reference surfaces are the surface of revolution are called shells of revolution.

A surface which is obtained by rotation of a plane curve about an axis lying in the plane of the curve is called surface of revolution. The plane curve is called a meridian of the surface, and its plane is the meridian plane. The intersection of the surface with planes perpendicular to the axis of

rotation are parallel circles and are called parallels. For the shells of revolution, the lines of principal curvature are its meridians and parallels.

Figure 2.7 shows the geometry and coordinate system of the shells of revolution. The orthogonal curvilinear coordinate system,  $\alpha_1, \alpha_2$ , and  $\zeta$ , of the reference surface of the shell, is replaced by  $\phi, \theta$ , and  $\zeta$ , respectively for the shells of revolution. The angle  $\phi$  shown in the Figure 2.7 is the angle between the normal to the reference surface and the axis of rotation, and the angle  $\theta$  shown in the Figure 2.7 is the angle determining the position of a point on the corresponding parallel circle.

The position vector  $\vec{r}$  of the point P on the reference surface of the shells of revolution is given by [14]:

$$\vec{r} = \vec{r}(\phi, \theta) = \left( \frac{R_0}{\sin \phi} \right) (\cos \theta \vec{e}_i + \sin \theta \vec{e}_j + \cos \phi \vec{e}_k) \quad (2.73)$$

where  $R_0$  is the radius of the parallel at position  $x_3$ , and  $\vec{e}_i, \vec{e}_j, \vec{e}_k$  are the unit normal vectors of the rectangular coordinate system.

Differentiating the position vector with respect to  $\phi$  and  $\theta$  separately, we get the followings

$$\frac{\partial \vec{r}}{\partial \phi} = \vec{r}_{,1} = \left( \frac{-R_0}{\sin^2 \phi} \right) (\cos \phi \cos \theta \vec{e}_i + \cos \phi \sin \theta \vec{e}_j + \vec{e}_k) \quad (2.74)$$

$$\frac{\partial \vec{r}}{\partial \theta} = \vec{r}_{,2} = \left( \frac{R_0}{\sin \phi} \right) (-\sin \theta \vec{e}_i + \cos \theta \vec{e}_j) \quad (2.75)$$

The first fundamental magnitudes,  $E$  and  $G$ , of the shells of revolutions can be determined by using Equations (2.74) and (2.75) in Equation (2.18).

$$E = \vec{r}_{,1} \cdot \vec{r}_{,1} = \left( \frac{R_0^2}{\sin^4 \phi} \right) (\cos^2 \phi + 1) \quad (2.76)$$

$$G = \vec{r}_{,2} \cdot \vec{r}_{,2} = \left( \frac{R_0^2}{\sin^2 \phi} \right) \quad (2.77)$$

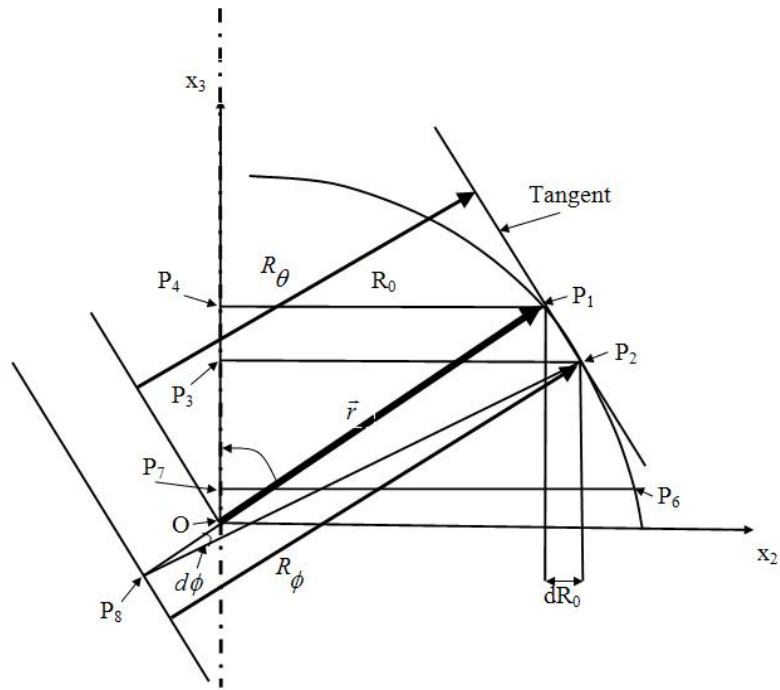
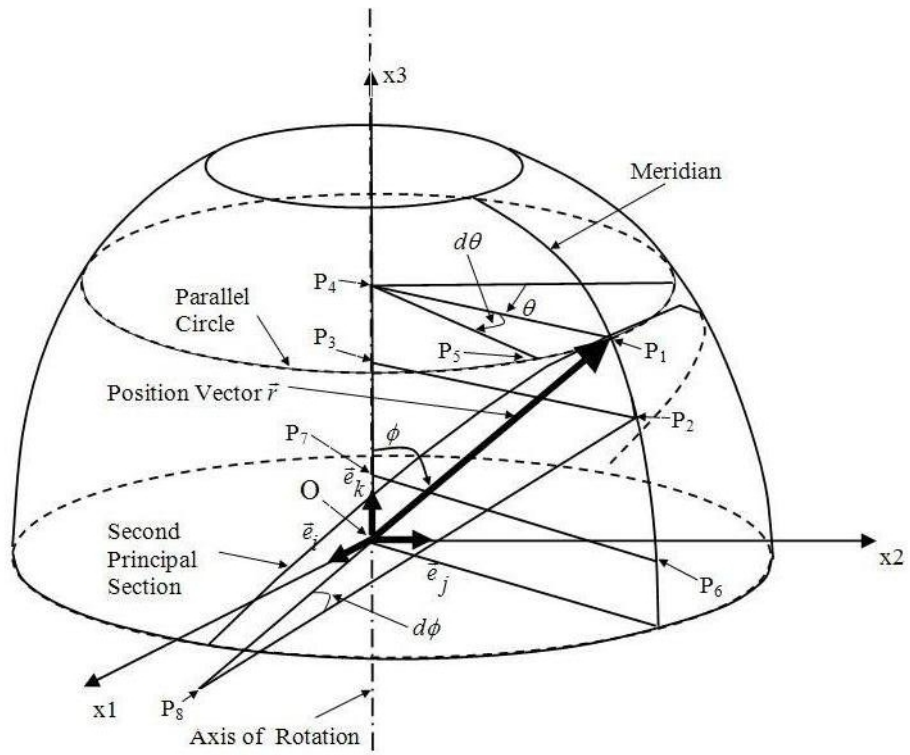


**Figure 2.7** Geometry and coordinate system of shells of revolution

The unit normal vector of the surface of revolution is obtained by substituting Equations (2.74), (2.75), (2.76), and (2.77) into Equation (2.27) and taking  $F = 0$ .

$$H = \sqrt{EG} = \left( \frac{R_0^2}{\sin^3 \phi} \right) \sqrt{\cos^2 \phi + 1} \quad (2.78)$$

$$\vec{n} = \left( \frac{\vec{r}_{,1} \times \vec{r}_{,2}}{H} \right) = \left( \frac{1}{\sqrt{\cos^2 \phi + 1}} \right) (\cos \theta \vec{e}_i + \sin \theta \vec{e}_j - \cos \phi \vec{e}_k) \quad (2.79)$$

We get the derivatives of the unit normal vector  $\vec{n}$  with respect to  $\phi$  and  $\theta$  as follows:

$$\frac{\partial \vec{n}}{\partial \phi} = \vec{n}_{,1} = \left( \frac{1}{\sqrt{\cos^2 \phi + 1}} \right) \left( \left( \frac{\cos \phi \sin \phi}{\cos^2 \phi + 1} \right) \cos \theta \vec{e}_i + \left( \frac{\cos \phi \sin \phi}{\cos^2 \phi + 1} \right) \sin \theta \vec{e}_j - \sin \phi \vec{e}_k \right) \quad (2.80)$$

$$\frac{\partial \vec{n}}{\partial \theta} = \vec{n}_{,2} = \left( \frac{1}{\sqrt{\cos^2 \phi + 1}} \right) (-\sin \theta \vec{e}_i + \cos \theta \vec{e}_j) \quad (2.81)$$

We have the second fundamental magnitudes,  $L$  and  $N$  for the shells of revolution by inserting Equations (2.74), (2.75), (2.80), and (2.81) into Equation (2.36).

$$L = \vec{r}_{,1} \cdot \vec{n}_{,1} = \left( \frac{1}{\sqrt{\cos^2 \phi + 1}} \right) \left( \frac{1}{\cos^2 \phi + 1} \right) \left( \frac{R_0}{\sin \phi} \right) \quad (2.82)$$

$$N = \vec{r}_{,2} \cdot \vec{n}_{,2} = \left( \frac{1}{\sqrt{\cos^2 \phi + 1}} \right) \left( \frac{R_0}{\sin \phi} \right) \quad (2.83)$$

$K_1$  and  $K_2$ , the principal curvatures are given by Equation (2.84), and  $R_1$  and  $R_2$ , the principal radii of curvatures are given by Equation (2.85) for shells of revolution.

$$K_1 = \frac{1}{R_1} = \frac{L}{E} = \frac{\left( \frac{1}{\sqrt{\cos^2 \phi + 1}} \right) \left( \frac{1}{\cos^2 \phi + 1} \right) \left( \frac{R_0}{\sin \phi} \right)}{\left( \frac{R_0^2}{\sin^4 \phi} \right) (\cos^2 \phi + 1)} \quad (2.84)$$

$$K_2 = \frac{1}{R_2} = \frac{N}{G} = \frac{\left( \frac{1}{\sqrt{\cos^2 \phi + 1}} \right) \left( \frac{R_0}{\sin \phi} \right)}{\left( \frac{R_0^2}{\sin^2 \phi} \right)} \quad (2.85)$$

Recalling Equation (2.21), and inserting Equations (2.76) and (2.77) into it, we get

$$A_1 = \sqrt{E} = \left( \frac{R_0}{\sin^2 \phi} \right) \sqrt{\cos^2 \phi + 1} \quad (2.86)$$

$$A_2 = \sqrt{G} = \left( \frac{R_0}{\sin \phi} \right) \quad (2.87)$$

Rewriting Equation (2.69) which is Gauss condition,

$$\left[ \left( \frac{1}{A_1} A_{2,1} \right) \right]_{,1} + \left[ \left( \frac{1}{A_2} A_{1,2} \right) \right]_{,2} = \left[ -\frac{A_1 A_2}{R_1 R_2} \right]$$

Substituting Equations (2.84), (2.85), (2.86), and (2.87) into Equation (2.69), we can write the Gauss condition for shells of revolution as

$$-\frac{\sin \phi}{\sqrt{\cos^2 \phi + 1}} = -\frac{\sin \phi}{\sqrt{\cos^2 \phi + 1}} \quad (2.88)$$

Also, rewriting Equation (2.71) which is Codazzi condition,

$$\left[ \frac{1}{R_2} A_{1,2} \right] = \left[ \left( \frac{A_1}{R_1} \right) \right]_{,2}, \quad \left[ \frac{1}{R_1} A_{2,1} \right] = \left[ \left( \frac{A_2}{R_2} \right) \right]_{,1}$$

Again, substituting Equations (2.84), (2.85), (2.86), and (2.87) into Equation (2.71), we can write the two components of Codazzi condition of shells of revolution in the form

$$0 = 0, \quad \frac{-\cos \phi \sin \phi}{(\cos^2 \phi + 1)^{5/2}} = \frac{-\cos \phi \sin \phi}{(\cos^2 \phi + 1)^{5/2}} \quad (2.89)$$

The left and right sides of Equations (2.88) and (2.89) are similar after substituting the expressions for  $A_1, A_2, R_1, R_2$  obtained for shells of revolution into Gauss-Codazzi conditions. In other words, the Gauss-Codazzi conditions are clearly satisfied for shells of revolution.

The infinitesimal distance  $\overline{P_2P_5}$  between two arbitrary points on the reference surface of the shells of revolution is given by (refer to Figure 2.7)

$$(ds)^2 = (\overline{P_2P_5})^2 + (\overline{P_1P_5})^2 \quad (2.90)$$

and from Figure 2.7 it is clear that

$$\overline{P_1P_2} = R_\phi d\phi \quad (2.91)$$

$$\overline{P_1P_5} = R_\theta \sin \phi d\theta \quad (2.92)$$

Hence

$$(ds)^2 = (R_\phi d\phi)^2 + (R_\theta \sin \phi d\theta)^2 \quad (2.93)$$

On the other hand, from Equation (2.20) the distance between any two points on the reference surface of a shell is given by

$$(ds)^2 = A_1^2 (d\alpha_1)^2 + A_2^2 (d\alpha_2)^2 \quad (2.94)$$

where  $A_1$  and  $A_2$  are sometimes called Lamé parameters which are related with the first fundamental magnitudes of the reference surface of the shell. Switching the notation of curvilinear coordinates to the notation of  $\phi$  and  $\theta$

$$(ds)^2 = A_\phi^2 (d\phi)^2 + A_\theta^2 (d\theta)^2 \quad (2.95)$$

Thus, comparing Equations (2.93) and (2.95), the Lamé parameters  $A_\phi$  and  $A_\theta$  for a shell of revolution are given by

$$A_\phi = R_\phi \quad (2.96)$$

$$A_\theta = R_\theta \sin \phi \quad (2.97)$$

Furthermore, from Figure 2.7 the following relationships can readily be seen

$$R_\theta \sin \phi = R_0 \quad (2.98)$$

and

$$d(R_\theta \sin \phi) = R_\theta \cos \phi d\phi \quad (2.99)$$

It should be noted that since the shell geometry is rotationally symmetric  $A_\phi, A_\theta, R_\phi, R_\theta$  are functions of  $\phi$  only. Therefore,

$$\frac{\partial}{\partial \theta} (A_\phi, A_\theta, R_\phi, R_\theta) = 0 \quad (2.100)$$

## 2.5 THEORY OF LAMINATED COMPOSITE ELASTIC SHELLS FOR DYNAMIC ANALYSIS

After reviewing the necessary preliminaries presented so far to understand the thin elastic shell theory, we can start to formulate the governing equations for dynamic analysis of laminated composite elastic shells with free vibration definition. Subsequently, the analysis of thin-walled structural elements, particularly shells of revolution in this thesis, made of laminated composite materials is presented.

A detailed study of the theoretical formulations of governing equations of laminated composite elastic shells constitutes the objective of the remaining part of this chapter. The methods of solution for the dynamic analysis of laminated composite shells will be expressed in the next chapter.

In this thesis, the free vibration analysis of laminated composite elastic shells is taken into consideration.

In dynamic analysis of the elastic structure, the task is to determine its response, namely the behavior of it, when subjected to a certain excitation. The excitation can be divided into forcing functions, initial displacements and velocities, and moving supports. The vibration resulting from the action of forcing upon a system is known as forced vibration, and the one resulting from initial conditions is called free vibration. Moving supports result in forcing functions in the form of inertia forces and elastic forces and, as such, they lead to forced vibration problems. The response is taken as

periodic in time.

When an elastic structure is displaced from its equilibrium position and then released, it will oscillate about that position before returning to state of rest. The elastic structure is said to be exhibiting free vibration when it is given an initial displacement from its equilibrium position and thereafter allowed to oscillate with no further imposed force.

It is known that the theory of shells is the subclass of the theory of elasticity. There are various shell theories pertaining to their different aspects. They can generally be divided into two groups: three-dimensional shell theories and two-dimensional shell theories. “The two-dimensional shell theories are derived from three-dimensional elasticity theory by making suitable assumptions concerning the kinematics of deformation through the thickness of the shell. These assumptions allow the reduction of a three-dimensional problem to a two-dimensional problem. The two-dimensional shell theories include thin and thick shell theories, shallow and deep shell theories, linear and nonlinear shell theories defined according to the ratio of the thickness of shell to the shortest of the span length or radii of curvatures, the ratio of the shortest span length to one of the radii of curvature or vice versa, and the magnitude of linear and rotational displacements, respectively” [42].

Aeronautical structures, which are considered as thin-walled structures, consist of various shell and plate configurations as basic structural elements. In this thesis, we make use of thin elastic shell theory. The thin elastic shell theory is interested with the study of small elastic deformations of thin elastic bodies under the influence of loads. By small deformations, it is assumed that the equilibrium conditions for deformed elements are the same as if they were not deformed. The relationships governing the behavior of thin elastic shells are based upon the equations of the theory of linear elasticity. However, the consideration of the complete three-dimensional elasticity field equations which are equilibrium (motion) equations, strain-displacement geometrical equations, compatibility equations and constitutive equations, do not assure the analytical solutions of thin elastic shells. “In fact, the three-dimensional equations of elasticity in rectangular coordinate system are complicated when written in curvilinear coordinate system defining shell geometry. There are two main “difficulty factors” involved in achieving an analytical solution of the boundary value problem using the three-dimensional elasticity theory. The first of these factors deals with the “degree of the geometrical complexity” of the shells, for example prescribed in the circular coordinate system. The number of boundaries in the shell geometry can lead to difficulties in the application of boundary conditions. The second “difficulty factor” involved in the solution of the three-dimensional equations of motion and the strain-displacement relations of shells in the circular coordinate system deals with the “degree of material complexity”. In fact, the most general form of the constitutive equations, do not have analytical solutions available in the literature. Therefore, almost all shell theories for thin elastic shells reduce the three-dimensional elasticity problem into a two-dimensional problem by making suitable assumptions. This is done usually by eliminating the coordinate normal to the shell

surface in the development of the two-dimensional shell theories” [42].

A number of theories have arisen and are used for thin homogeneous elastic shells. Leissa’s monograph [11] gives a summary and comparison of shell theories used in vibration of shell. All theories presented in the monograph [11] are considered to be classical shell theories. The linear differential equations of classical shell theories which describe the deformations of a thin elastic shell do not agree generally with each other. They have some differences due to the various assumptions made about the form of small terms and the order of terms which are returned in the analysis. Furthermore, the classical shell theories are based on the Love-Kirchhoff assumptions (or first approximation theory). These assumptions can be itemed as:

- (1) Straight lines normal to the undeformed reference surface remain straight and normal to the deformed reference surface;
- (2) The normal stresses perpendicular to the reference surface can be neglected in the stress-strain relation (plane stress condition in the two-dimensional elasticity);
- (3) The transverse displacement is independent of the thickness coordinate (the transverse normal of the reference surface is inextensible).

“The classical shell theories are expected to yield sufficiently accurate results when (i) the lateral and/or longitudinal dimension, or the radii of curvature-to-thickness ratio is large (thin elastic shell); (ii) the dynamic excitations are within the low-frequency range (in the scope of small deformations); (iii) the material anisotropy (isotropic or orthotropic) is not severe. However, the application of Love-Kirchhoff assumptions based theories to laminated composite shells could lead to errors in deflections, stresses, buckling loads and natural frequencies. These errors are occurred due to the anisotropy and heterogeneity of the materials of different layers and the existence of layers which exhibit weak resistance to transverse shear and normal deformations. A remedy for decreasing errors to some extent is to account for transverse shear deformations in two-dimensional shells theories for the laminated composite shell analysis. As a matter of fact that the experiments have revealed that neglecting transverse shear strains in the modeling leads to underestimations of deflection and overestimates of natural frequencies and buckling loads. In the case of plates and shells made of advanced laminated composite materials such as graphite-epoxy and boron-epoxy, where the ratio of elastic in-plane moduli to transverse shear moduli are very great (i.e., of the order 25-40 instead of 2.6 for isotropic materials), the transverse shear deformation becomes significant. Actually, as pointed out by Koiter [18], refinement of Love-Kirchhoff assumptions based theory, namely classical shell theory, of thin elastic shells is meaningless unless the effects of transverse shear and normal stresses are taken into consideration. Transverse shear deformation plays a very important role in reducing the effective flexural stiffness of anisotropic and laminated plate and shell structures than in corresponding isotropic plate and shell structures”[39]. Therefore, refined shell theories and computational models are developed to predict the response and failure characteristics of anisotropic and laminated

composite shells accurately. “Roughly, they can be splitted into three categories: the three-dimensional elasticity models, the quasi-three-dimensional models, and the two-dimensional shear-flexible models. In the three-dimensional elasticity models, the 15 unknowns (3 displacements, 6 normal and shear stresses, and 6 normal and shear strains) are tried to be found out directly by 15 available equations of elasticity (3 equilibrium equations, 6 stress-strain relations, and 6 strain-displacement relations) without any assumptions whereas in quasi-three-dimensional models, simplifying assumptions are made regarding the stress (or strain) state in the shell (or in the individual layers), but no a priori assumptions are made about the distribution of the different response quantities in the thickness direction. The use of both three-dimensional and quasi-three-dimensional models for predicting the response characteristics of anisotropic and laminated composite shells with complicated geometry is computationally cumbersome; therefore, they are only applied to shells with simple geometries, loading and boundary conditions. On the other hand, the two-dimensional shell theories are adequate and practical for predicting the gross response characteristics such as natural frequencies, buckling loads, and average through-the-thickness displacements and rotations of anisotropic and laminated composite shells. But they are not adequate for the precise accurate prediction of the transverse stresses and deformations. There are four approaches for constructing two-dimensional shell theories for laminated composite shells which can be listed as:

1. Method of hypotheses;
2. Method of expansion;
3. Asymptotic integration technique;
4. Iterative methods and methods of successive corrections.

The first approach is an extension of the Kirchhoff-Love approach and is based on introducing a priori plausible kinematic or static assumptions regarding the variation of displacements, strains and/or stresses in the thickness direction. The simplest of these hypotheses is the linear variation of the displacement components used in conjunction with first-order shear deformation theories. Although the method of hypotheses has the advantages of physical clarity and simplicity of applications, it has the drawback of not providing an estimate of the error in the response predictions.

The second approach is based on a series expansion, in terms of the thickness coordinate for displacements and/or stresses. It also includes the method of initial functions in which the displacements and stresses are expanded in a Taylor series in the thickness coordinate. The relations between the higher-order derivatives of each of the displacements and stresses and their lower-order derivatives are obtained by successive differentiation of the three-dimensional elasticity relations.

In the third approach, appropriate length scales are introduced in the three-dimensional elasticity equations for the different response quantities, followed by parametric (asymptotic) expansions of these quantities in power series in terms of a small thickness parameter. The three-

dimensional elasticity equations are thereby reduced to recursive sets of two-dimensional equations, governing the interior and edge zone responses of the shell. The edge zone (or boundary layer) is produced by self-equilibrated boundary stresses in the thickness direction. The lowest-order system of two-dimensional equations, depending on the choice of the length of scales, corresponds to the thin-shell assumptions. The higher-order systems introduce thickness correction effects in a systematic and consistent manner.

The fourth approach includes various iterative approximations of the three-dimensional elasticity equations, and predictor-corrector procedures based on a single correction or successive corrections of the two-dimensional equations”[32].

This study focuses on a two-dimensional shell theory including shear deformation based on the method of hypotheses in association with the smeared continuum approach. “The smeared continuum approach is defined with the simplifying assumption of laminated anisotropy which is often used in applying two-dimensional theory to plates and shells consisting of layers of composite materials. In this approach, the individual properties of composite constituents, the fibers and the matrix, are “smeared” and thus each lamina is treated as an orthotropic material”[39]. “The two-dimensional laminated composite shell theories including shear deformation vary among themselves due to different assumptions. These different assumptions can be classified such that:

- (1) global through-the-thickness, or piecewise, layer-by-layer, approximations;
- (2) purely kinematic assumptions (on displacements and strains), or a hybrid combination of kinematic and stress assumptions;
- (3) linear or nonlinear, through-the-thickness, variation of the response of quantities;
- (4) including or neglecting the transverse normal strains.

In our computational modeling, we are concerned with the first-order shear deformation theory which is a particular case of global approximation theories. In global approximation theories, global through-the-thickness displacement, strain and/or stress approximations are carried out; and the laminated composite shell is replaced by an equivalent single-layer anisotropic shell”[32].

The equivalent single-layer theories are developed by assuming the form of the displacement field or stress field as a linear combination of unknown functions and the thickness coordinate:

$$\varphi_i(x, y, z, t) = \sum_{j=0}^N (z)^j \varphi_i^j(x, y, t) \quad (2.101)$$

where  $\varphi_i$  is the  $i^{\text{th}}$  component of displacement or stress,  $(x, y)$  are the in-plane coordinates,  $z$  is the

thickness coordinate,  $t$  denotes the time, and  $\varphi_i^j$  are functions to be determined [4].

The following assumptions and considerations are made during the derivation of governing equations using Reissner-Naghdi's thin elastic shell theory for the free vibration analysis of anisotropic

laminated composite, thin, doubly curved shells:

- (1) The shell is considered to be thin when the ratio of the shell thickness to the wavelength of the deformation mode and/or radii of curvature is less than 1/10.
- (2) The thickness is constant throughout the shell.
- (3) The shell undergoes geometrical linear deformation. In other words, all the displacement terms and their derivatives are linear in the kinematic relations.
- (4) There is no change in the temperature of the shell during the analysis (isothermal state).
- (5) The shell is to be linear elastic; namely, there is a one-to-one relation between the state of stress and the state of strain. Thus, the Hooke's Law is applicable.
- (6) The displacements are prescribed with the assumed displacement field using consistent two-dimensional shell theory.
- (7) The system of curvilinear coordinates  $(\xi_1, \xi_2, \zeta)$  is chosen in a manner that at each point the elastically equivalent directions coincide with coordinate directions, noting that, infinitesimally small elements defined at different points of the body by three pairs of coordinate surfaces, being anisotropic possess identical elastic properties.
- (8) The doubly curved shell has mutually orthogonal curvilinear coordinate system. The two of the curvilinear coordinates,  $\xi_1$  and  $\xi_2$  coincides with the orthogonal lines of principal curvature of its reference surface. The third coordinate, the thickness coordinate, is normal to the reference surface at that point.
- (9) The normal stresses perpendicular to the reference surface of the shell are small when compared to other stress so that they can be neglected in the stress-strain relation. This leads to plane stress elasticity problem.
- (10) A linear element normal to the undeformed reference surface undergoes at most a translation and a rotation and suffers no extension. Thus, a linear element normal to the reference surface before deformation remains linear but does not necessarily remain normal to the reference surface after the deformation of the shell. This phenomena results in the inclusion of the shear deformation effects in the formulation whereas this does not exist in the classical shell theory. In addition to shear deformation, the rotary inertias are included in the formulation. In this study, the first-order shear deformation theory is used.
- (11) The assumed displacement field does not satisfy the transverse shear boundary conditions on the top and bottom surfaces of the shell since a constant shear angle through the thickness is assumed, and plane sections remain plane. Therefore, shear correction factors are usually required

for equilibrium consideration. The shear correction factors are only functions of lamination parameters (number of layers, stacking sequence, degree of orthotropy and fiber orientation in each layer).

(12) The transverse normals of the shell are considered to be inextensible. This results in zero transverse normal strain. In other words, the transverse displacement of the shell is independent of the thickness.

(13) The laminated composite shell is replaced by an equivalent single-layer which is statically and dynamically in equilibrium.

(14) The reference surface of the laminated composite doubly curved shell is taken at the middle of the laminate.

(15) An anisotropic body is one which has different values of a material property in different directions at a point; namely, material properties are directionally dependent, the functions of position. In laminated anisotropic shells, the individual layers are, in general, anisotropic and/or orthotropic depending on the fiber orientation angle, and the principal axes of material symmetry of the individual layers coincide with only one of the principal coordinates of the shell (the thickness normal coordinate).

(16) The layers of the lamination are assumed to be perfectly bonded. The perfectly bonding between layers exists when there is no gap or flaw between layers, no lamina can slip relative to another, and the laminate acts as a single lamina with special integrated properties.

(17) The material properties of the equivalent single-layer are constant along  $\xi_1$  and  $\xi_2$  directions, or  $\phi$  and  $\theta$  directions for doubly curved shells or shells of revolution, respectively.

(18) The shell structure is physically linear; that is, there are no discontinuities and complexities such as holes, stiffeners or being crack-free and invariable cross-sectional area in any direction. However, shells with circumferential stiffeners or rings can be considered in the further analysis.

In the following sections, the differential element and the curvilinear coordinate system are defined for doubly curved shells at first. In addition, the expressions studied in the differential geometry section are presented for an arbitrary point on the surface located  $\zeta$  away up to the reference surface in the shell space. Then, the field equations of doubly curved shell are derived. Subsequently, these derived equations are transformed to the governing equations of a shell of revolution.

### 2.5.1 THE COORDINATE SYSTEM AND DIFFERENTIAL ELEMENT OF A SINGLE-LAYER DOUBLY CURVED THIN SHELL AND ITS SURFACE RELATED FEATURES

Figure 2.8 shows the curvilinear coordinate system and differential element of a doubly curved thin shell and its reference surface. Here, the middle surface is chosen as the reference surface of the shell. Let  $\xi_1, \xi_2$  and  $\zeta$  define the mutually orthogonal curvilinear coordinate system. As stated previously, the two of the curvilinear coordinates,  $\xi_1$  and  $\xi_2$  coincides with the orthogonal lines of principal curvature of reference surface of the shell. The third coordinate  $\zeta$ , the thickness coordinate, is normal to the reference surface.

The position vector describing the location of an arbitrary point in the space occupied by the thin doubly curved shell is defined as:

$$\vec{R}(\xi_1, \xi_2, \zeta) = \vec{r}(\xi_1, \xi_2) + \zeta \vec{n}(\xi_1, \xi_2), \quad \xi_1^0 \leq \xi_1 \leq \xi_1^1, \quad \xi_2^0 \leq \xi_2 \leq \xi_2^1 \quad (2.102)$$

where  $\vec{r}$  is the position vector of a corresponding point on the reference surface,  $\vec{n}$  is the unit normal vector from the reference surface to the point, and  $\zeta$  denotes the distance of the point from the corresponding point on reference surface along  $\vec{n}$  and ranges over the local thickness  $h(\xi_1, \xi_2)$ . The quantities  $\xi_1^0, \xi_1^1, \xi_2^0$  and  $\xi_2^1$ , in Equation (2.102), are bounding parametric lines which define, on the reference surface, the extent of the shell.

Inserting Equation (2.102) into Equation (2.17), we find out the magnitude of the distance between two arbitrary points in the shell space.

$$(dS)^2 = d\vec{R} \cdot d\vec{R} = (d\vec{r} + \zeta d\vec{n} + \vec{n} d\zeta) \cdot (d\vec{r} + \zeta d\vec{n} + \vec{n} d\zeta) \quad (2.103)$$

Recalling Equations (2.34) and (2.102) we make the dot product of Equation (2.103) explicitly

$$\begin{aligned} (dS)^2 &= (d\vec{r} \cdot d\vec{r}) + \zeta (d\vec{r} \cdot d\vec{n}) + (d\vec{r} \cdot \vec{n}) d\zeta \\ &+ \zeta (d\vec{n} \cdot d\vec{r}) + \zeta^2 (d\vec{n} \cdot d\vec{n}) + \zeta (d\vec{n} \cdot \vec{n}) d\zeta \\ &+ (\vec{n} \cdot d\vec{r}) d\zeta + \zeta (\vec{n} \cdot d\vec{n}) d\zeta + (\vec{n} \cdot \vec{n}) (d\zeta)^2 \end{aligned} \quad (2.104)$$

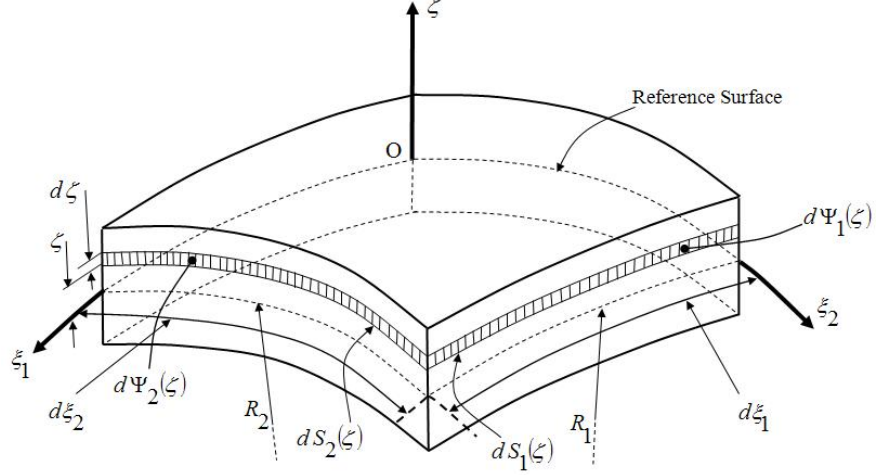


**Figure 2.8** Differential element and coordinate system of a doubly curved thin shell [12].

Incorporating the orthogonality of curvilinear coordinate system, Equations (2.94), (2.48), (2.54), and (2.55) with Equation (2.104) yields

$$\begin{aligned}
(dS)^2 &= \left\{ A_1^2 (d\xi_1)^2 + A_2^2 (d\xi_2)^2 \right\} + \left\{ \zeta \left[ \left( \frac{A_1}{R_1} \bar{t}_1 d\xi_1 + \frac{A_2}{R_2} \bar{t}_2 d\xi_2 \right) \cdot (\bar{t}_1 A_1 d\xi_1 + \bar{t}_2 A_2 d\xi_2) \right] \right\} \\
&+ \left\{ \bar{n} \cdot (\bar{t}_1 A_1 d\xi_1 + \bar{t}_2 A_2 d\xi_2) \right\} d\zeta + \left\{ \zeta \left[ \left( \frac{A_1}{R_1} \bar{t}_1 d\xi_1 + \frac{A_2}{R_2} \bar{t}_2 d\xi_2 \right) \cdot (\bar{t}_1 A_1 d\xi_1 + \bar{t}_2 A_2 d\xi_2) \right] \right\} \\
&+ \left\{ \zeta^2 \left[ \left( \frac{A_1}{R_1} \frac{\bar{r}_1}{A_1} d\xi_1 + \frac{A_2}{R_2} \frac{\bar{r}_2}{A_2} d\xi_2 \right) \cdot \left( \frac{A_1}{R_1} \frac{\bar{r}_1}{A_1} d\xi_1 + \frac{A_2}{R_2} \frac{\bar{r}_2}{A_2} d\xi_2 \right) \right] \right\} \\
&+ \left\{ \zeta \left[ \left( \frac{A_1}{R_1} \bar{t}_1 d\xi_1 + \frac{A_2}{R_2} \bar{t}_2 d\xi_2 \right) \cdot \bar{n} \right] d\zeta \right\} + \left\{ \bar{n} \cdot (\bar{t}_1 A_1 d\xi_1 + \bar{t}_2 A_2 d\xi_2) \right\} d\zeta \\
&+ \left\{ \zeta \left[ \bar{n} \cdot \left( \frac{A_1}{R_1} \bar{t}_1 d\xi_1 + \frac{A_2}{R_2} \bar{t}_2 d\xi_2 \right) \right] d\zeta \right\} + \left\{ (d\zeta)^2 \right\} \\
(dS)^2 &= \left\{ A_1^2 (d\xi_1)^2 + A_2^2 (d\xi_2)^2 \right\} + 2\zeta \left\{ \left( \frac{A_1^2}{R_1} \right) (d\xi_1)^2 + \left( \frac{A_2^2}{R_2} \right) (d\xi_2)^2 \right\} \\
&+ \zeta^2 \left\{ \left( \frac{A_1}{R_1} \right)^2 (d\xi_1)^2 + \left( \frac{A_2}{R_2} \right)^2 (d\xi_2)^2 \right\} + \left\{ (d\zeta)^2 \right\}
\end{aligned} \tag{2.105}$$

Simplifying Equation (2.105) yields

$$(dS)^2 = A_1^2 \left(1 + \frac{\zeta}{R_1}\right)^2 (d\xi_1)^2 + A_2^2 \left(1 + \frac{\zeta}{R_2}\right)^2 (d\xi_2)^2 + (d\zeta)^2 \quad (2.106)$$

Making analogy with the Equation (2.20), the first two terms on the right-hand side of Equation (2.106) can be considered as the first fundamental form of a surface located a distance  $\zeta$  from the reference surface. Let  $\vec{T}_1$  and  $\vec{T}_2$  defining two tangent unit vectors passing through an arbitrary point on that surface. There exists  $\vec{n}$ , the normal unit vector, at that point which is perpendicular to both  $\vec{T}_1$  and  $\vec{T}_2$ . Here,  $\vec{n}, \vec{T}_1$  and  $\vec{T}_2$  are orthogonal to each other. Substituting Equation (2.102) into Equation (2.48), the expressions for  $\vec{n}, \vec{T}_1$  and  $\vec{T}_2$  are given by:

$$\vec{T}_1 = \vec{R}_{,1} / |\vec{R}_{,1}|, \quad \vec{T}_2 = \vec{R}_{,2} / |\vec{R}_{,2}|, \quad \vec{n} = (\vec{T}_1 \times \vec{T}_2) \quad (2.107)$$

where

$$\vec{R}_{,1} = \frac{\partial \vec{R}}{\partial \xi_1} = \vec{r}_{,1} + \zeta \vec{n}_{,1} \quad (2.108)$$

$$\vec{R}_{,2} = \frac{\partial \vec{R}}{\partial \xi_2} = \vec{r}_{,2} + \zeta \vec{n}_{,2} \quad (2.109)$$

and

$$|\vec{R}_{,1}| = [(\vec{R}_{,1}) \cdot (\vec{R}_{,1})]^{1/2} \quad (2.110)$$

$$|\vec{R}_{,2}| = [(\vec{R}_{,2}) \cdot (\vec{R}_{,2})]^{1/2} \quad (2.111)$$

Substituting Equations (2.108) and (2.109) into Equations (2.110) and (2.111), respectively, we get

$$\begin{aligned} |\vec{R}_{,1}| &= [(\vec{r}_{,1} + \zeta \vec{n}_{,1}) \cdot (\vec{r}_{,1} + \zeta \vec{n}_{,1})]^{1/2} \\ |\vec{R}_{,1}| &= [(\vec{r}_{,1}) \cdot (\vec{r}_{,1}) + 2\zeta (\vec{r}_{,1}) \cdot (\vec{n}_{,1}) + \zeta^2 (\vec{n}_{,1}) \cdot (\vec{n}_{,1})]^{1/2} \end{aligned} \quad (2.112)$$

$$\begin{aligned} |\vec{R}_{,2}| &= [(\vec{r}_{,2} + \zeta \vec{n}_{,2}) \cdot (\vec{r}_{,2} + \zeta \vec{n}_{,2})]^{1/2} \\ |\vec{R}_{,2}| &= [(\vec{r}_{,2}) \cdot (\vec{r}_{,2}) + 2\zeta (\vec{r}_{,2}) \cdot (\vec{n}_{,2}) + \zeta^2 (\vec{n}_{,2}) \cdot (\vec{n}_{,2})]^{1/2} \end{aligned} \quad (2.113)$$

Recalling Equations (2.20), (2.48), (2.54) and (2.55), Equations (2.112) and (2.113) become

$$|\vec{R}_{,1}| = \left[ A_1^2 + 2\zeta \frac{A_1^2}{R_1} + \zeta^2 \left( \frac{A_1}{R_1} \right)^2 \right]^{1/2} \quad (2.114)$$

$$|\vec{R}_{,1}| = \left[ A_1^2 \left( 1 + \frac{\zeta}{R_1} \right)^2 \right]^{1/2} = A_1 \left( 1 + \frac{\zeta}{R_1} \right)$$

$$|\vec{R}_{,2}| = \left[ A_2^2 + 2\zeta \frac{A_2^2}{R_2} + \zeta^2 \left( \frac{A_2}{R_2} \right)^2 \right]^{1/2} \quad (2.115)$$

$$|\vec{R}_{,2}| = \left[ A_2^2 \left( 1 + \frac{\zeta}{R_2} \right)^2 \right]^{1/2} = A_2 \left( 1 + \frac{\zeta}{R_2} \right)$$

$\vec{T}_1$  and  $\vec{T}_2$  can be expressed finally as follows:

$$\vec{T}_1 = \frac{1}{A_1 \left( 1 + \frac{\zeta}{R_1} \right)} \vec{R}_{,1} \quad (2.116)$$

$$\vec{T}_2 = \frac{1}{A_2 \left( 1 + \frac{\zeta}{R_2} \right)} \vec{R}_{,2} \quad (2.117)$$

From the Figure 2.8 and the Equation (2.106), the length of the shaded surface whose unit normal is in  $\xi_2$  is

$$dS_1(\zeta) = A_1 \left( 1 + \frac{\zeta}{R_1} \right) d\xi_1 \quad (2.118)$$

and for the one whose unit normal vector is in  $\xi_1$  is given by:

$$dS_2(\zeta) = A_2 \left( 1 + \frac{\zeta}{R_2} \right) d\xi_2 \quad (2.119)$$

The areas of the shaded strips shown in the Figure 2.8 are

$$d\psi_1 = A_1 \left( 1 + \frac{1}{R_1} \right) d\xi_1 d\zeta \quad (2.120)$$

$$d\psi_2 = A_2 \left( 1 + \frac{1}{R_2} \right) d\xi_2 d\zeta \quad (2.121)$$

We presume that the Equation (2.102), the position vector, has continuous second derivatives such that  $\vec{R}_{,12} = \vec{R}_{,21}$ . Inserting Equation (2.116) and (2.117) into that relation, and making necessary manipulations, we obtain

$$(\vec{R}_{,1})_{,2} = (\vec{R}_{,2})_{,1}$$

$$\left[ A_1 \left( 1 + \frac{\zeta}{R_1} \right) \vec{T}_1 \right]_{,2} = \left[ A_2 \left( 1 + \frac{\zeta}{R_2} \right) \vec{T}_2 \right]_{,1} \quad (2.122)$$

$$\left[ A_1 \left( 1 + \frac{\zeta}{R_1} \right) \right]_{,2} \vec{T}_1 + \left[ A_1 \left( 1 + \frac{\zeta}{R_1} \right) \right] \vec{T}_{1,2} = \left[ A_2 \left( 1 + \frac{\zeta}{R_2} \right) \right]_{,1} \vec{T}_2 + \left[ A_2 \left( 1 + \frac{\zeta}{R_2} \right) \right] \vec{T}_{2,1}$$

From Equation (2.122), we obtain two relations which will be used afterwards.

$$\vec{T}_{1,2} = \frac{1}{\left[ A_1 \left( 1 + \frac{\zeta}{R_1} \right) \right]} \left\{ \left[ A_2 \left( 1 + \frac{\zeta}{R_2} \right) \right]_{,1} \vec{T}_2 + \left[ A_2 \left( 1 + \frac{\zeta}{R_2} \right) \right] \vec{T}_{2,1} - \left[ A_1 \left( 1 + \frac{\zeta}{R_1} \right) \right]_{,2} \vec{T}_1 \right\} \quad (2.123)$$

and

$$\vec{T}_{2,1} = \frac{1}{\left[ A_2 \left( 1 + \frac{\zeta}{R_2} \right) \right]} \left\{ \left[ A_1 \left( 1 + \frac{\zeta}{R_1} \right) \right]_{,2} \vec{T}_1 + \left[ A_1 \left( 1 + \frac{\zeta}{R_1} \right) \right] \vec{T}_{1,2} - \left[ A_2 \left( 1 + \frac{\zeta}{R_2} \right) \right]_{,1} \vec{T}_2 \right\} \quad (2.124)$$

To get the derivatives of the normal vector  $\vec{n}$  with respect to  $\xi_1$  and  $\xi_2$  using the position vector  $\vec{R}$ , we follow the same methodology that we used to get Equations (2.54) and (2.55). The derivatives of  $\vec{n}$  with respect to  $\xi_1$  and  $\xi_2$  can be written as:

$$\frac{\vec{n}}{d\xi_1} = \vec{n}_{,1} = \frac{A_1 \left(1 + \frac{\zeta}{R_1}\right)}{R_1 + \zeta} \vec{T}_1 \quad (2.125)$$

$$\frac{\vec{n}}{d\xi_2} = \vec{n}_{,2} = \frac{A_2 \left(1 + \frac{\zeta}{R_2}\right)}{R_2 + \zeta} \vec{T}_2 \quad (2.126)$$

The Codazzi relations using the position vector,  $\vec{R}$ , are found out in a similar procedure which used to derive Equation (2.69). In this perspective,  $\vec{T}_{1,1}, \vec{T}_{1,2}$  are perpendicular to  $\vec{T}_1$  and will therefore lie in the plane formed by  $\vec{T}_2$  and  $\vec{n}$ , and  $\vec{T}_{1,1}$  and  $\vec{T}_{1,2}$  can be expressed one by one in terms of  $\vec{T}_2$  and  $\vec{n}$  as

$$\vec{T}_{1,1} = c_1 \vec{n} + c_2 \vec{T}_2 \quad (2.127)$$

and

$$\vec{T}_{1,2} = c_3 \vec{n} + c_4 \vec{T}_2 \quad (2.128)$$

where  $c_1, c_2$  and  $c_3, c_4$  are unknown projections of  $\vec{T}_{1,1}$  and  $\vec{T}_{1,2}$ , respectively, on  $\vec{n}$  and  $\vec{T}_2$ . Similarly,  $\vec{T}_{2,1}$  and  $\vec{T}_{2,2}$  can be written in terms of  $\vec{T}_1$  and  $\vec{n}$

$$\vec{T}_{2,1} = c_5 \vec{n} + c_6 \vec{T}_1 \quad (2.129)$$

and

$$\vec{T}_{2,2} = c_7 \vec{n} + c_8 \vec{T}_1 \quad (2.130)$$

where  $c_5, c_6$  and  $c_7, c_8$  are unknown projections of  $\vec{T}_{2,1}$  and  $\vec{T}_{2,2}$ , respectively, on  $\vec{n}$  and  $\vec{T}_1$ .

Since  $\vec{T}_1, \vec{T}_2$  and  $\vec{n}$  are orthonormal vectors, the following relations are valid

$$(\vec{T}_1 \cdot \vec{n}) = 0 \quad (2.131)$$

$$\frac{\partial}{\partial \xi_1} (\vec{T}_1 \cdot \vec{n}) = (\vec{T}_1 \cdot \vec{n})_{,1} = \vec{T}_{1,1} \cdot \vec{n} + \vec{T}_1 \cdot \vec{n}_{,1} = 0 \quad (2.132)$$

$$\frac{\partial}{\partial \xi_2} (\vec{T}_1 \cdot \vec{n}) = (\vec{T}_1 \cdot \vec{n})_{,2} = \vec{T}_{1,2} \cdot \vec{n} + \vec{T}_1 \cdot \vec{n}_{,2} = 0 \quad (2.133)$$

$$(\vec{T}_2 \cdot \vec{n}) = 0 \quad (2.134)$$

$$\frac{\partial}{\partial \xi_1} (\vec{T}_2 \cdot \vec{n}) = (\vec{T}_2 \cdot \vec{n})_{,1} = \vec{T}_{2,1} \cdot \vec{n} + \vec{T}_2 \cdot \vec{n}_{,1} = 0 \quad (2.135)$$

$$\frac{\partial}{\partial \xi_2} (\vec{T}_2 \cdot \vec{n}) = (\vec{T}_2 \cdot \vec{n})_{,2} = \vec{T}_{2,2} \cdot \vec{n} + \vec{T}_2 \cdot \vec{n}_{,2} = 0 \quad (2.136)$$

To find the coefficients  $c_1, c_2$ , we multiply both sides of Equations (2.127) with  $\vec{n}$  and  $\vec{T}_2$  one by one. For  $c_3$  and  $c_4$ , both sides of Equation (2.128) are multiplied with  $\vec{n}$  and  $\vec{T}_2$  separately. Note that the orthogonality of unit vectors does exist.

$$\vec{n} \cdot \vec{T}_{1,1} = c_1 (\vec{n} \cdot \vec{n}) + c_2 (\vec{n} \cdot \vec{T}_2) = c_1 \quad (2.137)$$

$$\vec{T}_2 \cdot \vec{T}_{1,1} = c_1 (\vec{T}_2 \cdot \vec{n}) + c_2 (\vec{T}_2 \cdot \vec{T}_2) = c_2 \quad (2.138)$$

and

$$\vec{n} \cdot \vec{T}_{1,2} = c_3 (\vec{n} \cdot \vec{n}) + c_4 (\vec{n} \cdot \vec{T}_2) = c_3 \quad (2.139)$$

$$\vec{T}_2 \cdot \vec{T}_{1,2} = c_3 (\vec{T}_2 \cdot \vec{n}) + c_4 (\vec{T}_2 \cdot \vec{T}_2) = c_4 \quad (2.140)$$

Substituting, Equation (2.125) and Equation (2.132) into Equation (2.137),  $c_1$  become

$$c_1 = -\frac{A_1 \left(1 + \frac{\zeta}{R_1}\right)}{R_1 + \zeta} \quad (2.141)$$

Also, substituting Equation (2.124) into Equation (2.138),  $c_2$  is found to be

$$c_2 = -\frac{1}{A_2 \left(1 + \frac{\zeta}{R_2}\right)} \left\{ \left[ A_1 \left(1 + \frac{\zeta}{R_1}\right) \right]_{,2} \right\} \quad (2.142)$$

The Equation (2.127) is written finally as

$$\vec{T}_{1,1} = \left[ -\frac{A_1 \left(1 + \frac{\zeta}{R_1}\right)}{R_1 + \zeta} \right] \vec{n} + \left[ -\frac{1}{A_2 \left(1 + \frac{\zeta}{R_2}\right)} \left\{ \left[ A_1 \left(1 + \frac{\zeta}{R_1}\right) \right]_{1,2} \right\} \right] \vec{T}_2 \quad (2.143)$$

Substituting, Equation (2.126) and Equation (2.133) into Equation (2.139),  $c_3$  become

$$c_3 = 0 \quad (2.144)$$

Also, substituting Equation (2.123) into Equation (2.140),  $c_4$  is found to be

$$c_4 = \frac{1}{A_1 \left(1 + \frac{\zeta}{R_1}\right)} \left\{ \left[ A_2 \left(1 + \frac{\zeta}{R_2}\right) \right]_{1,1} \right\} \quad (2.145)$$

The Equation (2.128) is written finally as

$$\vec{T}_{1,2} = \left[ \frac{1}{A_1 \left(1 + \frac{\zeta}{R_1}\right)} \left\{ \left[ A_2 \left(1 + \frac{\zeta}{R_2}\right) \right]_{1,1} \right\} \right] \vec{T}_2 \quad (2.146)$$

In a similar manner, the coefficients  $c_5$ , and  $c_6$  are determined by multiplying both sides of Equations (2.129) with  $\vec{n}$  and  $\vec{T}_1$  one by one. For  $c_7$  and  $c_8$ , both sides of Equation (2.130) are multiplied with  $\vec{n}$  and  $\vec{T}_1$  separately. We again keep the orthogonality condition of unit vectors in mind.

$$\vec{n} \cdot \vec{T}_{2,1} = c_5 (\vec{n} \cdot \vec{n}) + c_6 (\vec{n} \cdot \vec{T}_1) = c_5 \quad (2.147)$$

$$\vec{T}_1 \cdot \vec{T}_{2,1} = c_5 (\vec{T}_1 \cdot \vec{n}) + c_6 (\vec{T}_1 \cdot \vec{T}_1) = c_6 \quad (2.148)$$

and

$$\vec{n} \cdot \vec{T}_{2,2} = c_7 (\vec{n} \cdot \vec{n}) + c_8 (\vec{n} \cdot \vec{T}_1) = c_7 \quad (2.149)$$

$$\vec{T}_1 \cdot \vec{T}_{2,2} = c_7 (\vec{T}_1 \cdot \vec{n}) + c_8 (\vec{T}_1 \cdot \vec{T}_1) = c_8 \quad (2.150)$$

Substituting, Equation (2.125) and Equation (2.135) into Equation (2.147),  $c_5$  become

$$c_5 = 0 \quad (2.151)$$

Also, substituting Equation (2.124) into Equation (2.148),  $c_6$  is found to be

$$c_6 = \frac{1}{A_2 \left(1 + \frac{\zeta}{R_2}\right)} \left\{ \left[ A_1 \left(1 + \frac{\zeta}{R_1}\right) \right]_{,2} \right\} \quad (2.152)$$

The Equation (2.129) is written finally as

$$\vec{T}_{2,1} = \left[ \frac{1}{A_2 \left(1 + \frac{\zeta}{R_2}\right)} \left\{ \left[ A_1 \left(1 + \frac{\zeta}{R_1}\right) \right]_{,2} \right\} \right] \vec{T}_1 \quad (2.153)$$

Substituting, Equation (2.126) and Equation (2.136) into Equation (2.149),  $c_7$  become

$$c_7 = - \frac{A_2 \left(1 + \frac{\zeta}{R_2}\right)}{R_2 + \zeta} \quad (2.154)$$

We take the dot product of  $\vec{T}_1$  with  $\vec{T}_2$  and get the derivative of it with respect to  $\xi_2$

$$\left( \vec{T}_1 \cdot \vec{T}_2 \right) = 0 \quad (2.155)$$

$$\left( \vec{T}_1 \cdot \vec{T}_2 \right)_{,2} = \vec{T}_{1,2} \cdot \vec{T}_2 + \vec{T}_1 \cdot \vec{T}_{2,2} = 0 \quad (2.156)$$

Substituting Equations (2.150) and (2.123) into Equation (2.156),  $c_8$  is found to be

$$c_8 = -\frac{1}{A_1 \left(1 + \frac{\zeta}{R_1}\right)} \left\{ \left[ A_2 \left(1 + \frac{\zeta}{R_2}\right) \right]_{,1} \right\} \quad (2.157)$$

The Equation (2.130) is written finally as

$$\vec{T}_{2,2} = \left[ -\frac{A_2 \left(1 + \frac{\zeta}{R_2}\right)}{R_2 + \zeta} \right]_1 \vec{n} + \left[ -\frac{1}{A_1 \left(1 + \frac{\zeta}{R_1}\right)} \left\{ \left[ A_2 \left(1 + \frac{\zeta}{R_2}\right) \right]_{,1} \right\} \right] \vec{T}_1 \quad (2.158)$$

Inserting Equations (2.125) and (2.126) into Equation (2.66) and expanding that

$$\begin{aligned} \left[ \frac{A_1 \left(1 + \frac{\zeta}{R_1}\right)}{R_1 + \zeta} \vec{T}_1 \right]_{,2} &= \left[ \frac{A_2 \left(1 + \frac{\zeta}{R_2}\right)}{R_2 + \zeta} \vec{T}_2 \right]_{,1} \\ \left[ \frac{A_1 \left(1 + \frac{\zeta}{R_1}\right)}{R_1 + \zeta} \right]_{,2} \vec{T}_1 + \vec{T}_{1,2} \left[ \frac{A_1 \left(1 + \frac{\zeta}{R_1}\right)}{R_1 + \zeta} \right] &= \\ \left[ \frac{A_2 \left(1 + \frac{\zeta}{R_2}\right)}{R_2 + \zeta} \right]_{,1} \vec{T}_2 + \vec{T}_{2,1} \left[ \frac{A_2 \left(1 + \frac{\zeta}{R_2}\right)}{R_2 + \zeta} \right] & \end{aligned} \quad (2.159)$$

Substituting Equations (2.146) and (2.153) into Equation (2.159), we get

$$\left[ \frac{A_1 \left( 1 + \frac{\zeta}{R_1} \right)}{R_1 + \zeta} \right]_{,2} \bar{T}_1 + \bar{T}_2 \left[ \frac{1}{A_1 \left( 1 + \frac{\zeta}{R_1} \right)} \left\{ \left[ A_2 \left( 1 + \frac{\zeta}{R_2} \right) \right]_{,1} \right\} \right] \left[ \frac{A_1 \left( 1 + \frac{\zeta}{R_1} \right)}{R_1 + \zeta} \right] =$$

(2.160)

$$\left[ \frac{A_2 \left( 1 + \frac{\zeta}{R_2} \right)}{R_2 + \zeta} \right]_{,1} \bar{T}_2 + \left[ \frac{A_2 \left( 1 + \frac{\zeta}{R_2} \right)}{R_2 + \zeta} \right] \left[ \frac{1}{A_2 \left( 1 + \frac{\zeta}{R_2} \right)} \left\{ \left[ A_1 \left( 1 + \frac{\zeta}{R_1} \right) \right]_{,2} \right\} \right] \bar{T}_1$$

Collecting the coefficients of  $\bar{T}_1$  and  $\bar{T}_2$ , we can write a similar expression like Equation (2.68) to derive the Codazzi condition

$$\left\{ \left[ \frac{A_1 \left( 1 + \frac{\zeta}{R_1} \right)}{R_1 + \zeta} \right]_{,2} - \left[ \frac{1}{R_2 + \zeta} \right] \left[ A_1 \left( 1 + \frac{\zeta}{R_1} \right) \right]_{,2} \right\} \bar{T}_1$$

(2.161)

$$- \left\{ \left[ \frac{1}{R_1 + \zeta} \right] \left[ A_2 \left( 1 + \frac{\zeta}{R_2} \right) \right]_{,1} - \left[ \frac{A_2 \left( 1 + \frac{\zeta}{R_2} \right)}{R_2 + \zeta} \right]_{,1} \right\} \bar{T}_2 = 0$$

The equality in Equation (2.161) holds when the coefficients of  $\bar{T}_1$  and  $\bar{T}_2$  are both zero. Thus, it results in

$$\left[ \frac{A_1 \left( 1 + \frac{\zeta}{R_1} \right)}{R_1 + \zeta} \right]_{,2} = \left[ \frac{1}{R_2 + \zeta} \right] \left[ A_1 \left( 1 + \frac{\zeta}{R_1} \right) \right]_{,2}$$

(2.162)

$$\left[ \frac{1}{R_1 + \zeta} \right] \left[ A_2 \left( 1 + \frac{\zeta}{R_2} \right) \right]_{,1} = \left[ \frac{A_2 \left( 1 + \frac{\zeta}{R_2} \right)}{R_2 + \zeta} \right]_{,1}$$

(2.163)

We substitute the two terms of Equation (2.69) appropriately into Equations (2.162) and (2.163), and make necessary simplifications.

$$\left[ A_1 \left( 1 + \frac{\zeta}{R_1} \right) \right]_{,2} = \left( 1 + \frac{\zeta}{R_2} \right) A_{1,2} \quad (2.164)$$

$$\left[ A_2 \left( 1 + \frac{\zeta}{R_2} \right) \right]_{,1} = \left( 1 + \frac{\zeta}{R_1} \right) A_{2,1} \quad (2.165)$$

The Equations (2.164) and (2.165) are the Codazzi conditions. They will be used in the strain-displacement relations.

## 2.5.2 KINEMATIC RELATIONS OF A LAMINATED COMPOSITE DOUBLY CURVED SHELL

Since the current developed shell theory is a displacement-based approach, the derivation of governing equations is initiated by stating a suitable displacement field. Thus, the displacement field using First Order Shear Deformation Theory is defined with

$$U(\xi_1, \xi_2, \zeta, t) = u^0(\xi_1, \xi_2, t) + \zeta \beta_1(\xi_1, \xi_2, t) \quad (2.166)$$

$$V(\xi_1, \xi_2, \zeta, t) = v^0(\xi_1, \xi_2, t) + \zeta \beta_2(\xi_1, \xi_2, t) \quad (2.167)$$

$$W(\xi_1, \xi_2, \zeta, t) = w^0(\xi_1, \xi_2, t) \quad (2.168)$$

where  $U$ ,  $V$  and  $W$  are the displacements along the  $\xi_1$ ,  $\xi_2$ , and  $\zeta$  coordinates, respectively, and  $t$  is the time variable.  $u^0$ ,  $v^0$  and  $w^0$  denote the displacements of a point on the reference surface of the shell in the  $\xi_1$ ,  $\xi_2$ , and  $\zeta$  directions, respectively.  $\beta_1$  and  $\beta_2$  are the rotations of a transverse normal about the  $\xi_2$ - and  $\xi_1$ - curvilinear coordinates. All these quantities  $(u^0, v^0, w^0, \beta_1, \beta_2)$  are called the generalized displacements. Also,  $u^0$ ,  $v^0$  and  $w^0$  can be expressed as:

$$u^0(\xi_1, \xi_2, t) = U^0(\xi_1, \xi_2) e^{i\omega_m t} \quad (2.169)$$

$$v^0(\xi_1, \xi_2, t) = V^0(\xi_1, \xi_2) e^{i\omega_m t} \quad (2.170)$$

$$\begin{aligned} w^0(\xi_1, \xi_2, t) &= W^0(\xi_1, \xi_2) e^{i\omega_m t}, \\ \beta_1(\xi_1, \xi_2, t) &= \beta_1(\xi_1, \xi_2) e^{i\omega_m t}, \quad \beta_2(\xi_1, \xi_2, t) = \beta_2(\xi_1, \xi_2) e^{i\omega_m t} \end{aligned} \quad (2.171)$$

where  $\omega_m$  is the natural frequency corresponding to the  $m^{\text{th}}$  mode, and  $U^0, V^0, W^0$  are unknown functions to be determined.

The strain-displacement relations by the theory of elasticity in the orthogonal curvilinear coordinate system are expressed as [39]:

$$\varepsilon_i = \frac{\partial}{\partial \alpha_i} \left( \frac{u_i}{\sqrt{g_i}} \right) + \frac{1}{2g_i} \sum_{k=1}^3 \frac{\partial g_i}{\partial \alpha_k} \frac{u_k}{\sqrt{g_k}}, \quad i = 1, 2, 3 \quad (2.172)$$

$$\gamma_{ij} = \frac{1}{\sqrt{g_i g_j}} \left[ g_i \frac{\partial}{\partial \alpha_j} \left( \frac{u_i}{\sqrt{g_i}} \right) + g_j \frac{\partial}{\partial \alpha_i} \left( \frac{u_j}{\sqrt{g_j}} \right) \right], \quad j = 1, 2, 3, \quad i \neq j \quad (2.173)$$

where  $\alpha_{i(\text{or } j)}, u_{i(\text{or } j)}$  and  $g_{i(\text{or } j)}$  are, respectively, the curvilinear coordinates of the geometry, components of the displacement vector and geometrical scale factor quantities. When the Equations (2.172) and (2.173) are applied to shells, the variables in the normal and shearing strain components turn into following:

$$\begin{aligned} \alpha_1 &= \xi_1, \quad \alpha_2 = \xi_2, \quad \alpha_3 = \zeta, \\ u_1 &= U, \quad u_2 = V, \quad u_3 = W, \\ g_1 &= A_1^2 \left( 1 + \frac{\zeta}{R_1} \right)^2, \quad g_2 = A_2^2 \left( 1 + \frac{\zeta}{R_2} \right)^2, \quad g_3 = 1 \end{aligned} \quad (2.174)$$

where  $U, V, W, A_i, R_i$ , and  $\zeta$  are the displacement vector components, Lamé coefficients, the principal radii of curvatures and the thickness coordinate, respectively. Substituting the relations in Equation (2.174) into Equations (2.172) and (2.173), the following strain-displacement relations are obtained in the shell space.

The normal strain components are:

$$\varepsilon_1 = \frac{1}{A_1 \left( 1 + \frac{\zeta}{R_1} \right)} \left( \frac{\partial U}{\partial \xi_1} + \frac{V}{A_2} \frac{\partial A_1}{\partial \xi_2} + \frac{A_1 W}{R_1} \right) \quad (2.175)$$

$$\varepsilon_2 = \frac{1}{A_2 \left( 1 + \frac{\zeta}{R_2} \right)} \left( \frac{\partial V}{\partial \xi_2} + \frac{U}{A_1} \frac{\partial A_2}{\partial \xi_1} + \frac{A_2 W}{R_2} \right) \quad (2.176)$$

$$\varepsilon_\zeta = \frac{\partial W}{\partial \zeta} \quad (2.177)$$

and, the shearing strain components are:

$$\gamma_{12} = \frac{A_2(1+\zeta/R_2)}{A_1(1+\zeta/R_1)} \frac{\partial}{\partial \xi_1} \left[ \frac{V}{A_2(1+\zeta/R_2)} \right] + \frac{A_1(1+\zeta/R_1)}{A_2(1+\zeta/R_2)} \frac{\partial}{\partial \xi_2} \left[ \frac{U}{A_1(1+\zeta/R_1)} \right] \quad (2.178)$$

$$\gamma_{1\zeta} = \frac{1}{A_1(1+\zeta/R_1)} \left[ \frac{\partial W}{\partial \xi_1} + \left[ \frac{\partial U}{\partial \zeta} (A_1(1+\zeta/R_1)) - U \frac{\partial}{\partial \zeta} (A_1(1+\zeta/R_1)) \right] \right] \quad (2.179)$$

$$\gamma_{2\zeta} = \frac{1}{A_2(1+\zeta/R_2)} \left[ \frac{\partial W}{\partial \xi_2} + \left[ \frac{\partial V}{\partial \zeta} (A_2(1+\zeta/R_2)) - V \frac{\partial}{\partial \zeta} (A_2(1+\zeta/R_2)) \right] \right] \quad (2.180)$$

Since the terms  $(\zeta/R_1)$  and  $(\zeta/R_2)$  are assumed to be much less than unity in the Naghdi-Reissner Shell Theory, they are neglected in the Equations (2.175), (2.176), and (2.178). In addition, the first  $(\zeta/R_1)$  and  $(\zeta/R_2)$  terms appearing in Equations (2.179) and (2.180), respectively, are neglected. The strain displacement equations turn into the following

$$\varepsilon_1 = \frac{1}{A_1} \left( \frac{\partial U}{\partial \xi_1} + \frac{V}{A_2} \frac{\partial A_1}{\partial \xi_2} + \frac{A_1 W}{R_1} \right) \quad (2.181)$$

$$\varepsilon_2 = \frac{1}{A_2} \left( \frac{\partial V}{\partial \xi_2} + \frac{U}{A_1} \frac{\partial A_2}{\partial \xi_1} + \frac{A_2 W}{R_2} \right) \quad (2.182)$$

$$\varepsilon_\zeta = \frac{\partial W}{\partial \zeta} \quad (2.183)$$

$$\gamma_{12} = \frac{A_2}{A_1} \frac{\partial}{\partial \xi_1} \left[ \frac{V}{A_2} \right] + \frac{A_1}{A_2} \frac{\partial}{\partial \xi_2} \left[ \frac{U}{A_1} \right] \quad (2.184)$$

$$\gamma_{1\zeta} = \frac{1}{A_1} \left[ \frac{\partial W}{\partial \xi_1} + \left[ \frac{\partial U}{\partial \zeta} (A_1(1+\zeta/R_1)) - U \frac{\partial}{\partial \zeta} (A_1(1+\zeta/R_1)) \right] \right] \quad (2.185)$$

$$\gamma_{2\zeta} = \frac{1}{A_2} \left[ \frac{\partial W}{\partial \xi_2} + \left[ \frac{\partial V}{\partial \zeta} (A_2(1+\zeta/R_2)) - V \frac{\partial}{\partial \zeta} (A_2(1+\zeta/R_2)) \right] \right] \quad (2.186)$$

Equations (2.164), (2.165), (2.166), (2.167) and (2.168) are substituted properly into Equations from (2.181) to (2.186), then the strain displacement relations can be represented as the sum of extensional (or membrane) strains and flexural (or bending) strains.

$$\varepsilon_1 = \varepsilon_1^0 + \zeta \kappa_1 \quad (2.187)$$

$$\varepsilon_2 = \varepsilon_2^0 + \zeta \kappa_2 \quad (2.188)$$

$$\gamma_{12} = (\gamma_1^0 + \gamma_2^0) + \zeta (\tau_1 + \tau_2) = \gamma_{12}^0 + \zeta \kappa_{12} \quad (2.189)$$

$$\gamma_{1\zeta} = \eta_1 \quad (2.190)$$

$$\gamma_{2\zeta} = \eta_2 \quad (2.191)$$

where  $\varepsilon_i^0$ , normal strains of the reference surface are

$$\varepsilon_1^0 = \frac{1}{A_1} \frac{\partial u^0}{\partial \xi_1} + \frac{v^0}{A_1 A_2} \frac{\partial A_1}{\partial \xi_2} + \frac{w^0}{R_1} \quad (2.192)$$

$$\varepsilon_2^0 = \frac{1}{A_2} \frac{\partial v^0}{\partial \xi_2} + \frac{u^0}{A_1 A_2} \frac{\partial A_2}{\partial \xi_1} + \frac{w^0}{R_2} \quad (2.193)$$

$\kappa_i$ , the curvature changes of the reference surface are

$$\kappa_1 = \frac{1}{A_1} \frac{\partial \beta_1}{\partial \xi_1} + \frac{\beta_2}{A_1 A_2} \frac{\partial A_1}{\partial \xi_2} \quad (2.194)$$

$$\kappa_2 = \frac{1}{A_2} \frac{\partial \beta_2}{\partial \xi_2} + \frac{\beta_1}{A_1 A_2} \frac{\partial A_2}{\partial \xi_1} \quad (2.195)$$

$\gamma_i^0$ , shearing strains of the reference surface are

$$\gamma_1^0 = \frac{1}{A_1} \frac{\partial v^0}{\partial \xi_1} - \frac{u^0}{A_1 A_2} \frac{\partial A_1}{\partial \xi_2} \quad (2.196)$$

$$\gamma_2^0 = \frac{1}{A_2} \frac{\partial u^0}{\partial \xi_2} - \frac{v^0}{A_1 A_2} \frac{\partial A_2}{\partial \xi_1} \quad (2.197)$$

$\tau_i$ , the twist changes of the reference surface are

$$\tau_1 = \frac{1}{A_1} \frac{\partial \beta_2}{\partial \xi_1} - \frac{\beta_1}{A_1 A_2} \frac{\partial A_1}{\partial \xi_2} \quad (2.198)$$

$$\tau_2 = \frac{1}{A_2} \frac{\partial \beta_1}{\partial \xi_2} - \frac{\beta_2}{A_1 A_2} \frac{\partial A_2}{\partial \xi_1} \quad (2.199)$$

and, finally,  $\eta_i$ , the transverse shear strains are

$$\eta_1 = \frac{1}{A_1} \frac{\partial w^0}{\partial \xi_1} - \frac{u^0}{R_1} + \beta_1 \quad (2.200)$$

$$\eta_2 = \frac{1}{A_2} \frac{\partial w^0}{\partial \xi_2} - \frac{v^0}{R_2} + \beta_2 \quad (2.201)$$

It is seen throughout the present section that the kinematic relations are independent of the material of the shell. In other words, the defined displacement field and the strain-displacement relations are valid for isotropic, orthotropic and/or anisotropic shell configurations.

### 2.5.3 CONSTITUTIVE RELATIONS OF AN ANISOTROPIC LAMINATED COMPOSITE DOUBLY CURVED SHELL

After determining governing equations for the state of deformation in the previous section, the constitutive relations; viz. force and moment resultants will be examined in this section.

In general, the stress-strain relation for a linear elastic material is given in tensor (uncontracted) notation as [4]

$$\sigma_{ij} = C_{ijkl} \epsilon_{kl} \quad (2.202)$$

$i, j = 1-3 \text{ and } k, l = 1-3$

where  $\sigma_{ij}$ ,  $\epsilon_{kl}$ ,  $C_{ijkl}$  are the Cauchy stress components ( $\sigma_{11}, \sigma_{22}, \sigma_{33}, \sigma_{23}, \sigma_{32}, \sigma_{31}, \sigma_{13}, \sigma_{12}, \sigma_{21}$ ), are the infinitesimal strain components ( $\epsilon_{11}, \epsilon_{22}, \epsilon_{33}, \epsilon_{23}, \epsilon_{32}, \epsilon_{31}, \epsilon_{13}, \epsilon_{12}, \epsilon_{21}$ ), and are the material coefficients or stiffness tensor, respectively. It is seen that  $C_{ijkl}$  has 81 components; however, there exist only 36 independent elastic coefficients due to the symmetry of both  $\sigma_{ij}$  and  $\epsilon_{kl}$ .

Equation (2.202) can be expressed in the contracted notation for the stress-strain relations or generalized Hooke's Law:

$$\begin{aligned}\sigma_i &= C_{ij}\varepsilon_j \\ i, j &= 1-6\end{aligned}\tag{2.203}$$

or

$$\begin{Bmatrix} \sigma_1 \\ \sigma_2 \\ \sigma_3 \\ \sigma_4 \\ \sigma_5 \\ \sigma_6 \end{Bmatrix} = \begin{bmatrix} C_{11} & C_{12} & C_{13} & C_{14} & C_{15} & C_{16} \\ C_{21} & C_{22} & C_{23} & C_{24} & C_{25} & C_{26} \\ C_{31} & C_{32} & C_{33} & C_{34} & C_{35} & C_{36} \\ C_{41} & C_{42} & C_{43} & C_{44} & C_{45} & C_{46} \\ C_{51} & C_{52} & C_{53} & C_{54} & C_{55} & C_{56} \\ C_{61} & C_{62} & C_{63} & C_{64} & C_{65} & C_{66} \end{bmatrix} \begin{Bmatrix} \varepsilon_1 \\ \varepsilon_2 \\ \varepsilon_3 \\ \varepsilon_4 \\ \varepsilon_5 \\ \varepsilon_6 \end{Bmatrix}\tag{2.204}$$

where  $C_{ij}$  are the elastic constants, and are obtained from  $C_{ijkl}$  by the following change of subscripts:

$$11 \rightarrow 1, \quad 22 \rightarrow 2, \quad 33 \rightarrow 3, \quad 23 \rightarrow 4, \quad 13 \rightarrow 5, \quad 12 \rightarrow 6$$

and the stress tensor

$$\sigma_1 = \sigma_{11}, \quad \sigma_2 = \sigma_{22}, \quad \sigma_3 = \sigma_{33}, \quad \sigma_4 = \sigma_{23}, \quad \sigma_5 = \sigma_{13}, \quad \sigma_6 = \sigma_{12}$$

and the strain tensor

$$\varepsilon_1 = \varepsilon_{11}, \quad \varepsilon_2 = \varepsilon_{22}, \quad \varepsilon_3 = \varepsilon_{33}, \quad \varepsilon_4 = \varepsilon_{23}, \quad \varepsilon_5 = \varepsilon_{13}, \quad \varepsilon_6 = \varepsilon_{12}$$

The resulting  $C_{ij}$  are also symmetric,  $C_{ij} = C_{ji}$ ; therefore, there are only 21 independent coefficients of the matrix  $[C]$ .

The shell configuration in this thesis is considered to be laminated composite which is made of layers of fiber-reinforced lamina. A lamina or ply represents the basic building block of a composite laminate, and a fiber-reinforced lamina consists of many unidirectional fibers embedded in a matrix material. Unidirectional fiber-reinforced lamina exhibits the highest strength and modulus in the direction of the fibers, but it has very low strength and modulus in the direction transverse to the fibers. It should be noted that the individual properties of the composite constituents, the continuous fibers and the matrix, are smeared and thus each lamina can be treated as an orthotropic material. This assumption is often used in the application of the two-dimensional shell theory to shells having layers of composite materials. Since the orthotropic material has three orthogonal planes of material symmetry, the number of independent elastic coefficients in the Equation (2.204) is reduced to 9. As a

result, the stress-strain relations for orthotropic materials can be written in the form of

$$\begin{Bmatrix} \sigma_1 \\ \sigma_2 \\ \sigma_3 \\ \sigma_4 \\ \sigma_5 \\ \sigma_6 \end{Bmatrix} = \begin{bmatrix} C_{11} & C_{12} & C_{13} & 0 & 0 & 0 \\ C_{21} & C_{22} & C_{23} & 0 & 0 & 0 \\ C_{31} & C_{32} & C_{33} & 0 & 0 & 0 \\ 0 & 0 & 0 & C_{44} & 0 & 0 \\ 0 & 0 & 0 & 0 & C_{55} & 0 \\ 0 & 0 & 0 & 0 & 0 & C_{66} \end{bmatrix} \begin{Bmatrix} \varepsilon_1 \\ \varepsilon_2 \\ \varepsilon_3 \\ \varepsilon_4 \\ \varepsilon_5 \\ \varepsilon_6 \end{Bmatrix} \quad (2.205)$$

The elastic coefficients in the stiffness matrix  $C_{ij}$  in Equation (2.205) in terms of the engineering constants  $E_i$ ,  $\nu_{ij}$ , and  $G_{ij}$  are [39]

$$\begin{aligned} C_{11} &= \frac{E_1(1-\nu_{23}\nu_{32})}{\Delta}, & C_{12} &= \frac{E_1(\nu_{21}+\nu_{31}\nu_{23})}{\Delta} = \frac{E_2(\nu_{12}+\nu_{32}\nu_{13})}{\Delta}, \\ C_{13} &= \frac{E_1(\nu_{31}+\nu_{21}\nu_{32})}{\Delta} = \frac{E_3(\nu_{13}+\nu_{12}\nu_{23})}{\Delta}, & C_{22} &= \frac{E_2(1-\nu_{13}\nu_{31})}{\Delta}, \\ C_{23} &= \frac{E_2(\nu_{32}+\nu_{12}\nu_{31})}{\Delta} = \frac{E_3(\nu_{23}+\nu_{21}\nu_{13})}{\Delta}, & C_{33} &= \frac{E_3(1-\nu_{12}\nu_{21})}{\Delta}, \\ C_{44} &= G_{23}, & C_{55} &= G_{13}, & C_{66} &= G_{12}, \\ \Delta &= 1-\nu_{12}\nu_{21}-\nu_{23}\nu_{32}-\nu_{31}\nu_{13}-2\nu_{21}\nu_{32}\nu_{13} \end{aligned} \quad (2.206)$$

where  $E_1, E_2, E_3$  are Young's moduli in 1, 2, and 3 directions, respectively,  $\nu_{ij}$  is Poisson's ratio defined as ratio of transverse strain in the  $j^{\text{th}}$  direction to the axial strain in the  $i^{\text{th}}$  direction, when stressed in the  $i$ -direction  $-\varepsilon_j/\varepsilon_i$  (for  $\sigma_i = \sigma$  and all other stresses are zero) ( $i, j=1,2,3$ ), and  $G_{23}, G_{13}, G_{12}$  are shear moduli in the 2-3, 1-3, and 1-2 planes, respectively. Due to fact that the normal stress is assumed to be negligible in the present computational model, the plane stress state is prevailed in the stress-strain relations of the lamina. Accordingly, the linear Hooke's Law according to plane stress state is given by

$$\begin{Bmatrix} \sigma_1 \\ \sigma_2 \\ \sigma_6 \end{Bmatrix} = \begin{bmatrix} Q_{11} & Q_{12} & 0 \\ Q_{12} & Q_{22} & 0 \\ 0 & 0 & Q_{66} \end{bmatrix} \begin{Bmatrix} \varepsilon_1 \\ \varepsilon_2 \\ \varepsilon_6 \end{Bmatrix} \quad (2.207)$$

and

$$\begin{Bmatrix} \sigma_4 \\ \sigma_5 \end{Bmatrix} = \begin{bmatrix} Q_{44} & 0 \\ 0 & Q_{55} \end{bmatrix} \begin{Bmatrix} \varepsilon_4 \\ \varepsilon_5 \end{Bmatrix} \quad (2.208)$$

where the  $Q_{ij}$  are the reduced stiffnesses, and are written in terms of engineering constants

$$Q_{11} = \frac{E_1}{1 - \nu_{12}\nu_{21}}, \quad Q_{12} = \frac{\nu_{12}E_2}{1 - \nu_{12}\nu_{21}}, \quad Q_{22} = \frac{E_2}{1 - \nu_{12}\nu_{21}}, \quad (2.209)$$

$$Q_{66} = G_{12}, \quad Q_{44} = G_{23}, \quad Q_{55} = G_{13}$$

Let's consider a small element of a lamina of constant thickness  $h$ , in which the principal material axes are denoted as 1, 2, and 3; that is, 1, also called longitudinal, direction is parallel to the fibers, 2, also called transverse, direction is perpendicular to it and 3, also called thickness, direction is normal to the plane formed by 1 and 2. Further, consider this lamina specimen is a part of the shell configuration which has geometric axes of  $\xi_1, \xi_2$  and  $\zeta$ . This consideration is shown in the Figure 2.9. If the principal material coordinate system of a lamina coincides with the shell coordinate system, shown in the Figure 2.9a, this kind of lamina is known to be specially orthotropic lamina. In laminated composites, each layer of the laminate may not actually get the principal material directions to coincide with the shell coordinates. Actually, each lamina in the laminate may be located with different orientation of their principal material directions with respect to the shell coordinates. The difference in orientation between the principal material directions and the shell coordinates is called the orientation angle,  $\alpha$ , and it is measured in counter-clockwise direction from the shell coordinates to the principal material coordinates. The lamina, shown in the Figure 2.9b, is called generally orthotropic lamina when the orientation angle is different than zero.

When there is an angle,  $\alpha$ , between the shell coordinates and the principal material coordinates, the stress-strain relations for Specially Orthotropic Lamina given by Equations (2.207) and (2.208) are transformed into ones for Generally Orthotropic Lamina.

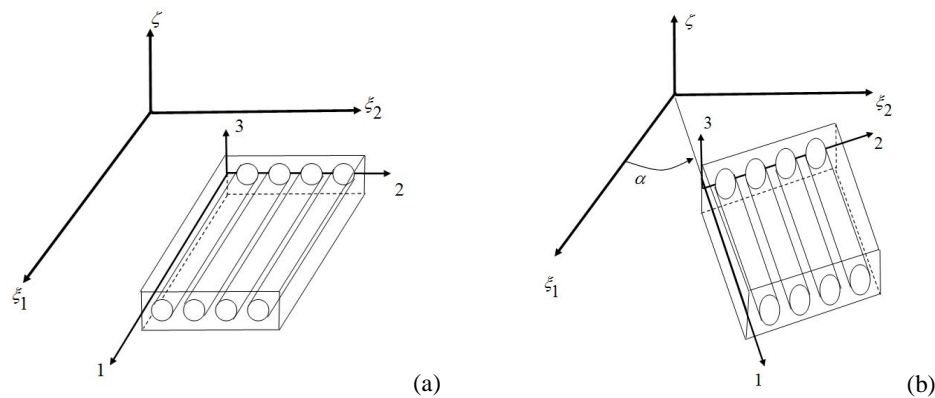


**Figure 2.9** (a) Specially Orthotropic Lamina, (b) Generally Orthotropic Lamina.

$$\begin{Bmatrix} \sigma_1 \\ \sigma_2 \\ \sigma_6 \end{Bmatrix} = \begin{bmatrix} \bar{Q}_{11} & \bar{Q}_{12} & \bar{Q}_{16} \\ \bar{Q}_{12} & \bar{Q}_{22} & \bar{Q}_{26} \\ \bar{Q}_{16} & \bar{Q}_{26} & \bar{Q}_{66} \end{bmatrix} \begin{Bmatrix} \varepsilon_1 \\ \varepsilon_2 \\ \varepsilon_6 \end{Bmatrix} \quad (2.210)$$

$$\begin{Bmatrix} \sigma_4 \\ \sigma_5 \end{Bmatrix} = \begin{bmatrix} \bar{Q}_{44} & \bar{Q}_{45} \\ \bar{Q}_{45} & \bar{Q}_{55} \end{bmatrix} \begin{Bmatrix} \varepsilon_4 \\ \varepsilon_5 \end{Bmatrix} \quad (2.211)$$

where the coefficients of the transformed reduced stiffness,  $\bar{Q}_{ij}$ , are [4]

$$\begin{aligned} \bar{Q}_{11} &= Q_{11} \cos^4 \alpha + 2(Q_{12} + 2Q_{66}) \sin^2 \alpha \cos^2 \alpha + Q_{22} \sin^4 \alpha \\ \bar{Q}_{12} &= (Q_{11} + Q_{22} - 4Q_{66}) \sin^2 \alpha \cos^2 \alpha + Q_{12} (\sin^4 \alpha + \cos^4 \alpha) \\ \bar{Q}_{16} &= (Q_{11} - Q_{12} - 2Q_{66}) \sin \alpha \cos^3 \alpha + (Q_{12} - Q_{22} + 2Q_{66}) \sin^3 \alpha \cos \alpha \\ \bar{Q}_{22} &= Q_{11} \sin^4 \alpha + 2(Q_{12} + 2Q_{66}) \sin^2 \alpha \cos^2 \alpha + Q_{22} \cos^4 \alpha \\ \bar{Q}_{26} &= (Q_{11} - Q_{12} - 2Q_{66}) \sin^3 \alpha \cos \alpha + (Q_{12} - Q_{22} + 2Q_{66}) \sin \alpha \cos^3 \alpha \\ \bar{Q}_{66} &= (Q_{11} + Q_{22} - 2Q_{12} - 2Q_{66}) \sin^2 \alpha \cos^2 \alpha + Q_{66} (\sin^4 \alpha + \cos^4 \alpha) \\ \bar{Q}_{44} &= Q_{44} \cos^2 \alpha + Q_{55} \sin^2 \alpha \\ \bar{Q}_{45} &= (Q_{55} - Q_{44}) \sin \alpha \cos \alpha \\ \bar{Q}_{55} &= Q_{55} \cos^2 \alpha + Q_{44} \sin^2 \alpha \end{aligned} \quad (2.212)$$

with  $\alpha$  being the rotation angle measured from the lamina body or shell coordinates to the lamina principal material coordinates.

The transformation of stresses and strains between the shell coordinates and the principal material coordinates is done by using the following relations.

$$\begin{Bmatrix} \sigma_{\xi_1} \\ \sigma_{\xi_2} \\ \tau_{\xi_1 \xi_2} \end{Bmatrix} = [T_1]^T \begin{Bmatrix} \sigma_1 \\ \sigma_2 \\ \sigma_6 \end{Bmatrix} [T_1] \quad (2.213)$$

$$\begin{Bmatrix} \tau_{\xi_2 \zeta} \\ \tau_{\xi_1 \zeta} \end{Bmatrix} = [T_2]^T \begin{Bmatrix} \sigma_4 \\ \sigma_5 \end{Bmatrix} [T_2] \quad (2.214)$$

and

$$\begin{Bmatrix} \varepsilon_{\xi_1} \\ \varepsilon_{\xi_2} \\ \gamma_{\xi_1 \xi_2} \end{Bmatrix} = [T_1]^T \begin{Bmatrix} \varepsilon_1 \\ \varepsilon_2 \\ \varepsilon_6 \end{Bmatrix} [T_1] \quad (2.215)$$

$$\begin{Bmatrix} \gamma_{\xi_1 \zeta} \\ \gamma_{\xi_2 \zeta} \end{Bmatrix} = [T_2]^T \begin{Bmatrix} \varepsilon_4 \\ \varepsilon_5 \end{Bmatrix} [T_2] \quad (2.216)$$

where  $\{\sigma_1, \sigma_2, \sigma_6\}^T$ ,  $\{\sigma_4, \sigma_5\}^T$ ,  $\{\sigma_{\xi_1}, \sigma_{\xi_2}, \tau_{\xi_1 \xi_2}\}^T$ , and  $\{\tau_{\xi_1 \zeta}, \tau_{\xi_2 \zeta}\}^T$  are the material in-plane stresses, the material transverse stresses, the shell in-plane stresses and the shell transverse stresses, respectively. In addition,  $\{\varepsilon_1, \varepsilon_2, \varepsilon_6\}^T$ ,  $\{\varepsilon_4, \varepsilon_5\}^T$ ,  $\{\varepsilon_{\xi_1}, \varepsilon_{\xi_2}, \gamma_{\xi_1 \xi_2}\}^T$ , and  $\{\gamma_{\xi_1 \zeta}, \gamma_{\xi_2 \zeta}\}^T$  are the material in-plane strains, the material transverse strains, the shell in-plane strains and the shell transverse strains, respectively.  $[T_1]$  and  $[T_2]$  are transformation matrices obtained from the direction cosines and are written as

$$[T_1] = \begin{bmatrix} \cos \alpha & \sin \alpha & 0 \\ -\sin \alpha & \cos \alpha & 0 \\ 0 & 0 & \cos \alpha \end{bmatrix} \quad (2.217)$$

$$[T_2] = \begin{bmatrix} \cos \alpha & \sin \alpha \\ \sin \alpha & \cos \alpha \end{bmatrix} \quad (2.218)$$

where  $\alpha = 0$ .

The figure 2.10 shows the internal stresses on a single layer doubly curved shell element. The internal stresses are in their positive directions. Due to defined displacement field by Equations (2.166), (2.167), and (2.168), the displacements are determined to vary linearly through the thickness of the lamina. In order to obtain a two-dimensional shell theory like the present computational model, it will be convenient to introduce statically equivalent forces and moments instead of internal stresses. Forces and moments acting on the edges of the shell element shown in the Figure 2.10 can be derived by integration of the stresses over the thickness. It can be shown that the stresses are known functions of thickness coordinate,  $\zeta$ , if we substitute displacement field into strain-displacement relations, then the strains into stress using Hooke's Law. As a result, the introduction of stress resultants and moment resultants permits the elimination of  $\zeta$  coordinate in the equilibrium equations to assure two-dimensional computational model. The reference surface is taken at the middle surface of the laminate.

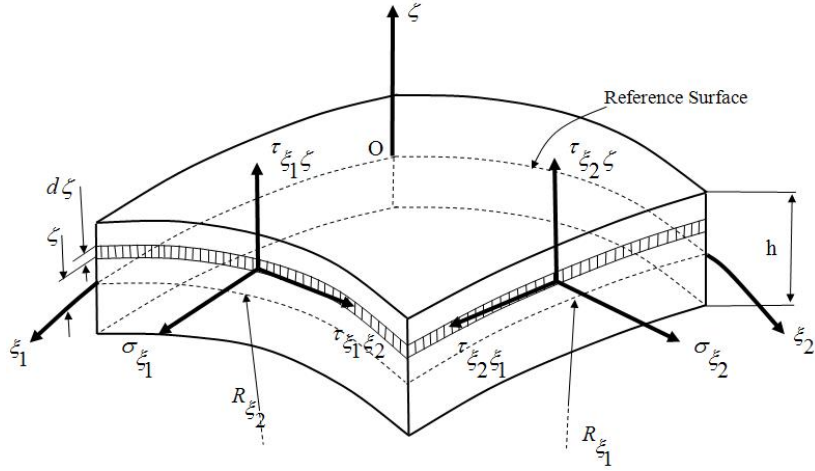


**Figure 2.10** Internal Stresses on a Doubly Curved Shell Element

The normal and shear force resultants acting on the face perpendicular to the  $\xi_1$  coordinate are given by

$$N_{\xi_1} = \int_{-h/2}^{h/2} \left\{ \sigma_{\xi_1}^{\zeta} \right\} \left( 1 + \frac{\zeta}{R_{\xi_2}^{\zeta}} \right) d\zeta \quad (2.219)$$

$$N_{\xi_1 \xi_2} = \int_{-h/2}^{h/2} \left\{ \tau_{\xi_1 \xi_2}^{\zeta} \right\} \left( 1 + \frac{\zeta}{R_{\xi_2}^{\zeta}} \right) d\zeta \quad (2.220)$$

$$Q_{\xi_1} = \int_{-h/2}^{h/2} \left\{ \tau_{\xi_1 \zeta} \right\} \left( 1 + \frac{\zeta}{R_{\xi_2}^{\zeta}} \right) d\zeta \quad (2.221)$$

and the normal and shear force resultants acting on the face perpendicular to the  $\xi_2$  coordinate are given by

$$N_{\xi_2} = \int_{-h/2}^{h/2} \left\{ \sigma_{\xi_2}^{\zeta} \right\} \left( 1 + \frac{\zeta}{R_{\xi_1}^{\zeta}} \right) d\zeta \quad (2.222)$$

$$N_{\xi_2 \xi_1} = \int_{-h/2}^{h/2} \left\{ \tau_{\xi_2 \xi_1}^{\zeta} \right\} \left( 1 + \frac{\zeta}{R_{\xi_1}^{\zeta}} \right) d\zeta \quad (2.223)$$

$$Q_{\xi_2} = \int_{-h/2}^{h/2} \left\{ \tau_{\xi_2 \zeta} \right\} \left( 1 + \frac{\zeta}{R_{\xi_1}^{\zeta}} \right) d\zeta \quad (2.224)$$

The force resultants acting on the reference surface are shown in Figure 2.11. These forces act at the reference surface and have units of force/length (N/m).

Similarly, the bending and twisting moment resultants having unit surface normals in the  $\xi_1$ -direction are

$$M_{\xi_1} = \int_{-h/2}^{h/2} \left\{ \sigma_{\xi_1} \right\} \left( 1 + \frac{\zeta}{R_{\xi_2}} \right) \zeta d\zeta \quad (2.225)$$

$$M_{\xi_1 \xi_2} = \int_{-h/2}^{h/2} \left\{ \tau_{\xi_1 \xi_2} \right\} \left( 1 + \frac{\zeta}{R_{\xi_2}} \right) \zeta d\zeta \quad (2.226)$$

and the bending and twisting moment resultants having unit surface normals in the  $\xi_2$ -direction are

$$M_{\xi_2} = \int_{-h/2}^{h/2} \left\{ \sigma_{\xi_2} \right\} \left( 1 + \frac{\zeta}{R_{\xi_1}} \right) \zeta d\zeta \quad (2.227)$$

$$M_{\xi_2 \xi_1} = \int_{-h/2}^{h/2} \left\{ \tau_{\xi_2 \xi_1} \right\} \left( 1 + \frac{\zeta}{R_{\xi_1}} \right) \zeta d\zeta \quad (2.228)$$

Also, the moment resultants acting on the reference surface are shown in Figure 2.12. They have dimensions of moment/length (Nm/m). Note that even though  $\tau_{\xi_1 \xi_2} = \tau_{\xi_2 \xi_1}$  from the symmetry of the stress tensor, the same does not hold for stress and moment resultants;  $N_{\xi_1 \xi_2} \neq N_{\xi_2 \xi_1}$  &  $M_{\xi_1 \xi_2} \neq M_{\xi_2 \xi_1}$ , unless  $R_{\xi_1} = R_{\xi_2}$  because the areas over which the stresses  $\tau_{\xi_1 \xi_2}$ ,  $\tau_{\xi_2 \xi_1}$  act are different on the different edges of the shell elements shown in the Figure 2.10. The expressions for force and moments resultants when Reissner's shell theory are obtained by neglecting  $\zeta/R_{\xi_1}$  and  $\zeta/R_{\xi_2}$  in comparison to unity. Therefore, for Reissner's shell theory,  $N_{\xi_1 \xi_2} = N_{\xi_2 \xi_1}$  and  $M_{\xi_1 \xi_2} = M_{\xi_2 \xi_1}$ .

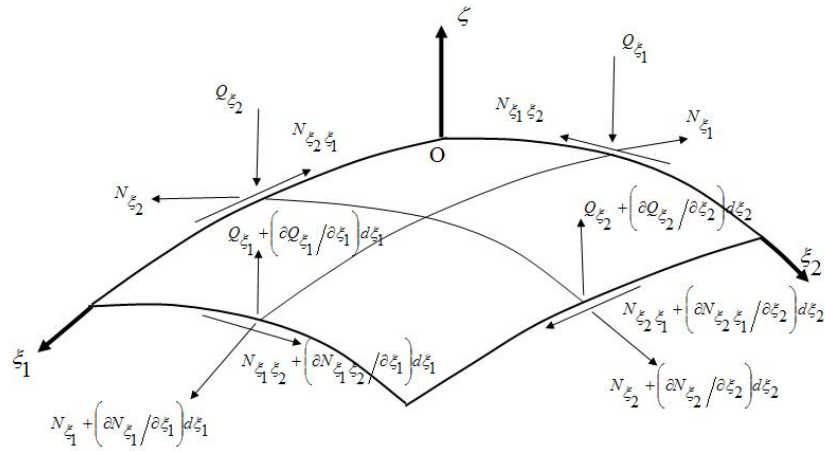


**Figure 2.11** Force resultants in the shell coordinates.

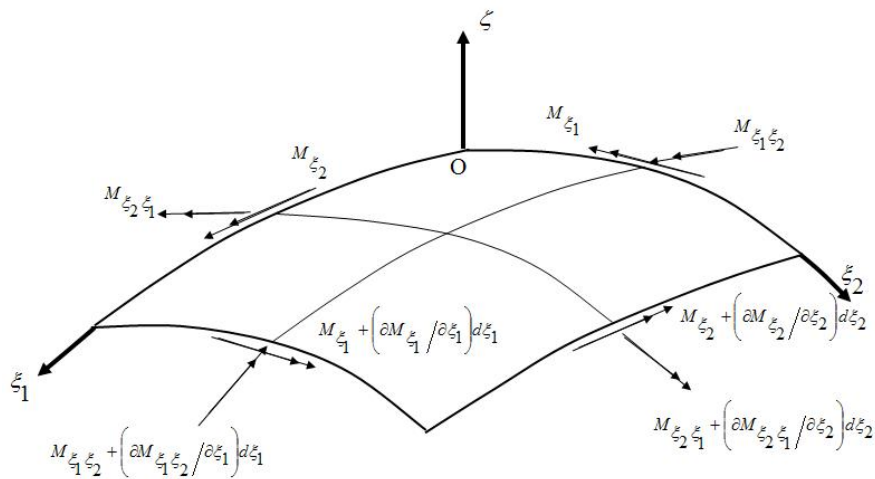


**Figure 2.12** Moment resultants in the shell coordinates.

A laminate of doubly curved shell element is shown in Figure 2.13. For a laminated shell, the stress components can be integrated across each lamina, then must be added together. In the lamination, laminae are assumed to be bonded perfectly to each other so that the displacements are continuous across the laminate. However, since each lamina might have different elastic moduli, the stresses will be discontinuous across the interface of two laminae.

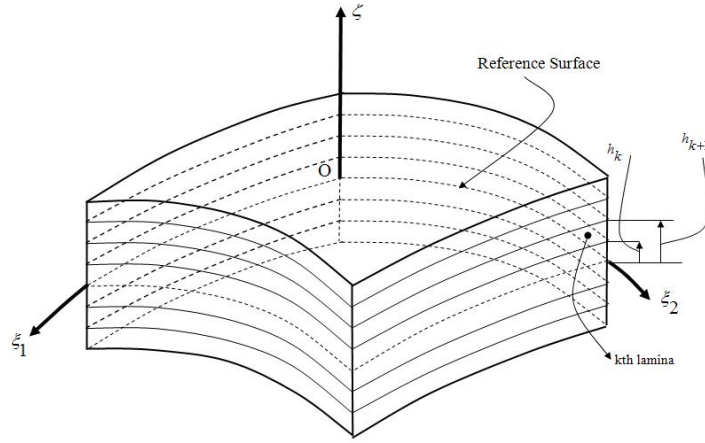


**Figure 2.13** N-layered laminate of a doubly curved shell element.

Since the transverse shear strains are represented as constant through the laminate thickness due to the assumed displacement field, it follows that the transverse shear stresses will also be constant. The constant transverse shear stresses do not satisfy the transverse shear boundary conditions on the top and bottom surfaces of the shell. However, it is well known from elementary theory of beams that the transverse shear stress varies parabolically through the beam thickness and is zero at the top and bottom surfaces. Accordingly, the following continuous function  $f(\zeta)$  [8] is used as a weighting function in order to provide the parabolic distribution of the transverse shear stresses throughout the thickness of the laminated composite shell and their top and bottom surface boundary conditions.

$$f(\zeta) = \frac{5}{4} \left[ 1 - \left( \frac{\zeta}{h/2} \right)^2 \right] \quad (2.229)$$

It should be noted that the coefficient (5/4) in the Equation (2.229) can be called the shear correction factor and it is consistent with the established shear factor from previous work of Reissner and Mindlin for isotropic case.

Consequently, the normal and shear resultants for the complete laminate of N-layers using Reissner's shell theory are given by

$$N_{\xi_1} = \sum_{k=1}^N \int_{h_k}^{h_{k+1}} \{ \sigma_{\xi_1}^{\zeta} \} d\zeta \quad (2.230)$$

$$N_{\xi_2} = \sum_{k=1}^N \int_{h_k}^{h_{k+1}} \{\sigma_{\xi_2}\} d\zeta \quad (2.231)$$

$$N_{\xi_1 \xi_2} = N_{\xi_2 \xi_1} = \sum_{k=1}^N \int_{h_k}^{h_{k+1}} \{\tau_{\xi_1 \xi_2}\} d\zeta \quad (2.232)$$

$$Q_{\xi_1} = \sum_{k=1}^N \int_{h_k}^{h_{k+1}} \{\tau_{\xi_1 \zeta}\} f(\zeta) d\zeta \quad (2.233)$$

$$Q_{\xi_2} = \sum_{k=1}^N \int_{h_k}^{h_{k+1}} \{\tau_{\xi_2 \zeta}\} f(\zeta) d\zeta \quad (2.234)$$

$$M_{\xi_1} = \sum_{k=1}^N \int_{h_k}^{h_{k+1}} \{\sigma_{\xi_1}\} \zeta d\zeta \quad (2.235)$$

$$M_{\xi_2} = \sum_{k=1}^N \int_{h_k}^{h_{k+1}} \{\sigma_{\xi_2}\} \zeta d\zeta \quad (2.236)$$

$$M_{\xi_1 \xi_2} = M_{\xi_2 \xi_1} = \sum_{k=1}^N \int_{h_k}^{h_{k+1}} \{\tau_{\xi_1 \xi_2}\} \zeta d\zeta \quad (2.237)$$

Combining Equations (2.187) to (2.191), (2.210), (2.211), (2.213) to (2.216) with Equations (2.230) to (2.37) and making necessary changes for the some subscripts, we obtain the expressions for the force and moments resultants as

$$\begin{Bmatrix} N_{\xi_1} \\ N_{\xi_2} \\ N_{\xi_1 \xi_2} \end{Bmatrix} = \sum_{k=1}^N \begin{bmatrix} \bar{Q}_{11} & \bar{Q}_{12} & \bar{Q}_{16} \\ \bar{Q}_{12} & \bar{Q}_{22} & \bar{Q}_{26} \\ \bar{Q}_{16} & \bar{Q}_{26} & \bar{Q}_{66} \end{bmatrix}_k \left\{ \int_{h_k}^{h_{k+1}} \begin{Bmatrix} \epsilon_{\xi_1}^0 \\ \epsilon_{\xi_2}^0 \\ \gamma_{\xi_1 \xi_2}^0 \end{Bmatrix} d\zeta + \int_{h_k}^{h_{k+1}} \begin{Bmatrix} \kappa_{\xi_1} \\ \kappa_{\xi_2} \\ \kappa_{\xi_1 \xi_2} \end{Bmatrix} \zeta d\zeta \right\} \quad (2.238)$$

$$\begin{Bmatrix} M_{\xi_1} \\ M_{\xi_2} \\ M_{\xi_1 \xi_2} \end{Bmatrix} = \sum_{k=1}^N \begin{bmatrix} \bar{Q}_{11} & \bar{Q}_{12} & \bar{Q}_{16} \\ \bar{Q}_{12} & \bar{Q}_{22} & \bar{Q}_{26} \\ \bar{Q}_{16} & \bar{Q}_{26} & \bar{Q}_{66} \end{bmatrix}_k \left\{ \int_{h_k}^{h_{k+1}} \begin{Bmatrix} \epsilon_{\xi_1}^0 \\ \epsilon_{\xi_2}^0 \\ \gamma_{\xi_1 \xi_2}^0 \end{Bmatrix} \zeta d\zeta + \int_{h_k}^{h_{k+1}} \begin{Bmatrix} \kappa_{\xi_1} \\ \kappa_{\xi_2} \\ \kappa_{\xi_1 \xi_2} \end{Bmatrix} \zeta^2 d\zeta \right\} \quad (2.239)$$

$$\begin{Bmatrix} Q_{\xi_2} \\ Q_{\xi_1} \end{Bmatrix} = \sum_{k=1}^N \begin{bmatrix} \bar{Q}_{44} & \bar{Q}_{45} \\ \bar{Q}_{45} & \bar{Q}_{55} \end{bmatrix}_k \left\{ \int_{h_k}^{h_{k+1}} \begin{Bmatrix} \eta_{\xi_2} \\ \eta_{\xi_1} \end{Bmatrix} \left( \frac{5}{4} \right) \left[ 1 - \left( \frac{\zeta}{h/2} \right)^2 \right] d\zeta \right\} \quad (2.240)$$

As a result, the constitutive equations for the anisotropic laminated composite doubly curved shell are

$$\begin{Bmatrix} N_{\xi_1} \\ N_{\xi_2} \\ N_{\xi_1 \xi_2} \\ M_{\xi_1} \\ M_{\xi_2} \\ M_{\xi_1 \xi_2} \end{Bmatrix} = \begin{bmatrix} A_{11} & A_{12} & A_{16} & B_{11} & B_{12} & B_{16} \\ A_{12} & A_{22} & A_{26} & B_{12} & B_{22} & B_{26} \\ A_{16} & A_{26} & A_{66} & B_{16} & B_{26} & B_{66} \\ B_{11} & B_{12} & B_{16} & D_{11} & D_{12} & D_{16} \\ B_{12} & B_{22} & B_{26} & D_{12} & D_{22} & D_{26} \\ B_{16} & B_{26} & B_{66} & D_{16} & D_{26} & D_{66} \end{bmatrix} \begin{Bmatrix} \varepsilon_{\xi_1}^0 \\ \varepsilon_{\xi_2}^0 \\ \gamma_{\xi_1 \xi_2}^0 \\ \kappa_{\xi_1} \\ \kappa_{\xi_2} \\ \kappa_{\xi_1 \xi_2} \end{Bmatrix} \quad (2.241)$$

and

$$\begin{Bmatrix} Q_{\xi_2} \\ Q_{\xi_1} \end{Bmatrix} = \begin{bmatrix} As_{44} & As_{45} \\ As_{45} & As_{55} \end{bmatrix} \begin{Bmatrix} \eta_{\xi_2} \\ \eta_{\xi_1} \end{Bmatrix} \quad (2.242)$$

where  $A_{ij}$ , the extensional stiffness matrix which relates the in-plane stress resultants to the reference surface strains, are given by

$$A_{ij} = \sum_{k=1}^N (\bar{Q}_{ij})_k (h_{k+1} - h_k), \quad i, j = 1, 2, 6 \quad (2.243)$$

and  $B_{ij}$ , the bending-stretching coupling matrix which relates the in-plane stress resultants and bending and twisting moment resultants to curvature and twist changes of the reference surface, respectively, are given by

$$B_{ij} = \left( \frac{1}{2} \right) \sum_{k=1}^N (\bar{Q}_{ij})_k (h_{k+1}^2 - h_k^2), \quad i, j = 1, 2, 6 \quad (2.244)$$

and  $D_{ij}$ , bending stiffness matrix which relates the bending and twisting moments to curvature and twist changes of the reference surface, are given by

$$D_{ij} = \left( \frac{1}{3} \right) \sum_{k=1}^N (\bar{Q}_{ij})_k (h_{k+1}^3 - h_k^3), \quad i, j = 1, 2, 6 \quad (2.245)$$

and  $As_{ij}$ , transverse shear stiffness matrix which relates the transverse shear resultants to transverse shear strains, are given by

$$As_{ij} = \frac{5}{4} \sum_{k=1}^N (\bar{Q}_{ij})_k \left[ h_{k+1} - h_k - \frac{4}{3} \left[ h_{k+1}^3 - h_k^3 \right] \frac{1}{h^2} \right], \quad i, j = 4, 5 \quad (2.246)$$

The presence of each term in the  $A_{ij}, B_{ij}, D_{ij}, As_{ij}$  stiffness matrices result in different types of deformation couplings in the anisotropic laminated composite shell with orthotropic symmetry in each lamina.

Extension-shear couplings take place when the elements  $A_{16}, A_{26}$  are not zero, in-plane normal force resultants  $N_{\xi_1}, N_{\xi_2}$  cause shear deformation  $\gamma_{\xi_1 \xi_2}^0$ , and a shear (or twist) force resultant  $N_{\xi_1 \xi_2}$  causes elongations in the  $\xi_1$  and  $\xi_2$  directions.

Bending-twist coupling takes place when the elements  $D_{16}, D_{26}$  are not zero, bending moment resultants  $M_{\xi_1}, M_{\xi_2}$  cause the twist of the laminate  $\kappa_{\xi_1 \xi_2}$ , and a twist moment resultant  $M_{\xi_1 \xi_2}$  causes curvatures in the  $\xi_1 - \zeta$  and  $\xi_2 - \zeta$  planes, namely  $\kappa_{\xi_1}$  and  $\kappa_{\xi_2}$ .

Extension-twist and bending-shear coupling exist when the elements  $B_{16}, B_{26}$  are not zero, in-plane normal force resultants  $N_{\xi_1}, N_{\xi_2}$  cause twist  $\kappa_{\xi_1 \xi_2}$ , and bending moment resultants  $M_{\xi_1}, M_{\xi_2}$  result in in-plane shear deformation  $\gamma_{\xi_1 \xi_2}^0$ .

In-plane—out-of-plane coupling exists when the elements  $B_{ij}$  are not zero, in-plane force resultants  $N_{\xi_1}, N_{\xi_2}, N_{\xi_1 \xi_2}$  cause out-of-plane deformations (curvatures), namely  $\kappa_{\xi_1}, \kappa_{\xi_2}, \kappa_{\xi_1 \xi_2}$ , of the laminate, and moment resultants  $M_{\xi_1}, M_{\xi_2}, M_{\xi_1 \xi_2}$  cause in-plane deformations, that is  $\epsilon_{\xi_1}^0, \epsilon_{\xi_2}^0, \gamma_{\xi_1 \xi_2}^0$ , in the  $\xi_1 - \xi_2$  plane.

The preceding four types of coupling are characteristic of composite materials and do not occur in homogeneous isotropic materials. The following two couplings occur in both composite and isotropic materials.

Extension-extension coupling happen when the element  $A_{12}$  is not zero, a normal force resultant  $N_{\xi_1}$  causes elongation in the  $\xi_2$  direction  $\epsilon_{\xi_2}^0$ , and a normal force resultant  $N_{\xi_2}$  causes elongation in the  $\xi_1$  direction  $\epsilon_{\xi_1}^0$ .

Bending-bending coupling occurs when the element  $D_{12}$  is not zero, a bending moment resultant  $M_{\xi_1}$  causes curvatures of the laminate in the  $\xi_2 - \zeta$  plane  $\kappa_{\xi_2}$ , and a bending moment

resultant  $M_{\xi_2}$  causes curvature of the laminate in the  $\xi_1$ - $\zeta$  plane  $\kappa_{\xi_1}$ .

#### 2.5.4 EQUATIONS OF MOTION OF AN ANISOTROPIC LAMINATED COMPOSITE DOUBLY CURVED SHELL

The last set of the governing equations for free vibration analysis of anisotropic laminated composite doubly curved shell is obtained in the present section. For this purpose, the Hamilton's Principle is used to derive the equations of motion and the corresponding boundary conditions. The Hamilton Principle can be written as

$$\delta \int_{t_0}^{t_1} (K - \Pi) dt = 0 \quad (2.247)$$

where  $\Pi$  is known as the total potential energy and is given by

$$\Pi = U - U_{ABR} - U_{DL} \quad (2.248)$$

and  $K$  is called the kinetic energy of the elastic body and is given by

$$K = \frac{1}{2} \int_V \rho (\dot{\vec{U}} \cdot \dot{\vec{U}}) dV \quad (2.249)$$

where  $\dot{\vec{U}}$  is described as the displacement vector at equilibrium, and obtained by adding the described displacement field given in Equations (2.166) to (2.168).

$$\dot{\vec{U}} = \dot{U} + \dot{V} + \dot{W} = (\dot{u}^0 + \zeta \dot{\beta}_{\xi_1}) \vec{i}_{\xi_1} + (\dot{v}^0 + \zeta \dot{\beta}_{\xi_2}) \vec{i}_{\xi_2} + (\dot{w}^0) \vec{i}_{\zeta} \quad (2.250)$$

and

$$dV = A_{\xi_1} A_{\xi_2} \left(1 + \zeta/R_{\xi_1}\right) \left(1 + \zeta/R_{\xi_2}\right) d\xi_1 d\xi_2 d\zeta \quad (2.251)$$

The kinetic energy  $K$  can be written explicitly as

$$K = \frac{1}{2} \int_{\xi_1} \int_{\xi_2} \int_{\zeta} \sum_{k=1}^N \rho_k \left[ (\dot{u}^0 + \zeta \dot{\beta}_{\xi_1})^2 + (\dot{v}^0 + \zeta \dot{\beta}_{\xi_2})^2 + (\dot{w}^0)^2 \right] A_{\xi_1} A_{\xi_2} \left(1 + \zeta/R_{\xi_1}\right) \left(1 + \zeta/R_{\xi_2}\right) d\xi_1 d\xi_2 d\zeta \quad (2.252)$$

Neglecting the terms  $\left(1 + \zeta/R_{\xi_1}\right)$  and  $\left(1 + \zeta/R_{\xi_2}\right)$  in comparison to unity yields

$$K = \frac{1}{2} \sum_{k=1}^N \int_{\xi_1} \int_{\xi_2} \int_{\zeta} \rho_k \left\{ \begin{aligned} & \left[ (\dot{u}^0)^2 + (\dot{v}^0)^2 + (\dot{w}^0)^2 + 2\zeta \left[ (\dot{u}^0)(\dot{\beta}_{\xi_1}) + (\dot{v}^0)(\dot{\beta}_{\xi_2}) \right] \right] \\ & + \zeta^2 \left[ (\dot{\beta}_{\xi_1})^2 + (\dot{\beta}_{\xi_2})^2 \right] \end{aligned} \right\} A_{\xi_1} A_{\xi_2} d\xi_1 d\xi_2 d\zeta \quad (2.253)$$

If we take the middle surface of the shell laminate as the reference surface, the integration in the  $\zeta$ , thickness, direction is done from  $-h/2$  to  $h/2$ ,  $K$  turns out to be

$$K = \frac{1}{2} \rho h \int_{\xi_1} \int_{\xi_2} \left\{ (\dot{u}^0)^2 + (\dot{v}^0)^2 + (\dot{w}^0)^2 + \frac{h^2}{12} \left[ (\dot{\beta}_{\xi_1})^2 + (\dot{\beta}_{\xi_2})^2 \right] \right\} A_{\xi_1} A_{\xi_2} d\xi_1 d\xi_2 \quad (2.254)$$

where  $\rho$  is the overall density of the composite laminate, and given by

$$\rho = \sum_{k=1}^N \int_{h_k}^{h_{k+1}} \rho_k d\zeta \quad (2.255)$$

The second term of Equation (2.247) can be written as follows

$$\delta \int_{t_0}^{t_1} K dt = \int_{t_0}^{t_1} \delta K dt \quad (2.256)$$

Taking variation of Equation (2.254)

$$\delta K = \rho h \int_{t_0}^{t_1} \int_{\xi_1} \int_{\xi_2} \left\{ \begin{aligned} & \left[ (\dot{u}^0)(\delta \dot{u}^0) + (\dot{v}^0)(\delta \dot{v}^0) + (\dot{w}^0)(\delta \dot{w}^0) \right] \\ & + \frac{h^2}{12} \left[ (\dot{\beta}_{\xi_1})(\delta \dot{\beta}_{\xi_1}) + (\dot{\beta}_{\xi_2})(\delta \dot{\beta}_{\xi_2}) \right] \end{aligned} \right\} A_{\xi_1} A_{\xi_2} d\xi_1 d\xi_2 dt \quad (2.257)$$

Applying integration by parts to the first term on the right hand side of Equation (2.257)

$$\begin{aligned} \rho h \int_{t_0}^{t_1} \int_{\xi_1} \int_{\xi_2} (\dot{u}^0)(\delta \dot{u}^0) A_{\xi_1} A_{\xi_2} d\xi_1 d\xi_2 dt &= \rho h \int_{\xi_1} \int_{\xi_2} \left[ (\dot{u}^0)(\delta u^0) \right]_{t=t_0}^{t=t_1} A_{\xi_1} A_{\xi_2} d\xi_1 d\xi_2 \\ &\quad - \rho h \int_{t_0}^{t_1} \int_{\xi_1} \int_{\xi_2} (\ddot{u}^0)(\delta u^0) A_{\xi_1} A_{\xi_2} d\xi_1 d\xi_2 dt \end{aligned} \quad (2.258)$$

Since the variational displacements and rotations at  $t = t_0$  and  $t = t_1$  are zero, the Equation

(2.258) turns out to be

$$\rho h \int_{t_0}^{t_1} \iint_{\xi_1 \xi_2} (\dot{u}^0) (\delta \dot{u}^0) A_{\xi_1} A_{\xi_2} d\xi_1 d\xi_2 dt = -\rho h \int_{t_0}^{t_1} \iint_{\xi_1 \xi_2} (\ddot{u}^0) (\delta u^0) A_{\xi_1} A_{\xi_2} d\xi_1 d\xi_2 dt \quad (2.259)$$

Similarly applying the same procedure to the remaining terms of Equation (2.257),  $\delta K$  becomes

$$\int_{t_0}^{t_1} \delta K dt = -\rho h \int_{t_0}^{t_1} \iint_{\xi_1 \xi_2} \left\{ (\ddot{u}^0) (\delta u^0) + (\ddot{v}^0) (\delta v^0) + (\ddot{w}^0) (\delta w^0) \right. \\ \left. + \frac{h^2}{12} [(\ddot{\beta}_{\xi_1}) (\delta \beta_{\xi_1}) + (\ddot{\beta}_{\xi_2}) (\delta \beta_{\xi_2})] \right\} A_{\xi_1} A_{\xi_2} d\xi_1 d\xi_2 dt \quad (2.260)$$

In Equation (2.248), the terms  $U$ ,  $U_{ABR}$ , and  $U_{DL}$  is described as the strain energy, the energy input to the shell due to the applied boundary resultant, and the energy input due to the distributed loading applied on the surface of the shell, respectively. In this study, it is assumed that there are no applied boundary resultants and distributed loading. Hence, there is only strain energy left in the total potential energy expression.  $U$ , the strain energy of the shell is defined in terms of a strain energy density function  $P$  as:

$$U = \int_V P dV \quad (2.261)$$

where

$$P = \frac{1}{2} [\sigma_{\xi_1} \varepsilon_{\xi_1} + \sigma_{\xi_2} \varepsilon_{\xi_2} + \sigma_{\zeta} \varepsilon_{\zeta} + \tau_{\xi_1 \xi_2} \gamma_{\xi_1 \xi_2} + \tau_{\xi_1 \zeta} \gamma_{\xi_1 \zeta} + \tau_{\xi_2 \zeta} \gamma_{\xi_2 \zeta}] \quad (2.262)$$

The variation of the strain energy is

$$\delta U = \iiint_{\xi_1 \xi_2 \zeta} \delta P A_{\xi_1} A_{\xi_2} d\xi_1 d\xi_2 d\zeta \quad (2.263)$$

The variation of the strain energy function is given by

$$\delta P = \frac{\partial P}{\partial \varepsilon_{\xi_1}} \delta \varepsilon_{\xi_1} + \frac{\partial P}{\partial \varepsilon_{\xi_2}} \delta \varepsilon_{\xi_2} + \frac{\partial P}{\partial \varepsilon_{\zeta}} \delta \varepsilon_{\zeta} + \frac{\partial P}{\partial \gamma_{\xi_1 \xi_2}} \delta \gamma_{\xi_1 \xi_2} + \frac{\partial P}{\partial \gamma_{\xi_1 \zeta}} \delta \gamma_{\xi_1 \zeta} + \frac{\partial P}{\partial \gamma_{\xi_2 \zeta}} \delta \gamma_{\xi_2 \zeta} \quad (2.264)$$

It can be shown from the definition of the strain energy function  $P$  that

$$\sigma_{ij} = \frac{\partial P}{\partial \varepsilon_{ij}} \quad (2.265)$$

As a result,

$$\delta P = \sigma_{\xi_1} \delta \varepsilon_{\xi_1} + \sigma_{\xi_2} \delta \varepsilon_{\xi_2} + \sigma_{\zeta} \delta \varepsilon_{\zeta} + \tau_{\xi_1 \xi_2} \delta \gamma_{\xi_1 \xi_2} + \tau_{\xi_1 \zeta} \delta \gamma_{\xi_1 \zeta} + \tau_{\xi_2 \zeta} \delta \gamma_{\xi_2 \zeta} \quad (2.266)$$

Since  $\sigma_{\zeta}$  is assumed to be negligible when compared to other stresses, Equation (2.266) is written as

$$\delta P = \sigma_{\xi_1} \delta \varepsilon_{\xi_1} + \sigma_{\xi_2} \delta \varepsilon_{\xi_2} + \tau_{\xi_1 \xi_2} \delta \gamma_{\xi_1 \xi_2} + \tau_{\xi_1 \zeta} \delta \gamma_{\xi_1 \zeta} + \tau_{\xi_2 \zeta} \delta \gamma_{\xi_2 \zeta} \quad (2.267)$$

Thus, the expression for the variation of the strain energy takes the form

$$\delta U = \iiint_{\xi_1 \xi_2 \zeta} (\sigma_{\xi_1} \delta \varepsilon_{\xi_1} + \sigma_{\xi_2} \delta \varepsilon_{\xi_2} + \tau_{\xi_1 \xi_2} \delta \gamma_{\xi_1 \xi_2} + \tau_{\xi_1 \zeta} \delta \gamma_{\xi_1 \zeta} + \tau_{\xi_2 \zeta} \delta \gamma_{\xi_2 \zeta}) A_{\xi_1} A_{\xi_2} d\xi_1 d\xi_2 d\zeta \quad (2.268)$$

Substituting the strain-displacement relations, (2.187) to (2.191) into Equation (2.268) yields

$$\int_{t_0}^{t_1} \iiint_{\xi_1 \xi_2 \zeta} \left\{ \begin{aligned} & \sigma_{\xi_1} \delta \left[ \frac{1}{A_{\xi_1}} \frac{\partial u^0}{\partial \xi_1} + \frac{v^0}{A_{\xi_1} A_{\xi_2}} \frac{\partial A_{\xi_1}}{\partial \xi_2} + \frac{w^0}{R_{\xi_1}} \right] + \sigma_{\xi_2} \delta \left[ \frac{1}{A_{\xi_2}} \frac{\partial v^0}{\partial \xi_2} + \frac{u^0}{A_{\xi_1} A_{\xi_2}} \frac{\partial A_{\xi_2}}{\partial \xi_1} + \frac{w^0}{R_{\xi_2}} \right] \\ & + \zeta \left( \frac{1}{A_{\xi_1}} \frac{\partial \beta_{\xi_1}}{\partial \xi_1} + \frac{\beta_{\xi_2}}{A_{\xi_1} A_{\xi_2}} \frac{\partial A_{\xi_1}}{\partial \xi_2} \right) \left[ \frac{1}{A_{\xi_1}} \frac{\partial v^0}{\partial \xi_1} - \frac{u^0}{A_{\xi_1} A_{\xi_2}} \frac{\partial A_{\xi_1}}{\partial \xi_2} + \frac{1}{A_{\xi_2}} \frac{\partial u^0}{\partial \xi_2} - \frac{v^0}{A_{\xi_1} A_{\xi_2}} \frac{\partial A_{\xi_2}}{\partial \xi_1} \right] \\ & + \zeta \left( \frac{1}{A_{\xi_1}} \frac{\partial \beta_{\xi_2}}{\partial \xi_1} - \frac{\beta_{\xi_1}}{A_{\xi_1} A_{\xi_2}} \frac{\partial A_{\xi_1}}{\partial \xi_2} \right) \left[ \frac{1}{A_{\xi_1}} \frac{\partial v^0}{\partial \xi_1} - \frac{u^0}{A_{\xi_1} A_{\xi_2}} \frac{\partial A_{\xi_1}}{\partial \xi_2} + \frac{1}{A_{\xi_2}} \frac{\partial u^0}{\partial \xi_2} - \frac{v^0}{A_{\xi_1} A_{\xi_2}} \frac{\partial A_{\xi_2}}{\partial \xi_1} \right] \\ & + \zeta \left( \frac{1}{A_{\xi_2}} \frac{\partial \beta_{\xi_1}}{\partial \xi_2} - \frac{\beta_{\xi_2}}{A_{\xi_1} A_{\xi_2}} \frac{\partial A_{\xi_2}}{\partial \xi_1} \right) \left[ \frac{1}{A_{\xi_1}} \frac{\partial v^0}{\partial \xi_1} - \frac{u^0}{A_{\xi_1} A_{\xi_2}} \frac{\partial A_{\xi_1}}{\partial \xi_2} + \frac{1}{A_{\xi_2}} \frac{\partial u^0}{\partial \xi_2} - \frac{v^0}{A_{\xi_1} A_{\xi_2}} \frac{\partial A_{\xi_2}}{\partial \xi_1} \right] \\ & + \tau_{\xi_1 \xi_2} \delta \left[ \frac{1}{A_{\xi_1}} \frac{\partial w^0}{\partial \xi_1} - \frac{u^0}{R_{\xi_1}} + \beta_{\xi_1} \right] + \tau_{\xi_2 \zeta} \delta \left[ \frac{1}{A_{\xi_2}} \frac{\partial w^0}{\partial \xi_2} - \frac{u^0}{R_{\xi_2}} + \beta_{\xi_2} \right] \end{aligned} \right\} d\xi_1 d\xi_2 d\zeta dt \quad (2.269)$$

Combining the constitutive equations (2.230) to (2.237) with Equation (2.269) and taking variation and whenever necessary applying the integration by parts, the Equation (2.247) results in

$$\begin{aligned}
& \int_{t_0}^{t_1} \int_{\xi_1} \int_{\xi_2} (-1) \left[ \begin{aligned}
& \left[ -\frac{\partial(N_{\xi_1}^{\xi} A_{\xi_2}^{\xi})}{\partial \xi_1} + N_{\xi_2}^{\xi} \frac{\partial A_{\xi_2}^{\xi}}{\partial \xi_1} - N_{\xi_1 \xi_2}^{\xi} \frac{\partial A_{\xi_1}^{\xi}}{\partial \xi_2} - \frac{\partial(N_{\xi_1 \xi_2}^{\xi} A_{\xi_1}^{\xi})}{\partial \xi_2} - Q_{\xi_1}^{\xi} \frac{A_{\xi_1}^{\xi} A_{\xi_2}^{\xi}}{R_{\xi_1}^{\xi}} \right] \delta u^0 \\
& + \rho h A_{\xi_1}^{\xi} A_{\xi_2}^{\xi} \ddot{u}^0 \\
& \left[ N_{\xi_1}^{\xi} \frac{\partial A_{\xi_1}^{\xi}}{\partial \xi_2} - \frac{\partial(N_{\xi_2}^{\xi} A_{\xi_1}^{\xi})}{\partial \xi_2} - \frac{\partial(N_{\xi_1 \xi_2}^{\xi} A_{\xi_2}^{\xi})}{\partial \xi_1} - N_{\xi_1 \xi_2}^{\xi} \frac{\partial(A_{\xi_2}^{\xi})}{\partial \xi_1} - Q_{\xi_2}^{\xi} \frac{A_{\xi_1}^{\xi} A_{\xi_2}^{\xi}}{R_{\xi_2}^{\xi}} \right] \delta v^0 \\
& + \rho h A_{\xi_1}^{\xi} A_{\xi_2}^{\xi} \ddot{v}^0 \\
& \left[ N_{\xi_1}^{\xi} \frac{A_{\xi_1}^{\xi} A_{\xi_2}^{\xi}}{R_{\xi_1}^{\xi}} + N_{\xi_2}^{\xi} \frac{A_{\xi_1}^{\xi} A_{\xi_2}^{\xi}}{R_{\xi_2}^{\xi}} - \frac{\partial(Q_{\xi_1}^{\xi} A_{\xi_2}^{\xi})}{\partial \xi_1} - \frac{\partial(Q_{\xi_2}^{\xi} A_{\xi_1}^{\xi})}{\partial \xi_2} + \rho h A_{\xi_1}^{\xi} A_{\xi_2}^{\xi} \ddot{w}^0 \right] \delta w^0 \\
& \left[ -\frac{\partial(M_{\xi_1}^{\xi} A_{\xi_2}^{\xi})}{\partial \xi_1} + M_{\xi_2}^{\xi} \frac{\partial A_{\xi_2}^{\xi}}{\partial \xi_1} - M_{\xi_1 \xi_2}^{\xi} \frac{\partial A_{\xi_1}^{\xi}}{\partial \xi_2} - \frac{\partial(M_{\xi_1 \xi_2}^{\xi} A_{\xi_1}^{\xi})}{\partial \xi_2} + Q_{\xi_1}^{\xi} A_{\xi_1}^{\xi} A_{\xi_2}^{\xi} \right] \delta \beta_{\xi_1} \\
& + \rho \frac{h^3}{12} A_{\xi_1}^{\xi} A_{\xi_2}^{\xi} \ddot{\beta}_{\xi_1} \\
& \left[ M_{\xi_1}^{\xi} \frac{\partial A_{\xi_2}^{\xi}}{\partial \xi_1} - \frac{\partial(M_{\xi_2}^{\xi} A_{\xi_1}^{\xi})}{\partial \xi_2} - \frac{\partial(M_{\xi_1 \xi_2}^{\xi} A_{\xi_2}^{\xi})}{\partial \xi_1} - M_{\xi_1 \xi_2}^{\xi} \frac{\partial A_{\xi_2}^{\xi}}{\partial \xi_1} + Q_{\xi_2}^{\xi} A_{\xi_1}^{\xi} A_{\xi_2}^{\xi} \right] \delta \beta_{\xi_2} \\
& + \rho \frac{h^3}{12} A_{\xi_1}^{\xi} A_{\xi_2}^{\xi} \ddot{\beta}_{\xi_2}
\end{aligned} \right] d\xi_1 d\xi_2 dt \\
& + \int_{t_0}^{t_1} \int_{\xi_1} [N_{\xi_2}^{\xi} \delta v^0 + M_{\xi_2}^{\xi} \delta \beta_{\xi_2} + N_{\xi_1 \xi_2}^{\xi} \delta u^0 + M_{\xi_1 \xi_2}^{\xi} \delta \beta_{\xi_1} + Q_{\xi_2}^{\xi} \delta w^0] A_{\xi_1}^{\xi} d\xi_1 dt \\
& + \int_{t_0}^{t_1} \int_{\xi_2} [N_{\xi_1}^{\xi} \delta u^0 + M_{\xi_1}^{\xi} \delta \beta_{\xi_1} + N_{\xi_1 \xi_2}^{\xi} \delta v^0 + M_{\xi_1 \xi_2}^{\xi} \delta \beta_{\xi_2} + Q_{\xi_1}^{\xi} \delta w^0] A_{\xi_2}^{\xi} d\xi_2 dt = 0
\end{aligned} \tag{2.270}$$

The detailed derivation of Equation (2.270) is given in Appendix A. The equation (2.270) can only be satisfied if each of the triple and double integral parts is equal to zero. Furthermore, since the variational displacements and rotations; namely  $\delta u^0$ ,  $\delta v^0$ ,  $\delta w^0$ ,  $\delta \beta_{\xi_1}$ ,  $\delta \beta_{\xi_2}$ , are arbitrary, each integral equation can only vanish only if the coefficients of the variational displacements and rotations are zero. Therefore, when the coefficients of the triple integral are set to zero, the following five equations of motion for free vibration analysis of an anisotropic laminated composite doubly curved shell are obtained

$$\frac{\partial(N_{\xi_1} A_{\xi_2})}{\partial \xi_1} - N_{\xi_2} \frac{\partial A_{\xi_2}}{\partial \xi_1} + \frac{\partial(N_{\xi_1 \xi_2} A_{\xi_1})}{\partial \xi_2} + N_{\xi_1 \xi_2} \frac{\partial A_{\xi_1}}{\partial \xi_2} + Q_{\xi_1} \frac{A_{\xi_1} A_{\xi_2}}{R_{\xi_1}} = \rho h A_{\xi_1} A_{\xi_2} \ddot{u}^0 \quad (2.271)$$

$$\frac{\partial(N_{\xi_2} A_{\xi_1})}{\partial \xi_2} - N_{\xi_1} \frac{\partial A_{\xi_1}}{\partial \xi_2} + \frac{\partial(N_{\xi_1 \xi_2} A_{\xi_2})}{\partial \xi_1} + N_{\xi_1 \xi_2} \frac{\partial(A_{\xi_2})}{\partial \xi_1} + Q_{\xi_2} \frac{A_{\xi_1} A_{\xi_2}}{R_{\xi_2}} = \rho h A_{\xi_1} A_{\xi_2} \ddot{v}^0 \quad (2.272)$$

$$-N_{\xi_1} \frac{A_{\xi_1} A_{\xi_2}}{R_{\xi_1}} - N_{\xi_2} \frac{A_{\xi_1} A_{\xi_2}}{R_{\xi_2}} + \frac{\partial(Q_{\xi_1} A_{\xi_2})}{\partial \xi_1} + \frac{\partial(Q_{\xi_2} A_{\xi_1})}{\partial \xi_2} = \rho h A_{\xi_1} A_{\xi_2} \ddot{w}^0 \quad (2.273)$$

$$\frac{\partial(M_{\xi_1} A_{\xi_2})}{\partial \xi_1} - M_{\xi_2} \frac{\partial A_{\xi_2}}{\partial \xi_1} + M_{\xi_1 \xi_2} \frac{\partial A_{\xi_1}}{\partial \xi_2} + \frac{\partial(M_{\xi_1 \xi_2} A_{\xi_1})}{\partial \xi_2} - Q_{\xi_1} A_{\xi_1} A_{\xi_2} = \rho \frac{h^3}{12} A_{\xi_1} A_{\xi_2} \ddot{\beta}_{\xi_1} \quad (2.274)$$

$$-M_{\xi_1} \frac{\partial A_{\xi_2}}{\partial \xi_1} + \frac{\partial(M_{\xi_2} A_{\xi_1})}{\partial \xi_2} + \frac{\partial(M_{\xi_1 \xi_2} A_{\xi_2})}{\partial \xi_1} + M_{\xi_1 \xi_2} \frac{\partial A_{\xi_2}}{\partial \xi_1} - Q_{\xi_2} A_{\xi_1} A_{\xi_2} = \rho \frac{h^3}{12} A_{\xi_1} A_{\xi_2} \ddot{\beta}_{\xi_2} \quad (2.275)$$

It should be noted that each of the double integrals given in Equation (2.270) is equal to zero only if the coefficients of the variational displacements, variational displacements or one of the two for each term are zero. Since variational displacements are only zero at all times when the boundary displacements are prescribed, this translates into the following possible boundary conditions for an  $\xi_1$ =constant edge.

$$\text{Either } N_{\xi_1} \text{ or } u^0 = 0 \quad (2.276)$$

$$\text{Either } N_{\xi_1 \xi_2} \text{ or } v^0 = 0 \quad (2.277)$$

$$\text{Either } Q_{\xi_1} \text{ or } w^0 = 0 \quad (2.278)$$

$$\text{Either } M_{\xi_1} \text{ or } \beta_{\xi_1} = 0 \quad (2.279)$$

$$\text{Either } M_{\xi_1 \xi_2} \text{ or } \beta_{\xi_2} = 0 \quad (2.280)$$

This states the intuitively obvious fact that one has to prescribe at a boundary either forces (moments) or displacements (rotations). However, five conditions have to be identified per edge. Similarly, examining Equation (2.270) for an  $\xi_2$ =constant edge, the five boundary conditions have to be

$$\text{Either } N_{\xi_1 \xi_2} \text{ or } u^0 = 0 \quad (2.281)$$

$$\text{Either } N_{\xi_2} \text{ or } v^0 = 0 \quad (2.282)$$

$$\text{Either } Q_{\xi_2} \text{ or } w^0 = 0 \quad (2.283)$$

$$\text{Either } M_{\xi_1 \xi_2} \text{ or } \beta_{\xi_1} = 0 \quad (2.284)$$

$$\text{Either } M_{\xi_2} \text{ or } \beta_{\xi_2} = 0 \quad (2.285)$$

Equations (2.271) to (2.275) together with the associated boundary conditions (Equations (2.276) to (2.285)) given above constitutes the equations of motion for free vibrations of an anisotropic laminated composite doubly curved shell.

## 2.6 GOVERNING EQUATIONS FOR FREE VIBRATION ANALYSIS OF ANISOTROPIC LAMINATED COMPOSITE SHELLS OF REVOLUTION

In the preceding sections, the governing equations for free vibration analysis of anisotropic laminated composite doubly curved shells are derived using First Order Shear Deformation Theory. These formulations can be translated to the governing equations for free vibration analysis of anisotropic laminated shells of revolution by first replacing the coordinates  $\xi_1, \xi_2$  and  $\zeta$  with  $\phi, \theta$ , and  $\zeta$ ; then substituting the Equations (2.96), (2.97) and (2.100) conveniently into the governing equations. After performing these transactions, the following governing equations for shells of revolutions are obtained.

The strain-displacement relations are:

$$\varepsilon_{\phi\phi} = \varepsilon_{\phi\phi}^0 + \zeta \kappa_{\phi\phi}^0 \quad (2.286)$$

where

$$\varepsilon_{\phi\phi}^0 = \left[ \frac{1}{R_\phi} \frac{\partial u_\phi^0}{\partial \phi} + \frac{1}{R_\phi} w^0 \right] \quad (2.287)$$

and

$$\kappa_{\phi\phi}^0 = \left[ \frac{1}{R_\phi} \frac{\partial \beta_\phi}{\partial \phi} \right] \quad (2.288)$$

$$\varepsilon_{\theta\theta} = \varepsilon_{\theta\theta}^0 + \zeta \kappa_{\theta\theta}^0 \quad (2.289)$$

where

$$\varepsilon_{\theta\theta}^0 = \left[ \frac{1}{R_\theta} \frac{\cos \phi}{\sin \phi} u_\phi^0 + \frac{1}{R_\theta \sin \phi} \frac{\partial u_\theta^0}{\partial \theta} + \frac{1}{R_\theta} w^0 \right] \quad (2.290)$$

and

$$\kappa_{\theta\theta}^0 = \left[ \frac{\cos \phi}{\sin \phi R_\theta} \beta_\phi + \frac{1}{R_\theta \sin \phi} \frac{\partial \beta_\theta}{\partial \theta} \right] \quad (2.291)$$

$$\gamma_{\phi\theta} = \gamma_{\phi\theta}^0 + \zeta \kappa_{\phi\theta}^0 \quad (2.292)$$

where

$$\gamma_{\phi\theta}^0 = \left[ \frac{1}{R_\theta \sin \phi} \frac{\partial u_\phi^0}{\partial \theta} + \frac{1}{R_\phi} \frac{\partial u_\theta^0}{\partial \phi} - \frac{\cos \phi}{\sin \phi R_\theta} u_\theta^0 \right] \quad (2.293)$$

and

$$\kappa_{\phi\theta}^0 = \left[ \frac{1}{R_\theta \sin \phi} \frac{\partial \beta_\phi^0}{\partial \theta} + \frac{1}{R_\phi} \frac{\partial \beta_\theta^0}{\partial \phi} - \frac{\cos \phi}{\sin \phi R_\theta} \beta_\theta^0 \right] \quad (2.294)$$

$$\gamma_{\phi\zeta} = \eta_\phi^0 \quad (2.295)$$

where

$$\eta_\phi^0 = \left[ \beta_\phi - \frac{u_\phi^0}{R_\phi} + \frac{1}{R_\phi} \frac{\partial w^0}{\partial \phi} \right] \quad (2.296)$$

$$\gamma_{\theta\zeta} = \eta_\theta^0 \quad (2.297)$$

where

$$\eta_\theta^0 = \left[ \beta_\theta - \frac{u_\theta^0}{R_\theta} + \frac{1}{R_\theta \sin \phi} \frac{\partial w^0}{\partial \theta} \right] \quad (2.298)$$

The constitutive equations are

$$\begin{Bmatrix} N_{\phi\phi} \\ N_{\theta\theta} \\ N_{\phi\theta} \\ M_{\phi\phi} \\ M_{\theta\theta} \\ M_{\phi\theta} \end{Bmatrix} = \begin{bmatrix} A_{11} & A_{12} & A_{16} & B_{11} & B_{12} & B_{16} \\ A_{12} & A_{22} & A_{26} & B_{12} & B_{22} & B_{26} \\ A_{16} & A_{26} & A_{66} & B_{16} & B_{26} & B_{66} \\ B_{11} & B_{12} & B_{16} & D_{11} & D_{12} & D_{16} \\ B_{12} & B_{22} & B_{26} & D_{12} & D_{22} & D_{26} \\ B_{16} & B_{26} & B_{66} & D_{16} & D_{26} & D_{66} \end{bmatrix} \begin{Bmatrix} \varepsilon_{\phi\phi}^0 \\ \varepsilon_{\theta\theta}^0 \\ \gamma_{\phi\theta}^0 \\ \kappa_{\phi\phi} \\ \kappa_{\theta\theta} \\ \kappa_{\phi\theta} \end{Bmatrix} \quad (2.299)$$

and

$$\begin{Bmatrix} Q_\theta \\ Q_\phi \end{Bmatrix} = \begin{bmatrix} As_{55} & As_{45} \\ As_{45} & As_{44} \end{bmatrix} \begin{Bmatrix} \eta_\theta \\ \eta_\phi \end{Bmatrix} \quad (2.300)$$

where

$$A_{ij} = \sum_{k=1}^N (\overline{Q}_{ij})_k (h_{k+1} - h_k), \quad i, j = 1, 2, 6 \quad (2.301)$$

$$B_{ij} = \sum_{k=1}^N (\overline{Q}_{ij})_k (h_{k+1}^2 - h_k^2), \quad i, j = 1, 2, 6 \quad (2.302)$$

$$D_{ij} = \sum_{k=1}^N (\overline{Q}_{ij})_k (h_{k+1}^3 - h_k^3), \quad i, j = 1, 2, 6 \quad (2.303)$$

$$As_{ij} = \frac{5}{4} \sum_{k=1}^N (\overline{Q}_{ij})_k \left[ h_{k+1} - h_k - \frac{4}{3} \left[ h_{k+1}^3 - h_k^3 \right] \frac{1}{h^2} \right], \quad i, j = 4, 5 \quad (2.304)$$

Writing the each element of the left hand side of Equation (2.299) in terms of strain components

$$N_{\phi\phi} = A_{11}\epsilon_{\phi\phi}^0 + A_{12}\epsilon_{\theta\theta}^0 + A_{16}\gamma_{\phi\theta}^0 + B_{11}\kappa_{\phi\phi}^0 + B_{12}\kappa_{\theta\theta}^0 + B_{16}\kappa_{\phi\theta}^0 \quad (2.305)$$

$$N_{\theta\theta} = A_{12}\epsilon_{\phi\phi}^0 + A_{22}\epsilon_{\theta\theta}^0 + A_{26}\gamma_{\phi\theta}^0 + B_{12}\kappa_{\phi\phi}^0 + B_{22}\kappa_{\theta\theta}^0 + B_{26}\kappa_{\phi\theta}^0 \quad (2.306)$$

$$N_{\phi\theta} = A_{16}\epsilon_{\phi\phi}^0 + A_{26}\epsilon_{\theta\theta}^0 + A_{66}\gamma_{\phi\theta}^0 + B_{16}\kappa_{\phi\phi}^0 + B_{26}\kappa_{\theta\theta}^0 + B_{66}\kappa_{\phi\theta}^0 \quad (2.307)$$

$$M_{\phi\phi} = B_{11}\epsilon_{\phi\phi}^0 + B_{12}\epsilon_{\theta\theta}^0 + B_{16}\gamma_{\phi\theta}^0 + D_{11}\kappa_{\phi\phi}^0 + D_{12}\kappa_{\theta\theta}^0 + D_{16}\kappa_{\phi\theta}^0 \quad (2.308)$$

$$M_{\theta\theta} = B_{12}\epsilon_{\phi\phi}^0 + B_{22}\epsilon_{\theta\theta}^0 + B_{26}\gamma_{\phi\theta}^0 + D_{12}\kappa_{\phi\phi}^0 + D_{22}\kappa_{\theta\theta}^0 + D_{26}\kappa_{\phi\theta}^0 \quad (2.309)$$

$$M_{\phi\theta} = B_{16}\epsilon_{\phi\phi}^0 + B_{26}\epsilon_{\theta\theta}^0 + B_{66}\gamma_{\phi\theta}^0 + D_{16}\kappa_{\phi\phi}^0 + D_{26}\kappa_{\theta\theta}^0 + D_{66}\kappa_{\phi\theta}^0 \quad (2.310)$$

The equations of motion are

$$\begin{aligned} \frac{\partial N_{\phi\phi}}{\partial \phi} R_\theta \sin \phi + N_{\phi\phi} R_\phi \cos \phi + \frac{\partial N_{\theta\theta}}{\partial \theta} R_\phi - N_{\theta\theta} R_\phi \cos \phi \\ + Q_\phi R_\theta \sin \phi = \rho h \ddot{u}_\phi^0 R_\theta R_\phi \sin \phi \end{aligned} \quad (2.311)$$

$$\begin{aligned} \frac{\partial N_{\theta\theta}}{\partial \phi} R_\theta \sin \phi + N_{\theta\theta} R_\phi \cos \phi + \frac{\partial N_{\phi\phi}}{\partial \theta} R_\phi + N_{\phi\phi} R_\phi \cos \phi \\ + Q_\theta R_\phi \sin \phi = \rho h \ddot{u}_\theta^0 R_\theta R_\phi \sin \phi \end{aligned} \quad (2.312)$$

$$\begin{aligned}
& \frac{\partial Q_\theta}{\partial \theta} R_\phi + \frac{\partial Q_\phi}{\partial \phi} R_\theta \sin \phi + Q_\phi R_\phi \cos \phi - N_{\theta\theta} R_\phi \sin \phi \\
& - N_{\phi\phi} R_\theta \sin \phi = \rho h \ddot{w}^0 R_\theta R_\phi \sin \phi
\end{aligned} \tag{2.313}$$

$$\begin{aligned}
& \frac{\partial M_\phi}{\partial \phi} R_\theta \sin \phi + \frac{\partial M_{\phi\theta}}{\partial \theta} R_\phi + M_\phi R_\phi \cos \phi - M_\theta R_\phi \cos \phi \\
& - Q_\phi R_\phi R_\theta \sin \phi = \frac{1}{12} \rho h^3 \ddot{\beta}_\phi R_\theta R_\phi \sin \phi
\end{aligned} \tag{2.314}$$

$$\begin{aligned}
& \frac{\partial M_{\phi\theta}}{\partial \phi} R_\theta \sin \phi + \frac{\partial M_\theta}{\partial \theta} R_\phi + 2M_{\phi\theta} R_\phi \cos \phi \\
& - Q_\theta R_\phi R_\theta \sin \phi = \frac{1}{12} \rho h^3 \ddot{\beta}_\theta R_\theta R_\phi \sin \phi
\end{aligned} \tag{2.315}$$

## **CHAPTER 3**

### **METHOD OF SOLUTION**

#### **3.1 INTRODUCTION**

The objective of the current chapter is to present a method of solution to the governing equations derived for free vibration analysis of anisotropic laminated composite shells of revolution in the previous chapter. At first, methods of solution used for free vibration of shells of revolution are discussed briefly. Then, the governing equations given in the section 2.6 are formulated into a suitable form to carry out determined numerical method in this thesis in order to compute the free vibration characteristics; namely, natural frequencies and mode shapes. For this reason, the governing equations for free vibration of a laminated shell of revolution using First Order Shear Deformation Theory are initially formulated into the system of partial differential equations in terms of fundamental variables. Then, this formulated fundamental system of equations is reduced to an equivalent system of first order ordinary differential equations with respect to  $\phi$  by applying the method of Finite Exponential Fourier Transform. In addition, the procedure to get the nondimensional form of the resulting system of first order ordinary differential equations is presented. The system of first order ordinary differential equations with the prescribed boundary conditions at the two edges of shell of revolution is considered as a two-point boundary value problem. Subsequently, this boundary value problem is turned into a set of initial value problems. Finally, a particular numerical integration method in combination with Frequency Trial Method is explained comprehensively as the method of solution.

#### **3.2 OVERVIEW OF THE METHODS OF SOLUTION FOR FREE VIBRATION OF HOMOGENEOUS OR LAMINATED SHELLS OF REVOLUTION**

The methods of solution for free vibration of homogeneous or laminated shells can be divided into two: exact and numerical methods. Qatu [42, 43] reviewed the various methods of solution for dynamic behavior of homogeneous and laminated composite shells in terms of experimental investigations and analytical methods. Moreover, Soldatos [62] presented a survey of three dimensional dynamic analyses of circular cylinders and cylindrical shells.

“The most commonly used approach for the free vibration analysis of shells of revolution is based on the representation of shell variables by a Fourier series in the circumferential coordinate  $\theta$ , combined with the use of a numerical discretization technique such as finite elements, finite differences or numerical integration in the meridional direction”[58]. The one can refer to the Literature Survey section of Chapter 1 for a comprehensive review of methods used. For shells with uniform circumferential properties, the Fourier series representation permits separation of variables for isotropic and laminated shells having specially orthotropic layers, and equations uncouple in harmonics.

“The fundamental problem of the theory of free vibration analysis of laminated composite thin elastic shells is the formulation of a two-dimensional system of differential equations and boundary conditions, for a rational approximate determination of stresses and deformations in three-dimensional elastic bodies shaped as a thin elastic layer surrounding a surface in space, the middle or reference surface of the shell”[36]. The equations governing the free vibration analysis of an anisotropic laminated composite shell of revolution consist of ten differential equations which are five equations of motion and five strain-displacement equations plus eight algebraic constitutive equations. Any method of analysis of shells must start with the reduction of these 18 equations to a manageable system of equations. Two methods of obtaining such a manageable system have been successfully employed for shells of revolution: (A) reduction of the 18 equations to a single  $m$ -th order differential equation involving a single unknown; and (B) reduction to an equivalent system of  $m$  first order differential equations involving  $m$  unknowns. The number  $m$  depends on the type of a shell theory employed. In this study,  $m=10$  when using the First Order Shear Deformation Theory for shell with cross ply or specially orthotropic lamination whereas  $m=20$  for shell with angle ply or generally orthotropic lamination [65].

Method (A) has been successfully applied to some simple shell configurations, such as cylindrical and spherical shells with constant thickness and elastic properties. The usual procedure is to eliminate from the system of equations all dependent variables except one, which is usually taken as the transverse displacement of the reference surface denoted here by  $w$ . In principle, it should be possible to carry out such elimination for any arbitrary shell, but in practice this has been mainly done for cylindrical and spherical shells. By means of this approach, the resulting single differential equation may be written in the form

$$\left[ k_{m/2} (\ )^m + \dots + k_2 (\ )^4 + k_1 (\ )^2 + k_0 \right] w = 0 \quad (3.1)$$

where  $(\ )^2$  denotes a second order differential operator and the  $k_i$  are constants with respect to meridional and circumferential coordinates ( $\phi$  and  $\theta$ ) which contain the geometric and elastic

parameters of the shell and derivatives with respect to time. Upon separation of variables in the circumferential direction  $\theta$  for a shell of revolution equation (3.1) becomes an ordinary  $m$ -th order differential equation in the meridional coordinate  $\phi$  with constant coefficients  $k_i$ , whose general solution consists of a sum of solutions of

$$\left[ (\frac{d}{d\phi})^2 - \lambda_i \right] W(\phi) = 0 \quad (3.2)$$

The  $m/2$  numbers  $\lambda_i$  are the  $m/2$  roots of the algebraic equation

$$k_{m/2} (\frac{d}{d\phi})^m + \dots + k_2 (\frac{d}{d\phi})^4 + k_1 (\frac{d}{d\phi})^2 + k_0 = 0 \quad (3.3)$$

The general solution of the homogeneous boundary value problem can be written for every dependent variable  $y_j$  as

$$y_j = \sum_{i=1}^m C_{ij} A_i W_i(\phi) \quad (3.4)$$

where  $C_{ij}$  are constant factors and  $A_i$  are  $m$  arbitrary constants. With the use of (3.4), the frequency equation is easily constructed from the  $m$  homogeneous boundary conditions which must be given with the statement of the problem. The general solution in the form of (3.4) has been derived explicitly for cylindrical and spherical shells. The solutions  $W_i(\phi)$  for these shells are given by the usual hyper geometric series expansions; in particular,  $W_i(\phi)$  for a cylindrical shell are trigonometric functions, for a shallow spherical shell they are Bessel functions, while for a nonshallow spherical shell they are Legendre functions.

Method (B) is based on the idea that the boundary value problem of a shell of revolution can be stated in the form of a system of  $m$  first order differential equations, containing  $m$  unknowns, subject to  $m$  boundary conditions. Since the basic shell equations are at most first order to begin with, such a system can be derived for a general shell of revolution much easier with much more generality than the uncoupled equations required by method (A). The only restriction of method (B) is that the shell (but not the vibration) must be rotationally symmetric; that is, all geometric and elastic properties of the shell can vary arbitrarily (even discontinuously) along the meridian of the reference surface of the shell but not along its circumference.

According to method (B) as given in [65], the boundary value problem is stated in terms

of exactly  $m$  unknowns denoted by  $y_i(\phi)$  in the form

$$\frac{dy_i(\phi)}{d\phi} = F_i(\phi, y_1, y_2, \dots, y_m) \quad (i = 1, 2, \dots, m) \quad (3.5)$$

and  $m$  boundary conditions at two values of  $\phi$ . It is very convenient to choose the  $m$  unknowns  $y_i(\phi)$  as those quantities which appear in the natural boundary conditions on a rotationally symmetric edge of the shell of revolution, because the boundary conditions can involve either  $y_i$  or their linear combinations, but not their derivatives.

After deriving the  $m$  first order equations for the method (B), the boundary value problem is replaced by  $m$  initial value problems to which the solution can be obtained by means of either hyper geometric series (which is at present possible for cylindrical and spherical shells) or direct numerical integration (for arbitrary rotationally symmetric shells). Of course, method (B) is most powerful for the cases where the hyper geometric series solutions are not known and therefore numerical integration must be employed. However, since very accurate numerical integration codes are available through various computer program libraries, the direct integration phase of method (B) can be handled very easily.

### 3.3 FORMULATION OF THE SYSTEM OF FIRST ORDER ORDINARY DIFFERENTIAL EQUATIONS

The governing equations for free vibration analysis of anisotropic laminated composite shells of revolution are given in Section 2.6. In this section, they are attempted to be reduced to a system of first order, ordinary differential equations which can be written in the form

$$\frac{dy(\phi)}{d\phi} = A(n, \Omega, \phi)y(\phi) \quad (3.6)$$

where  $y(\phi)$  is an  $(m,1)$  column matrix which contains  $m$  unknown dependent variables,  $A$  is an  $m \times m$  coefficient matrix,  $\Omega$  is dimensional natural frequency, and  $n$  is the wave number in the circumferential direction.

If we take an arbitrary cut which is perpendicular to axial direction, the displacement and rotation variables of  $w^0, u_\phi^0, u_\theta^0, \beta_\phi, \beta_\theta$ , and the force and moment resultant variables, which are

$Q_\phi, N_\phi, N_{\phi\theta}, M_\phi, M_{\phi\theta}$ , exist in the normal and parallel direction of the corresponding cut. Furthermore, these variables should be prescribed at the two boundary edges of shells of revolution.

As a result,  $\{\psi\} = \{w^0, u_\phi^0, u_\theta^0, \beta_\phi, \beta_\theta, Q_\phi, N_\phi, N_{\phi\theta}, M_\phi, M_{\phi\theta}\}^T$  is referred as column vector of fundamental variables.

The reduction of governing equations into a system of first order ordinary differential equations with respect to the axial direction,  $\phi$ , in terms of the fundamental variables is done in two consecutive steps. In the first step, the governing equations of free vibration analysis of anisotropic laminated composite shells of revolution are reduced into the system of partial differential equations. Then, in the second step, the system of partial differential equations is turned into the system of first order ordinary differential equations using Method of Finite Exponential Fourier Transform. The dependency in the circumferential direction is removed with the second step.

### 3.3.1 SYSTEM OF PARTIAL DIFFERENTIAL EQUATIONS

The system of partial differential equations in terms of fundamental variables will be obtained in this section. The fundamental set of equations is started with the first term which is  $\frac{\partial w^0}{\partial \phi}$  by getting the shear force resultant,  $Q_\phi$  in Equation (2.300) in terms of displacements and rotations variables in Equations (2.296) and (2.298) into (2.300). It yields

$$Q_\phi = As_{45} \left( \beta_\theta - \frac{u_\theta^0}{R_\theta} + \frac{1}{R_\theta \sin \phi} \frac{\partial w^0}{\partial \theta} \right) + As_{44} \left( \beta_\phi - \frac{u_\phi^0}{R_\phi} + \frac{1}{R_\phi} \frac{\partial w^0}{\partial \phi} \right) \quad (3.7)$$

After necessary manipulation and leaving the term  $\partial w^0 / \partial \phi$  on the left hand side, we get

$$\frac{\partial w^0}{\partial \phi} = (cp_{11}) \left( \frac{\partial w^0}{\partial \theta} \right) + (c_{12}) (u_\phi^0) + (c_{13}) (u_\theta^0) + (c_{14}) (\beta_\phi) + (c_{15}) (\beta_\theta) + (c_{16}) (Q_\phi) \quad (3.8)$$

where the coefficients  $cp_{11}, c_{12}, c_{13}, c_{14}, c_{15}$  and  $c_{16}$  are given in Appendix C. All the coefficients following in this section are also listed in the Appendix C.

The equations,  $(\partial u_\phi^0 / \partial \phi, \partial u_\theta^0 / \partial \phi, \partial \beta_\phi / \partial \phi, \partial \beta_\theta / \partial \phi)$  can be easily derived from (2.305),

(2.307), (2.308), and (2.310). After combining the strain-displacement equations with (2.305), (2.307), (2.308) and (2.310), we can write following four equations.

$$\begin{aligned}
& \left[ (A_{11}) \left( \frac{1}{R_\phi} \right) \right] \left( \frac{\partial u_\phi^0}{\partial \phi} \right) + \left[ (A_{16}) \left( \frac{1}{R_\phi} \right) \right] \left( \frac{\partial u_\theta^0}{\partial \phi} \right) + \left[ (B_{11}) \left( \frac{1}{R_\phi} \right) \right] \left( \frac{\partial \beta_\phi}{\partial \phi} \right) + \left[ (B_{16}) \left( \frac{1}{R_\phi} \right) \right] \left( \frac{\partial \beta_\theta}{\partial \phi} \right) \\
&= [N_\phi] - \left[ (A_{11}) \left( \frac{1}{R_\phi} \right) (w^0) \right] - \left[ (A_{12}) \left( \frac{1}{R_\theta} \frac{\cos \phi}{\sin \phi} u_\phi^0 + \frac{1}{R_\theta} \frac{1}{\sin \phi} \frac{\partial u_\theta^0}{\partial \theta} + \frac{1}{R_\theta} w^0 \right) \right] \\
&- \left[ (A_{16}) \left( \frac{1}{R_\theta} \frac{1}{\sin \phi} \frac{\partial u_\phi^0}{\partial \theta} - \frac{1}{R_\theta} \frac{\cos \phi}{\sin \phi} u_\theta^0 \right) \right] - \left[ (B_{12}) \left( \frac{1}{R_\theta} \frac{\cos \phi}{\sin \phi} \beta_\phi + \frac{1}{R_\theta} \frac{1}{\sin \phi} \frac{\partial \beta_\theta}{\partial \theta} \right) \right] \\
&- \left[ (B_{16}) \left( \frac{1}{R_\theta} \frac{1}{\sin \phi} \frac{\partial \beta_\phi}{\partial \theta} - \frac{1}{R_\theta} \frac{\cos \phi}{\sin \phi} \beta_\theta \right) \right]
\end{aligned} \tag{3.9}$$

$$\begin{aligned}
& \left[ (A_{16}) \left( \frac{1}{R_\phi} \right) \right] \left( \frac{\partial u_\phi^0}{\partial \phi} \right) + \left[ (A_{66}) \left( \frac{1}{R_\phi} \right) \right] \left( \frac{\partial u_\theta^0}{\partial \phi} \right) + \left[ (B_{16}) \left( \frac{1}{R_\phi} \right) \right] \left( \frac{\partial \beta_\phi}{\partial \phi} \right) + \left[ (B_{66}) \left( \frac{1}{R_\phi} \right) \right] \left( \frac{\partial \beta_\theta}{\partial \phi} \right) \\
&= [N_{\phi\theta}] - \left[ (A_{16}) \left( \frac{1}{R_\phi} \right) (w^0) \right] - \left[ (A_{26}) \left( \frac{1}{R_\theta} \frac{\cos \phi}{\sin \phi} u_\phi^0 + \frac{1}{R_\theta} \frac{1}{\sin \phi} \frac{\partial u_\theta^0}{\partial \theta} + \frac{1}{R_\theta} w^0 \right) \right] \\
&- \left[ (A_{66}) \left( \frac{1}{R_\theta} \frac{1}{\sin \phi} \frac{\partial u_\phi^0}{\partial \theta} - \frac{1}{R_\theta} \frac{\cos \phi}{\sin \phi} u_\theta^0 \right) \right] - \left[ (B_{26}) \left( \frac{1}{R_\theta} \frac{\cos \phi}{\sin \phi} \beta_\phi + \frac{1}{R_\theta} \frac{1}{\sin \phi} \frac{\partial \beta_\theta}{\partial \theta} \right) \right] \\
&- \left[ (B_{16}) \left( \frac{1}{R_\theta} \frac{1}{\sin \phi} \frac{\partial \beta_\phi}{\partial \theta} - \frac{1}{R_\theta} \frac{\cos \phi}{\sin \phi} \beta_\theta \right) \right]
\end{aligned} \tag{3.10}$$

$$\begin{aligned}
& \left[ (B_{11}) \left( \frac{1}{R_\phi} \right) \right] \left( \frac{\partial u_\phi^0}{\partial \phi} \right) + \left[ (B_{16}) \left( \frac{1}{R_\phi} \right) \right] \left( \frac{\partial u_\theta^0}{\partial \phi} \right) + \left[ (D_{11}) \left( \frac{1}{R_\phi} \right) \right] \left( \frac{\partial \beta_\phi}{\partial \phi} \right) + \left[ (D_{16}) \left( \frac{1}{R_\phi} \right) \right] \left( \frac{\partial \beta_\theta}{\partial \phi} \right) \\
&= [M_\phi] - \left[ (B_{11}) \left( \frac{1}{R_\phi} \right) (w^0) \right] - \left[ (B_{12}) \left( \frac{1}{R_\theta} \frac{\cos \phi}{\sin \phi} u_\phi^0 + \frac{1}{R_\theta} \frac{1}{\sin \phi} \frac{\partial u_\theta^0}{\partial \theta} + \frac{1}{R_\theta} w^0 \right) \right] \\
&- \left[ (B_{16}) \left( \frac{1}{R_\theta} \frac{1}{\sin \phi} \frac{\partial u_\phi^0}{\partial \theta} - \frac{1}{R_\theta} \frac{\cos \phi}{\sin \phi} u_\theta^0 \right) \right] - \left[ (D_{12}) \left( \frac{1}{R_\theta} \frac{\cos \phi}{\sin \phi} \beta_\phi + \frac{1}{R_\theta} \frac{1}{\sin \phi} \frac{\partial \beta_\theta}{\partial \theta} \right) \right] \\
&- \left[ (D_{16}) \left( \frac{1}{R_\theta} \frac{1}{\sin \phi} \frac{\partial \beta_\phi}{\partial \theta} - \frac{1}{R_\theta} \frac{\cos \phi}{\sin \phi} \beta_\theta \right) \right]
\end{aligned} \tag{3.11}$$

$$\begin{aligned}
& \left[ (B_{16}) \left( \frac{1}{R_\phi} \right) \right] \left( \frac{\partial u_\phi^0}{\partial \phi} \right) + \left[ (B_{66}) \left( \frac{1}{R_\phi} \right) \right] \left( \frac{\partial u_\theta^0}{\partial \phi} \right) + \left[ (D_{16}) \left( \frac{1}{R_\phi} \right) \right] \left( \frac{\partial \beta_\phi}{\partial \phi} \right) + \left[ (D_{66}) \left( \frac{1}{R_\phi} \right) \right] \left( \frac{\partial \beta_\theta}{\partial \phi} \right) \\
&= [M_{\phi\theta}] - \left[ (B_{16}) \left( \frac{1}{R_\phi} \right) (w^0) \right] - \left[ (B_{26}) \left( \frac{1}{R_\theta} \frac{\cos \phi}{\sin \phi} u_\phi^0 + \frac{1}{R_\theta} \frac{1}{\sin \phi} \frac{\partial u_\theta^0}{\partial \theta} + \frac{1}{R_\theta} w^0 \right) \right] \\
&- \left[ (B_{66}) \left( \frac{1}{R_\theta} \frac{1}{\sin \phi} \frac{\partial u_\phi^0}{\partial \theta} - \frac{1}{R_\theta} \frac{\cos \phi}{\sin \phi} u_\theta^0 \right) \right] - \left[ (D_{26}) \left( \frac{1}{R_\theta} \frac{\cos \phi}{\sin \phi} \beta_\phi + \frac{1}{R_\theta} \frac{1}{\sin \phi} \frac{\partial \beta_\theta}{\partial \theta} \right) \right] \\
&- \left[ (D_{66}) \left( \frac{1}{R_\theta} \frac{1}{\sin \phi} \frac{\partial \beta_\phi}{\partial \theta} - \frac{1}{R_\theta} \frac{\cos \phi}{\sin \phi} \beta_\theta \right) \right]
\end{aligned} \tag{3.12}$$

The equations (3.9) to (3.12) can be written in compact form as:

$$\begin{bmatrix} h_{11} & h_{12} & h_{13} & h_{14} \\ h_{21} & h_{22} & h_{23} & h_{24} \\ h_{31} & h_{32} & h_{33} & h_{34} \\ h_{41} & h_{42} & h_{43} & h_{44} \end{bmatrix} \begin{Bmatrix} (\partial u_\phi^0 / \partial \phi) \\ (\partial u_\theta^0 / \partial \phi) \\ (\partial \beta_\phi / \partial \phi) \\ (\partial \beta_\theta / \partial \phi) \end{Bmatrix} = \begin{Bmatrix} j_{11} \\ j_{21} \\ j_{31} \\ j_{41} \end{Bmatrix} \tag{3.13}$$

or

$$\begin{Bmatrix} (\partial u_\phi^0 / \partial \phi) \\ (\partial u_\theta^0 / \partial \phi) \\ (\partial \beta_\phi / \partial \phi) \\ (\partial \beta_\theta / \partial \phi) \end{Bmatrix} = \begin{bmatrix} h_{11} & h_{12} & h_{13} & h_{14} \\ h_{21} & h_{22} & h_{23} & h_{24} \\ h_{31} & h_{32} & h_{33} & h_{34} \\ h_{41} & h_{42} & h_{43} & h_{44} \end{bmatrix}^{-1} \begin{Bmatrix} j_{11} \\ j_{21} \\ j_{31} \\ j_{41} \end{Bmatrix} \tag{3.14}$$

The Equation (3.14) is solved symbolically by implementing the Symbolic Toolbox of Matlab. Matlab is a trademark of Mathworks Inc. [68]. The results are given in the Appendix B. The

equations for  $\left( \frac{\partial u_\phi^0}{\partial \phi}, \frac{\partial u_\theta^0}{\partial \phi}, \frac{\partial \beta_\phi}{\partial \phi}, \frac{\partial \beta_\theta}{\partial \phi} \right)$  are written in terms of fundamental variables as follows:

$$\begin{aligned}
\frac{\partial u_\phi^0}{\partial \phi} &= (c_{21})(w^0) + (c_{22})(u_\phi^0) + (cp_{22}) \left( \frac{\partial u_\phi^0}{\partial \theta} \right) + (c_{23})(u_\theta^0) + (cp_{23}) \left( \frac{\partial u_\theta^0}{\partial \theta} \right) \\
&+ (c_{24})(\beta_\phi) + (cp_{24}) \left( \frac{\partial \beta_\phi}{\partial \theta} \right) + (c_{25})(\beta_\theta) + (cp_{25}) \left( \frac{\partial \beta_\theta}{\partial \theta} \right) \\
&+ (c_{27})(N_\phi) + (c_{28})(N_{\phi\theta}) + (c_{29})(M_\phi) + (c_{210})(M_{\phi\theta})
\end{aligned} \tag{3.15}$$

$$\begin{aligned}
\frac{\partial u_\theta^0}{\partial \phi} &= (c_{31})(w^0) + (c_{32})(u_\phi^0) + (cp_{32})\left(\frac{\partial u_\phi^0}{\partial \theta}\right) + (c_{33})(u_\theta^0) + (cp_{33})\left(\frac{\partial u_\theta^0}{\partial \theta}\right) \\
&+ (c_{34})(\beta_\phi) + (cp_{34})\left(\frac{\partial \beta_\phi}{\partial \theta}\right) + (c_{35})(\beta_\theta) + (cp_{35})\left(\frac{\partial \beta_\theta}{\partial \theta}\right) \\
&+ (c_{37})(N_\phi) + (c_{38})(N_{\phi\theta}) + (c_{39})(M_\phi) + (c_{310})(M_{\phi\theta})
\end{aligned} \tag{3.16}$$

$$\begin{aligned}
\frac{\partial \beta_\phi^0}{\partial \phi} &= (c_{41})(w^0) + (c_{42})(u_\phi^0) + (cp_{42})\left(\frac{\partial u_\phi^0}{\partial \theta}\right) + (c_{43})(u_\theta^0) + (cp_{43})\left(\frac{\partial u_\theta^0}{\partial \theta}\right) \\
&+ (c_{44})(\beta_\phi) + (cp_{44})\left(\frac{\partial \beta_\phi}{\partial \theta}\right) + (c_{45})(\beta_\theta) + (cp_{45})\left(\frac{\partial \beta_\theta}{\partial \theta}\right) \\
&+ (c_{47})(N_\phi) + (c_{48})(N_{\phi\theta}) + (c_{49})(M_\phi) + (c_{410})(M_{\phi\theta})
\end{aligned} \tag{3.17}$$

$$\begin{aligned}
\frac{\partial \beta_\theta^0}{\partial \phi} &= (c_{51})(w^0) + (c_{52})(u_\phi^0) + (cp_{52})\left(\frac{\partial u_\phi^0}{\partial \theta}\right) + (c_{53})(u_\theta^0) + (cp_{53})\left(\frac{\partial u_\theta^0}{\partial \theta}\right) \\
&+ (c_{54})(\beta_\phi) + (cp_{54})\left(\frac{\partial \beta_\phi}{\partial \theta}\right) + (c_{55})(\beta_\theta) + (cp_{55})\left(\frac{\partial \beta_\theta}{\partial \theta}\right) \\
&+ (c_{57})(N_\phi) + (c_{58})(N_{\phi\theta}) + (c_{59})(M_\phi) + (c_{510})(M_{\phi\theta})
\end{aligned} \tag{3.18}$$

Up to this point, the displacements and rotations terms of the system of partial differential equations are found in terms of fundamental variables and their derivatives with respect to  $\theta$ . The desired stress resultants terms can now be extracted from equations of motion derived for free vibration analysis of anisotropic laminated shells of revolution.

$$\frac{\partial Q_\phi}{\partial \phi}, \frac{\partial N_\phi}{\partial \phi}, \frac{\partial N_{\phi\theta}}{\partial \phi}, \frac{\partial M_\phi}{\partial \phi}, \text{ and } \frac{\partial M_{\phi\theta}}{\partial \phi}$$

are obtained from Equations (2.313), (2.311), (2.312), (2.314) and (2.315), respectively. The required term is placed on the left hand of its relevant equation. Then, we substitute not only the stress resultants other than existing in the column vector of fundamental variables in terms of displacement field variables such that  $w^0, u_\phi^0, u_\theta^0, \beta_\phi$ , and  $\beta_\theta$  but also Equations (3.8) and (3.15) to (3.18) whenever necessary into the right hand side of the equations of motion. After making necessary manipulations and collecting similar terms together, we get the following equations for the remaining terms of the system of partial differential equations in terms of fundamental variables and their derivatives with respect to  $\theta$ .

$$\begin{aligned}
\frac{\partial Q_\phi}{\partial \phi} &= (c_{61})\chi(w^0) + (cdp_{61})\left(\frac{\partial^2 w^0}{\partial \theta^2}\right) + (c_{62})\chi(u_\phi^0) + (cp_{62})\left(\frac{\partial u_\phi^0}{\partial \theta}\right) + (c_{63})\chi(u_\theta^0) + (cp_{63})\left(\frac{\partial u_\theta^0}{\partial \theta}\right) \\
&+ (c_{64})\chi(\beta_\phi) + (cp_{64})\left(\frac{\partial \beta_\phi}{\partial \theta}\right) + (c_{65})\chi(\beta_\theta) + (cp_{65})\left(\frac{\partial \beta_\theta}{\partial \theta}\right) + (c_{66})\chi(Q_\phi) + (cp_{66})\left(\frac{\partial Q_\phi}{\partial \theta}\right) \\
&+ (c_{67})\chi(N_\phi) + (c_{68})\chi(N_{\phi\theta}) + (c_{69})\chi(M_\phi) + (c_{610})\chi(M_{\phi\theta})
\end{aligned} \tag{3.19}$$

$$\begin{aligned}
\frac{\partial N_\phi}{\partial \phi} &= (c_{71})\chi(w^0) + (c_{72})\chi(u_\phi^0) + (cp_{72})\left(\frac{\partial u_\phi^0}{\partial \theta}\right) + (c_{73})\chi(u_\theta^0) + (cp_{73})\left(\frac{\partial u_\theta^0}{\partial \theta}\right) \\
&+ (c_{74})\chi(\beta_\phi) + (cp_{74})\left(\frac{\partial \beta_\phi}{\partial \theta}\right) + (c_{75})\chi(\beta_\theta) + (cp_{75})\left(\frac{\partial \beta_\theta}{\partial \theta}\right) \\
&+ (c_{76})\chi(Q_\phi) + (c_{77})\chi(N_\phi) + (c_{78})\chi(N_{\phi\theta}) + (cp_{78})\left(\frac{\partial N_{\phi\theta}}{\partial \theta}\right) + (c_{79})\chi(M_\phi) + (c_{710})\chi(M_{\phi\theta})
\end{aligned} \tag{3.20}$$

$$\begin{aligned}
\frac{\partial N_{\phi\theta}}{\partial \phi} &= (cp_{81})\left(\frac{\partial w^0}{\partial \theta}\right) + (c_{82})\chi(u_\phi^0) + (cp_{82})\left(\frac{\partial u_\phi^0}{\partial \theta}\right) + (cdp_{82})\left(\frac{\partial^2 u_\phi^0}{\partial \theta^2}\right) + (c_{83})\chi(u_\theta^0) + (cp_{83})\left(\frac{\partial u_\theta^0}{\partial \theta}\right) \\
&+ (cdp_{83})\left(\frac{\partial^2 u_\theta^0}{\partial \theta^2}\right) + (c_{84})\chi(\beta_\phi) + (cp_{84})\left(\frac{\partial \beta_\phi}{\partial \theta}\right) + (cdp_{84})\left(\frac{\partial^2 \beta_\phi}{\partial \theta^2}\right) + (c_{85})\chi(\beta_\theta) \\
&+ (cp_{85})\left(\frac{\partial \beta_\theta}{\partial \theta}\right) + (cdp_{85})\left(\frac{\partial^2 \beta_\theta}{\partial \theta^2}\right) + (c_{86})\chi(Q_\phi) + (cp_{87})\left(\frac{\partial N_\phi}{\partial \theta}\right) + (c_{88})\chi(N_{\phi\theta}) \\
&+ (cp_{88})\left(\frac{\partial N_{\phi\theta}}{\partial \theta}\right) + (cp_{89})\left(\frac{\partial M_\phi}{\partial \theta}\right) + (cp_{810})\left(\frac{\partial M_{\phi\theta}}{\partial \theta}\right)
\end{aligned} \tag{3.21}$$

$$\begin{aligned}
\frac{\partial M_\phi}{\partial \theta} &= (c_{91})\chi(w^0) + (c_{92})\chi(u_\phi^0) + (cp_{92})\left(\frac{\partial u_\phi^0}{\partial \theta}\right) + (c_{93})\chi(u_\theta^0) + (cp_{93})\left(\frac{\partial u_\theta^0}{\partial \theta}\right) \\
&+ (c_{94})\chi(\beta_\phi) + (cp_{94})\left(\frac{\partial \beta_\phi}{\partial \theta}\right) + (c_{95})\chi(\beta_\theta) + (cp_{95})\left(\frac{\partial \beta_\theta}{\partial \theta}\right) + (c_{96})\chi(Q_\phi) \\
&+ (c_{97})\chi(N_\phi) + (c_{98})\chi(N_{\phi\theta}) + (c_{99})\chi(M_\phi) + (c_{910})\chi(M_{\phi\theta}) + (cp_{910})\left(\frac{\partial M_{\phi\theta}}{\partial \theta}\right)
\end{aligned} \tag{3.22}$$

$$\begin{aligned}
\frac{\partial M_{\phi\theta}}{\partial \phi} &= (cp_{101})\left(\frac{\partial w^0}{\partial \theta}\right) + (c_{102})\chi(u_\phi^0) + (cp_{102})\left(\frac{\partial u_\phi^0}{\partial \theta}\right) + (cdp_{102})\left(\frac{\partial^2 u_\phi^0}{\partial \theta^2}\right) + (c_{103})\chi(u_\theta^0) \\
&+ (cp_{103})\left(\frac{\partial u_\theta^0}{\partial \theta}\right) + (cdp_{103})\left(\frac{\partial^2 u_\theta^0}{\partial \theta^2}\right) + (c_{104})\chi(\beta_\phi) + (cp_{104})\left(\frac{\partial \beta_\phi}{\partial \theta}\right) + (cdp_{104})\left(\frac{\partial^2 \beta_\phi}{\partial \theta^2}\right) \\
&+ (c_{105})\chi(\beta_\theta) + (cp_{105})\left(\frac{\partial \beta_\theta}{\partial \theta}\right) + (cdp_{105})\left(\frac{\partial^2 \beta_\theta}{\partial \theta^2}\right) + (c_{106})\chi(Q_\phi) \\
&+ (cp_{107})\left(\frac{\partial N_\phi}{\partial \theta}\right) + (cp_{108})\left(\frac{\partial N_{\phi\theta}}{\partial \theta}\right) + (cp_{109})\left(\frac{\partial M_\phi}{\partial \theta}\right) + (c_{1010})\chi(M_{\phi\theta}) + (cp_{1010})\left(\frac{\partial M_{\phi\theta}}{\partial \theta}\right)
\end{aligned} \tag{3.23}$$

### 3.3.2 SYSTEM OF FIRST ORDER ORDINARY DIFFERENTIAL EQUATIONS

In the preceding section, the system of partial differential equations for free vibrations of an anisotropic laminated composite shell of revolution is obtained from the corresponding governing equations. In this system, the fundamental variables have dependency with both the axial coordinate  $\phi$ , and the circumferential coordinate,  $\theta$ . Furthermore, for free vibration problem, assuming harmonic vibration in time, the dependence of each fundamental variable on time appears in a factor  $e^{i\omega t}$ , where  $\omega$  is the natural frequency,  $t$  is time, and  $i = \sqrt{-1}$ . Since the shell of revolution is rotationally symmetric, the motion must be periodic in  $\theta$ . For the shell of revolution which is laminated in cross-ply (specially orthotropic) configurations, each variable in the governing equations for free vibrations of the laminated composite shell of revolution can be separated in  $\theta$  as a function of  $\cos(n\theta)$  or  $\sin(n\theta)$ , where  $n$  is the circumferential wave number, commonly known as the Fourier components. This type of separation of variables like Navier-type or Levy-type solutions is known as traditional Fourier decomposition procedure. For example, Kalnins [66] used the traditional Fourier decomposition procedures for analysis of shells of revolution subjected to symmetrical and unsymmetrical loads. Moreover, he applied the same procedure in the free vibration of rotationally symmetric shells [67]. The other scientific works using traditional Fourier decomposition procedure are presented in [71-75]. However, the traditional Fourier decomposition procedure is inapplicable for laminated composite shells of revolution possessing the material anisotropy in each layer due to the existence of deformation couplings. The deformation couplings are such as extensional-shear  $(A_{16}, A_{26})$ , extensional-bending  $(B_{16}, B_{26})$ , bending-twisting  $(D_{16}, D_{26})$  couplings, and transverse shear coupling  $(A_{45})$  between shear strain in the  $\phi - \zeta$  plane and shear strain in the  $\theta - \zeta$  plane.

In the manner of Lestingi and Padovan [64], the system of partial differential equations for free vibration analysis of an anisotropic laminated composite shell of revolution can be converted into a system of first order ordinary differential equations in real form so as to apply the multisegment numerical integration procedure as the method of solution. In the works of Lestingi and Padovan [64], governing equations derived by the classical shell theory for static analysis were reduced to sixteen first-order ordinary differential equations after applying the Finite Exponential Fourier Transform Method. For our study, the governing equations for free vibration analysis of anisotropic laminated composite shells of revolution are reduced to the system of first order ordinary differential equations having 20 homogeneous linear first order ordinary differential equations and 20 unknowns with the application of Finite Exponential Fourier Transform Method. This system of equations and the unknowns are called the fundamental system and the fundamental variables, respectively, because they are necessary and sufficient for a complete statement of the problem. The conversion from system of partial differential equations to system of first order ordinary differential equations is

accomplished with the use of method of Finite Exponential Fourier Transform. Consequently, the fundamental variables are only function of the axial coordinate which is  $\phi$ . The application of the method of finite exponential Fourier Transform will now be demonstrated by carrying out it to the first equation (Equation (3.8)) of the fundamental system of partial differential equations for free vibrations of an anisotropic laminated composite axisymmetric shell. The application of method of Finite Exponential Fourier Transform to arbitrary functions is given in Appendix D.

Let us consider the dimensional transverse displacement  $w^0 = w^0(\phi, \theta, t)$ . It can be expanded as

$$w^0(\phi, \theta, t) = \sum_{-\infty}^{\infty} w_n^0(\phi, t) e^{in\theta} \quad (3.24)$$

where

$$w_n^0(\phi, t) = \frac{1}{2\Pi} \int_0^{2\Pi} w^0(\phi, \theta, t) e^{-in\theta} d\theta \quad (3.25)$$

Actually, Equations (3.24) and (3.25) are the exponential form of Fourier series given by

$$f(t) = \sum_{-\infty}^{\infty} C_n e^{int} \quad (3.26)$$

$$C_n = \frac{1}{T} \int_{-T/2}^{T/2} f(t) e^{-int} dt \quad (3.27)$$

where  $f(t)$  is any periodic function with a period of  $T$ . Equation (3.25) can further be written as

$$w_n^0(\phi, t) = \frac{1}{2\Pi} \int_0^{2\Pi} w^0(\phi, \theta, t) e^{-in\theta} d\theta = [w^0(\phi, t)]_{nc} - i [w^0(\phi, t)]_{ns} \quad (3.28)$$

where

$$[w^0(\phi, t)]_{nc} = \frac{1}{2\Pi} \int_0^{2\Pi} w^0(\phi, \theta, t) \cos n\theta d\theta \quad (3.29)$$

$$[w^0(\phi, t)]_{ns} = \frac{1}{2\Pi} \int_0^{2\Pi} w^0(\phi, \theta, t) \sin n\theta d\theta \quad (3.30)$$

$$e^{\pm in\theta} = \cos n\theta \pm i \sin n\theta \quad (3.31)$$

Rewriting the first equation of the system of partial differential equations (Equation (3.8)):

$$\frac{\partial w^0}{\partial \phi} = (c_{p_{11}}) \left( \frac{\partial w^0}{\partial \theta} \right) + (c_{12})(u_\phi^0) + (c_{13})(u_\theta^0) + (c_{14})(\beta_\phi) + (c_{15})(\beta_\theta) + (c_{16})(Q_\phi) \quad (3.8)$$

Carrying out the Finite Exponential Fourier Transform to Equation (3.8)

$$\begin{aligned} \frac{1}{2\Pi} \int_0^{2\Pi} \left[ \frac{\partial w^0(\phi, \theta, t)}{\partial \phi} e^{-in\theta} \right] d\theta &= (c_{p_{11}}) \frac{1}{2\Pi} \int_0^{2\Pi} \left[ \frac{\partial w^0(\phi, \theta, t)}{\partial \theta} e^{-in\theta} \right] d\theta \\ + (c_{12}) \frac{1}{2\Pi} \int_0^{2\Pi} [u_\phi^0(\phi, \theta, t) e^{-in\theta}] d\theta &+ (c_{13}) \frac{1}{2\Pi} \int_0^{2\Pi} [u_\theta^0(\phi, \theta, t) e^{-in\theta}] d\theta \\ + (c_{14}) \frac{1}{2\Pi} \int_0^{2\Pi} [\beta_\phi(\phi, \theta, t) e^{-in\theta}] d\theta &+ (c_{15}) \frac{1}{2\Pi} \int_0^{2\Pi} [\beta_\theta(\phi, \theta, t) e^{-in\theta}] d\theta \\ + (c_{16}) \frac{1}{2\Pi} \int_0^{2\Pi} [Q_\phi(\phi, \theta, t) e^{-in\theta}] d\theta & \end{aligned} \quad (3.32)$$

Using Equation (3.28), (3.29) and (3.30) in Equation (3.32) yields

$$\begin{aligned} \int_0^{2\Pi} \left[ \begin{array}{l} \frac{\partial w^0(\phi, \theta, t)}{\partial \phi} \cos n\theta \\ -i \frac{\partial w^0(\phi, \theta, t)}{\partial \phi} \sin n\theta \end{array} \right] d\theta &= (c_{p_{11}}) \int_0^{2\Pi} (in) \left[ \begin{array}{l} w^0(\phi, \theta, t) \cos n\theta \\ -i w^0(\phi, \theta, t) \sin n\theta \end{array} \right] d\theta \\ + (c_{12}) \int_0^{2\Pi} \left[ \begin{array}{l} u_\phi^0(\phi, \theta, t) \cos n\theta \\ -i u_\phi^0(\phi, \theta, t) \sin n\theta \end{array} \right] d\theta &+ (c_{13}) \int_0^{2\Pi} \left[ \begin{array}{l} u_\theta^0(\phi, \theta, t) \cos n\theta \\ -i u_\theta^0(\phi, \theta, t) \sin n\theta \end{array} \right] d\theta \\ + (c_{14}) \int_0^{2\Pi} \left[ \begin{array}{l} \beta_\phi(\phi, \theta, t) \cos n\theta \\ -i \beta_\phi(\phi, \theta, t) \sin n\theta \end{array} \right] d\theta &+ (c_{15}) \frac{1}{2\Pi} \int_0^{2\Pi} \left[ \begin{array}{l} \beta_\theta(\phi, \theta, t) \cos n\theta \\ -i \beta_\theta(\phi, \theta, t) \sin n\theta \end{array} \right] d\theta \\ + (c_{16}) \frac{1}{2\Pi} \int_0^{2\Pi} \left[ \begin{array}{l} Q_\phi(\phi, \theta, t) \cos n\theta \\ -i Q_\phi(\phi, \theta, t) \sin n\theta \end{array} \right] d\theta & \end{aligned} \quad (3.33)$$

Writing Equation (3.33) in terms of (3.29) and (3.30)

$$\begin{aligned}
& \left[ \frac{dw^0(\phi, t)}{d\phi} \right]_{nc} - i \left[ \frac{dw^0(\phi, t)}{d\phi} \right]_{ns} = (cp_{11})(n) \{ i [w^0(\phi, t)]_{nc} + [w^0(\phi, t)]_{ns} \} \\
& + (c_{12}) \{ [u_\phi^0(\phi, t)]_{nc} - i [u_\phi^0(\phi, t)]_{ns} \} + (c_{13}) \{ [u_\theta^0(\phi, t)]_{nc} - i [u_\theta^0(\phi, t)]_{ns} \} \\
& + (c_{14}) \{ [\beta_\phi(\phi, t)]_{nc} - i [\beta_\phi(\phi, t)]_{ns} \} + (c_{15}) \{ [\beta_\theta(\phi, t)]_{nc} - i [\beta_\theta(\phi, t)]_{ns} \} \\
& + (c_{16}) \{ [\varrho_\phi(\phi, t)]_{nc} - i [\varrho_\phi(\phi, t)]_{ns} \}
\end{aligned} \tag{3.34}$$

We separate the real and imaginary parts of Equation (3.34). First, writing real parts of Equation (3.34) term by term:

$$\begin{aligned}
& \left[ \frac{dw^0(\phi, t)}{d\phi} \right]_{nc} = (cp_{11})(n) [w^0(\phi, t)]_{ns} + (c_{12}) [u_\phi^0(\phi, t)]_{nc} + (c_{13}) [u_\theta^0(\phi, t)]_{nc} \\
& + (c_{14}) [\beta_\phi(\phi, t)]_{nc} + (c_{15}) [\beta_\theta(\phi, t)]_{nc} + (c_{16}) [\varrho_\phi(\phi, t)]_{nc}
\end{aligned} \tag{3.35}$$

Then, writing imaginary parts of Equation (3.34) term by term:

$$\begin{aligned}
& \left[ \frac{dw^0(\phi, t)}{d\phi} \right]_{ns} = -(cp_{11})(n) [w^0(\phi, t)]_{nc} + (c_{12}) [u_\phi^0(\phi, t)]_{ns} + (c_{13}) [u_\theta^0(\phi, t)]_{ns} \\
& + (c_{14}) [\beta_\phi(\phi, t)]_{ns} + (c_{15}) [\beta_\theta(\phi, t)]_{ns} + (c_{16}) [\varrho_\phi(\phi, t)]_{ns}
\end{aligned} \tag{3.36}$$

The application of the method of Finite Exponential Fourier Transform to the remaining elements of the system of partial differential equations is done in Appendix E.

As a result, the system of partial differential equations for the free vibration of an anisotropic laminated composite shell of revolution is transformed into the system of first order ordinary differential equations. The resulting system can be written in the following form.

$$\frac{d}{d\phi} \begin{Bmatrix} \psi_1 \\ \psi_2 \end{Bmatrix} = [K] \begin{Bmatrix} \psi_1 \\ \psi_2 \end{Bmatrix} \tag{3.37}$$

where

$$\psi_1 = \left\{ \begin{array}{l} [w^0(\phi, t)]_{nc} \\ [w^0(\phi, t)]_{ns} \\ [u_\phi^0(\phi, t)]_{nc} \\ [u_\phi^0(\phi, t)]_{ns} \\ [u_\theta^0(\phi, t)]_{nc} \\ [u_\theta^0(\phi, t)]_{ns} \\ [\beta_\phi(\phi, t)]_{nc} \\ [\beta_\phi(\phi, t)]_{ns} \\ [\beta_\theta(\phi, t)]_{nc} \\ [\beta_\theta(\phi, t)]_{ns} \end{array} \right\}; \quad \psi_2 = \left\{ \begin{array}{l} [Q_\phi(\phi, t)]_{nc} \\ [Q_\phi(\phi, t)]_{ns} \\ [N_\phi(\phi, t)]_{nc} \\ [N_\phi(\phi, t)]_{ns} \\ [N_{\phi\theta}(\phi, t)]_{nc} \\ [N_{\phi\theta}(\phi, t)]_{ns} \\ [M_\phi(\phi, t)]_{nc} \\ [M_\phi(\phi, t)]_{ns} \\ [M_{\phi\theta}(\phi, t)]_{nc} \\ [M_{\phi\theta}(\phi, t)]_{ns} \end{array} \right\} \quad (3.38)$$

The elements of the coefficient matrix K are given in the Appendix F.

### 3.4 NONDIMENSIONALIZATION OF THE SYSTEM OF FIRST ORDER ORDINARY DIFFERENTIAL EQUATIONS

The Equation (3.37) can be put into nondimensional form by using the following scheme

$$(\bar{w}^0, \bar{u}_\phi^0, \bar{u}_\theta^0) = (w^0, u_\phi^0, u_\theta^0)/h \quad (3.39)$$

$$(\bar{R}_\phi, \bar{R}_\theta, \bar{R}) = (R_\phi, R_\theta, R)/h \quad (3.40)$$

and

$$\bar{A}_{ij} = A_{ij}/(E_{11}h) \quad (i, j = 1, 2, 6, 4, 5) \quad (3.41)$$

$$\bar{B}_{ij} = B_{ij}/(E_{11}h^2) \quad (i, j = 1, 2, 6) \quad (3.42)$$

$$\bar{D}_{ij} = D_{ij}/(E_{11}h^3) \quad (i, j = 1, 2, 6) \quad (3.43)$$

and

$$(\bar{Q}_\phi, \bar{N}_\phi, \bar{N}_{\phi\theta}) = (Q_\phi, N_\phi, N_{\phi\theta})/(E_{11}h) \quad (3.44)$$

$$(\bar{M}_\phi, \bar{M}_{\phi\theta}) = (M_\phi, M_{\phi\theta})/(E_{11}h^2) \quad (3.45)$$

Similarly, the nondimensional form of the fundamental system of first order ordinary differential equations for free vibration analysis of an anisotropic laminated composite shell of revolution may be cast in a matrix form as

$$\frac{d}{d\phi} \begin{Bmatrix} \bar{\psi}_1 \\ \bar{\psi}_2 \end{Bmatrix} = [\bar{K}] \begin{Bmatrix} \bar{\psi}_1 \\ \bar{\psi}_2 \end{Bmatrix} \quad (3.46)$$

where  $\bar{K}$  is a 20x20 coefficient matrix, and  $\{\bar{\psi}\}$  is the column vector of nondimensional fundamental variables. The matrix  $\bar{K}$  incorporates the nondimensional natural frequency,  $\bar{\Omega}$  implicitly. When the Equations (3.39) to (3.45) are applied to the Equation (3.37) so as to obtain the Equation (3.46), it is found that the elements of matrix  $\bar{K}$  look as same as the elements of matrix  $K$  in Equation (3.37). They differ in two aspects. The first difference is that all variables in the matrix  $\bar{K}$  are the barred form of the corresponding variables of the matrix  $K$ . The second difference is that the dimensional natural frequency in Equation (3.37) is denoted by  $\omega$  whereas the nondimensional natural frequency in Equation (3.46) is represented with  $\bar{\Omega} = \omega h \sqrt{\rho/E_{11}}$ .

### 3.5 NUMERICAL SOLUTION FOR THE TWO POINT BOUNDARY VALUE PROBLEMS

When a problem involves a system of homogeneous ordinary differential equations like Equation (3.37), we can not solve it numerically without specifying boundary conditions. The nature of boundary conditions determines which numerical methods will be used.

Boundary conditions are divided into two broad categories [70]:

- The initial value problem is a type of boundary value problems in which all the fundamental dependent variables,  $\psi(\phi)$  are given at the some starting value, say at  $\phi_{\min}$ , and it is desired to find  $\psi(\phi)$ 's at some arbitrary point  $\phi$ , or at some discrete list of  $\phi$  coordinates.
- The two point boundary value problem is a type of boundary value problems in which boundary conditions are specified at more than one  $\phi$ , sometimes at two points that give the name. Typically, some of conditions will be specified at  $\phi_{\min}$ , and the remainder at  $\phi_{\max}$ .

Numerical methods for solving the boundary value problems depend on which type they are. For the initial value problems, we consider three major types of practical methods for solving initial value problems for the system of ordinary differential equations:

- (i) single-step methods
- (ii) extrapolation methods (Bulirsch-Stoer methods)
- (iii) multi-step methods

On the other hand, there are two distinct classes of numerical methods for solving two point boundary value problems:

- (i) shooting methods
- (ii) relaxation methods (finite-difference equations)

“The crucial distinction between initial value problems and two point boundary value problems is that in the former case we are able to start an acceptable solution at its beginning (initial values) and just march it along by numerical integration to its end (final values); while in the later case, the boundary conditions at the starting point do not determine a unique solution to start with and a random choice among the solutions that satisfy these (incomplete) starting boundary conditions is almost certain not to satisfy the boundary conditions at the other specified point(s). Thus two point boundary value problems require considerably more effort to solve than done for initial value problems because iteration is needed in general to satisfy these spatially scattered boundary conditions into a single global solution of the system of ordinary differential equations”[70].

The theory of boundary value problems for ordinary differential equations relies rather heavily on the initial value problems. The existence and uniqueness theories for two point boundary value problems are quite complicated than corresponding theories for initial value problems. Therefore, theories of initial value problems are utilized generally in order to derive the theories for two point or general boundary value problems. Moreover, it is a significant fact that initial value problems are used in some of the most generally applicable numerical methods for solving boundary value problems.

In previous sections, it is shown that equations governing the free vibrations of anisotropic laminated composite shells of revolution can be reduced to a system of first order ordinary differential equations. The equation (3.37) represents the dimensional form of this system. Also, nondimensional form of this reduced system is written in the Equation (3.46). Either dimensional system of differential equations or nondimensional system of differential equations together with prescribed boundary conditions at the two edges of the shell constitutes a two point boundary value problem.

Here, if we take into consideration the dimensional system of first order ordinary differential equations for the present study which can be written as

$$\frac{d}{d\phi} \{\psi(\phi)\} = [K(\phi)]\{\psi(\phi)\} \quad (3.47)$$

where  $\{\psi(\phi)\}$  is a (20,1) column matrix which contains 20 unknown dependent variables, and  $K$  is a 20x20 coefficient matrix whose elements have been already given in Appendix F. The unknown dependent variables are the fundamental variables of First Order Shear Deformation Theory by using the Reissner-Naghdi shell theory at any meridional coordinate. The fundamental variables are given completely in Equation (3.38).

The object is to determine the  $\{\psi(\phi)\}$  in the interval  $\phi_{\min} \leq \phi \leq \phi_{\max}$  subject to 10 boundary conditions at each end of the axisymmetric shell. In this regard, some of the fundamental variables in the column vector  $\psi(\phi)$  at each edge of the shell must be prescribed. If edges of the shell are taken as  $\phi = \phi_{\min}$  and  $\phi = \phi_{\max}$  then 10 elements of  $\psi(\phi_{\min})$  and 10 elements of  $\psi(\phi_{\max})$  are considered to be known. For different conservative boundary conditions which are SS=simply supported, C=clamped, and F=free, the prescribed fundamental variables in  $\psi(\phi)$  vary. They are

$$w^0 = u_\theta^0 = \beta_\theta = N_\phi = M_\phi = 0 \quad (3.48)$$

for the case of simply supported boundary conditions,

$$w^0 = u_\phi^0 = u_\theta^0 = \beta_\phi = \beta_\theta = 0 \quad (3.49)$$

for the case of clamped boundary conditions, and

$$Q_\phi = N_\phi = N_{\phi\theta} = M_\phi = M_{\phi\theta} = 0 \quad (3.50)$$

for the case of free boundary conditions.

For the present study, the prescribed boundary conditions of the free vibration analysis of an anisotropic laminated composite axisymmetric shell are

$$\begin{aligned} [w^0(\phi, t)]_{nc} &= [w^0(\phi, t)]_{ns} = [u_\theta^0(\phi, t)]_{nc} = [u_\theta^0(\phi, t)]_{ns} = [\beta_\theta(\phi, t)]_{nc} = \\ [\beta_\theta(\phi, t)]_{ns} &= [N_\phi(\phi, t)]_{nc} = [N_\phi(\phi, t)]_{ns} = [M_\phi(\phi, t)]_{nc} = [M_\phi(\phi, t)]_{ns} = 0 \end{aligned} \quad (3.51)$$

for simply supported boundary conditions,

$$\begin{aligned} [w^0(\phi, t)]_{nc} &= [w^0(\phi, t)]_{ns} = [u_\phi^0(\phi, t)]_{nc} = [u_\phi^0(\phi, t)]_{ns} = [u_\theta^0(\phi, t)]_{nc} = \\ [u_\theta^0(\phi, t)]_{ns} &= [\beta_\phi(\phi, t)]_{nc} = [\beta_\phi(\phi, t)]_{ns} = [\beta_\theta(\phi, t)]_{nc} = [\beta_\theta(\phi, t)]_{ns} = 0 \end{aligned} \quad (3.52)$$

for clamped boundary conditions, and

$$\begin{aligned} [Q_\phi(\phi, t)]_{nc} &= [Q_\phi(\phi, t)]_{ns} = [N_\phi(\phi, t)]_{nc} = [N_\phi(\phi, t)]_{ns} = [N_{\phi\theta}(\phi, t)]_{nc} = \\ [N_{\phi\theta}(\phi, t)]_{ns} &= [M_\phi(\phi, t)]_{nc} = [M_\phi(\phi, t)]_{ns} = [M_{\phi\theta}(\phi, t)]_{nc} = [M_{\phi\theta}(\phi, t)]_{ns} = 0 \end{aligned} \quad (3.53)$$

for free boundary conditions.

Consequently, Equation (3.47) with appropriate boundary conditions at the two edges of the shell represents a two point boundary value problem. A numerical method for this two point boundary value problem is explained in the next section.

### 3.5.1 REDUCTION TO INITIAL VALUE PROBLEMS

In this section, the two point boundary value problem (Equation (3.47)) will be reduced to a series of initial value problems. “The solution for the fundamental variables of a shell of revolution in the Equation (3.47) can be written in the form

$$\{\psi(\phi)\} = [W(\phi)]C \quad (3.54)$$

where  $W(\phi)$  is a 20x20 matrix whose columns represent 20 linearly independent solutions of the homogeneous governing equations, and  $C$  denotes a column matrix of 20 arbitrary constants. The solution is obtained by defining the columns of  $W(\phi)$  as the solutions of 20 initial value problems in the interval  $(\phi_{\min}, \phi_{\max})$  governed by the system of equations in Equation (3.47) and subjected to arbitrary linearly independent initial conditions at  $\phi = \phi_{\min}$ . If the independence requirement is met at  $\phi = \phi_{\min}$ , then the solutions will be independent at any other value of  $\phi$  in the interval  $(\phi_{\min}, \phi_{\max})$ .

Since the only requirement of the columns of  $W(\phi)$  is that they be linearly independent solutions of the system of equations (3.47), in place of  $W(\phi)$  we may employ in the interval  $(\phi_{\min}, \phi_{\max})$  a matrix of linear combinations of the solutions of equations (3.47), which at  $\phi = \phi_{\min}$  reduces to a unit matrix  $I$ . This is done by evaluating Equation (3.54) at  $\phi = \phi_{\min}$ .

$$\{\psi(\phi_{\min})\} = [W(\phi_{\min})]C \quad (3.55)$$

Solving for  $C$

$$C = [W(\phi_{\min})]^{-1} \{\psi(\phi_{\min})\} \quad (3.56)$$

and replacing  $C$  in (3.54) by (3.56) to give

$$\{\psi(\phi)\} = [W(\phi)][W(\phi_{\min})]^{-1} \{\psi(\phi_{\min})\} \quad (3.57)$$

Defining

$$[T(\phi)] = [W(\phi)][W(\phi_{\min})]^{-1} \quad (3.58)$$

The expression for the solution is obtained in the form

$$\{\psi(\phi)\} = [T(\phi)]\{\psi(\phi_{\min})\} \quad (3.59)$$

where  $T(\phi)$  is the transfer matrix of the shell and  $\psi(\phi)$  is a column vector of fundamental dependent variables at any arbitrary  $\phi$ .

It should be noted that if the columns of  $W(\phi)$  are homogeneous solutions of (3.47) then the columns of  $T(\phi)$  are linear combinations of  $W(\phi)$ ; therefore, also homogeneous solutions of (3.47).

Substituting Equation (3.59) into Equation (3.47) the columns of  $T(\phi)$  are given as the solutions of 20 initial value problems

$$\frac{d}{d\phi} \{T(\phi)\} = [K(\phi)]\{T(\phi)\} \quad (3.60)$$

The initial values for  $T(\phi)$  at  $\phi = \phi_{\min}$  is obtained from

$$[T(\phi_{\min})] = [W(\phi_{\min})][W(\phi_{\min})]^{-1} = I \quad (3.61)$$

The elements of the rows of  $T(\phi)$  in Equation (3.60) represent those fundamental variables that are contained in the corresponding rows of  $\psi(\phi)$  in Equation (3.47). It is important to note that the solutions  $T(\phi)$  depend only on the geometric and material properties of the shell given by coefficient matrix  $K(\phi)$  but not on the boundary conditions. The same solutions  $T(\phi)$  can be used for any appropriate boundary conditions imposed at the edges of a given shell. For this reason, the solution of the free vibration problem of a shell of revolution is completely determined by  $T(\phi)$ .

The solution of Equation (3.47) in the interval  $\phi_{\min} \leq \phi \leq \phi_{\max}$  is formally given by Equation (3.59) where  $T(\phi)$  is obtained from the 20 solutions of the initial value problems defined by Equations (3.60) and (3.61). In order to make such a solution also satisfying the prescribed boundary conditions given in section 3.5, one evaluates Equation (3.59) at  $\phi = \phi_{\max}$ ,

$$\{\psi(\phi_{\max})\} = [T(\phi_{\max})]\{\psi(\phi_{\min})\} \quad (3.62)$$

Once  $\{\psi(\phi_{\min})\}$  is known, the solution at any value of  $\phi$  is obtained from Equation (3.59) provided that the values of  $T(\phi)$  at that particular  $\phi$  are stored. This completes the reduction of a two point boundary value problem defined by Equation (3.47) to 20 initial value problems given by Equations (3.60) and (3.61)"[71].

### 3.5.2 METHOD OF SOLUTION FOR A ONE SEGMENT SHELL

"In order to solve Equation (3.47) numerically, at each edge of the shell, that is, at  $\phi = \phi_{\min}$  and  $\phi = \phi_{\max}$ , 10 fundamental variables in  $\psi(\phi_{\min})$  and  $\psi(\phi_{\max})$  must be prescribed as boundary conditions. Therefore, 10 elements of  $\psi(\phi_{\min})$  and 10 elements of  $\psi(\phi_{\max})$  in our case are considered to be known, and the remaining ones in  $\psi(\phi_{\min})$  and  $\psi(\phi_{\max})$  are unknown. Furthermore, we need to arrange the elements of  $\psi(\phi)$  at  $\phi = \phi_{\min}$  and  $\phi = \phi_{\max}$  in such way that the known and unknown fundamental variables of  $\psi(\phi_{\min})$  and  $\psi(\phi_{\max})$  are separated into two partitioned matrices.

When the first 10 elements of  $\psi(\phi_{\min})$ , denoted by  $\psi_1(\phi_{\min})$ , and the last 10 elements of  $\psi(\phi_{\max})$ , denoted by  $\psi_2(\phi_{\max})$ , are determined as the prescribed fundamental variables, the Equation (3.62) can be written as a partitioned matrix product in the form

$$\begin{Bmatrix} \psi_1(\phi_{\max}) \\ \psi_2(\phi_{\max}) \end{Bmatrix} = \begin{bmatrix} T^1(\phi_{\max}) & T^2(\phi_{\max}) \\ T^3(\phi_{\max}) & T^4(\phi_{\max}) \end{bmatrix} \begin{Bmatrix} \psi_1(\phi_{\min}) \\ \psi_2(\phi_{\min}) \end{Bmatrix} \quad (3.63)$$

where the 10 by 10 matrices  $T^j(\phi_{\max})$  are the partitioned matrices of  $T(\phi_{\max})$ . If we assume that for the free vibration  $\psi_1(\phi_{\min}) = \psi_2(\phi_{\max}) = 0$  when basic boundary conditions such as simply supported, clamped or free are applied appropriately at the two edges of shell, then the unknowns  $\psi_2(\phi_{\min})$  are directly obtained from

$$[T^4(\phi_{\max})] \{\psi_2(\phi_{\min})\} = 0 \quad (3.64)$$

The above matrix equation gives a set of linear homogeneous equations with unknown coefficients which are given by  $\{\psi_2(\phi_{\min})\}$ .

Since a nontrivial solution for  $\{\psi_2(\phi_{\min})\}$  is possible if the matrix  $T^4(\phi_{\max})$  is of rank 9, the frequency equation of the system is given by

$$| [T^4(\phi_{\max})] | = 0 \quad (3.65)$$

There exist natural frequencies implicitly in Equation (3.65). The Equation (3.65) is called as characteristics equation of the given system. Once a frequency is found that satisfies Equation (3.65), the corresponding solution for  $\{\psi_2(\phi_{\min})\}$  is obtained from

$$\psi_2^i(\phi_{\min}) = r(-1)^{i+1} |M_i| \quad (3.66)$$

where  $\psi_2^i(\phi_{\min})$  denotes the  $i$ th element of  $\{\psi_2(\phi_{\min})\}$ ,  $r$  is an arbitrary constant, and  $|M_i|$  is the determinant obtained from any [9,10] submatrix of rank 9 contained in  $[T^4(\phi_{\max})]$  by deleting the  $i$ th column. After  $\{\psi_2(\phi_{\min})\}$  is calculated from Equation (3.66), the corresponding mode shapes for a particular natural frequency are found from Equation (3.59). The necessary computation of the matrix

$T(\phi)$  at any  $\phi$  can be done by numerical integration of Equation (3.60) with initial values given by Equation (3.61).

The method so far is essentially a generalization of the one employed in the analysis of axisymmetric vibration of a conical shell in [76]. It works very well for a shell with a relatively short interval  $(\phi_{\min}, \phi_{\max})$ . However, when the length of the meridian of the shell is increased, the elements of  $T(\phi_{\max})$  increase rapidly in magnitude while the value of the frequency determinant does not, and, consequently, an increasing number of significant digits is subtracted out in the process of calculation of the determinant of  $T^4(\phi_{\max})$ . Furthermore, if any required number of significant digits were kept in all initial value integrations, and matrix operations, then the method would give correct solution for any size of the interval  $\phi_{\min} \leq \phi \leq \phi_{\max}$ . However, if only a fixed number of significant digits like in digital computers are kept in the calculation, the solution loses all accuracy beyond a critical length of the interval. The loss of accuracy is not caused by cumulative errors in the integration process, rather caused by the subtraction of almost equal very large numbers. Similarly, because of the large values of the elements of  $T(\phi)$  at large values of  $\phi$ , accuracy is invariably lost when the mode shapes are obtained from Equation (3.59). Therefore, the loss of accuracy of the solution can be avoided and shells of revolution with much larger meridional lengths can be analyzed by means of the direct integration technique if the multisegment method discussed in the next section is used”[71].

### 3.5.3 EXTENSION OF PRESENT METHOD OF SOLUTION TO A MULTISEGMENT SHELL

“Let the shell be divided into  $M$  segments denoted by  $S_i$ , where  $i = 1, 2, \dots, M$ . The coordinates of the ends of the segments are denoted by  $\phi_i$ . The left-hand edge of the shell is at  $\phi = \phi_1$  and the right-hand edge at  $\phi = \phi_{M+1}$ , as shown in Figure 3.1. In analogy to Equation (3.59), the solution within each segment  $S_i$  is given by

$$\{\psi(\phi)\} = [T_i(\phi)]\{\psi(\phi_i)\} \quad (3.67)$$

where  $\{T_i(\phi)\}$  are obtained from the initial value problems defined in  $S_i$  by

$$\frac{d}{d\phi} \{T_i(\phi)\} = [K(\phi)]\{T_i(\phi)\} \quad (3.68)$$

$$\{T_i(\phi_i)\} = I \quad (3.69)$$

Continuity requirements on all fundamental variables at the end point of the segments lead, from Equation (3.67), to

$$\{\psi(\phi_{i+1})\} = [T_i(\phi_{i+1})]\{\psi(\phi_i)\} \quad (3.70)$$

where  $i = 1, 2, \dots, M$ .

Using the partitioned matrix product of as given by Equation (3.63) for the single segment of shell, Equation (3.70) can be written as

$$T_i^1(\phi_{i+1})\psi_1(\phi_i) + T_i^2(\phi_{i+1})\psi_2(\phi_i) - \psi_1(\phi_{i+1}) = 0 \quad (3.71)$$

$$T_i^3(\phi_{i+1})\psi_1(\phi_i) + T_i^4(\phi_{i+1})\psi_2(\phi_i) - \psi_2(\phi_{i+1}) = 0 \quad (3.72)$$

where  $i = 1, 2, \dots, M$ .

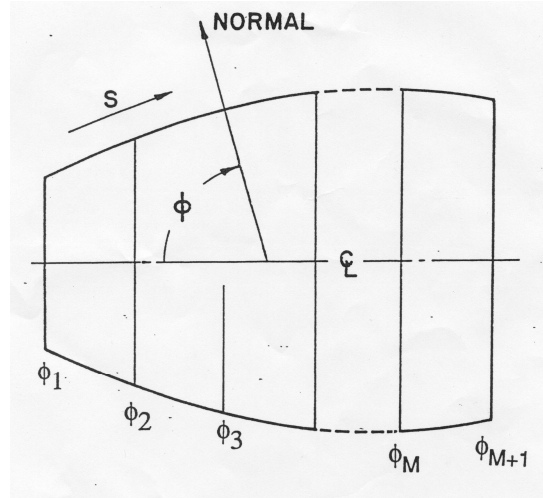


**Figure 3.1** Division of meridional length of the shell of revolution into segments [71].

Equations (3.71) and (3.72) constitute a system of  $2M$  linear homogeneous matrix equations with  $2M$  unknowns:  $\psi_1(\phi_i)$  for  $i = 2, 3, \dots, M + 1$  and  $\psi_2(\phi_{i+1})$  for  $i = 1, 2, \dots, M$ . For free vibration problems, we assume that the prescribed quantities  $\psi_1(\phi_1) = \psi_2(\phi_{M+1}) = 0$  designating

boundary conditions. By means of Gauss elimination, the system of Equations (3.71) and (3.72) are brought to the form

$$\begin{bmatrix} E_1 & -I & 0 & \cdot & \cdot & 0 \\ 0 & C_1 & -I & 0 & \cdot & 0 \\ \cdot & \cdot & \cdot & \cdot & \cdot & \cdot \\ \cdot & \cdot & \cdot & \cdot & \cdot & \cdot \\ 0 & \cdot & \cdot & 0 & E_M & -I \\ 0 & \cdot & \cdot & 0 & 0 & C_M \end{bmatrix} \begin{Bmatrix} \psi_2(\phi_1) \\ \psi_1(\phi_2) \\ \cdot \\ \cdot \\ \psi_2(\phi_M) \\ \psi_1(\phi_{M+1}) \end{Bmatrix} = 0 \quad (3.73)$$

where the (10,10) matrices  $E_1, C_1$  are defined by

$$[E_1] = [T_1^2] \quad (3.74)$$

$$[C_1] = [T_1^4][E_1]^{-1} \quad (3.75)$$

and for  $i = 2, 3, \dots, M$

$$[E_i] = [T_i^2] + [T_i^1][C_{i-1}]^{-1} \quad (3.76)$$

$$[C_i] = ([T_i^4] + [T_i^3])[C_{i-1}]^{-1}[E_i]^{-1} \quad (3.77)$$

A nontrivial solution of the system of Equations (3.73) is possible if the (10, 10) matrix  $C_M$  is of rank 9

$$|[C_M]| = 0 \quad (3.78)$$

and then the solution for elements of  $\{\psi_1(\phi_{M+1})\}$ , denoted by  $\psi_1^i(\phi_{M+1})$ , where  $i = 1, 2, \dots, 10$  is given by

$$\psi_1^i(\phi_{M+1}) = r(-1)^{i+1} |M_i| \quad (3.79)$$

where  $r$  is again an arbitrary constant and the determinant  $|M_i|$  is obtained from any (9,10) submatrix of rank 9 contained in  $C_M$  by deleting the  $i$ th column. Once  $\{\psi_1(\phi_{M+1})\}$  is known, the remaining unknowns can be found successively from Equation (3.73) as

$$\{\psi_2(\phi_M)\} = [E_M]^{-1} \{\psi_1(\phi_{M+1})\} \quad (3.80)$$

and for  $i = 1, 2, \dots, M - 1$

$$\{\psi_1(\phi_{M-i+1})\} = [C_{M-i}]^{-1} \{\psi_2(\phi_{M-i+1})\} \quad (3.81)$$

$$\{\psi_2(\phi_{M-i})\} = [E_{M-i}]^{-1} \{\psi_1(\phi_{M-i+1})\} \quad (3.82)$$

describing the corresponding mode shapes in terms of both displacements, rotations and stress resultants”[71].

### 3.6 FREQUENCY TRIAL METHOD

Frequency trial method is essentially a systematized process of trial and error in which the input to each iteration step is a trial value of the frequency. This method has been successfully applied for the solution of free vibration problem of isotropic shells of revolution by Kalnins [67]. In this study, the frequency trial method is extended to compute the mode shapes and their corresponding natural frequencies of the anisotropic laminated composite shell of revolution with appropriate boundary conditions and given mechanical and geometrical properties.

The frequency trial method is considered to have two main parts. The first part deals with the determination of the system of homogeneous first order ordinary differential equations for the free vibration analysis of an anisotropic laminated composite shell of revolution by using mathematical modeling presented in Chapter 2 in combination with the method of Finite Exponential Fourier Transform given in this chapter. Then, in the second part, the system of differential equations formulated in the first part is reduced to the series of initial value problems, and the shell is divided into segments. After then, the multisegment integration method is carried out to solve the conceived problem numerically to find out the free vibration characteristics. It should be noted that the proposed numerical solution procedure cannot provide free vibration results directly as the undetermined natural frequency  $\omega$  is included in matrix  $K$  in Equation (3.47).

Some steps of the numerical solution method of the second part of the frequency trial method are repeated in order to determine the free vibration characteristics such as natural frequencies and mode shapes. In particular, the determinant of  $C_M$  in Equation (3.78) for the given corresponding natural frequency in the prescribed natural frequency range is needed to be computed iteratively. The subparts of the second part of the Frequency Trial Method are depicted in Figure 3.2.

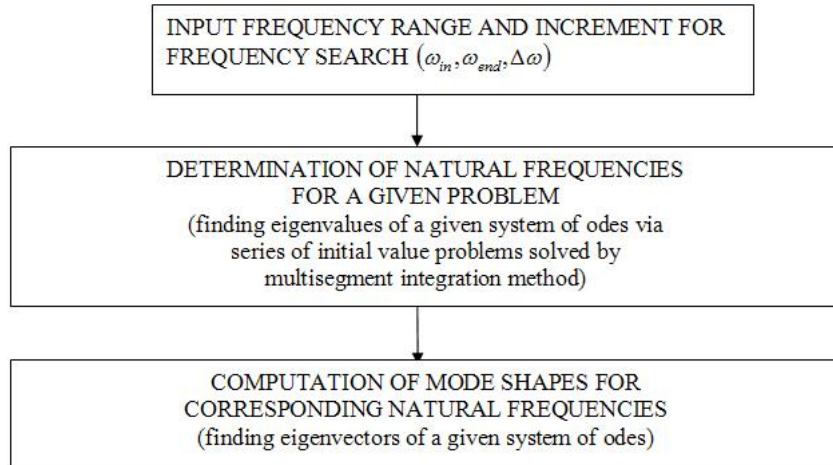


**Figure 3.2** The subparts of the second part of Frequency Trial Method.

It is better to explain how the natural frequency is determined by the second block given in Figure 3.2 with an example. Consider a single layer simply supported isotropic circular cylindrical shell. It has the following mechanical and geometrical properties such that Young's modulus, density, Poisson's ratio, thickness, radius, length are given as  $E = 10.145 \text{ Mpa}$ ,  $\rho = 2.5338 \times 10^4 \text{ kg/m}^3$ ,  $\nu = 0.33$ ,  $h = 0.05 \text{ cm}$ ,  $R = 10 \text{ cm}$ ,  $L = 20 \text{ cm}$ , respectively. The first natural frequency  $\omega_1$  for circumferential wave number  $n = 1$  is calculated as  $11972.28 \text{ rad/sec}$  by using traditional Fourier Decomposition procedure. The frequency search is started with an initial value. Then the determinant of the given trial frequency is calculated. The behavior of calculated determinant of the given natural frequency is examined. For our example, some natural frequencies with their computed determinant in order to find the first natural frequency of the problem for  $n=1$  are given in Table 3.1.

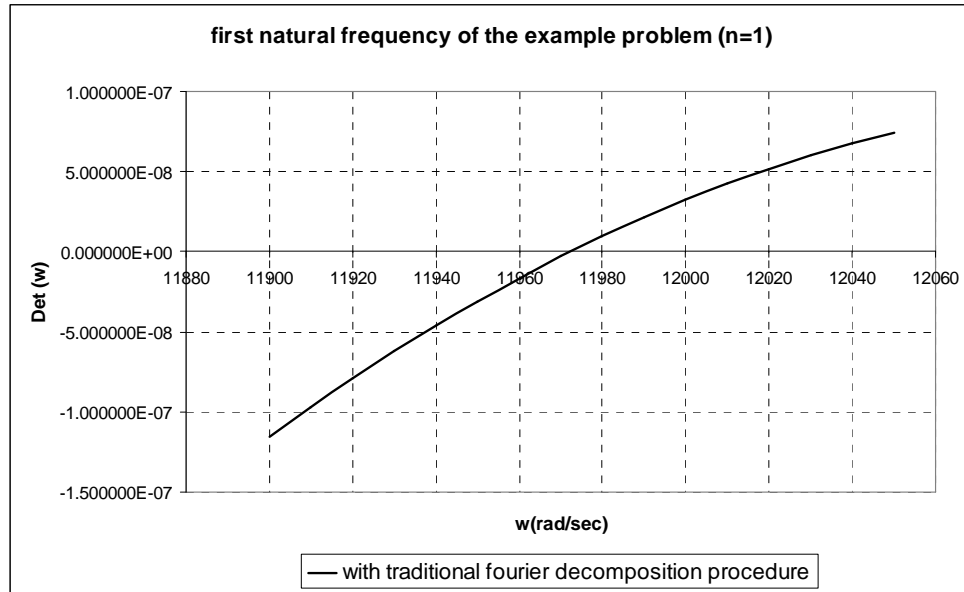
Whenever the determinant changes sign, in our case its sign changes from negative to positive, a relatively small frequency range is determined around the first natural frequency, then a standard Regula-Falsi root determination routine is employed to find the first natural frequency accurately. The standard Regula-Falsi root determination procedure can be studied from [69]. Furthermore, the geometric representation of behavior of natural frequency versus computed determinant is given in Figure 3.3a with traditional Fourier Decomposition procedure used as a method of solution.

In our study, as presented in this chapter, the method of Finite Exponential Fourier Transform is employed in order to decouple the fundamental variables of free vibration analysis of an

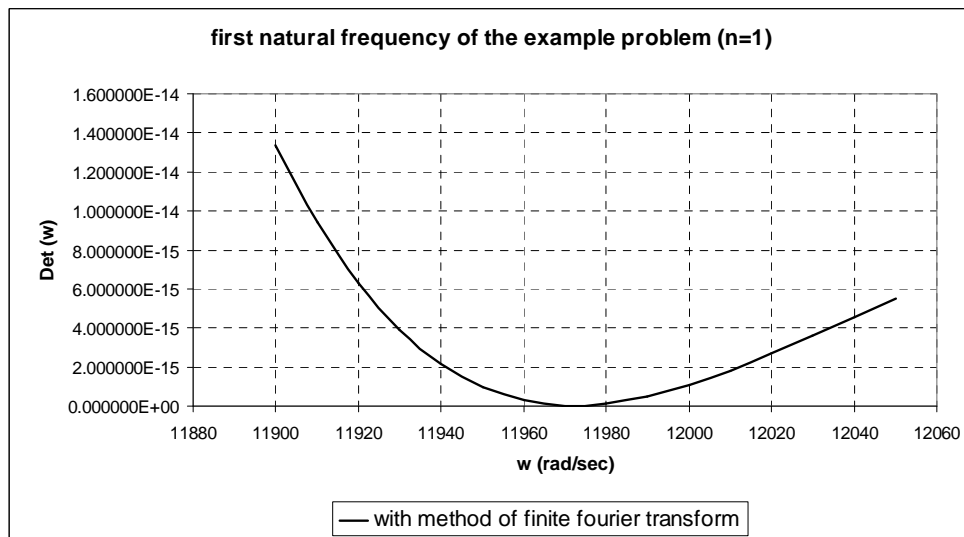
anisotropic laminated composite axisymmetric shell. In our example, there is no coupling effect; however, it is also solved using the Method of Finite Exponential Fourier Transform. The dimension of the system of first order differential equations for free vibration analysis of the isotropic single layer circular cylindrical shell is 10 by 10 using traditional Fourier Decomposition procedure whereas it becomes 20 by 20 after the application of Method of Finite Exponential Fourier Transform. A Fortran program which is prepared to calculate the free vibration characteristics of anisotropic laminated composite circular cylindrical shells is run in the frequency range of (11900,12050) for our example which was already solved by the classical Fourier decomposition method of solution. The values of the trial natural frequencies and their computed determinants using Method of Finite Exponential Fourier Transform are given in Table 3.2. The first natural frequency for  $n=1$  is found to be  $\omega = 11972.39 \text{ rad/sec}$  with the method of Finite Exponential Fourier Transform. The graphical representation of them is shown in Figure 3.3b.

**Table 3.1** Trial natural frequencies and their computed determinants in order to find first natural frequency of the example problem with traditional Fourier Decomposition procedure.

Trial Natural Frequencies $\omega$ (rad/sec)	Corresponding computed determinants $\det(\omega)$
11900	-1.156926E-07
11910	-9.704969E-08
11920	-7.924888E-08
11930	-6.229280E-08
11940	-4.618408E-08
11950	-3.092539E-08
11960	-1.651947E-08
11970	-2.969108E-09
11980	9.722855E-09
11990	2.155352E-08
12000	3.251994E-08
12010	4.261911E-08
12020	5.184795E-08
12030	6.020336E-08
12040	6.768214E-08
12050	7.428107E-08



(a)



(b)

**Figure 3.3** Finding first natural frequency of the example problem with (a)traditional Fourier Decomposition Method, and (b) Method of Finite Exponential Fourier Transform.

Comparison of the determinants in Tables 3.1 and 3.2 reveal that the determinant values given in Table 3.2 is the square of the corresponding values given in Table 3.1. Graphically, this is clearly seen in Figure 3.3(b). Proof of this is demonstrated in Appendix G for a generic two-point boundary value problem composed of 2 fundamental variables.

**Table 3.2** Trial natural frequencies and their computed determinants in order to find first natural frequency of the example problem with method of Finite Exponential Fourier Transform.

Trial Natural Frequencies $\omega$ (rad/sec)	Corresponding computed determinants $\det(\omega)$
11900	1.338479E-14
11910	9.418642E-15
11920	6.280386E-15
11930	3.880393E-15
11940	2.132969E-15
11950	9.563798E-16
11960	2.728929E-16
11970	8.815602E-18
11980	9.453392E-17
11990	4.645544E-16
12000	1.057547E-15
12010	1.816388E-15
12020	2.688210E-15
12030	3.624444E-15
12040	4.580872E-15
12050	5.517678E-15

Based on Figure 3.3, it can be said that in order to determine the root by the application of Finite Exponential Fourier Transform Method (doubling the total number of equations), standard Regula-falsi method can not be applied. Rather a slope change algorithm is necessary to pin the natural frequency as shown in Figure 3.3(b).

In the present study, a computer code, DALSOR is developed in FORTRAN 77. The DALSOR stands for (Dynamic Analysis of Anisotropic Laminated Shells of Revolution). The DALSOR performs the following main tasks:

- Multisegment numerical integration of the equations of general anisotropic shells of revolution (Equations 3.37 or 3.46).
- Determination of the characteristic matrix  $C_M$  given in Equation 3.78.
- A slope change algorithm to determine the natural frequency which is graphically shown in Figure 3.3(b) for a particular example.
- Mode shape determination algorithm to determine the displacements, rotations and force/moment resultants across the shell meridional axis.

In addition to the above mentioned main blocks, the slope change algorithm is also modified such that the method for the determination of the natural frequency is brought into a form to which classical regula-falsi method can be applied easily. This method actually makes use of the fact that the values of the determinant of the characteristic matrix determined by the Finite Exponential Fourier Transform Method is square of the value of the determinant of the characteristic matrix obtained by the traditional Fourier decomposition procedure for the same shell and for the same trial frequency. Notice that as it is seen in Figure 3.3, one can actually take the square root of the determinant of Figure 3.3(b) and switch signs of the determinant either above or below the root, and employ the traditional Regula-falsi method to pin the natural frequency. This way, much faster convergence to the root can be achieved by employing standard Regula-falsi method to Figure 3.3(a) as compared to the slope change algorithm employed in Figure 3.3(b).

### **3.7 DESCRIPTION AND FLOW-CHART OF THE DEVELOPED CODE, DALSOR**

The developed code DALSOR (Dynamic Analysis of Anisotropic Laminated Shells of Revolution) is written in Fortran 77 in order to determine the free vibration characteristics; namely, mode shapes and their corresponding natural frequencies, of the anisotropic laminated composite shells of revolution. The DALSOR has 3 main programs and 8 subprograms. Laminate, Natural Frequency, Mode Shape are the main programs. The flow-chart of Laminate and Natural Frequency programs, and the flow-chart of Mode Shape Program of the developed FORTRAN code DALSOR is given in Figure 3.4, and Figure 3.5, respectively. Among the 8 subprograms, one external subprogram, DIVPAG, is called as an external subroutine in both Natural Frequency and Mode Shape Programs. DIVPAG carries out the numerical integration of Equation (3.60). DIVPAG is a subroutine of the IMSL FORTRAN Numerical Libraries v.5. DIVPAG solves initial-value problems for ordinary differential equations using either Adams-Moulton's or Gear's BDF method. The Adams-Moulton's method is chosen to take numerical integration of Equation (3.60) in the DALSOR. The IMSL FORTRAN Numerical Libraries v.5, which is a product of Visual Numerics Inc. [77], is a collection of FORTRAN routines and functions useful in mathematical analysis research and application development.

The DALSOR is based on the computational model discussed in the Chapter 2. The computational model is the Reissner-Naghdi shell theory with transverse shear deformation effects included. It also includes full anisotropic form of constitutive equation based on lamination theory. The governing equations of free vibration analysis of an anisotropic laminated composite shell of revolution are derived in the Chapter 2. In the current chapter, the method of solution for those governing equations is presented. One can refer to the previous section for the tasks performed by the DALSOR. Generally speaking, the main capabilities of the developed code DALSOR have been

already given in the section 1.3.2 of Chapter 1.

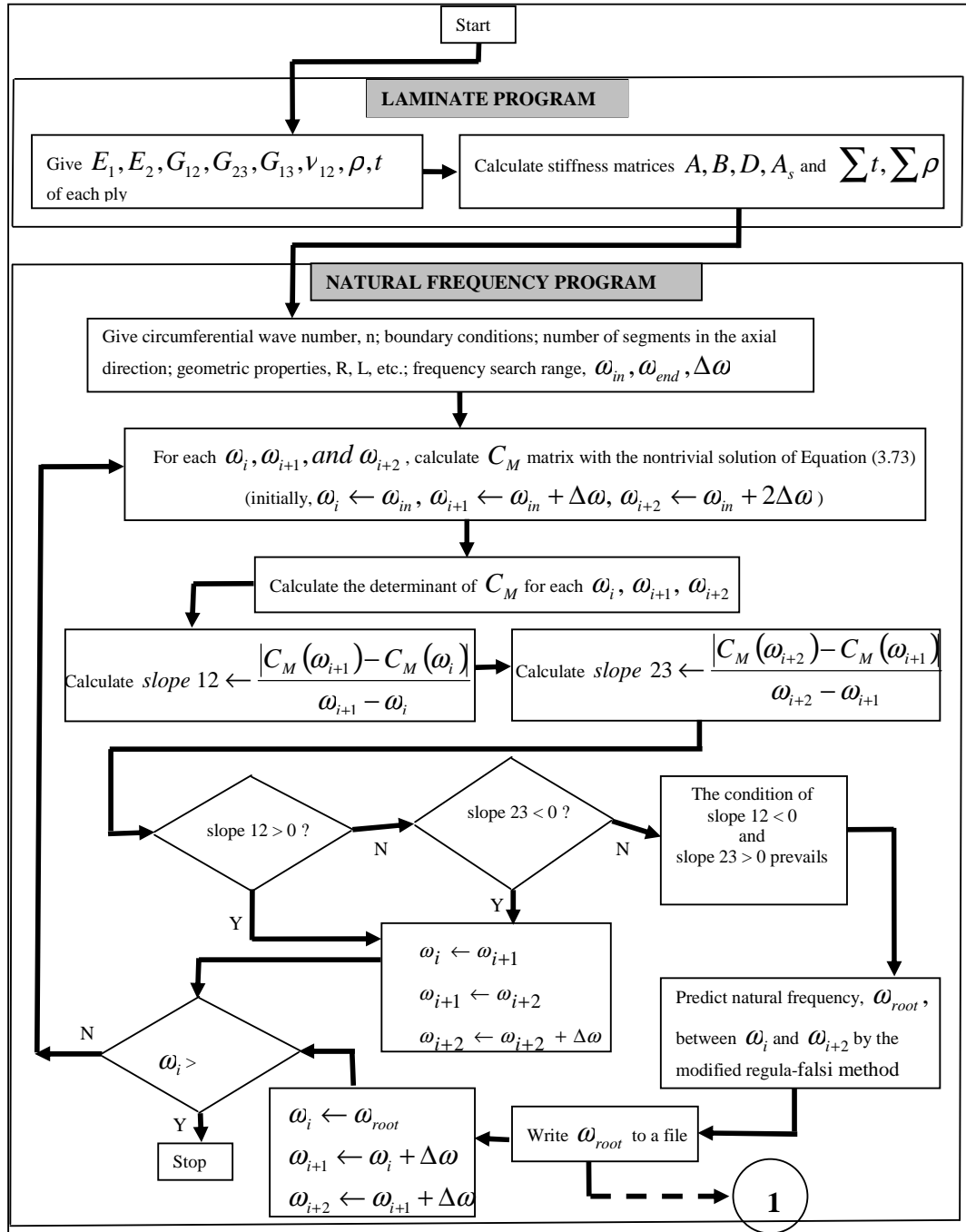


Figure 3.4 Flow-chart of Laminate and Natural Frequency Programs of the DALSOR.

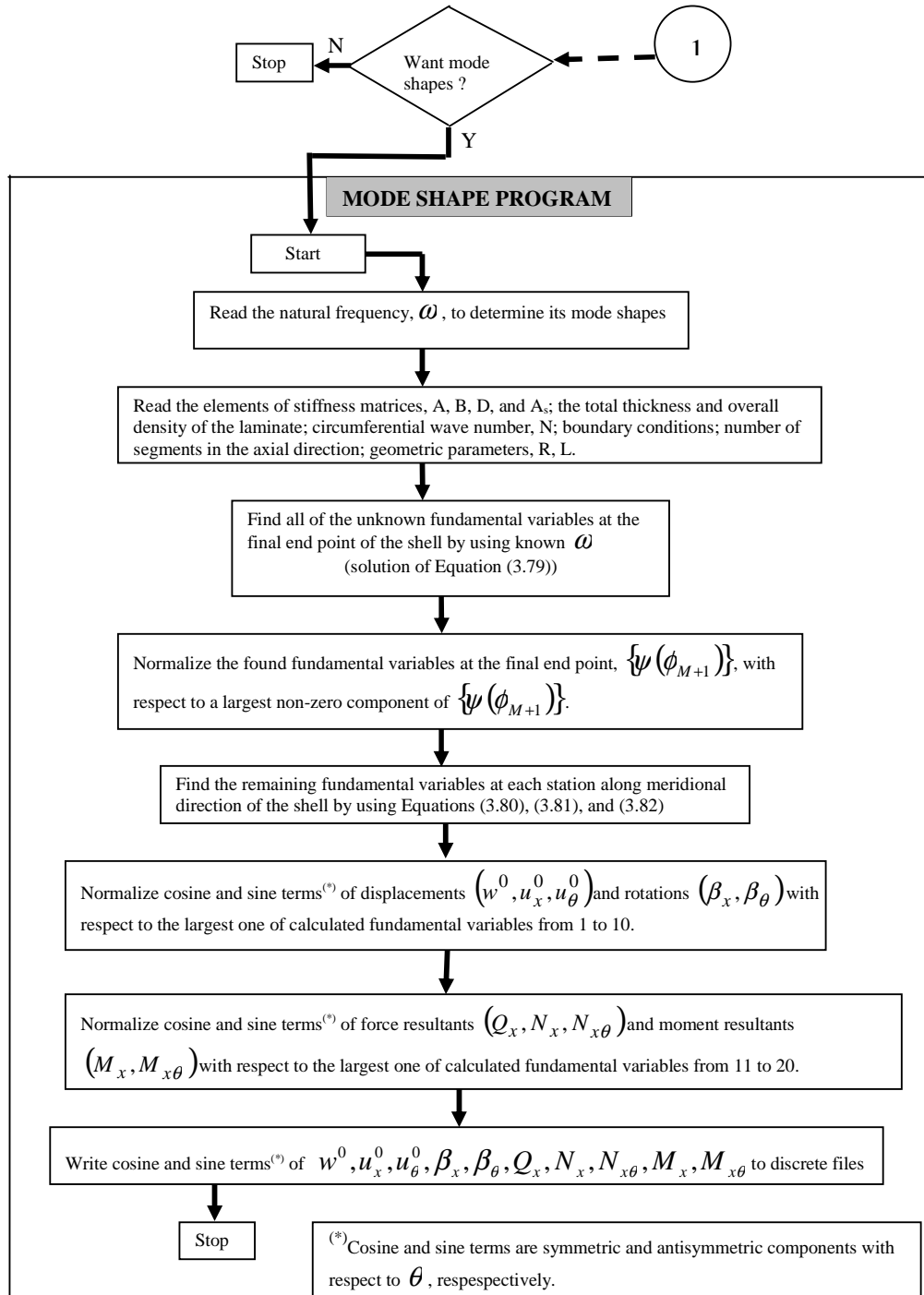


Figure 3.5 Flow-chart of Mode Shape Program of the DALSOR.

## CHAPTER 4

### NUMERICAL RESULTS AND DISCUSSIONS

#### 4.1 INTRODUCTION

In the previous two chapters, the governing equations for free vibration analysis of an anisotropic laminated composite shell of revolution and solution procedure to those equations were presented. A computer code named DALSOR (Dynamic Analysis of Anisotropic Laminated Shells of Revolution) is developed so as to determine the free vibration characteristics; namely natural frequencies and their mode shapes, of the anisotropic laminated composite shell of revolution. In this chapter, numerical results produced with the developed code DALSOR are presented and discussed. It can be seen from the coefficient matrix  $K$  in Equations (3.47) and (3.60) that the free vibration characteristics are dependent on the boundary conditions at each edges of the shell, circumferential wave number, laminate properties, material and geometrical properties of the shell. The laminated composite circular cylindrical shell, which is the one of laminated composite shells of revolution mostly studied in the literature, is taken as an illustrative example in this thesis in order to investigate the effects of primarily fiber orientation angle, stacking sequence, boundary conditions at the edges of the shell, thickness-to-radius ratio on the natural frequencies of a laminated composite circular cylindrical shell. Therefore, studies are carried out for the following cases:

- For comparison of present method of solution with the exact method of solution, a simply supported single layer orthotropic circular cylindrical shell.
- The variation of fiber orientation angle in a simply supported laminated composite circular cylindrical shell.
- The laminated composite circular cylindrical shell having six different stacking sequence:  $[0_2/90_2/\pm 45_2]_s$ ,  $[0_2/\pm 45_2/90_2]_s$ ,  $[\pm 45_2/0_2/90_2]_s$ ,  $[\pm 45_2/90_2/0_2]_s$ ,  $[90_2/\pm 45_2/0_2]_s$ ,  $[90_2/0_2/\pm 45_2]_s$ .
- (i) Boundary condition: Clamped-Clamped  
Thickness to radius ratio: approximately 0.01
- (ii) Boundary condition: Clamped-free  
Thickness to radius ratio: approximately 0.01

- The laminated composite circular cylindrical shell having six different stacking sequence:  $[0_2/90_2/\pm 45_2]_k$ ,  $[0_2/\pm 45_2/90_2]_k$ ,  $[\pm 45_2/0_2/90_2]_k$ ,  $[\pm 45_2/90_2/0_2]_k$ ,  $[90_2/\pm 45_2/0_2]_k$ ,  $[90_2/0_2/\pm 45_2]_s$ 
  - (i) Boundary condition: Clamped-Clamped  
Thickness to radius ratio: approximately 0.1
  - (ii) Boundary condition: Clamped-free  
Thickness to radius ratio: approximately 0.1
- The simply supported laminated composite circular cylindrical shell with symmetrical, antisymmetrical and unsymmetrical laminate schemes for the purpose of identifying the coupling effects.
- The laminated composite spherical shell with clamped-free (CF) boundary condition.

In the following section, the laminated composite circular cylindrical shell is described before the presentation of the numerical results for free vibration analysis of the anisotropic laminated composite circular cylindrical shell.

## 4.2 LAMINATED COMPOSITE CIRCULAR CYLINDRICAL SHELL

Static and dynamic analysis of circular cylindrical shells built up composite materials are mostly studied by the researchers. The ease of manufacturing and widespread usage of circular cylindrical shells made of advanced composite materials as a primary and secondary structural components in various structural applications, especially in aeronautical and space structures, are undoubtedly the reasons for those studies.

The governing equations for the free vibration analysis of anisotropic laminated composite shells of revolution are derived in Chapter 2. The strain-displacement relations are given from Equation (2.286) to Equation (2.298), the constitutive equations from Equation (2.299) to (2.310), and the equations of motion from Equation (2.311) to Equation (2.315). Thereafter, those governing equations are reduced to a system of first-order differential equations given by Equation (3.37). This system of first-order differential equations for general shells of revolution can be transformed into circular cylindrical shells by applying the following scheme

$$\begin{aligned}
 \frac{1}{R_\phi} \frac{\partial}{\partial \phi} &\rightarrow \frac{\partial}{\partial x}, \\
 R_\phi &\rightarrow \infty, \\
 R_\theta &\rightarrow R, \\
 \phi &\rightarrow x \text{ and } \theta \rightarrow \theta
 \end{aligned}
 \tag{4.1}$$

where  $R$  is the mean radius of laminated composite circular cylindrical shell.

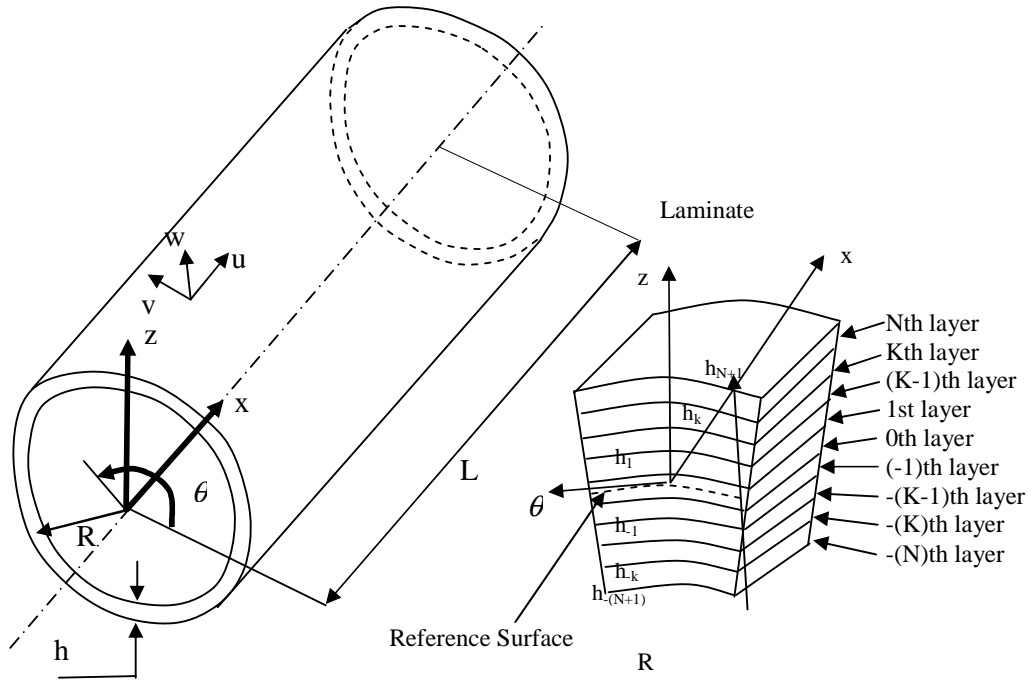


**Figure 4.1** General Configuration and Coordinate System of Laminated Composite Circular Cylindrical Shell and its Laminate.

General configuration and coordinate system of laminated composite circular cylindrical shell and its laminate used in the numerical results of free vibration analysis are shown in Figure 4.1.  $x, \theta,$  and  $z$  denote the axial, circumferential, and thickness coordinates, respectively. Also,  $R, h, u, v,$  and  $w$  denote the mean radius, laminate total thickness, axial displacement, circumferential displacement, and transverse displacement of the laminated composite circular cylindrical shell, respectively.

The circular cylindrical shell is known to vibrate axisymmetrically when the circumferential wave number,  $n$ , is zero. Also, it undergoes asymmetrical vibration when the value of circumferential wave number is equal to or greater than one. Figure 4.2 shows the mode shapes of a simply supported circular cylindrical shell when the axial wave number,  $m$ , changing from one to three, and the circumferential wave number,  $n$ , changing from zero to four.

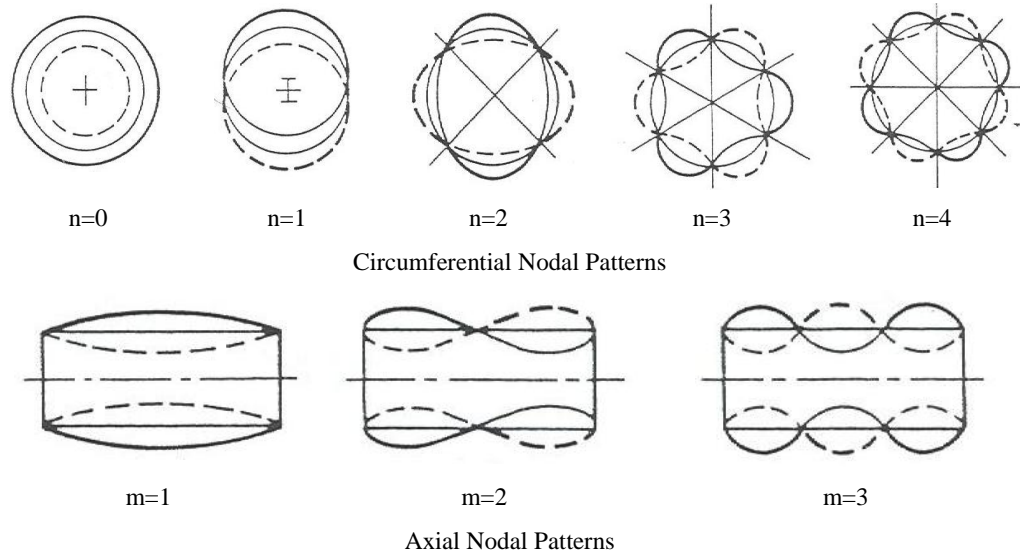


**Figure 4.2** Circumferential Nodal Patterns and Axial Nodal Patterns for a Simply Supported Circular Cylindrical Shell without axial constraint [78].

In the particular case of axisymmetric vibrational motion, the displacements are only functions of the axial or meridional coordinate,  $x$ . Two systems of equations can be obtained. The first one is the torsional system. It is a function of the circumferential displacement  $V$ , and the rotation of the transverse normal about  $x$  coordinate  $\beta_\theta$ , and the torsional system gives zero mode shapes of  $U, W, \text{ and } \beta_x$ . The other system which is a function of the axial displacement  $U$ , the transverse displacement  $W$ , and the rotation of the transverse normal about  $\theta$  coordinate  $\beta_x$ , is called non-torsional system. The non-torsional system gives zero mode shapes of  $V$  and  $\beta_\theta$ .

### 4.3 VERIFICATION OF THE DALSOR

In order to show the accuracy and efficiency of the numerical results obtained by developed code

DALSOR for the free vibration analysis of anisotropic laminated composite shells of revolution, one case study is conducted. This study is a comparison study of the present method of solution presented in Chapter 3 with an exact method of solution in [13].

#### 4.3.1 VERIFICATION OF THE PRESENT METHOD OF SOLUTION

In this section, the comparison study of the present method of solution presented in Chapter 3

with an exact method of solution is carried out with a single layer simply supported specially orthotropic circular cylindrical shell. Soedel [13] gives the exact solution for the free vibrations of circular cylindrical shell which is simply supported at  $x = 0$ , and  $x = L$  in the section 5.5 of his book. The geometrical and material properties of the problem studied in this subsection are given in Table 4.1. It should be noted that the same shell theory is used in DALSOR as that of Soedel [13]. In addition, Soedel's solution can only be produced for a special boundary condition case; simply supported, at both ends. Soedel's solution is exact for the shell theory used. However, the assumptions of the shell theory do still exist there.

**Table 4.1** Geometrical and material properties of the single layer, simply supported circular cylindrical shell used in comparison study of the method of solution.

Geometrical properties		Mechanical Properties [52]	
Radius [m]	0.1	$E_1$ [GPa]	206.9
Meridional Length [m]	0.22	$E_2$ [GPa]	18.62
Thickness [m]	0.002	$G_{12}$ [Gpa]	4.48
		$G_{13}$ [Gpa]	4.48
		$G_{23}$ [Gpa]	2.24
		$\nu_{12}$	0.28
		$\rho$ [kg/m <sup>3</sup> ]	2048

Figure 4.3 shows the comparison of natural frequencies calculated by the exact method of solution [13] with those calculated by the present method of solution from  $n=0$  to  $n=10$  for three lowest natural frequencies which correspond to each  $n$ . For brevity, these three lowest natural frequencies are depicted as  $m=1, 2,$  and  $3$  in the tables and figures in this section and in this chapter. The numerical values of Figure 4.3 is given in Table 4.2. It can be clearly seen from Figure 4.3 and relative percentage difference values in Table 4.2 that the natural frequencies of the single layer simply supported specially orthotropic circular cylindrical shell obtained with the DALSOR are in good agreement with the results of the exact method of solution for the axial wave numbers,  $m$ , from one to three and the circumferential wave numbers,  $n$ , from zero to ten.

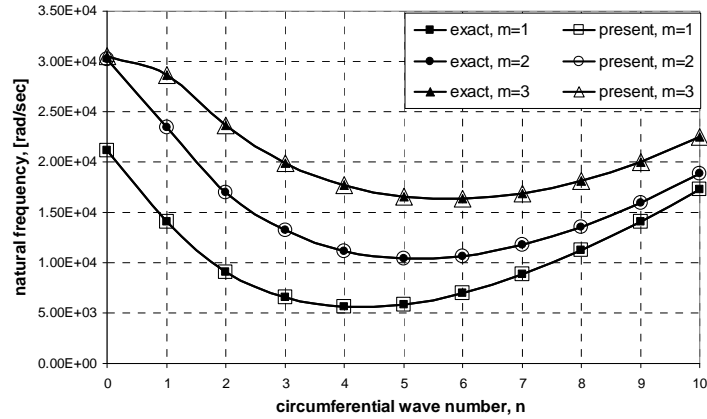


**Figure 4.3** The comparison of natural frequencies calculated by the exact method of solution [13] with those calculated by the present method of solution from  $n=0$  to  $n=10$  for  $m=1, 2,$  and  $3.$

**Table 4.2** Natural Frequencies (rad/sec) calculated with DALSOR as the present method of solution and calculated with the exact solution in [13] and the relative % differences between them for  $m=1-3$  and  $n=0-10.$

	<b>m</b>	<b>exact method of solution</b>	<b>present method of solution</b>	<b>relative % diff.*</b>		<b>m</b>	<b>exact method of solution</b>	<b>present method of solution</b>	<b>relative % diff.*</b>
<b>n=0</b>	1	21120.355	21120.454	4.67E-04	<b>n=1</b>	1	14010.545	14010.631	6.16E-04
	2	30169.964	30169.890	2.47E-04		2	23410.345	23410.411	2.83E-04
	3	30513.722	30513.671	1.70E-04		3	28636.483	28636.522	1.38E-04
<b>n=2</b>	1	9045.061	9044.961	1.11E-03	<b>n=3</b>	1	6575.209	6575.114	1.45E-03
	2	16986.293	16986.364	4.23E-04		2	13222.606	13222.522	6.35E-04
	3	23619.471	23619.371	4.20E-04		3	19943.890	19943.838	2.57E-04
<b>n=4</b>	1	5587.279	5587.187	1.66E-03	<b>n=5</b>	1	5809.237	5809.143	1.62E-03
	2	11179.295	11179.346	4.51E-04		2	10377.671	10377.756	8.19E-04
	3	17683.947	17684.035	4.99E-04		3	16542.672	16542.771	6.01E-04
<b>n=6</b>	1	7009.775	7009.709	9.39E-04	<b>n=7</b>	1	8903.127	8902.972	1.74E-03
	2	10611.252	10611.171	7.68E-04		2	11726.976	11726.982	4.91E-05
	3	16315.327	16315.386	3.59E-04		3	16881.355	16881.475	7.08E-04
<b>n=8</b>	1	11298.669	11298.815	1.29E-03	<b>n=9</b>	1	14100.779	14100.932	1.08E-03
	2	13563.910	13563.753	1.16E-03		2	15981.332	15981.455	7.68E-04
	3	18153.247	18153.116	7.26E-04		3	20051.677	20051.775	4.88E-04
<b>n=10</b>	1	17262.576	17262.716	8.09E-04	* relative percentage difference $rel. \% diff. = \frac{ (exact sol.) - (present sol.) }{(exact sol.)} \times 100$				
	2	18878.118	18877.979	7.36E-04					
	3	22503.035	22502.875	7.08E-04					

## 4.4 CASE STUDIES

After performing comparison study of the present method of solution to check the efficiency and accuracy of the DALSOR, we will investigate the effects of the fiber orientation angle, the stacking sequence, the boundary conditions, the thickness-to-radius ratios in the following sections.

### 4.4.1 CASE STUDY ON THE EFFECT OF FIBER ORIENTATION ANGLE

The free vibration characteristics are determined for each case while changing the fiber orientation angle in the laminate from 0 degree to 90 degrees with the increment of 10 degrees in the present case study. The simply supported laminated circular cylindrical shell is used and its geometrical, mechanical and laminate properties are given in Table 4.3.

**Table 4.3** Geometrical, material properties, and laminate properties of the simply supported laminated composite circular cylindrical shell used for the case study on the fiber orientation angle.

Geometrical properties		Mechanical Properties of E-glass/Epoxy[55]	
Radius [m]	0.1	$E_1$ [GPa]	38.704963
Meridional Length [m]	0.22	$E_2=E_3$ [GPa]	8.293963
Thickness [m]	0.002	$G_{12}$ [Gpa]	4.146981
<b>Laminate Properties</b>		$G_{13}$ [Gpa]	4.146981
		$G_{23}$ [Gpa]	4.146981
Ply thickness [m]	0.0005	$\nu_{12} = \nu_{13} = \nu_{23}$	0.26
Layup	$[\alpha/\alpha]_s$ , where $\alpha$ changes from 0 to 90 with the increment of 10 degree	$\rho$ [kg/m <sup>3</sup> ]	2550.60

When ply stacking sequence, material, and geometry (ply thickness) are symmetric about the midplane of the laminate like in this case, the laminate is called a symmetric laminate. For a symmetric laminate, the upper half through the laminate thickness is a mirror image of the lower half. Hence, in our case, the stacking sequence of  $[\alpha/\alpha]_s$  is a short display of the present symmetric laminate of  $[\alpha/\alpha/\alpha/\alpha]$ . The subscript “s” stands for symmetric.

First of all, we will investigate the effect of the variation of the fiber orientation angle on laminate stiffness coefficients such as the extensional stiffness coefficients,  $A_{ij}$  (Equation(2.243)) ;

the bending-stretching coupling coefficients,  $B_{ij}$  (Equation(2.244)) ; the bending stiffness coefficients,  $D_{ij}$  (Equation(2.245)) ; and the transverse shear stiffness coefficients,  $As_{ij}$  (Equation(2.246)). The extensional stiffness coefficients,  $A_{ij}$  depend only the thicknesses and stiffnesses of the plies but not on their placement through the thickness. On the other hand, the bending stiffness coefficients,  $B_{ij}$ , and the transverse shear stiffness coefficients,  $As_{ij}$  depend not only on the layer thicknesses and stiffnesses but also on their location relative to the midplane. Dependency on the layer thicknesses, stiffnesses and their location relative to the midplane is also valid for the bending-stretching coupling coefficients.

When the laminate is a symmetric laminate, all terms of the bending-stretching coupling coefficients  $B_{ij}$  become zero due to the symmetry of the layer transformed reduced stiffness coefficients,  $(\bar{Q}_{ij})_k$ , distances,  $\zeta_k$ , and thicknesses  $h_k$  about the midplane of the laminate for every layer or ply. From production point of view, symmetrical laminates do not have the tendency to twist from the thermally induced contractions that occur during cooling following the curing process.

The effect of the fiber orientation angle on the coefficients of the stretching stiffness, the transverse shear stiffness and the bending stiffness are shown in Figures 4.4, 4.5 and 4.6, respectively for this case study. Since the laminate used in this section is a symmetric laminate, all coefficients of the bending-stretching coupling stiffness,  $B_{ij}$  are zero. As seen in Figure 4.4, the value of the coefficient  $A_{11}$  decreases as the fiber orientation angle  $\alpha$  increases. In contrast, the value of the  $A_{22}$  increases as  $\alpha$  increases.  $A_{66}$  is zero when  $\alpha = 0^\circ$ , then has its maximum value when  $\alpha = 45^\circ$ , and becomes zero when  $\alpha = 90^\circ$ . It can be seen that the coupling coefficient  $A_{16}$  is maximum at approximately  $\alpha = 30^\circ$ . In addition, the  $A_{26}$  takes its maximum value at approximately  $\alpha = 60^\circ$ . From Figure 4.5, the transverse shear coefficients,  $A_{44}, A_{45}, A_{55}$  keep constant due to the same values of  $G_{13}$  and  $G_{23}$ . Variation of bending stiffness coefficients  $D_{ij}$  follow the similar variation as extensional stiffness coefficients, and they are shown in Figure 4.6.

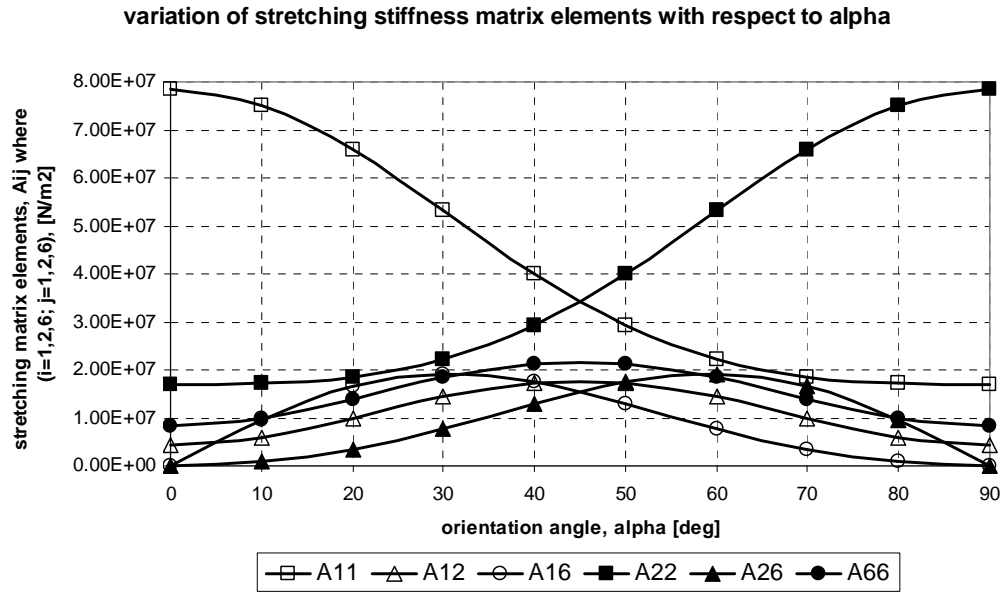


**Figure 4.4** Effect of the fiber orientation angle on the elements of stretching stiffness matrix.

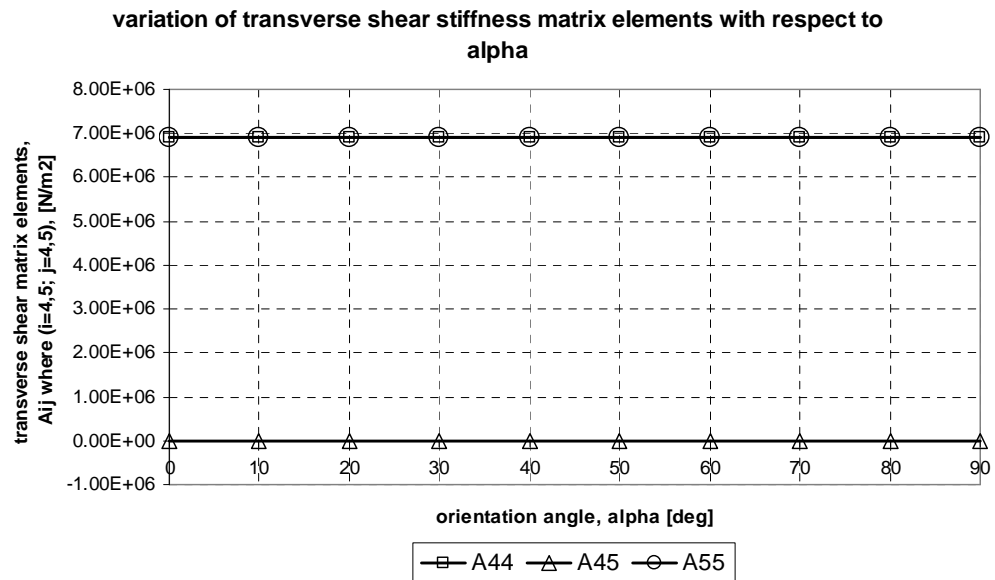


**Figure 4.5** Effect of the fiber orientation angle on the elements of transverse shear stiffness matrix.

variation of flexural stiffness matrix elements with respect to alpha

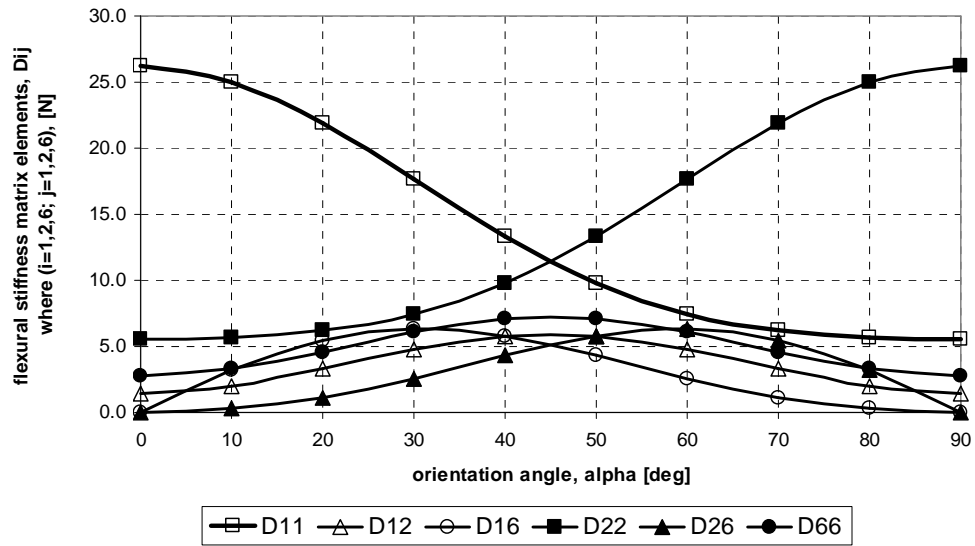


Figure 4.6 Effect of the fiber orientation angle on the elements of flexural stiffness matrix.

Natural frequencies (rad/sec) when the fiber orientation angle changes from 0° to 90° with the increment of 10 degrees for the first three lowest frequency modes (for m=1,2, and 3) are given in Tables 4.4, 4.5, 4.6, 4.7, 4.8, 4.9, 4.10, 4.11, 4.12, 4.13, and 4.14 for n=0-10, respectively.

Table 4.4 Natural Frequencies (rad/sec) when the fiber orientation angle changing from 0 to 90 with the increment of 10 degrees for n=0, and m=1,2, and 3.

n=0										
m	$\alpha = 0$	$\alpha = 10$	$\alpha = 20$	$\alpha = 30$	$\alpha = 40$	$\alpha = 50$	$\alpha = 60$	$\alpha = 70$	$\alpha = 80$	$\alpha = 90$
1	18023	18045	18137	18207	18305	18396	18449	18421	18300	18209
2	18121	18110	18163	18539	19398	20827	22929	24898	25512	25610
3	18208	18509	18609	18707	19872	21648	24143	27073	31619	36417

**Table 4.5** Natural Frequencies (rad/sec) when the fiber orientation angle changing from 0 to 90 with the increment of 10 degrees for n=1, and m=1,2, and 3.

n=1										
m	$\alpha = 0$	$\alpha = 10$	$\alpha = 20$	$\alpha = 30$	$\alpha = 40$	$\alpha = 50$	$\alpha = 60$	$\alpha = 70$	$\alpha = 80$	$\alpha = 90$
1	11153	11209	11376	11582	11695	11650	11494	11327	11222	11191
2	12751	13120	14142	15371	15970	15927	15235	14102	13133	12751
3	15976	16129	16618	17586	18565	19113	19706	20667	21915	22608

**Table 4.6** Natural Frequencies (rad/sec) when the fiber orientation angle changing from 0 to 90 with the increment of 10 degrees for n=2, and m=1,2, and 3.

n=2										
m	$\alpha = 0$	$\alpha = 10$	$\alpha = 20$	$\alpha = 30$	$\alpha = 40$	$\alpha = 50$	$\alpha = 60$	$\alpha = 70$	$\alpha = 80$	$\alpha = 90$
1	7076	7091	7110	7077	6940	6691	6378	6077	5857	5775
2	12561	12812	13473	14168	14493	14487	14348	14201	14082	14025
3	15547	15731	16365	17533	18407	18681	18942	19530	20330	20762

**Table 4.7** Natural Frequencies (rad/sec) when the fiber orientation angle changing from 0 to 90 with the increment of 10 degrees for n=3, and m=1,2, and 3.

n=3										
m	$\alpha = 0$	$\alpha = 10$	$\alpha = 20$	$\alpha = 30$	$\alpha = 40$	$\alpha = 50$	$\alpha = 60$	$\alpha = 70$	$\alpha = 80$	$\alpha = 90$
1	4805	4752	4620	4451	4271	4096	3938	3811	3728	3698
2	9868	10122	10698	11168	11251	10966	10469	9944	9546	9394
3	13456	13724	14580	15815	16480	16358	15892	15439	15143	15035

**Table 4.8** Natural Frequencies (rad/sec) when the fiber orientation angle changing from 0 to 90 with the increment of 10 degrees for n=4, and m=1,2, and 3.

n=4										
m	$\alpha = 0$	$\alpha = 10$	$\alpha = 20$	$\alpha = 30$	$\alpha = 40$	$\alpha = 50$	$\alpha = 60$	$\alpha = 70$	$\alpha = 80$	$\alpha = 90$
1	3725	3681	3601	3557	3571	3635	3726	3826	3908	3941
2	8070	8294	8740	9023	8991	8692	8248	7794	7455	7329
3	11793	12108	13039	14159	14621	14295	13522	12665	12009	11761

**Table 4.9** Natural Frequencies (rad/sec) when the fiber orientation angle changing from 0 to 90 with the increment of 10 degrees for n=5, and m=1,2, and 3.

n=5										
m	$\alpha = 0$	$\alpha = 10$	$\alpha = 20$	$\alpha = 30$	$\alpha = 40$	$\alpha = 50$	$\alpha = 60$	$\alpha = 70$	$\alpha = 80$	$\alpha = 90$
1	3619	3625	3683	3842	4099	4425	4790	5157	5459	5583
2	7094	7300	7702	7984	8051	7947	7753	7550	7402	7347
3	10707	11043	11972	12963	13321	12985	12237	11399	10747	10499

**Table 4.10** Natural Frequencies (rad/sec) when the fiber orientation angle changing from 0 to 90 with the increment of 10 degrees for n=6, and m=1,2, and 3.

n=6										
m	$\alpha = 0$	$\alpha = 10$	$\alpha = 20$	$\alpha = 30$	$\alpha = 40$	$\alpha = 50$	$\alpha = 60$	$\alpha = 70$	$\alpha = 80$	$\alpha = 90$
1	4274	4321	4486	4793	5231	5776	6402	7071	7670	7938
2	6888	7092	7525	7931	8223	8422	8574	8721	8858	8915
3	10233	10577	11485	12420	12816	12647	12153	11591	11162	11002

**Table 4.11** Natural Frequencies (rad/sec) when the fiber orientation angle changing from 0 to 90 with the increment of 10 degrees for n=7, and m=1,2, and 3.

n=7										
m	$\alpha = 0$	$\alpha = 10$	$\alpha = 20$	$\alpha = 30$	$\alpha = 40$	$\alpha = 50$	$\alpha = 60$	$\alpha = 70$	$\alpha = 80$	$\alpha = 90$
1	5419	5488	5715	6118	6697	7440	8337	9353	10327	10799
2	7371	7577	8060	8613	9145	9653	10167	10714	11224	11443
3	10360	10702	11595	12545	13089	13206	13093	12949	12881	12867

**Table 4.12** Natural Frequencies (rad/sec) when the fiber orientation angle changing from 0 to 90 with the increment of 10 degrees for n=8, and m=1,2, and 3.

n=8										
m	$\alpha = 0$	$\alpha = 10$	$\alpha = 20$	$\alpha = 30$	$\alpha = 40$	$\alpha = 50$	$\alpha = 60$	$\alpha = 70$	$\alpha = 80$	$\alpha = 90$
1	6889	6972	7239	7719	8429	9377	10572	11980	13389	14108
2	8410	8616	9138	9813	10553	11344	12216	13199	14166	14609
3	11038	11374	12256	13261	14002	14451	14767	15110	15492	15671

**Table 4.13** Natural Frequencies (rad/sec) when the fiber orientation angle changing from 0 to 90 with the increment of 10 degrees for n=9, and m=1,2, and 3.

<b>n=9</b>										
m	$\alpha = 0$	$\alpha = 10$	$\alpha = 20$	$\alpha = 30$	$\alpha = 40$	$\alpha = 50$	$\alpha = 60$	$\alpha = 70$	$\alpha = 80$	$\alpha = 90$
1	8614	8707	9009	9566	10415	11587	13109	14955	16851	17843
2	9871	10076	10626	11399	12320	13380	14621	16077	17560	18277
3	12191	12521	13397	14469	15415	16199	16955	17822	18725	19146

**Table 4.14** Natural Frequencies (rad/sec) when the fiber orientation angle changing from 0 to 90 with the increment of 10 degrees for n=10, and m=1,2, and 3.

<b>n=10</b>										
m	$\alpha = 0$	$\alpha = 10$	$\alpha = 20$	$\alpha = 30$	$\alpha = 40$	$\alpha = 50$	$\alpha = 60$	$\alpha = 70$	$\alpha = 80$	$\alpha = 90$
1	10564	10668	11009	11650	12651	14068	15950	18276	20704	21992
2	11662	11868	12443	13303	14396	15728	17358	19325	21368	22392
3	13742	14068	14946	16089	17234	18347	19549	20968	22448	23154

For the first three lowest frequency modes, the variation of natural frequency with respect to circumferential wave number is plotted in Figures 4.7, 4.8, and 4.9 for m=1,2, and 3, respectively. It is seen that natural frequencies initially decrease with n until a certain circumferential mode, after then the natural frequencies increase with n. This general behavior is common in shells and referred to by Warburton in [79]. It was shown in [79] that bending strain energy associated with vibratory motion increases with n whereas stretching strain energy decreases with n. Therefore, the total strain energy curve shows a somewhat parabolic form having a minimum at a particular circumferential mode. Figure 7 of [79] is given in Figure 4.10 which displays the strain energy variation of a particular cylindrical shell. This general behavior was observed for all fiber orientation cases given in Figures 4.7, 4.8, and 4.9 for the lowest frequency modes. It should also be stressed that as n gets larger, we have 2n number of nodes in the circumferential direction (see Figure 4.2). These nodes actually correspond to points of zero displacement. Considering that bending energy dominates at high n values, we should expect higher natural frequencies for shells which are circumferentially stiffer. This effect is clearly seen in Figures 4.7, 4.8, and 4.9. In the portions of the graphs where bending strain energy dominates (after a certain n), it is seen that as the fiber orientation angle  $\alpha$  is made more circumferential, the natural frequencies increase with the largest difference in natural frequencies being between  $\alpha = 90^{\circ}$  and  $\alpha = 0^{\circ}$ .

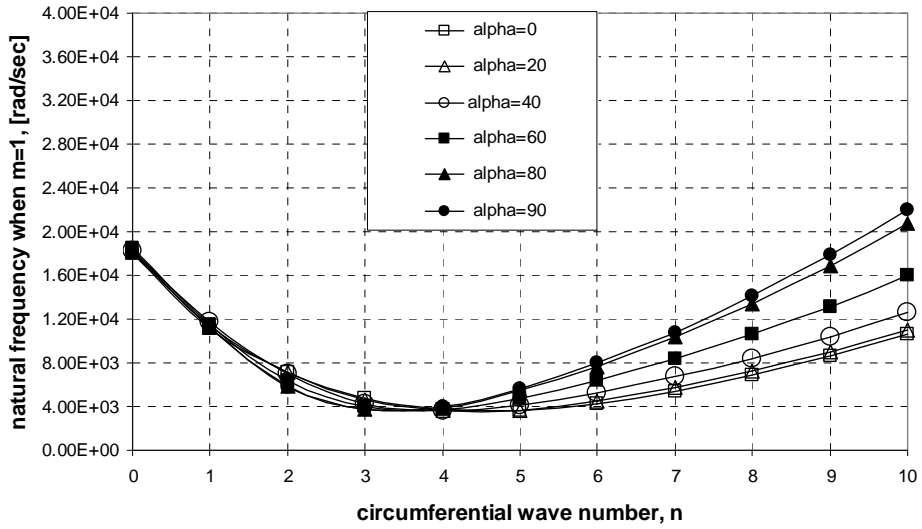


**Figure 4.7** Natural Frequency versus circumferential wave number changing from 0 to 10 for fiber orientation angle of  $0^\circ$  to  $90^\circ$  with the increment of 20 degrees when  $m=1$ .

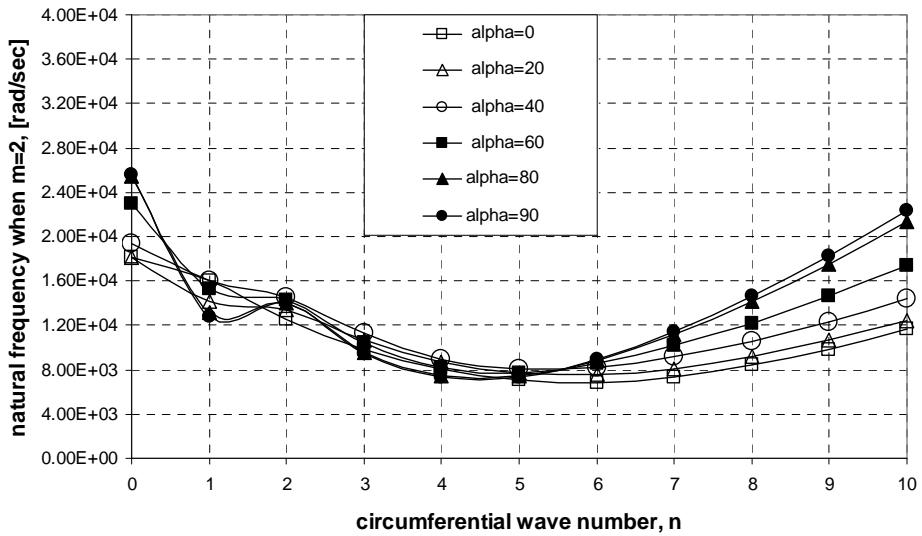


**Figure 4.8** Natural Frequency versus circumferential wave number changing from 0 to 10 for fiber orientation angle of  $0^\circ$  to  $90^\circ$  with the increment of 20 degrees when  $m=2$ .

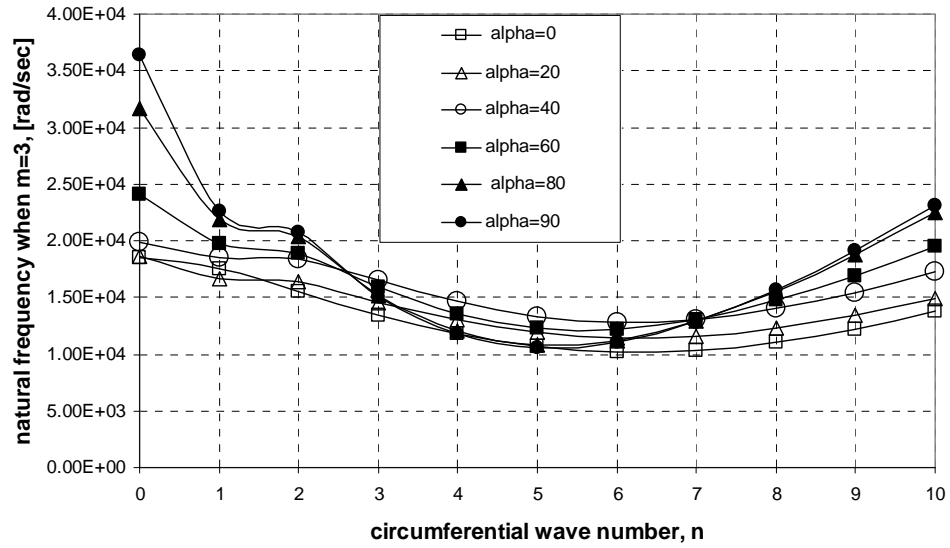


**Figure 4.9** Natural Frequency versus circumferential wave number changing from 0 to 10 for fiber orientation angle of  $0^\circ$  to  $90^\circ$  with the increment of 20 degrees when  $m=3$ .

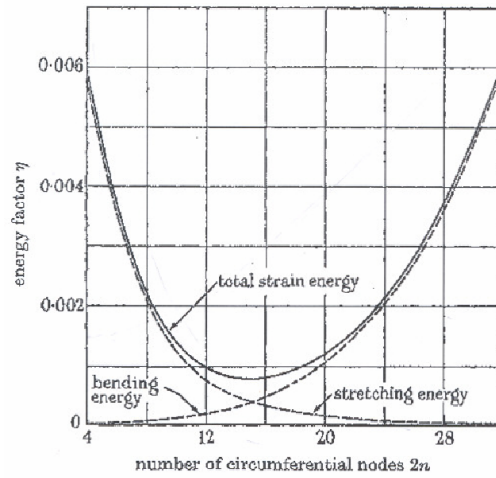


**Figure 4.10** Variation in strain energy in a particular cylindrical shell with increasing number of circumferential modes [79].

Natural frequency versus fiber orientation angle is plotted for  $m=1, 2,$  and  $3$  in Figures 4.11, 4.12, and 4.13, respectively for different values of the circumferential wave number ranging from 0 to 10.

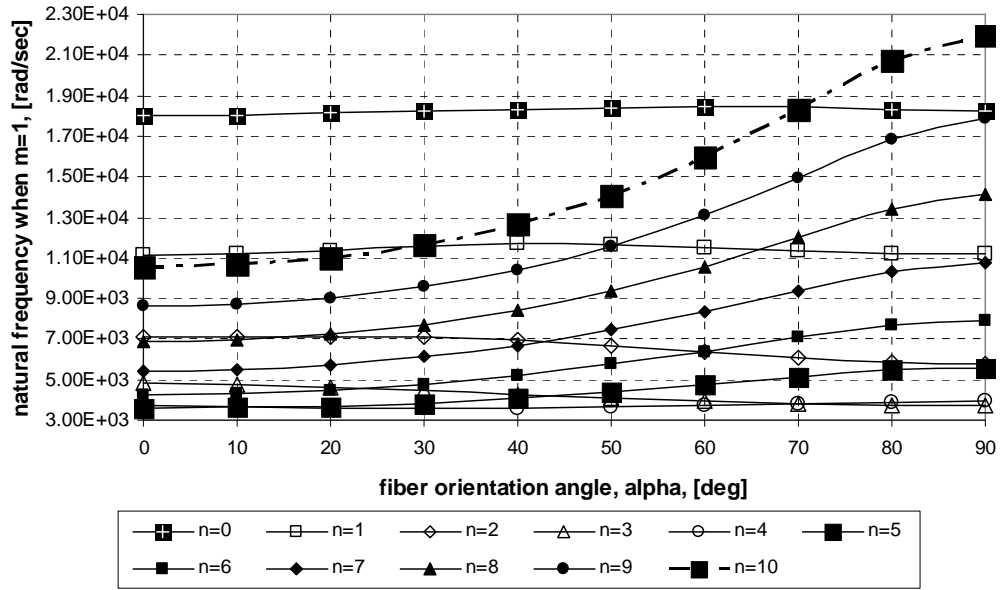


Figure 4.11 Natural Frequency versus fiber orientation angle for the first lowest fundamental mode ( $m=1$ ).

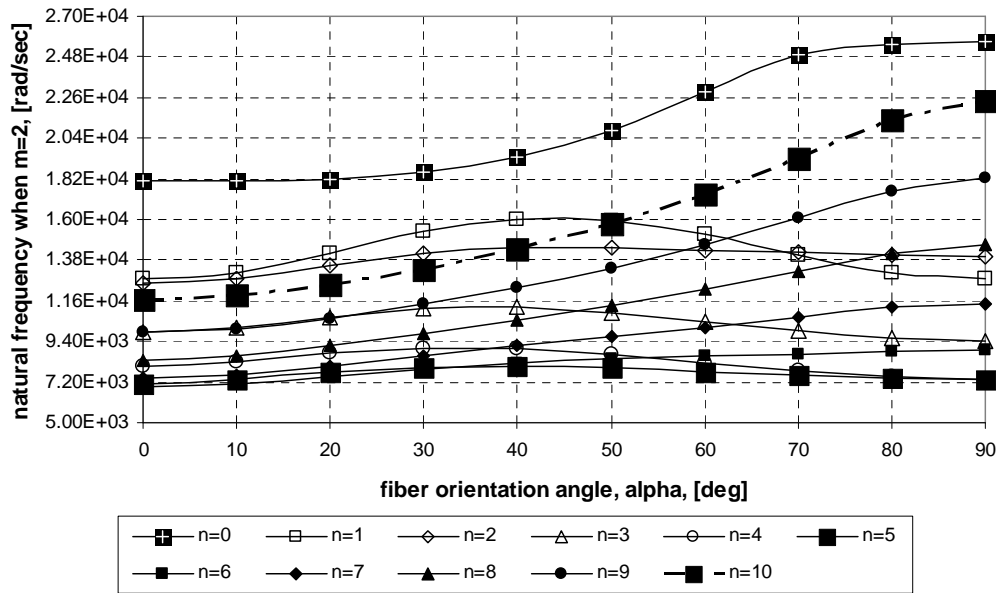
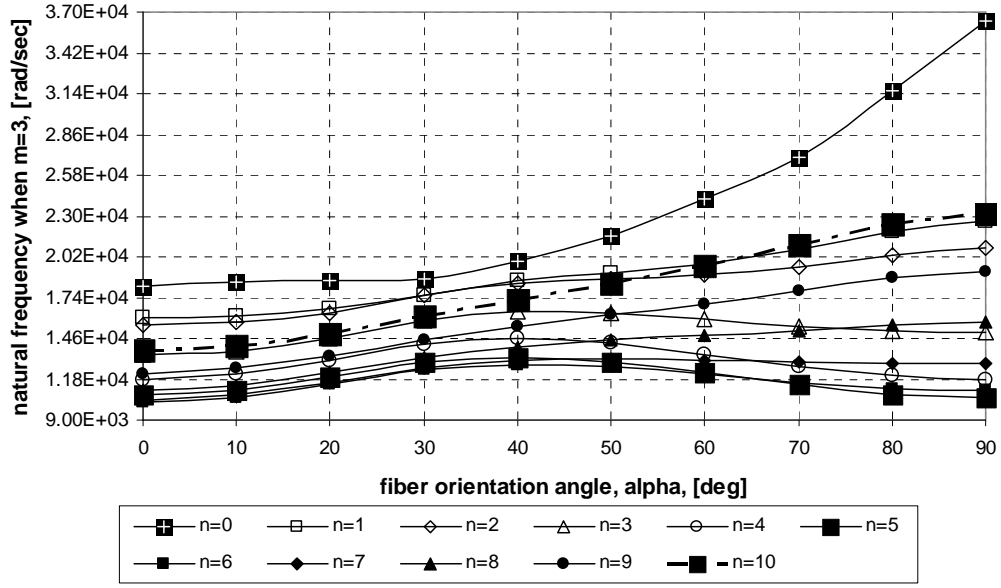


Figure 4.12 Natural Frequency versus fiber orientation angle for the second lowest fundamental mode ( $m=2$ ).



**Figure 4.13** Natural Frequency versus fiber orientation angle for the third lowest fundamental mode ( $m=3$ ).

Figures 4.11, 4.12, and 4.13 show that for asymmetric modes ( $n>0$ ), after a certain circumferential wave number there is a marked increase in natural frequencies as the fiber orientation angle approaches  $90^\circ$ . If one were to take a slice of cylinder and unwrap, it would resemble to a beam with high number of nodes for large  $n$ . Thus, by orienting the fibers in the circumferential direction we would actually make this beam stiffer and for high number of nodes along the circumference, this would result in a marked increase in natural frequency compared to axial fiber orientation case. It can be deduced that for large  $n$ , bending strain energy dominates, a shell with fibers oriented in the circumferential direction would have a much higher bending stiffness compared to a shell with axial fiber orientation leading to a marked increase in natural frequency. On the other hand, as  $n$  gets lower, the stretching strain energy also becomes dominant and the effect of fiber orientation angle on the natural frequencies decrease.

It is also noted that for  $n=0$ , axisymmetric vibration case, most of the first three lowest natural frequency modes were transverse displacement dominant. Since  $n=0$ , these modes actually correspond to breathing modes. It has been observed that for the breathing modes as we go to higher axial bending modes ( $m=1, 2, 3$ ), the effect of fiber orientation becomes significant again with increasing natural frequencies as the fibers are oriented in the circumferential direction.

However, it is warned that for the lower circumferential modes, especially axisymmetric mode ( $n=0$ ), due to high contribution of the extensional strain energy to the total strain energy, the lowest natural frequencies may also turn out to be axial displacement  $u_x$  or circumferential

displacement  $u_\theta$  dominant, as well, depending on boundary conditions, material and geometrical properties of the shell. In those cases the effect of fiber orientation angle may be different from the breathing mode case. Therefore, different conclusions can be inferred with regard to the effect of fiber orientation angle on the natural frequencies of low n modes depending on dominant displacement mode. For instance, for n=1 in Table 4.5 m=2 case, natural frequencies corresponding to different fiber orientation angle conditions have extensional displacement ( $u_x$ ) dominant modes. On the other hand, the first (m=1) and the third (m=3) lowest frequency modes for n=1 are transverse displacement ( $w$ ) dominant modes.

Mode shapes for the first fundamental transverse mode corresponding to three different circumferential modes; namely n=1,2, and 3, are given in Figures 4.14, 4.15, and 4.16, respectively. It should be noted that, as explained in section 3.3.2, the application of method of the finite exponential Fourier transform to the first order system of partial differential equations yields 20 first order ordinary differential equations in terms of cosine and sine Fourier components as the fundamental variables.

The magnitude of the fundamental variables is constructed using Equation (4.2)

$$(w\_mag)_n = \sqrt{(w\_c)_n^2 + (w\_s)_n^2} \quad (4.2)$$

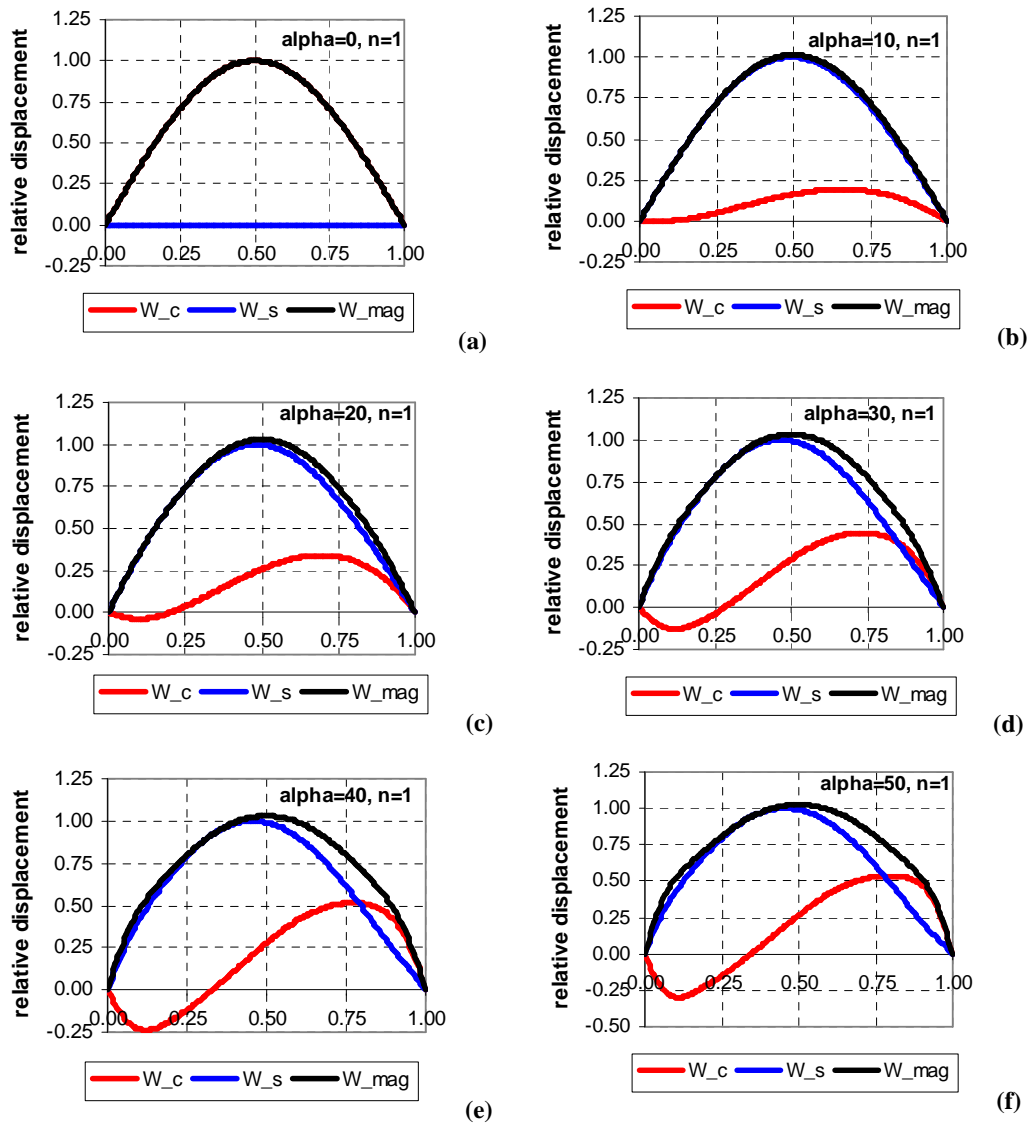
where the Equation (4.2) is written for the finite exponential transform of the transverse displacement as an example. Equation (4.2) lets us calculate the actual finite exponential transform of the transverse displacement from its cosine and sine Fourier components for any particular circumferential wave number.

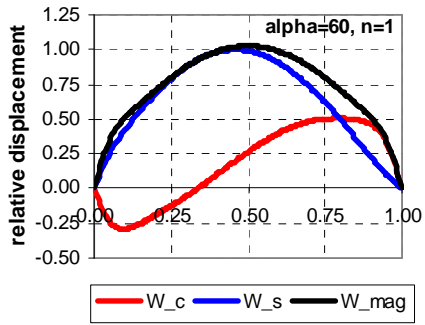
Figures 4.14, 4.15, and 4.16 give the mode shape for the transverse displacement, which corresponds to the fundamental frequency (m=1), for different fiber orientation angles. On the same figures, the cosine and sine Fourier components are also plotted since they are actually the output the mode shape program of the DALSOR.

Notice that  $\alpha = 0^\circ$  corresponds to the orthotropic case since we have a symmetric laminate. This case is shown in Figures 4.14-16 (a). For this case, it is seen that sine Fourier component is zero as it should be. This fact can be studied in [13]. Increase in fiber orientation angle results in nonzero sine and cosine Fourier components. Notice that although the sine and cosine Fourier components are not symmetric with respect to midspan of the symmetric configured circular cylindrical shell, the actual finite exponential transform of the transverse displacement determined by Equation (4.2) is symmetric with respect to the midspan of the same shell as it should be.

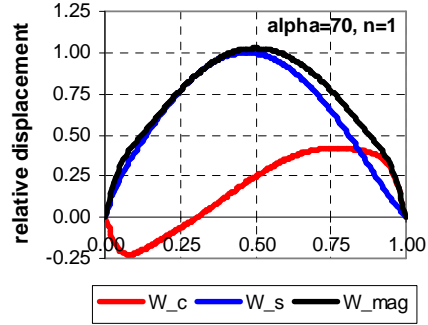
Mode shape algorithm developed within the scope of the thesis determines the sine and cosine Fourier components along the meridional direction of the shell for all fundamental variables. Once they are determined, the actual finite exponential transform of the each fundamental variable is determined by calculating the magnitude.

Figures 4.14, 4.15, and 4.16 are intended to demonstrate that for different circumferential wave numbers, the finite exponential transform of the transverse displacement is indeed symmetric with respect to midspan of the symmetric configured shell for all fiber orientation angle cases.

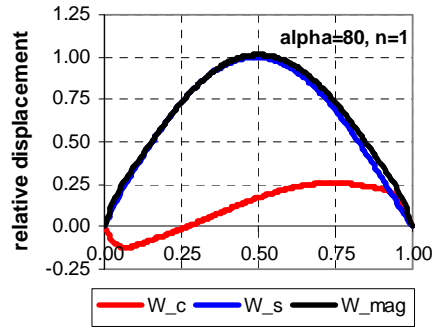




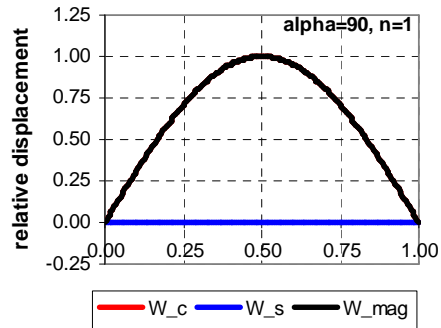
(g)



(h)

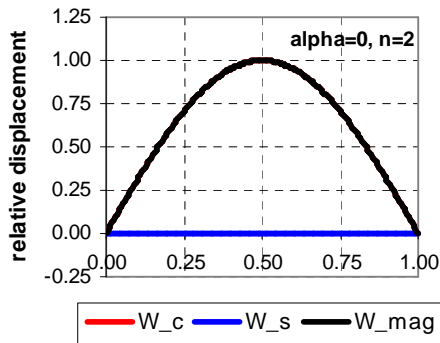


(i)

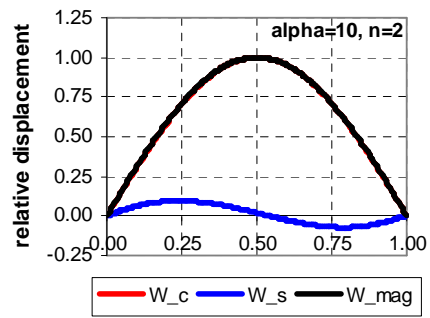


(j)

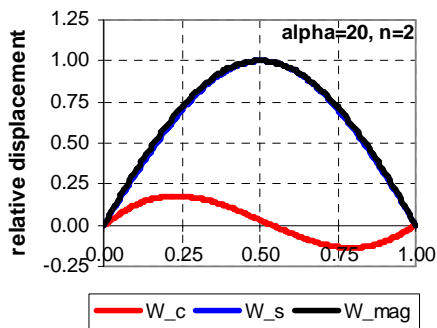
Figure 4.14 Mode shapes for the first fundamental transverse mode when  $\alpha$  changes from  $0^\circ$  to  $90^\circ$  with the increment of  $10^\circ$  ( $n=1$ ).



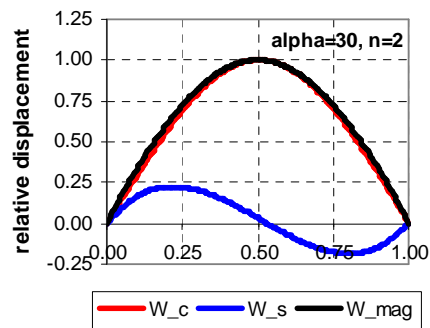
(a)



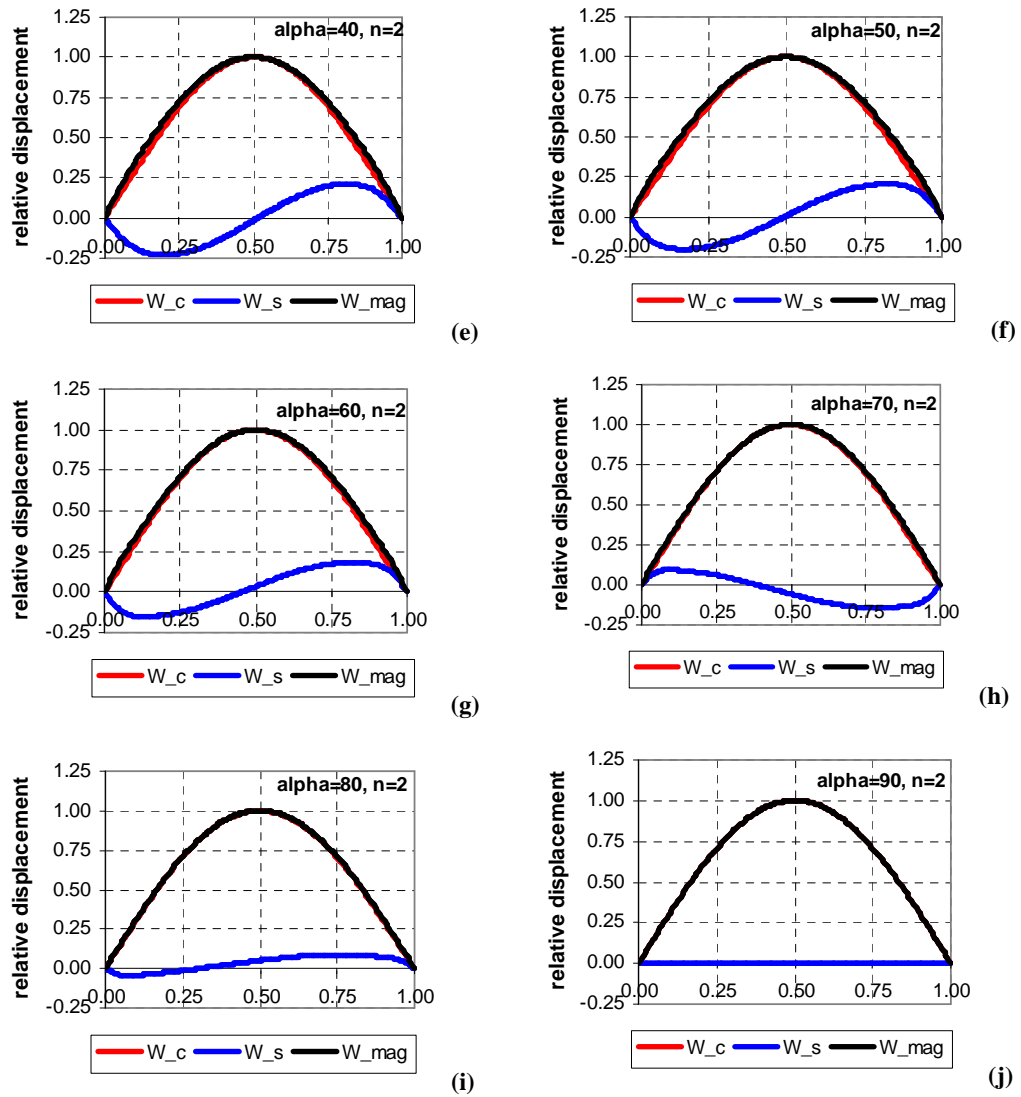
(b)



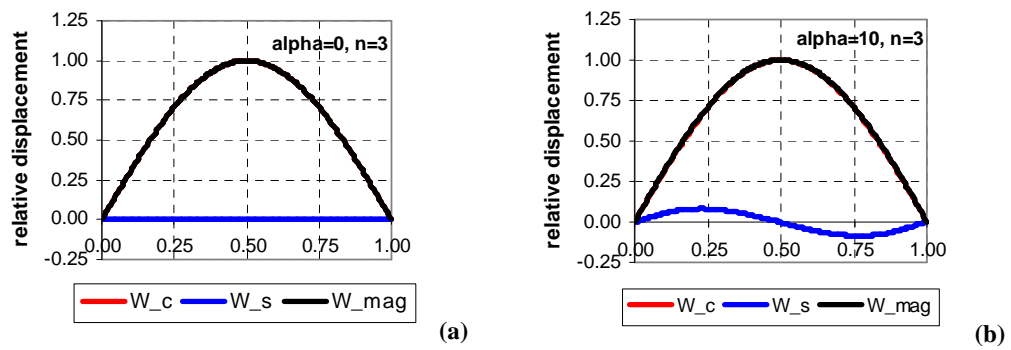
(c)



(d)



**Figure 4.15** Mode shapes for the first fundamental transverse mode when  $\alpha$  changes from  $0^\circ$  to  $90^\circ$  with the increment of  $10^\circ$  ( $n=2$ ).



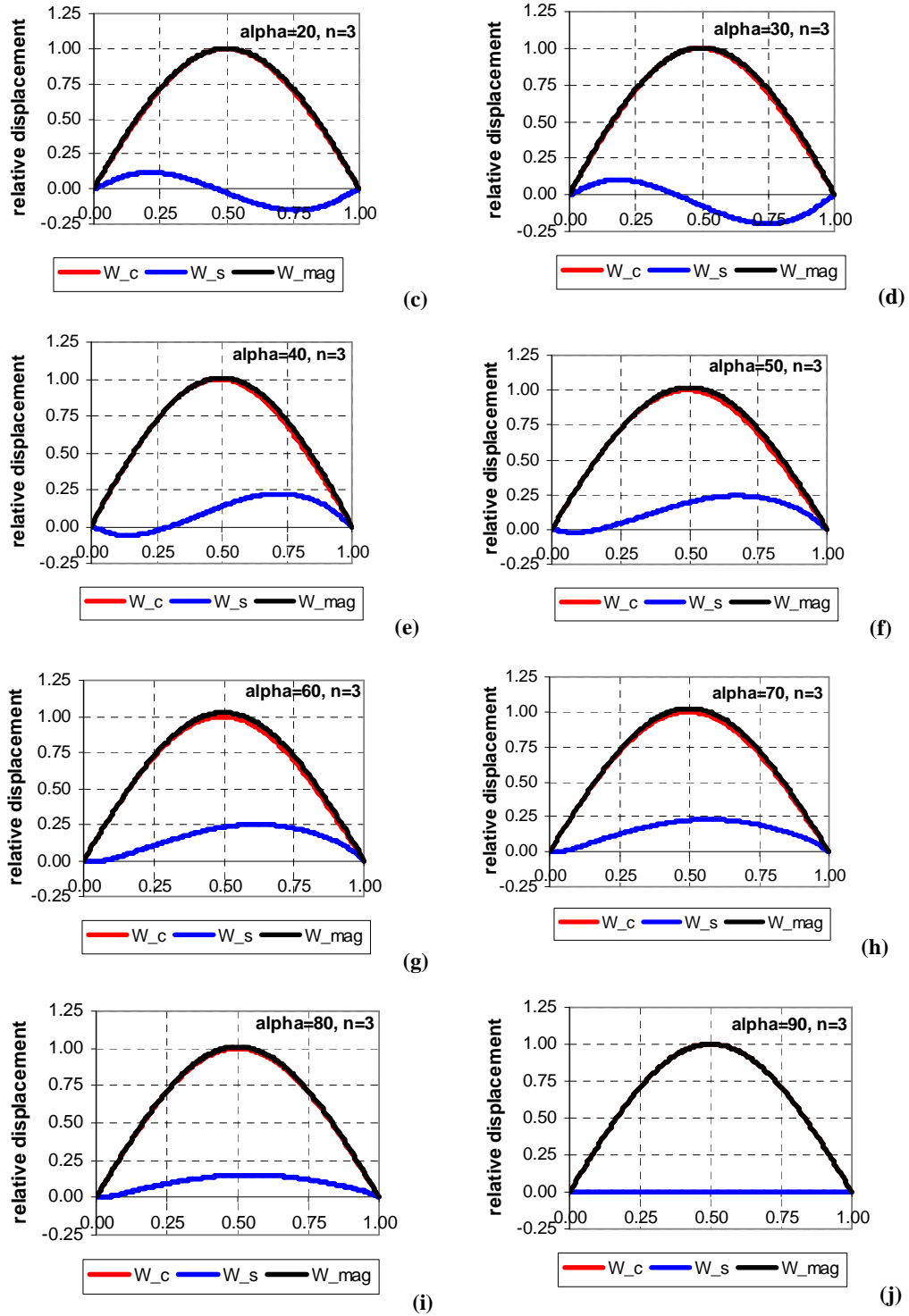


**Figure 4.16** Mode shapes for the first fundamental transverse mode when  $\alpha$  changes from  $0^\circ$  to  $90^\circ$  with the increment of  $10^\circ$  ( $n=3$ ).

#### 4.4.2 CASE STUDY ON STACKING SEQUENCE

The effect of the stacking sequence on the natural frequencies of a laminated composite circular cylindrical shell clamped at both edges is studied herein. Six different symmetric layups listed in Table 4.15 are utilized.  $0^\circ / 90^\circ / \pm 45^\circ$  lamination scheme is a widely used scheme in practical applications. Especially for hand layup/vacuum bagging applications.  $0^\circ / 90^\circ / \pm 45^\circ$  is the common scheme because manufacturing of such a laminate is relatively easy. While  $0^\circ$  and  $90^\circ$  layers give axial and transverse strengths,  $\pm 45^\circ$  layers account for strength in shear. Symmetric laminate configuration is a preferred configuration in most structural applications because of the nonexistence of bending-stretching coupling.

**Table 4.15** Six symmetric layups used in the case study on the stacking sequence.

$\text{layup 1: } [0_2 / 90_2 / \pm 45_2]_s$ $\text{layup 2: } [0_2 / \pm 45_2 / 90_2]_s$ $\text{layup 3: } [\pm 45_2 / 0_2 / 90_2]_s$ $\text{layup 4: } [\pm 45_2 / 90_2 / 0_2]_s$ $\text{layup 5: } [90_2 / \pm 45_2 / 0_2]_s$ $\text{layup 6: } [90_2 / 0_2 / \pm 45_2]_s$
---

The geometrical, mechanical and laminate properties of the clamped laminated composite circular cylindrical shell are given in Table 4.16.

Figures from 4.17 to 4.19 show the effect of stacking sequence on the laminate stiffness coefficients. As seen from Figure 4.17, the stretching stiffness coefficients of  $A_{11}$  and  $A_{22}$  are the largest for all stacking sequence listed in Table 4.15. Note that the stretching and transverse shear stiffness coefficients are same for all layups. This is because extensional stiffness coefficients  $A_{ij}$  do not depend on the placement of the plies within the laminate [1]. Moreover, all layups are symmetric laminates, the stretching-bending coupling stiffness coefficients are zero. The coefficients  $A_{16}$  and  $A_{26}$  are zero, and since the  $G_{13}$  and  $G_{23}$  are equal to each other, the coefficient  $A_{45}$  is also zero. In terms of the flexural stiffness coefficients,  $D_{11}$  is maximum for layup 2,  $D_{22}$  is maximum for layup 5. Also, the coupling coefficients  $D_{16}$  and  $D_{26}$ , are maximum for layups 3 and 4. In contrast to

the extensional stiffness coefficients, the bending stiffness coefficients  $D_{ij}$  depend on the placement of the plies within the laminate [1].

**Table 4.16** Geometrical, material properties, and laminate properties of the clamped-clamped laminated composite circular cylindrical shell used for the case study on stacking sequence.

Geometrical properties		Mechanical Properties of High Modulus Graphite/Epoxy[55]	
Radius [m]	0.21	$E_1$ [GPa]	207.348182
Meridional Length [m]	1.20	$E_2=E_3$ [GPa]	5.183702
Thickness [m]	0.00192	$G_{12}$ [Gpa]	3.110261
<b>Laminate Properties</b>		$G_{13}$ [Gpa]	3.110261
Layup	For each, refer to Table 4.19	$G_{23}$ [Gpa]	3.110261
Ply thickness [m]	0.00012	$\nu_{12} = \nu_{13} = \nu_{23}$	0.25
		$\rho$ [kg/m <sup>3</sup> ]	1524.4740

The results of the six different stacking sequence for the lowest three natural frequencies ( $m=1,2,3$ ) corresponding to ten circumferential modes ( $n=0-9$ ) are given for layup 1, layup 2, layup 3, layup 4, layup 5, and layup 6 in Tables 4.17, 4.18, 4.19, 4.20, 4.21, and 4.22, respectively when ( $h/R$ ) is approximately equal to 0.01 for clamped-clamped (CC) boundary condition. For  $n>1$ , all the three lowest natural frequencies turned out to be the first three transverse displacement modes ( $w$ ). This is confirmed by plotting the mode shapes as done in Figures 4.14 to 4.16. Since the mode shape algorithm scales the values with respect to the maximum displacement, the displacement component having maximum displacement of unity is the governing mode. However, for the axisymmetric mode, it is turned out that the lowest three modes primarily consisted of extensional modes. In other words, the substantial modes become  $u_\theta$  and  $u_x$  dominant.

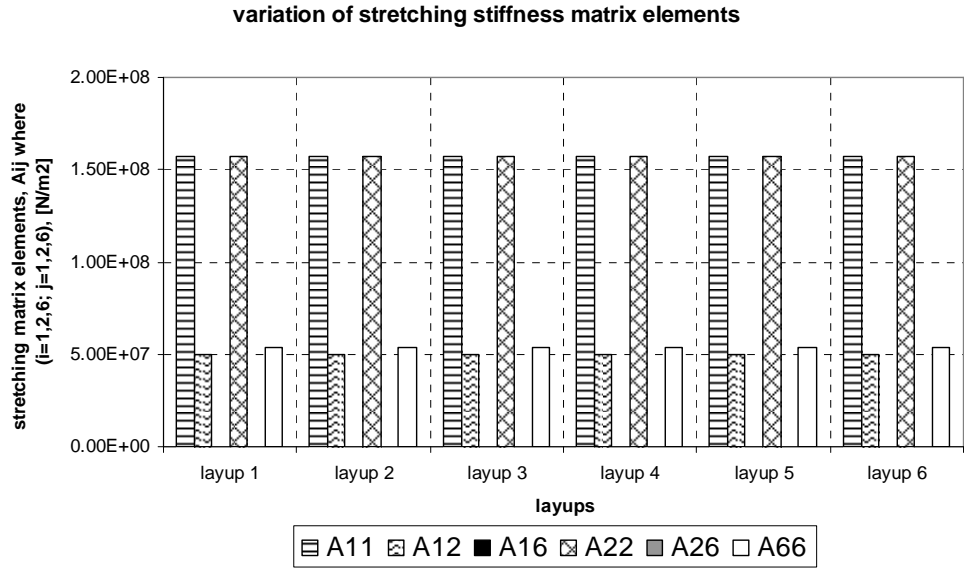


**Figure 4.17** Effect of the stacking sequence on the elements of stretching stiffness matrix ( $h/R=0.01$ ).

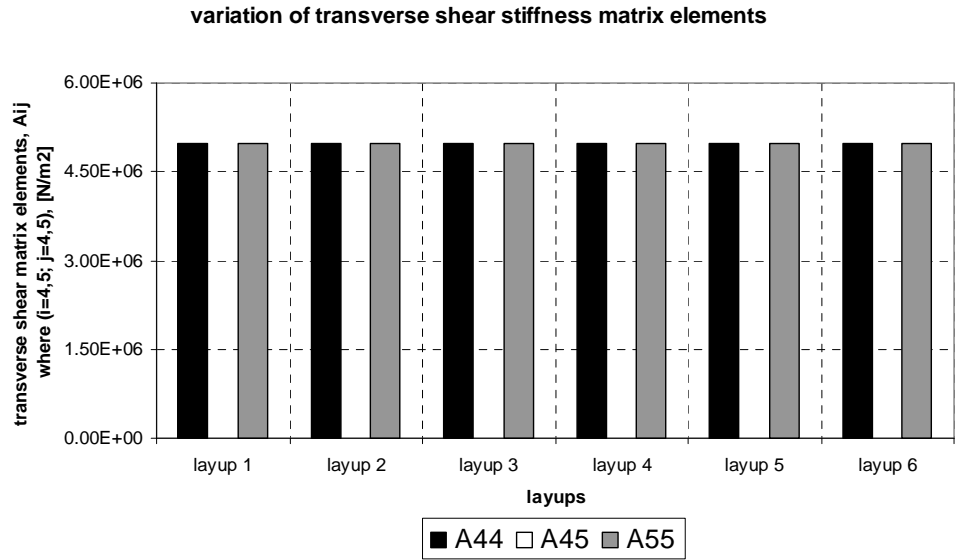


**Figure 4.18** Effect of the stacking sequence on the elements of transverse shear stiffness matrix ( $h/R=0.01$ ).

variation of flexural stiffness matrix elements

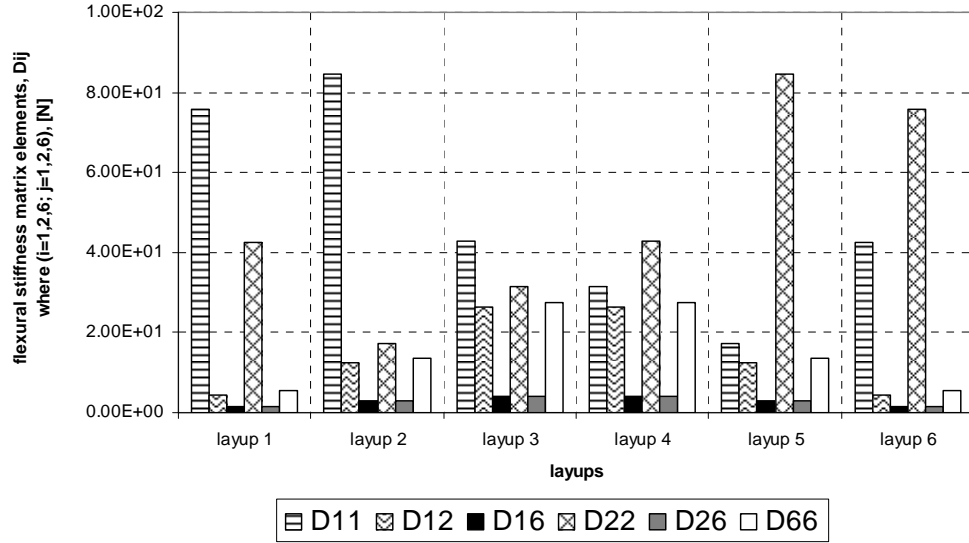


Figure 4.19 Effect of the stacking sequence on the elements of flexural stiffness matrix (h/R=0.01)

Table 4.17 Natural frequencies (rad/sec) for n 0 to 9 for the layup 1 in Table 4.15 for CC (h/R=0.01).

$[0_2/90_2/\pm 45_2]_s$ (layup 1)										
m	n=0	n=1	n=2	n=3	n=4	n=5	n=6	n=7	n=8	n=9
1	11187	7088	3609	2114	1771	2199	3035	4110	5373	6807
2	17872	13951	7862	4807	3358	2980	3391	4287	5478	6882
3	22375	20706	12563	8079	5626	4435	4214	4729	5729	7041

Table 4.18 Natural frequencies (rad/sec) for n 0 to 9 for the layup 2 in Table 4.15 for CC (h/R=0.01).

$[0_2/\pm 45_2/90_2]_s$ (layup 2)										
m	n=0	n=1	n=2	n=3	n=4	n=5	n=6	n=7	n=8	n=9
1	11187	7089	3606	2059	1503	1579	2031	2686	3477	4387
2	17874	13951	7863	4790	3244	2596	2592	3023	3716	4578
3	22375	20706	12566	8077	5577	4225	3666	3712	4183	4932

**Table 4.19** Natural frequencies (rad/sec) for n 0 to 9 for the layup 3 in Table 4.15 for CC (h/R=0.01).

$[\pm 45_2 / 0_2 / 90_2]_s$ (layup 3)										
m	n=0	n=1	n=2	n=3	n=4	n=5	n=6	n=7	n=8	n=9
1	11187	7086	3607	2099	1688	1995	2691	3607	4689	5925
2	17863	13948	7860	4810	3355	2916	3206	3944	4950	6148
3	22375	20702	12560	8087	5656	4471	4199	4596	5428	6540

**Table 4.20** Natural frequencies (rad/sec) for n 0 to 9 for the layup 4 in Table 4.15 for CC (h/R=0.01).

$[\pm 45_2 / 90_2 / 0_2]_s$ (layup 4)										
m	n=0	n=1	n=2	n=3	n=4	n=5	n=6	n=7	n=8	n=9
1	11187	7085	3607	2125	1805	2249	3091	4168	5432	6870
2	17859	13947	7858	4819	3413	3093	3546	4461	5657	7061
3	22375	20700	12557	8090	5687	4584	4461	5044	6076	7402

**Table 4.21** Natural frequencies (rad/sec) for n 0 to 9 for the layup 5 in Table 4.15 for CC (h/R=0.01).

$[90_2 / \pm 45_2 / 0_2]_s$ (layup 5)										
m	n=0	n=1	n=2	n=3	n=4	n=5	n=6	n=7	n=8	n=9
1	11187	7083	3611	2211	2173	2989	4235	5765	7539	9543
2	17852	13946	7855	4844	3590	3620	4523	5924	7646	9628
3	22375	20698	12550	8091	5764	4900	5196	6289	7872	9791

**Table 4.22** Natural frequencies (rad/sec) for n 0 to 9 for the layup 6 in Table 4.15 for CC (h/R=0.01).

$[90_2 / 0_2 / \pm 45_2]_s$ (layup 6)										
m	n=0	n=1	n=2	n=3	n=4	n=5	n=6	n=7	n=8	n=9
1	11187	7086	3612	2190	2090	2838	4013	5465	7151	9057
2	17863	13948	7859	4835	3531	3473	4284	5596	7228	9111
3	22375	20701	12556	8087	5721	4771	4953	5935	7414	9228

Natural frequencies versus circumferential wave numbers for all stacking sequence for clamped-clamped (CC) boundary condition are plotted in Figures 4.20, 4.21, and 4.22 for the lowest three modes ( $m=1$ ,  $m=2$ , and  $m=3$ ), respectively. Up to a certain  $n$ , every stacking sequence gives almost closer natural frequencies. Because the laminate stiffness coefficients are similar except the flexural stiffness coefficients for all layups, the differences in the flexural stiffness coefficients determine which laminate has the higher or lower natural frequencies. In this respect, as seen from Figures 4.22 to 4.24, the laminated composite circular cylindrical shell with  $[0_2/\pm 45_2/90_2]_5$  is less stiff whereas the shell with  $[90_2/\pm 45_2/0_2]_5$  is most stiff. As it was explained previously, as the circumferential wave number gets higher, bending strain energy dominates whereas for lower circumferential modes extensional strain energy dominates.

From the laminate stiffness coefficients shown in Figures 4.17, 4.18, and 4.19, it is clearly seen that layup 5 has the highest bending stiffness coefficient  $D_{22}$  in the transverse direction, implying circumferential direction. Hence, as  $n$  gets higher a shell with a high  $D_{22}$  bending stiffness value is expected to have the highest natural frequency. Figures 4.20, 4.21, and 4.22 verify this expectation. It should also be noted that the difference between the natural frequencies of the layup 5 (with the highest  $D_{22}$ ) and layup 2 (with the highest  $D_{11}$ ) slowly diminishes as we go to higher axial modes. Because, as we go to higher axial modes ( $m=2$ , and 3), the number of nodal points along the meridional axis of the shell increases and bending along the meridional axis of the shell becomes significant. Therefore, one should expect the natural frequencies of layup 5 and layup 2 get close to each other. This behavior is obviously seen when one investigates Figures from 4.17 to 4.19. It is also pointed out that for  $n=9$ ,  $m=3$  case  $D_{22}$  still dominates the bending stiffness such that layup 5 has the highest natural frequency. However, as one goes to higher axial modes, it is expected that this trend would change. On the other hand, for low circumferential wave numbers we almost have the same natural frequency for all six different stacking sequence cases. This result is also expected because for low  $n$  extensional strain energy prevails and extensional stiffness coefficients have the primary effect on the natural frequencies. Since extensional stiffness coefficients are same for all six different layups, the natural frequencies are nearly same for low circumferential modes.

Careful observation of the results in Tables 4.17 to 4.22 reveals that for low circumferential modes (low  $n$ ) natural frequencies are very close to each other for every layup of six different stacking sequences. However, for high circumferential modes (high  $n$ ) natural frequencies differ from one stacking sequence to another. This behavior is attributed to the fact that for low circumferential modes the extensional strain energy prevails, and thus extensional stiffness of the laminate plays a significant role on the natural frequency compared to bending stiffness. Since for each of the six stacking sequences the extensional stiffnesses are the same we have close natural frequencies for low circumferential modes. However, as the higher circumferential modes we get, the more influence of

bending strain energy takes place. The different values of the bending stiffness of each of the six stacking sequences will result in different amount of contributions to the magnitudes of the natural frequencies.

Furthermore, for  $n=0$ , axisymmetric modes, natural frequencies are almost equal to each other for all six stacking sequences. As it was stated before, for axisymmetric modes ( $n=0$ ), for the six different stacking sequences, the three lowest modes were extensional modes, and the associated natural frequencies are mainly dependent on extensional stiffnesses of the layups. The natural frequencies are almost same since the extensional stiffnesses of the six different stacking sequences are same.

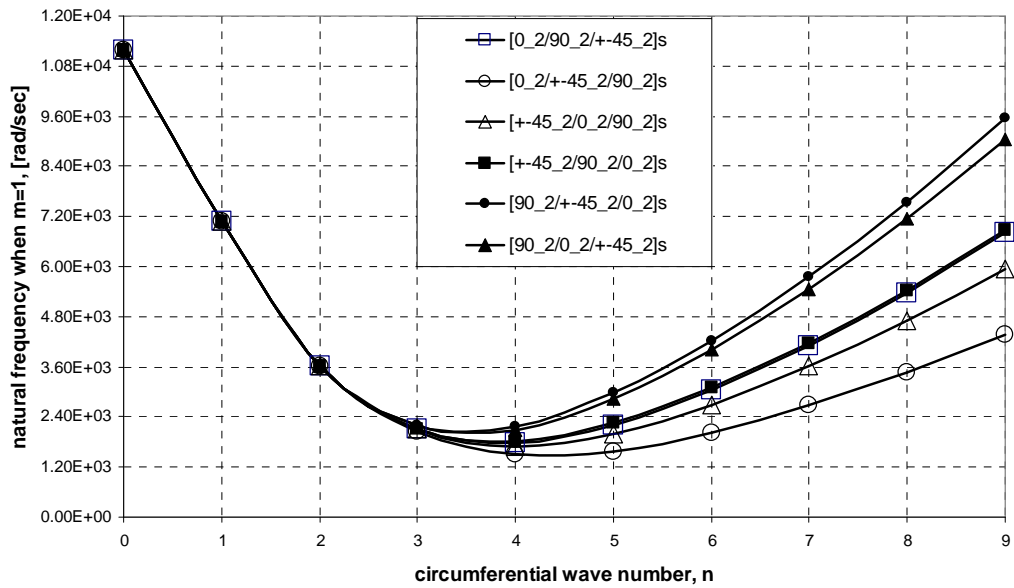


**Figure 4.20** Natural frequencies versus circumferential wave numbers for all stacking sequence for clamped-clamped (CC) boundary condition ( $m=1$  and  $h/R=0.01$ ).

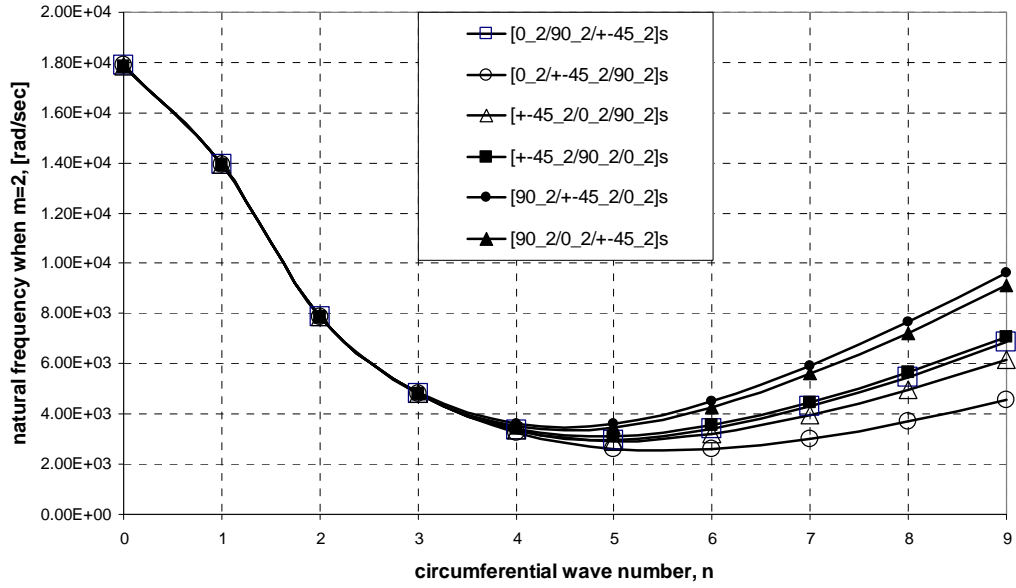


**Figure 4.21** Natural frequencies versus circumferential wave numbers for all stacking sequence for clamped-clamped (CC) boundary condition (m=2 and h/R=0.01).

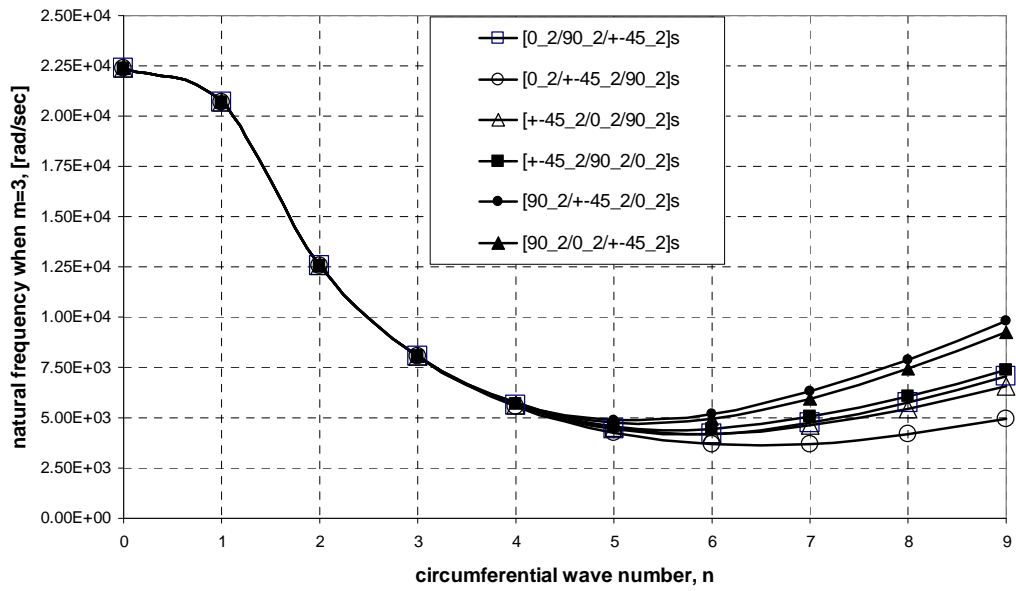


**Figure 4.22** Natural frequencies versus circumferential wave numbers for all stacking sequence for clamped-clamped (CC) boundary condition (m=3 and h/R=0.01).

#### 4.4.3 CASE STUDY ON BOUNDARY CONDITION

In the previous section, the natural frequencies of the laminated composite circular cylindrical shell clamped at both edges with six different stacking sequence were presented. In this section, the only difference from the previous problem will be the boundary condition, and the laminated composite circular cylindrical shell will have the boundary conditions of clamped at  $x = 0$  and free at  $x = L$ .

Natural frequencies of the results of the case study on stacking sequence for clamped-free (CF) are given for layup 1, layup 2, layup 3, layup 4, layup 5, and layup 6 in Tables 4.23, 4.24, 4.25, 4.26, 4.27, and 4.28, respectively. Additionally, natural frequencies versus circumferential wave numbers for all stacking sequence for this boundary condition are plotted in Figures 4.23, 4.24, and 4.25 for the three lowest axial modes ( $m=1,2$ , and 3).

**Table 4.23** Natural frequencies (rad/sec) for n 0 to 9 for the layup 1 in Table 4.15 for CF ( $h/R=0.01$ ).

$[0_2/90_2/\pm 45_2]_s$ (layup 1)										
m	n=0	n=1	n=2	n=3	n=4	n=5	n=6	n=7	n=8	n=9
1	5594	2096	794	752	1273	2031	2967	4073	5347	6786
2	9060	7915	3883	2191	1795	2213	3050	4126	5390	6823
3	16781	15974	8805	5192	3522	3052	3428	4313	5501	6905

**Table 4.24** Natural frequencies (rad/sec) for n 0 to 9 for the layup 2 in Table 4.15 for CF ( $h/R=0.01$ ).

$[0_2/\pm 45_2/90_2]_s$ (layup 2)										
m	n=0	n=1	n=2	n=3	n=4	n=5	n=6	n=7	n=8	n=9
1	5594	2096	775	564	837	1306	1896	2595	3404	4321
2	9061	7916	3881	2143	1546	1623	2080	2736	3525	4430
3	16781	15974	8806	5181	3423	2700	2674	3100	3792	4654

**Table 4.25** Natural frequencies (rad/sec) for n 0 to 9 for the layup 3 in Table 4.15 for CF (h/R=0.01).

$[\pm 45_2 / 0_2 / 90_2]_s$ (layup 3)										
m	n=0	n=1	n=2	n=3	n=4	n=5	n=6	n=7	n=8	n=9
1	5594	2095	788	681	1106	1745	2539	3478	4558	5779
2	9059	7914	3884	2191	1745	2051	2744	3654	4729	5959
3	16781	15972	8806	5206	3545	3037	3305	4034	5034	6227

**Table 4.26** Natural frequencies (rad/sec) for n 0 to 9 for the layup 4 in Table 4.15 for CF (h/R=0.01).

$[\pm 45_2 / 90_2 / 0_2]_s$ (layup 4)										
m	n=0	n=1	n=2	n=3	n=4	n=5	n=6	n=7	n=8	n=9
1	5594	2095	796	759	1277	2027	2953	4045	5302	6719
2	9058	7914	3885	2215	1858	2295	3133	4204	5462	6894
3	16781	15971	8805	5215	3600	3206	3632	4537	5725	7124

**Table 4.27** Natural frequencies (rad/sec) for n 0 to 9 for the layup 5 in Table 4.15 for CF (h/R=0.01).

$[90_2 / \pm 45_2 / 0_2]_s$ (layup 5)										
m	n=0	n=1	n=2	n=3	n=4	n=5	n=6	n=7	n=8	n=9
1	5594	2094	827	996	1781	2854	4169	5717	7496	9499
2	9057	7913	3887	2291	2201	3008	4254	5783	7554	9556
3	16781	15970	8802	5234	3755	3694	4566	5957	7676	9655

**Table 4.28** Natural frequencies (rad/sec) for n 0 to 9 for the layup 6 in Table 4.15 for CF (h/R=0.01).

$[90_2 / 0_2 / \pm 45_2]_s$ (layup 6)										
m	n=0	n=1	n=2	n=3	n=4	n=5	n=6	n=7	n=8	n=9
1	5594	2095	820	951	1691	2710	3962	5437	7131	9042
2	9059	7914	3886	2264	2110	2848	4023	5476	7163	9069
3	16781	15972	8803	5220	3687	3535	4313	5615	7245	9128

As it is seen from Figures 4.23, 4.24, and 4.25, we have the same trend of the variation of the natural frequency with the circumferential wave number as in the clamped-clamped. As  $n$  gets larger, layup 5 has the highest natural frequency and layup 2 has the lowest natural frequency; trend being the same for the three lowest axial modes. The discussion regarding the behavior of natural frequency with  $n$  is the same as that of the case for the clamped-clamped boundary condition.

Comparison of the natural frequencies of the laminated composite circular cylindrical shell with clamped-clamped boundary condition with the clamped-free boundary condition is shown in Figures 4.26, 4.27, and 4.28 for the three lowest axial modes for the most stiff layup and the less stiff layup. As expected, the natural frequencies of the shell with clamped-clamped (CC) boundary condition are higher than the shell with clamped-free (CF) boundary condition for the two layups.

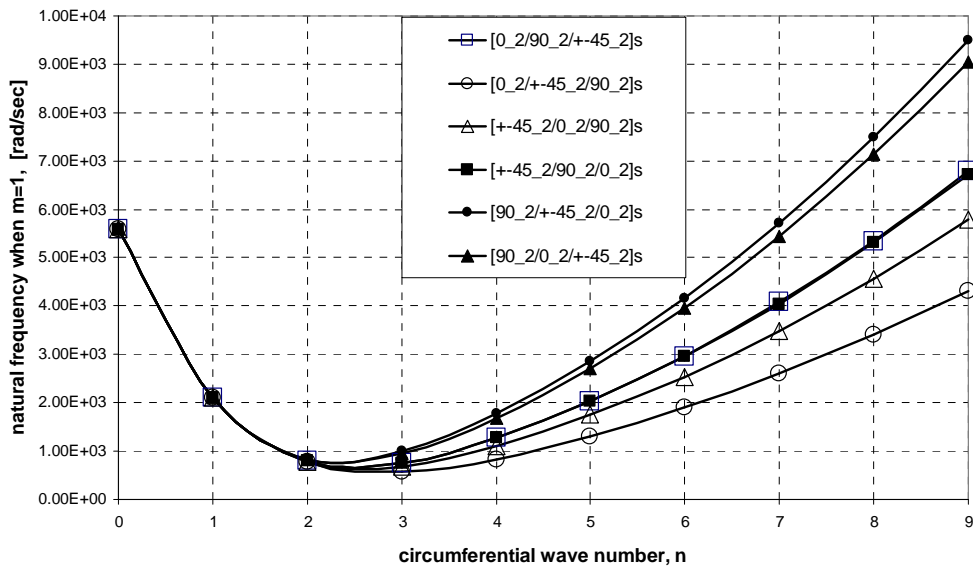


**Figure 4.23** Natural frequencies versus circumferential wave numbers for all stacking sequence for clamped-free (CF) boundary condition ( $m=1$  and  $h/R=0.01$ ).

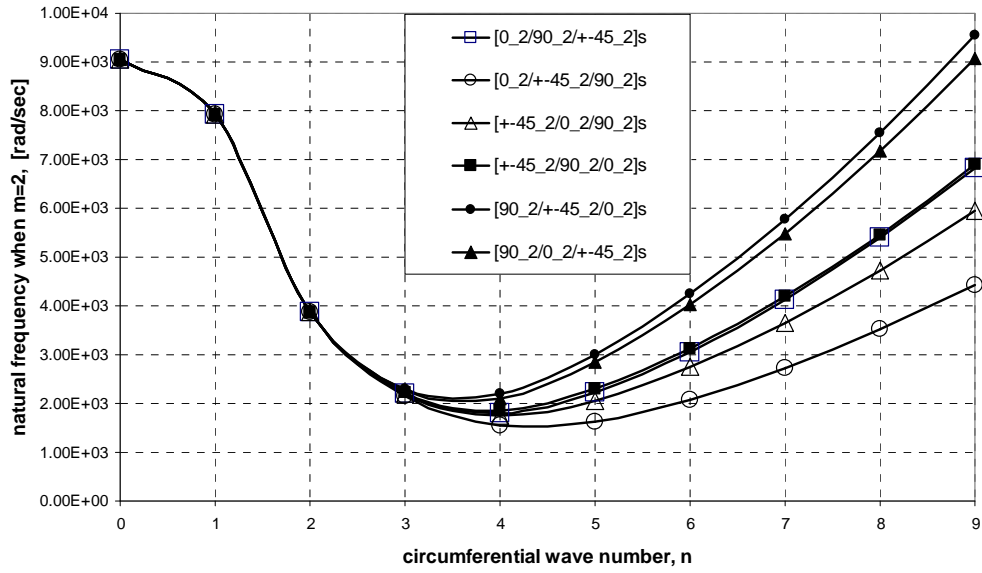


**Figure 4.24** Natural frequencies versus circumferential wave numbers for all stacking sequence for clamped-free (CF) boundary condition ( $m=2$  and  $h/R=0.01$ ).

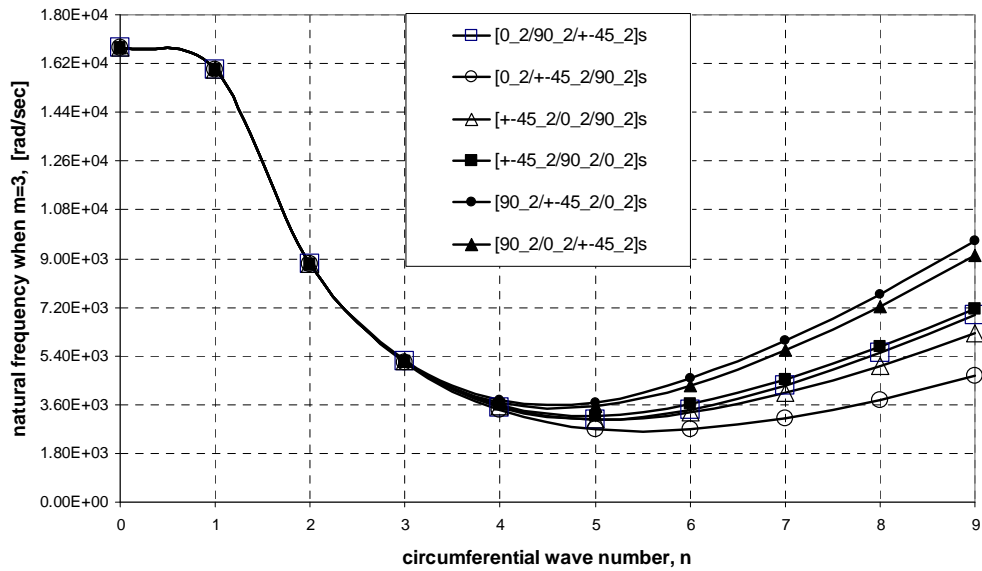


**Figure 4.25** Natural frequencies versus circumferential wave numbers for all stacking sequence for clamped-free (CF) boundary condition ( $m=3$  and  $h/R=0.01$ ).

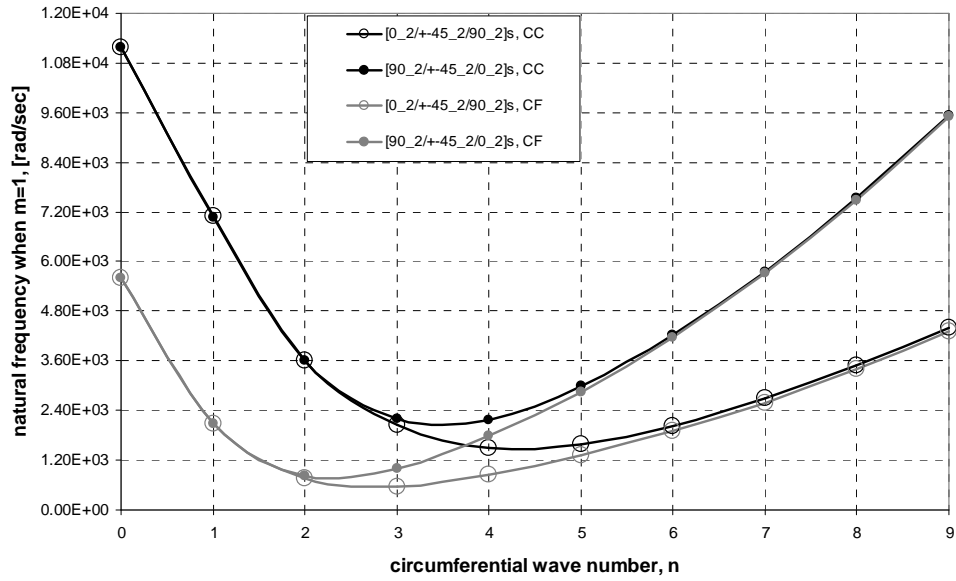


**Figure 4.26** Comparison of the natural frequencies of the laminated composite circular cylindrical shell having CC boundary conditions with the ones having CF boundary conditions ( $m=1$  and  $h/R=0.01$ ).

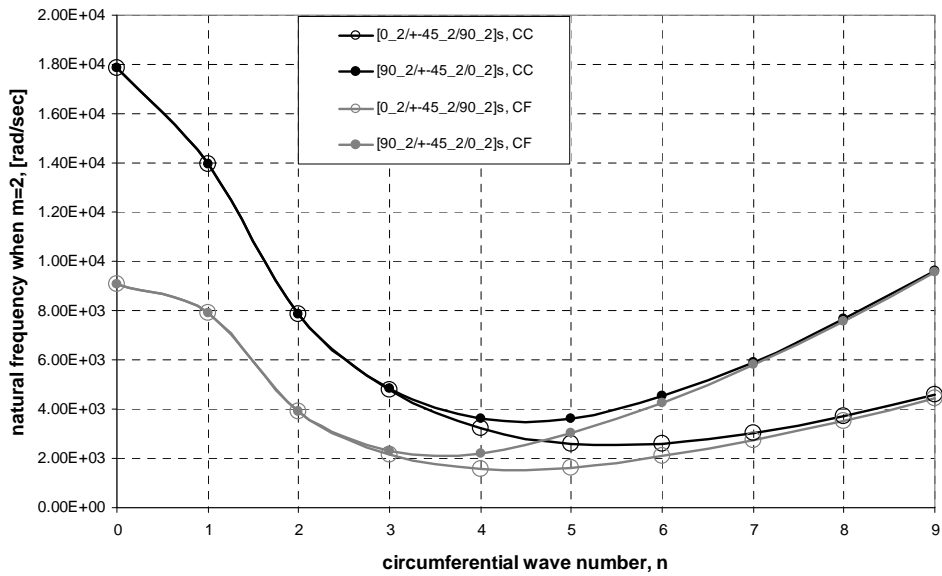


**Figure 4.27** Comparison of the natural frequencies of the laminated composite circular cylindrical shell having CC boundary conditions with the ones having CF boundary conditions ( $m=2$  and  $h/R=0.01$ ).

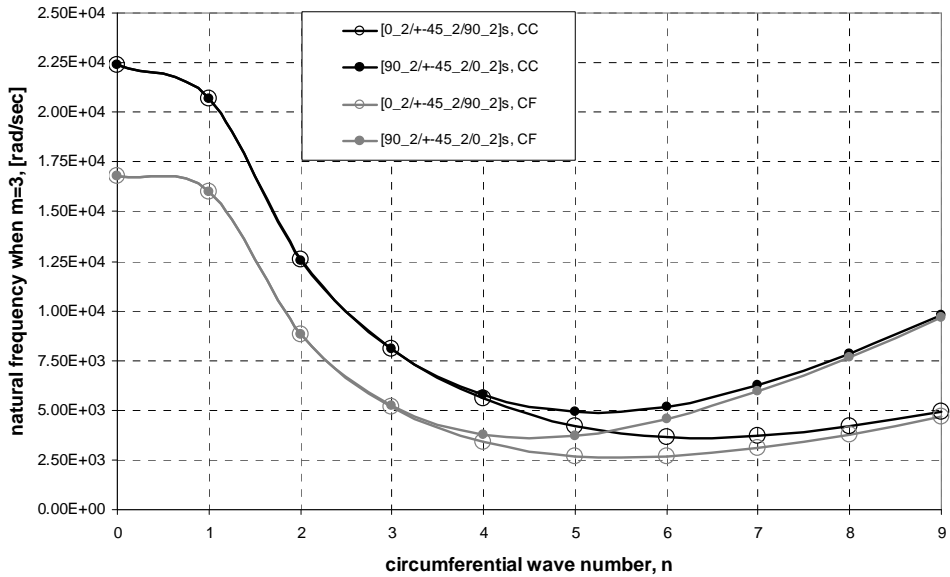


**Figure 4.28** Comparison of the natural frequencies of the laminated composite circular cylindrical shell having CC boundary conditions with the ones having CF boundary conditions ( $m=3$  and  $h/R=0.01$ ).

#### 4.4.4 CASE STUDY ON THICKNESS-TO-RADIUS RATIO

In the previous two sections, various parametric studies are performed to investigate the effect of the stacking sequence, which is given in Table 4.15, boundary conditions on the free vibration characteristics of laminated composite circular cylindrical shells. The geometrical and material characteristics of those shells are given in Table 4.16. All of those shells have the laminate thickness to radius ratio of approximately 0.01. In this section we will analyze the same shell with the same geometrical (except thickness) and material properties as in the previous section. The layup stacking sequence is also kept as in Table 4.15. To achieve a thicker shell the only change made is in the layup thickness. In this case each ply thickness is increased to 1.2 mm from 0.12 mm. These properties are practical properties taken from Hexcel Composites catalogues. 0.12 mm ply thickness approximately corresponds to a fabric with approximately 100 grams per square meter weight. On the other hand 1.2 mm ply thickness corresponds to a fabric with approximately 900-1000 grams per square meter weight. In the following the shell having a thickness to radius ratio of about 0.01 will be named as thin shell whereas the shell with the thickness to radius ratio of approximately 0.1 will be named as thick shell.

Figures from 4.29 to 4.31 show the effect of stacking sequence on the laminate stiffness

coefficients for thick shell. The variations of the laminate stiffness coefficients for thick shell are as similar as those for thin shell except the values.

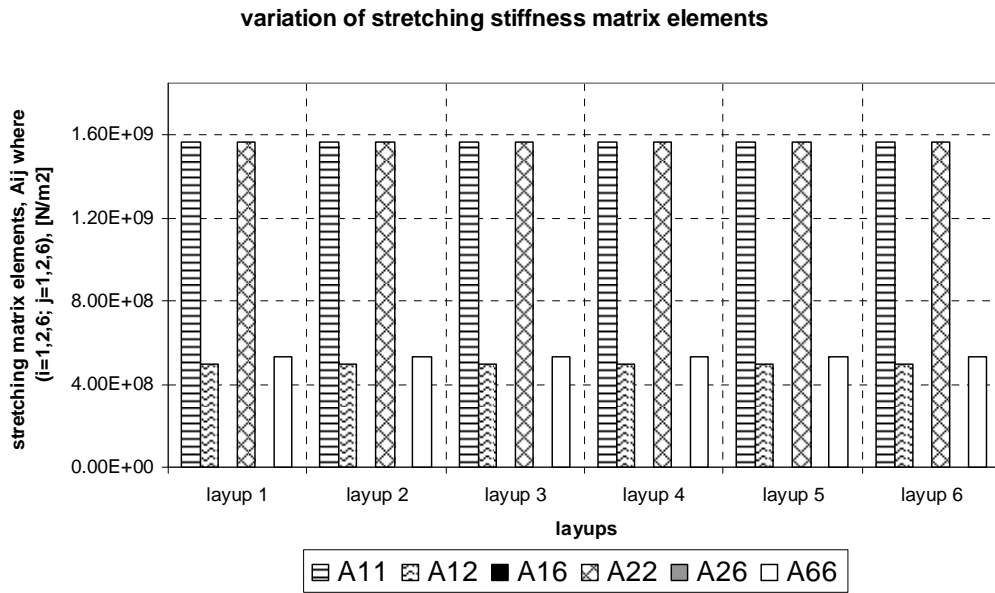


**Figure 4.29** Effect of the stacking sequence on the elements of stretching stiffness matrix ( $h/R=0.1$ ).

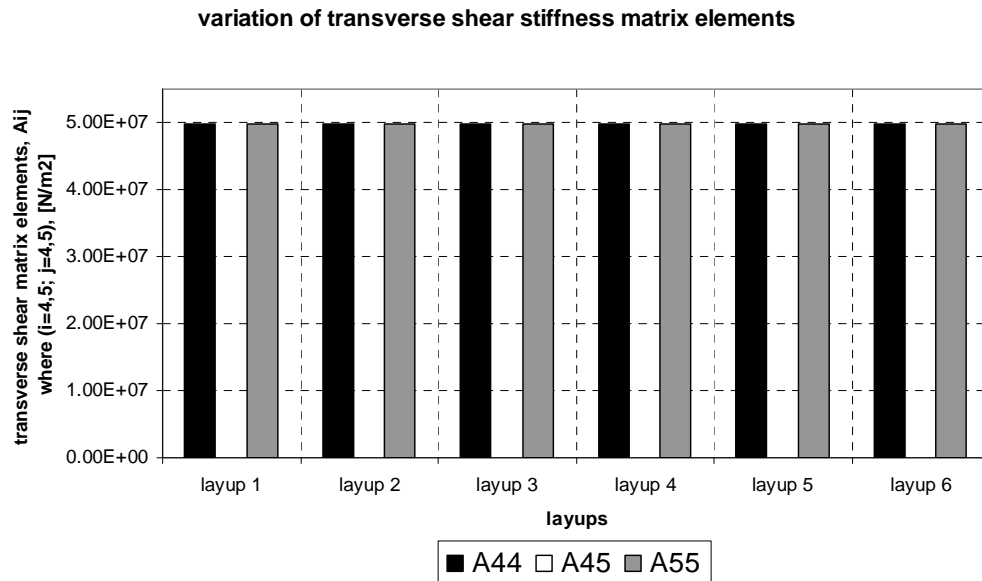


**Figure 4.30** Effect of the stacking sequence on the elements of transverse shear stiffness matrix ( $h/R=0.1$ ).

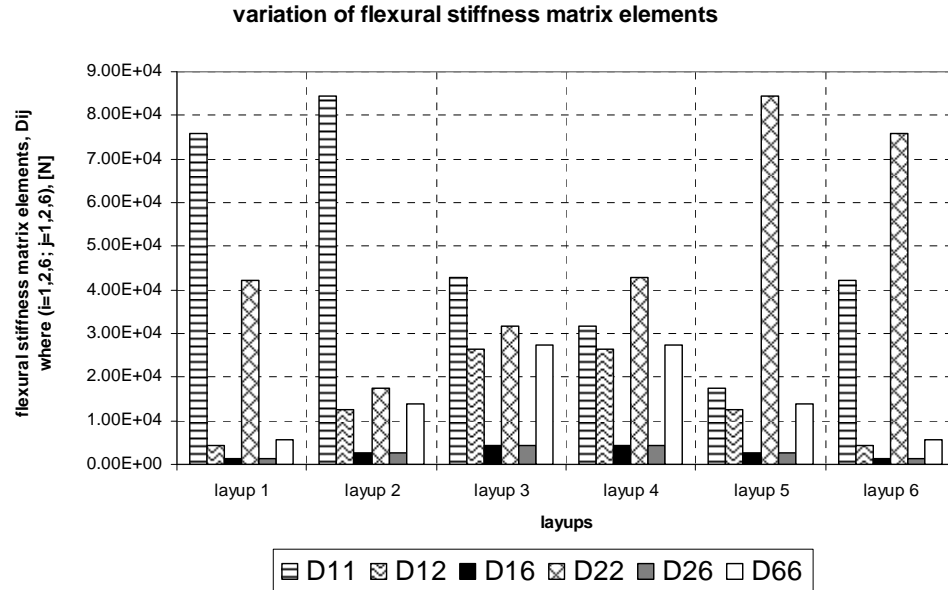


**Figure 4.31** Effect of the stacking sequence on the elements of flexural stiffness matrix ( $h/R=0.1$ ).

Natural frequencies of the results of the thick shell configurations for the clamped-clamped (CC) boundary condition are given for layups 1-6 in Tables 4.29, 4.30, 4.31, 4.32, 4.33, and 4.34, respectively. In addition, natural frequencies of thick shell configuration versus circumferential wave numbers for clamped-clamped (CC) boundary condition are shown in Figure 4.32, 4.33, and 4.34 for the three lowest modes (for  $m=1, 2$ , and  $3$ ), respectively. Furthermore, natural frequencies of the results of the thick shell configurations for clamped-free (CF) boundary condition are given for layups 1-6 in Tables 4.35-40, respectively. Additionally, natural frequencies of thick shell configuration versus circumferential wave numbers for clamped-free (CF) boundary condition are shown in Figure 4.35, 4.36, and 4.37 for the three lowest axial modes (for  $m=1, 2$ , and  $3$ ), respectively.

For thick shell, comparison of the natural frequencies of the laminated composite circular cylindrical shell with clamped-clamped (CC) boundary condition with the clamped-free (CF) boundary condition is shown in Figures 4.38, 4.39, and 4.40 for the three lowest axial modes for the most stiff layup and the less stiff layup. As expected, it is valid for thick shell that the natural frequencies of the shell with clamped-clamped (CC) boundary condition are higher than the shell with clamped-free (CF) boundary condition for the two layups.

We know from the study of Warburton [79] that the bending strain energy of the shell is proportional to the cube of the shell thickness whereas the stretching strain energy of the shell is proportional to the thickness itself. Therefore, if one carefully studies Figure 4.10 by increasing the thickness we would actually be pulling the bending strain energy up much higher than the stretching

strain energy. This effect obviously causes the lowest point of the total strain energy to occur at lower circumferential wave numbers. This effect is clearly seen if one compares Figures 4.20, 4.21, and 4.22 with Figures 4.32, 4.33, and 4.34 for the clamped-clamped (CC) configuration, and Figures 4.23, 4.24, and 4.25 with Figures 4.35, 4.36, and 4.37 for the clamped-free (CF) configuration. Figures 4.32 to 4.34 and 4.35 to 4.37 display the similar trend of the variation of natural frequencies with the circumferential wave number for the thicker shell configuration as in the thin shell configuration. The careful study of the curves for thin shells (Figures 4.20-4.22 for CC and Figures 4.23-4.25 for CF) and thick shells (Figures 4.32-4.34 for CC and Figures 4.35-4.37 for CF) reveals that for the thick shell configuration the lowest natural frequency occurs at a smaller circumferential wave number compared to the thin shell configuration. It should also be noticed that for both boundary condition configurations layup 5  $[90_2 / \pm 45_2 / 0_2]_s$  gives the highest natural frequencies over the circumferential wave number range studied for the three lowest axial modes (for  $m=1, 2,$  and  $3$ ). Additionally, the natural frequencies of layup 5 (most stiff) and layup 2 (less stiff) still get closer to each other as we go to higher modes. However, for the thick shell natural frequencies get close to each other much slowly as compared to the thin shell. These effects are more clearly seen in the comparison curves drawn for both thick and thin shell configurations in Figures 4.41 to 4.46.

Comparison of the natural frequencies of the thick shell configurations with clamped-clamped (CC) boundary conditions with the thin shell configurations with clamped-clamped (CC) boundary conditions is shown in Figures 4.41, 4.42, and 4.43 for the three lowest axial modes (for  $m=1, 2,$  and  $3$ ). Also, comparison of the natural frequencies of the thick shell configurations with clamped-free (CF) boundary conditions with the thin shell configurations with clamped-free (CF) boundary conditions is shown in Figures 4.44, 4.45, and 4.46 for the three lowest axial modes (for  $m=1, 2,$  and  $3$ ). As one can see from those comparison curves for the thicker shell configuration, natural frequencies are higher than the thin shell configuration as we go to the higher circumferential wave numbers. This behavior is expected because as the number of nodal points along the circumference ( $2n$ ) and along the span of the shell ( $m$ ) increase we actually experience substantially bending action. Higher thickness leads to the higher bending stiffness and higher natural frequencies. It is also noted that for both boundary condition cases for low circumferential modes the difference in natural frequencies between the thick and thin shell becomes very small, and natural frequencies are almost identical with thin and thick shells for axisymmetric vibration case. It is well known (from simplified shell equations on page 125 of Soedel [13] and [80]) that all natural frequencies in the absence of the effects of bending are independent of the thickness of the shell. Although this conclusion was made for isotropic shells, for laminated composite shells it still applies especially for low circumferential modes in which extensional strain energy prevails. One can actually show the elimination of thickness through the equilibrium equation if one sets the bending stiffness coefficients ( $D_{ij}$ ) to zero. By this way, thickness term passes through all the equations and the resulting equations will actually be independent of the thickness. This approximation is called as membrane or extensiona

extensional approximation.

**Table 4.29** Natural frequencies (rad/sec) for n 0 to 9 for the layup 1 in Table 4.15 for CC (h/R=0.1).

$[0_2/90_2/\pm 45_2]_s$ (layup 1)										
m	n=0	n=1	n=2	n=3	n=4	n=5	n=6	n=7	n=8	n=9
1	11185	7147	4354	6462	11086	16680	22813	29267	35905	42640
2	17956	14074	8513	8149	11783	17093	23121	29522	36128	42840
3	22370	20995	13418	11080	13259	17950	23723	29999	36532	43196

**Table 4.30** Natural frequencies (rad/sec) for n 0 to 9 for the layup 2 in Table 4.15 for CC (h/R=0.1).

$[0_2/\pm 45_2/90_2]_s$ (layup 2)										
m	n=0	n=1	n=2	n=3	n=4	n=5	n=6	n=7	n=8	n=9
1	11187	7152	4094	4843	7922	12031	16821	22128	27833	33841
2	17958	14087	8486	7269	9341	13071	17671	22852	28461	34391
3	22374	21027	13510	10768	11677	14793	19068	24039	29490	35293

**Table 4.31** Natural frequencies (rad/sec) for n 0 to 9 for the layup 3 in Table 4.15 for CC (h/R=0.1).

$[\pm 45_2/0_2/90_2]_s$ (layup 3)										
m	n=0	n=1	n=2	n=3	n=4	n=5	n=6	n=7	n=8	n=9
1	11190	7136	4358	6093	10177	15262	20968	27087	33480	40046
2	17947	14045	8670	8414	11622	16348	21843	27811	34087	40561
3	22380	20928	13628	11779	13914	18093	23258	28989	35080	41408

**Table 4.32** Natural frequencies (rad/sec) for n 0 to 9 for the layup 4 in Table 4.15 for CC (h/R=0.1).

$[\pm 45_2/90_2/0_2]_s$ (layup 4)										
m	n=0	n=1	n=2	n=3	n=4	n=5	n=6	n=7	n=8	n=9
1	11190	7130	4485	6736	11351	16917	23023	29455	36074	42793
2	17941	14030	8707	8845	12606	17843	23767	30072	36596	43241
3	22380	20889	13609	12029	14668	19367	24988	31087	37456	43981

**Table 4.33** Natural frequencies (rad/sec) for n 0 to 9 for the layup 5 in Table 4.15 for CC (h/R=0.1).

$[90_2 / \pm 45_2 / 0_2]_s$ (layup 5)										
m	n=0	n=1	n=2	n=3	n=4	n=5	n=6	n=7	n=8	n=9
1	11187	7118	4823	8323	14065	20506	27225	34042	40871	47671
2	17930	14000	8709	9739	14709	20928	27558	34327	41123	47900
3	22374	20814	13405	12246	15958	21711	28149	34818	41553	48287

**Table 4.34** Natural frequencies (rad/sec) for n 0 to 9 for the layup 6 in Table 4.15 for CC (h/R=0.1).

$[90_2 / 0_2 / \pm 45_2]_s$ (layup 6)										
m	n=0	n=1	n=2	n=3	n=4	n=5	n=6	n=7	n=8	n=9
1	11185	7133	4705	7956	13547	19891	26557	33351	40178	46990
2	17946	14036	8626	9294	14048	20172	26760	33519	40325	47124
3	22370	20897	13375	11795	15165	20778	27172	33841	40599	47367

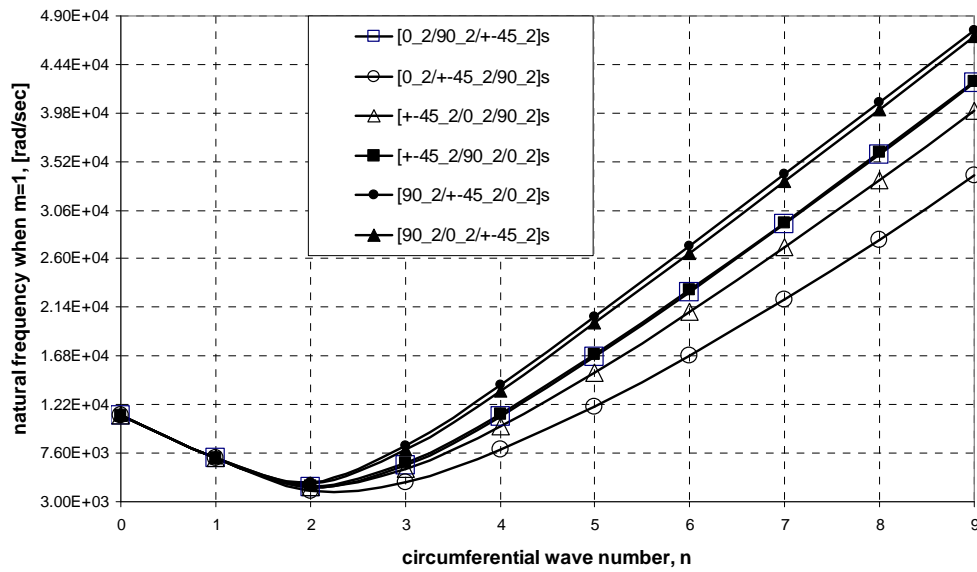


**Figure 4.32** Natural frequencies versus circumferential wave numbers for all stacking sequence for clamped-clamped (CC) boundary condition (m=1 and h/R=0.1).

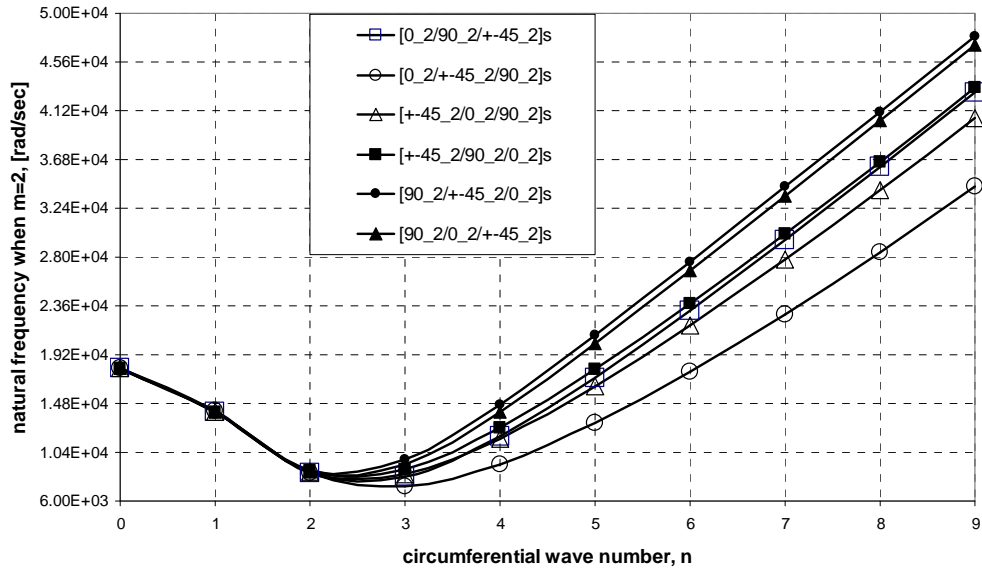


**Figure 4.33** Natural frequencies versus circumferential wave numbers for all stacking sequence for clamped-clamped (CC) boundary condition ( $m=2$  and  $h/R=0.1$ ).

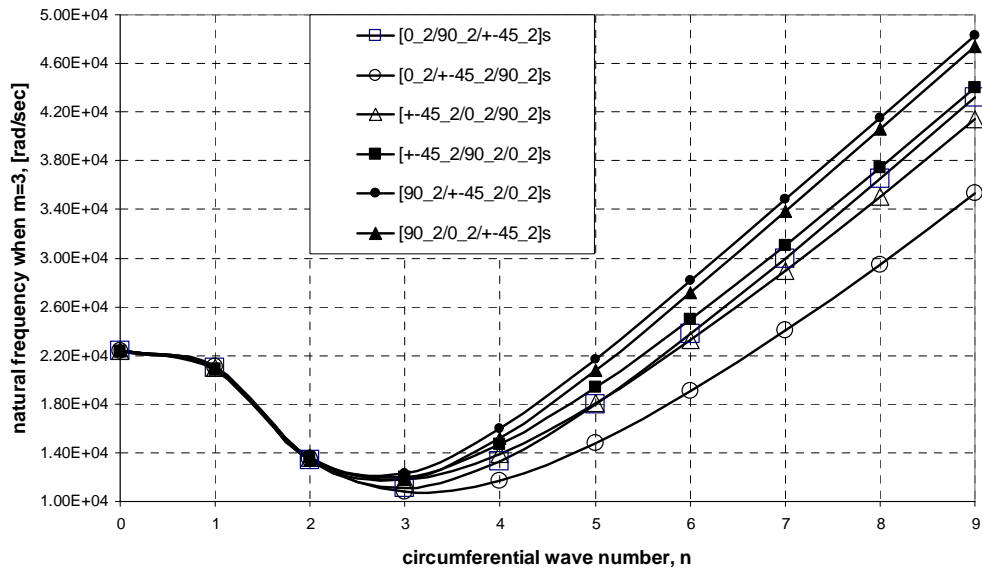


**Figure 4.34** Natural frequencies versus circumferential wave numbers for all stacking sequence for clamped-clamped (CC) boundary condition ( $m=3$  and  $h/R=0.1$ ).

**Table 4.35** Natural frequencies (rad/sec) for n 0 to 9 for the layup 1 in Table 4.15 for CF (h/R=0.1).

$[0_2/90_2/\pm 45_2]_s$ (layup 1)										
m	n=0	n=1	n=2	n=3	n=4	n=5	n=6	n=7	n=8	n=9
1	5593	2106	2373	6048	10925	16575	22729	29195	35840	42581
2	9076	7954	4606	6565	11180	16767	22891	29338	35970	42700
3	16777	16079	9411	8475	11960	17240	23256	29647	36244	42949

**Table 4.36** Natural frequencies (rad/sec) for n 0 to 9 for the layup 2 in Table 4.15 for CF (h/R=0.1).

$[0_2/\pm 45_2/90_2]_s$ (layup 2)										
m	n=0	n=1	n=2	n=3	n=4	n=5	n=6	n=7	n=8	n=9
1	5593	2108	1707	4070	7479	11667	16484	21802	27512	33522
2	9076	7959	4446	5177	8236	12300	17047	22315	27987	33968
3	16780	16092	9443	7832	9846	13544	18100	23232	28792	34679

**Table 4.37** Natural frequencies (rad/sec) for n 0 to 9 for the layup 3 in Table 4.15 for CF (h/R=0.1).

$[\pm 45_2/0_2/90_2]_s$ (layup 3)										
m	n=0	n=1	n=2	n=3	n=4	n=5	n=6	n=7	n=8	n=9
1	5595	2108	2393	5963	9483	14521	20129	26142	32431	38912
2	9073	7945	4882	7043	10456	15460	21106	27185	33550	40098
3	16785	16044	9703	9437	12167	16799	22202	28091	34305	40731

**Table 4.38** Natural frequencies (rad/sec) for n 0 to 9 for the layup 4 in Table 4.15 for CF (h/R=0.1).

$[\pm 45_2/90_2/0_2]_s$ (layup 4)										
m	n=0	n=1	n=2	n=3	n=4	n=5	n=6	n=7	n=8	n=9
1	5593	2104	3148	5963	10714	16228	22253	28609	35175	41859
2	9071	7934	5095	7043	11571	17070	23132	29534	36134	42839
3	16780	16016	9628	9437	13069	18214	24061	30304	36781	43391

**Table 4.39** Natural frequencies (rad/sec) for n 0 to 9 for the layup 5 in Table 4.15 for CF (h/R=0.1).

$[90_2 / \pm 45_2 / 0_2]_s$ (layup 5)										
m	n=0	n=1	n=2	n=3	n=4	n=5	n=6	n=7	n=8	n=9
1	5593	2105	3009	7943	13865	20345	27081	33912	40752	47564
2	9074	7943	4928	8455	14171	20593	27300	34110	40933	47730
3	16777	16044	9507	10091	14926	21108	27717	34471	41258	48027

**Table 4.40** Natural frequencies (rad/sec) for n 0 to 9 for the layup 6 in Table 4.15 for CF (h/R=0.1).

$[90_2 / 0_2 / \pm 45_2]_s$ (layup 6)										
m	n=0	n=1	n=2	n=3	n=4	n=5	n=6	n=7	n=8	n=9
1	5595	2109	2133	7648	13437	19823	26503	33305	40137	46953
2	9074	7950	4776	8022	13607	19947	26607	33398	40222	47032
3	16785	16058	9674	9558	14169	20268	26848	33601	40403	47198

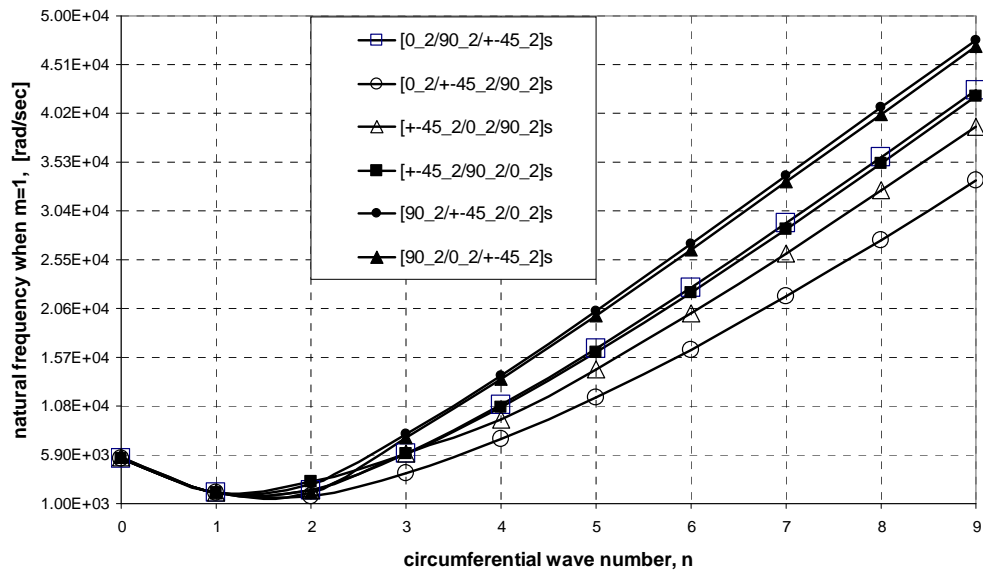


**Figure 4.35** Natural frequencies versus circumferential wave numbers for all stacking sequence for clamped-free (CF) boundary condition (m=1 and h/R=0.1).

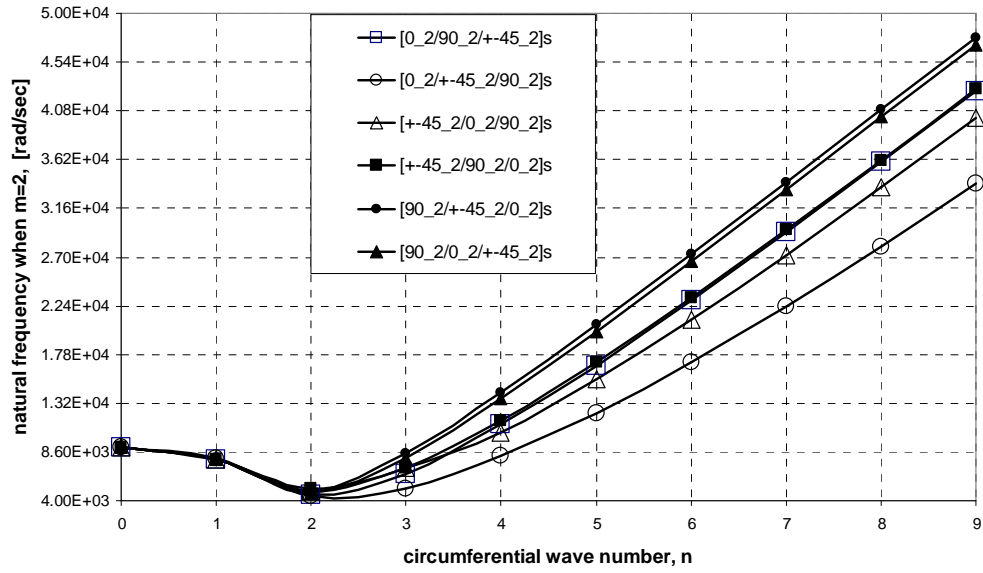


Figure 4.36 Natural frequencies versus circumferential wave numbers for all stacking sequence for clamped-free (CF) boundary condition (m=2 and h/R=0.1).

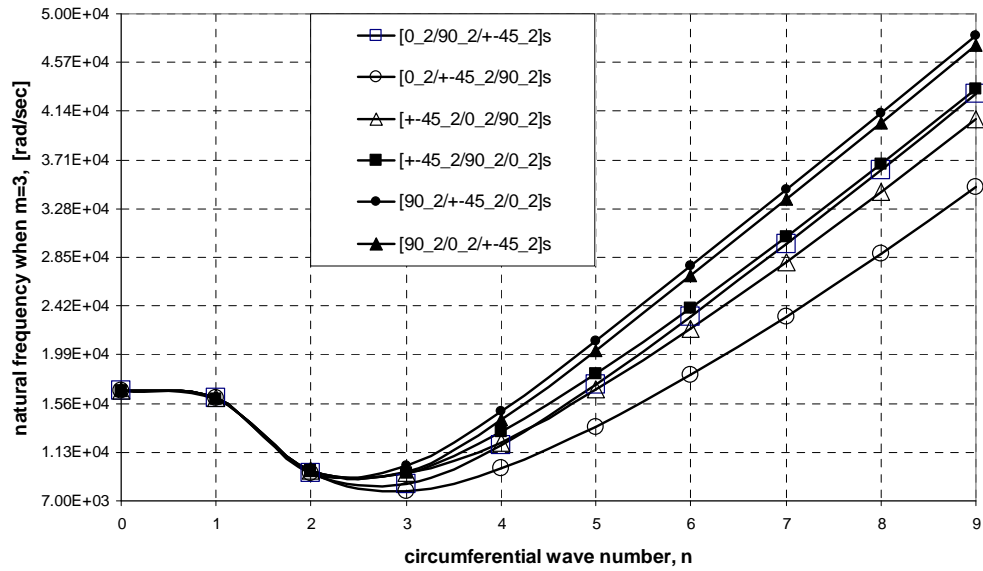
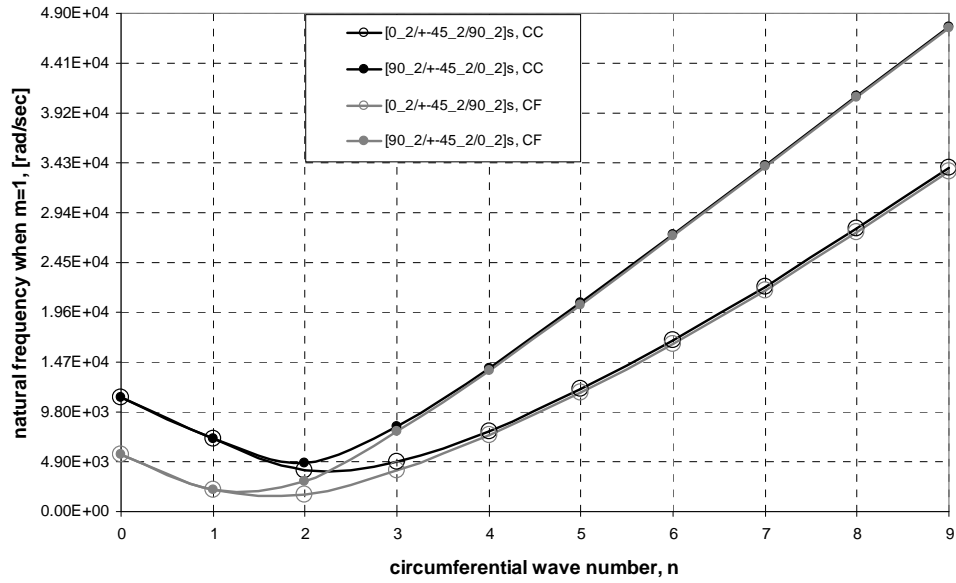
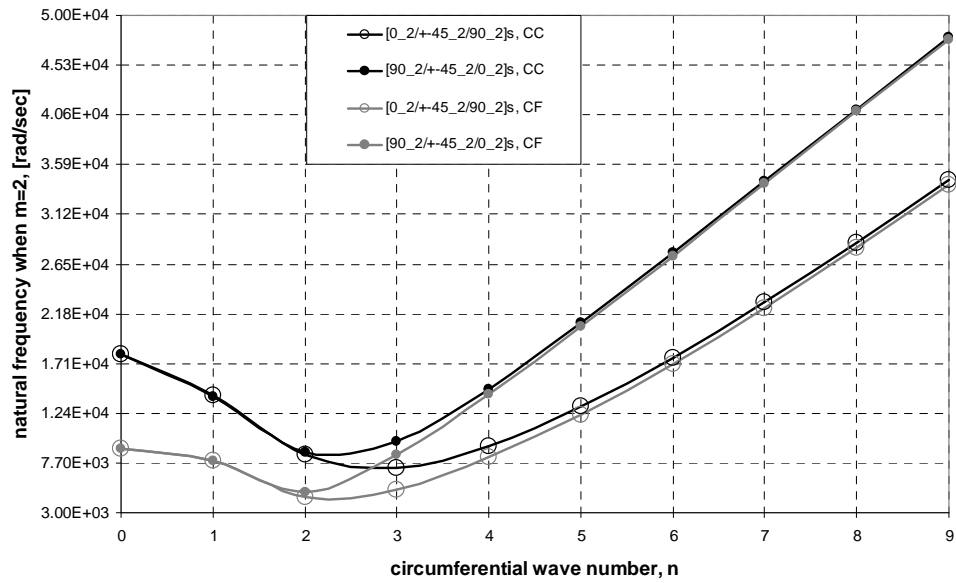


Figure 4.37 Natural frequencies versus circumferential wave numbers for all stacking sequence for clamped-free (CF) boundary condition (m=3 and h/R=0.1).



**Figure 4.38** Comparison of the natural frequencies of the laminated composite circular cylindrical shell having CC boundary conditions with the ones having CF boundary conditions ( $m=1$  and  $h/R=0.1$ ).



**Figure 4.39** Comparison of the natural frequencies of the laminated composite circular cylindrical shell having CC boundary conditions with the ones having CF boundary conditions ( $m=2$  and  $h/R=0.1$ ).

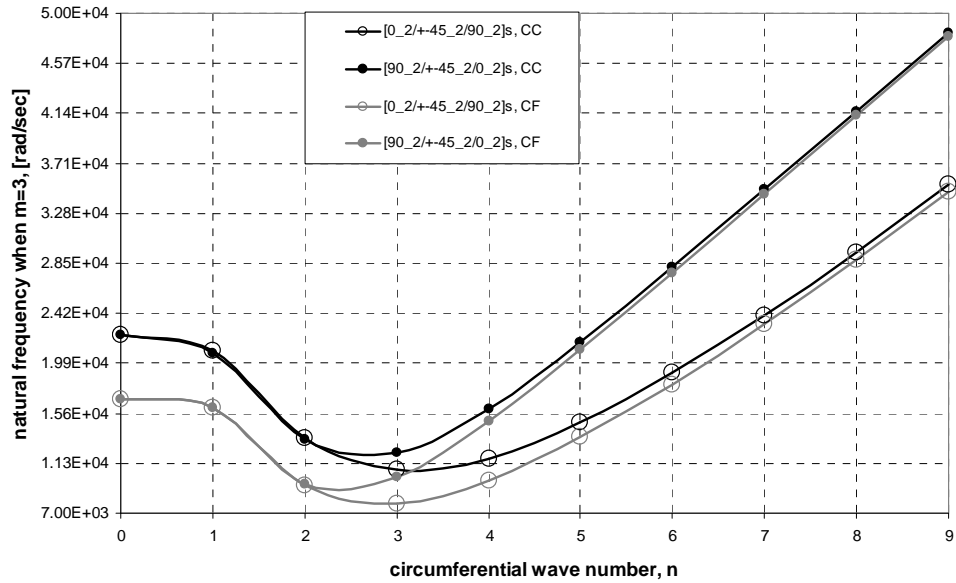


**Figure 4.40** Comparison of the natural frequencies of the laminated composite circular cylindrical shell having CC boundary conditions with the ones having CF boundary conditions ( $m=3$  and  $h/R=0.1$ ).

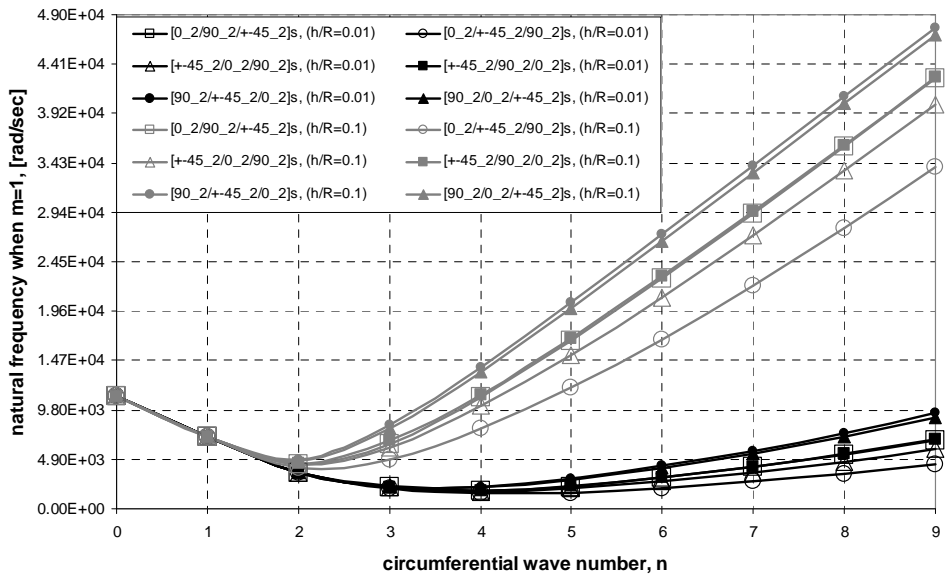


**Figure 4.41** Comparison of the natural frequencies of the thick and thin shell configurations for clamped-clamped (CC) boundary condition ( $m=1$ ).

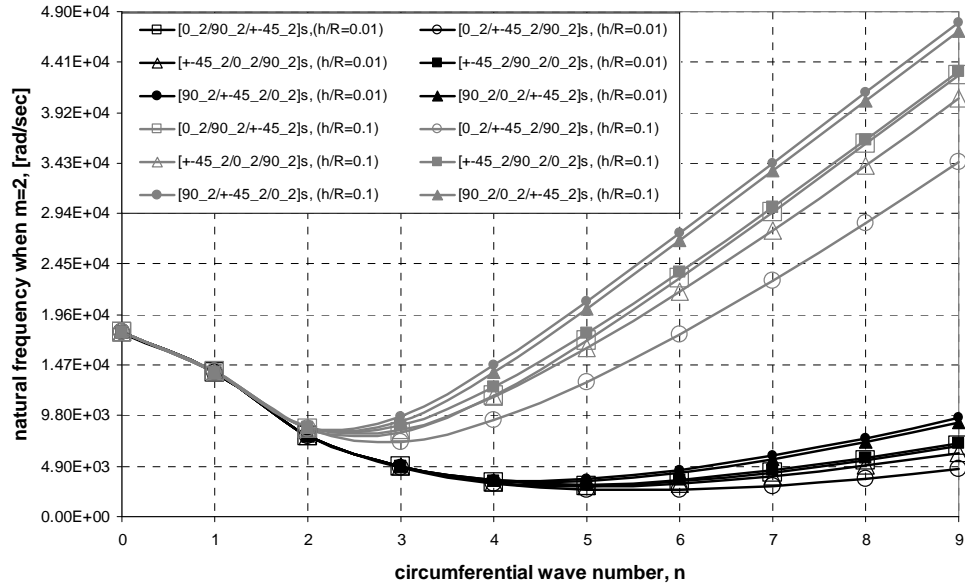


Figure 4.42 Comparison of the natural frequencies of the thick and thin shell configurations for clamped-clamped (CC) boundary condition ( $m=2$ ).

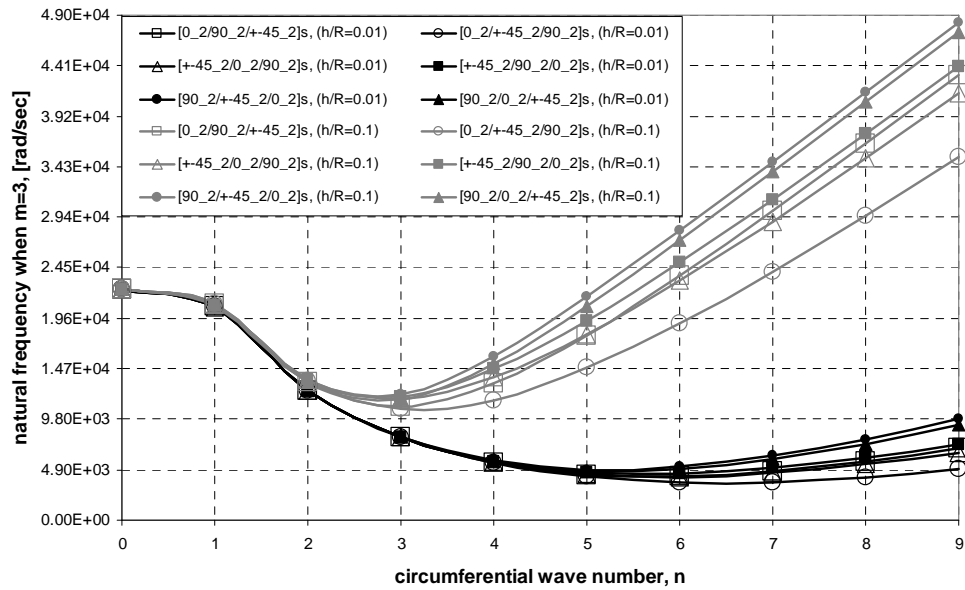
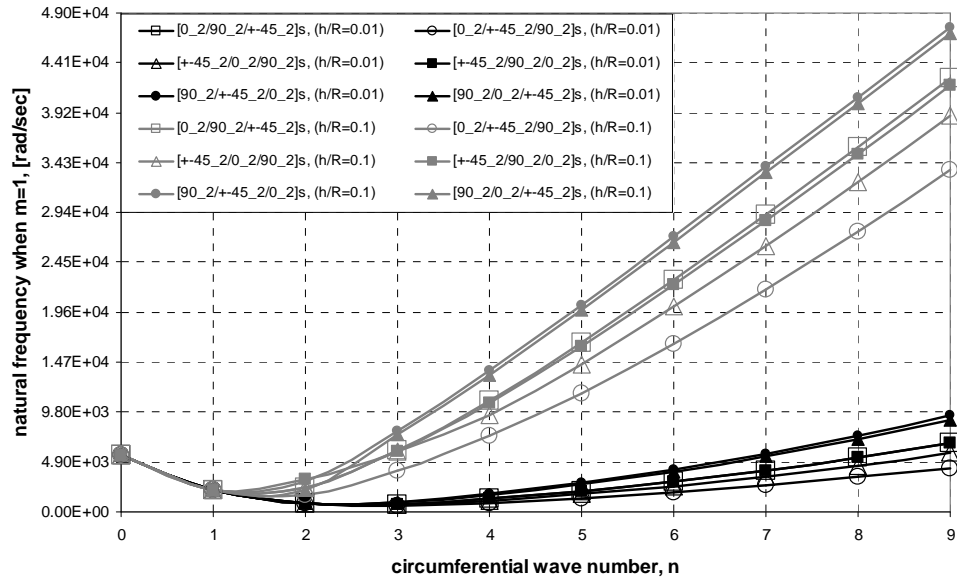
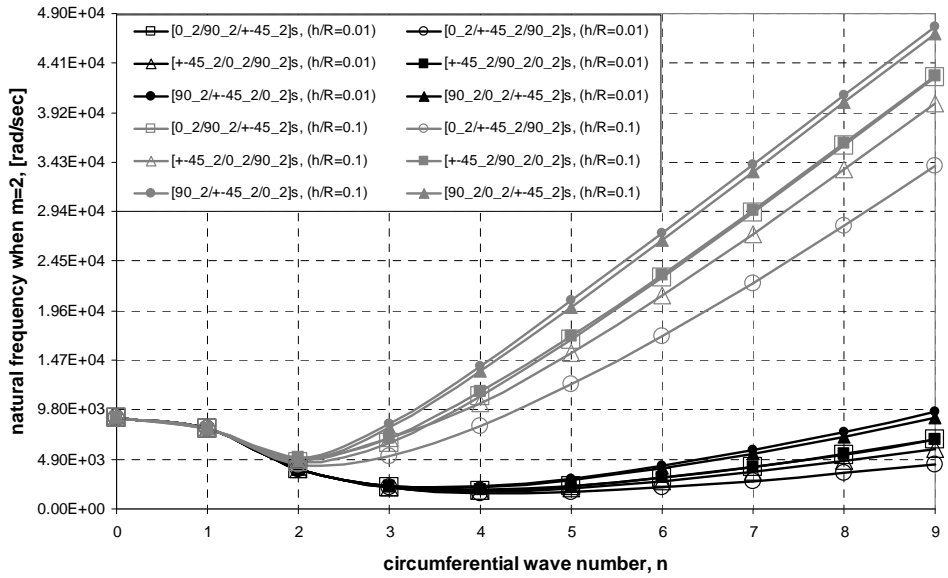


Figure 4.43 Comparison of the natural frequencies of the thick and thin shell configurations for clamped-clamped (CC) boundary condition ( $m=3$ ).



**Figure 4.44** Comparison of the natural frequencies of the thick and thin shell configurations for clamped-free (CF) boundary condition ( $m=1$ ).



**Figure 4.45** Comparison of the natural frequencies of the thick and thin shell configurations for clamped-free (CF) boundary condition ( $m=2$ ).

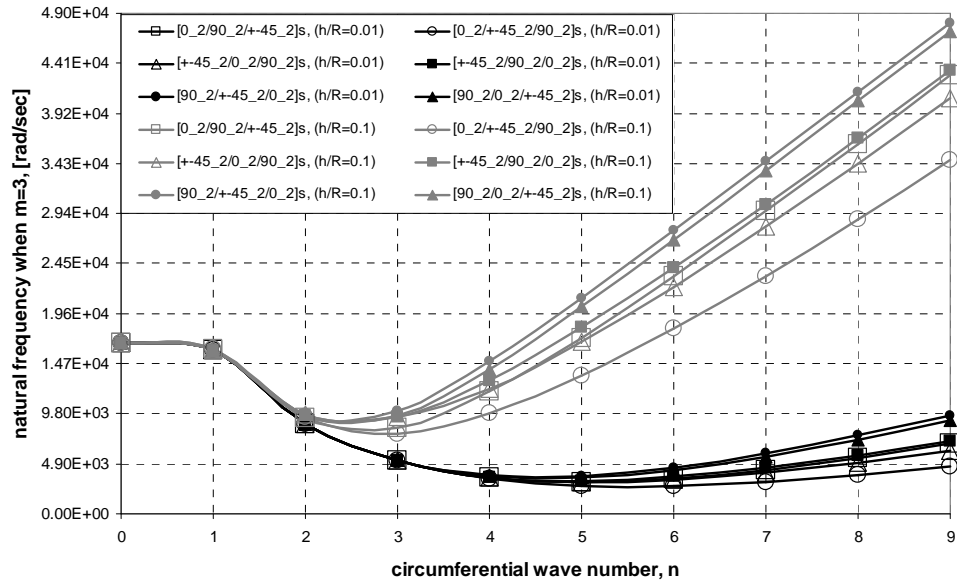


**Figure 4.46** Comparison of the natural frequencies of the thick and thin shell configurations for clamped-free (CF) boundary condition ( $m=3$ ).

#### 4.4.5 CASE STUDY ON EFFECT OF COUPLING TERMS

To study the effect of coupling terms on the natural frequencies three different stacking sequences are used to get numerical results for the laminated composite circular cylindrical shells which has the geometrical, material and laminate properties given in Table 4.42. In order to get all the coupling terms with non-zero values highly orthotropic Boron/Epoxy is used in each ply as the material. For the test cases the circular cylindrical shell is taken as simply supported at both ends. Three different stacking sequences given in Table 4.41 are used, and in each of them  $0^\circ$ ,  $30^\circ$ ,  $60^\circ$  and  $90^\circ$  fiber orientations are utilized for each ply.

**Table 4.41** Three different layups used in the case study on effect of coupling terms.

Layup 1-symmetric	$[0/30/90/60]_s$
Layup 2-antisymmetric	$[0/30/90/60/-60/-90/-30/0]$
Layup 3-unsymmetric	$[0/30/90/60/0/30/90/60]$

**Table 4.42** Geometrical, material properties, and laminate properties of the simply supported laminated composite circular cylindrical shell used for the case study on effect of coupling terms.

Geometrical properties		Mechanical Properties of Boron/Epoxy [71]	
Radius [m]	0.21	$E_1$ [GPa]	224.0
Meridional Length [m]	1.20	$E_2=E_3$ [GPa]	12.7
Thickness [m]	0.0016	$G_{12}$ [Gpa]	4.42
<b>Laminate Properties</b>		$G_{13}$ [Gpa]	4.42
Layup	For each, refer to Table 4.41	$G_{23}$ [Gpa]	2.48
Ply thickness [m]	0.0002	$\nu_{12} = \nu_{13} = \nu_{23}$	0.256
		$\rho$ [kg/m <sup>3</sup> ]	2527.0

Stretching, transverse shear, stretching-flexural coupling, and flexural stiffness coefficients for each of the three different layup cases are given in Figures 4.47, 4.48, 4.49, and 4.50, respectively.

Tables 4.43, 4.44, and 4.45 give the natural frequencies of these three different stacking sequence cases for the circumferential wave number ranging from zero to nine. For each circumferential wave number first three ( $m=1, 2, 3$ ) natural frequencies are tabulated in Tables 4.43, 4.44, and 4.45.

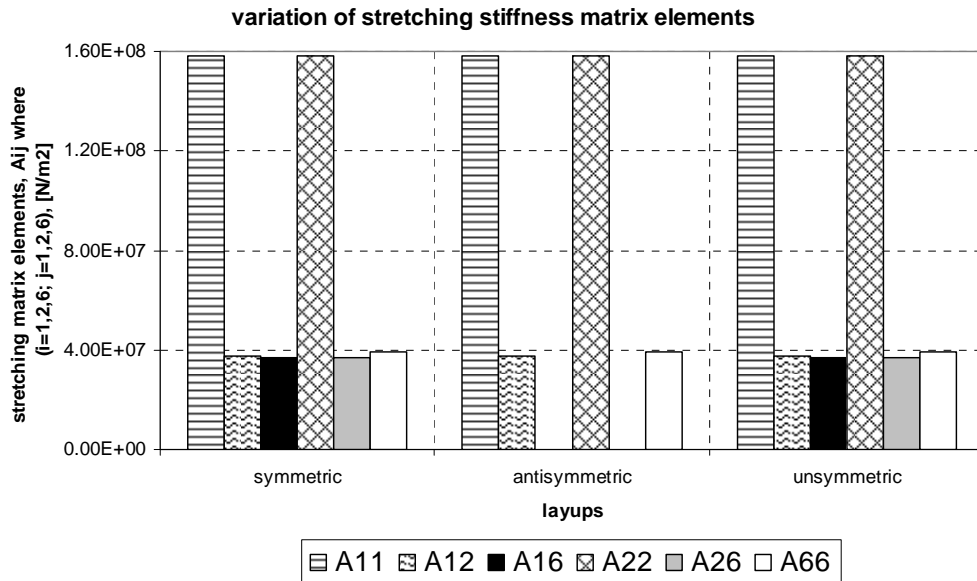


**Figure 4.47** Effect of the stacking sequence on the elements of stretching stiffness matrix for three different layups in the case study on effect of coupling terms.

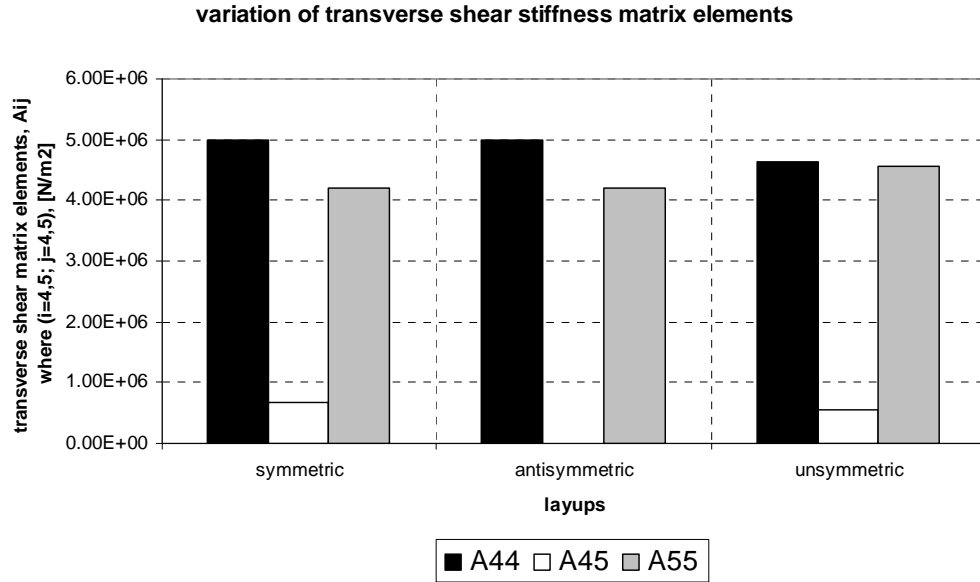


**Figure 4.48** Effect of the stacking sequence on the elements of transverse shear stiffness matrix for three different layups in the case study on effect of coupling terms.

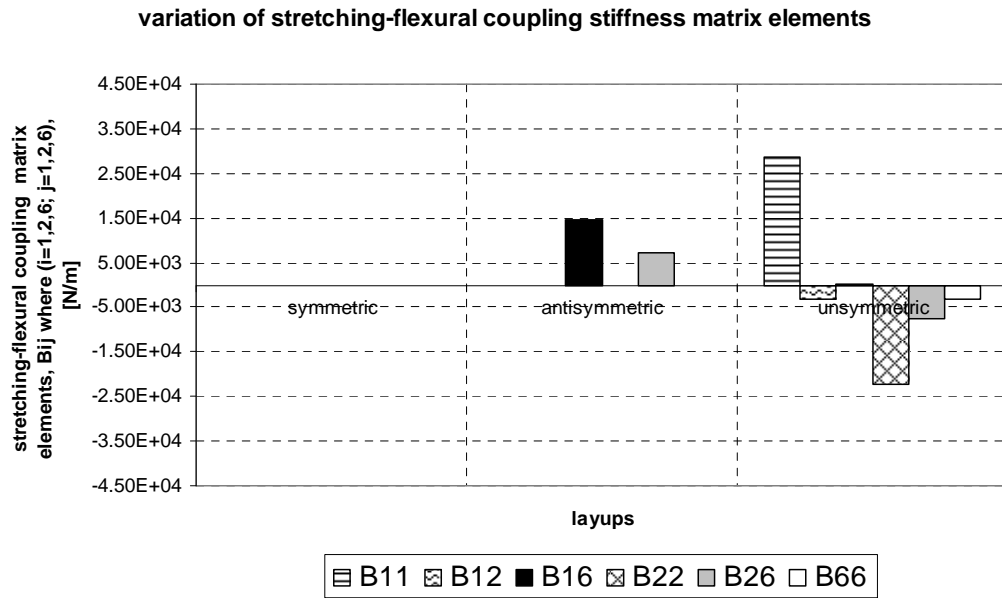


**Figure 4.49** Effect of the stacking sequence on the elements of stretching-flexural coupling stiffness matrix for three different layups in the case study on effect of coupling terms.

variation of flexural stiffness matrix elements

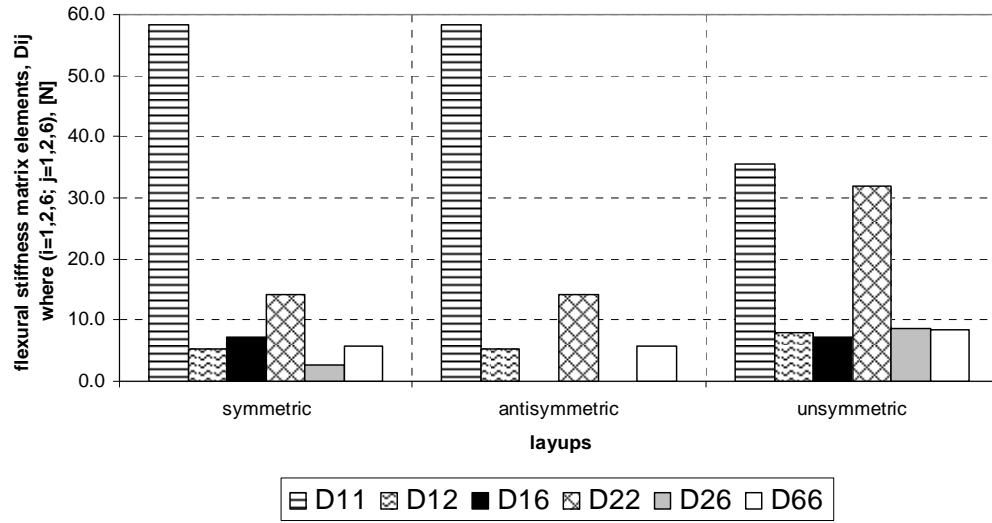


Figure 4.50 Effect of the stacking sequence on the elements of flexural stiffness matrix for three different layups in the case study on effect of coupling terms.

Table 4.43 Natural frequencies (rad/sec) of circular cylindrical shell with symmetric layup  $[0/30/90/60]_s$ .

Symmetric layup $[0/30/90/60]_s$										
m	n=0	n=1	n=2	n=3	n=4	n=5	n=6	n=7	n=8	n=9
1	6501	3477	1513	847	786	1060	1492	2021	2634	3328
2	12397	8316	4503	2644	1799	1564	1747	2179	2755	3432
3	16080	12124	7555	4829	3336	2587	2374	2558	3006	3622

Table 4.44 Natural frequencies (rad/sec) of circular cylindrical shell with antisymmetric layup  $[0/30/90/60/-60/-90/-30/0]$ .

Antisymmetric layup $[0/30/90/60/-60/-90/-30/0]$										
m	n=0	n=1	n=2	n=3	n=4	n=5	n=6	n=7	n=8	n=9
1	8127	4189	1735	927	789	1018	1424	1936	2536	3218
2	15726	10265	5364	3051	1990	1613	1700	2075	2618	3276
3	16251	14792	9182	5719	3829	2832	2435	2491	2860	3430

**Table 4.45** Natural frequencies (rad/sec) of circular cylindrical shell with unsymmetric layup [0/30/90/60/0/30/90/60].

Unsymmetric layup [0/30/90/60/0/30/90/60]										
m	n=0	n=1	n=2	n=3	n=4	n=5	n=6	n=7	n=8	n=9
1	6506	3485	1537	944	1038	1481	2093	2822	3659	4598
2	12408	8342	4545	2729	1996	1957	2364	3019	3824	4744
3	16079	12131	7619	4932	3525	2939	2959	3402	4106	4979

Natural frequencies for the three layup cases are plotted with respect to circumferential wave number in Figures 4.51, 4.52, and 4.53 for m=1,2, and 3, respectively.

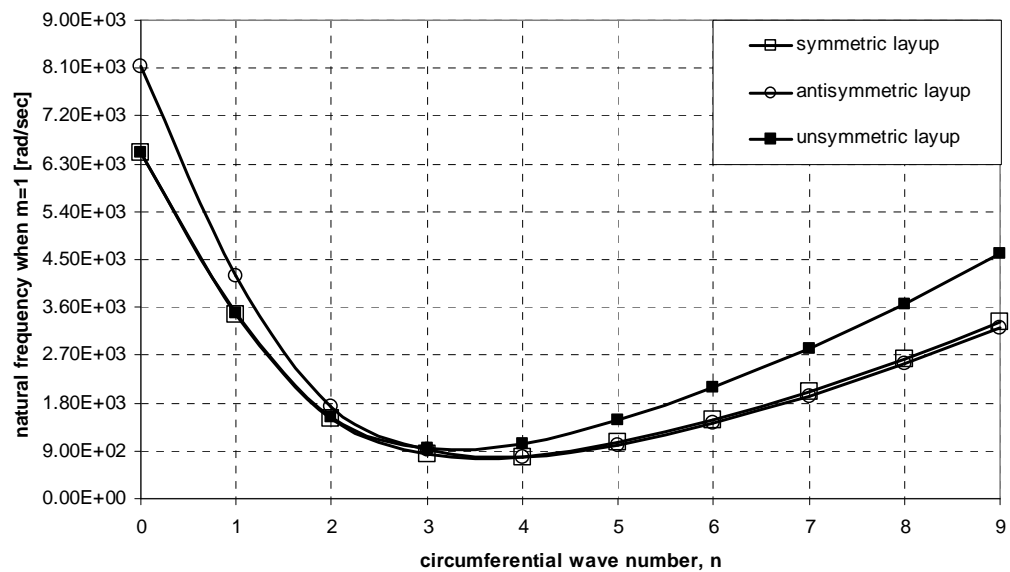


**Figure 4.51** Effect of coupling terms on the natural frequencies of the simply supported laminated composite circular cylindrical shell (m=1).

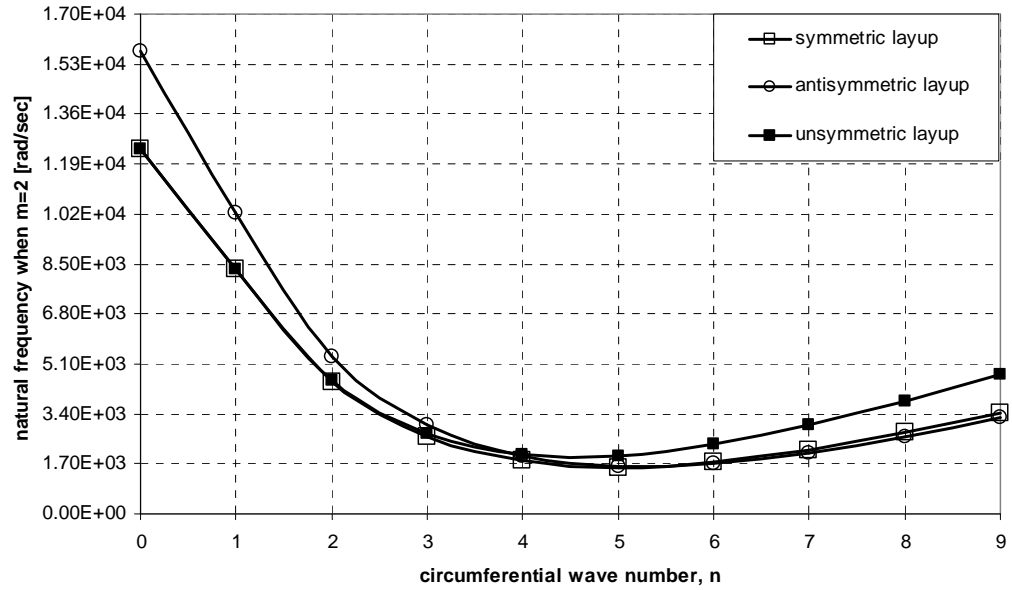


**Figure 4.52** Effect of coupling terms on the natural frequencies of the simply supported laminated composite circular cylindrical shell ( $m=2$ ).

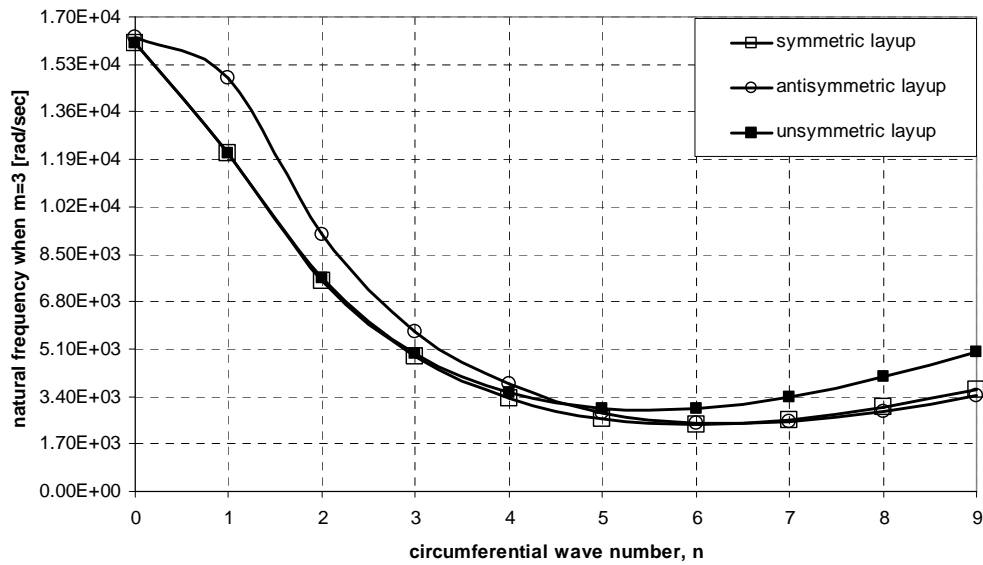


**Figure 4.53** Effect of coupling terms on the natural frequencies of the simply supported laminated composite circular cylindrical shell ( $m=3$ ).

In order to make meaningful explanations about the variation of natural frequencies, one needs to identify the dominant displacement component of the mode shapes. As discussed before after a certain  $n$  value the dominant displacement mode always become the transverse displacement  $w$  because bending strain energy starts to prevail. Results given in Tables 4.43, 4.44, and 4.45 revealed that for  $n \geq 2$  the first three lowest axial modes ( $m=1,2,3$ ) were transverse displacement dominant mode shapes. It is noticed that as  $n$  gets larger the natural frequencies of symmetric and antisymmetric layups, although not equal, were very close to each other. However, the natural frequencies of the unsymmetric layup get higher and higher compared to symmetric and antisymmetric layups as the circumferential wave number gets higher. This behavior can easily be explained by looking at the stiffness coefficients of these layups given graphically in Figures 4.47 to 4.50. For large  $n$ , bending strain energy prevails and we have  $2n$  nodal points around the circumference of the shell. Therefore, as it was discussed previously that bending stiffness coefficient  $D_{22}$  becomes the key element influencing the natural frequency. Because  $D_{22}$  for the unsymmetric layup is higher than either the symmetric layup or the antisymmetric layup, the natural frequencies associated with unsymmetric layup gets higher and higher as we go to higher circumferential wave numbers. Also, in general one should expect the natural frequency to decrease when coupling terms are introduced. When one compares the natural frequencies of symmetric layup and unsymmetric layup, it is seen that the effect of bending stiffness coefficient  $D_{22}$  in increasing the natural frequencies of the unsymmetric layup is more dominant and effective than the effect of stretching-flexural coupling coefficients  $(B_{ij})$  in reducing the natural frequencies.

Careful study of Tables 4.43, 4.44, and 4.45 and Figures 4.51, 4.52, and 4.53 reveals that at low circumferential wave numbers antisymmetric layup has higher natural frequencies compared to symmetric and unsymmetric layups. It is noted that at low  $n$  values the extensional strain energy becomes more dominant and effective; therefore, stretching stiffness coefficients have significant impact on the natural frequencies. It is seen from Figure 4.47, which is the graphical representation of the stretching stiffness coefficients of the each layup, that the stretching-shear coupling terms  $(A_{16}, A_{26})$  are absent for an antisymmetric layup in contrast to symmetric and unsymmetric layups. Thus, relative stiffness of the antisymmetric layup becomes higher at low  $n$  values leading to an increase in natural frequencies. The dominance of the extensional strain energy is also seen when one compares the natural frequencies of symmetric and unsymmetric layups. At low  $n$  values natural frequencies of symmetric and unsymmetric layups are very close to each other. Because symmetric and unsymmetric layups consist of same number of orientation plies but in different stacking sequences. It is well known and also shown in Figure 4.47 that the stretching stiffness coefficients do not depend on the placement of plies within a laminate. Therefore, the stretching stiffness coefficients of the symmetric and unsymmetric layups are equal to each other. Hence, natural frequencies at low  $n$  values are predominantly governed by the stretching stiffness terms, and due to equality of those terms

for symmetric and unsymmetric layups natural frequencies are very close to each other. The slight difference in the natural frequencies is due to the difference in other stiffness coefficients such as  $B_{ij}$  and  $D_{ij}$  between the symmetric and unsymmetric layups.

For  $n=0, 1,$  and  $2$  the mode shapes of  $u_x, u_\theta,$  and  $w$  of the symmetric, antisymmetric, and unsymmetric layups for each three lowest axial modes ( $m=1, 2, 3$ ) are given in Appendix H. For  $n=0$  and  $1,$  the dominant mode shapes related to displacements determined by the mode shape program of the DALSOR are given in Table 4.46 below. For the other  $n$  values, the mode shapes are  $w$  dominant.

**Table 4.46** Dominant mode shapes for three layups for  $n=0,$  and  $n=1.$

m	Symmetric layup		Antisymmetric layup		Unsymmetric layup	
	n=0	n=1	n=0	n=1	n=0	n=1
1	$u_\theta$	$w$	$u_\theta$	$u_\theta$	$u_\theta$	$w$
2	$u_\theta$	$w$	$u_x$	$w$	$u_\theta$	$w$
3	$u_x$	$u_x$	$u_\theta$	$u_x$	$u_x$	$u_x$

As one can see from Table 4.46 for  $n=0,$  axisymmetric case, the dominant modes are all extensional modes  $u_x$  and  $u_\theta.$  Therefore, the natural frequencies of the symmetric and unsymmetric layups are very close to each other, natural frequency being predominantly governed by the extensional stiffness coefficients for  $n=0$  case. It can be seen that for  $n=0$  the first 2 modes for the three layups are  $u_\theta$  dominant. Because  $u_\theta$  is the tangential displacement, this mode implies torsional vibration mode. Kayran [74] has shown that for shells of revolution, for the axisymmetric vibration case ( $n=0$ ), torsional modes totally uncouple from bending and extensional modes only when coupling stiffness coefficients with subscripts 16 and 26 are zero. Under those circumstances the torsional vibration natural frequencies depend on  $A_{66}, B_{66},$  and  $D_{66}$  stiffness coefficients. Kayran has also shown that bending stiffness coefficient  $D_{66},$  bending-twisting coefficient  $B_{66}$  has very little effect on the torsional natural frequency, and for all cross-ply layups the torsional natural frequencies are the same. In the current case study, because the 16 and 26 stiffness coefficients are not zero, one can not talk about the uncoupling of torsional modes from the extensional-bending modes. It is clearly seen that the existence of  $A_{16}$  and  $A_{26}$  terms for the symmetric and unsymmetric layups causes the torsional natural frequencies to be different from the antisymmetric layup. As a matter of fact that first two lowest torsional natural frequencies are seen to differ quite significantly when the layup stacking

sequence is changed such that  $A_{16}$  and  $A_{26}$  coupling terms vanished. The lowest frequency is increased from a value of about 6500 rad/sec to 8127 rad/sec which is a substantial increase demonstrating the significant effect of ply orientations on the dynamic characteristics of the laminated composite shell for a particular mode of vibration studied here.

#### 4.4.6 CASE STUDY ON THE EXISTENCE OF COUPLING TERMS

In this section, the effect of the existence of the coupling terms on the free vibration characteristics is further studied. For this respect, the results of the unsymmetric layup case studied in the previous section are compared with the results of a hypothetical layup in which all the coupling terms of the unsymmetric layup are taken as zero. The stiffness coefficients for the unsymmetric layup when all the coupling terms are set to zero are given in Figures from 4.54 to 4.57. In Figures 4.54-4.57, all coefficients with subscripts 16 and 26 and all stretching-flexural coupling coefficients  $B_{ij}$  are set to zero at the right hand sides for the unsymmetric layup. The three lowest natural frequencies ( $m=1,2,3$ ) for different circumferential wave numbers are listed in Table 4.47 for the unsymmetric layup with all coupling terms omitted.

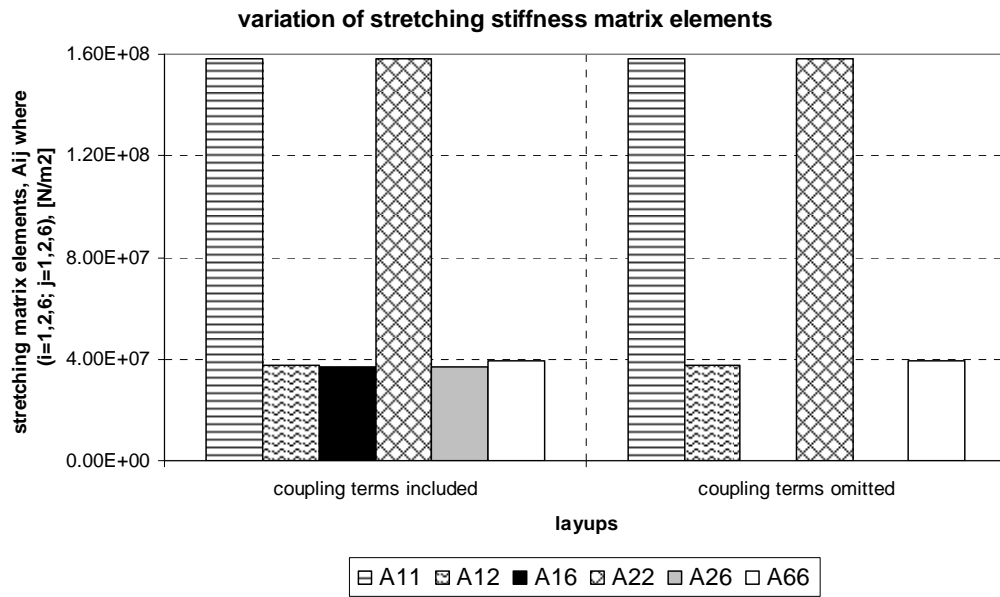


**Figure 4.54** Elements of stretching stiffness matrix for the layups used in the case study on the existence of coupling terms.

variation of transverse shear stiffness matrix elements

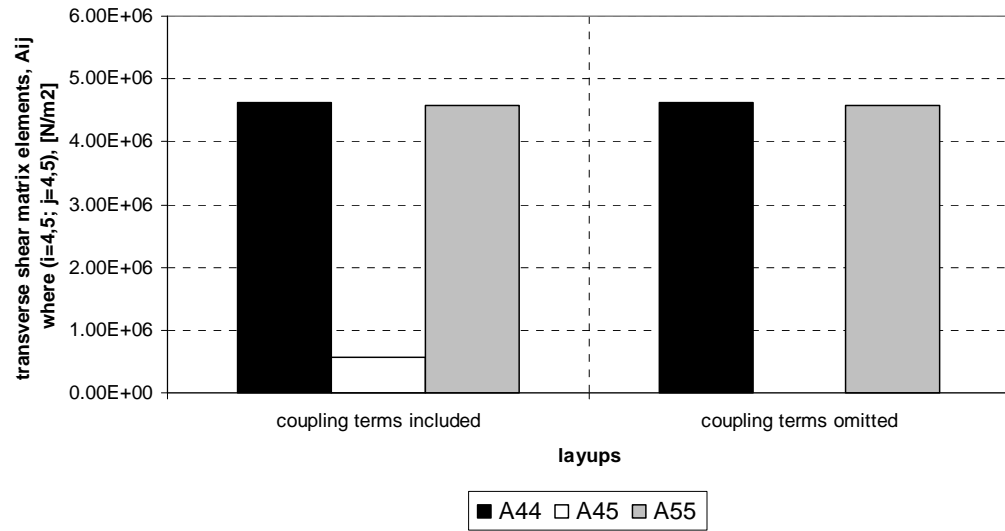


Figure 4.55 Elements of transverse shear stiffness matrix for the layups used in the case study on the existence of coupling terms.

variation of stretching-flexural coupling stiffness matrix elements

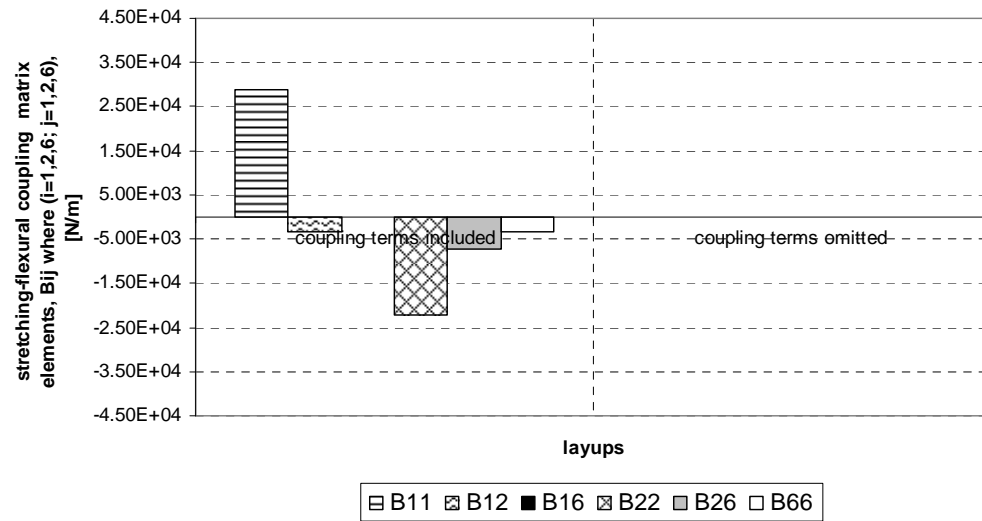


Figure 4.56 Elements of stretching-flexural coupling stiffness matrix for the layups used in the case study on the existence of coupling terms.

variation of flexural stiffness matrix elements

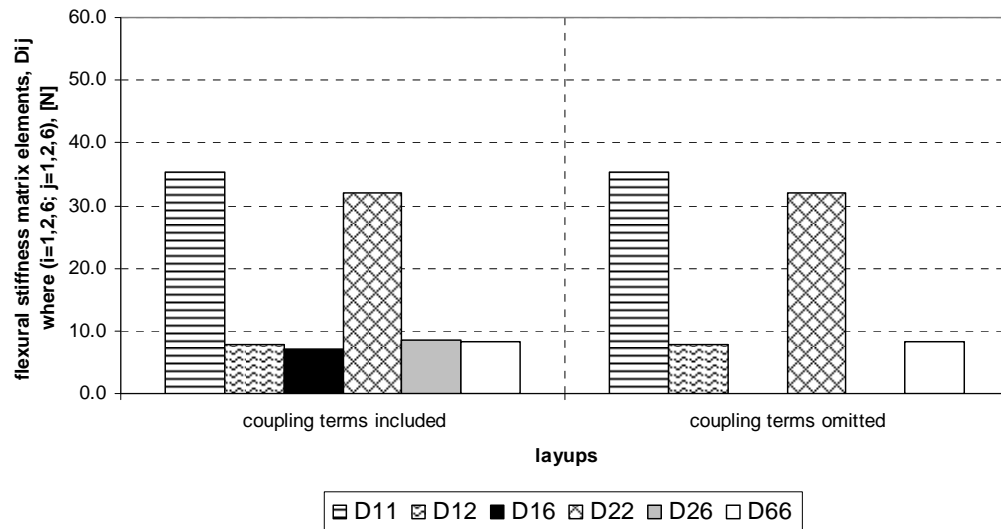


Figure 4.57 Elements of flexural stiffness matrix for the layups used in the case study on the existence of coupling terms.

Table 4.47 Natural frequencies (rad/sec) of circular cylindrical shell with unsymmetric layup  $[0/30/90/60/0/30/90/60]$  with all coupling terms omitted.

Unsymmetric laminate $[0/30/90/60/0/30/90/60]$ with all coupling terms omitted										
m	n=0	n=1	n=2	n=3	n=4	n=5	n=6	n=7	n=8	n=9
1	8139	4193	1741	1003	1072	1550	2223	3040	3985	5057
2	15726	10278	5371	3079	2128	2009	2430	3152	4061	5116
3	16278	14804	9194	5741	3913	3093	3018	3472	4255	5252

The variation of the natural frequencies versus circumferential wave number is given in Figures 4.58, 4.59, and 4.60 for the three lowest modes (for  $m=1,2,3$ ), respectively. Also, the variation of the natural frequency for the unsymmetric layup with coupling terms included is simultaneously given on the same figures. Figures 4.58, 4.59, and 4.60 reveal that when the coupling terms are omitted in the analysis, natural frequencies increase. This increase is due to the absence of coupling terms. The absence of coupling terms make the shell less stiff. It can be seen that after a certain circumferential wave number, further increase in  $n$  results in a larger difference in the natural frequency (for  $m=1$  condition). Yet, when one goes to higher modes at each circumferential wave

number, the difference between the natural frequencies of coupling terms included and those of coupling terms omitted becomes less and less. For the low circumferential wave numbers the difference between the unsymmetric layup case and unsymmetric layup case with the coupling terms omitted is seen to be higher.

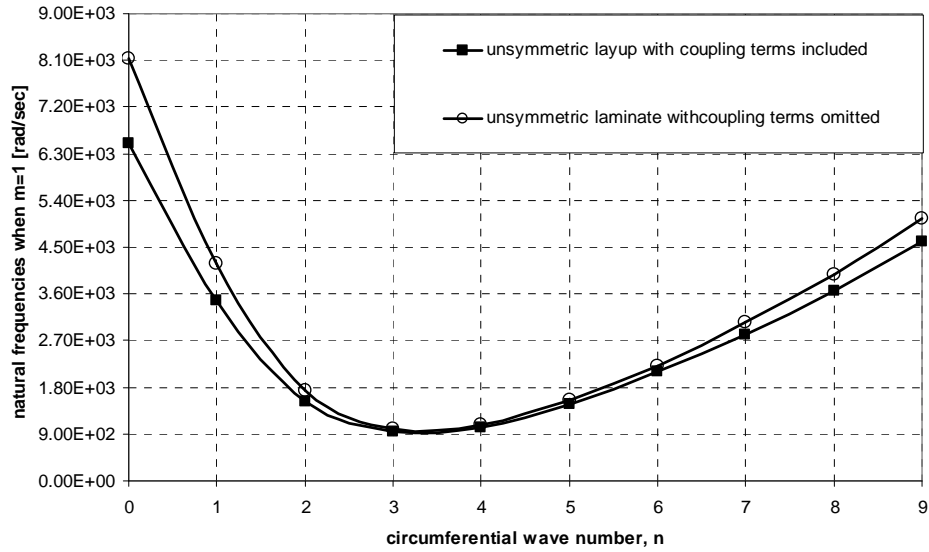


Figure 4.58 Effect of the coupling terms on the natural frequencies over n range of 0-9 (m=1).

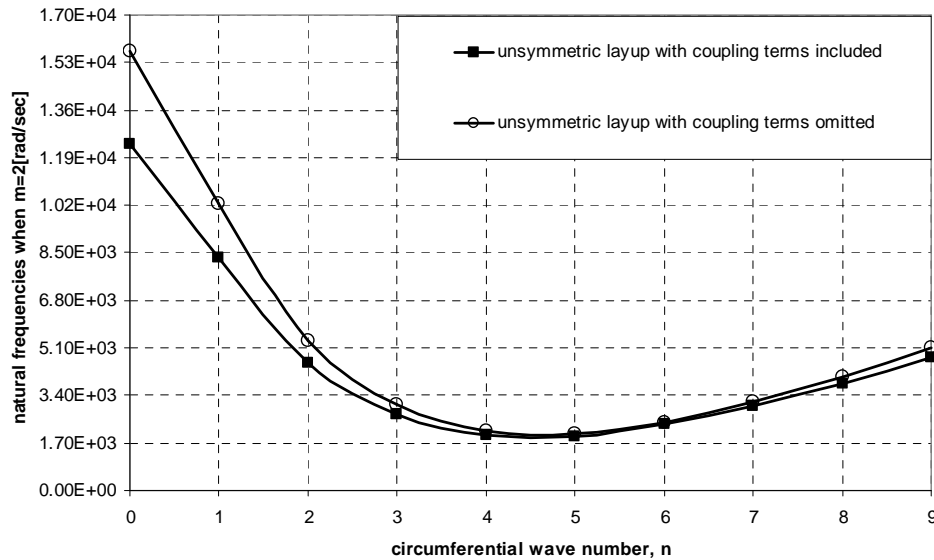
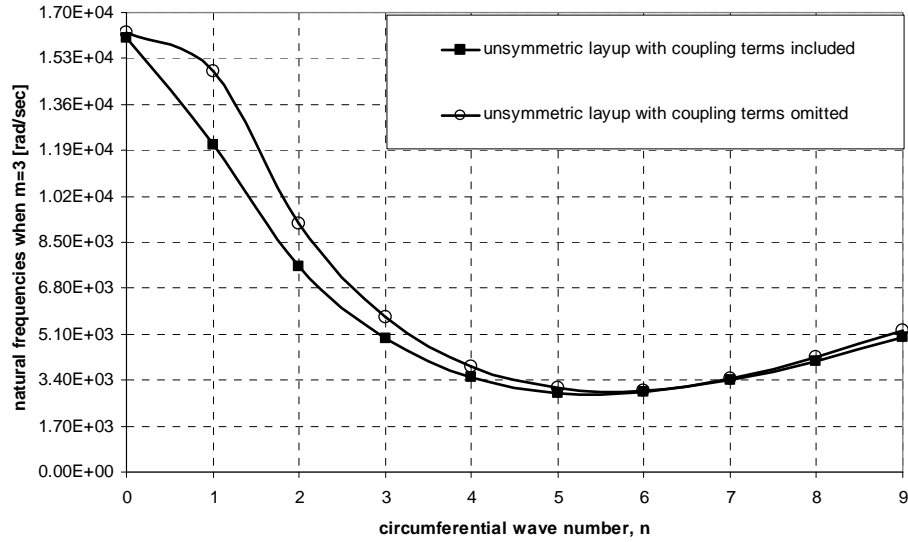


Figure 4.59 Effect of the coupling terms on the natural frequencies over n range of 0-9 (m=2).



**Figure 4.60** Effect of the coupling terms on the natural frequencies over n range of 0-9 (m=3).

As seen from Figures 4.58-4.60, omitting coupling terms may introduce significant errors for certain modes. When one omits the coupling terms, the resulting equations look like the governing equations of orthotropic layup case for which quite easier solutions can be obtained. However, one actually needs to verify the actual difference in a forced vibration problem and build up a solution from the free vibration modes. In a forced vibration or transient loading problem one would start from the lower modes and superimpose the results and cut the modal participation after a certain mode. Since lower modes have considerable differences between the natural frequencies, it is expected that forced vibration or transient loading solutions for the unsymmetric layup case without coupling terms and the unsymmetric layup with coupling terms case would differ in a proportion that is not negligible. However, this is needed to be verified.

One last interesting discussion can be made after comparing the results of the antisymmetric layup case with the unsymmetric layup case with coupling terms omitted. Comparison of the figures of stiffness coefficients (Figures 4.47-4.50 and Figures 4.54-4.57) shows us the followings:

- Extensional stiffness terms  $(A_{ij})$  are identical. Because in an antisymmetric layup  $A_{16}$  and  $A_{26}$  terms turn out to be zero and they are omitted in the unsymmetric layup case.
- Transverse shear stiffness terms  $(A_{44}$  and  $A_{55})$ , although not the same, are very close to each other.
- In terms of extensional-bending coupling terms  $B_{ij}$ , antisymmetric layup has nonzero

$B_{16}$  and  $B_{26}$  terms only. The other terms are zero for both case.

- From bending stiffness terms ( $D_{ij}$ ),  $D_{11}$ ,  $D_{22}$ ,  $D_{12}$ , and  $D_{66}$  have different values from each other, but  $D_{16}$  and  $D_{26}$  terms are zero for both cases.

Considering that at low circumferential modes extensional strain energy dominates, when one compares the layup stiffnesses given above, one can conclude that for low  $n$  values . natural frequencies should be very close to each other. This conclusion could actually be verified by extracting the natural frequencies of low  $n$  values, for instance for  $n=0,1$ , and  $2$ , from the respective natural frequency tables of the antisymmetric layup case (Table 4.44) and the unsymmetric layup case with coupling terms omitted (Table 4.47).

**Table 4.48** Comparison of the natural frequencies (rad/sec) between antisymmetric layup case and unsymmetric layup with coupling terms omitted for  $n=0,1$ , and  $2$ .

	[0/30/90/60/-60/-90/-30/0]			[0/30/90/60/0/30/90/60]		
	Antisymmetric layup			Unsymmetric layup with coupling terms omitted		
	n=0	n=1	n=2	n=0	n=1	n=2
m=1	8127	4189	1735	8139	4193	1741
m=2	15726	10265	5364	15726	10278	5371
m=3	16251	14792	9182	16278	14804	9194

The results given in Table 4.48 also confirm that at low circumferential modes (low  $n$ ) the influence of bending stiffness  $D_{ij}$  is very little. Although these two layups have different bending stiffness coefficients, due to dominance of the extensional strain energy at low  $n$ , natural frequencies are governed largely by the extensional stiffness coefficients.

## 4.5 LAMINATED COMPOSITE SPHERICAL SHELL

In this section, it is intended to show a solution for free vibration analysis of a spherical shell to demonstrate the applicability of the method of solution to any general shape of shell of revolution. Up to this point in this chapter, the numerical results for the free vibration analysis of anisotropic laminated composite shells of revolution are performed for a circular cylindrical shell. Like the circular cylindrical shell, a spherical shell is a typical example for the shells of revolution. Spherical

shells are also structural elements of the aeronautical and space structures such as an antenna of a satellite or a nose of an aircraft, etc. The geometrical, material, and material properties of the clamped-free (CF) laminated composite spherical shell are given in Table 4.49. The side and perspective views of the laminated composite spherical shell is shown in Figure 4.61. The natural frequencies for  $n=1$  and  $m=1,2$ , and 3 are given in Table 4.50. Also, the mode shapes corresponding to those natural frequencies are given in Figures 4.62.

**Table 4.49** Geometrical, material properties, and laminate properties of the clamped-free laminated composite spherical shell.

Geometrical properties		Mechanical Properties of High Modulus Graphite/Epoxy[55]	
Radius [m]	1.0	$E_1$ [GPa]	207.348182
Thickness [m]	0.00192	$E_2=E_3$ [GPa]	5.183702
		$G_{12}$ [Gpa]	3.110261
		$G_{13}$ [Gpa]	3.110261
Layup	$[90_2 / \pm 45_2 / 0_2]_s$	$G_{23}$ [Gpa]	3.110261
Ply thickness [m]	0.00012	$\nu_{12} = \nu_{13} = \nu_{23}$	0.25
		$\rho$ [kg/m <sup>3</sup> ]	1524.4740

**Table 4.50** Natural Frequencies for the laminated composite spherical shell ( $n=1$ ).

m	Natural Frequency [rad/sec]
1	281
2	4850
3	6695

As one can see from the mode shape plots, first three modes for  $n=1$  correspond to transverse displacement modes. It is further seen that for a particular layup the sine Fourier components are much smaller than the cosine Fourier components in magnitude. Therefore, when both Fourier components are overlayed on the same figure (Figure 4.62) sine Fourier components almost seem to be nonexistent. Thus, practically one can regard variation of the cosine Fourier component as the actual mode shape.

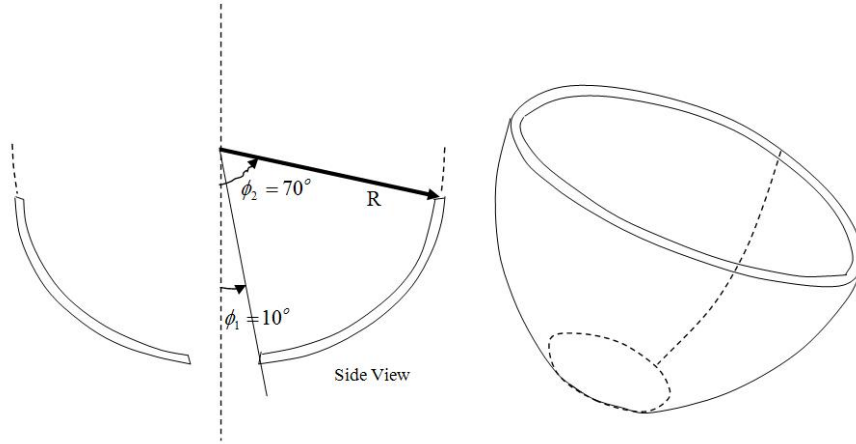


**Figure 4.61** The side and perspective views of the laminated composite spherical shell.

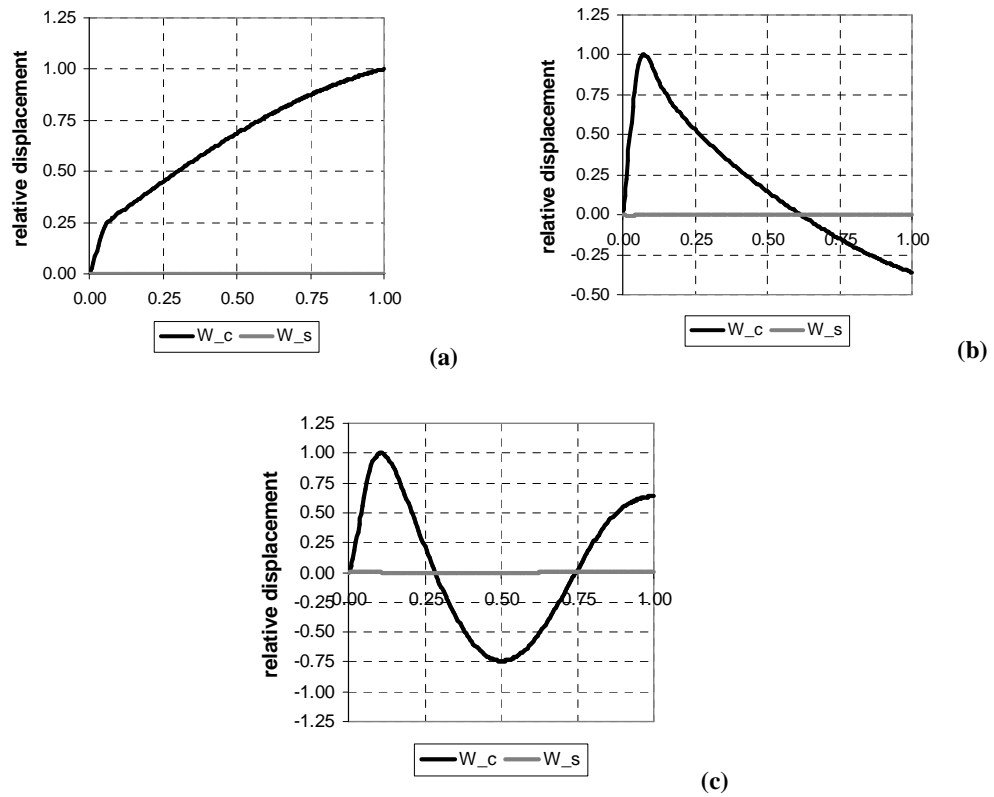


**Figure 4.62** Dominant mode shapes (transverse displacement) of the corresponding natural frequencies given in Table 4.50 for (a)  $m=1$ , (b)  $m=2$ , and (c)  $m=3$ .

It can be considered that for the layup  $[90_2 / \pm 45_2 / 0_2]_s$  actually has stiffness coefficients very similar to a layup with no coupling terms. For layups with no coupling terms we have previously mentioned that sine Fourier components vanish. Therefore, low values for the sine Fourier component of the transverse displacement is verified.

## CHAPTER 5

### CONCLUSIONS AND RECOMMENDATIONS

In this thesis, the free vibration analysis of anisotropic laminated composite shells of revolution was studied. Shells of revolution made of advanced composite materials such as graphite/epoxy and/or boron/epoxy have been utilizing as primary and secondary structural components in aeronautical and space structures for more than forty years. The advanced composite materials are preferred in the design and manufacture over metallic materials due to their high strength-to-weight and stiffness-to-weight ratios compared to metallic counterparts. For the sake of performance and structural integrity, the dynamic behavior of these structural components is needed to be investigated and to be understood comprehensively. Thus, it is essential to determine dynamic characteristics such as natural frequencies and associated mode shapes. For this purpose a computer code named DALSOR (Dynamic Analysis of Anisotropic Laminated Shells of Revolution) was developed. The description and flow-chart of the DALSOR are given in Section 3.7.

The governing equations for the free vibration analysis of anisotropic laminated composite shells of revolution were derived in Chapter 2. A displacement-based two dimensional shell theory; namely, Reissner-Naghdi shell theory with geometrically linear strain-displacement equations was used in combination with first-order shear deformation theory in which transverse shear and rotatory inertia effects are taken into consideration. Statically equivalent force and moment resultants instead of internal stresses for a single layer were introduced in the constitutive relations of the macroscopically anisotropic laminated composite shells of revolution. Equations of motion for the free vibration problem under consideration were derived with the help of the Hamilton's principle.

Chapter 3 presented the method of solution to the derived governing equations for the free vibration analysis of anisotropic laminated composite shells of revolution. Those equations were initially formulated into a system of partial differential equations in terms of fundamental variables which are displacements  $(w^o, u_\phi^o, u_\theta^o)$  and rotations  $(\beta_\phi, \beta_\theta)$  of the reference surface of the shell, force resultants  $(Q_\phi, N_\phi, N_{\phi\theta})$ , and moment resultants  $(M_\phi, M_{\phi\theta})$ . Then, the formulated system of partial differential equations was reduced to a system of first order ordinary differential equations with

the application of Finite Exponential Fourier Transform Method. Since the shell of revolution is rotationally symmetric, the motion must be periodic in  $\theta$ . For the shell of revolution which is laminated in cross-ply (specially orthotropic) configurations, each fundamental variable in the governing equations for free vibrations of the laminated composite shell of revolution can be separated in  $\theta$  as a function of  $\cos(n\theta)$  or  $\sin(n\theta)$ , where  $n$  is the circumferential wave number, commonly known as the Fourier components. This type of separation of variables is known as traditional Fourier decomposition procedure. However, the traditional Fourier decomposition procedure is inapplicable for laminated composite shells of revolution possessing the material anisotropy in each layer due to the existence of deformation couplings as a result of fiber orientation making an angle  $\alpha$  with the meridional direction of the shell. After the application of the finite exponential Fourier transform method, a two point boundary value problem was obtained including 20 homogeneous linear first order ordinary differential equations and 20 unknowns which were actually the finite exponential Fourier transform of the fundamental variables. This way, the finite exponential Fourier transform of the fundamental variables in the system of first order ordinary differential equations became only functions of the axial coordinate  $\phi$  of the shell of revolution. Then, this two point boundary value problem was reduced to a series of initial value problems. The multisegment numerical integration, in which Adam's predictor-corrector method was utilized, was carried out via dividing the shell into segments so as to solve the obtained series of initial value problems. Natural frequencies were calculated by the Frequency Trial Method which is essentially a systematized process of trial and error in which the input to each iteration step is a trial value of the natural frequency. Within the given range of natural frequencies, a probable natural frequency (or frequencies) was (were) sought through the change of slopes calculated from the determinant of  $C_M$  in Equation 3.78 of consecutive natural frequencies.

The scope of Chapter 4 was numerical results produced by the developed code DALSOR for the free vibration analysis of anisotropic laminated composite shells of revolution, and also the discussions made regarding those results. Various case studies were performed in order to investigate the effects of primarily fiber orientation angle, stacking sequence, arbitrary boundary conditions at the edges of the shell, thickness-to-radius ratio on the natural frequencies of a laminated composite circular cylindrical shell in Chapter 4. Additionally, mode shapes were determined for some cases.

The following general conclusions can be drawn from the present research documented with this thesis:

- It was aimed to build up an accurate and efficient tool for determining the free vibration characteristics of anisotropic laminated composite shells of revolution. The accuracy of the method of solution of the developed code was verified with the exact method of solution for a simply supported laminated composite shells of revolution whose procedure is given by Soedel [13] (refer to Table 4.2).

The frequency trial method coupled with multisegment numerical integration technique was extended to the vibration problem of macroscopically anisotropic shells of revolution including the transverse shear deformation and rotatory inertia. When the full anisotropic form of constitutive equations was included it has been demonstrated that the determinant of the frequency matrix  $C_M$  (Equation 3.78) does not change sign. Therefore, a slope change algorithm was designed to solve the resulting eigenvalue problem. Although the method of solution utilized is a trial method, for the particular shell theory the method developed in this thesis is actually exact. Therefore, high accuracy should be expected, and the accuracy of the method was verified. Thus, the method of solution can actually be used to verify results of different finite element codes. It should be noted that analytical solution of general shell of revolution which include all coupling terms in the stiffness coefficients does not exist. Therefore, finite element method is a common tool to solve the dynamic problems associated with anisotropic shells of revolution. However, in finite element approach there is a need to verify the accuracy of the developed code. This verification can only be done either comparing the results with the experimental results or by comparing the results of the finite element method with the results of other means whose accuracy can be relied on. Because there are so many design parameters for laminated composite shells of revolution, performing experiments for all combinations of design parameters is not feasible. Therefore, there is a definite need to have alternative method of solution to verify the results of finite element codes. It is claimed that the code developed DALSOR will provide an alternative solution method which can be used to verify the results of the finite element codes. In the current thesis, the laminated composite circular cylindrical shells without complicating effects were studied. However, we can encounter engineering problems having complicating effects and complex configurations in the real world. In order to solve those complex problems, the finite element tool is an effective and practical tool. It is believed in that the present developed code DALSOR will help one to determine an accurate finite element type for the dynamic analysis. First, a laminated composite shell of revolution, for instance a circular cylindrical shell, without complicating effects is solved with both the DALSOR and determined standard finite element software. During the dynamic analysis, the accurate finite element type can be searched among the available finite element types of the determined standard finite element software. Consequently, the determined finite element type can be used in the dynamic analysis of complex problems.

For design problems in which the critical excitation frequency is known the method can be utilized very effectively and the dynamic characteristics of the structure modeled as a shell of revolution can be determined very accurately in a very short time. A priori knowledge of the critical frequency interval significantly reduces the work load with the present method and identification of natural frequencies in a frequency interval can be performed effectively.

For dynamic loading or transient vibration type of problems one only requires certain number of low frequency modes for accurate determination of the response of the structure. Complete

spectrum of frequencies and modes shapes is not required in most dynamic problems. Therefore, the present method of solution can be regarded as a comparable method to the finite element method for extracting the dynamic characteristics. However, because the present method is actually an exact method for the particular shell theory used, compared to a finite element method utilizing the same shell theory the present method is expected to provide more accurate results.

- Shell theories must incorporate both flexural and extensional deformations due to the existence of a curvature. In fact, the curvature of the shell results in coupling of the extensional and flexural deformations of the shell. The deformation of a shell can vary from purely extensional to purely flexural. It was shown by Warburton [79] (Fig. 4.10) that bending (or flexural) strain energy associated with vibratory motion increases with the circumferential wave number  $n$ , whereas stretching (or extensional) strain energy decreases with  $n$ . For all case studies performed in Chapter 4, the variation of natural frequencies with respect to circumferential wave number looked similar with the finding of Warburton given in Figure 4.10. In other words, it can be concluded that for larger  $n$  the bending strain energy dominates in the free vibration, and for lower  $n$  the extensional strain energy dominates in the free vibration. This fact is also confirmed by the determined mode shapes for each  $n$ .
- In general, at low circumferential wave numbers, the natural frequencies of shells with meridional fiber orientation are higher than the natural frequencies of shells with circumferential fiber orientation. This can be explained with the higher extensional stiffness coefficient  $A_{11}$  and the higher flexural stiffness coefficient  $D_{11}$  for lower fiber orientation angles. However, for high circumferential modes the natural frequencies of circumferentially laminated shells become higher than the natural frequencies of meridionally laminated shells due to higher extensional stiffness coefficient  $A_{22}$  and higher flexural stiffness coefficient  $D_{22}$  for higher fiber orientation angles. However, depending on the particular mode of vibration and on dominant vibration mode, different conclusions can be inferred with regard to the effect of fiber orientation angle on the natural frequencies at low circumferential modes. For instance, for axisymmetric breathing mode of vibration for higher modes circumferential fiber orientation causes frequencies to increase. Therefore, for low circumferential modes the effect of fiber orientation should be analyzed case by case.
- The natural frequencies of the thick shells are higher than the ones of the thin shells, for higher circumferential modes, when all mechanical, laminate, and geometrical properties except the thickness-to-radius ratio are kept same. However, at low circumferential modes the effect of thickness on the natural frequencies diminishes. The reason for this behavior is explained in detail in the thesis and it was primarily attributed to extensional vibration character of shells at low circumferential modes. It was observed that anisotropy did not alter this behavior. It has also been shown that for

thicker shells lowest natural frequencies occur at lower circumferential modes compared to a thin shell.

- The effect of coupling terms on the natural frequencies can be very significant especially at low circumferential modes. Therefore, especially for transient vibration problems such as buffeting, dynamic loading or store flutter type of problems full anisotropic form of the constitutive equations should be kept. Failure to do so could result in incorrect structural response because lower modes usually have higher modal participation to the response.

## **RECOMMENDATIONS FOR FUTURE WORK**

The method presented can also be extended to the static problems. Thus, stress analysis of any macroscopically anisotropic laminated composite shell of revolution with general boundary conditions can be carried out by the shell theory used; first order transverse shear deformation theory of Reissner and Naghdi.

The method of solution can further be extended to higher order transverse shear deformation theories by modifying the coefficient matrix  $K$  given in equation 3.47. There is no need of using the shear correction factor when higher order transverse shear deformation theories are used. Table 1.2 gives the various higher order transverse shear deformation theories.

Possibility of extending the present method of solution the laminated shells of revolution which are modeled as layerwise rather than as an equivalent single layer can be sought.

The power of present method of solution can be demonstrated by applying it to problems in which meridional variation of shell design parameters such as thickness, layup, stacking sequence are taken into consideration. Circumferential stiffeners can also be incorporated into the analysis by slight modification of the code DALSOR. The procedure for including the stiffeners in the computational modeling of free vibration analysis of anisotropic laminated composite shells of revolution is explained with the aid of Figure 5.1 which displays the cross-sections of the laminated composite circular cylindrical shells with a single stiffener or more than one stiffener. Figure 5.1a shows the cross-section of the circular cylindrical shell with a single stiffener. The corresponding coefficient matrices of the stiffener part, the left non-stiffener part, and the right non-stiffener part, which are given in Equations (3.47) and (3.60), are computed properly by taking a continuous reference surface for the shell including every part. The meridional length of the shell should be divided into segments appropriately. The starting and final coordinates of each part are known; therefore, changing coefficient matrices  $K$ 's of the parts should be incorporated properly into Equation (3.73). The similar considerations can be taken when studying laminated composite circular cylindrical shells with more than one stiffener.

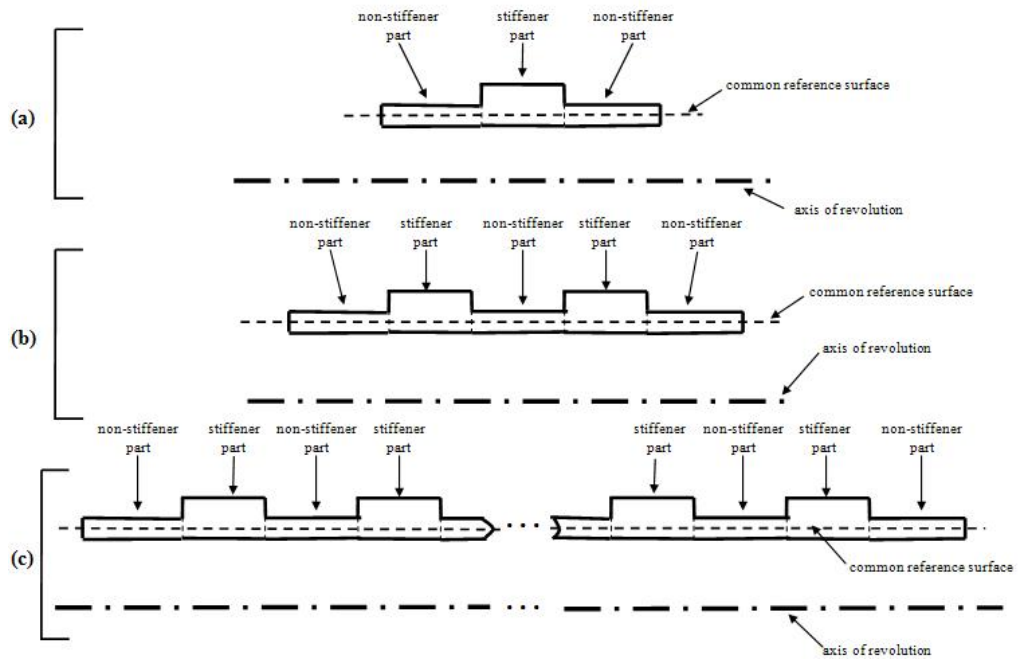


**Figure 5.1** Cross-sections of the circular cylindrical shells with  
 (a) a single stiffener, (b) two stiffeners or, (c) multi-stiffeners.

## REFERENCES

- [1] Jones, Robert M., "*Mechanics of Composite Materials*," Washington, Scripta Book Co., 1975.
  
- [2] ASM International Handbook Committee, "*Engineered Material Handbook, Volume 1: Composites*," ASM International, Metals Park, Ohio, 1988.
  
- [3] Niu, Michael Chun-Yung, "*Composite Airframe Structures*," Hong Kong Conmilit Press Ltd., Hong Kong, 1992.
  
- [4] Reddy, J. N., "*Mechanics of Laminated Composite Plates-Theory and Analysis*," Boca Raton, USA, CRC Press, 1997.
  
- [5] Tsai, Stephen W., "*Theory of Composite Design*," Dayton, Ohio: Think Composite, 1992.
  
- [6] Tsai, Stephen W., "*Introduction to Composite Materials*," Westport, Conn: Technomic Pub., 1980.
  
- [7] Scaled Composites, LLC., "*Scaled Composites, LLC: composite aircraft design, prototyping and flight test*," <http://www.scaled.com/index.html>, last visited on June 2005.
  
- [8] Vinson, J.R., and Sierakowski, R.L., "*The Behaviour of Structures Composed of Composite Materials*," Martinus Nijhoff, Hingham, Massachusetts, 1986.
  
- [9] Meirovitch, L., "*Analytical Methods in Vibrations*," New York, Macmillan, 1967.
  
- [10] Love, A. E. H., "*The Small Free Vibrations and Deformations of a Thin Elastic Shell*," Phil. Trans. Roy. Soc., London, ser. A, 179, pp. 491-549, 1888.
  
- [11] Leissa, A. W., "*Vibrations of Shells*," NASA SP-288, U.S. Government Printing Office, Washington, D.C., 1973.
  
- [12] Kraus, H., "*Thin Elastic Shells*," John Wiley, New York, 1967.
  
- [13] Soedel, W., "*Vibrations of Shells and Plates*," 2nd Edition, Marcel Dekker Inc., New York, 1993.
  
- [14] Doghri, I., "*Mechanics of Deformable Solids: Linear, Nonlinear, Analytical, and Computational Aspects*," Springer, Berlin; New York, 2000.

- [15] Kellar, J., Sewell, Robert T., “*Fundamentals of the Analysis and Design of Shell Structures*,” Englewood Cliffs, N.J. : Prentice-Hall, 1987.
- [16] Bushnell, D., “*Computerized Analysis of Shells-Governing Equations*,” Computers and Structures, 18(3), pp. 471-536, 1984.
- [17] Ambartsumyan, S. A., “*Theory of Anisotropic Shells*,” NASA TT F-118, 1964.
- [18] Koiter, W. T., “*A Consistent First Approximation in the General Theory of Thin Elastic Shells*,” Proceedings of the Symposium on the Theory of Thin Elastic Shells, Amsterdam, North Holland, pp. 12-32, 1960.
- [19] Timoshenko, S. P., “*On the Correction for Shear of the Differential Equation for Transverse Vibrations of Prismatic Bars*,” Philosophical Magazine, 41, pp. 744-746, 1921.
- [20] Reissner, E., “*The effect of transverse shear deformation on the bending of elastic plates*,” Journal of Applied Mechanics, 12, pp. 37-45, 1945.
- [21] Mindlin, R. D., “*Influence of rotary inertia and shear on the flexural motions of isotropic elastic plates*,” Journal of Applied Mechanics, 18, pp. 31-38, 1951.
- [22] Dong, S. B., and Tso, F. K., “*On a laminated orthotropic shell theory including transverse shear deformation*,” Journal of Applied Mechanics, 39, pp. 1091-1096, 1972.
- [23] Whitney, J. M., “*Shear Correction Factors for Orthotropic Laminates Under Static Loads*,” Journal of Applied Mechanics, 40, pp. 302-304, 1973.
- [24] Bert, C. W., “*Simplified Analysis of Static Shear Factors for Beams of Nonhomogeneous Cross Section*,” Journal of Composite Materials, 7, pp. 525-529, 1973.
- [25] Vlachoutsis, S., “*Shear Correction Factors for Plates and Shells*,” International Journal for Numerical Methods in Engineering, 33, pp. 1537-1552, 1992.
- [26] Whitney, J. M., and Sun, C. T., “*A Higher Order Theory for Extensional Motion of Laminated Anisotropic Shells and Plates*,” Journal of Sound and Vibration, 30, pp. 85-97, 1973.
- [27] Whitney, J. M., and Sun, C. T., “*A Refined Theory for Laminated Anisotropic Cylindrical Shells*,” Journal of Applied Mechanics, 41, pp. 47-53, 1974.
- [28] Reddy, J. N., and Liu, C. F., “*A Higher-order Shear Deformation Theory of Laminated Elastic Shells*,” International Journal of Engineering Science, 23(3), pp. 319-330, 1985.
- [29] Bhimarraddi, A., “*Dynamic Response of Orthotropic, Homogeneous and Laminated Cylindrical Shells*,” AIAA Journal, 23(11), pp. 1834-1837, 1985.

- [30] Librescu, L., “*Elastostatics and Kinetics of Anisotropic and Heterogeneous Shell-Type Structures*,” Noordhoff International, Leyden, the Netherlands, 1975.
- [31] Librescu, L., Khedir, A. A., and Frederick D., “*A Shear Deformable Theory of Laminated Composite Shallow Shell-Type Panels and Their Response Analysis I: Free Vibration and Buckling*,” *Acta Mechanica*, 76, pp. 1-33, 1989.
- [32] Noor, Ahmed K., and Burton, W. Scott, “*Assessment of Computational Models for Multilayered Composite Shells*,” *Applied Mechanics Reviews*, 43(4), pp. 67-97, 1990.
- [33] Noor, Ahmed K., Burton, W. Scott, and Peters Jeanne M., “*Assessment of Computational Models for Multilayered Composite Cylinders*,” *International Journal of Solids Structures*, 27(10), pp. 1269-1286, 1991.
- [34] Noor Ahmed K., and Burton W. Scott, “*Assesment of Computational Models for Multilayered Anisotropic Plates*,” *Composite Structures*, 14, pp. 233-265, 1990.
- [35] Noor Ahmed K., and Burton W. Scott, “*Stress and Free Vibration Analyses of Multilayered Composite Plates*,” *Composite Structures*, 11, pp. 183-204, 1989.
- [36] Touratier, Maurice, “*A Generalization of Shear Deformation Theories for Axisymmetric Multilayered Shells*,” *International Journal of Solids and Structures*, 29(11), pp. 1379-1399, 1992.
- [37] Soldatos, K. P., and Timarci, T., “*A Unified Formulation of Laminated Composite, Shear Deformable, Five-degrees-of-freedom Cylindrical Shell Theories*,” *Composite Structures*, 25, pp. 165-171, 1993.
- [38] Soldatos, K. P., “*A Refined Laminated Plate and Shell Theory with Applications*,” *Journal of Sound and Vibration*, 144(1), pp. 109-129, 1991.
- [39] Toorani, M. H. ,and Lakis, A. A., “*General Equations of Anisotropic Plates and Shells Including Transverse Shear Deformations, Rotatory Inertia and Initial Curvature Effects*,” *Journal of Sound and Vibration*, 237(4), pp. 561-615, 2000.
- [40] Toorani, M. H. ,and Lakis, A. A., “*Dynamics Behavior of Axisymmetric and Beam-like Anisotropic Cylindrical Shells Conveying Fluid*,” *Journal of Sound and Vibration*, 259(2), pp. 265-298, 2003.
- [41] Noor, Ahmed K. ,”*Mechanics of Anisotropic Plates and Shells- A New Look at an Old Subject*,” *Computers and Structures*, 44(3), pp. 499-514, 1992.
- [42] Quatu, Mohamad S. , “*Recent Research Advances in the Dynamic Behavoi of Shells: 1989-2000, Part 1: Laminated Composite Shells*,” *Applied Mechanics Reviews*, 55(4), pp. 325-349, 2002.
- [43] Quatu, Mohamad S. , “*Recent Research Advances in the Dynamic Behavoi of Shells: 1989-2000, Part 2: Homogeneous Shells*,” *Applied Mechanics Reviews*, 55(5), pp. 415-434, 2002.

- [44] Qatu, Mohammed S., “*Vibrations of Laminated Shells and Plates*,” Elsevier Academic Press, 2004.
- [45] Cohen, Gerald A., “*FASOR- A Second Generation Shell of Revolution Code*,” *Computers and Structures*, 10, pp. 301-309, 1979.
- [46] Bert, Charles, W., “*Structural Theory for Laminated Anisotropic Elastic Shells*,” *Journal of Composite Materials*, 1, pp. 414-423, 1963.
- [47] Bert, C. W., Baker, J. L., and Egle, D. M., “*Free Vibrations of Multilayer Anisotropic Cylindrical Shells*,” *Journal of Composite Materials*, 3, pp. 480-499, 1969.
- [48] Reddy, J. N., “*On Refined Computational Models of Composite Laminates*,” *International Journal for Numerical Methods in Engineering*, 27, pp. 361-382, 1989.
- [49] Padovan, J., “*Quasi-Analytical Finite Element Procedures for Axisymmetric Anisotropic Shells and Solids*,” *Computers & Structures*, 4, pp. 467-483, 1974.
- [50] Padovan, Joseph., and Lestingi, Joseph F., “*Complex Numerical Integration Procedure for Static Loading of Anisotropic Shells of Revolution*,” *Computers and Structures*, 4, pp. 1159-1172, 1974.
- [51] Tan, D. Y., “*Free Vibration Analysis of Shells of Revolution*,” *Journal of Sound and Vibration*, 213(1), pp.15-33, 1998.
- [52] Ganesan, N., and Sivadas, K. R., “*Effect of Coupling Between In-plane Strains and Twist Due to Anisotropy on Vibrations of Composite Shells*,” *Computers & Structures*, 49(3), pp. 481-493, 1993.
- [53] Correia, I. F. Pinto, Barbosa, J. I., Soares, Cristovao M. Mota, and Soares, Carlos, A. Mota, “*A Finite Element Semi-analytical Model for Laminated Axisymmetric Shells: Statics, Dynamics and Buckling*,” *Computers and Structures*, 76, pp. 299-317, 2000.
- [54] Xi, Z. C., Yam, L. H., and Leung, T. P., “*Semi-analytical Study of Free Vibration of Composite Shells of Revolution Based on the Reissner-Mindlin Assumption*,” *International Journal of Solids and Structures*, 33(6), pp. 851-863, 1996.
- [55] Lakshminarayana, H. V., and Dwarakanath, K., “*Free Vibration Characteristics of Cylindrical Shells Made of Composite Materials*,” *Journal of Sound and Vibration*, 154(3), pp. 431-439, 1992.
- [56] Heyliger, P. R., and Jilani, A., “*Free Vibrations of Laminated Anisotropic Cylindrical Shells*,” *Journal of Engineering Mechanics*, 119(5), pp. 1062-1077, 1993.
- [57] Heyliger, P. R., “*Axisymmetric Free Vibrations of Finite Anisotropic Cylinders*,” *Journal of Sound and Vibration*, 148(3), pp. 507-520, 1991.

- [58] Noor, Ahmed K., and Peters Jeanne M., “*Vibration Analysis of Laminated Anisotropic Shells of Revolutions*,” Computer Methods in Applied Mechanics and Engineering, 61, pp. 277-301, 1987.
- [59] Noor, Ahmed K., and Peters Jeanne M., “*Stress and Vibration Analyses of Anisotropic Shells of Revolution*,” International Journal for Numerical Methods in Engineering, 26, pp. 1145-1167, 1988.
- [60] Noor, Ahmed K., and Peters Jeanne M., “*Stress, Vibration, and Buckling of Multilayered Cylinders*,” ASCE, Journal of Structural Engineering, 115(1), pp. 69-88, 1989.
- [61] Noor, Ahmed K., and Rarig, Pamela, “*Three-dimensional Solutions of Laminated Cylinders*,” Computer Methods in Applied Mechanics and Engineering, 3, pp. 319-334, 1974.
- [62] Soldatos, Kostas P., “*Review of Three-dimensional Dynamic Analyses of Circular Cylinders and Cylindrical Shells*,” Applied Mechanics Reviews, 47(10), pp. 501-516, 1994.
- [63] Xiaoyu, Jiang, “*3-D Vibration Analysis of Fiber Reinforced Composite Laminated Cylindrical Shells*,” ASME, Journal of Vibration and Acoustics, 119, pp. 46-51, 1997.
- [64] Lestingi, Joseph, and Paldovan, Joseph, “*Numerical Analysis of Anisotropic Rotational Shells Subjected to Nonsymmetrical Loads*,” Computers and Structures, 3, pp. 133-147, 1973.
- [65] Kalnins, A., “*Dynamic Problems of Elastic Shells*,” Applied Mechanics Reviews, 18, pp. 867-872, 1965.
- [66] Kalnins, A., “*Analysis of Shells of Revolution Subjected to Symmetrical and Nonsymmetrical Loads*,” Journal of Applied Mechanics, 31, pp. 467-476, 1964.
- [67] Kalnins, A., “*Free Vibration of Rotationally Symmetric Shells*,” Journal of the Acoustical Society of America, 36(7), pp.1355-1365, 1964.
- [68] The MathWorks Inc., “*The Mathworks- MATLAB and Simulink for Technical Computing*,” <http://www.mathwoks.com>, last visited on June 2005.
- [69] Kreyszig, E., “*Advanced Engineering Mathematics*,” New York: John Wiley & Sons, Inc., 8th Edition, 1999.
- [70] Press, William H., et al, “*Numerical Recipes in FORTRAN: The Art of Scientific Computing*,” Cambridge [England]; New York, N.Y., USA: Cambridge University, 2nd Edition, 1992.
- [71] Kayran, Altan, “*Free Vibration Analysis of Laminated Composite Shells of Revolution Including Transverse Shear Deformation*,” Ph. D. Dissertation, Department of Mechanical Engineering, University of Delaware, 1990.

- [72] Kayran, A., and Vinson, J.R., “*Free Vibration Analysis of Laminated Composite Truncated Circular Conical Shells*,” AIAA Journal, 28(7), pp. 1259-1269, 1990.
- [73] Kayran, A., and Anlaş, G. ,”*Effect of Stacking Sequence on Free Vibration Frequencies of Laminated Composite Circular Cylindrical Shells*,” Journal of Vibration and Control, 5(3), pp. 355-372, 1999.
- [74] Kayran, A., and Vinson, J.R., “*Torsional Vibrations of Layered Composite Paraboloidal Shells*,” Journal of Sound and Vibration, 141(2), pp. 231-244, 1990.
- [75] Kayran, A., and Vinson, J.R., “*The Effect of Transverse-Shear Deformation on the Natural Frequencies of Layered Composite Paraboloidal Shells*,” Journal of Vibration and Acoustics-Transactions of the ASME, 112(4), pp. 429-439, 1990.
- [76] Goldberg, J. E., and Bogdanoff, J. L., “*Static and Dynamic Analysis of Nonuniform Conical Shells under Symmetrical and Unsymmetrical Conditions*,” Proceedings of the Sixth Symposium on Ballistic Missile and Aerospace Technology, Academic Press, New York, N.Y., vol. 1, pp.219-238, 1961.
- [77] Visual Numerics Inc., “Visual Numerics- Developers of IMSL and PV-WAVE,” <http://www.vni.com>, last visited on June 2005.
- [78] Blevins, Robert D., “*Formulas for Natural Frequency and Mode Shape*,” Malabar, Florida: Krieger Publishing, 1979.
- [79] Arnold, R. N., and Warburton, G. B., “*Flexural Vibrations of the Walls of Thin Cylindrical Shells Having Freely Supported Ends*,” Proceedings of the Royal Society of London, Series A, Mathematical and Physical Sciences, Vol. 197, No. 1049, pp. 238-256, 1949.
- [80] Kalnins, A., “*Effect of Bending on Vibrations of Spherical Shells*,” Journal of the Acoustical Society of America, 36, pp. 74-81, 1964.

## APPENDIX A

### VARIATIONAL COMPUTATION OF THE STRAIN ENERGY

( $\delta U$ )

The application of integration by parts to two different example equations is given as

$$\begin{aligned} & \int_{t_0}^{t_1} \int_{\xi_1}^{\xi_2} \int C_1 \frac{\partial(\delta C_2)}{\partial \xi_1} d\xi_1 d\xi_2 dt \\ &= \int_{t_0}^{t_1} \left[ \int_{\xi_2} C_1 \delta C_2 d\xi_2 - \int_{\xi_1} \frac{\partial(C_1)}{\partial \xi_1} \delta C_2 d\xi_1 d\xi_2 \right] dt \end{aligned} \quad (\text{A.1})$$

$$\begin{aligned} & \int_{t_0}^{t_1} \int_{\xi_1} \int_{\xi_2} C_3 \frac{\partial(\delta C_4)}{\partial \xi_2} d\xi_2 d\xi_1 dt \\ &= \int_{t_0}^{t_1} \left[ \int_{\xi_1} C_3 \delta C_4 d\xi_1 - \int_{\xi_1} \frac{\partial(C_3)}{\partial \xi_2} \delta C_4 d\xi_1 d\xi_2 \right] dt \end{aligned} \quad (\text{A.2})$$

where  $C_1, C_2, C_3$ , and  $C_4$  are functions of  $\xi_1$  and  $\xi_2$

Rewriting Equation (2.269), and carrying out the variation and taking the force and moment resultants into account, we obtain

$$\begin{aligned}
& \int_{t_0}^{t_1} \int_{\xi_1} \int_{\xi_2} \left\{ \underbrace{N_{\xi_1} \left[ \frac{1}{A_{\xi_1}} \frac{\partial(\delta u^0)}{\partial \xi_1} + \frac{(\delta v^0)}{A_{\xi_1} A_{\xi_2}} \frac{\partial A_{\xi_1}}{\partial \xi_2} + \frac{(\delta w^0)}{R_{\xi_1}} \right]}_{\text{I}} \right. \\
& \quad \left. + \underbrace{M_{\xi_1} \left[ \frac{1}{A_{\xi_1}} \frac{\partial(\delta \beta_{\xi_1})}{\partial \xi_1} + \frac{(\delta \beta_{\xi_2})}{A_{\xi_1} A_{\xi_2}} \frac{\partial A_{\xi_1}}{\partial \xi_2} \right]}_{\text{I}} \right. \\
& \quad + \underbrace{N_{\xi_2} \left[ \frac{1}{A_{\xi_2}} \frac{\partial(\delta v^0)}{\partial \xi_2} + \frac{(\delta u^0)}{A_{\xi_1} A_{\xi_2}} \frac{\partial A_{\xi_2}}{\partial \xi_1} + \frac{(\delta w^0)}{R_{\xi_2}} \right]}_{\text{II}} \\
& \quad \left. + \underbrace{M_{\xi_2} \left[ \frac{1}{A_{\xi_2}} \frac{\partial(\delta \beta_{\xi_2})}{\partial \xi_2} + \frac{(\delta \beta_{\xi_1})}{A_{\xi_1} A_{\xi_2}} \frac{\partial A_{\xi_2}}{\partial \xi_1} \right]}_{\text{II}} \right. \\
& \quad + \underbrace{N_{\xi_1 \xi_2} \left[ \frac{1}{A_{\xi_1}} \frac{\partial(\delta v^0)}{\partial \xi_1} - \frac{(\delta u^0)}{A_{\xi_1} A_{\xi_2}} \frac{\partial A_{\xi_1}}{\partial \xi_2} + \frac{1}{A_{\xi_2}} \frac{\partial(\delta u^0)}{\partial \xi_2} - \frac{(\delta v^0)}{A_{\xi_1} A_{\xi_2}} \frac{\partial A_{\xi_2}}{\partial \xi_1} \right]}_{\text{III}} \\
& \quad \left. + \underbrace{M_{\xi_1 \xi_2} \left[ \frac{1}{A_{\xi_1}} \frac{\partial(\delta \beta_{\xi_2})}{\partial \xi_1} - \frac{(\delta \beta_{\xi_1})}{A_{\xi_1} A_{\xi_2}} \frac{\partial A_{\xi_1}}{\partial \xi_2} + \frac{1}{A_{\xi_2}} \frac{\partial(\delta \beta_{\xi_1})}{\partial \xi_2} - \frac{(\delta \beta_{\xi_2})}{A_{\xi_1} A_{\xi_2}} \frac{\partial A_{\xi_2}}{\partial \xi_1} \right]}_{\text{III}} \right. \\
& \quad \left. + \underbrace{Q_{\xi_1} \left[ \frac{1}{A_{\xi_1}} \frac{\partial(\delta w^0)}{\partial \xi_1} - \frac{(\delta u^0)}{R_{\xi_1}} + (\delta \beta_{\xi_1}) \right]}_{\text{IV}} \right. \\
& \quad \left. + \underbrace{Q_{\xi_2} \left[ \frac{1}{A_{\xi_2}} \frac{\partial(\delta w^0)}{\partial \xi_2} - \frac{(\delta v^0)}{R_{\xi_2}} + (\delta \beta_{\xi_2}) \right]}_{\text{V}} \right\} A_{\xi_1} A_{\xi_2} d\xi_1 d\xi_2 d\zeta dt
\end{aligned} \tag{A.3}$$

Let us split the Equation (A.3) and do the variational computations term by term, and carrying out the integration by parts ((A.1) or (A.2)) when necessary

$$\begin{aligned}
& \int_{t_0}^{t_1} \int_{\xi_1} \int_{\xi_2} \left\{ \underbrace{N_{\xi_1} \left[ \frac{1}{A_{\xi_1}} \frac{\partial(\delta u^0)}{\partial \xi_1} + \frac{(\delta v^0)}{A_{\xi_1} A_{\xi_2}} \frac{\partial A_{\xi_1}}{\partial \xi_2} + \frac{(\delta w^0)}{R_{\xi_1}} \right]}_{\mathbf{I}} + M_{\xi_1} \left[ \frac{1}{A_{\xi_1}} \frac{\partial(\delta \beta_{\xi_1})}{\partial \xi_1} + \frac{(\delta \beta_{\xi_2})}{A_{\xi_1} A_{\xi_2}} \frac{\partial A_{\xi_1}}{\partial \xi_2} \right]} \right\} A_{\xi_1} A_{\xi_2} d\xi_1 d\xi_2 dt \\
& = \int_{t_0}^{t_1} \int_{\xi_1} \int_{\xi_2} \left\{ \underbrace{N_{\xi_1} \left[ A_{\xi_2} \frac{\partial(\delta u^0)}{\partial \xi_1} + (\delta v^0) \frac{\partial A_{\xi_1}}{\partial \xi_2} + \frac{A_{\xi_1} A_{\xi_2}}{R_{\xi_1}} (\delta w^0) \right]}_{\mathbf{I}} + M_{\xi_1} \left[ A_{\xi_2} \frac{\partial(\delta \beta_{\xi_1})}{\partial \xi_1} + (\delta \beta_{\xi_2}) \frac{\partial A_{\xi_1}}{\partial \xi_2} \right]} \right\} d\xi_1 d\xi_2 dt
\end{aligned} \tag{A.4}$$

$$\begin{aligned}
& \int_{t_0}^{t_1} \int_{\xi_1} \int_{\xi_2} \left\{ \underbrace{N_{\xi_1} \left[ A_{\xi_2} \frac{\partial(\delta u^0)}{\partial \xi_1} + (\delta v^0) \frac{\partial A_{\xi_1}}{\partial \xi_2} + \frac{A_{\xi_1} A_{\xi_2}}{R_{\xi_1}} (\delta w^0) \right]}_{\mathbf{I}} + M_{\xi_1} \left[ A_{\xi_2} \frac{\partial(\delta \beta_{\xi_1})}{\partial \xi_1} + (\delta \beta_{\xi_2}) \frac{\partial A_{\xi_1}}{\partial \xi_2} \right]} \right\} d\xi_1 d\xi_2 dt \\
& = \int_{t_0}^{t_1} \left\{ \begin{aligned} & \left[ \int_{\xi_2} N_{\xi_1} A_{\xi_2} \delta u^0 d\xi_2 - \int_{\xi_1} \int_{\xi_2} \frac{\partial(N_{\xi_1} A_{\xi_2})}{\partial \xi_1} \delta u^0 d\xi_1 d\xi_2 \right] \\ & + \left[ \int_{\xi_1} \int_{\xi_2} N_{\xi_1} \frac{\partial A_{\xi_1}}{\partial \xi_2} (\delta v^0) d\xi_1 d\xi_2 \right] \\ & + \left[ \int_{\xi_1} \int_{\xi_2} N_{\xi_1} \frac{A_{\xi_1} A_{\xi_2}}{R_{\xi_1}} (\delta w^0) d\xi_1 d\xi_2 \right] \\ & + \left[ \int_{\xi_2} M_{\xi_1} A_{\xi_2} \delta \beta_{\xi_1} d\xi_2 - \int_{\xi_1} \int_{\xi_2} \frac{\partial(M_{\xi_1} A_{\xi_2})}{\partial \xi_1} \delta \beta_{\xi_1} d\xi_1 d\xi_2 \right] \\ & + \left[ \int_{\xi_1} \int_{\xi_2} M_{\xi_1} \frac{\partial A_{\xi_1}}{\partial \xi_2} \delta \beta_{\xi_2} d\xi_1 d\xi_2 \right] \end{aligned} \right\} dt
\end{aligned} \tag{A.5}$$

$$\begin{aligned}
& \left. \int_{t_0}^{t_1} \int_{\xi_1} \int_{\xi_2} \left\{ \begin{aligned} & N_{\xi_2} \left[ \frac{1}{A_{\xi_2}} \frac{\partial(\delta v^0)}{\partial \xi_2} + \frac{(\delta u^0)}{A_{\xi_1} A_{\xi_2}} \frac{\partial A_{\xi_2}}{\partial \xi_1} + \frac{(\delta w^0)}{R_{\xi_2}} \right] \right. \\ & \left. + M_{\xi_2} \left[ \frac{1}{A_{\xi_2}} \frac{\partial(\delta \beta_{\xi_2})}{\partial \xi_2} + \frac{(\delta \beta_{\xi_1})}{A_{\xi_1} A_{\xi_2}} \frac{\partial A_{\xi_2}}{\partial \xi_1} \right] \right\} A_{\xi_1} A_{\xi_2} d\xi_1 d\xi_2 dt}{II} \right. \\
& = \int_{t_0}^{t_1} \int_{\xi_1} \int_{\xi_2} \left\{ \begin{aligned} & N_{\xi_2} \left[ A_{\xi_1} \frac{\partial(\delta v^0)}{\partial \xi_2} + (\delta u^0) \frac{\partial A_{\xi_2}}{\partial \xi_1} + \frac{A_{\xi_1} A_{\xi_2}}{R_{\xi_2}} (\delta w^0) \right] \\ & + M_{\xi_2} \left[ A_{\xi_1} \frac{\partial(\delta \beta_{\xi_2})}{\partial \xi_2} + (\delta \beta_{\xi_1}) \frac{\partial A_{\xi_2}}{\partial \xi_1} \right] \end{aligned} \right\} d\xi_1 d\xi_2 dt
\end{aligned} \tag{A.6}$$

$$\begin{aligned}
& \int_{t_0}^{t_1} \int_{\xi_1} \int_{\xi_2} \left\{ \begin{aligned} & N_{\xi_2} \left[ A_{\xi_1} \frac{\partial(\delta v^0)}{\partial \xi_2} + (\delta u^0) \frac{\partial A_{\xi_2}}{\partial \xi_1} + \frac{A_{\xi_1} A_{\xi_2}}{R_{\xi_2}} (\delta w^0) \right] \\ & + M_{\xi_2} \left[ A_{\xi_1} \frac{\partial(\delta \beta_{\xi_2})}{\partial \xi_2} + (\delta \beta_{\xi_1}) \frac{\partial A_{\xi_2}}{\partial \xi_1} \right] \end{aligned} \right\} d\xi_1 d\xi_2 dt \\
& = \int_{t_0}^{t_1} \left\{ \begin{aligned} & \left[ \int_{\xi_1} N_{\xi_2} A_{\xi_1} \delta v^0 d\xi_1 - \int_{\xi_1 \xi_2} \frac{\partial(N_{\xi_2} A_{\xi_1})}{\partial \xi_2} \delta v^0 d\xi_1 d\xi_2 \right] \\ & + \left[ \int_{\xi_1 \xi_2} N_{\xi_2} \frac{\partial A_{\xi_2}}{\partial \xi_1} (\delta u^0) d\xi_1 d\xi_2 \right] \\ & + \left[ \int_{\xi_1 \xi_2} N_{\xi_2} \frac{A_{\xi_1} A_{\xi_2}}{R_{\xi_2}} (\delta w^0) d\xi_1 d\xi_2 \right] \\ & + \left[ \int_{\xi_1} M_{\xi_2} A_{\xi_1} \delta \beta_{\xi_2} d\xi_1 - \int_{\xi_1 \xi_2} \frac{\partial(M_{\xi_2} A_{\xi_1})}{\partial \xi_2} \delta \beta_{\xi_2} d\xi_1 d\xi_2 \right] \\ & + \left[ \int_{\xi_1 \xi_2} M_{\xi_2} \frac{\partial A_{\xi_2}}{\partial \xi_1} \delta \beta_{\xi_1} d\xi_1 d\xi_2 \right] \end{aligned} \right\} dt
\end{aligned} \tag{A.7}$$

$$\int_{t_0}^{t_1} \int_{\xi_1} \int_{\xi_2} \left\{ \begin{array}{l} N_{\xi_1 \xi_2} \\ + M_{\xi_1 \xi_2} \end{array} \right\} \left[ \begin{array}{l} \frac{1}{A_{\xi_1}} \frac{\partial(\delta v^0)}{\partial \xi_1} \\ - \frac{(\delta u^0)}{A_{\xi_1} A_{\xi_2}} \frac{\partial A_{\xi_1}}{\partial \xi_2} \\ + \frac{1}{A_{\xi_2}} \frac{\partial(\delta u^0)}{\partial \xi_2} \\ - \frac{(\delta v^0)}{A_{\xi_1} A_{\xi_2}} \frac{\partial A_{\xi_2}}{\partial \xi_1} \end{array} \right] \left[ \begin{array}{l} \frac{1}{A_{\xi_1}} \frac{\partial(\delta \beta_{\xi_2})}{\partial \xi_1} \\ - \frac{(\delta \beta_{\xi_1})}{A_{\xi_1} A_{\xi_2}} \frac{\partial A_{\xi_1}}{\partial \xi_2} \\ + \frac{1}{A_{\xi_2}} \frac{\partial(\delta \beta_{\xi_1})}{\partial \xi_2} \\ - \frac{(\delta \beta_{\xi_2})}{A_{\xi_1} A_{\xi_2}} \frac{\partial A_{\xi_2}}{\partial \xi_1} \end{array} \right] A_{\xi_1} A_{\xi_2} d\xi_1 d\xi_2 dt$$

**III**

(A.8)

$$= \int_{t_0}^{t_1} \int_{\xi_1} \int_{\xi_2} \left\{ \begin{array}{l} N_{\xi_1 \xi_2} \\ + M_{\xi_1 \xi_2} \end{array} \right\} \left[ \begin{array}{l} A_{\xi_2} \frac{\partial(\delta v^0)}{\partial \xi_1} \\ - (\delta u^0) \frac{\partial A_{\xi_1}}{\partial \xi_2} \\ + A_{\xi_1} \frac{\partial(\delta u^0)}{\partial \xi_2} \\ - (\delta v^0) \frac{\partial A_{\xi_2}}{\partial \xi_1} \end{array} \right] \left[ \begin{array}{l} A_{\xi_2} \frac{\partial(\delta \beta_{\xi_2})}{\partial \xi_1} \\ - (\delta \beta_{\xi_1}) \frac{\partial A_{\xi_1}}{\partial \xi_2} \\ + A_{\xi_1} \frac{\partial(\delta \beta_{\xi_1})}{\partial \xi_2} \\ - (\delta \beta_{\xi_2}) \frac{\partial A_{\xi_2}}{\partial \xi_1} \end{array} \right] d\xi_1 d\xi_2 dt$$

**III**

$$\int_{t_0}^{t_1} \int_{\xi_1} \int_{\xi_2} \left\{ \underbrace{N_{\xi_1 \xi_2} \left[ A_{\xi_2} \frac{\partial(\delta v^0)}{\partial \xi_1} - (\delta u^0) \frac{\partial A_{\xi_1}}{\partial \xi_2} + A_{\xi_1} \frac{\partial(\delta u^0)}{\partial \xi_2} - (\delta v^0) \frac{\partial A_{\xi_2}}{\partial \xi_1} \right] + M_{\xi_1 \xi_2} \left[ A_{\xi_2} \frac{\partial(\delta \beta_{\xi_2})}{\partial \xi_1} - (\delta \beta_{\xi_1}) \frac{\partial A_{\xi_1}}{\partial \xi_2} + A_{\xi_1} \frac{\partial(\delta \beta_{\xi_1})}{\partial \xi_2} - (\delta \beta_{\xi_2}) \frac{\partial A_{\xi_2}}{\partial \xi_1} \right]}_{III} \right\} d\xi_1 d\xi_2 dt$$

$$= \int_{t_0}^{t_1} \left\{ \begin{aligned} & \left[ \int_{\xi_2} N_{\xi_1 \xi_2} A_{\xi_2} \delta v^0 d\xi_2 - \int \int_{\xi_1 \xi_2} \frac{\partial(N_{\xi_1 \xi_2} A_{\xi_2})}{\partial \xi_1} \delta v^0 d\xi_1 d\xi_2 \right] \\ & - \left[ \int \int_{\xi_1 \xi_2} N_{\xi_1 \xi_2} \frac{\partial A_{\xi_1}}{\partial \xi_2} \delta u^0 d\xi_1 d\xi_2 \right] \\ & + \left[ \int_{\xi_1} N_{\xi_1 \xi_2} A_{\xi_1} \delta u^0 d\xi_1 - \int \int_{\xi_1 \xi_2} \frac{\partial(N_{\xi_1 \xi_2} A_{\xi_1})}{\partial \xi_2} \delta u^0 d\xi_1 d\xi_2 \right] \\ & - \left[ \int \int_{\xi_1 \xi_2} N_{\xi_1 \xi_2} \frac{\partial A_{\xi_2}}{\partial \xi_1} \delta v^0 d\xi_1 d\xi_2 \right] \\ & + \left[ \int_{\xi_2} M_{\xi_1 \xi_2} A_{\xi_2} \delta \beta_{\xi_2} d\xi_2 - \int \int_{\xi_1 \xi_2} \frac{\partial(M_{\xi_1 \xi_2} A_{\xi_2})}{\partial \xi_1} \delta \beta_{\xi_2} d\xi_1 d\xi_2 \right] \\ & - \left[ \int \int_{\xi_1 \xi_2} M_{\xi_1 \xi_2} \frac{\partial A_{\xi_1}}{\partial \xi_2} \delta \beta_{\xi_1} d\xi_1 d\xi_2 \right] \\ & + \left[ \int_{\xi_1} M_{\xi_1 \xi_2} A_{\xi_1} \delta \beta_{\xi_1} d\xi_1 - \int \int_{\xi_1 \xi_2} \frac{\partial(M_{\xi_1 \xi_2} A_{\xi_1})}{\partial \xi_2} \delta \beta_{\xi_1} d\xi_1 d\xi_2 \right] \\ & - \left[ \int \int_{\xi_1 \xi_2} M_{\xi_1 \xi_2} \frac{\partial A_{\xi_2}}{\partial \xi_1} \delta \beta_{\xi_2} d\xi_1 d\xi_2 \right] \end{aligned} \right\} dt \quad (A.9)$$

$$\begin{aligned}
& \int_{t_0}^{t_1} \int_{\xi_1} \int_{\xi_2} \left\{ \underbrace{Q_{\xi_1} \left[ \frac{1}{A_{\xi_1}} \frac{\partial(\delta w^0)}{\partial \xi_1} - \frac{(\delta u^0)}{R_{\xi_1}} + (\delta \beta_{\xi_1}) \right]}_{IV} \right\} A_{\xi_1} A_{\xi_2} d\xi_1 d\xi_2 dt \\
& = \int_{t_0}^{t_1} \int_{\xi_1} \int_{\xi_2} \left\{ \underbrace{Q_{\xi_1} \left[ A_{\xi_2} \frac{\partial(\delta w^0)}{\partial \xi_1} - \frac{A_{\xi_1} A_{\xi_2}}{R_{\xi_1}} (\delta u^0) + A_{\xi_1} A_{\xi_2} (\delta \beta_{\xi_1}) \right]}_{IV} \right\} d\xi_1 d\xi_2 dt
\end{aligned} \tag{A.10}$$

$$\begin{aligned}
& \int_{t_0}^{t_1} \int_{\xi_1} \int_{\xi_2} \left\{ \underbrace{Q_{\xi_1} \left[ A_{\xi_2} \frac{\partial(\delta w^0)}{\partial \xi_1} - \frac{A_{\xi_1} A_{\xi_2}}{R_{\xi_1}} (\delta u^0) + A_{\xi_1} A_{\xi_2} (\delta \beta_{\xi_1}) \right]}_{IV} \right\} d\xi_1 d\xi_2 dt \\
& = \int_{t_0}^{t_1} \left\{ \begin{aligned} & \left[ \int_{\xi_2} Q_{\xi_1} A_{\xi_2} \delta w^0 d\xi_2 - \int_{\xi_1} \int_{\xi_2} \frac{\partial(Q_{\xi_1} A_{\xi_2})}{\partial \xi_1} \delta w^0 d\xi_1 d\xi_2 \right] \\ & - \left[ \int_{\xi_1} \int_{\xi_2} Q_{\xi_1} \frac{A_{\xi_1} A_{\xi_2}}{R_{\xi_1}} \delta u^0 d\xi_1 d\xi_2 \right] \\ & + \left[ \int_{\xi_1} \int_{\xi_2} Q_{\xi_1} A_{\xi_1} A_{\xi_2} \delta \beta_{\xi_1} d\xi_1 d\xi_2 \right] \end{aligned} \right\} dt
\end{aligned} \tag{A.11}$$

$$\begin{aligned}
& \int_{t_0}^{t_1} \int_{\xi_1} \int_{\xi_2} \left\{ \underbrace{Q_{\xi_2} \left[ \frac{1}{A_{\xi_2}} \frac{\partial(\delta w^0)}{\partial \xi_2} - \frac{(\delta v^0)}{R_{\xi_2}} + (\delta \beta_{\xi_2}) \right]}_V \right\} A_{\xi_1} A_{\xi_2} d\xi_1 d\xi_2 dt \\
& = \int_{t_0}^{t_1} \int_{\xi_1} \int_{\xi_2} \left\{ \underbrace{Q_{\xi_2} \left[ A_{\xi_1} \frac{\partial(\delta w^0)}{\partial \xi_2} - \frac{A_{\xi_1} A_{\xi_2}}{R_{\xi_2}} (\delta v^0) + A_{\xi_1} A_{\xi_2} (\delta \beta_{\xi_2}) \right]}_V \right\} d\xi_1 d\xi_2 dt
\end{aligned} \tag{A.12}$$

$$\begin{aligned}
& \int_{t_0}^{t_1} \int_{\xi_1} \int_{\xi_2} \left\{ \underbrace{Q_{\xi_2} \left[ A_{\xi_1} \frac{\partial(\delta w^0)}{\partial \xi_2} - \frac{A_{\xi_1} A_{\xi_2}}{R_{\xi_2}} (\delta v^0) + A_{\xi_1} A_{\xi_2} (\delta \beta_{\xi_2}) \right]}_V \right\} d\xi_1 d\xi_2 dt \\
& = \int_{t_0}^{t_1} \left\{ \begin{aligned} & \left[ \int_{\xi_1} Q_{\xi_2} A_{\xi_1} \delta w^0 d\xi_1 - \int_{\xi_1 \xi_2} \frac{\partial(Q_{\xi_2} A_{\xi_1})}{\partial \xi_2} \delta w^0 d\xi_1 d\xi_2 \right] \\ & - \left[ \int_{\xi_1 \xi_2} Q_{\xi_2} \frac{A_{\xi_1} A_{\xi_2}}{R_{\xi_2}} \delta v^0 d\xi_1 d\xi_2 \right] \\ & + \left[ \int_{\xi_1 \xi_2} Q_{\xi_2} A_{\xi_1} A_{\xi_2} \delta \beta_{\xi_2} d\xi_1 d\xi_2 \right] \end{aligned} \right\} dt
\end{aligned} \tag{A.13}$$

## APPENDIX B

### SYMBOLIC COMPUTATION OF EQUATION (3.14)

The m-code written for the symbolic computation of Equation (3.9) in order to get the relations

$\left( \frac{\partial u_\phi^0}{\partial \phi}, \frac{\partial u_\theta^0}{\partial \phi}, \frac{\partial \beta_\phi}{\partial \phi}, \frac{\partial \beta_\theta}{\partial \phi} \right)$  is given below.

```
syms h11 h12 h13 h14 h21 h22 h23 h24 h31 h32 h33 h34 h41 h42 h43 h44
syms j11 j21 j31 j41
H=[h11 h12 h13 h14;h21 h22 h23 h24;h31 h32 h33 h34;h41 h42 h43 h44];
J=[j11;j21;j31;j41];
B=H^-1*J;
b11=B(1,1);
pretty(b11)
pause
clc
pause
b21=B(2,1);
pretty(b21)
pause
clc
pause
b31=B(3,1);
pretty(b31)
pause
clc
pause
b41=B(4,1);
pretty(b41)
pause
clc
```

The results are given as follow

$\partial u_\phi^0 / \partial \phi$ :

```
(h22 h33 h44 - h22 h34 h43 - h32 h23 h44 + h32 h24 h43 + h42 h23 h34
- h42 h24 h33) j11/(%1) - (h12 h33 h44 - h12 h34 h43 - h32 h13 h44
+ h32 h14 h43 + h42 h13 h34 - h42 h14 h33) j21/(%1) + (h12 h23 h44
- h12 h24 h43 - h22 h13 h44 + h22 h14 h43 + h42 h13 h24 - h42 h14 h23
) j31/(%1) - (h12 h23 h34 - h12 h24 h33 - h22 h13 h34 + h22 h14 h33
+ h32 h13 h24 - h32 h14 h23) j41/(%1)
%1 := h11 h22 h33 h44 - h11 h22 h34 h43 - h11 h32 h23 h44 + h11 h32 h24 h43
+ h11 h42 h23 h34 - h11 h42 h24 h33 - h21 h12 h33 h44
+ h21 h12 h34 h43 + h21 h32 h13 h44 - h21 h32 h14 h43
- h21 h42 h13 h34 + h21 h42 h14 h33 + h31 h12 h23 h44
- h31 h12 h24 h43 - h31 h22 h13 h44 + h31 h22 h14 h43
+ h31 h42 h13 h24 - h31 h42 h14 h23 - h41 h12 h23 h34
+ h41 h12 h24 h33 + h41 h22 h13 h34 - h41 h22 h14 h33
- h41 h32 h13 h24 + h41 h32 h14 h23
```

(B.1)

The expressions % 1 in (B.2), (B.3) and (B.4) are similar to the one given in (B.1).

$\partial u_\theta^0 / \partial \phi$ :

```
- (h21 h33 h44 - h21 h34 h43 - h31 h23 h44 + h31 h24 h43 + h41 h23 h34
- h41 h24 h33) j11/(%1) + (h11 h33 h44 - h11 h34 h43 - h31 h13 h44
+ h31 h14 h43 + h41 h13 h34 - h41 h14 h33) j21/(%1) - (h11 h23 h44
- h11 h24 h43 - h21 h13 h44 + h21 h14 h43 + h41 h13 h24 - h41 h14 h23
) j31/(%1) + (h11 h23 h34 - h11 h24 h33 - h21 h13 h34 + h21 h14 h33
+ h31 h13 h24 - h31 h14 h23) j41/(%1)
```

(B.2)

$\partial\beta_\phi/\partial\phi$ :

$$\begin{aligned}
& (h_{21} h_{32} h_{44} - h_{21} h_{34} h_{42} - h_{31} h_{22} h_{44} + h_{31} h_{24} h_{42} + h_{41} h_{22} h_{34} \\
& - h_{41} h_{24} h_{32}) j_{11}/(*1) - (h_{11} h_{32} h_{44} - h_{11} h_{34} h_{42} - h_{31} h_{12} h_{44} \\
& + h_{31} h_{14} h_{42} + h_{41} h_{12} h_{34} - h_{41} h_{14} h_{32}) j_{21}/(*1) + (h_{11} h_{22} h_{44} \\
& - h_{11} h_{24} h_{42} - h_{21} h_{12} h_{44} + h_{21} h_{14} h_{42} + h_{41} h_{12} h_{24} - h_{41} h_{14} h_{22} \\
& ) j_{31}/(*1) - (h_{11} h_{22} h_{34} - h_{11} h_{24} h_{32} - h_{21} h_{12} h_{34} + h_{21} h_{14} h_{32} \\
& + h_{31} h_{12} h_{24} - h_{31} h_{14} h_{22}) j_{41}/(*1)
\end{aligned} \tag{B.3}$$

$\partial\beta_\theta/\partial\phi$ :

$$\begin{aligned}
& - (h_{21} h_{32} h_{43} - h_{21} h_{33} h_{42} - h_{31} h_{22} h_{43} + h_{31} h_{23} h_{42} + h_{41} h_{22} h_{33} \\
& - h_{41} h_{23} h_{32}) j_{11}/(*1) + (h_{11} h_{32} h_{43} - h_{11} h_{33} h_{42} - h_{31} h_{12} h_{43} \\
& + h_{31} h_{13} h_{42} + h_{41} h_{12} h_{33} - h_{41} h_{13} h_{32}) j_{21}/(*1) - (h_{11} h_{22} h_{43} \\
& - h_{11} h_{23} h_{42} - h_{21} h_{12} h_{43} + h_{21} h_{13} h_{42} + h_{41} h_{12} h_{23} - h_{41} h_{13} h_{22} \\
& ) j_{31}/(*1) + (h_{11} h_{22} h_{33} - h_{11} h_{23} h_{32} - h_{21} h_{12} h_{33} + h_{21} h_{13} h_{32} \\
& + h_{31} h_{12} h_{23} - h_{31} h_{13} h_{22}) j_{41}/(*1)
\end{aligned} \tag{B.4}$$

## APPENDIX C

### COEFFICIENTS OF THE SYSTEM OF PARTIAL DIFFERENTIAL EQUATIONS DERIVED IN SECTION 3.3.1

The coefficients of  $\frac{\partial w_\phi^0}{\partial \phi}$  given in Equation (3.8)

$$c_{p11} = -\frac{R_\phi A s_{45}}{R_\phi A s_{55}} \quad (C.1)$$

$$c_{12} = 1 \quad (C.2)$$

$$c_{13} = -\frac{R_\phi A s_{45}}{R_\phi A s_{55}} \quad (C.3)$$

$$c_{14} = -R_\phi \quad (C.4)$$

$$c_{15} = -\frac{A s_{45} R_\phi}{A s_{55}} \quad (C.5)$$

$$c_{16} = \frac{R_\phi}{A s_{55}} \quad (C.6)$$

The coefficients of  $\frac{\partial u_\phi^0}{\partial \phi}$  given in Equation (3.15)

$$\Delta = \left( \frac{1}{R_\phi} \right) \left[ \begin{aligned} & (A_{11} A_{66} D_{11} D_{66}) - (A_{11} A_{66} D_{16} D_{16}) - (A_{11} B_{16} B_{16} D_{66}) + (A_{11} B_{16} B_{66} D_{16}) \\ & + (A_{11} B_{66} B_{16} D_{16}) - (A_{11} B_{66} B_{66} D_{11}) - (A_{16} A_{16} D_{11} D_{66}) + (A_{16} A_{16} D_{16} D_{16}) \\ & + (A_{16} B_{16} B_{11} D_{66}) - (A_{16} B_{16} B_{16} D_{16}) - (A_{16} B_{66} B_{11} D_{16}) + (A_{16} B_{66} B_{16} D_{11}) \\ & + (B_{11} A_{16} B_{16} D_{66}) - (B_{11} A_{16} B_{66} D_{16}) - (B_{11} A_{66} B_{11} D_{66}) + (B_{11} A_{66} B_{16} D_{16}) \\ & + (B_{11} B_{66} B_{11} B_{66}) - (B_{11} B_{66} B_{16} B_{16}) - (B_{16} A_{16} B_{16} D_{16}) + (B_{16} A_{16} B_{66} D_{11}) \\ & + (B_{16} A_{66} B_{11} D_{16}) - (B_{16} A_{66} B_{16} D_{11}) - (B_{16} B_{16} B_{11} B_{66}) + (B_{16} B_{16} B_{16} B_{16}) \end{aligned} \right] \quad (C.7)$$

$$U1 = \begin{bmatrix} (A_{66}D_{11}D_{66}) - (A_{66}D_{16}D_{16}) - (B_{16}B_{16}D_{66}) \\ + (B_{16}B_{66}D_{16}) + (B_{66}B_{16}D_{16}) - (B_{66}B_{66}D_{11}) \end{bmatrix} \quad (C.8)$$

$$U2 = \begin{bmatrix} (-A_{16}D_{11}D_{66}) + (A_{16}D_{16}D_{16}) + (B_{16}B_{11}D_{66}) \\ - (B_{16}B_{16}D_{16}) - (B_{66}B_{11}D_{16}) + (B_{66}B_{16}D_{11}) \end{bmatrix} \quad (C.9)$$

$$U3 = \begin{bmatrix} (A_{16}B_{16}D_{66}) - (A_{16}B_{66}D_{16}) - (A_{66}B_{11}D_{66}) \\ + (A_{66}B_{16}D_{16}) + (B_{66}B_{11}B_{66}) - (B_{66}B_{16}B_{16}) \end{bmatrix} \quad (C.10)$$

$$U4 = \begin{bmatrix} (-A_{16}B_{16}D_{16}) + (A_{16}B_{66}D_{11}) + (A_{66}B_{11}D_{16}) \\ - (A_{66}B_{16}D_{11}) - (B_{16}B_{11}B_{66}) + (B_{16}B_{16}B_{16}) \end{bmatrix} \quad (C.11)$$

$$c_{21} = \left( \frac{1}{\Delta} \right) \left\{ \begin{array}{l} \left( \frac{1}{R_\phi} \right) [(-A_{11})(U1) + (-A_{16})(U2) + (-B_{11})(U3) + (-B_{16})(U4)] \\ + \left( \frac{1}{R_\theta} \right) [(-A_{12})(U1) + (-A_{26})(U2) + (-B_{12})(U3) + (-B_{26})(U4)] \end{array} \right\} \quad (C.12)$$

$$c_{22} = \left( \frac{1}{\Delta} \right) \left( \frac{1 \cos \phi}{R_\theta \sin \phi} \right) \left\{ \begin{array}{l} (-A_{12})(U1) + (-A_{26})(U2) \\ + (-B_{12})(U3) + (-B_{26})(U4) \end{array} \right\} \quad (C.13)$$

$$cP_{22} = \left( \frac{1}{\Delta} \right) \left( \frac{1 \quad 1}{R_\theta \sin \phi} \right) \left\{ \begin{array}{l} (-A_{16})(U1) + (-A_{66})(U2) \\ + (-B_{16})(U3) + (-B_{66})(U4) \end{array} \right\} \quad (C.14)$$

$$c_{23} = \left( \frac{1}{\Delta} \right) \left( \frac{1 \cos \phi}{R_\theta \sin \phi} \right) \left\{ \begin{array}{l} (A_{16})(U1) + (A_{66})(U2) \\ + (B_{16})(U3) + (B_{66})(U4) \end{array} \right\} \quad (C.15)$$

$$cP_{23} = \left( \frac{1}{\Delta} \right) \left( \frac{1 \quad 1}{R_\theta \sin \phi} \right) \left\{ \begin{array}{l} (-A_{12})(U1) + (-A_{26})(U2) \\ + (-B_{12})(U3) + (-B_{26})(U4) \end{array} \right\} \quad (C.16)$$

$$c_{24} = \left( \frac{1}{\Delta} \right) \left( \frac{1 \cos \phi}{R_\theta \sin \phi} \right) \left\{ \begin{array}{l} (-B_{12})(U1) + (-B_{26})(U2) \\ + (-D_{12})(U3) + (-D_{26})(U4) \end{array} \right\} \quad (C.17)$$

$$cP_{24} = \left( \frac{1}{\Delta} \right) \left( \frac{1 \quad 1}{R_\theta \sin \phi} \right) \left\{ \begin{array}{l} (-B_{16})(U1) + (-B_{66})(U2) \\ + (-D_{16})(U3) + (-D_{66})(U4) \end{array} \right\} \quad (C.18)$$

$$c_{25} = \left( \frac{1}{\Delta} \right) \left( \frac{1 \cos \phi}{R_\theta \sin \phi} \right) \left\{ \begin{array}{l} (B_{16})(U1) + (B_{66})(U2) \\ + (D_{16})(U3) + (D_{66})(U4) \end{array} \right\} \quad (C.19)$$

$$cP_{25} = \left( \frac{1}{\Delta} \right) \left( \frac{1}{R_\theta \sin \phi} \right) \left\{ \begin{aligned} & [(-B_{12})(U1) + (-B_{26})(U2)] \\ & [ + (-D_{12})(U3) + (-D_{26})(U4) ] \end{aligned} \right\} \quad (C.20)$$

$$c_{27} = \left( \frac{1}{\Delta} \right) \{U1\} \quad (C.21)$$

$$c_{28} = \left( \frac{1}{\Delta} \right) \{U2\} \quad (C.22)$$

$$c_{29} = \left( \frac{1}{\Delta} \right) \{U3\} \quad (C.23)$$

$$c_{210} = \left( \frac{1}{\Delta} \right) \{U4\} \quad (C.24)$$

The coefficients of  $\frac{\partial u_\theta^0}{\partial \phi}$  given in Equation (3.16)

$$V1 = \left[ \begin{aligned} & (-A_{16}D_{11}D_{66}) + (A_{16}D_{16}D_{16}) + (B_{11}B_{16}D_{66}) \\ & - (B_{11}B_{66}D_{16}) - (B_{16}B_{16}D_{16}) + (B_{16}B_{66}D_{11}) \end{aligned} \right] \quad (C.25)$$

$$V2 = \left[ \begin{aligned} & (A_{11}D_{11}D_{66}) - (A_{11}D_{16}D_{16}) - (B_{11}B_{11}D_{66}) \\ & + (B_{11}B_{16}D_{16}) + (B_{16}B_{11}D_{16}) - (B_{16}B_{16}D_{11}) \end{aligned} \right] \quad (C.26)$$

$$V3 = \left[ \begin{aligned} & (-A_{11}B_{16}D_{66}) + (A_{11}B_{66}D_{16}) + (A_{16}B_{11}D_{66}) \\ & - (A_{16}B_{16}D_{16}) - (B_{16}B_{11}B_{66}) + (B_{16}B_{16}B_{16}) \end{aligned} \right] \quad (C.27)$$

$$V4 = \left[ \begin{aligned} & (A_{11}B_{16}D_{16}) - (A_{11}B_{66}D_{11}) - (A_{16}B_{11}D_{16}) \\ & + (A_{16}B_{16}D_{11}) + (B_{11}B_{11}B_{66}) - (B_{11}B_{16}B_{16}) \end{aligned} \right] \quad (C.28)$$

$$c_{31} = \left( \frac{1}{\Delta} \right) \left\{ \begin{aligned} & \left( \frac{1}{R_\phi} \right) [(-A_{11})(V1) + (-A_{16})(V2) + (-B_{11})(V3) + (-B_{16})(V4)] \\ & + \left( \frac{1}{R_\theta} \right) [(-A_{12})(V1) + (-A_{26})(V2) + (-B_{12})(V3) + (-B_{26})(V4)] \end{aligned} \right\} \quad (C.29)$$

$$c_{32} = \left( \frac{1}{\Delta} \right) \left( \frac{1}{R_\theta \sin \phi} \right) \left\{ \begin{aligned} & [(-A_{12})(V1) + (-A_{26})(V2)] \\ & [ + (-B_{12})(V3) + (-B_{26})(V4) ] \end{aligned} \right\} \quad (C.30)$$

$$cP_{32} = \left( \frac{1}{\Delta} \left( \frac{1}{R_\theta} \frac{1}{\sin \phi} \right) \right) \left\{ \begin{aligned} &(-A_{16})(V1) + (-A_{66})(V2) \\ &+ (-B_{16})(V3) + (-B_{66})(V4) \end{aligned} \right\} \quad (C.31)$$

$$c_{33} = \left( \frac{1}{\Delta} \left( \frac{1}{R_\theta} \frac{\cos \phi}{\sin \phi} \right) \right) \left\{ \begin{aligned} &(A_{16})(V1) + (A_{66})(V2) \\ &+ (B_{16})(V3) + (B_{66})(V4) \end{aligned} \right\} \quad (C.32)$$

$$cP_{33} = \left( \frac{1}{\Delta} \left( \frac{1}{R_\theta} \frac{1}{\sin \phi} \right) \right) \left\{ \begin{aligned} &(-A_{12})(V1) + (-A_{26})(V2) \\ &+ (-B_{12})(V3) + (-B_{26})(V4) \end{aligned} \right\} \quad (C.33)$$

$$c_{34} = \left( \frac{1}{\Delta} \left( \frac{1}{R_\theta} \frac{\cos \phi}{\sin \phi} \right) \right) \left\{ \begin{aligned} &(-B_{12})(V1) + (-B_{26})(V2) \\ &+ (-D_{12})(V3) + (-D_{26})(V4) \end{aligned} \right\} \quad (C.34)$$

$$cP_{34} = \left( \frac{1}{\Delta} \left( \frac{1}{R_\theta} \frac{1}{\sin \phi} \right) \right) \left\{ \begin{aligned} &(-B_{16})(V1) + (-B_{66})(V2) \\ &+ (-D_{16})(V3) + (-D_{66})(V4) \end{aligned} \right\} \quad (C.35)$$

$$c_{35} = \left( \frac{1}{\Delta} \left( \frac{1}{R_\theta} \frac{\cos \phi}{\sin \phi} \right) \right) \left\{ \begin{aligned} &(B_{16})(V1) + (B_{66})(V2) \\ &+ (D_{16})(V3) + (D_{66})(V4) \end{aligned} \right\} \quad (C.36)$$

$$cP_{35} = \left( \frac{1}{\Delta} \left( \frac{1}{R_\theta} \frac{1}{\sin \phi} \right) \right) \left\{ \begin{aligned} &(-B_{12})(V1) + (-B_{26})(V2) \\ &+ (-D_{12})(V3) + (-D_{26})(V4) \end{aligned} \right\} \quad (C.37)$$

$$c_{37} = \left( \frac{1}{\Delta} \right) \{V1\} \quad (C.38)$$

$$c_{38} = \left( \frac{1}{\Delta} \right) \{V2\} \quad (C.39)$$

$$c_{39} = \left( \frac{1}{\Delta} \right) \{V3\} \quad (C.40)$$

$$c_{310} = \left( \frac{1}{\Delta} \right) \{V4\} \quad (C.41)$$

The coefficients of  $\frac{\partial \beta_\phi}{\partial \phi}$  given in Equation (3.17)

$$Y1 = \left[ \begin{aligned} &(A_{16}B_{16}D_{66}) - (A_{16}D_{16}B_{66}) - (B_{11}A_{66}D_{66}) \\ &+ (B_{11}B_{66}B_{66}) + (B_{16}A_{66}D_{16}) - (B_{16}B_{66}B_{16}) \end{aligned} \right] \quad (C.42)$$

$$Y2 = \begin{bmatrix} (-A_{11}B_{16}D_{66}) + (A_{11}D_{16}B_{66}) + (B_{11}A_{16}D_{66}) \\ -(B_{11}B_{16}B_{66}) - (B_{16}A_{16}D_{16}) + (B_{16}B_{16}B_{16}) \end{bmatrix} \quad (C.43)$$

$$Y3 = \begin{bmatrix} (A_{11}A_{66}D_{66}) - (A_{11}B_{66}B_{66}) - (A_{16}A_{16}D_{66}) \\ + (A_{16}B_{16}B_{66}) + (B_{16}A_{16}B_{66}) - (B_{16}B_{16}A_{66}) \end{bmatrix} \quad (C.44)$$

$$Y4 = \begin{bmatrix} (-A_{11}A_{66}D_{16}) + (A_{11}B_{66}B_{16}) + (A_{16}A_{16}D_{16}) \\ -(A_{16}B_{16}B_{16}) - (B_{11}A_{16}B_{66}) + (B_{11}B_{16}A_{66}) \end{bmatrix} \quad (C.45)$$

$$c_{41} = \left( \frac{1}{\Delta} \right) \left\{ \begin{array}{l} \left( \frac{1}{R_\phi} \right) [(-A_{11})(Y1) + (-A_{16})(Y2) + (-B_{11})(Y3) + (-B_{16})(Y4)] \\ + \left( \frac{1}{R_\theta} \right) [(-A_{12})(Y1) + (-A_{26})(Y2) + (-B_{12})(Y3) + (-B_{26})(Y4)] \end{array} \right\} \quad (C.46)$$

$$c_{42} = \left( \frac{1}{\Delta} \right) \left( \frac{1 \cos \phi}{R_\theta \sin \phi} \right) \left\{ (-A_{12})(Y1) + (-A_{26})(Y2) \right\} + (-B_{12})(Y3) + (-B_{26})(Y4) \quad (C.47)$$

$$cP_{42} = \left( \frac{1}{\Delta} \right) \left( \frac{1}{R_\theta \sin \phi} \right) \left\{ (-A_{16})(Y1) + (-A_{66})(Y2) \right\} + (-B_{16})(Y3) + (-B_{66})(Y4) \quad (C.48)$$

$$c_{43} = \left( \frac{1}{\Delta} \right) \left( \frac{1 \cos \phi}{R_\theta \sin \phi} \right) \left\{ (A_{16})(Y1) + (A_{66})(Y2) \right\} + (B_{16})(Y3) + (B_{66})(Y4) \quad (C.49)$$

$$cP_{43} = \left( \frac{1}{\Delta} \right) \left( \frac{1}{R_\theta \sin \phi} \right) \left\{ (-A_{12})(Y1) + (-A_{26})(Y2) \right\} + (-B_{12})(Y3) + (-B_{26})(Y4) \quad (C.50)$$

$$c_{44} = \left( \frac{1}{\Delta} \right) \left( \frac{1 \cos \phi}{R_\theta \sin \phi} \right) \left\{ (-B_{12})(Y1) + (-B_{26})(Y2) \right\} + (-D_{12})(Y3) + (-D_{26})(Y4) \quad (C.51)$$

$$cP_{44} = \left( \frac{1}{\Delta} \right) \left( \frac{1}{R_\theta \sin \phi} \right) \left\{ (-B_{16})(Y1) + (-B_{66})(Y2) \right\} + (-D_{16})(Y3) + (-D_{66})(Y4) \quad (C.52)$$

$$c_{45} = \left( \frac{1}{\Delta} \right) \left( \frac{1 \cos \phi}{R_\theta \sin \phi} \right) \left\{ (B_{16})(Y1) + (B_{66})(Y2) \right\} + (D_{16})(Y3) + (D_{66})(Y4) \quad (C.53)$$

$$cP_{45} = \left( \frac{1}{\Delta} \right) \left( \frac{1}{R_\theta \sin \phi} \right) \left\{ (-B_{12})(Y1) + (-B_{26})(Y2) \right\} + (-D_{12})(Y3) + (-D_{26})(Y4) \quad (C.54)$$

$$c_{47} = \left( \frac{1}{\Delta} \right) \{Y1\} \quad (C.55)$$

$$c_{48} = \left( \frac{1}{\Delta} \right) \{Y2\} \quad (C.56)$$

$$c_{49} = \left( \frac{1}{\Delta} \right) \{Y3\} \quad (C.57)$$

$$c_{410} = \left( \frac{1}{\Delta} \right) \{Y4\} \quad (C.58)$$

The coefficients of  $\frac{\partial \beta_\theta}{\partial \phi}$  given in Equation (3.18)

$$Z1 = \left[ \begin{array}{l} (-A_{16}B_{16}D_{16}) + (A_{16}D_{11}B_{66}) + (B_{11}A_{66}D_{16}) \\ -(B_{11}B_{16}B_{66}) - (B_{16}A_{66}D_{11}) + (B_{16}B_{16}B_{16}) \end{array} \right] \quad (C.59)$$

$$Z2 = \left[ \begin{array}{l} (A_{11}B_{16}D_{16}) - (A_{11}D_{11}B_{66}) - (B_{11}A_{16}D_{16}) \\ + (B_{11}B_{11}B_{66}) + (B_{16}A_{16}D_{11}) - (B_{16}B_{11}B_{16}) \end{array} \right] \quad (C.60)$$

$$Z3 = \left[ \begin{array}{l} (-A_{11}A_{66}D_{16}) + (A_{11}B_{16}B_{66}) + (A_{16}A_{16}D_{16}) \\ -(A_{16}B_{11}B_{66}) - (B_{16}A_{16}B_{16}) + (B_{16}B_{11}A_{66}) \end{array} \right] \quad (C.61)$$

$$Z4 = \left[ \begin{array}{l} (A_{11}A_{66}D_{11}) - (A_{11}B_{16}B_{16}) - (A_{16}A_{16}D_{11}) \\ + (A_{16}B_{11}B_{16}) + (B_{11}A_{16}B_{16}) - (B_{11}B_{11}A_{66}) \end{array} \right] \quad (C.62)$$

$$c_{51} = \left( \frac{1}{\Delta} \right) \left\{ \begin{array}{l} \left( \frac{1}{R_\phi} \right) [(-A_{11})(Z1) + (-A_{16})(Z2) + (-B_{11})(Z3) + (-B_{16})(Z4)] \\ + \left( \frac{1}{R_\theta} \right) [(-A_{12})(Z1) + (-A_{26})(Z2) + (-B_{12})(Z3) + (-B_{26})(Z4)] \end{array} \right\} \quad (C.63)$$

$$c_{52} = \left( \frac{1}{\Delta} \right) \left( \frac{1 \cos \phi}{R_\theta \sin \phi} \right) \left\{ \begin{array}{l} (-A_{12})(Z1) + (-A_{26})(Z2) \\ + (-B_{12})(Z3) + (-B_{26})(Z4) \end{array} \right\} \quad (C.64)$$

$$cp_{52} = \left( \frac{1}{\Delta} \right) \left( \frac{1}{R_\theta \sin \phi} \right) \left\{ \begin{array}{l} (-A_{16})(Z1) + (-A_{66})(Z2) \\ + (-B_{16})(Z3) + (-B_{66})(Z4) \end{array} \right\} \quad (C.65)$$

$$c_{53} = \left( \frac{1}{\Delta} \right) \left( \frac{1 \cos \phi}{R_\theta \sin \phi} \right) \left\{ \begin{array}{l} (A_{16})(Z1) + (A_{66})(Z2) \\ + (B_{16})(Z3) + (B_{66})(Z4) \end{array} \right\} \quad (C.66)$$

$$cp_{53} = \left( \frac{1}{\Delta} \right) \left( \frac{1}{R_\theta} \frac{1}{\sin \phi} \right) \left\{ \begin{aligned} &(-A_{12})(Z1) + (-A_{26})(Z2) \\ &+ (-B_{12})(Z3) + (-B_{26})(Z4) \end{aligned} \right\} \quad (C.67)$$

$$c_{54} = \left( \frac{1}{\Delta} \right) \left( \frac{1}{R_\theta} \frac{\cos \phi}{\sin \phi} \right) \left\{ \begin{aligned} &(-B_{12})(Z1) + (-B_{26})(Z2) \\ &+ (-D_{12})(Z3) + (-D_{26})(Z4) \end{aligned} \right\} \quad (C.68)$$

$$cp_{54} = \left( \frac{1}{\Delta} \right) \left( \frac{1}{R_\theta} \frac{1}{\sin \phi} \right) \left\{ \begin{aligned} &(-B_{16})(Z1) + (-B_{66})(Z2) \\ &+ (-D_{16})(Z3) + (-D_{66})(Z4) \end{aligned} \right\} \quad (C.69)$$

$$c_{55} = \left( \frac{1}{\Delta} \right) \left( \frac{1}{R_\theta} \frac{\cos \phi}{\sin \phi} \right) \left\{ \begin{aligned} &(B_{16})(Z1) + (B_{66})(Z2) \\ &+ (D_{16})(Z3) + (D_{66})(Z4) \end{aligned} \right\} \quad (C.70)$$

$$cp_{55} = \left( \frac{1}{\Delta} \right) \left( \frac{1}{R_\theta} \frac{1}{\sin \phi} \right) \left\{ \begin{aligned} &(-B_{12})(Z1) + (-B_{26})(Z2) \\ &+ (-D_{12})(Z3) + (-D_{26})(Z4) \end{aligned} \right\} \quad (C.71)$$

$$c_{57} = \left( \frac{1}{\Delta} \right) \{Z1\} \quad (C.72)$$

$$c_{58} = \left( \frac{1}{\Delta} \right) \{Z2\} \quad (C.73)$$

$$c_{59} = \left( \frac{1}{\Delta} \right) \{Z3\} \quad (C.74)$$

$$c_{510} = \left( \frac{1}{\Delta} \right) \{Z4\} \quad (C.75)$$

The coefficients of  $\frac{\partial Q_\phi}{\partial \phi}$  given in Equation (3.19)

$$c_{61} = \left\{ \begin{aligned} &(-\rho h \omega^2 R_\phi) + \left( \frac{1}{R_\theta} \right) \left[ \begin{aligned} &(A_{12})(c_{21}) + (A_{12}) + (A_{26})(c_{31}) \\ &+ (B_{12})(c_{41}) + (B_{26})(c_{51}) \end{aligned} \right] + \left( \frac{R_\phi}{R_\theta^2} \right) (A_{22}) \end{aligned} \right\} \quad (C.76)$$

$$cdp_{61} = \left\{ \begin{aligned} &\left( -\frac{1}{R_\theta} \right) \left( \frac{As_{45}}{\sin \phi} \right) (cp_{11}) + \left( -\frac{R_\phi}{R_\theta^2} \right) \left( \frac{As_{44}}{\sin^2 \phi} \right) \end{aligned} \right\} \quad (C.77)$$

$$c_{62} = \left\{ \left[ \begin{aligned} &\left( \frac{1}{R_\theta} \right) \left[ \begin{aligned} &(A_{12})(c_{22}) + (A_{22}) \left( \frac{\cos \phi}{\sin \phi} \right) + (A_{26})(c_{32}) + (B_{12})(c_{42}) + (B_{26})(c_{52}) \end{aligned} \right] \end{aligned} \right] \right\} \quad (C.78)$$

$$cp_{62} = \left\{ \left( \frac{1}{R_\theta} \right) \left[ \left( \frac{As_{45}}{\sin \phi} \right) + \left( -\frac{As_{45}}{\sin \phi} \right) (c_{12}) + (A_{12})(cp_{22}) + \left( \frac{R_\phi}{R_\theta} \right) \left( \frac{A_{26}}{\sin \phi} \right) \right] \right. \\ \left. + (A_{26})(cp_{32}) + (B_{12})(cp_{42}) + (B_{26})(cp_{52}) \right\} \quad (C.79)$$

$$c_{63} = \left\{ \left( \frac{1}{R_\theta} \right) \left[ (A_{12})(c_{23}) + (A_{26})(c_{33}) + (-A_{26}) \left( \frac{\cos \phi}{\sin \phi} \right) + (B_{12})(c_{43}) + (B_{26})(c_{53}) \right] \right\} \quad (C.80)$$

$$cp_{63} = \left\{ \left( \frac{1}{R_\theta} \right) \left[ \left( -\frac{As_{45}}{\sin \phi} \right) (c_{13}) + \left( \frac{R_\phi}{R_\theta} \right) \left( \frac{As_{44}}{\sin \phi} \right) + (A_{12})(cp_{23}) + \left( \frac{R_\phi}{R_\theta} \right) \left( \frac{A_{22}}{\sin \phi} \right) \right] \right. \\ \left. + (A_{26})(cp_{33}) + (B_{12})(cp_{43}) + (B_{26})(cp_{53}) \right\} \quad (C.81)$$

$$c_{64} = \left\{ \left( \frac{1}{R_\theta} \right) \left[ (A_{12})(c_{24}) + (A_{26})(c_{34}) + (B_{12})(c_{44}) + (B_{26})(c_{54}) + (B_{22}) \left( \frac{\cos \phi}{\sin \phi} \right) \right] \right\} \quad (C.82)$$

$$cp_{64} = \left\{ \left( \frac{1}{R_\theta} \right) \left[ \left( -R_\phi \right) \left( \frac{As_{45}}{\sin \phi} \right) + \left( -\frac{As_{45}}{\sin \phi} \right) (c_{14}) + (A_{12})(cp_{24}) + (A_{26})(cp_{34}) \right] \right. \\ \left. + (B_{12})(cp_{44}) + \left( \frac{R_\phi}{R_\theta} \right) \left( \frac{B_{26}}{\sin \phi} \right) + (B_{26})(cp_{54}) \right\} \quad (C.83)$$

$$c_{65} = \left\{ \left( \frac{1}{R_\theta} \right) \left[ (A_{12})(c_{25}) + (A_{26})(c_{35}) + (B_{12})(c_{45}) + (B_{26})(c_{55}) + (-B_{26}) \left( \frac{\cos \phi}{\sin \phi} \right) \right] \right\} \quad (C.84)$$

$$cp_{65} = \left\{ \left( \frac{1}{R_\theta} \right) \left[ \left( -\frac{As_{45}}{\sin \phi} \right) (c_{15}) + \left( -R_\phi \right) \left( \frac{As_{44}}{\sin \phi} \right) + (A_{12})(cp_{25}) + (A_{26})(cp_{35}) \right] \right. \\ \left. + (B_{12})(cp_{45}) + \left( \frac{R_\phi}{R_\theta} \right) \left( \frac{B_{22}}{\sin \phi} \right) + (B_{26})(cp_{55}) \right\} \quad (C.85)$$

$$c_{66} = \left\{ \left( -\frac{R_\phi}{R_\theta} \right) \left( \frac{\cos \phi}{\sin \phi} \right) \right\} \quad (C.86)$$

$$cp_{66} = \left\{ \left( -\frac{1}{R_\theta} \right) \left[ \left( \frac{As_{45}}{\sin \phi} \right) (c_{16}) \right] \right\} \quad (C.87)$$

$$c_{67} = \left\{ \left( \frac{1}{R_\theta} \right) \left[ (A_{12})(c_{27}) + (A_{26})(c_{37}) + (B_{12})(c_{47}) + (B_{26})(c_{57}) \right] + (1) \right\} \quad (C.88)$$

$$c_{68} = \left\{ \left( \frac{1}{R_\theta} \right) \left[ (A_{12})(c_{28}) + (A_{26})(c_{38}) + (B_{12})(c_{48}) + (B_{26})(c_{58}) \right] \right\} \quad (\text{C.89})$$

$$c_{69} = \left\{ \left( \frac{1}{R_\theta} \right) \left[ (A_{12})(c_{29}) + (A_{26})(c_{39}) + (B_{12})(c_{49}) + (B_{26})(c_{59}) \right] \right\} \quad (\text{C.90})$$

$$c_{610} = \left\{ \left( \frac{1}{R_\theta} \right) \left[ (A_{12})(c_{210}) + (A_{26})(c_{310}) + (B_{12})(c_{410}) + (B_{26})(c_{510}) \right] \right\} \quad (\text{C.91})$$

The coefficients of  $\frac{\partial N_\phi}{\partial \phi}$  given in Equation (3.20)

$$c_{71} = \left\{ \left( \frac{1}{R_\theta} \right) \left( \frac{\cos \phi}{\sin \phi} \right) \left[ (A_{12})(c_{21}) + (A_{12}) + (A_{26})(c_{31}) + (B_{12})(c_{41}) \right] + (B_{26})(c_{51}) + \left( \frac{R_\phi}{R_\theta} \right) (A_{22}) \right\} \quad (\text{C.92})$$

$$c_{72} = \left\{ (-\rho h \omega^2 R_\phi) + \left( \frac{1}{R_\theta} \right) \left( \frac{\cos \phi}{\sin \phi} \right) \left[ (A_{12})(c_{22}) + \left( \frac{R_\phi}{R_\theta} \right) (A_{22}) \left( \frac{\cos \phi}{\sin \phi} \right) + (A_{26})(c_{32}) \right] + (B_{12})(c_{42}) + (B_{26})(c_{52}) \right\} \quad (\text{C.93})$$

$$cp_{72} = \left\{ \left( \frac{1}{R_\theta} \right) \left( \frac{\cos \phi}{\sin \phi} \right) \left[ (A_{12})(cp_{22}) + (A_{26})(cp_{32}) + (B_{12})(cp_{42}) \right] + \left( \frac{R_\phi}{R_\theta} \right) \left( \frac{1}{\sin \phi} \right) (A_{26}) + (B_{26})(cp_{52}) \right\} \quad (\text{C.94})$$

$$c_{73} = \left\{ \left( \frac{1}{R_\theta} \right) \left( \frac{\cos \phi}{\sin \phi} \right) \left[ (A_{12})(c_{23}) + (A_{26})(c_{33}) + (-A_{26}) \left( \frac{\cos \phi}{\sin \phi} \right) \right] + (B_{12})(c_{43}) + (B_{26})(c_{53}) \right\} \quad (\text{C.95})$$

$$cp_{73} = \left\{ \left( \frac{1}{R_\theta} \right) \left( \frac{\cos \phi}{\sin \phi} \right) \left[ (A_{12})(cp_{23}) + \left( \frac{R_\phi}{R_\theta} \right) (A_{22}) \left( \frac{1}{\sin \phi} \right) + (A_{26})(cp_{33}) \right] + (B_{12})(cp_{43}) + (B_{26})(cp_{53}) \right\} \quad (\text{C.96})$$

$$c_{74} = \left\{ \left( \frac{1}{R_\theta} \right) \left( \frac{\cos \phi}{\sin \phi} \right) \left[ (A_{12})(c_{24}) + (A_{26})(c_{34}) + (B_{12})(c_{44}) \right] + (B_{22}) \left( \frac{\cos \phi}{\sin \phi} \right) + (B_{26})(c_{54}) \right\} \quad (\text{C.97})$$

$$cp_{74} = \left\{ \left( \frac{1}{R_\theta} \right) \left( \frac{\cos \phi}{\sin \phi} \right) \left[ (A_{12})(cp_{24}) + (A_{26})(cp_{34}) + (B_{12})(cp_{44}) \right] + \left( \frac{R_\phi}{R_\theta} \right) (B_{26}) \left( \frac{1}{\sin \phi} \right) + (B_{26})(cp_{54}) \right\} \quad (C.98)$$

$$c_{75} = \left\{ \left( \frac{1}{R_\theta} \right) \left( \frac{\cos \phi}{\sin \phi} \right) \left[ (A_{12})(c_{25}) + (A_{26})(c_{35}) + (B_{12})(c_{45}) \right] + (B_{26})(c_{55}) + (-B_{26}) \left( \frac{\cos \phi}{\sin \phi} \right) \right\} \quad (C.99)$$

$$cp_{75} = \left\{ \left( \frac{1}{R_\theta} \right) \left( \frac{\cos \phi}{\sin \phi} \right) \left[ (A_{12})(cp_{25}) + (A_{26})(cp_{35}) + (B_{12})(cp_{45}) \right] + \left( \frac{R_\phi}{R_\theta} \right) (B_{22}) \left( \frac{1}{\sin \phi} \right) + (B_{26})(cp_{55}) \right\} \quad (C.100)$$

$$c_{76} = \{-1\} \quad (C.101)$$

$$c_{77} = \left\{ \left( \frac{1}{R_\theta} \right) \left( \frac{\cos \phi}{\sin \phi} \right) \left[ (-R_\phi) + (A_{12})(c_{27}) + (A_{26})(c_{37}) + (B_{12})(c_{47}) + (B_{26})(c_{57}) \right] \right\} \quad (C.102)$$

$$c_{78} = \left\{ \left( \frac{1}{R_\theta} \right) \left( \frac{\cos \phi}{\sin \phi} \right) \left[ (A_{12})(c_{28}) + (A_{26})(c_{38}) + (B_{12})(c_{48}) + (B_{26})(c_{58}) \right] \right\} \quad (C.103)$$

$$cp_{78} = \left\{ \left( -\frac{R_\phi}{R_\theta} \right) \left( \frac{1}{\sin \phi} \right) \right\} \quad (C.104)$$

$$c_{79} = \left\{ \left( \frac{1}{R_\theta} \right) \left( \frac{\cos \phi}{\sin \phi} \right) \left[ (A_{12})(c_{29}) + (A_{26})(c_{39}) + (B_{12})(c_{49}) + (B_{26})(c_{59}) \right] \right\} \quad (C.105)$$

$$c_{710} = \left\{ \left( \frac{1}{R_\theta} \right) \left( \frac{\cos \phi}{\sin \phi} \right) \left[ (A_{12})(c_{210}) + (A_{26})(c_{310}) + (B_{12})(c_{410}) + (B_{26})(c_{510}) \right] \right\} \quad (C.106)$$

The coefficients of  $\frac{\partial N_{\phi\phi}}{\partial \phi}$  given in Equation (3.21)

$$cp_{81} = \left\{ \left( \frac{1}{R_\theta} \right) \left[ (-As_{45})(cp_{11}) + \left( -\frac{R_\phi}{R_\theta \sin \phi} \right) (As_{44}) \right] + \left( \frac{1}{R_\theta} \right) \left( \frac{1}{\sin \phi} \right) \left[ (-A_{12})(c_{21}) + (-A_{12}) + \left( -\frac{R_\phi}{R_\theta} \right) (A_{22}) + (-A_{26})(c_{31}) \right] + (-B_{12})(c_{41}) + (-B_{26})(c_{51}) \right\} \quad (C.107)$$

$$c_{82} = \left\{ \left( \frac{1}{R_\theta} \right) \left[ (As_{45}) + (-As_{45})(c_{12}) \right] \right\} \quad (C.108)$$

$$cp_{82} = \left\{ \left( \frac{1}{R_\theta} \right) \left( \frac{1}{\sin \phi} \right) \left[ (-A_{12})(c_{22}) + (-A_{22}) \left( \frac{\cos \phi}{\sin \phi} \right) + (-A_{26})(c_{32}) \right] \right. \\ \left. + (-B_{12})(c_{42}) + (-B_{26})(c_{52}) \right\} \quad (C.109)$$

$$cdp_{82} = \left\{ \left( \frac{1}{R_\theta} \right) \left( \frac{1}{\sin \phi} \right) \left[ (-A_{12})(cp_{22}) + \left( -\frac{R_\phi}{R_\theta} \right) \left( A_{26} \left( \frac{1}{\sin \phi} \right) + (-A_{26})(cp_{32}) \right) \right] \right. \\ \left. + (-B_{12})(cp_{42}) + (-B_{26})(cp_{52}) \right\} \quad (C.110)$$

$$c_{83} = \left\{ (-\rho h \omega^2 R_\phi) + \left( \frac{1}{R_\theta} \right) \left[ (-As_{45})(c_{13}) + \left( \frac{R_\phi}{R_\theta} \right) (As_{44}) \right] \right\} \quad (C.111)$$

$$cp_{83} = \left\{ \left( \frac{1}{R_\theta} \right) \left( \frac{1}{\sin \phi} \right) \left[ (-A_{12})(c_{23}) + (-A_{26})(c_{33}) + \left( A_{26} \left( \frac{\cos \phi}{\sin \phi} \right) \right) \right] \right. \\ \left. + (-B_{12})(c_{43}) + (-B_{26})(c_{53}) \right\} \quad (C.112)$$

$$cdp_{83} = \left\{ \left( \frac{1}{R_\theta} \right) \left( \frac{1}{\sin \phi} \right) \left[ (-A_{12})(cp_{23}) + \left( -\frac{R_\phi}{R_\theta} \right) \left( A_{22} \left( \frac{1}{\sin \phi} \right) + (-A_{26})(cp_{33}) \right) \right] \right. \\ \left. + (-B_{12})(cp_{43}) + (-B_{26})(cp_{53}) \right\} \quad (C.113)$$

$$c_{84} = \left\{ \left( \frac{1}{R_\theta} \right) \left[ (-R_\phi)(As_{45}) + (-As_{45})(c_{14}) \right] \right\} \quad (C.114)$$

$$cp_{84} = \left\{ \left( \frac{1}{R_\theta} \right) \left( \frac{1}{\sin \phi} \right) \left[ (-A_{12})(c_{24}) + (-A_{26})(c_{34}) + (-B_{12})(c_{44}) \right] \right. \\ \left. + (-B_{22}) \left( \frac{\cos \phi}{\sin \phi} \right) + (-B_{26})(c_{54}) \right\} \quad (C.115)$$

$$cdp_{84} = \left\{ \left( \frac{1}{R_\theta} \right) \left( \frac{1}{\sin \phi} \right) \left[ (-A_{12})(cp_{24}) + (-A_{26})(cp_{34}) + (-B_{12})(cp_{44}) \right] \right. \\ \left. + \left( -\frac{R_\phi}{R_\theta} \right) (B_{26}) \left( \frac{1}{\sin \phi} \right) + (-B_{26})(cp_{54}) \right\} \quad (C.116)$$

$$c_{85} = \left\{ \left( \frac{1}{R_\theta} \right) \left[ (-As_{45})(c_{15}) + (-R_\phi)(As_{44}) \right] \right\} \quad (C.117)$$

$$cp_{85} = \left\{ \left( \frac{1}{R_\theta} \right) \frac{1}{\sin \phi} \left[ (-A_{12})(c_{25}) + (-A_{26})(c_{35}) + (-B_{12})(c_{45}) \right] \right. \\ \left. + (-B_{26})(c_{55}) + (B_{26}) \left( \frac{\cos \phi}{\sin \phi} \right) \right\} \quad (\text{C.118})$$

$$cdp_{85} = \left\{ \left( \frac{1}{R_\theta} \right) \frac{1}{\sin \phi} \left[ (-A_{12})(cp_{25}) + (-A_{26})(cp_{35}) + (-B_{12})(cp_{45}) \right] \right. \\ \left. + \left( -\frac{R_\phi}{R_\theta} \right) (B_{22}) \left( \frac{1}{\sin \phi} \right) + (-B_{26})(cp_{55}) \right\} \quad (\text{C.119})$$

$$c_{86} = \left\{ \left( \frac{1}{R_\theta} \right) [(-As_{45})(c_{16})] \right\} \quad (\text{C.120})$$

$$cp_{87} = \left\{ \left( \frac{1}{R_\theta} \right) \left( \frac{1}{\sin \phi} \right) [(-A_{12})(c_{27}) + (-A_{26})(c_{37}) + (-B_{12})(c_{47}) + (-B_{26})(c_{57})] \right\} \quad (\text{C.121})$$

$$c_{88} = \left\{ \left( \frac{1}{R_\theta} \right) \left[ (-2R_\phi) \left( \frac{\cos \phi}{\sin \phi} \right) \right] \right\} \quad (\text{C.122})$$

$$cp_{88} = \left\{ \left( \frac{1}{R_\theta} \right) \left( \frac{1}{\sin \phi} \right) [(-A_{12})(c_{28}) + (-A_{26})(c_{38}) + (-B_{12})(c_{48}) + (-B_{26})(c_{58})] \right\} \quad (\text{C.123})$$

$$cp_{89} = \left\{ \left( \frac{1}{R_\theta} \right) \left( \frac{1}{\sin \phi} \right) [(-A_{12})(c_{29}) + (-A_{26})(c_{39}) + (-B_{12})(c_{49}) + (-B_{26})(c_{59})] \right\} \quad (\text{C.124})$$

$$cp_{810} = \left\{ \left( \frac{1}{R_\theta} \right) \left( \frac{1}{\sin \phi} \right) [(-A_{12})(c_{210}) + (-A_{26})(c_{310}) + (-B_{12})(c_{410}) + (-B_{26})(c_{510})] \right\} \quad (\text{C.125})$$

The coefficients of  $\frac{\partial M_\phi}{\partial \phi}$  given in Equation (3.22)

$$c_{91} = \left\{ \left( \frac{1}{R_\theta} \right) \left( \frac{\cos \phi}{\sin \phi} \right) \left[ (B_{12}) + \left( \frac{R_\phi}{R_\theta} \right) (B_{22}) + (B_{12})(c_{21}) + (B_{26})(c_{31}) \right] \right. \\ \left. + (D_{12})(c_{41}) + (D_{26})(c_{51}) \right\} \quad (\text{C.126})$$

$$cp_{91} = \left\{ \left( \frac{1}{R_\theta} \right) \left( \frac{1}{\sin \phi} \right) \left[ (-B_{16})(c_{21}) + (-B_{16}) + \left( -\frac{R_\phi}{R_\theta} \right) (B_{26}) + (-B_{66})(c_{31}) \right] \right. \\ \left. + (-D_{16})(c_{41}) + (-D_{66})(c_{51}) \right\} \quad (C.127)$$

$$c_{92} = \left\{ \left( \frac{1}{R_\theta} \right) \left( \frac{\cos \phi}{\sin \phi} \right) \left[ (B_{12})(c_{22}) + (B_{22}) \left( \frac{\cos \phi}{\sin \phi} \right) + (B_{26})(c_{32}) \right] \right. \\ \left. + (D_{12})(c_{42}) + (D_{26})(c_{52}) \right\} \quad (C.128)$$

$$cp_{92} = \left\{ \left( \frac{1}{R_\theta} \right) \left( \frac{1}{\sin \phi} \right) \left[ (-B_{16})(c_{22}) + \left( -\frac{R_\phi}{R_\theta} \right) (B_{26}) \left( \frac{\cos \phi}{\sin \phi} \right) + (-B_{66})(c_{32}) \right] \right. \\ \left. + \left( \frac{1}{R_\theta} \right) \left( \frac{\cos \phi}{\sin \phi} \right) \left[ (B_{12})(cp_{22}) + \left( \frac{R_\phi}{R_\theta} \right) \left( \frac{1}{\sin \phi} \right) (B_{26}) + (B_{26})(cp_{32}) \right] \right. \\ \left. + (D_{12})(cp_{42}) + (D_{26})(cp_{52}) \right\} \quad (C.129)$$

$$cdp_{92} = \left\{ \left( \frac{1}{R_\theta} \right) \left( \frac{1}{\sin \phi} \right) \left[ (-B_{16})(cp_{22}) + \left( -\frac{R_\phi}{R_\theta} \right) \left( \frac{1}{\sin \phi} \right) (B_{66}) + (-B_{66})(cp_{32}) \right] \right. \\ \left. + (-D_{16})(cp_{42}) + (-D_{66})(cp_{52}) \right\} \quad (C.130)$$

$$c_{93} = \left\{ \left( \frac{1}{R_\theta} \right) \left( \frac{\cos \phi}{\sin \phi} \right) \left[ (B_{12})(c_{23}) + (B_{26})(c_{33}) + (-B_{26}) \left( \frac{\cos \phi}{\sin \phi} \right) \right] \right. \\ \left. + (D_{12})(c_{43}) + (D_{26})(c_{53}) \right\} \quad (C.131)$$

$$cp_{93} = \left\{ \left( \frac{1}{R_\theta} \right) \left( \frac{1}{\sin \phi} \right) \left[ (-B_{16})(c_{23}) + (-B_{66})(c_{33}) + \left( -\frac{R_\phi}{R_\theta} \right) (-B_{66}) \left( \frac{\cos \phi}{\sin \phi} \right) \right] \right. \\ \left. + \left( \frac{1}{R_\theta} \right) \left( \frac{\cos \phi}{\sin \phi} \right) \left[ (B_{12})(cp_{23}) + \left( \frac{R_\phi}{R_\theta} \right) \left( \frac{1}{\sin \phi} \right) (B_{22}) + (B_{26})(cp_{33}) \right] \right. \\ \left. + (D_{12})(cp_{43}) + (D_{26})(cp_{53}) \right\} \quad (C.132)$$

$$cdp_{93} = \left\{ \left( \frac{1}{R_\theta} \right) \left( \frac{1}{\sin \phi} \right) \left[ (-B_{16})(cp_{23}) + \left( -\frac{R_\phi}{R_\theta} \right) \left( \frac{1}{\sin \phi} \right) (B_{26}) + (-B_{66})(cp_{33}) \right] \right. \\ \left. + (-D_{16})(cp_{43}) + (-D_{66})(cp_{53}) \right\} \quad (C.133)$$

$$c_{94} = \left\{ \left( -\frac{1}{12} \rho h^3 \omega^2 R_\phi \right) + \left( \frac{1}{R_\theta} \right) \left( \frac{\cos \phi}{\sin \phi} \right) \left[ (B_{12})(c_{24}) + (B_{26})(c_{34}) + (D_{12})(c_{44}) \right] \right. \\ \left. + (D_{22}) \left( \frac{\cos \phi}{\sin \phi} \right) + (D_{26})(c_{54}) \right\} \quad (C.134)$$

$$cp_{94} = \left\{ \left( \frac{1}{R_\theta} \right) \left( \frac{1}{\sin \phi} \right) \left[ (-B_{16})(c_{24}) + (-B_{66})(c_{34}) + (-D_{16})(c_{44}) \right] \right. \\ \left. + \left( -\frac{R_\phi}{R_\theta} \right) (D_{26}) \left( \frac{\cos \phi}{\sin \phi} \right) + (-D_{66})(c_{54}) \right\} \\ + \left\{ \left( \frac{1}{R_\theta} \right) \left( \frac{\cos \phi}{\sin \phi} \right) \left[ (B_{12})(cp_{24}) + (B_{26})(cp_{34}) + (D_{12})(cp_{44}) \right] \right. \\ \left. + \left( \frac{R_\phi}{R_\theta} \right) \left( \frac{1}{\sin \phi} \right) (D_{26}) + (D_{26})(cp_{54}) \right\} \quad (C.135)$$

$$cdp_{94} = \left\{ \left( \frac{1}{R_\theta} \right) \left( \frac{1}{\sin \phi} \right) \left[ (-B_{16})(cp_{24}) + (-B_{66})(cp_{34}) + (-D_{16})(cp_{44}) \right] \right. \\ \left. + \left( -\frac{R_\phi}{R_\theta} \right) \left( \frac{1}{\sin \phi} \right) (D_{66}) + (-D_{66})(cp_{54}) \right\} \quad (C.136)$$

$$c_{95} = \left\{ \left( \frac{1}{R_\theta} \right) \left( \frac{\cos \phi}{\sin \phi} \right) \left[ (B_{12})(c_{25}) + (B_{26})(c_{35}) + (D_{12})(c_{45}) \right] \right. \\ \left. + (D_{26})(c_{55}) + \left( -D_{26} \right) \left( \frac{\cos \phi}{\sin \phi} \right) \right\} \quad (C.137)$$

$$cp_{95} = \left\{ \left( \frac{1}{R_\theta} \right) \left( \frac{1}{\sin \phi} \right) \left[ (-B_{16})(c_{25}) + (-B_{66})(c_{35}) + (-D_{16})(c_{45}) \right] \right. \\ \left. + (-D_{66})(c_{55}) + \left( -\frac{R_\phi}{R_\theta} \right) \left( -D_{66} \right) \left( \frac{\cos \phi}{\sin \phi} \right) \right\} \\ + \left\{ \left( \frac{1}{R_\theta} \right) \left( \frac{\cos \phi}{\sin \phi} \right) \left[ (B_{12})(cp_{25}) + (B_{26})(cp_{35}) + (D_{12})(cp_{45}) \right] \right. \\ \left. + \left( \frac{R_\phi}{R_\theta} \right) \left( \frac{1}{\sin \phi} \right) (D_{22}) + (D_{26})(cp_{55}) \right\} \quad (C.138)$$

$$cdp_{95} = \left\{ \left[ \left( \frac{1}{R_\theta} \right) \left( \frac{1}{\sin \phi} \right) \left[ (-B_{16})(cp_{25}) + (-B_{66})(cp_{35}) + (-D_{16})(cp_{45}) \right] \right] \right. \\ \left. + \left[ -\frac{R_\phi}{R_\theta} \left( \frac{1}{\sin \phi} \right) (D_{26}) + (-D_{66})(cp_{55}) \right] \right\} \quad (C.139)$$

$$c_{96} = \{R_\phi\} \quad (C.140)$$

$$c_{97} = \left\{ \left[ \left( \frac{1}{R_\theta} \right) \left( \frac{\cos \phi}{\sin \phi} \right) \left[ (B_{12})(c_{27}) + (B_{26})(c_{37}) + (D_{12})(c_{47}) + (D_{26})(c_{57}) \right] \right] \right\} \quad (C.141)$$

$$c_{98} = \left\{ \left[ \left( \frac{1}{R_\theta} \right) \left( \frac{\cos \phi}{\sin \phi} \right) \left[ (B_{12})(c_{28}) + (B_{26})(c_{38}) + (D_{12})(c_{48}) + (D_{26})(c_{58}) \right] \right] \right\} \quad (C.142)$$

$$c_{99} = \left\{ \left[ -\frac{R_\phi}{R_\theta} \left( \frac{\cos \phi}{\sin \phi} \right) + \left( \frac{1}{R_\theta} \right) \left( \frac{\cos \phi}{\sin \phi} \right) \left[ (B_{12})(c_{29}) + (B_{26})(c_{39}) \right] \right] \right. \\ \left. + \left[ (D_{12})(c_{49}) + (D_{26})(c_{59}) \right] \right\} \quad (C.143)$$

$$c_{910} = \left\{ \left[ \left( \frac{1}{R_\theta} \right) \left( \frac{\cos \phi}{\sin \phi} \right) \left[ (B_{12})(c_{210}) + (B_{26})(c_{310}) + (D_{12})(c_{410}) + (D_{26})(c_{510}) \right] \right] \right\} \quad (C.144)$$

$$cp_{910} = \left\{ \left[ -\frac{R_\phi}{R_\theta} \left( \frac{1}{\sin \phi} \right) \right] \right\} \quad (C.145)$$

The coefficients of  $\frac{\partial M_{\phi\theta}}{\partial \phi}$  given in Equation (3.23)

$$cp_{101} = \left\{ \left[ \left( \frac{1}{R_\theta} \right) \left( \frac{1}{\sin \phi} \right) \left[ (-B_{12})(c_{21}) + (-B_{12}) + \left( -\frac{R_\phi}{R_\theta} \right) (B_{22}) \right] \right] \right. \\ \left. + \left[ (-B_{26})(c_{31}) + (-D_{12})(c_{41}) + (-D_{26})(c_{51}) \right] \right\} \quad (C.146)$$

$$c_{102} = \{ \{ (-As_{45}) + (As_{45})(c_{12}) \} \} \quad (C.147)$$

$$cp_{102} = \left\{ \left( \frac{1}{R_\theta} \right) \left( \frac{1}{\sin \phi} \right) \left[ (-B_{12})(c_{22}) + (-B_{22}) \left( \frac{\cos \phi}{\sin \phi} \right) + (-B_{26})(c_{32}) \right] \right. \\ \left. + (-D_{12})(c_{42}) + (-D_{26})(c_{52}) \right\} \quad (\text{C.148})$$

$$cdp_{102} = \left\{ \left( \frac{1}{R_\theta} \right) \left( \frac{1}{\sin \phi} \right) \left[ (-B_{12})(cp_{22}) + \left( -\frac{R_\phi}{R_\theta} \right) (B_{26}) \left( \frac{1}{\sin \phi} \right) + (-B_{26})(cp_{32}) \right] \right. \\ \left. + (-D_{12})(cp_{42}) + (-D_{26})(cp_{52}) \right\} \quad (\text{C.149})$$

$$c_{103} = \left\{ \left[ (As_{45})(c_{13}) + \left( -\frac{R_\phi}{R_\theta} \right) (As_{44}) \right] \right\} \quad (\text{C.150})$$

$$cp_{103} = \left\{ \left( \frac{1}{R_\theta} \right) \left( \frac{1}{\sin \phi} \right) \left[ (-B_{12})(c_{23}) + (-B_{26})(c_{33}) + (B_{26}) \left( \frac{\cos \phi}{\sin \phi} \right) \right] \right. \\ \left. + (-D_{12})(c_{43}) + (-D_{26})(c_{53}) \right\} \quad (\text{C.151})$$

$$cdp_{103} = \left\{ \left( \frac{1}{R_\theta} \right) \left( \frac{1}{\sin \phi} \right) \left[ (-B_{12})(cp_{23}) + \left( -\frac{R_\phi}{R_\theta} \right) (B_{22}) \left( \frac{1}{\sin \phi} \right) + (-B_{26})(cp_{33}) \right] \right. \\ \left. + (-D_{12})(cp_{43}) + (-D_{26})(cp_{53}) \right\} \quad (\text{C.152})$$

$$c_{104} = \left\{ \left[ (As_{45})(c_{14}) + (As_{45})(R_\phi) \right] \right\} \quad (\text{C.153})$$

$$cp_{104} = \left\{ \left( \frac{1}{R_\theta} \right) \left( \frac{1}{\sin \phi} \right) \left[ (-B_{12})(c_{24}) + (-B_{26})(c_{34}) + (-D_{12})(c_{44}) \right] \right. \\ \left. + (-D_{22}) \left( \frac{\cos \phi}{\sin \phi} \right) + (-D_{26})(c_{54}) \right\} \quad (\text{C.154})$$

$$cdp_{104} = \left\{ \left( \frac{1}{R_\theta} \right) \left( \frac{1}{\sin \phi} \right) \left[ (-B_{12})(cp_{24}) + (-B_{26})(cp_{34}) + (-D_{12})(cp_{44}) \right] \right. \\ \left. + \left( -\frac{R_\phi}{R_\theta} \right) (D_{26}) \left( \frac{1}{\sin \phi} \right) + (-D_{26})(cp_{54}) \right\} \quad (\text{C.155})$$

$$c_{105} = \left\{ \left[ -\frac{1}{12} \rho h^3 \omega^2 R_\phi \right] + \left[ (As_{45})(c_{15}) + (As_{44})(R_\phi) \right] \right\} \quad (\text{C.156})$$

$$cp_{105} = \left\{ \left( \frac{1}{R_\theta} \right) \left( \frac{1}{\sin \phi} \right) \left[ (-B_{12})(c_{25}) + (-B_{26})(c_{35}) + (-D_{12})(c_{45}) \right] \right. \\ \left. + (-D_{26})(c_{55}) + (D_{26}) \left( \frac{\cos \phi}{\sin \phi} \right) \right\} \quad (C.157)$$

$$cdp_{105} = \left\{ \left( \frac{1}{R_\theta} \right) \left( \frac{1}{\sin \phi} \right) \left[ (-B_{12})(cp_{25}) + (-B_{26})(cp_{35}) + (-D_{12})(cp_{45}) \right] \right. \\ \left. + (-D_{26})(cp_{55}) + \left( -\frac{R_\phi}{R_\theta} \right) \left( D_{22} \left( \frac{1}{\sin \phi} \right) \right) \right\} \quad (C.158)$$

$$c_{106} = \{ \{ (As_{45})(c_{16}) \} \} \quad (C.159)$$

$$cp_{107} = \left\{ \left( \frac{1}{R_\theta} \right) \left( \frac{1}{\sin \phi} \right) \left[ (-B_{12})(c_{27}) + (-B_{26})(c_{37}) + (-D_{12})(c_{47}) + (-D_{26})(c_{57}) \right] \right\} \quad (C.160)$$

$$cp_{108} = \left\{ \left( \frac{1}{R_\theta} \right) \left( \frac{1}{\sin \phi} \right) \left[ (-B_{12})(c_{28}) + (-B_{26})(c_{38}) + (-D_{12})(c_{48}) + (-D_{26})(c_{58}) \right] \right\} \quad (C.161)$$

$$cp_{109} = \left\{ \left( \frac{1}{R_\theta} \right) \left( \frac{1}{\sin \phi} \right) \left[ (-B_{12})(c_{29}) + (-B_{26})(c_{39}) + (-D_{12})(c_{49}) + (-D_{26})(c_{59}) \right] \right\} \quad (C.162)$$

$$c_{1010} = \left\{ (-2) \left( \frac{R_\phi}{R_\theta} \right) \left( \frac{\cos \phi}{\sin \phi} \right) \right\} \quad (C.163)$$

$$cp_{1010} = \left\{ \left( \frac{1}{R_\theta} \right) \left( \frac{1}{\sin \phi} \right) \left[ (-B_{12})(c_{210}) + (-B_{26})(c_{310}) \right] \right. \\ \left. + (-D_{12})(c_{410}) + (-D_{26})(c_{510}) \right\} \quad (C.164)$$

## APPENDIX D

### METHOD OF FINITE EXPONENTIAL FOURIER TRANSFORM

Carrying out Method of Finite Fourier Transform to some functions  $[V_1, V_2, V_3, V_4, V_5]$  and their derivatives up to order 2 with respect to  $\phi$  and/or  $\theta$ . During these operations the integration by parts is done whenever necessary.

$$V_1(\phi) = \frac{1}{2\pi} \int_0^{2\pi} V_1(\phi, \theta) e^{-in\theta} d\theta \quad (D.1)$$

$$\frac{dV_2(\phi)}{d\phi} = \frac{1}{2\pi} \int_0^{2\pi} \frac{\partial V_2(\phi, \theta)}{\partial \phi} e^{-in\theta} d\theta \quad (D.2)$$

$$\frac{d^2V_3(\phi)}{d\phi^2} = \frac{1}{2\pi} \int_0^{2\pi} \frac{\partial^2 V_3(\phi, \theta)}{\partial \phi^2} e^{-in\theta} d\theta \quad (D.3)$$

$$V_4(\phi) = \frac{1}{2\pi} \int_0^{2\pi} \frac{\partial V_4(\phi, \theta)}{\partial \theta} e^{-in\theta} d\theta$$

$$V_4(\phi) = \frac{1}{2\pi} \left\{ e^{-in\theta} V_4(\phi, \theta) \Big|_0^{2\pi} - \int_0^{2\pi} V_4(\phi, \theta) (-ine^{-in\theta}) d\theta \right\}$$

$$\text{because } V_4(\phi, \theta) \Big|_{\theta=0} = V_4(\phi, \theta) \Big|_{\theta=2\pi} \quad (D.4)$$

$$V_4(\phi) = \frac{in}{2\pi} \int_0^{2\pi} V_4(\phi, \theta) e^{-in\theta} d\theta$$

$$V_5(\phi) = \frac{1}{2\pi} \int_0^{2\pi} \frac{\partial^2 V_5(\phi, \theta)}{\partial \theta^2} e^{-in\theta} d\theta$$

$$V_5(\phi) = \frac{1}{2\pi} \left\{ e^{-in\theta} \frac{\partial V_5(\phi, \theta)}{\partial \theta} \Big|_0^{2\pi} + in \int_0^{2\pi} \frac{\partial V_5}{\partial \theta} e^{-in\theta} d\theta \right\}$$

$$\text{yet } \frac{\partial V_5(\phi, \theta)}{\partial \theta} \Big|_{\theta=0} = \frac{\partial V_5(\phi, \theta)}{\partial \theta} \Big|_{\theta=2\pi} \quad (\text{D.5})$$

$$V_5(\phi) = in \left\{ e^{-in\theta} V_5(\phi, \theta) \Big|_0^{2\pi} - \int_0^{2\pi} V_5(\phi, \theta) (-ine^{-in\theta}) d\theta \right\}$$

$$V_5(\phi) = \frac{(in)^2}{2\pi} \int_0^{2\pi} V_5(\phi, \theta) e^{-in\theta} d\theta = -\frac{(n)^2}{2\pi} \int_0^{2\pi} V_5(\phi, \theta) e^{-in\theta} d\theta$$

## APPENDIX E

### APPLICATION OF METHOD OF FINITE EXPONENTIAL FOURIER TRANSFORM TO THE SYSTEM OF DIFFERENTIAL EQUATIONS DERIVED IN SECTION 3.3.1

Rewriting Equation (3.15)

$$\begin{aligned}
 \frac{\partial u_\phi^0}{\partial \phi} &= (c_{21})(w^0) + (c_{22})(u_\phi^0) + (cp_{22})\left(\frac{\partial u_\phi^0}{\partial \theta}\right) + (c_{23})(u_\theta^0) + (cp_{23})\left(\frac{\partial u_\theta^0}{\partial \theta}\right) + (c_{24})(\beta_\phi) \\
 &+ (cp_{24})\left(\frac{\partial \beta_\phi}{\partial \theta}\right) + (c_{25})(\beta_\theta) + (cp_{25})\left(\frac{\partial \beta_\theta}{\partial \theta}\right) + (c_{27})(N_{\phi\phi}) + (c_{28})(N_{\phi\theta}) + (c_{29})(M_{\phi\phi}) \\
 &+ (c_{210})(M_{\phi\theta})
 \end{aligned} \tag{E.1}$$

Carrying out the Finite exponential Fourier transform to Equation (E.1)

$$\begin{aligned}
 \frac{1}{2\Pi} \int_0^{2\Pi} \left[ \frac{\partial u_\phi^0(\phi, \theta, t)}{\partial \phi} e^{-in\theta} \right] d\theta &= (c_{21}) \frac{1}{2\Pi} \int_0^{2\Pi} [w^0(\phi, \theta, t) e^{-in\theta}] d\theta \\
 &+ (c_{22}) \frac{1}{2\Pi} \int_0^{2\Pi} [u_\phi^0(\phi, \theta, t) e^{-in\theta}] d\theta + (cp_{22}) \frac{1}{2\Pi} \int_0^{2\Pi} \left[ \frac{\partial u_\phi^0(\phi, \theta, t)}{\partial \theta} e^{-in\theta} \right] d\theta \\
 &+ (c_{23}) \frac{1}{2\Pi} \int_0^{2\Pi} [u_\theta^0(\phi, \theta, t) e^{-in\theta}] d\theta + (cp_{23}) \frac{1}{2\Pi} \int_0^{2\Pi} \left[ \frac{\partial u_\theta^0(\phi, \theta, t)}{\partial \theta} e^{-in\theta} \right] d\theta \\
 &+ (c_{24}) \frac{1}{2\Pi} \int_0^{2\Pi} [\beta_\phi(\phi, \theta, t) e^{-in\theta}] d\theta + (cp_{24}) \frac{1}{2\Pi} \int_0^{2\Pi} \left[ \frac{\partial \beta_\phi(\phi, \theta, t)}{\partial \theta} e^{-in\theta} \right] d\theta \\
 &+ (c_{25}) \frac{1}{2\Pi} \int_0^{2\Pi} [\beta_\theta(\phi, \theta, t) e^{-in\theta}] d\theta + (cp_{25}) \frac{1}{2\Pi} \int_0^{2\Pi} \left[ \frac{\partial \beta_\theta(\phi, \theta, t)}{\partial \theta} e^{-in\theta} \right] d\theta \\
 &+ (c_{27}) \frac{1}{2\Pi} \int_0^{2\Pi} [N_\phi(\phi, \theta, t) e^{-in\theta}] d\theta + (c_{28}) \frac{1}{2\Pi} \int_0^{2\Pi} [N_{\phi\theta}(\phi, \theta, t) e^{-in\theta}] d\theta \\
 &+ (c_{29}) \frac{1}{2\Pi} \int_0^{2\Pi} [M_\phi(\phi, \theta, t) e^{-in\theta}] d\theta + (c_{210}) \frac{1}{2\Pi} \int_0^{2\Pi} [M_{\phi\theta}(\phi, \theta, t) e^{-in\theta}] d\theta
 \end{aligned} \tag{E.2}$$

Using Equation (3.28) in Equation (E.2) yield

$$\begin{aligned}
& \int_0^{2\pi} \begin{bmatrix} \frac{\partial u_\phi^0(\phi, \theta, t)}{\partial \phi} \cos n\theta \\ -i \frac{\partial u_\phi^0(\phi, \theta, t)}{\partial \phi} \sin n\theta \end{bmatrix} d\theta = (c_{21}) \int_0^{2\pi} \begin{bmatrix} w^0(\phi, \theta, t) \cos n\theta \\ -i w^0(\phi, \theta, t) \sin n\theta \end{bmatrix} d\theta \\
& + (c_{22}) \int_0^{2\pi} \begin{bmatrix} u_\phi^0(\phi, \theta, t) \cos n\theta \\ -i u_\phi^0(\phi, \theta, t) \sin n\theta \end{bmatrix} d\theta + (cp_{22}) \int_0^{2\pi} (in) \begin{bmatrix} u_\phi^0(\phi, \theta, t) \cos n\theta \\ -i u_\phi^0(\phi, \theta, t) \sin n\theta \end{bmatrix} d\theta \\
& + (c_{23}) \int_0^{2\pi} \begin{bmatrix} u_\theta^0(\phi, \theta, t) \cos n\theta \\ -i u_\theta^0(\phi, \theta, t) \sin n\theta \end{bmatrix} d\theta + (cp_{23}) \int_0^{2\pi} (in) \begin{bmatrix} u_\theta^0(\phi, \theta, t) \cos n\theta \\ -i u_\theta^0(\phi, \theta, t) \sin n\theta \end{bmatrix} d\theta \\
& + (c_{24}) \int_0^{2\pi} \begin{bmatrix} \beta_\phi(\phi, \theta, t) \cos n\theta \\ -i \beta_\phi(\phi, \theta, t) \sin n\theta \end{bmatrix} d\theta + (cp_{24}) \int_0^{2\pi} (in) \begin{bmatrix} \beta_\phi(\phi, \theta, t) \cos n\theta \\ -i \beta_\phi(\phi, \theta, t) \sin n\theta \end{bmatrix} d\theta \\
& + (c_{25}) \int_0^{2\pi} \begin{bmatrix} \beta_\theta(\phi, \theta, t) \cos n\theta \\ -i \beta_\theta(\phi, \theta, t) \sin n\theta \end{bmatrix} d\theta + (cp_{25}) \int_0^{2\pi} (in) \begin{bmatrix} \beta_\theta(\phi, \theta, t) \cos n\theta \\ -i \beta_\theta(\phi, \theta, t) \sin n\theta \end{bmatrix} d\theta \\
& + (c_{27}) \int_0^{2\pi} \begin{bmatrix} N_\phi(\phi, \theta, t) \cos n\theta \\ -i N_\phi(\phi, \theta, t) \sin n\theta \end{bmatrix} d\theta + (c_{28}) \int_0^{2\pi} \begin{bmatrix} N_{\phi\theta}(\phi, \theta, t) \cos n\theta \\ -i N_{\phi\theta}(\phi, \theta, t) \sin n\theta \end{bmatrix} d\theta \\
& + (c_{29}) \int_0^{2\pi} \begin{bmatrix} M_\phi(\phi, \theta, t) \cos n\theta \\ -i M_\phi(\phi, \theta, t) \sin n\theta \end{bmatrix} d\theta + (c_{210}) \int_0^{2\pi} \begin{bmatrix} M_{\phi\theta}(\phi, \theta, t) \cos n\theta \\ -i M_{\phi\theta}(\phi, \theta, t) \sin n\theta \end{bmatrix} d\theta
\end{aligned} \tag{E.3}$$

$$\begin{aligned}
& \left[ \frac{du_\phi^0(\phi, t)}{d\phi} \right]_{nc} - i \left[ \frac{du_\phi^0(\phi, t)}{d\phi} \right]_{ns} = (c_{21}) \{ [w^0(\phi, t)]_{nc} - i [w^0(\phi, t)]_{ns} \} \\
& + (c_{22}) \{ [u_\phi^0(\phi, t)]_{nc} - i [u_\phi^0(\phi, t)]_{ns} \} + (cp_{22})(n) \{ i [u_\phi^0(\phi, t)]_{nc} + [u_\phi^0(\phi, t)]_{ns} \} \\
& + (c_{23}) \{ [u_\theta^0(\phi, t)]_{nc} - i [u_\theta^0(\phi, t)]_{ns} \} + (cp_{23})(n) \{ i [u_\theta^0(\phi, t)]_{nc} + [u_\theta^0(\phi, t)]_{ns} \} \\
& + (c_{24}) \{ [\beta_\phi(\phi, t)]_{nc} - i [\beta_\phi(\phi, t)]_{ns} \} + (cp_{24})(n) \{ i [\beta_\phi(\phi, t)]_{nc} + [\beta_\phi(\phi, t)]_{ns} \} \\
& + (c_{25}) \{ [\beta_\theta(\phi, t)]_{nc} - i [\beta_\theta(\phi, t)]_{ns} \} + (cp_{25})(n) \{ i [\beta_\theta(\phi, t)]_{nc} + [\beta_\theta(\phi, t)]_{ns} \} \\
& + (c_{27}) \{ [N_\phi(\phi, t)]_{nc} - i [N_\phi(\phi, t)]_{ns} \} + (c_{28}) \{ [N_{\phi\theta}(\phi, t)]_{nc} - i [N_{\phi\theta}(\phi, t)]_{ns} \} \\
& + (c_{29}) \{ [M_\phi(\phi, t)]_{nc} - i [M_\phi(\phi, t)]_{ns} \} + (c_{210}) \{ [M_{\phi\theta}(\phi, t)]_{nc} - i [M_{\phi\theta}(\phi, t)]_{ns} \}
\end{aligned} \tag{E.4}$$

Separating the real and imaginary parts of Equation (E.4)

First, writing real parts of Equation (E.4) term by term

$$\begin{aligned}
\left[ \frac{du_\phi^0(\phi, t)}{d\phi} \right]_{nc} &= (c_{21})[w^0(\phi, t)]_{nc} + (c_{22})[u_\phi^0(\phi, t)]_{nc} + (cp_{22})(n)[u_\phi^0(\phi, t)]_{ns} \\
&+ (c_{23})[u_\theta^0(\phi, t)]_{nc} + (cp_{23})(n)[u_\theta^0(\phi, t)]_{ns} + (c_{24})[\beta_\phi(\phi, t)]_{nc} + (cp_{24})(n)[\beta_\phi(\phi, t)]_{ns} \\
&+ (c_{25})[\beta_\theta(\phi, t)]_{nc} + (cp_{25})(n)[\beta_\theta(\phi, t)]_{ns} + (c_{27})[N_\phi(\phi, t)]_{nc} + (c_{28})[N_{\phi\theta}(\phi, t)]_{nc} \\
&+ (c_{29})[M_\phi(\phi, t)]_{nc} + (c_{210})[M_{\phi\theta}(\phi, t)]_{nc}
\end{aligned} \tag{E.5}$$

Then, writing imaginary parts of Equation (E.4) term by term.

$$\begin{aligned}
\left[ \frac{du_\phi^0(\phi, t)}{d\phi} \right]_{ns} &= (c_{21})[w^0(\phi, t)]_{ns} + (c_{22})[u_\phi^0(\phi, t)]_{ns} - (cp_{22})(n)[u_\phi^0(\phi, t)]_{nc} \\
&+ (c_{23})[u_\theta^0(\phi, t)]_{ns} - (cp_{23})(n)[u_\theta^0(\phi, t)]_{nc} + (c_{24})[\beta_\phi(\phi, t)]_{ns} - (cp_{24})(n)[\beta_\phi(\phi, t)]_{nc} \\
&+ (c_{25})[\beta_\theta(\phi, t)]_{ns} - (cp_{25})(n)[\beta_\theta(\phi, t)]_{nc} + (c_{27})[N_\phi(\phi, t)]_{ns} + (c_{28})[N_{\phi\theta}(\phi, t)]_{ns} \\
&+ (c_{29})[M_\phi(\phi, t)]_{ns} + (c_{210})[M_{\phi\theta}(\phi, t)]_{ns}
\end{aligned} \tag{E.6}$$

Rewriting Equation (3.16)

$$\begin{aligned}
\frac{\partial u_\phi^0}{\partial \phi} &= (c_{31})(w^0) + (c_{32})(u_\phi^0) + (cp_{32})\left(\frac{\partial u_\phi^0}{\partial \theta}\right) + (c_{33})(u_\theta^0) + (cp_{33})\left(\frac{\partial u_\theta^0}{\partial \theta}\right) \\
&+ (c_{34})(\beta_\phi) + (cp_{34})\left(\frac{\partial \beta_\phi}{\partial \theta}\right) + (c_{35})(\beta_\theta) + (cp_{35})\left(\frac{\partial \beta_\theta}{\partial \theta}\right) \\
&+ (c_{37})(N_{\phi\phi}) + (c_{38})(N_{\phi\theta}) + (c_{39})(M_{\phi\phi}) + (c_{310})(M_{\phi\theta})
\end{aligned} \tag{E.7}$$

Carrying out the Finite exponential Fourier transform to Equation (E.7)

$$\begin{aligned}
& \frac{1}{2\Pi} \int_0^{2\Pi} \left[ \frac{\partial u_\theta^0(\phi, \theta, t)}{\partial \phi} e^{-in\theta} \right] d\theta = (c_{31}) \frac{1}{2\Pi} \int_0^{2\Pi} \left[ w^0(\phi, \theta, t) e^{-in\theta} \right] d\theta \\
& + (c_{32}) \frac{1}{2\Pi} \int_0^{2\Pi} \left[ u_\phi^0(\phi, \theta, t) e^{-in\theta} \right] d\theta + (cp_{32}) \frac{1}{2\Pi} \int_0^{2\Pi} \left[ \frac{\partial u_\phi^0(\phi, \theta, t)}{\partial \theta} e^{-in\theta} \right] d\theta \\
& + (c_{33}) \frac{1}{2\Pi} \int_0^{2\Pi} \left[ u_\theta^0(\phi, \theta, t) e^{-in\theta} \right] d\theta + (cp_{33}) \frac{1}{2\Pi} \int_0^{2\Pi} \left[ \frac{\partial u_\theta^0(\phi, \theta, t)}{\partial \theta} e^{-in\theta} \right] d\theta \\
& + (c_{24}) \frac{1}{2\Pi} \int_0^{2\Pi} \left[ \beta_\phi(\phi, \theta, t) e^{-in\theta} \right] d\theta + (cp_{24}) \frac{1}{2\Pi} \int_0^{2\Pi} \left[ \frac{\partial \beta_\phi(\phi, \theta, t)}{\partial \theta} e^{-in\theta} \right] d\theta \\
& + (c_{35}) \frac{1}{2\Pi} \int_0^{2\Pi} \left[ \beta_\theta(\phi, \theta, t) e^{-in\theta} \right] d\theta + (cp_{35}) \frac{1}{2\Pi} \int_0^{2\Pi} \left[ \frac{\partial \beta_\theta(\phi, \theta, t)}{\partial \theta} e^{-in\theta} \right] d\theta \\
& + (c_{37}) \frac{1}{2\Pi} \int_0^{2\Pi} \left[ N_\phi(\phi, \theta, t) e^{-in\theta} \right] d\theta + (c_{38}) \frac{1}{2\Pi} \int_0^{2\Pi} \left[ N_{\phi\theta}(\phi, \theta, t) e^{-in\theta} \right] d\theta \\
& + (c_{39}) \frac{1}{2\Pi} \int_0^{2\Pi} \left[ M_\phi(\phi, \theta, t) e^{-in\theta} \right] d\theta + (c_{310}) \frac{1}{2\Pi} \int_0^{2\Pi} \left[ M_{\phi\theta}(\phi, \theta, t) e^{-in\theta} \right] d\theta
\end{aligned} \tag{E.8}$$

Using Equation (3.28) in Equation (E.8) yields

$$\begin{aligned}
& \int_0^{2\Pi} \left[ \begin{array}{l} \frac{\partial u_\theta^0(\phi, \theta, t)}{\partial \phi} \cos n\theta \\ -i \frac{\partial u_\theta^0(\phi, \theta, t)}{\partial \phi} \sin n\theta \end{array} \right] d\theta = (c_{31}) \int_0^{2\Pi} \left[ \begin{array}{l} w^0(\phi, \theta, t) \cos n\theta \\ -i w^0(\phi, \theta, t) \sin n\theta \end{array} \right] d\theta \\
& + (c_{32}) \int_0^{2\Pi} \left[ \begin{array}{l} u_\phi^0(\phi, \theta, t) \cos n\theta \\ -i u_\phi^0(\phi, \theta, t) \sin n\theta \end{array} \right] d\theta + (cp_{32}) \int_0^{2\Pi} (in) \left[ \begin{array}{l} u_\phi^0(\phi, \theta, t) \cos n\theta \\ -i u_\phi^0(\phi, \theta, t) \sin n\theta \end{array} \right] d\theta \\
& + (c_{33}) \int_0^{2\Pi} \left[ \begin{array}{l} u_\theta^0(\phi, \theta, t) \cos n\theta \\ -i u_\theta^0(\phi, \theta, t) \sin n\theta \end{array} \right] d\theta + (cp_{33}) \int_0^{2\Pi} (in) \left[ \begin{array}{l} u_\theta^0(\phi, \theta, t) \cos n\theta \\ -i u_\theta^0(\phi, \theta, t) \sin n\theta \end{array} \right] d\theta \\
& + (c_{34}) \int_0^{2\Pi} \left[ \begin{array}{l} \beta_\phi(\phi, \theta, t) \cos n\theta \\ -i \beta_\phi(\phi, \theta, t) \sin n\theta \end{array} \right] d\theta + (cp_{34}) \int_0^{2\Pi} (in) \left[ \begin{array}{l} \beta_\phi(\phi, \theta, t) \cos n\theta \\ -i \beta_\phi(\phi, \theta, t) \sin n\theta \end{array} \right] d\theta \\
& + (c_{35}) \int_0^{2\Pi} \left[ \begin{array}{l} \beta_\theta(\phi, \theta, t) \cos n\theta \\ -i \beta_\theta(\phi, \theta, t) \sin n\theta \end{array} \right] d\theta + (cp_{35}) \int_0^{2\Pi} (in) \left[ \begin{array}{l} \beta_\theta(\phi, \theta, t) \cos n\theta \\ -i \beta_\theta(\phi, \theta, t) \sin n\theta \end{array} \right] d\theta \\
& + (c_{37}) \int_0^{2\Pi} \left[ \begin{array}{l} N_\phi(\phi, \theta, t) \cos n\theta \\ -i N_\phi(\phi, \theta, t) \sin n\theta \end{array} \right] d\theta + (c_{38}) \int_0^{2\Pi} \left[ \begin{array}{l} N_{\phi\theta}(\phi, \theta, t) \cos n\theta \\ -i N_{\phi\theta}(\phi, \theta, t) \sin n\theta \end{array} \right] d\theta \\
& + (c_{39}) \int_0^{2\Pi} \left[ \begin{array}{l} M_\phi(\phi, \theta, t) \cos n\theta \\ -i M_\phi(\phi, \theta, t) \sin n\theta \end{array} \right] d\theta + (c_{310}) \int_0^{2\Pi} \left[ \begin{array}{l} M_{\phi\theta}(\phi, \theta, t) \cos n\theta \\ -i M_{\phi\theta}(\phi, \theta, t) \sin n\theta \end{array} \right] d\theta
\end{aligned} \tag{E.9}$$

$$\begin{aligned}
& \left[ \frac{du_\theta^0(\phi, t)}{d\phi} \right]_{nc} - i \left[ \frac{du_\theta^0(\phi, t)}{d\phi} \right]_{ns} = (c_{31}) \{ [w^0(\phi, t)]_{nc} - i [w^0(\phi, t)]_{ns} \} \\
& + (c_{32}) \{ [u_\phi^0(\phi, t)]_{nc} - i [u_\phi^0(\phi, t)]_{ns} \} + (cp_{32}) \chi(n) \{ i [u_\phi^0(\phi, t)]_{nc} + [u_\phi^0(\phi, t)]_{ns} \} \\
& + (c_{33}) \{ [u_\theta^0(\phi, t)]_{nc} - i [u_\theta^0(\phi, t)]_{ns} \} + (cp_{33}) \chi(n) \{ i [u_\theta^0(\phi, t)]_{nc} + [u_\theta^0(\phi, t)]_{ns} \} \\
& + (c_{34}) \{ [\beta_\phi(\phi, t)]_{nc} - i [\beta_\phi(\phi, t)]_{ns} \} + (cp_{34}) \chi(n) \{ i [\beta_\phi(\phi, t)]_{nc} + [\beta_\phi(\phi, t)]_{ns} \} \\
& + (c_{35}) \{ [\beta_\theta(\phi, t)]_{nc} - i [\beta_\theta(\phi, t)]_{ns} \} + (cp_{35}) \chi(n) \{ i [\beta_\theta(\phi, t)]_{nc} + [\beta_\theta(\phi, t)]_{ns} \} \\
& + (c_{37}) \{ [N_\phi(\phi, t)]_{nc} - i [N_\phi(\phi, t)]_{ns} \} + (c_{38}) \{ [N_{\phi\theta}(\phi, t)]_{nc} - i [N_{\phi\theta}(\phi, t)]_{ns} \} \\
& + (c_{39}) \{ [M_\phi(\phi, t)]_{nc} - i [M_\phi(\phi, t)]_{ns} \} + (c_{310}) \{ [M_{\phi\theta}(\phi, t)]_{nc} - i [M_{\phi\theta}(\phi, t)]_{ns} \}
\end{aligned} \tag{E.10}$$

We now separate the real and imaginary parts of Equation (E.10). First, writing real parts of Equation (E.10) term by term.

$$\begin{aligned}
& \left[ \frac{du_\theta^0(\phi, t)}{d\phi} \right]_{nc} = (c_{31}) [w^0(\phi, t)]_{nc} + (c_{32}) [u_\phi^0(\phi, t)]_{nc} + (cp_{32}) \chi(n) [u_\phi^0(\phi, t)]_{ns} \\
& + (c_{33}) [u_\theta^0(\phi, t)]_{nc} + (cp_{33}) \chi(n) [u_\theta^0(\phi, t)]_{ns} + (c_{34}) [\beta_\phi(\phi, t)]_{nc} + (cp_{34}) \chi(n) [\beta_\phi(\phi, t)]_{ns} \\
& + (c_{35}) [\beta_\theta(\phi, t)]_{nc} + (cp_{35}) \chi(n) [\beta_\theta(\phi, t)]_{ns} + (c_{37}) [N_\phi(\phi, t)]_{nc} + (c_{38}) [N_{\phi\theta}(\phi, t)]_{nc} \\
& + (c_{39}) [M_\phi(\phi, t)]_{nc} + (c_{310}) [M_{\phi\theta}(\phi, t)]_{nc}
\end{aligned} \tag{E.11}$$

Then, writing imaginary parts of Equation (E.10) term by term.

$$\begin{aligned}
& \left[ \frac{du_\theta^0(\phi, t)}{d\phi} \right]_{ns} = (c_{31}) [w^0(\phi, t)]_{ns} + (c_{32}) [u_\phi^0(\phi, t)]_{ns} - (cp_{32}) \chi(n) [u_\phi^0(\phi, t)]_{nc} \\
& + (c_{33}) [u_\theta^0(\phi, t)]_{ns} - (cp_{33}) \chi(n) [u_\theta^0(\phi, t)]_{nc} + (c_{34}) [\beta_\phi(\phi, t)]_{ns} - (cp_{34}) \chi(n) [\beta_\phi(\phi, t)]_{nc} \\
& + (c_{35}) [\beta_\theta(\phi, t)]_{ns} - (cp_{35}) \chi(n) [\beta_\theta(\phi, t)]_{nc} + (c_{37}) [N_\phi(\phi, t)]_{ns} + (c_{38}) [N_{\phi\theta}(\phi, t)]_{ns} \\
& + (c_{39}) [M_\phi(\phi, t)]_{ns} + (c_{310}) [M_{\phi\theta}(\phi, t)]_{ns}
\end{aligned} \tag{E.12}$$

Rewriting Equation (3.17)

$$\begin{aligned}
\frac{\partial \beta_\phi^0}{\partial \phi} &= (c_{41})(w^0) + (c_{42})(u_\phi^0) + (cp_{42})\left(\frac{\partial u_\phi^0}{\partial \theta}\right) + (c_{43})(u_\theta^0) + (cp_{43})\left(\frac{\partial u_\theta^0}{\partial \theta}\right) \\
&+ (c_{44})(\beta_\phi) + (cp_{44})\left(\frac{\partial \beta_\phi}{\partial \theta}\right) + (c_{45})(\beta_\theta) + (cp_{45})\left(\frac{\partial \beta_\theta}{\partial \theta}\right) \\
&+ (c_{47})(N_{\phi\phi}) + (c_{48})(N_{\phi\theta}) + (c_{49})(M_{\phi\phi}) + (c_{410})(M_{\phi\theta})
\end{aligned} \tag{E.13}$$

Carrying out the Finite exponential Fourier transform to Equation (E.13)

$$\begin{aligned}
\frac{1}{2\Pi} \int_0^{2\Pi} \left[ \frac{\partial \beta_\phi(\phi, \theta, t)}{\partial \phi} e^{-in\theta} \right] d\theta &= (c_{41}) \frac{1}{2\Pi} \int_0^{2\Pi} [w^0(\phi, \theta, t) e^{-in\theta}] d\theta \\
+ (c_{42}) \frac{1}{2\Pi} \int_0^{2\Pi} [u_\phi^0(\phi, \theta, t) e^{-in\theta}] d\theta &+ (cp_{42}) \frac{1}{2\Pi} \int_0^{2\Pi} \left[ \frac{\partial u_\phi^0(\phi, \theta, t)}{\partial \theta} e^{-in\theta} \right] d\theta \\
+ (c_{43}) \frac{1}{2\Pi} \int_0^{2\Pi} [u_\theta^0(\phi, \theta, t) e^{-in\theta}] d\theta &+ (cp_{43}) \frac{1}{2\Pi} \int_0^{2\Pi} \left[ \frac{\partial u_\theta^0(\phi, \theta, t)}{\partial \theta} e^{-in\theta} \right] d\theta \\
+ (c_{44}) \frac{1}{2\Pi} \int_0^{2\Pi} [\beta_\phi(\phi, \theta, t) e^{-in\theta}] d\theta &+ (cp_{44}) \frac{1}{2\Pi} \int_0^{2\Pi} \left[ \frac{\partial \beta_\phi(\phi, \theta, t)}{\partial \theta} e^{-in\theta} \right] d\theta \\
+ (c_{45}) \frac{1}{2\Pi} \int_0^{2\Pi} [\beta_\theta(\phi, \theta, t) e^{-in\theta}] d\theta &+ (cp_{45}) \frac{1}{2\Pi} \int_0^{2\Pi} \left[ \frac{\partial \beta_\theta(\phi, \theta, t)}{\partial \theta} e^{-in\theta} \right] d\theta \\
+ (c_{47}) \frac{1}{2\Pi} \int_0^{2\Pi} [N_{\phi\phi}(\phi, \theta, t) e^{-in\theta}] d\theta &+ (c_{48}) \frac{1}{2\Pi} \int_0^{2\Pi} [N_{\phi\theta}(\phi, \theta, t) e^{-in\theta}] d\theta \\
+ (c_{49}) \frac{1}{2\Pi} \int_0^{2\Pi} [M_{\phi\phi}(\phi, \theta, t) e^{-in\theta}] d\theta &+ (c_{410}) \frac{1}{2\Pi} \int_0^{2\Pi} [M_{\phi\theta}(\phi, \theta, t) e^{-in\theta}] d\theta
\end{aligned} \tag{E.14}$$

Using Equation (3.28) in Equation (E.14) yields

$$\begin{aligned}
& \int_0^{2\Pi} \begin{bmatrix} \frac{\partial \beta_\phi(\phi, \theta, t)}{\partial \phi} \cos n\theta \\ -i \frac{\partial \beta_\phi(\phi, \theta, t)}{\partial \phi} \sin n\theta \end{bmatrix} d\theta = (c_{41}) \int_0^{2\Pi} \begin{bmatrix} w^0(\phi, \theta, t) \cos n\theta \\ -i w^0(\phi, \theta, t) \sin n\theta \end{bmatrix} d\theta \\
& + (c_{42}) \int_0^{2\Pi} \begin{bmatrix} u_\phi^0(\phi, \theta, t) \cos n\theta \\ -i u_\phi^0(\phi, \theta, t) \sin n\theta \end{bmatrix} d\theta + (cp_{42}) \int_0^{2\Pi} (in) \begin{bmatrix} u_\phi^0(\phi, \theta, t) \cos n\theta \\ -i u_\phi^0(\phi, \theta, t) \sin n\theta \end{bmatrix} d\theta \\
& + (c_{43}) \int_0^{2\Pi} \begin{bmatrix} u_\theta^0(\phi, \theta, t) \cos n\theta \\ -i u_\theta^0(\phi, \theta, t) \sin n\theta \end{bmatrix} d\theta + (cp_{43}) \int_0^{2\Pi} (in) \begin{bmatrix} u_\theta^0(\phi, \theta, t) \cos n\theta \\ -i u_\theta^0(\phi, \theta, t) \sin n\theta \end{bmatrix} d\theta \\
& + (c_{44}) \int_0^{2\Pi} \begin{bmatrix} \beta_\phi(\phi, \theta, t) \cos n\theta \\ -i \beta_\phi(\phi, \theta, t) \sin n\theta \end{bmatrix} d\theta + (cp_{44}) \int_0^{2\Pi} (in) \begin{bmatrix} \beta_\phi(\phi, \theta, t) \cos n\theta \\ -i \beta_\phi(\phi, \theta, t) \sin n\theta \end{bmatrix} d\theta \\
& + (c_{45}) \int_0^{2\Pi} \begin{bmatrix} \beta_\theta(\phi, \theta, t) \cos n\theta \\ -i \beta_\theta(\phi, \theta, t) \sin n\theta \end{bmatrix} d\theta + (cp_{45}) \int_0^{2\Pi} (in) \begin{bmatrix} \beta_\theta(\phi, \theta, t) \cos n\theta \\ -i \beta_\theta(\phi, \theta, t) \sin n\theta \end{bmatrix} d\theta \\
& + (c_{47}) \int_0^{2\Pi} \begin{bmatrix} N_\phi(\phi, \theta, t) \cos n\theta \\ -i N_\phi(\phi, \theta, t) \sin n\theta \end{bmatrix} d\theta + (c_{48}) \int_0^{2\Pi} \begin{bmatrix} N_{\phi\theta}(\phi, \theta, t) \cos n\theta \\ -i N_{\phi\theta}(\phi, \theta, t) \sin n\theta \end{bmatrix} d\theta \\
& + (c_{49}) \int_0^{2\Pi} \begin{bmatrix} M_\phi(\phi, \theta, t) \cos n\theta \\ -i M_\phi(\phi, \theta, t) \sin n\theta \end{bmatrix} d\theta + (c_{410}) \int_0^{2\Pi} \begin{bmatrix} M_{\phi\theta}(\phi, \theta, t) \cos n\theta \\ -i M_{\phi\theta}(\phi, \theta, t) \sin n\theta \end{bmatrix} d\theta
\end{aligned} \tag{E.15}$$

$$\begin{aligned}
& \left[ \frac{d\beta_\phi(\phi, t)}{d\phi} \right]_{nc} - i \left[ \frac{d\beta_\phi(\phi, t)}{d\phi} \right]_{ns} = (c_{41}) \{ [w^0(\phi, t)]_{nc} - i [w^0(\phi, t)]_{ns} \} \\
& + (c_{42}) \{ [u_\phi^0(\phi, t)]_{nc} - i [u_\phi^0(\phi, t)]_{ns} \} + (cp_{42}) (n) \{ i [u_\phi^0(\phi, t)]_{nc} + [u_\phi^0(\phi, t)]_{ns} \} \\
& + (c_{43}) \{ [u_\theta^0(\phi, t)]_{nc} - i [u_\theta^0(\phi, t)]_{ns} \} + (cp_{43}) (n) \{ i [u_\theta^0(\phi, t)]_{nc} + [u_\theta^0(\phi, t)]_{ns} \} \\
& + (c_{44}) \{ [\beta_\phi(\phi, t)]_{nc} - i [\beta_\phi(\phi, t)]_{ns} \} + (cp_{44}) (n) \{ i [\beta_\phi(\phi, t)]_{nc} + [\beta_\phi(\phi, t)]_{ns} \} \\
& + (c_{45}) \{ [\beta_\theta(\phi, t)]_{nc} - i [\beta_\theta(\phi, t)]_{ns} \} + (cp_{45}) (n) \{ i [\beta_\theta(\phi, t)]_{nc} + [\beta_\theta(\phi, t)]_{ns} \} \\
& + (c_{47}) \{ [N_\phi(\phi, t)]_{nc} - i [N_\phi(\phi, t)]_{ns} \} + (c_{48}) \{ [N_{\phi\theta}(\phi, t)]_{nc} - i [N_{\phi\theta}(\phi, t)]_{ns} \} \\
& + (c_{49}) \{ [M_\phi(\phi, t)]_{nc} - i [M_\phi(\phi, t)]_{ns} \} + (c_{410}) \{ [M_{\phi\theta}(\phi, t)]_{nc} - i [M_{\phi\theta}(\phi, t)]_{ns} \}
\end{aligned} \tag{E.16}$$

We separate the real and imaginary parts of Equation (E.16)

First, writing real parts of Equation (E.16) term by term.

$$\begin{aligned}
\left[ \frac{d\beta_\phi(\phi, t)}{d\phi} \right]_{nc} &= (c_{41})[w^0(\phi, t)]_{nc} + (c_{42})[u_\phi^0(\phi, t)]_{nc} + (cp_{42})(n)[u_\phi^0(\phi, t)]_{ns} \\
&+ (c_{43})[u_\theta^0(\phi, t)]_{nc} + (cp_{43})(n)[u_\theta^0(\phi, t)]_{ns} + (c_{44})[\beta_\phi(\phi, t)]_{nc} + (cp_{44})(n)[\beta_\phi(\phi, t)]_{ns} \\
&+ (c_{45})[\beta_\theta(\phi, t)]_{nc} + (cp_{45})(n)[\beta_\theta(\phi, t)]_{ns} + (c_{47})[N_\phi(\phi, t)]_{nc} + (c_{48})[N_{\phi\theta}(\phi, t)]_{nc} \\
&+ (c_{49})[M_\phi(\phi, t)]_{nc} + (c_{410})[M_{\phi\theta}(\phi, t)]_{nc}
\end{aligned} \tag{E.17}$$

Then, writing imaginary parts of Equation (E.16) term by term.

$$\begin{aligned}
\left[ \frac{d\beta_\phi(\phi, t)}{d\phi} \right]_{ns} &= (c_{41})[w^0(\phi, t)]_{ns} + (c_{42})[u_\phi^0(\phi, t)]_{ns} - (cp_{42})(n)[u_\phi^0(\phi, t)]_{nc} \\
&+ (c_{43})[u_\theta^0(\phi, t)]_{ns} - (cp_{43})(n)[u_\theta^0(\phi, t)]_{nc} + (c_{44})[\beta_\phi(\phi, t)]_{ns} - (cp_{44})(n)[\beta_\phi(\phi, t)]_{nc} \\
&+ (c_{45})[\beta_\theta(\phi, t)]_{ns} - (cp_{45})(n)[\beta_\theta(\phi, t)]_{nc} + (c_{47})[N_\phi(\phi, t)]_{ns} + (c_{48})[N_{\phi\theta}(\phi, t)]_{ns} \\
&+ (c_{49})[M_\phi(\phi, t)]_{ns} + (c_{410})[M_{\phi\theta}(\phi, t)]_{ns}
\end{aligned} \tag{E.18}$$

Rewriting Equation (3.18)

$$\begin{aligned}
\frac{\partial \beta_\theta^0}{\partial \phi} &= (c_{51})(w^0) + (c_{52})(u_\phi^0) + (cp_{52})\left(\frac{\partial u_\phi^0}{\partial \theta}\right) + (c_{53})(u_\theta^0) + (cp_{53})\left(\frac{\partial u_\theta^0}{\partial \theta}\right) \\
&+ (c_{54})(\beta_\phi) + (cp_{54})\left(\frac{\partial \beta_\phi}{\partial \theta}\right) + (c_{55})(\beta_\theta) + (cp_{55})\left(\frac{\partial \beta_\theta}{\partial \theta}\right) \\
&+ (c_{57})(N_{\phi\phi}) + (c_{58})(N_{\phi\theta}) + (c_{59})(M_{\phi\phi}) + (c_{510})(M_{\phi\theta})
\end{aligned} \tag{E.19}$$

Carrying out the Finite exponential Fourier transform to Equation (E.19)

$$\begin{aligned}
& \frac{1}{2\Pi} \int_0^{2\Pi} \left[ \frac{\partial \beta_\theta(\phi, \theta, t)}{\partial \phi} e^{-in\theta} \right] d\theta = (c_{51}) \frac{1}{2\Pi} \int_0^{2\Pi} \left[ w^0(\phi, \theta, t) e^{-in\theta} \right] d\theta \\
& + (c_{52}) \frac{1}{2\Pi} \int_0^{2\Pi} \left[ u_\phi^0(\phi, \theta, t) e^{-in\theta} \right] d\theta + (cp_{52}) \frac{1}{2\Pi} \int_0^{2\Pi} \left[ \frac{\partial u_\phi^0(\phi, \theta, t)}{\partial \theta} e^{-in\theta} \right] d\theta \\
& + (c_{53}) \frac{1}{2\Pi} \int_0^{2\Pi} \left[ u_\theta^0(\phi, \theta, t) e^{-in\theta} \right] d\theta + (cp_{53}) \frac{1}{2\Pi} \int_0^{2\Pi} \left[ \frac{\partial u_\theta^0(\phi, \theta, t)}{\partial \theta} e^{-in\theta} \right] d\theta \\
& + (c_{54}) \frac{1}{2\Pi} \int_0^{2\Pi} \left[ \beta_\phi(\phi, \theta, t) e^{-in\theta} \right] d\theta + (cp_{54}) \frac{1}{2\Pi} \int_0^{2\Pi} \left[ \frac{\partial \beta_\phi(\phi, \theta, t)}{\partial \theta} e^{-in\theta} \right] d\theta \\
& + (c_{55}) \frac{1}{2\Pi} \int_0^{2\Pi} \left[ \beta_\theta(\phi, \theta, t) e^{-in\theta} \right] d\theta + (cp_{55}) \frac{1}{2\Pi} \int_0^{2\Pi} \left[ \frac{\partial \beta_\theta(\phi, \theta, t)}{\partial \theta} e^{-in\theta} \right] d\theta \\
& + (c_{57}) \frac{1}{2\Pi} \int_0^{2\Pi} \left[ N_\phi(\phi, \theta, t) e^{-in\theta} \right] d\theta + (c_{58}) \frac{1}{2\Pi} \int_0^{2\Pi} \left[ N_{\phi\theta}(\phi, \theta, t) e^{-in\theta} \right] d\theta \\
& + (c_{59}) \frac{1}{2\Pi} \int_0^{2\Pi} \left[ M_\phi(\phi, \theta, t) e^{-in\theta} \right] d\theta + (c_{510}) \frac{1}{2\Pi} \int_0^{2\Pi} \left[ M_{\phi\theta}(\phi, \theta, t) e^{-in\theta} \right] d\theta
\end{aligned} \tag{E.20}$$

Using Equation (3.28) in Equation (E.20) yields

$$\begin{aligned}
& \int_0^{2\Pi} \left[ \begin{array}{c} \frac{\partial \beta_\theta(\phi, \theta, t)}{\partial \phi} \cos n\theta \\ -i \frac{\partial \beta_\theta(\phi, \theta, t)}{\partial \phi} \sin n\theta \end{array} \right] d\theta = (c_{51}) \int_0^{2\Pi} \left[ \begin{array}{c} w^0(\phi, \theta, t) \cos n\theta \\ -i w^0(\phi, \theta, t) \sin n\theta \end{array} \right] d\theta \\
& + (c_{52}) \int_0^{2\Pi} \left[ \begin{array}{c} u_\phi^0(\phi, \theta, t) \cos n\theta \\ -i u_\phi^0(\phi, \theta, t) \sin n\theta \end{array} \right] d\theta + (cp_{52}) \int_0^{2\Pi} (in) \left[ \begin{array}{c} u_\phi^0(\phi, \theta, t) \cos n\theta \\ -i u_\phi^0(\phi, \theta, t) \sin n\theta \end{array} \right] d\theta \\
& + (c_{53}) \int_0^{2\Pi} \left[ \begin{array}{c} u_\theta^0(\phi, \theta, t) \cos n\theta \\ -i u_\theta^0(\phi, \theta, t) \sin n\theta \end{array} \right] d\theta + (cp_{53}) \int_0^{2\Pi} (in) \left[ \begin{array}{c} u_\theta^0(\phi, \theta, t) \cos n\theta \\ -i u_\theta^0(\phi, \theta, t) \sin n\theta \end{array} \right] d\theta \\
& + (c_{54}) \int_0^{2\Pi} \left[ \begin{array}{c} \beta_\phi(\phi, \theta, t) \cos n\theta \\ -i \beta_\phi(\phi, \theta, t) \sin n\theta \end{array} \right] d\theta + (cp_{54}) \int_0^{2\Pi} (in) \left[ \begin{array}{c} \beta_\phi(\phi, \theta, t) \cos n\theta \\ -i \beta_\phi(\phi, \theta, t) \sin n\theta \end{array} \right] d\theta \\
& + (c_{55}) \int_0^{2\Pi} \left[ \begin{array}{c} \beta_\theta(\phi, \theta, t) \cos n\theta \\ -i \beta_\theta(\phi, \theta, t) \sin n\theta \end{array} \right] d\theta + (cp_{55}) \int_0^{2\Pi} (in) \left[ \begin{array}{c} \beta_\theta(\phi, \theta, t) \cos n\theta \\ -i \beta_\theta(\phi, \theta, t) \sin n\theta \end{array} \right] d\theta \\
& + (c_{57}) \int_0^{2\Pi} \left[ \begin{array}{c} N_\phi(\phi, \theta, t) \cos n\theta \\ -i N_\phi(\phi, \theta, t) \sin n\theta \end{array} \right] d\theta + (c_{58}) \int_0^{2\Pi} \left[ \begin{array}{c} N_{\phi\theta}(\phi, \theta, t) \cos n\theta \\ -i N_{\phi\theta}(\phi, \theta, t) \sin n\theta \end{array} \right] d\theta \\
& + (c_{59}) \int_0^{2\Pi} \left[ \begin{array}{c} M_\phi(\phi, \theta, t) \cos n\theta \\ -i M_\phi(\phi, \theta, t) \sin n\theta \end{array} \right] d\theta + (c_{510}) \int_0^{2\Pi} \left[ \begin{array}{c} M_{\phi\theta}(\phi, \theta, t) \cos n\theta \\ -i M_{\phi\theta}(\phi, \theta, t) \sin n\theta \end{array} \right] d\theta
\end{aligned} \tag{E.21}$$

$$\begin{aligned}
& \left[ \frac{d\beta_\theta(\phi, t)}{d\phi} \right]_{nc} - i \left[ \frac{d\beta_\theta(\phi, t)}{d\phi} \right]_{ns} = (c_{51}) \{ [w^0(\phi, t)]_{nc} - i [w^0(\phi, t)]_{ns} \} \\
& + (c_{52}) \{ [u_\phi^0(\phi, t)]_{nc} - i [u_\phi^0(\phi, t)]_{ns} \} + (cp_{52})(n) \{ i [u_\phi^0(\phi, t)]_{nc} + [u_\phi^0(\phi, t)]_{ns} \} \\
& + (c_{53}) \{ [u_\theta^0(\phi, t)]_{nc} - i [u_\theta^0(\phi, t)]_{ns} \} + (cp_{53})(n) \{ i [u_\theta^0(\phi, t)]_{nc} + [u_\theta^0(\phi, t)]_{ns} \} \\
& + (c_{54}) \{ [\beta_\phi(\phi, t)]_{nc} - i [\beta_\phi(\phi, t)]_{ns} \} + (cp_{54})(n) \{ i [\beta_\phi(\phi, t)]_{nc} + [\beta_\phi(\phi, t)]_{ns} \} \\
& + (c_{55}) \{ [\beta_\theta(\phi, t)]_{nc} - i [\beta_\theta(\phi, t)]_{ns} \} + (cp_{55})(n) \{ i [\beta_\theta(\phi, t)]_{nc} + [\beta_\theta(\phi, t)]_{ns} \} \\
& + (c_{57}) \{ [N_\phi(\phi, t)]_{nc} - i [N_\phi(\phi, t)]_{ns} \} + (c_{58}) \{ [N_{\phi\theta}(\phi, t)]_{nc} - i [N_{\phi\theta}(\phi, t)]_{ns} \} \\
& + (c_{59}) \{ [M_\phi(\phi, t)]_{nc} - i [M_\phi(\phi, t)]_{ns} \} + (c_{510}) \{ [M_{\phi\theta}(\phi, t)]_{nc} - i [M_{\phi\theta}(\phi, t)]_{ns} \}
\end{aligned} \tag{E.22}$$

We separate the real and imaginary parts of Equation (E.22). First, writing real parts of Equation (E.22) term by term.

$$\begin{aligned}
& \left[ \frac{d\beta_\theta(\phi, t)}{d\phi} \right]_{nc} = (c_{51}) [w^0(\phi, t)]_{nc} + (c_{52}) [u_\phi^0(\phi, t)]_{nc} + (cp_{52})(n) [u_\phi^0(\phi, t)]_{ns} \\
& + (c_{53}) [u_\theta^0(\phi, t)]_{nc} + (cp_{53})(n) [u_\theta^0(\phi, t)]_{ns} + (c_{54}) [\beta_\phi(\phi, t)]_{nc} + (cp_{54})(n) [\beta_\phi(\phi, t)]_{ns} \\
& + (c_{55}) [\beta_\theta(\phi, t)]_{nc} + (cp_{55})(n) [\beta_\theta(\phi, t)]_{ns} + (c_{57}) [N_\phi(\phi, t)]_{nc} + (c_{58}) [N_{\phi\theta}(\phi, t)]_{nc} \\
& + (c_{59}) [M_\phi(\phi, t)]_{nc} + (c_{510}) [M_{\phi\theta}(\phi, t)]_{nc}
\end{aligned} \tag{E.23}$$

Then, writing imaginary parts of Equation (E.22) term by term.

$$\begin{aligned}
& \left[ \frac{d\beta_\theta(\phi, t)}{d\phi} \right]_{ns} = (c_{51}) [w^0(\phi, t)]_{ns} + (c_{52}) [u_\phi^0(\phi, t)]_{ns} - (cp_{52})(n) [u_\phi^0(\phi, t)]_{nc} \\
& + (c_{53}) [u_\theta^0(\phi, t)]_{ns} - (cp_{53})(n) [u_\theta^0(\phi, t)]_{nc} + (c_{54}) [\beta_\phi(\phi, t)]_{ns} - (cp_{54})(n) [\beta_\phi(\phi, t)]_{nc} \\
& + (c_{55}) [\beta_\theta(\phi, t)]_{ns} - (cp_{55})(n) [\beta_\theta(\phi, t)]_{nc} + (c_{57}) [N_\phi(\phi, t)]_{ns} + (c_{58}) [N_{\phi\theta}(\phi, t)]_{ns} \\
& + (c_{59}) [M_\phi(\phi, t)]_{ns} + (c_{510}) [M_{\phi\theta}(\phi, t)]_{ns}
\end{aligned} \tag{E.24}$$

Rewriting Equation (3.19)

$$\begin{aligned}
\frac{\partial Q_\phi}{\partial \phi} = & (c_{61})w^0 + (cdp_{61})\left(\frac{\partial^2 w^0}{\partial \theta^2}\right) + (c_{62})u_\phi^0 + (cp_{62})\left(\frac{\partial u_\phi^0}{\partial \theta}\right) \\
& + (c_{63})u_\theta^0 + (cp_{63})\left(\frac{\partial u_\theta^0}{\partial \theta}\right) + (c_{64})\beta_\phi + (cp_{64})\left(\frac{\partial \beta_\phi}{\partial \theta}\right) \\
& + (c_{65})\beta_\theta + (cp_{65})\left(\frac{\partial \beta_\theta}{\partial \theta}\right) + (c_{66})Q_\phi + (cp_{66})\left(\frac{\partial Q_\phi}{\partial \theta}\right) \\
& + (c_{67})N_\phi + (c_{68})N_{\phi\theta} + (c_{69})M_\phi + (c_{610})M_{\phi\theta}
\end{aligned} \tag{E.25}$$

Carrying out the Finite exponential Fourier transform to Equation (E.25).

$$\begin{aligned}
& \frac{1}{2\Pi} \int_0^{2\Pi} \left[ \frac{\partial Q_\phi(\phi, \theta, t)}{\partial \phi} e^{-in\theta} \right] d\theta = \\
& (c_{61}) \frac{1}{2\Pi} \int_0^{2\Pi} [w^0(\phi, \theta, t) e^{-in\theta}] d\theta + (cdp_{61}) \frac{1}{2\Pi} \int_0^{2\Pi} \left[ \frac{\partial^2 w^0(\phi, \theta, t)}{\partial \theta^2} e^{-in\theta} \right] d\theta \\
& + (c_{62}) \frac{1}{2\Pi} \int_0^{2\Pi} [u_\phi^0(\phi, \theta, t) e^{-in\theta}] d\theta + (cp_{62}) \frac{1}{2\Pi} \int_0^{2\Pi} \left[ \frac{\partial u_\phi^0(\phi, \theta, t)}{\partial \theta} e^{-in\theta} \right] d\theta \\
& + (c_{63}) \frac{1}{2\Pi} \int_0^{2\Pi} [u_\theta^0(\phi, \theta, t) e^{-in\theta}] d\theta + (cp_{63}) \frac{1}{2\Pi} \int_0^{2\Pi} \left[ \frac{\partial u_\theta^0(\phi, \theta, t)}{\partial \theta} e^{-in\theta} \right] d\theta \\
& + (c_{64}) \frac{1}{2\Pi} \int_0^{2\Pi} [\beta_\phi(\phi, \theta, t) e^{-in\theta}] d\theta + (cp_{64}) \frac{1}{2\Pi} \int_0^{2\Pi} \left[ \frac{\partial \beta_\phi(\phi, \theta, t)}{\partial \theta} e^{-in\theta} \right] d\theta \\
& + (c_{65}) \frac{1}{2\Pi} \int_0^{2\Pi} [\beta_\theta(\phi, \theta, t) e^{-in\theta}] d\theta + (cp_{65}) \frac{1}{2\Pi} \int_0^{2\Pi} \left[ \frac{\partial \beta_\theta(\phi, \theta, t)}{\partial \theta} e^{-in\theta} \right] d\theta \\
& + (c_{66}) \frac{1}{2\Pi} \int_0^{2\Pi} [Q_\phi(\phi, \theta, t) e^{-in\theta}] d\theta + (cp_{66}) \frac{1}{2\Pi} \int_0^{2\Pi} \left[ \frac{\partial Q_\phi(\phi, \theta, t)}{\partial \theta} e^{-in\theta} \right] d\theta \\
& + (c_{67}) \frac{1}{2\Pi} \int_0^{2\Pi} [N_\phi(\phi, \theta, t) e^{-in\theta}] d\theta + (c_{68}) \frac{1}{2\Pi} \int_0^{2\Pi} [N_{\phi\theta}(\phi, \theta, t) e^{-in\theta}] d\theta \\
& + (c_{69}) \frac{1}{2\Pi} \int_0^{2\Pi} [M_\phi(\phi, \theta, t) e^{-in\theta}] d\theta + (c_{610}) \frac{1}{2\Pi} \int_0^{2\Pi} [M_{\phi\theta}(\phi, \theta, t) e^{-in\theta}] d\theta
\end{aligned} \tag{E.26}$$

Using Equation (3.28) in Equation (E.26) yields

$$\begin{aligned}
& \int_0^{2\Pi} \left[ \frac{\partial Q_\phi(\phi, \theta, t)}{\partial \phi} \cos n\theta \right. \\
& \left. - i \sin n\theta \frac{\partial Q_\phi(\phi, \theta, t)}{\partial \phi} \right] d\theta = (c_{61}) \int_0^{2\Pi} \left[ w^0(\phi, \theta, t) \cos n\theta \right. \\
& \left. - i w^0(\phi, \theta, t) \sin n\theta \right] d\theta \\
& + (cdp_{61}) \int_0^{2\Pi} (in)^2 \left[ w^0(\phi, \theta, t) \cos n\theta \right. \\
& \left. - i w^0(\phi, \theta, t) \sin n\theta \right] d\theta + (c_{62}) \int_0^{2\Pi} \left[ u_\phi^0(\phi, \theta, t) \cos n\theta \right. \\
& \left. - i u_\phi^0(\phi, \theta, t) \sin n\theta \right] d\theta \\
& + (cp_{62}) \int_0^{2\Pi} (in) \left[ u_\phi^0(\phi, \theta, t) \cos n\theta \right. \\
& \left. - i u_\phi^0(\phi, \theta, t) \sin n\theta \right] d\theta + (c_{63}) \int_0^{2\Pi} \left[ u_\theta^0(\phi, \theta, t) \cos n\theta \right. \\
& \left. - i u_\theta^0(\phi, \theta, t) \sin n\theta \right] d\theta \\
& + (cp_{63}) \int_0^{2\Pi} (in) \left[ u_\theta^0(\phi, \theta, t) \cos n\theta \right. \\
& \left. - i u_\theta^0(\phi, \theta, t) \sin n\theta \right] d\theta + (c_{64}) \int_0^{2\Pi} \left[ \beta_\phi(\phi, \theta, t) \cos n\theta \right. \\
& \left. - i \beta_\phi(\phi, \theta, t) \sin n\theta \right] d\theta \\
& + (cp_{64}) \int_0^{2\Pi} (in) \left[ \beta_\phi(\phi, \theta, t) \cos n\theta \right. \\
& \left. - i \beta_\phi(\phi, \theta, t) \sin n\theta \right] d\theta + (c_{65}) \int_0^{2\Pi} \left[ \beta_\theta(\phi, \theta, t) \cos n\theta \right. \\
& \left. - i \beta_\theta(\phi, \theta, t) \sin n\theta \right] d\theta \\
& + (cp_{65}) \int_0^{2\Pi} (in) \left[ \beta_\theta(\phi, \theta, t) \cos n\theta \right. \\
& \left. - i \beta_\theta(\phi, \theta, t) \sin n\theta \right] d\theta + (c_{66}) \int_0^{2\Pi} \left[ Q_\phi(\phi, \theta, t) \cos n\theta \right. \\
& \left. - i Q_\phi(\phi, \theta, t) \sin n\theta \right] d\theta \\
& + (cp_{66}) \int_0^{2\Pi} (in) \left[ Q_\phi(\phi, \theta, t) \cos n\theta \right. \\
& \left. - i Q_\phi(\phi, \theta, t) \sin n\theta \right] d\theta + (c_{67}) \int_0^{2\Pi} \left[ N_\phi(\phi, \theta, t) \cos n\theta \right. \\
& \left. - i N_\phi(\phi, \theta, t) \sin n\theta \right] d\theta \\
& + (c_{68}) \int_0^{2\Pi} \left[ N_{\phi\theta}(\phi, \theta, t) \cos n\theta \right. \\
& \left. - i N_{\phi\theta}(\phi, \theta, t) \sin n\theta \right] d\theta + (c_{69}) \int_0^{2\Pi} \left[ M_\phi(\phi, \theta, t) \cos n\theta \right. \\
& \left. - i M_\phi(\phi, \theta, t) \sin n\theta \right] d\theta \\
& + (c_{610}) \int_0^{2\Pi} \left[ M_{\phi\theta}(\phi, \theta, t) \cos n\theta \right. \\
& \left. - i M_{\phi\theta}(\phi, \theta, t) \sin n\theta \right] d\theta
\end{aligned} \tag{E.27}$$

$$\begin{aligned}
& \left[ \frac{dQ_\phi(\phi, t)}{d\phi} \right]_{nc} - i \left[ \frac{dQ_\phi(\phi, t)}{d\phi} \right]_{ns} = (c_{61}) \{ [w^0(\phi, t)]_{nc} - i [w^0(\phi, t)]_{ns} \} \\
& - (n^2) (cdp_{61}) \{ [w^0(\phi, t)]_{nc} - i [w^0(\phi, t)]_{ns} \} + (c_{62}) \{ [u_\phi^0(\phi, t)]_{nc} - i [u_\phi^0(\phi, t)]_{ns} \} \\
& + (cp_{62}) (n) \{ i [u_\phi^0(\phi, t)]_{nc} + [u_\phi^0(\phi, t)]_{ns} \} + (c_{63}) \{ [u_\theta^0(\phi, t)]_{nc} - i [u_\theta^0(\phi, t)]_{ns} \} \\
& + (cp_{63}) (n) \{ i [u_\theta^0(\phi, t)]_{nc} + [u_\theta^0(\phi, t)]_{ns} \} + (c_{64}) \{ [\beta_\phi(\phi, t)]_{nc} - i [\beta_\phi(\phi, t)]_{ns} \} \\
& + (cp_{64}) (n) \{ i [\beta_\phi(\phi, t)]_{nc} + [\beta_\phi(\phi, t)]_{ns} \} + (c_{65}) \{ [\beta_\theta(\phi, t)]_{nc} - i [\beta_\theta(\phi, t)]_{ns} \} \\
& + (cp_{65}) (n) \{ i [\beta_\theta(\phi, t)]_{nc} + [\beta_\theta(\phi, t)]_{ns} \} + (c_{66}) \{ [Q_\phi(\phi, t)]_{nc} - i [Q_\phi(\phi, t)]_{ns} \} \\
& + (cp_{66}) (n) \{ i [Q_\phi(\phi, t)]_{nc} + [Q_\phi(\phi, t)]_{ns} \} + (c_{67}) \{ [N_\phi(\phi, t)]_{nc} - i [N_\phi(\phi, t)]_{ns} \} \\
& + (c_{68}) \{ [N_{\phi\theta}(\phi, t)]_{nc} - i [N_{\phi\theta}(\phi, t)]_{ns} \} + (c_{69}) \{ [M_\phi(\phi, t)]_{nc} - i [M_\phi(\phi, t)]_{ns} \} \\
& + (c_{610}) \{ [M_{\phi\theta}(\phi, t)]_{nc} - i [M_{\phi\theta}(\phi, t)]_{ns} \}
\end{aligned} \tag{E.28}$$

We separate the real and imaginary parts of Equation (E.28).

First, writing real parts of Equation (E.28) term by term.

$$\begin{aligned}
\left[ \frac{dQ_\phi(\phi, t)}{d\phi} \right]_{nc} &= (c_{61}) [w^0(\phi, t)]_{nc} - (n^2) (cdp_{61}) [w^0(\phi, t)]_{nc} + (c_{62}) [u_\phi^0(\phi, t)]_{nc} \\
&+ (cp_{62})(n) [u_\phi^0(\phi, t)]_{ns} + (c_{63}) [u_\theta^0(\phi, t)]_{nc} + (cp_{63})(n) [u_\theta^0(\phi, t)]_{ns} + (c_{64}) [\beta_\phi(\phi, t)]_{nc} \\
&+ (cp_{64})(n) [\beta_\phi(\phi, t)]_{ns} + (c_{65}) [\beta_\theta(\phi, t)]_{nc} + (cp_{65})(n) [\beta_\theta(\phi, t)]_{ns} + (c_{66}) [Q_\phi(\phi, t)]_{nc} \\
&+ (cp_{66})(n) [Q_\phi(\phi, t)]_{ns} + (c_{67}) [N_\phi(\phi, t)]_{nc} + (c_{68}) [N_{\phi\theta}(\phi, t)]_{nc} + (c_{69}) [M_\phi(\phi, t)]_{nc} \\
&+ (c_{610}) [M_{\phi\theta}(\phi, t)]_{nc}
\end{aligned} \tag{E.29}$$

Then, writing imaginary parts of Equation (E.28) term by term.

$$\begin{aligned}
\left[ \frac{dQ_\phi(\phi, t)}{d\phi} \right]_{ns} &= (c_{61}) [w^0(\phi, t)]_{ns} - (n^2) (cdp_{61}) [w^0(\phi, t)]_{ns} + (c_{62}) [u_\phi^0(\phi, t)]_{ns} \\
&- (cp_{62})(n) [u_\phi^0(\phi, t)]_{nc} + (c_{63}) [u_\theta^0(\phi, t)]_{ns} - (cp_{63})(n) [u_\theta^0(\phi, t)]_{nc} + (c_{64}) [\beta_\phi(\phi, t)]_{ns} \\
&- (cp_{64})(n) [\beta_\phi(\phi, t)]_{nc} + (c_{65}) [\beta_\theta(\phi, t)]_{ns} - (cp_{65})(n) [\beta_\theta(\phi, t)]_{nc} + (c_{66}) [Q_\phi(\phi, t)]_{ns} \\
&- (cp_{66})(n) [Q_\phi(\phi, t)]_{nc} + (c_{67}) [N_\phi(\phi, t)]_{ns} + (c_{68}) [N_{\phi\theta}(\phi, t)]_{ns} + (c_{69}) [M_\phi(\phi, t)]_{ns} \\
&+ (c_{610}) [M_{\phi\theta}(\phi, t)]_{ns}
\end{aligned} \tag{E.30}$$

Rewriting Equation (3.20).

$$\begin{aligned}
\frac{\partial N_\phi}{\partial \phi} &= (c_{71})w^0 + (c_{72})u_\phi^0 + (cp_{72})\left(\frac{\partial u_\phi^0}{\partial \theta}\right) + (c_{73})u_\theta^0 + (cp_{73})\left(\frac{\partial u_\theta^0}{\partial \theta}\right) \\
&+ (c_{74})\beta_\phi + (cp_{74})\left(\frac{\partial \beta_\phi}{\partial \theta}\right) + (c_{75})\beta_\theta + (cp_{75})\left(\frac{\partial \beta_\theta}{\partial \theta}\right) + (c_{76})Q_\phi \\
&+ (c_{77})N_\phi + (c_{78})N_{\phi\theta} + (cp_{78})\left(\frac{\partial N_{\phi\theta}}{\partial \theta}\right) + (c_{79})M_\phi + (c_{710})M_{\phi\theta}
\end{aligned} \tag{E.31}$$

Carrying out the Finite exponential Fourier transform to Equation (E.31)

$$\begin{aligned}
\frac{1}{2\Pi} \int_0^{2\Pi} \left[ \frac{\partial N_\phi(\phi, \theta, t)}{\partial \phi} e^{-in\theta} \right] d\theta &= (c_{71}) \frac{1}{2\Pi} \int_0^{2\Pi} [w^0(\phi, \theta, t) e^{-in\theta}] d\theta \\
+ (c_{72}) \frac{1}{2\Pi} \int_0^{2\Pi} [u_\phi^0(\phi, \theta, t) e^{-in\theta}] d\theta &+ (cp_{72}) \frac{1}{2\Pi} \int_0^{2\Pi} \left[ \frac{\partial u_\phi^0(\phi, \theta, t)}{\partial \theta} e^{-in\theta} \right] d\theta \\
+ (c_{73}) \frac{1}{2\Pi} \int_0^{2\Pi} [u_\theta^0(\phi, \theta, t) e^{-in\theta}] d\theta &+ (cp_{73}) \frac{1}{2\Pi} \int_0^{2\Pi} \left[ \frac{\partial u_\theta^0(\phi, \theta, t)}{\partial \theta} e^{-in\theta} \right] d\theta \\
+ (c_{74}) \frac{1}{2\Pi} \int_0^{2\Pi} [\beta_\phi(\phi, \theta, t) e^{-in\theta}] d\theta &+ (cp_{74}) \frac{1}{2\Pi} \int_0^{2\Pi} \left[ \frac{\partial \beta_\phi(\phi, \theta, t)}{\partial \theta} e^{-in\theta} \right] d\theta \\
+ (c_{75}) \frac{1}{2\Pi} \int_0^{2\Pi} [\beta_\theta(\phi, \theta, t) e^{-in\theta}] d\theta &+ (cp_{75}) \frac{1}{2\Pi} \int_0^{2\Pi} \left[ \frac{\partial \beta_\theta(\phi, \theta, t)}{\partial \theta} e^{-in\theta} \right] d\theta \\
+ (c_{76}) \frac{1}{2\Pi} \int_0^{2\Pi} [Q_\phi(\phi, \theta, t) e^{-in\theta}] d\theta &+ (c_{77}) \frac{1}{2\Pi} \int_0^{2\Pi} [N_\phi(\phi, \theta, t) e^{-in\theta}] d\theta \\
+ (c_{78}) \frac{1}{2\Pi} \int_0^{2\Pi} [N_{\phi\theta}(\phi, \theta, t) e^{-in\theta}] d\theta &+ (cp_{78}) \frac{1}{2\Pi} \int_0^{2\Pi} \left[ \frac{\partial N_{\phi\theta}(\phi, \theta, t)}{\partial \theta} e^{-in\theta} \right] d\theta \\
+ (c_{79}) \frac{1}{2\Pi} \int_0^{2\Pi} [M_\phi(\phi, \theta, t) e^{-in\theta}] d\theta &+ (c_{710}) \frac{1}{2\Pi} \int_0^{2\Pi} [M_{\phi\theta}(\phi, \theta, t) e^{-in\theta}] d\theta
\end{aligned} \tag{E.32}$$

Using Equation (3.28) in Equation (E.32) yields

$$\begin{aligned}
& \int_0^{2\Pi} \left[ \frac{\partial N_\phi(\phi, \theta, t)}{\partial \phi} \cos n\theta \right. \\
& \left. -i \frac{\partial N_\phi(\phi, \theta, t)}{\partial \phi} \sin n\theta \right] d\theta = (c_{71}) \int_0^{2\Pi} \left[ w^0(\phi, \theta, t) \cos n\theta \right. \\
& \left. -i w^0(\phi, \theta, t) \sin n\theta \right] d\theta \\
& + (c_{72}) \int_0^{2\Pi} \left[ u_\phi^0(\phi, \theta, t) \cos n\theta \right. \\
& \left. -i u_\phi^0(\phi, \theta, t) \sin n\theta \right] d\theta + (cp_{72}) \int_0^{2\Pi} (in) \left[ u_\phi^0(\phi, \theta, t) \cos n\theta \right. \\
& \left. -i u_\phi^0(\phi, \theta, t) \sin n\theta \right] d\theta \\
& + (c_{73}) \int_0^{2\Pi} \left[ u_\theta^0(\phi, \theta, t) \cos n\theta \right. \\
& \left. -i u_\theta^0(\phi, \theta, t) \sin n\theta \right] d\theta + (cp_{73}) \int_0^{2\Pi} (in) \left[ u_\theta^0(\phi, \theta, t) \cos n\theta \right. \\
& \left. -i u_\theta^0(\phi, \theta, t) \sin n\theta \right] d\theta \\
& + (c_{74}) \int_0^{2\Pi} \left[ \beta_\phi(\phi, \theta, t) \cos n\theta \right. \\
& \left. -i \beta_\phi(\phi, \theta, t) \sin n\theta \right] d\theta + (cp_{74}) \int_0^{2\Pi} (in) \left[ \beta_\phi(\phi, \theta, t) \cos n\theta \right. \\
& \left. -i \beta_\phi(\phi, \theta, t) \sin n\theta \right] d\theta \tag{E.33} \\
& + (c_{75}) \int_0^{2\Pi} \left[ \beta_\theta(\phi, \theta, t) \cos n\theta \right. \\
& \left. -i \beta_\theta(\phi, \theta, t) \sin n\theta \right] d\theta + (cp_{75}) \int_0^{2\Pi} (in) \left[ \beta_\theta(\phi, \theta, t) \cos n\theta \right. \\
& \left. -i \beta_\theta(\phi, \theta, t) \sin n\theta \right] d\theta \\
& + (c_{76}) \int_0^{2\Pi} \left[ Q_\phi(\phi, \theta, t) \cos n\theta \right. \\
& \left. -i Q_\phi(\phi, \theta, t) \sin n\theta \right] d\theta + (c_{77}) \int_0^{2\Pi} \left[ N_\phi(\phi, \theta, t) \cos n\theta \right. \\
& \left. -i N_\phi(\phi, \theta, t) \sin n\theta \right] d\theta \\
& + (c_{78}) \int_0^{2\Pi} \left[ N_{\phi\theta}(\phi, \theta, t) \cos n\theta \right. \\
& \left. -i N_{\phi\theta}(\phi, \theta, t) \sin n\theta \right] d\theta + (cp_{78}) \int_0^{2\Pi} (in) \left[ N_{\phi\theta}(\phi, \theta, t) \cos n\theta \right. \\
& \left. -i N_{\phi\theta}(\phi, \theta, t) \sin n\theta \right] d\theta \\
& + (c_{79}) \int_0^{2\Pi} \left[ M_\phi(\phi, \theta, t) \cos n\theta \right. \\
& \left. -i M_\phi(\phi, \theta, t) \sin n\theta \right] d\theta + (c_{710}) \int_0^{2\Pi} \left[ M_{\phi\theta}(\phi, \theta, t) \cos n\theta \right. \\
& \left. -i M_{\phi\theta}(\phi, \theta, t) \sin n\theta \right] d\theta
\end{aligned}$$

$$\begin{aligned}
& \left[ \frac{dN_\phi(\phi, t)}{d\phi} \right]_{nc} -i \left[ \frac{dN_\phi(\phi, t)}{d\phi} \right]_{ns} = (c_{71}) \{ [w^0(\phi, t)]_{nc} -i [w^0(\phi, t)]_{ns} \} \\
& + (c_{72}) \{ [u_\phi^0(\phi, t)]_{nc} -i [u_\phi^0(\phi, t)]_{ns} \} + (cp_{72}) (n) \{ i [u_\phi^0(\phi, t)]_{nc} + [u_\phi^0(\phi, t)]_{ns} \} \\
& + (c_{73}) \{ [u_\theta^0(\phi, t)]_{nc} -i [u_\theta^0(\phi, t)]_{ns} \} + (cp_{73}) (n) \{ i [u_\theta^0(\phi, t)]_{nc} + [u_\theta^0(\phi, t)]_{ns} \} \\
& + (c_{74}) \{ [\beta_\phi(\phi, t)]_{nc} -i [\beta_\phi(\phi, t)]_{ns} \} + (cp_{74}) (n) \{ i [\beta_\phi(\phi, t)]_{nc} + [\beta_\phi(\phi, t)]_{ns} \} \\
& + (c_{75}) \{ [\beta_\theta(\phi, t)]_{nc} -i [\beta_\theta(\phi, t)]_{ns} \} + (cp_{75}) (n) \{ i [\beta_\theta(\phi, t)]_{nc} + [\beta_\theta(\phi, t)]_{ns} \} \\
& + (c_{76}) \{ [Q_\phi(\phi, t)]_{nc} -i [Q_\phi(\phi, t)]_{ns} \} + (c_{77}) \{ [N_\phi(\phi, t)]_{nc} -i [N_\phi(\phi, t)]_{ns} \} \\
& + (c_{78}) \{ [N_{\phi\theta}(\phi, t)]_{nc} -i [N_{\phi\theta}(\phi, t)]_{ns} \} + (cp_{78}) (n) \{ i [N_{\phi\theta}(\phi, t)]_{nc} + [N_{\phi\theta}(\phi, t)]_{ns} \} \\
& + (c_{79}) \{ [M_\phi(\phi, t)]_{nc} -i [M_\phi(\phi, t)]_{ns} \} + (c_{710}) \{ [M_{\phi\theta}(\phi, t)]_{nc} -i [M_{\phi\theta}(\phi, t)]_{ns} \}
\end{aligned} \tag{E.34}$$

Separating the real and imaginary parts of Equation (E.34)

First, writing real parts of Equation (E.34) term by term.

$$\begin{aligned}
\left[ \frac{dN_\phi(\phi, t)}{d\phi} \right]_{nc} &= (c_{71}) [w^0(\phi, t)]_{nc} + (c_{72}) [u_\phi^0(\phi, t)]_{nc} + (cp_{72}) (n) [u_\phi^0(\phi, t)]_{ns} \\
&+ (c_{73}) [u_\theta^0(\phi, t)]_{nc} + (cp_{73}) (n) [u_\theta^0(\phi, t)]_{ns} + (c_{74}) [\beta_\phi(\phi, t)]_{nc} + (cp_{74}) (n) [\beta_\phi(\phi, t)]_{ns} \\
&+ (c_{75}) [\beta_\theta(\phi, t)]_{nc} + (cp_{75}) (n) [\beta_\theta(\phi, t)]_{ns} + (c_{76}) [Q_\phi(\phi, t)]_{nc} + (c_{77}) [N_\phi(\phi, t)]_{nc} \\
&+ (c_{78}) [N_{\phi\theta}(\phi, t)]_{nc} + (cp_{78}) (n) [N_{\phi\theta}(\phi, t)]_{ns} + (c_{79}) [M_\phi(\phi, t)]_{nc} + (c_{710}) [M_{\phi\theta}(\phi, t)]_{nc}
\end{aligned} \tag{E.35}$$

Then, writing imaginary parts of Equation (E.34) term by term.

$$\begin{aligned}
\left[ \frac{dN_\phi(\phi, t)}{d\phi} \right]_{ns} &= (c_{71}) [w^0(\phi, t)]_{ns} + (c_{72}) [u_\phi^0(\phi, t)]_{ns} - (cp_{72}) (n) [u_\phi^0(\phi, t)]_{nc} \\
&+ (c_{73}) [u_\theta^0(\phi, t)]_{ns} - (cp_{73}) (n) [u_\theta^0(\phi, t)]_{nc} + (c_{74}) [\beta_\phi(\phi, t)]_{ns} - (cp_{74}) (n) [\beta_\phi(\phi, t)]_{nc} \\
&+ (c_{75}) [\beta_\theta(\phi, t)]_{ns} - (cp_{75}) (n) [\beta_\theta(\phi, t)]_{nc} + (c_{76}) [Q_\phi(\phi, t)]_{ns} + (c_{77}) [N_\phi(\phi, t)]_{ns} \\
&+ (c_{78}) [N_{\phi\theta}(\phi, t)]_{ns} - (cp_{78}) (n) [N_{\phi\theta}(\phi, t)]_{nc} + (c_{79}) [M_\phi(\phi, t)]_{ns} \\
&+ (c_{710}) [M_{\phi\theta}(\phi, t)]_{ns}
\end{aligned} \tag{E.36}$$

Rewriting Equation (3.21)

$$\begin{aligned}
\frac{\partial N_{\phi\theta}}{\partial \phi} &= (cp_{81}) \left( \frac{\partial w^0}{\partial \theta} \right) + (c_{82}) (u_\phi^0) + (cp_{82}) \left( \frac{\partial u_\phi^0}{\partial \theta} \right) + (cdp_{82}) \left( \frac{\partial^2 u_\phi^0}{\partial \theta^2} \right) + (c_{83}) (u_\theta^0) \\
&+ (cp_{83}) \left( \frac{\partial u_\theta^0}{\partial \theta} \right) + (cdp_{83}) \left( \frac{\partial^2 u_\theta^0}{\partial \theta^2} \right) + (c_{84}) (\beta_\phi) + (cp_{84}) \left( \frac{\partial \beta_\phi}{\partial \theta} \right) + (cdp_{84}) \left( \frac{\partial^2 \beta_\phi}{\partial \theta^2} \right) \\
&+ (c_{85}) (\beta_\theta) + (cp_{85}) \left( \frac{\partial \beta_\theta}{\partial \theta} \right) + (cdp_{85}) \left( \frac{\partial^2 \beta_\theta}{\partial \theta^2} \right) + (c_{86}) (Q_\phi) \\
&+ (cp_{87}) \left( \frac{\partial N_\phi}{\partial \theta} \right) + (c_{88}) (N_{\phi\theta}) + (cp_{88}) \left( \frac{\partial N_{\phi\theta}}{\partial \theta} \right) + (cp_{89}) \left( \frac{\partial M_\phi}{\partial \theta} \right) + (cp_{810}) \left( \frac{\partial M_{\phi\theta}}{\partial \theta} \right)
\end{aligned} \tag{E.37}$$

Carrying out the Finite exponential Fourier transform to Equation (E.37)

$$\begin{aligned}
\frac{1}{2\Pi} \int_0^{2\Pi} \left[ \frac{\partial N_{\phi\theta}(\phi, \theta, t)}{\partial \phi} e^{-in\theta} \right] d\theta &= (cp_{81}) \frac{1}{2\Pi} \int_0^{2\Pi} \left[ \frac{\partial w^0(\phi, \theta, t)}{\partial \theta} e^{-in\theta} \right] d\theta \\
+ (c_{82}) \frac{1}{2\Pi} \int_0^{2\Pi} [u_\phi^0(\phi, \theta, t) e^{-in\theta}] d\theta &+ (cp_{82}) \frac{1}{2\Pi} \int_0^{2\Pi} \left[ \frac{\partial u_\phi^0(\phi, \theta, t)}{\partial \theta} e^{-in\theta} \right] d\theta \\
+ (cdp_{82}) \frac{1}{2\Pi} \int_0^{2\Pi} \left[ \frac{\partial^2 u_\phi^0(\phi, \theta, t)}{\partial \theta^2} e^{-in\theta} \right] d\theta &+ (c_{83}) \frac{1}{2\Pi} \int_0^{2\Pi} [u_\theta^0(\phi, \theta, t) e^{-in\theta}] d\theta \\
+ (cp_{83}) \frac{1}{2\Pi} \int_0^{2\Pi} \left[ \frac{\partial u_\theta^0(\phi, \theta, t)}{\partial \theta} e^{-in\theta} \right] d\theta &+ (cdp_{83}) \frac{1}{2\Pi} \int_0^{2\Pi} \left[ \frac{\partial^2 u_\theta^0(\phi, \theta, t)}{\partial \theta^2} e^{-in\theta} \right] d\theta \\
+ (c_{84}) \frac{1}{2\Pi} \int_0^{2\Pi} [\beta_\phi(\phi, \theta, t) e^{-in\theta}] d\theta &+ (cp_{84}) \frac{1}{2\Pi} \int_0^{2\Pi} \left[ \frac{\partial \beta_\phi(\phi, \theta, t)}{\partial \theta} e^{-in\theta} \right] d\theta \\
+ (cdp_{84}) \frac{1}{2\Pi} \int_0^{2\Pi} \left[ \frac{\partial^2 \beta_\phi(\phi, \theta, t)}{\partial \theta^2} e^{-in\theta} \right] d\theta &+ (c_{85}) \frac{1}{2\Pi} \int_0^{2\Pi} [\beta_\theta(\phi, \theta, t) e^{-in\theta}] d\theta \\
+ (cp_{85}) \frac{1}{2\Pi} \int_0^{2\Pi} \left[ \frac{\partial \beta_\theta(\phi, \theta, t)}{\partial \theta} e^{-in\theta} \right] d\theta &+ (cdp_{85}) \frac{1}{2\Pi} \int_0^{2\Pi} \left[ \frac{\partial^2 \beta_\theta(\phi, \theta, t)}{\partial \theta^2} e^{-in\theta} \right] d\theta \\
+ (c_{86}) \frac{1}{2\Pi} \int_0^{2\Pi} [Q_\phi(\phi, \theta, t) e^{-in\theta}] d\theta &+ (cp_{87}) \frac{1}{2\Pi} \int_0^{2\Pi} \left[ \frac{\partial N_\phi(\phi, \theta, t)}{\partial \theta} e^{-in\theta} \right] d\theta \\
+ (c_{88}) \frac{1}{2\Pi} \int_0^{2\Pi} [N_{\phi\theta}(\phi, \theta, t) e^{-in\theta}] d\theta &+ (cp_{88}) \frac{1}{2\Pi} \int_0^{2\Pi} \left[ \frac{\partial N_{\phi\theta}(\phi, \theta, t)}{\partial \theta} e^{-in\theta} \right] d\theta \\
+ (cp_{89}) \frac{1}{2\Pi} \int_0^{2\Pi} \left[ \frac{\partial M_\phi(\phi, \theta, t)}{\partial \theta} e^{-in\theta} \right] d\theta &+ (cp_{810}) \frac{1}{2\Pi} \int_0^{2\Pi} \left[ \frac{\partial M_{\phi\theta}(\phi, \theta, t)}{\partial \theta} e^{-in\theta} \right] d\theta
\end{aligned} \tag{E.38}$$

Using Equation (3.28) in Equation (E.38) yields

$$\begin{aligned}
& \int_0^{2\Pi} \left[ \begin{array}{c} \frac{\partial N_{\phi\theta}(\phi, \theta, t)}{\partial \phi} \cos n\theta \\ -i \frac{\partial N_{\phi\theta}(\phi, \theta, t)}{\partial \phi} \sin n\theta \end{array} \right] d\theta = (cp_{81}) \int_0^{2\Pi} (in) \left[ \begin{array}{c} w^0(\phi, \theta, t) \cos n\theta \\ -i w^0(\phi, \theta, t) \sin n\theta \end{array} \right] d\theta \\
& + (c_{82}) \int_0^{2\Pi} \left[ \begin{array}{c} u_\phi^0(\phi, \theta, t) \cos n\theta \\ -i u_\phi^0(\phi, \theta, t) \sin n\theta \end{array} \right] d\theta + (cp_{82}) \int_0^{2\Pi} (in) \left[ \begin{array}{c} u_\phi^0(\phi, \theta, t) \cos n\theta \\ -i u_\phi^0(\phi, \theta, t) \sin n\theta \end{array} \right] d\theta \\
& - (cdp_{82})(n^2) \int_0^{2\Pi} \left[ \begin{array}{c} u_\phi^0(\phi, \theta, t) \cos n\theta \\ -i u_\phi^0(\phi, \theta, t) \sin n\theta \end{array} \right] d\theta + (c_{83}) \int_0^{2\Pi} \left[ \begin{array}{c} u_\theta^0(\phi, \theta, t) \cos n\theta \\ -i u_\theta^0(\phi, \theta, t) \sin n\theta \end{array} \right] d\theta \\
& + (cp_{83}) \int_0^{2\Pi} (in) \left[ \begin{array}{c} u_\theta^0(\phi, \theta, t) \cos n\theta \\ -i u_\theta^0(\phi, \theta, t) \sin n\theta \end{array} \right] d\theta - (cdp_{83})(n^2) \int_0^{2\Pi} \left[ \begin{array}{c} u_\theta^0(\phi, \theta, t) \cos n\theta \\ -i u_\theta^0(\phi, \theta, t) \sin n\theta \end{array} \right] d\theta \\
& + (c_{84}) \int_0^{2\Pi} \left[ \begin{array}{c} \beta_\phi(\phi, \theta, t) \cos n\theta \\ -i \beta_\phi(\phi, \theta, t) \sin n\theta \end{array} \right] d\theta + (cp_{84}) \int_0^{2\Pi} (in) \left[ \begin{array}{c} \beta_\phi(\phi, \theta, t) \cos n\theta \\ -i \beta_\phi(\phi, \theta, t) \sin n\theta \end{array} \right] d\theta \\
& - (cdp_{84})(n^2) \int_0^{2\Pi} \left[ \begin{array}{c} \beta_\phi(\phi, \theta, t) \cos n\theta \\ -i \beta_\phi(\phi, \theta, t) \sin n\theta \end{array} \right] d\theta + (c_{85}) \int_0^{2\Pi} \left[ \begin{array}{c} \beta_\theta(\phi, \theta, t) \cos n\theta \\ -i \beta_\theta(\phi, \theta, t) \sin n\theta \end{array} \right] d\theta \\
& + (cp_{85}) \int_0^{2\Pi} (in) \left[ \begin{array}{c} \beta_\theta(\phi, \theta, t) \cos n\theta \\ -i \beta_\theta(\phi, \theta, t) \sin n\theta \end{array} \right] d\theta - (cdp_{85})(n^2) \int_0^{2\Pi} \left[ \begin{array}{c} \beta_\theta(\phi, \theta, t) \cos n\theta \\ -i \beta_\theta(\phi, \theta, t) \sin n\theta \end{array} \right] d\theta \\
& + (c_{86}) \int_0^{2\Pi} \left[ \begin{array}{c} Q_\phi(\phi, \theta, t) \cos n\theta \\ -i Q_\phi(\phi, \theta, t) \sin n\theta \end{array} \right] d\theta + (cp_{87}) \int_0^{2\Pi} (in) \left[ \begin{array}{c} N_\phi(\phi, \theta, t) \cos n\theta \\ -i N_\phi(\phi, \theta, t) \sin n\theta \end{array} \right] d\theta \\
& + (c_{88}) \int_0^{2\Pi} \left[ \begin{array}{c} N_{\phi\theta}(\phi, \theta, t) \cos n\theta \\ -i N_{\phi\theta}(\phi, \theta, t) \sin n\theta \end{array} \right] d\theta + (cp_{88}) \int_0^{2\Pi} (in) \left[ \begin{array}{c} N_{\phi\theta}(\phi, \theta, t) \cos n\theta \\ -i N_{\phi\theta}(\phi, \theta, t) \sin n\theta \end{array} \right] d\theta \\
& + (cp_{89}) \int_0^{2\Pi} (in) \left[ \begin{array}{c} M_\phi(\phi, \theta, t) \cos n\theta \\ -i M_\phi(\phi, \theta, t) \sin n\theta \end{array} \right] d\theta + (cp_{810}) \int_0^{2\Pi} (in) \left[ \begin{array}{c} M_{\phi\theta}(\phi, \theta, t) \cos n\theta \\ -i M_{\phi\theta}(\phi, \theta, t) \sin n\theta \end{array} \right] d\theta
\end{aligned} \tag{E.39}$$

$$\begin{aligned}
& \left[ \frac{dN_{\phi\theta}(\phi, t)}{d\phi} \right]_{nc} - i \left[ \frac{dN_{\phi\theta}(\phi, t)}{d\phi} \right]_{ns} = (cp_{81})\chi(n)\{i[w^0(\phi, t)]_{nc} + [w^0(\phi, t)]_{ns}\} \\
& + (c_{82})\chi\{[u_\phi^0(\phi, t)]_{nc} - i[u_\phi^0(\phi, t)]_{ns}\} + (cp_{82})\chi(n)\{i[u_\phi^0(\phi, t)]_{nc} + [u_\phi^0(\phi, t)]_{ns}\} \\
& - (cdp_{82})\chi(n^2)\chi\{[u_\phi^0(\phi, t)]_{nc} - i[u_\phi^0(\phi, t)]_{ns}\} + (c_{83})\chi\{[u_\theta^0(\phi, t)]_{nc} - i[u_\theta^0(\phi, t)]_{ns}\} \\
& + (cp_{83})\chi(n)\{i[u_\theta^0(\phi, t)]_{nc} + [u_\theta^0(\phi, t)]_{ns}\} - (cdp_{83})\chi(n^2)\chi\{[u_\theta^0(\phi, t)]_{nc} - i[u_\theta^0(\phi, t)]_{ns}\} \\
& + (c_{84})\chi\{[\beta_\phi(\phi, t)]_{nc} - i[\beta_\phi(\phi, t)]_{ns}\} + (cp_{84})\chi(n)\{i[\beta_\phi(\phi, t)]_{nc} + [\beta_\phi(\phi, t)]_{ns}\} \\
& - (cdp_{84})\chi(n^2)\chi\{[\beta_\phi(\phi, t)]_{nc} - i[\beta_\phi(\phi, t)]_{ns}\} + (c_{85})\chi\{[\beta_\theta(\phi, t)]_{nc} - i[\beta_\theta(\phi, t)]_{ns}\} \\
& + (cp_{85})\chi(n)\{i[\beta_\theta(\phi, t)]_{nc} + [\beta_\theta(\phi, t)]_{ns}\} - (cdp_{85})\chi(n^2)\chi\{[\beta_\theta(\phi, t)]_{nc} - i[\beta_\theta(\phi, t)]_{ns}\} \\
& + (c_{86})\chi\{[Q_\phi(\phi, t)]_{nc} - i[Q_\phi(\phi, t)]_{ns}\} + (cp_{87})\chi(n)\{i[N_\phi(\phi, t)]_{nc} + [N_\phi(\phi, t)]_{ns}\} \\
& + (c_{88})\chi\{[N_{\phi\theta}(\phi, t)]_{nc} - i[N_{\phi\theta}(\phi, t)]_{ns}\} + (cp_{88})\chi(n)\{i[N_{\phi\theta}(\phi, t)]_{nc} + [N_{\phi\theta}(\phi, t)]_{ns}\} \\
& + (cp_{89})\chi(n)\{i[M_\phi(\phi, t)]_{nc} + [M_\phi(\phi, t)]_{ns}\} + (cp_{810})\chi(n)\{i[M_{\phi\theta}(\phi, t)]_{nc} + [M_{\phi\theta}(\phi, t)]_{ns}\}
\end{aligned} \tag{E.40}$$

We separate the real and imaginary parts of Equation (E.40). First, writing real parts of Equation (E.40) term by term.

$$\begin{aligned}
& \left[ \frac{dN_{\phi\theta}(\phi, t)}{d\phi} \right]_{nc} = (cp_{81})\chi(n)[w^0(\phi, t)]_{ns} + [(c_{82}) - (cdp_{82})\chi(n^2)]u_\phi^0(\phi, t)_{nc} + (cp_{82})\chi(n)u_\phi^0(\phi, t)_{ns} \\
& + [(c_{83}) - (cdp_{83})\chi(n^2)]u_\theta^0(\phi, t)_{nc} + (cp_{83})\chi(n)u_\theta^0(\phi, t)_{ns} + [(c_{84}) - (cdp_{84})\chi(n^2)]\beta_\phi(\phi, t)_{nc} \\
& + (cp_{84})\chi(n)\beta_\phi(\phi, t)_{ns} + [(c_{85}) - (cdp_{85})\chi(n^2)]\beta_\theta(\phi, t)_{nc} + (cp_{85})\chi(n)\beta_\theta(\phi, t)_{ns} \\
& + (c_{86})Q_\phi(\phi, t)_{nc} + (cp_{87})\chi(n)N_\phi(\phi, t)_{ns} + (c_{88})N_{\phi\theta}(\phi, t)_{nc} + (cp_{88})\chi(n)N_{\phi\theta}(\phi, t)_{ns} \\
& + (cp_{89})\chi(n)M_\phi(\phi, t)_{ns} + (cp_{810})\chi(n)M_{\phi\theta}(\phi, t)_{ns}
\end{aligned} \tag{E.41}$$

Then, writing imaginary parts of Equation (E.40) term by term.

$$\begin{aligned}
\left[ \frac{dN_{\phi\theta}(\phi, t)}{d\phi} \right]_{nS} &= -(cp_{81})(n)[w^0(\phi, t)]_{nC} + [(c_{82}) - (cdp_{82})(n^2)]u_{\phi}^0(\phi, t)_{nS} \\
&- (cp_{82})(n)[u_{\phi}^0(\phi, t)]_{nC} + [(c_{83}) - (cdp_{83})(n^2)]u_{\theta}^0(\phi, t)_{nS} - (cp_{83})(n)[u_{\theta}^0(\phi, t)]_{nC} \\
&+ [(c_{84}) - (cdp_{84})(n^2)]\beta_{\phi}(\phi, t)_{nS} - (cp_{84})(n)[\beta_{\phi}(\phi, t)]_{nC} + [(c_{85}) - (cdp_{85})(n^2)]\beta_{\theta}(\phi, t)_{nS} \\
&- (cp_{85})(n)[\beta_{\theta}(\phi, t)]_{nC} + (c_{86})Q_{\phi}(\phi, t)_{nS} - (cp_{87})(n)[N_{\phi}(\phi, t)]_{nC} + (c_{88})N_{\phi\theta}(\phi, t)_{nS} \\
&- (cp_{88})(n)[N_{\phi\theta}(\phi, t)]_{nC} - (cp_{89})(n)[M_{\phi}(\phi, t)]_{nC} - (cp_{810})(n)[M_{\phi\theta}(\phi, t)]_{nC}
\end{aligned} \tag{E.42}$$

Rewriting Equation (3.22)

$$\begin{aligned}
\frac{\partial M_{\phi}}{\partial \phi} &= (c_{91})(w^0) + (c_{92})(u_{\phi}^0) + (cp_{92}) \left( \frac{\partial u_{\phi}^0}{\partial \theta} \right) \\
&+ (c_{93})(u_{\theta}^0) + (cp_{93}) \left( \frac{\partial u_{\theta}^0}{\partial \theta} \right) \\
&+ (c_{94})(\beta_{\phi}) + (cp_{94}) \left( \frac{\partial \beta_{\phi}}{\partial \theta} \right) \\
&+ (c_{95})(\beta_{\theta}) + (cp_{95}) \left( \frac{\partial \beta_{\theta}}{\partial \theta} \right) \\
&+ (c_{96})(Q_{\phi\phi}) + (c_{97})(N_{\phi\phi}) \\
&+ (c_{98})(N_{\phi\theta}) + (c_{99})(M_{\phi\phi}) \\
&+ (c_{910})(M_{\phi\theta}) + (cp_{910}) \left( \frac{\partial M_{\phi\theta}}{\partial \theta} \right)
\end{aligned} \tag{E.43}$$

Carrying out the Finite exponential Fourier transform to Equation (E.43)

$$\begin{aligned}
& \frac{1}{2\Pi} \int_0^{2\Pi} \left[ \frac{\partial M_\phi(\phi, \theta, t)}{\partial \phi} e^{-in\theta} \right] d\theta = (c_{91}) \frac{1}{2\Pi} \int_0^{2\Pi} \left[ w^0(\phi, \theta, t) e^{-in\theta} \right] d\theta \\
& + (c_{92}) \frac{1}{2\Pi} \int_0^{2\Pi} \left[ u_\phi^0(\phi, \theta, t) e^{-in\theta} \right] d\theta + (cp_{92}) \frac{1}{2\Pi} \int_0^{2\Pi} \left[ \frac{\partial u_\phi^0(\phi, \theta, t)}{\partial \theta} e^{-in\theta} \right] d\theta \\
& + (c_{93}) \frac{1}{2\Pi} \int_0^{2\Pi} \left[ u_\theta^0(\phi, \theta, t) e^{-in\theta} \right] d\theta + (cp_{93}) \frac{1}{2\Pi} \int_0^{2\Pi} \left[ \frac{\partial u_\theta^0(\phi, \theta, t)}{\partial \theta} e^{-in\theta} \right] d\theta \\
& + (c_{94}) \frac{1}{2\Pi} \int_0^{2\Pi} \left[ \beta_\phi(\phi, \theta, t) e^{-in\theta} \right] d\theta + (cp_{94}) \frac{1}{2\Pi} \int_0^{2\Pi} \left[ \frac{\partial \beta_\phi(\phi, \theta, t)}{\partial \theta} e^{-in\theta} \right] d\theta \\
& + (c_{95}) \frac{1}{2\Pi} \int_0^{2\Pi} \left[ \beta_\theta(\phi, \theta, t) e^{-in\theta} \right] d\theta + (cp_{95}) \frac{1}{2\Pi} \int_0^{2\Pi} \left[ \frac{\partial \beta_\theta(\phi, \theta, t)}{\partial \theta} e^{-in\theta} \right] d\theta \\
& + (c_{96}) \frac{1}{2\Pi} \int_0^{2\Pi} \left[ Q_\phi(\phi, \theta, t) e^{-in\theta} \right] d\theta + (c_{97}) \frac{1}{2\Pi} \int_0^{2\Pi} \left[ N_\phi(\phi, \theta, t) e^{-in\theta} \right] d\theta \\
& + (c_{98}) \frac{1}{2\Pi} \int_0^{2\Pi} \left[ N_{\phi\theta}(\phi, \theta, t) e^{-in\theta} \right] d\theta + (c_{99}) \frac{1}{2\Pi} \int_0^{2\Pi} \left[ M_\phi(\phi, \theta, t) e^{-in\theta} \right] d\theta \\
& + (c_{910}) \frac{1}{2\Pi} \int_0^{2\Pi} \left[ M_{\phi\theta}(\phi, \theta, t) e^{-in\theta} \right] d\theta + (cp_{910}) \frac{1}{2\Pi} \int_0^{2\Pi} \left[ \frac{\partial M_{\phi\theta}(\phi, \theta, t)}{\partial \theta} e^{-in\theta} \right] d\theta
\end{aligned} \tag{E.44}$$

Using Equation (3.28) in Equation (E.44) yields

$$\begin{aligned}
& \int_0^{2\pi} \left[ \frac{\partial M_\phi(\phi, \theta, t)}{\partial \phi} \cos n\theta \right. \\
& \quad \left. - i \frac{\partial M_\phi(\phi, \theta, t)}{\partial \phi} \sin n\theta \right] d\theta = (c_{91}) \int_0^{2\pi} \left[ w^0(\phi, \theta, t) \cos n\theta \right. \\
& \quad \left. - i w^0(\phi, \theta, t) \sin n\theta \right] d\theta \\
& + (c_{92}) \int_0^{2\pi} \left[ u_\phi^0(\phi, \theta, t) \cos n\theta \right. \\
& \quad \left. - i u_\phi^0(\phi, \theta, t) \sin n\theta \right] d\theta + (cp_{92}) \int_0^{2\pi} (in) \left[ u_\phi^0(\phi, \theta, t) \cos n\theta \right. \\
& \quad \left. - i u_\phi^0(\phi, \theta, t) \sin n\theta \right] d\theta \\
& + (c_{93}) \int_0^{2\pi} \left[ u_\theta^0(\phi, \theta, t) \cos n\theta \right. \\
& \quad \left. - i u_\theta^0(\phi, \theta, t) \sin n\theta \right] d\theta + (cp_{93}) \int_0^{2\pi} (in) \left[ u_\theta^0(\phi, \theta, t) \cos n\theta \right. \\
& \quad \left. - i u_\theta^0(\phi, \theta, t) \sin n\theta \right] d\theta \\
& + (c_{94}) \int_0^{2\pi} \left[ \beta_\phi(\phi, \theta, t) \cos n\theta \right. \\
& \quad \left. - i \beta_\phi(\phi, \theta, t) \sin n\theta \right] d\theta + (cp_{94}) \int_0^{2\pi} (in) \left[ \beta_\phi(\phi, \theta, t) \cos n\theta \right. \\
& \quad \left. - i \beta_\phi(\phi, \theta, t) \sin n\theta \right] d\theta \tag{E.45} \\
& + (c_{95}) \int_0^{2\pi} \left[ \beta_\theta(\phi, \theta, t) \cos n\theta \right. \\
& \quad \left. - i \beta_\theta(\phi, \theta, t) \sin n\theta \right] d\theta + (cp_{95}) \int_0^{2\pi} (in) \left[ \beta_\theta(\phi, \theta, t) \cos n\theta \right. \\
& \quad \left. - i \beta_\theta(\phi, \theta, t) \sin n\theta \right] d\theta \\
& + (c_{96}) \int_0^{2\pi} \left[ Q_\phi(\phi, \theta, t) \cos n\theta \right. \\
& \quad \left. - i Q_\phi(\phi, \theta, t) \sin n\theta \right] d\theta + (c_{97}) \int_0^{2\pi} \left[ N_\phi(\phi, \theta, t) \cos n\theta \right. \\
& \quad \left. - i N_\phi(\phi, \theta, t) \sin n\theta \right] d\theta \\
& + (c_{98}) \int_0^{2\pi} \left[ N_{\phi\theta}(\phi, \theta, t) \cos n\theta \right. \\
& \quad \left. - i N_{\phi\theta}(\phi, \theta, t) \sin n\theta \right] d\theta + (c_{99}) \int_0^{2\pi} \left[ M_\phi(\phi, \theta, t) \cos n\theta \right. \\
& \quad \left. - i M_\phi(\phi, \theta, t) \sin n\theta \right] d\theta \\
& + (c_{910}) \int_0^{2\pi} \left[ M_{\phi\theta}(\phi, \theta, t) \cos n\theta \right. \\
& \quad \left. - i M_{\phi\theta}(\phi, \theta, t) \sin n\theta \right] + (cp_{910}) \int_0^{2\pi} (in) \left[ M_{\phi\theta}(\phi, \theta, t) \cos n\theta \right. \\
& \quad \left. - i M_{\phi\theta}(\phi, \theta, t) \sin n\theta \right] d\theta d\theta
\end{aligned}$$

$$\begin{aligned}
& \left[ \frac{dM_\phi(\phi, t)}{d\phi} \right]_{nc} - i \left[ \frac{dM_\phi(\phi, t)}{d\phi} \right]_{ns} = (c_{91}) \{ [w^0(\phi, t)]_{nc} - i [w^0(\phi, t)]_{ns} \} \\
& + (c_{92}) \{ [u_\phi^0(\phi, t)]_{nc} - i [u_\phi^0(\phi, t)]_{ns} \} + (cp_{92}) (n) \{ i [u_\phi^0(\phi, t)]_{nc} + [u_\phi^0(\phi, t)]_{ns} \} \\
& + (c_{93}) \{ [u_\theta^0(\phi, t)]_{nc} - i [u_\theta^0(\phi, t)]_{ns} \} + (cp_{93}) (n) \{ i [u_\theta^0(\phi, t)]_{nc} + [u_\theta^0(\phi, t)]_{ns} \} \\
& + (c_{94}) \{ [\beta_\phi(\phi, t)]_{nc} - i [\beta_\phi(\phi, t)]_{ns} \} + (cp_{94}) (n) \{ i [\beta_\phi(\phi, t)]_{nc} + [\beta_\phi(\phi, t)]_{ns} \} \\
& + (c_{95}) \{ [\beta_\theta(\phi, t)]_{nc} - i [\beta_\theta(\phi, t)]_{ns} \} + (cp_{95}) (n) \{ i [\beta_\theta(\phi, t)]_{nc} + [\beta_\theta(\phi, t)]_{ns} \} \\
& + (c_{96}) \{ [Q_\phi(\phi, t)]_{nc} - i [Q_\phi(\phi, t)]_{ns} \} + (c_{97}) \{ [N_\phi(\phi, t)]_{nc} - i [N_\phi(\phi, t)]_{ns} \} \\
& + (c_{98}) \{ [N_{\phi\theta}(\phi, t)]_{nc} - i [N_{\phi\theta}(\phi, t)]_{ns} \} + (c_{99}) \{ [M_\phi(\phi, t)]_{nc} - i [M_\phi(\phi, t)]_{ns} \} \\
& + (c_{910}) \{ [M_{\phi\theta}(\phi, t)]_{nc} - i [M_{\phi\theta}(\phi, t)]_{ns} \} + (cp_{910}) (n) \{ i [M_{\phi\theta}(\phi, t)]_{nc} + [M_{\phi\theta}(\phi, t)]_{ns} \}
\end{aligned} \tag{E.46}$$

We separate the real and imaginary parts of Equation (E.46)

First, writing real parts of Equation (E.46) term by term.

$$\begin{aligned}
\left[ \frac{dM_\phi(\phi, t)}{d\phi} \right]_{nc} &= (c_{91}) [w^0(\phi, t)]_{nc} + (c_{92}) [u_\phi^0(\phi, t)]_{nc} + (cp_{92}) (n) [u_\phi^0(\phi, t)]_{ns} \\
&+ (c_{93}) [u_\theta^0(\phi, t)]_{nc} + (cp_{93}) (n) [u_\theta^0(\phi, t)]_{ns} + (c_{94}) [\beta_\phi(\phi, t)]_{nc} + (cp_{94}) (n) [\beta_\phi(\phi, t)]_{ns} \\
&+ (c_{95}) [\beta_\theta(\phi, t)]_{nc} + (cp_{95}) (n) [\beta_\theta(\phi, t)]_{ns} + (c_{96}) [Q_\phi(\phi, t)]_{nc} + (c_{97}) [N_\phi(\phi, t)]_{nc} \\
&+ (c_{98}) [N_{\phi\theta}(\phi, t)]_{nc} + (c_{99}) [M_\phi(\phi, t)]_{nc} + (c_{910}) [M_{\phi\theta}(\phi, t)]_{nc} + (cp_{910}) (n) [M_{\phi\theta}(\phi, t)]_{ns}
\end{aligned} \tag{E.47}$$

Then, writing imaginary parts of Equation (E.46) term by term.

$$\begin{aligned}
\left[ \frac{dM_\phi(\phi, t)}{d\phi} \right]_{ns} &= (c_{91}) [w^0(\phi, t)]_{ns} + (c_{92}) [u_\phi^0(\phi, t)]_{ns} - (cp_{92}) (n) [u_\phi^0(\phi, t)]_{nc} \\
&+ (c_{93}) [u_\theta^0(\phi, t)]_{ns} - (cp_{93}) (n) [u_\theta^0(\phi, t)]_{nc} + (c_{94}) [\beta_\phi(\phi, t)]_{ns} - (cp_{94}) (n) [\beta_\phi(\phi, t)]_{nc} \\
&+ (c_{95}) [\beta_\theta(\phi, t)]_{ns} - (cp_{95}) (n) [\beta_\theta(\phi, t)]_{nc} + (c_{96}) [Q_\phi(\phi, t)]_{ns} + (c_{97}) [N_\phi(\phi, t)]_{ns} \\
&+ (c_{98}) [N_{\phi\theta}(\phi, t)]_{ns} + (c_{99}) [M_\phi(\phi, t)]_{ns} + (c_{910}) [M_{\phi\theta}(\phi, t)]_{ns} - (cp_{910}) (n) [M_{\phi\theta}(\phi, t)]_{nc}
\end{aligned} \tag{E.48}$$

Rewriting Equation (3.23)

$$\begin{aligned}
\frac{\partial M_{\phi\theta}}{\partial \phi} &= (cp_{101}) \left( \frac{\partial w^0}{\partial \theta} \right) + (c_{102}) (u_\phi^0) + (cp_{102}) \left( \frac{\partial u_\phi^0}{\partial \theta} \right) + (cdp_{102}) \left( \frac{\partial^2 u_\phi^0}{\partial \theta^2} \right) + (c_{103}) (u_\theta^0) \\
&+ (cp_{103}) \left( \frac{\partial u_\theta^0}{\partial \theta} \right) + (cdp_{103}) \left( \frac{\partial^2 u_\theta^0}{\partial \theta^2} \right) + (c_{104}) (\beta_\phi) + (cp_{104}) \left( \frac{\partial \beta_\phi}{\partial \theta} \right) + (cdp_{104}) \left( \frac{\partial^2 \beta_\phi}{\partial \theta^2} \right) \\
&+ (c_{105}) (\beta_\theta) + (cp_{105}) \left( \frac{\partial \beta_\theta}{\partial \theta} \right) + (cdp_{105}) \left( \frac{\partial^2 \beta_\theta}{\partial \theta^2} \right) + (c_{106}) (Q_\phi) \\
&+ (cp_{107}) \left( \frac{\partial N_\phi}{\partial \theta} \right) + (cp_{108}) \left( \frac{\partial N_{\phi\theta}}{\partial \theta} \right) + (cp_{109}) \left( \frac{\partial M_\phi}{\partial \theta} \right) + (c_{1010}) (M_{\phi\theta}) + (cp_{1010}) \left( \frac{\partial M_{\phi\theta}}{\partial \theta} \right)
\end{aligned} \tag{E.49}$$

Carrying out the Finite exponential Fourier transform to Equation (E.49)

$$\begin{aligned}
& \frac{1}{2\Pi} \int_0^{2\Pi} \left[ \frac{\partial M_{\phi\theta}(\phi, \theta, t)}{\partial \phi} e^{-in\theta} \right] d\theta = (cp_{101}) \frac{1}{2\Pi} \int_0^{2\Pi} \left[ \frac{\partial w^0(\phi, \theta, t)}{\partial \theta} e^{-in\theta} \right] d\theta \\
& + (c_{102}) \frac{1}{2\Pi} \int_0^{2\Pi} \left[ u_\phi^0(\phi, \theta, t) e^{-in\theta} \right] d\theta + (cp_{102}) \frac{1}{2\Pi} \int_0^{2\Pi} \left[ \frac{\partial u_\phi^0(\phi, \theta, t)}{\partial \theta} e^{-in\theta} \right] d\theta \\
& + (cdp_{102}) \frac{1}{2\Pi} \int_0^{2\Pi} \left[ \frac{\partial^2 u_\phi^0(\phi, \theta, t)}{\partial \theta^2} e^{-in\theta} \right] d\theta + (c_{103}) \frac{1}{2\Pi} \int_0^{2\Pi} \left[ u_\theta^0(\phi, \theta, t) e^{-in\theta} \right] d\theta \\
& + (cp_{103}) \frac{1}{2\Pi} \int_0^{2\Pi} \left[ \frac{\partial u_\theta^0(\phi, \theta, t)}{\partial \theta} e^{-in\theta} \right] d\theta + (cdp_{103}) \frac{1}{2\Pi} \int_0^{2\Pi} \left[ \frac{\partial^2 u_\theta^0(\phi, \theta, t)}{\partial \theta^2} e^{-in\theta} \right] d\theta \\
& + (c_{104}) \frac{1}{2\Pi} \int_0^{2\Pi} \left[ \beta_\phi(\phi, \theta, t) e^{-in\theta} \right] d\theta + (cp_{104}) \frac{1}{2\Pi} \int_0^{2\Pi} \left[ \frac{\partial \beta_\phi(\phi, \theta, t)}{\partial \theta} e^{-in\theta} \right] d\theta \\
& + (cdp_{104}) \frac{1}{2\Pi} \int_0^{2\Pi} \left[ \frac{\partial^2 \beta_\phi(\phi, \theta, t)}{\partial \theta^2} e^{-in\theta} \right] d\theta + (c_{105}) \frac{1}{2\Pi} \int_0^{2\Pi} \left[ \beta_\theta(\phi, \theta, t) e^{-in\theta} \right] d\theta \\
& + (cp_{105}) \frac{1}{2\Pi} \int_0^{2\Pi} \left[ \frac{\partial \beta_\theta(\phi, \theta, t)}{\partial \theta} e^{-in\theta} \right] d\theta + (cdp_{105}) \frac{1}{2\Pi} \int_0^{2\Pi} \left[ \frac{\partial^2 \beta_\theta(\phi, \theta, t)}{\partial \theta^2} e^{-in\theta} \right] d\theta \\
& + (c_{106}) \frac{1}{2\Pi} \int_0^{2\Pi} \left[ Q_\phi(\phi, \theta, t) e^{-in\theta} \right] d\theta + (cp_{107}) \frac{1}{2\Pi} \int_0^{2\Pi} \left[ \frac{\partial N_\phi(\phi, \theta, t)}{\partial \theta} e^{-in\theta} \right] d\theta \\
& + (cp_{108}) \frac{1}{2\Pi} \int_0^{2\Pi} \left[ \frac{\partial N_{\phi\theta}(\phi, \theta, t)}{\partial \theta} e^{-in\theta} \right] d\theta + (cp_{109}) \frac{1}{2\Pi} \int_0^{2\Pi} \left[ \frac{\partial M_\phi(\phi, \theta, t)}{\partial \theta} e^{-in\theta} \right] d\theta \\
& + (c_{1010}) \frac{1}{2\Pi} \int_0^{2\Pi} \left[ M_{\phi\theta}(\phi, \theta, t) e^{-in\theta} \right] d\theta + (cp_{1010}) \frac{1}{2\Pi} \int_0^{2\Pi} \left[ \frac{\partial M_{\phi\theta}(\phi, \theta, t)}{\partial \theta} e^{-in\theta} \right] d\theta
\end{aligned} \tag{E.50}$$

Using Equation (3.28) in (E.50) yields

$$\begin{aligned}
& \int_0^{2\Pi} \left[ \begin{array}{c} \frac{\partial M_{\phi\theta}(\phi, \theta, t)}{\partial \phi} \cos n\theta \\ -i \frac{\partial M_{\phi\theta}(\phi, \theta, t)}{\partial \phi} \sin n\theta \end{array} \right] d\theta = (cp_{101}) \int_0^{2\Pi} (in) \left[ \begin{array}{c} w^0(\phi, \theta, t) \cos n\theta \\ -i w^0(\phi, \theta, t) \sin n\theta \end{array} \right] d\theta \\
& + (c_{102}) \int_0^{2\Pi} \left[ \begin{array}{c} u_\phi^0(\phi, \theta, t) \cos n\theta \\ -i u_\phi^0(\phi, \theta, t) \sin n\theta \end{array} \right] d\theta + (cp_{102}) \int_0^{2\Pi} (in) \left[ \begin{array}{c} u_\phi^0(\phi, \theta, t) \cos n\theta \\ -i u_\phi^0(\phi, \theta, t) \sin n\theta \end{array} \right] d\theta \\
& - (cdp_{102})(n^2) \int_0^{2\Pi} \left[ \begin{array}{c} u_\phi^0(\phi, \theta, t) \cos n\theta \\ -i u_\phi^0(\phi, \theta, t) \sin n\theta \end{array} \right] d\theta + (c_{103}) \int_0^{2\Pi} \left[ \begin{array}{c} u_\theta^0(\phi, \theta, t) \cos n\theta \\ -i u_\theta^0(\phi, \theta, t) \sin n\theta \end{array} \right] d\theta \\
& + (cp_{103}) \int_0^{2\Pi} (in) \left[ \begin{array}{c} u_\theta^0(\phi, \theta, t) \cos n\theta \\ -i u_\theta^0(\phi, \theta, t) \sin n\theta \end{array} \right] d\theta - (cdp_{103})(n^2) \int_0^{2\Pi} \left[ \begin{array}{c} u_\theta^0(\phi, \theta, t) \cos n\theta \\ -i u_\theta^0(\phi, \theta, t) \sin n\theta \end{array} \right] d\theta \\
& + (c_{104}) \int_0^{2\Pi} \left[ \begin{array}{c} \beta_\phi(\phi, \theta, t) \cos n\theta \\ -i \beta_\phi(\phi, \theta, t) \sin n\theta \end{array} \right] d\theta + (cp_{104}) \int_0^{2\Pi} (in) \left[ \begin{array}{c} \beta_\phi(\phi, \theta, t) \cos n\theta \\ -i \beta_\phi(\phi, \theta, t) \sin n\theta \end{array} \right] d\theta \tag{E.51} \\
& - (cdp_{104})(n^2) \int_0^{2\Pi} \left[ \begin{array}{c} \beta_\phi(\phi, \theta, t) \cos n\theta \\ -i \beta_\phi(\phi, \theta, t) \sin n\theta \end{array} \right] d\theta + (c_{105}) \int_0^{2\Pi} \left[ \begin{array}{c} \beta_\theta(\phi, \theta, t) \cos n\theta \\ -i \beta_\theta(\phi, \theta, t) \sin n\theta \end{array} \right] d\theta \\
& + (cp_{105}) \int_0^{2\Pi} (in) \left[ \begin{array}{c} \beta_\theta(\phi, \theta, t) \cos n\theta \\ -i \beta_\theta(\phi, \theta, t) \sin n\theta \end{array} \right] d\theta - (cdp_{105})(n^2) \int_0^{2\Pi} \left[ \begin{array}{c} \beta_\theta(\phi, \theta, t) \cos n\theta \\ -i \beta_\theta(\phi, \theta, t) \sin n\theta \end{array} \right] d\theta \\
& + (c_{106}) \int_0^{2\Pi} \left[ \begin{array}{c} Q_\phi(\phi, \theta, t) \cos n\theta \\ -i Q_\phi(\phi, \theta, t) \sin n\theta \end{array} \right] d\theta + (cp_{107}) \int_0^{2\Pi} (in) \left[ \begin{array}{c} N_\phi(\phi, \theta, t) \cos n\theta \\ -i N_\phi(\phi, \theta, t) \sin n\theta \end{array} \right] d\theta \\
& + (cp_{108}) \int_0^{2\Pi} (in) \left[ \begin{array}{c} N_{\phi\theta}(\phi, \theta, t) \cos n\theta \\ -i N_{\phi\theta}(\phi, \theta, t) \sin n\theta \end{array} \right] d\theta + (cp_{109}) \int_0^{2\Pi} (in) \left[ \begin{array}{c} M_\phi(\phi, \theta, t) \cos n\theta \\ -i M_\phi(\phi, \theta, t) \sin n\theta \end{array} \right] d\theta \\
& + (c_{1010}) \int_0^{2\Pi} \left[ \begin{array}{c} M_{\phi\theta}(\phi, \theta, t) \cos n\theta \\ -i M_{\phi\theta}(\phi, \theta, t) \sin n\theta \end{array} \right] d\theta + (cp_{1010}) \int_0^{2\Pi} (in) \left[ \begin{array}{c} M_{\phi\theta}(\phi, \theta, t) \cos n\theta \\ -i M_{\phi\theta}(\phi, \theta, t) \sin n\theta \end{array} \right] d\theta
\end{aligned}$$

$$\begin{aligned}
& \left[ \frac{dM_{\phi\theta}(\phi, t)}{d\phi} \right]_{nc} - i \left[ \frac{dM_{\phi\theta}(\phi, t)}{d\phi} \right]_{ns} = (cp_{101}) \chi(n) \{ i [w^0(\phi, t)]_{nc} + [w^0(\phi, t)]_{ns} \} \\
& + (c_{102}) \chi \{ [u_\phi^0(\phi, t)]_{nc} - i [u_\phi^0(\phi, t)]_{ns} \} + (cp_{102}) \chi(n) \{ i [u_\phi^0(\phi, t)]_{nc} + [u_\phi^0(\phi, t)]_{ns} \} \\
& - (cdp_{102}) \chi(n^2) \{ [u_\phi^0(\phi, t)]_{nc} - i [u_\phi^0(\phi, t)]_{ns} \} + (c_{103}) \chi \{ [u_\theta^0(\phi, t)]_{nc} - i [u_\theta^0(\phi, t)]_{ns} \} \\
& + (cp_{103}) \chi(n) \{ i [u_\theta^0(\phi, t)]_{nc} + [u_\theta^0(\phi, t)]_{ns} \} - (cdp_{103}) \chi(n^2) \{ [u_\theta^0(\phi, t)]_{nc} - i [u_\theta^0(\phi, t)]_{ns} \} \\
& + (c_{104}) \chi \{ [\beta_\phi(\phi, t)]_{nc} - i [\beta_\phi(\phi, t)]_{ns} \} + (cp_{104}) \chi(n) \{ i [\beta_\phi(\phi, t)]_{nc} + [\beta_\phi(\phi, t)]_{ns} \} \\
& - (cdp_{104}) \chi(n^2) \{ [\beta_\phi(\phi, t)]_{nc} - i [\beta_\phi(\phi, t)]_{ns} \} + (c_{105}) \chi \{ [\beta_\theta(\phi, t)]_{nc} - i [\beta_\theta(\phi, t)]_{ns} \} \\
& + (cp_{105}) \chi(n) \{ i [\beta_\theta(\phi, t)]_{nc} + [\beta_\theta(\phi, t)]_{ns} \} - (cdp_{105}) \chi(n^2) \{ [\beta_\theta(\phi, t)]_{nc} - i [\beta_\theta(\phi, t)]_{ns} \} \\
& + (c_{106}) \chi \{ [\rho_\phi(\phi, t)]_{nc} - i [\rho_\phi(\phi, t)]_{ns} \} + (cp_{107}) \chi(n) \{ i [N_\phi(\phi, t)]_{nc} + [N_\phi(\phi, t)]_{ns} \} \\
& + (cp_{108}) \chi(n) \{ i [N_{\phi\theta}(\phi, t)]_{nc} + [N_{\phi\theta}(\phi, t)]_{ns} \} + (cp_{109}) \chi(n) \{ i [M_\phi(\phi, t)]_{nc} + [M_\phi(\phi, t)]_{ns} \} \\
& + (c_{1010}) \chi \{ [M_{\phi\theta}(\phi, t)]_{nc} - i [M_{\phi\theta}(\phi, t)]_{ns} \} + (cp_{1010}) \chi(n) \{ i [M_{\phi\theta}(\phi, t)]_{nc} + [M_{\phi\theta}(\phi, t)]_{ns} \}
\end{aligned} \tag{E.52}$$

We separate the real and imaginary parts of Equation (E.52).

First, writing real parts of Equation (E.52) term by term.

$$\begin{aligned}
& \left[ \frac{dM_{\phi\theta}(\phi, t)}{d\phi} \right]_{nc} = (cp_{101}) \chi(n) [w^0(\phi, t)]_{ns} + [(c_{102}) - (cdp_{102}) \chi(n^2)] [u_\phi^0(\phi, t)]_{nc} \\
& + (cp_{102}) \chi(n) [u_\phi^0(\phi, t)]_{ns} + [(c_{103}) - (cdp_{103}) \chi(n^2)] [u_\theta^0(\phi, t)]_{nc} + (cp_{103}) \chi(n) [u_\theta^0(\phi, t)]_{ns} \\
& + [(c_{104}) - (cdp_{104}) \chi(n^2)] [\beta_\phi(\phi, t)]_{nc} + (cp_{104}) \chi(n) [\beta_\phi(\phi, t)]_{ns} \\
& + [(c_{105}) - (cdp_{105}) \chi(n^2)] [\beta_\theta(\phi, t)]_{nc} + (cp_{105}) \chi(n) [\beta_\theta(\phi, t)]_{ns} + (c_{106}) [\rho_\phi(\phi, t)]_{nc} \\
& + (cp_{107}) \chi(n) [N_\phi(\phi, t)]_{ns} + (cp_{108}) \chi(n) [N_{\phi\theta}(\phi, t)]_{ns} + (cp_{109}) \chi(n) [M_\phi(\phi, t)]_{ns} \\
& + (c_{1010}) [M_{\phi\theta}(\phi, t)]_{nc} + (cp_{1010}) \chi(n) [M_{\phi\theta}(\phi, t)]_{ns}
\end{aligned} \tag{E.53}$$

Then, imaginary parts of Equation (E.52)

$$\begin{aligned}
\left[ \frac{dM_{\phi\theta}(\phi, t)}{d\phi} \right]_{n_S} &= -(c_{p_{101}})(n)[w^0(\phi, t)]_{n_C} + [(c_{102}) - (cdp_{102})(n^2)]u_\phi^0(\phi, t)_{n_S} \\
&- (cp_{102})(n)[u_\phi^0(\phi, t)]_{n_C} + [(c_{103}) - (cdp_{103})(n^2)]u_\theta^0(\phi, t)_{n_S} - (cp_{103})(n)[u_\theta^0(\phi, t)]_{n_C} \\
&+ [(c_{104}) - (cdp_{104})(n^2)]\beta_\phi(\phi, t)_{n_S} - (cp_{104})(n)[\beta_\phi(\phi, t)]_{n_C} \\
&+ [(c_{105}) - (cdp_{105})(n^2)]\beta_\theta(\phi, t)_{n_S} - (cp_{105})(n)[\beta_\theta(\phi, t)]_{n_C} + (c_{106})Q_\phi(\phi, t)_{n_S} \\
&- (cp_{107})(n)[N_\phi(\phi, t)]_{n_C} - (cp_{108})(n)[N_{\phi\theta}(\phi, t)]_{n_C} - (cp_{109})(n)[M_\phi(\phi, t)]_{n_C} \\
&+ (c_{1010})[M_{\phi\theta}(\phi, t)]_{n_S} - (cp_{1010})(n)[M_{\phi\theta}(\phi, t)]_{n_C}
\end{aligned} \tag{E.54}$$

## APPENDIX F

### THE ELEMENTS OF COEFFICIENT MATRIX K

The elements of 1<sup>st</sup> row are:

$$K_{11} = 0; K_{12} = ncp_{11}; K_{13} = c_{12}; K_{14} = 0; K_{15} = c_{13};$$

$$K_{16} = 0; K_{17} = c_{14}; K_{18} = 0; K_{19} = c_{15}; K_{110} = 0;$$

$$K_{111} = c_{16}; K_{112} = 0; K_{113} = 0; K_{114} = 0; K_{115} = 0;$$

$$K_{116} = 0; K_{117} = 0; K_{118} = 0; K_{119} = 0; K_{120} = 0;$$

(F.1-10)

The elements of 2<sup>nd</sup> row are:

$$K_{21} = -ncp_{11}; K_{22} = 0; K_{23} = 0; K_{24} = c_{12}; K_{25} = 0;$$

$$K_{26} = c_{13}; K_{27} = 0; K_{28} = c_{14}; K_{29} = 0; K_{210} = c_{15};$$

$$K_{211} = 0; K_{212} = c_{16}; K_{213} = 0; K_{214} = 0; K_{215} = 0;$$

$$K_{216} = 0; K_{217} = 0; K_{218} = 0; K_{219} = 0; K_{220} = 0$$

(F.11-20)

The elements of 3<sup>rd</sup> row are:

$$K_{31} = c_{21}; K_{32} = 0; K_{33} = c_{22}; K_{34} = ncp_{22}; K_{35} = c_{23};$$

$$K_{36} = ncp_{23}; K_{37} = c_{24}; K_{38} = ncp_{24}; K_{39} = c_{25}; K_{310} = ncp_{25};$$

$$K_{311} = 0; K_{312} = 0; K_{313} = c_{27}; K_{314} = 0; K_{315} = c_{28};$$

$$K_{316} = 0; K_{317} = c_{29}; K_{318} = 0; K_{319} = c_{210}; K_{320} = 0$$

(F.21-30)

The elements of 4<sup>th</sup> row are:

$$\begin{aligned}
K_{41} &= 0; K_{42} = c_{21}; K_{43} = -ncp_{22}; K_{44} = c_{22}; K_{45} = -ncp_{23}; \\
K_{46} &= c_{23}; K_{47} = -ncp_{24}; K_{48} = c_{24}; K_{49} = -ncp_{25}; K_{410} = c_{25}; \\
K_{411} &= 0; K_{412} = 0; K_{413} = 0; K_{414} = c_{27}; K_{415} = 0; \\
K_{416} &= c_{28}; K_{417} = 0; K_{418} = c_{29}; K_{419} = 0; K_{420} = c_{210}
\end{aligned}
\tag{F.31-40}$$

The elements of 5<sup>th</sup> row are:

$$\begin{aligned}
K_{51} &= c_{31}; K_{52} = 0; K_{53} = c_{32}; K_{54} = ncp_{32}; K_{55} = c_{33}; \\
K_{56} &= ncp_{33}; K_{57} = c_{34}; K_{58} = ncp_{34}; K_{59} = c_{35}; K_{510} = ncp_{35}; \\
K_{511} &= 0; K_{512} = 0; K_{513} = c_{37}; K_{514} = 0; K_{515} = c_{38}; \\
K_{516} &= 0; K_{517} = c_{39}; K_{518} = 0; K_{519} = c_{310}; K_{520} = 0
\end{aligned}
\tag{F.41-50}$$

The elements of 6<sup>th</sup> row are:

$$\begin{aligned}
K_{61} &= 0; K_{62} = c_{31}; K_{63} = -ncp_{32}; K_{64} = c_{32}; K_{65} = -ncp_{33}; \\
K_{66} &= c_{33}; K_{67} = -ncp_{34}; K_{68} = c_{34}; K_{69} = -ncp_{35}; K_{610} = c_{35}; \\
K_{611} &= 0; K_{612} = 0; K_{613} = 0; K_{614} = c_{37}; K_{615} = 0; \\
K_{616} &= c_{38}; K_{617} = 0; K_{618} = c_{39}; K_{619} = 0; K_{620} = c_{310}
\end{aligned}
\tag{F.51-60}$$

The elements of 7<sup>th</sup> row are:

$$K_{71} = c_{41}; K_{72} = 0; K_{73} = c_{42}; K_{74} = ncp_{42}; K_{75} = c_{43};$$

$$K_{76} = ncp_{43}; K_{77} = c_{44}; K_{78} = ncp_{43}; K_{79} = c_{45}; K_{710} = ncp_{45};$$

(F.61-70)

$$K_{711} = 0; K_{712} = 0; K_{713} = c_{47}; K_{714} = 0; K_{715} = c_{48};$$

$$K_{716} = 0; K_{717} = c_{49}; K_{718} = 0; K_{719} = c_{410}; K_{720} = 0$$

The elements of 8<sup>th</sup> row are:

$$K_{81} = 0; K_{82} = c_{41}; K_{83} = -ncp_{42}; K_{84} = c_{42}; K_{85} = -ncp_{43};$$

$$K_{86} = c_{43}; K_{87} = -ncp_{44}; K_{88} = c_{44}; K_{89} = -ncp_{45}; K_{810} = c_{45};$$

(F.71-80)

$$K_{811} = 0; K_{812} = 0; K_{813} = 0; K_{814} = c_{47}; K_{815} = 0;$$

$$K_{816} = c_{48}; K_{817} = 0; K_{818} = c_{49}; K_{819} = 0; K_{820} = c_{410}$$

The elements of 9<sup>th</sup> row are:

$$K_{91} = c_{51}; K_{92} = 0; K_{93} = c_{52}; K_{94} = ncp_{52}; K_{95} = c_{53};$$

$$K_{96} = ncp_{53}; K_{97} = c_{54}; K_{98} = ncp_{54}; K_{99} = c_{55}; K_{910} = ncp_{55};$$

(F.81-90)

$$K_{911} = 0; K_{912} = 0; K_{913} = c_{57}; K_{914} = 0; K_{915} = c_{58};$$

$$K_{916} = 0; K_{917} = c_{59}; K_{918} = 0; K_{919} = c_{510}; K_{920} = 0$$

The elements of 10<sup>th</sup> row are:

$$\begin{aligned}
K_{101} &= 0; K_{102} = c_{51}; K_{103} = -ncp_{52}; K_{104} = c_{52}; K_{105} = -ncp_{53}; \\
K_{106} &= c_{53}; K_{107} = -ncp_{54}; K_{108} = c_{54}; K_{109} = -ncp_{55}; K_{1010} = c_{55}; \\
K_{1011} &= 0; K_{1012} = 0; K_{1013} = 0; K_{1014} = c_{57}; K_{1015} = 0; \\
K_{1016} &= c_{58}; K_{1017} = 0; K_{1018} = c_{59}; K_{1019} = 0; K_{1020} = c_{510}
\end{aligned}
\tag{F.91-100}$$

The elements of 11<sup>th</sup> row are:

$$\begin{aligned}
K_{111} &= c_{61} - n^2cdp_{61}; K_{112} = 0; K_{113} = c_{62}; K_{114} = ncp_{62}; K_{115} = c_{63}; \\
K_{116} &= ncp_{63}; K_{117} = c_{64}; K_{118} = ncp_{64}; K_{119} = c_{65}; K_{1110} = ncp_{65}; \\
K_{1111} &= c_{66}; K_{1112} = ncp_{66}; K_{1113} = c_{67}; K_{1114} = 0; K_{1115} = c_{68}; \\
K_{1116} &= 0; K_{1117} = c_{69}; K_{1118} = 0; K_{1119} = c_{610}; K_{1120} = 0
\end{aligned}
\tag{F.101-110}$$

The elements of 12<sup>th</sup> row are:

$$\begin{aligned}
K_{121} &= 0; K_{122} = c_{61} - n^2cdp_{61}; K_{123} = -ncp_{62}; K_{124} = c_{62}; K_{125} = -ncp_{63}; \\
K_{126} &= c_{63}; K_{127} = -ncp_{64}; K_{128} = c_{64}; K_{129} = -ncp_{65}; K_{1210} = c_{65}; \\
K_{1211} &= -ncp_{66}; K_{1212} = c_{66}; K_{1213} = 0; K_{1214} = c_{67}; K_{1215} = 0; \\
K_{1216} &= c_{68}; K_{1217} = 0; K_{1218} = c_{69}; K_{1219} = 0; K_{1220} = c_{610}
\end{aligned}
\tag{F.111-120}$$

The elements of 13<sup>th</sup> row are:

$$K_{131} = c_{71}; K_{132} = 0; K_{133} = c_{72}; K_{134} = ncp_{72}; K_{135} = c_{73};$$

$$K_{136} = ncp_{73}; K_{137} = c_{74}; K_{138} = ncp_{74}; K_{139} = c_{75}; K_{1310} = ncp_{75};$$

(F.121-130)

$$K_{1311} = c_{76}; K_{1312} = 0; K_{1313} = c_{77}; K_{1314} = 0; K_{1315} = c_{78};$$

$$K_{1316} = ncp_{78}; K_{1317} = c_{79}; K_{1318} = 0; K_{1319} = c_{710}; K_{1320} = 0$$

The elements of 14<sup>th</sup> row are:

$$K_{141} = 0; K_{142} = c_{71}; K_{143} = -ncp_{72}; K_{144} = c_{72}; K_{145} = -ncp_{73};$$

$$K_{146} = c_{73}; K_{147} = -ncp_{74}; K_{148} = c_{74}; K_{149} = -ncp_{75}; K_{1410} = c_{75};$$

(F.131-140)

$$K_{1411} = 0; K_{1412} = c_{76}; K_{1413} = 0; K_{1414} = c_{77}; K_{1415} = -ncp_{78};$$

$$K_{1416} = c_{78}; K_{1417} = 0; K_{1418} = c_{79}; K_{1419} = 0; K_{1420} = c_{710}$$

The elements of 15<sup>th</sup> row are:

$$K_{151} = 0; K_{152} = ncp_{81}; K_{153} = c_{82} - n^2 cdp_{82}; K_{154} = ncp_{82};$$

$$K_{155} = c_{83} - n^2 cdp_{83}; K_{156} = ncp_{83}; K_{157} = c_{84} - n^2 cdp_{84}; K_{158} = ncp_{84};$$

$$K_{159} = c_{85} - n^2 cdp_{85}; K_{1510} = ncp_{85}; K_{1511} = c_{86}; K_{1512} = 0;$$

(F.141-150)

$$K_{1513} = 0; K_{1514} = ncp_{87}; K_{1515} = c_{88}; K_{1516} = ncp_{88};$$

$$K_{1517} = 0; K_{1518} = ncp_{89}; K_{1519} = 0; K_{1520} = ncp_{810}$$

The elements of 16<sup>th</sup> row are:

$$\begin{aligned}
K_{161} &= -ncp_{81}; K_{162} = 0; K_{163} = -ncp_{82}; K_{164} = c_{82} - n^2cdp_{82}; \\
K_{165} &= -ncp_{83}; K_{166} = c_{83} - n^2cdp_{83}; K_{167} = -ncp_{84}; K_{168} = c_{84} - n^2cdp_{84}; \\
K_{169} &= -ncp_{85}; K_{1610} = c_{85} - n^2cdp_{85}; K_{1611} = 0; K_{1612} = c_{86}; \\
K_{1613} &= -ncp_{87}; K_{1614} = 0; K_{1615} = -ncp_{88}; K_{1616} = c_{88}; \\
K_{1617} &= -ncp_{89}; K_{1618} = 0; K_{1619} = -ncp_{810}; K_{1620} = 0
\end{aligned} \tag{F.151-160}$$

The elements of 17<sup>th</sup> row are:

$$\begin{aligned}
K_{171} &= c_{91}; K_{172} = 0; K_{173} = c_{92}; K_{174} = ncp_{92}; K_{175} = c_{93}; \\
K_{176} &= ncp_{93}; K_{177} = c_{94}; K_{178} = ncp_{94}; K_{179} = c_{95}; K_{1710} = ncp_{95}; \\
K_{1711} &= c_{96}; K_{1712} = 0; K_{1713} = c_{97}; K_{1714} = 0; K_{1715} = c_{98}; \\
K_{1716} &= 0; K_{1717} = c_{99}; K_{1718} = 0; K_{1719} = c_{910}; K_{1720} = ncp_{910}
\end{aligned} \tag{F.161-170}$$

The elements of 18<sup>th</sup> row are:

$$\begin{aligned}
K_{181} &= 0; K_{182} = c_{91}; K_{183} = -ncp_{92}; K_{184} = c_{92}; K_{185} = -ncp_{93}; \\
K_{186} &= c_{93}; K_{187} = -ncp_{94}; K_{188} = c_{94}; K_{189} = -ncp_{95}; K_{1810} = c_{95}; \\
K_{1811} &= 0; K_{1812} = c_{96}; K_{1813} = 0; K_{1814} = c_{97}; K_{1815} = 0; \\
K_{1816} &= c_{98}; K_{1817} = 0; K_{1818} = c_{99}; K_{1819} = -ncp_{910}; K_{1820} = c_{910}
\end{aligned} \tag{F.171-180}$$

The elements of 19<sup>th</sup> row are:

$$K_{191} = 0; K_{192} = ncp_{101}; K_{193} = c_{102} - n^2cdp_{102}; K_{194} = ncp_{102};$$

$$K_{195} = c_{103} - n^2cdp_{103}; K_{196} = ncp_{103}; K_{197} = c_{104} - n^2cdp_{104}; K_{198} = ncp_{104};$$

$$K_{199} = c_{105} - n^2cdp_{105}; K_{1910} = ncp_{105}; K_{1911} = c_{106}; K_{1912} = 0; \quad (\text{F.181-190})$$

$$K_{1913} = 0; K_{1914} = ncp_{107}; K_{1915} = 0; K_{1916} = ncp_{108};$$

$$K_{1917} = 0; K_{1918} = ncp_{109}; K_{1919} = c_{1010}; K_{1920} = ncp_{1010}$$

The elements of 20<sup>th</sup> row are:

$$K_{201} = -ncp_{101}; K_{202} = 0; K_{203} = -ncp_{102}; K_{204} = c_{102} - n^2cdp_{102};$$

$$K_{205} = -ncp_{103}; K_{206} = c_{103} - n^2cdp_{103}; K_{207} = -ncp_{104}; K_{208} = c_{104} - n^2cdp_{104};$$

$$K_{209} = -ncp_{105}; K_{2010} = c_{105} - n^2cdp_{105}; K_{2011} = 0; K_{2012} = c_{106}; \quad (\text{F.191-200})$$

$$K_{2013} = -ncp_{107}; K_{2014} = 0; K_{2015} = -ncp_{108}; K_{2016} = 0;$$

$$K_{2017} = -ncp_{109}; K_{2018} = 0; K_{2019} = -ncp_{1010}; K_{2020} = c_{1010}$$

## APPENDIX G

### DEMONSTRATION OF THE RELATION BETWEEN THE DETERMINANT OF THE CHARACTERISTIC EQUATION DETERMINED BY THE TRADITIONAL FOURIER DECOMPOSITION METHOD AND THE ONE BY THE FINITE EXPONENTIAL FOURIER TRANSFORM METHOD

This demonstration, for ease of explanation, is performed for one segment shell with 2 fundamental variable case. Let us have a sample system of first order ordinary differential equations which is given by

$$\frac{d}{d\phi} \begin{Bmatrix} y_1(\phi) \\ y_2(\phi) \end{Bmatrix} = [A] \begin{Bmatrix} y_1(\phi) \\ y_2(\phi) \end{Bmatrix} \quad (\text{G.1})$$

where

$$[A] = \begin{bmatrix} a_{11} & a_{12} \\ a_{21} & a_{22} \end{bmatrix} \quad (\text{G.2})$$

If the solution of (G.1) in the interval  $(\phi_0, \phi_1)$  is expressed as:

$$\begin{Bmatrix} y_1(\phi) \\ y_2(\phi) \end{Bmatrix} = [T(\phi)] \begin{Bmatrix} y_1(\phi_0) \\ y_2(\phi_0) \end{Bmatrix} \quad (\text{G.3})$$

then, the system of differential equations given in (G.1) can be reduced to series of initial value problems when (G.3) is substituted into (G.1). The obtained 4 initial value problems are given by

$$\frac{d}{d\phi} \{T(\phi)\} = [A] \{T(\phi)\} \quad (\text{G.4})$$

The initial values for  $T(\phi)$  at  $\phi = \phi_0$  is obtained from

$$[T(\phi_0)] = I \quad (\text{G.5})$$

where  $I$  is a 2 by 2 unit matrix.

The formal solution of (G.1) in the interval  $(\phi_0, \phi_1)$  is given by (G.4) where  $T(\phi)$  is obtained from the 4 solutions of the initial value problems defined by (G.4) and (G.5). If this solution is also aimed

to satisfy the prescribed boundary conditions, then (G.3) is evaluated at  $\phi = \phi_1$ .

$$\begin{Bmatrix} y_1(\phi_1) \\ y_2(\phi_1) \end{Bmatrix} = [T(\phi_1)] \begin{Bmatrix} y_1(\phi_0) \\ y_2(\phi_0) \end{Bmatrix} \quad (\text{G.6})$$

where

$$[T(\phi_1)] = \begin{bmatrix} T^1(\phi_1) & T^2(\phi_1) \\ T^3(\phi_1) & T^4(\phi_1) \end{bmatrix} \quad (\text{G.7})$$

It can be seen that when variables at  $\phi_0$  is known, the solution for (G.1) at any value  $\phi$  is obtained from (G.3).

$[T(\phi_1)]$  can be obtained from (G.4) as:

$$\frac{d}{d\phi} [T(\phi_1)] = [A][T(\phi_0)] \quad (\text{G.8})$$

where

$$[T(\phi_0)] = \begin{bmatrix} T^1(\phi_0) & T^2(\phi_0) \\ T^3(\phi_0) & T^4(\phi_0) \end{bmatrix} = I = \begin{bmatrix} 1 & 0 \\ 0 & 1 \end{bmatrix} \quad (\text{G.9})$$

and

$$[T(\phi_1)] = \begin{bmatrix} T^1(\phi_1) & T^2(\phi_1) \\ T^3(\phi_1) & T^4(\phi_1) \end{bmatrix} \quad (\text{G.10})$$

Putting (G.8) into the following form

$$\frac{d}{d\phi} \begin{Bmatrix} T^1(\phi_1) \\ T^2(\phi_1) \\ T^3(\phi_1) \\ T^4(\phi_1) \end{Bmatrix} = \begin{bmatrix} a_{11} & 0 & a_{12} & 0 \\ 0 & a_{11} & 0 & a_{12} \\ a_{21} & 0 & a_{22} & 0 \\ 0 & a_{21} & 0 & a_{22} \end{bmatrix} \begin{Bmatrix} T^1(\phi_0) \\ T^2(\phi_0) \\ T^3(\phi_0) \\ T^4(\phi_0) \end{Bmatrix} \quad (\text{G.11})$$

$$\begin{Bmatrix} T^1(\phi_0) \\ T^2(\phi_0) \\ T^3(\phi_0) \\ T^4(\phi_0) \end{Bmatrix} = \begin{Bmatrix} 1 \\ 0 \\ 0 \\ 1 \end{Bmatrix} \quad (\text{G.12})$$

For brevity, the following terms are determined

$$\begin{aligned} T^1(\phi_1) &= T_{1-1}; T^2(\phi_1) = T_{2-1}; T^3(\phi_1) = T_{3-1}; T^4(\phi_1) = T_{4-1} \\ T^1(\phi_0) &= T_{1-0}; T^2(\phi_0) = T_{2-0}; T^3(\phi_0) = T_{3-0}; T^4(\phi_0) = T_{4-0} \end{aligned} \quad (\text{G.13})$$

Then, the 4th order Runge-Kutta is employed to calculate  $[T(\phi_1)]$ . The values of  $[T(\phi_0)]$  are already known as initial values given in (G.12). The scheme for the 4th order Runge-Kutta method for system of ODEs is given in [69]. As a result,  $[T(\phi_1)]$  is given by

$$[T(\phi_1)] = [T(\phi_0)] + \left(\frac{1}{6}\right) (\{K\} + 2\{L\} + 2\{M\} + \{N\}) \quad (\text{G.14})$$

where

$$\{K\} = \begin{Bmatrix} k_1 \\ k_2 \\ k_3 \\ k_4 \end{Bmatrix} = h \begin{Bmatrix} (a_{11}T_{1-0}) + (a_{12}T_{3-0}) \\ (a_{11}T_{2-0}) + (a_{12}T_{4-0}) \\ (a_{21}T_{1-0}) + (a_{22}T_{3-0}) \\ (a_{21}T_{2-0}) + (a_{22}T_{4-0}) \end{Bmatrix} \quad (\text{G.15})$$

$$\{L\} = \begin{Bmatrix} l_1 \\ l_2 \\ l_3 \\ l_4 \end{Bmatrix} = h \begin{Bmatrix} a_{11}\left(T_{1-0} + \frac{1}{2}k_1\right) + a_{12}\left(T_{3-0} + \frac{1}{2}k_3\right) \\ a_{11}\left(T_{2-0} + \frac{1}{2}k_2\right) + a_{12}\left(T_{4-0} + \frac{1}{2}k_4\right) \\ a_{21}\left(T_{1-0} + \frac{1}{2}k_1\right) + a_{22}\left(T_{3-0} + \frac{1}{2}k_3\right) \\ a_{21}\left(T_{2-0} + \frac{1}{2}k_2\right) + a_{22}\left(T_{4-0} + \frac{1}{2}k_4\right) \end{Bmatrix} \quad (\text{G.16})$$

$$\{M\} = \begin{Bmatrix} m_1 \\ m_2 \\ m_3 \\ m_4 \end{Bmatrix} = h \begin{bmatrix} a_{11} \left( T_{1-0} + \frac{1}{2} l_1 \right) + a_{12} \left( T_{3-0} + \frac{1}{2} l_3 \right) \\ a_{11} \left( T_{2-0} + \frac{1}{2} l_2 \right) + a_{12} \left( T_{4-0} + \frac{1}{2} l_4 \right) \\ a_{21} \left( T_{1-0} + \frac{1}{2} l_1 \right) + a_{22} \left( T_{3-0} + \frac{1}{2} l_3 \right) \\ a_{21} \left( T_{2-0} + \frac{1}{2} l_2 \right) + a_{22} \left( T_{4-0} + \frac{1}{2} l_4 \right) \end{bmatrix} \quad (\text{G.17})$$

and

$$\{N\} = \begin{Bmatrix} n_1 \\ n_2 \\ n_3 \\ n_4 \end{Bmatrix} = h \begin{bmatrix} a_{11} \left( T_{1-0} + \frac{1}{2} m_1 \right) + a_{12} \left( T_{3-0} + \frac{1}{2} m_3 \right) \\ a_{11} \left( T_{2-0} + \frac{1}{2} m_2 \right) + a_{12} \left( T_{4-0} + \frac{1}{2} m_4 \right) \\ a_{21} \left( T_{1-0} + \frac{1}{2} m_1 \right) + a_{22} \left( T_{3-0} + \frac{1}{2} m_3 \right) \\ a_{21} \left( T_{2-0} + \frac{1}{2} m_2 \right) + a_{22} \left( T_{4-0} + \frac{1}{2} m_4 \right) \end{bmatrix} \quad (\text{G.18})$$

When the above computations are done symbolically using Matlab, the terms of  $[T(\phi)]$  are computed as:

$T_{1-1}$ :

```

1 + 1/6 h a11 + 1/3 %1 + 1/3
h (a11 (1 + 1/2 %1) + 1/2 a12 h (a21 (1 + 1/2 h a11) + 1/2 a22 h a21))
+ 1/6 h (a11 (1 + 1/2
h (a11 (1 + 1/2 %1) + 1/2 a12 h (a21 (1 + 1/2 h a11) + 1/2 a22 h a21))
) + 1/2 a12 h
(a21 (1 + 1/2 %1) + 1/2 a22 h (a21 (1 + 1/2 h a11) + 1/2 a22 h a21)))
%1 := h (a11 (1 + 1/2 h a11) + 1/2 a12 h a21)

```

(G.19)

$T_{2-1}$ :

$$\begin{aligned}
& 1/6 h a_{12} + 1/3 h \%2 + 1/3 h (1/2 a_{11} h \%2 + a_{12} \%1) + 1/6 h ( \\
& \quad 1/2 a_{11} h (1/2 a_{11} h \%2 + a_{12} \%1) \\
& \quad + a_{12} (1 + 1/2 h (1/2 a_{21} h \%2 + a_{22} \%1))) \tag{G.20} \\
\%1 & := 1 + 1/2 h (1/2 a_{12} h a_{21} + a_{22} (1 + 1/2 h a_{22})) \\
\%2 & := 1/2 a_{11} h a_{12} + a_{12} (1 + 1/2 h a_{22})
\end{aligned}$$

$T_{3\_1}$ :

$$\begin{aligned}
& 1/6 h a_{21} + 1/3 h \%1 + 1/3 h (a_{21} \%2 + 1/2 a_{22} h \%1) + 1/6 h ( \\
& \quad a_{21} (1 + 1/2 h (a_{11} \%2 + 1/2 a_{12} h \%1)) \\
& \quad + 1/2 a_{22} h (a_{21} \%2 + 1/2 a_{22} h \%1)) \tag{G.21} \\
\%1 & := a_{21} (1 + 1/2 h a_{11}) + 1/2 a_{22} h a_{21} \\
\%2 & := 1 + 1/2 h (a_{11} (1 + 1/2 h a_{11}) + 1/2 a_{12} h a_{21})
\end{aligned}$$

and  $T_{4\_1}$ :

$$\begin{aligned}
& 1 + 1/6 h a_{22} + 1/3 \%1 + 1/3 \\
& \quad h (1/2 a_{21} h (1/2 a_{11} h a_{12} + a_{12} (1 + 1/2 h a_{22})) + a_{22} (1 + 1/2 \%1)) \\
& \quad + 1/6 h (1/2 a_{21} h \\
& \quad (1/2 a_{11} h (1/2 a_{11} h a_{12} + a_{12} (1 + 1/2 h a_{22})) + a_{12} (1 + 1/2 \%1)) \\
& \quad + a_{22} (1 + 1/2 \\
& \quad h (1/2 a_{21} h (1/2 a_{11} h a_{12} + a_{12} (1 + 1/2 h a_{22})) + a_{22} (1 + 1/2 \%1)) \\
& \quad )) \tag{G.22} \\
\%1 & := h (1/2 a_{12} h a_{21} + a_{22} (1 + 1/2 h a_{22}))
\end{aligned}$$

If  $y_1(\phi_1)$  and  $y_1(\phi_0)$  are assumed to be prescribed, then (G.6) results in

$$(T_{2-1})(y_2(\phi_0))=0 \quad (G.23)$$

The pertaining characteristic equation is obtained by finding the nontrivial solution of (G.23) by taking determinant of  $T_{2-1}$

$$|(T_{2-1})|=0 \quad (G.24)$$

When the method of Finite Fourier Transform is applied to (G.1), the new form of the system of differential equations in (G.1) can be written in terms of real variables as

$$\begin{aligned} \frac{d}{d\phi}[y_1(\phi)]_{nc} - i \frac{d}{d\phi}[y_1(\phi)]_{ns} &= a_{11} \{ [y_1(\phi)]_{nc} - i [y_1(\phi)]_{ns} \} \\ &\quad + a_{12} \{ [y_2(\phi)]_{nc} - i [y_2(\phi)]_{ns} \} \\ \frac{d}{d\phi}[y_2(\phi)]_{nc} - i \frac{d}{d\phi}[y_2(\phi)]_{ns} &= a_{21} \{ [y_1(\phi)]_{nc} - i [y_1(\phi)]_{ns} \} \\ &\quad + a_{22} \{ [y_2(\phi)]_{nc} - i [y_2(\phi)]_{ns} \} \end{aligned} \quad (G.25)$$

(G.25) is written in compact form

$$\frac{d}{d\phi} \begin{Bmatrix} [y_1(\phi)]_{nc} \\ [y_1(\phi)]_{ns} \\ [y_2(\phi)]_{nc} \\ [y_2(\phi)]_{ns} \end{Bmatrix} = [A_n] \begin{Bmatrix} [y_1(\phi)]_{nc} \\ [y_1(\phi)]_{ns} \\ [y_2(\phi)]_{nc} \\ [y_2(\phi)]_{ns} \end{Bmatrix} \quad (G.26)$$

where

$$[A_n] = \begin{bmatrix} a_{11} & 0 & a_{12} & 0 \\ 0 & a_{11} & 0 & a_{12} \\ a_{21} & 0 & a_{22} & 0 \\ 0 & a_{21} & 0 & a_{22} \end{bmatrix} \quad (G.27)$$

The formal solution of (G.26) in the interval  $(\phi_0, \phi_1)$  can be given by

$$\begin{Bmatrix} [y_1(\phi_1)]_{nc} \\ [y_1(\phi_1)]_{ns} \\ [y_2(\phi_1)]_{nc} \\ [y_2(\phi_1)]_{ns} \end{Bmatrix} = [T_n(\phi_1)] \begin{Bmatrix} [y_1(\phi_0)]_{nc} \\ [y_1(\phi_0)]_{ns} \\ [y_2(\phi_0)]_{nc} \\ [y_2(\phi_0)]_{ns} \end{Bmatrix} \quad (G.28)$$

$$[T_n(\phi_1)] = \begin{bmatrix} T_n^1(\phi_1) & T_n^2(\phi_1) & T_n^3(\phi_1) & T_n^4(\phi_1) \\ T_n^5(\phi_1) & T_n^6(\phi_1) & T_n^7(\phi_1) & T_n^8(\phi_1) \\ T_n^9(\phi_1) & T_n^{10}(\phi_1) & T_n^{11}(\phi_1) & T_n^{12}(\phi_1) \\ T_n^{13}(\phi_1) & T_n^{14}(\phi_1) & T_n^{15}(\phi_1) & T_n^{16}(\phi_1) \end{bmatrix} \quad (G.29)$$

$[T_n(\phi_1)]$  can be obtained from solutions of 16 initial value problems such that

$$\frac{d}{d\phi} [T_n(\phi_1)] = [A_n] [T_n(\phi_0)] \quad (G.30)$$

$$[T_n(\phi_0)] = \begin{bmatrix} T_n^1(\phi_1) & T_n^2(\phi_1) & T_n^3(\phi_1) & T_n^4(\phi_1) \\ T_n^5(\phi_1) & T_n^6(\phi_1) & T_n^7(\phi_1) & T_n^8(\phi_1) \\ T_n^9(\phi_1) & T_n^{10}(\phi_1) & T_n^{11}(\phi_1) & T_n^{12}(\phi_1) \\ T_n^{13}(\phi_1) & T_n^{14}(\phi_1) & T_n^{15}(\phi_1) & T_n^{16}(\phi_1) \end{bmatrix} = I = \begin{bmatrix} 1 & 0 & 0 & 0 \\ 0 & 1 & 0 & 0 \\ 0 & 0 & 1 & 0 \\ 0 & 0 & 0 & 1 \end{bmatrix} \quad (G.31)$$

(G.30) is expanded to let us carry out single step numerical integration as follows:

$$\frac{d}{d\phi} \{T_n(\phi_1)\} = \begin{bmatrix} a_{11} & 0 & 0 & 0 & 0 & 0 & 0 & 0 & a_{12} & 0 & 0 & 0 & 0 & 0 & 0 & 0 \\ 0 & a_{11} & 0 & 0 & 0 & 0 & 0 & 0 & 0 & a_{12} & 0 & 0 & 0 & 0 & 0 & 0 \\ 0 & 0 & a_{11} & 0 & 0 & 0 & 0 & 0 & 0 & 0 & a_{12} & 0 & 0 & 0 & 0 & 0 \\ 0 & 0 & 0 & a_{11} & 0 & 0 & 0 & 0 & 0 & 0 & 0 & a_{12} & 0 & 0 & 0 & 0 \\ 0 & 0 & 0 & 0 & a_{11} & 0 & 0 & 0 & 0 & 0 & 0 & 0 & a_{12} & 0 & 0 & 0 \\ 0 & 0 & 0 & 0 & 0 & a_{11} & 0 & 0 & 0 & 0 & 0 & 0 & 0 & a_{12} & 0 & 0 \\ 0 & 0 & 0 & 0 & 0 & 0 & a_{11} & 0 & 0 & 0 & 0 & 0 & 0 & 0 & a_{12} & 0 \\ 0 & 0 & 0 & 0 & 0 & 0 & 0 & a_{11} & 0 & 0 & 0 & 0 & 0 & 0 & 0 & a_{12} \\ a_{21} & 0 & 0 & 0 & 0 & 0 & 0 & 0 & a_{22} & 0 & 0 & 0 & 0 & 0 & 0 & 0 \\ 0 & a_{21} & 0 & 0 & 0 & 0 & 0 & 0 & 0 & a_{22} & 0 & 0 & 0 & 0 & 0 & 0 \\ 0 & 0 & a_{21} & 0 & 0 & 0 & 0 & 0 & 0 & 0 & a_{22} & 0 & 0 & 0 & 0 & 0 \\ 0 & 0 & 0 & a_{21} & 0 & 0 & 0 & 0 & 0 & 0 & 0 & a_{22} & 0 & 0 & 0 & 0 \\ 0 & 0 & 0 & 0 & a_{21} & 0 & 0 & 0 & 0 & 0 & 0 & 0 & a_{22} & 0 & 0 & 0 \\ 0 & 0 & 0 & 0 & 0 & a_{21} & 0 & 0 & 0 & 0 & 0 & 0 & 0 & a_{22} & 0 & 0 \\ 0 & 0 & 0 & 0 & 0 & 0 & a_{21} & 0 & 0 & 0 & 0 & 0 & 0 & 0 & a_{22} & 0 \\ 0 & 0 & 0 & 0 & 0 & 0 & 0 & a_{21} & 0 & 0 & 0 & 0 & 0 & 0 & 0 & a_{22} \end{bmatrix} \{T_n(\phi_0)\} \quad (G.32)$$

where

$$\{T_n(\phi_1)\} = \begin{Bmatrix} T_n^1(\phi_1) \\ T_n^2(\phi_1) \\ T_n^3(\phi_1) \\ T_n^4(\phi_1) \\ T_n^5(\phi_1) \\ T_n^6(\phi_1) \\ T_n^7(\phi_1) \\ T_n^8(\phi_1) \\ T_n^9(\phi_1) \\ T_n^{10}(\phi_1) \\ T_n^{11}(\phi_1) \\ T_n^{12}(\phi_1) \\ T_n^{13}(\phi_1) \\ T_n^{14}(\phi_1) \\ T_n^{15}(\phi_1) \\ T_n^{16}(\phi_1) \end{Bmatrix}; \quad \{T_n(\phi_0)\} = \begin{Bmatrix} T_n^1(\phi_0) \\ T_n^2(\phi_0) \\ T_n^3(\phi_0) \\ T_n^4(\phi_0) \\ T_n^5(\phi_0) \\ T_n^6(\phi_0) \\ T_n^7(\phi_0) \\ T_n^8(\phi_0) \\ T_n^9(\phi_0) \\ T_n^{10}(\phi_0) \\ T_n^{11}(\phi_0) \\ T_n^{12}(\phi_0) \\ T_n^{13}(\phi_0) \\ T_n^{14}(\phi_0) \\ T_n^{15}(\phi_0) \\ T_n^{16}(\phi_0) \end{Bmatrix} \quad (\text{G.33})$$

and

$$\begin{Bmatrix} T_n^1(\phi_0) \\ T_n^2(\phi_0) \\ T_n^3(\phi_0) \\ T_n^4(\phi_0) \\ T_n^5(\phi_0) \\ T_n^6(\phi_0) \\ T_n^7(\phi_0) \\ T_n^8(\phi_0) \\ T_n^9(\phi_0) \\ T_n^{10}(\phi_0) \\ T_n^{11}(\phi_0) \\ T_n^{12}(\phi_0) \\ T_n^{13}(\phi_0) \\ T_n^{14}(\phi_0) \\ T_n^{15}(\phi_0) \\ T_n^{16}(\phi_0) \end{Bmatrix} = \begin{Bmatrix} 1 \\ 0 \\ 0 \\ 0 \\ 0 \\ 1 \\ 0 \\ 0 \\ 0 \\ 0 \\ 1 \\ 0 \\ 0 \\ 0 \\ 0 \\ 1 \end{Bmatrix} \quad (\text{G.34})$$

The terms in (G.33) can be written in their short forms

$$\begin{aligned}
T_n^1(\phi_1) &= T_{1\_1n}; T_n^2(\phi_1) = T_{2\_1n}; T_n^3(\phi_1) = T_{3\_1n}; T_n^4(\phi_1) = T_{4\_1n}; \\
T_n^5(\phi_1) &= T_{5\_1n}; T_n^6(\phi_1) = T_{6\_1n}; T_n^7(\phi_1) = T_{7\_1n}; T_n^8(\phi_1) = T_{8\_1n}; \\
T_n^9(\phi_1) &= T_{9\_1n}; T_n^{10}(\phi_1) = T_{10\_1n}; T_n^{11}(\phi_1) = T_{11\_1n}; T_n^{12}(\phi_1) = T_{12\_1n}; \\
T_n^{13}(\phi_1) &= T_{13\_1n}; T_n^{14}(\phi_1) = T_{14\_1n}; T_n^{15}(\phi_1) = T_{15\_1n}; T_n^{16}(\phi_1) = T_{16\_1n} \\
T_n^1(\phi_0) &= T_{1\_0n}; T_n^2(\phi_0) = T_{2\_0n}; T_n^3(\phi_0) = T_{3\_0n}; T_n^4(\phi_0) = T_{4\_0n}; \\
T_n^5(\phi_0) &= T_{5\_0n}; T_n^6(\phi_0) = T_{6\_0n}; T_n^7(\phi_0) = T_{7\_0n}; T_n^8(\phi_0) = T_{8\_0n}; \\
T_n^9(\phi_0) &= T_{9\_0n}; T_n^{10}(\phi_0) = T_{10\_0n}; T_n^{11}(\phi_0) = T_{11\_0n}; T_n^{12}(\phi_0) = T_{12\_0n}; \\
T_n^{13}(\phi_0) &= T_{13\_0n}; T_n^{14}(\phi_0) = T_{14\_0n}; T_n^{15}(\phi_0) = T_{15\_0n}; T_n^{16}(\phi_0) = T_{16\_0n}
\end{aligned} \tag{G.35}$$

Again,  $[T_n(\phi_1)]$  is calculated with the following equation after employing 4<sup>th</sup> order Runge-Kutta Method.

$$[T_n(\phi_1)] = [T_n(\phi_0)] + \left(\frac{1}{6}\right) (\{K_n\} + 2\{L_n\} + 2\{M_n\} + \{N_n\}) \tag{G.36}$$

where

$$\{K_n\} = \begin{Bmatrix} k_1 \\ k_2 \\ k_3 \\ k_4 \\ k_5 \\ k_6 \\ k_7 \\ k_8 \\ k_9 \\ k_{10} \\ k_{11} \\ k_{12} \\ k_{13} \\ k_{14} \\ k_{15} \\ k_{16} \end{Bmatrix} = h \begin{Bmatrix} (a_{11}T_{1\_0n}) + (a_{12}T_{9\_0n}) \\ (a_{11}T_{2\_0n}) + (a_{12}T_{10\_0n}) \\ (a_{11}T_{3\_0n}) + (a_{12}T_{11\_0n}) \\ (a_{11}T_{4\_0n}) + (a_{12}T_{12\_0n}) \\ (a_{11}T_{5\_0n}) + (a_{12}T_{13\_0n}) \\ (a_{11}T_{6\_0n}) + (a_{12}T_{14\_0n}) \\ (a_{11}T_{7\_0n}) + (a_{12}T_{15\_0n}) \\ (a_{11}T_{8\_0n}) + (a_{12}T_{16\_0n}) \\ (a_{21}T_{1\_0n}) + (a_{22}T_{9\_0n}) \\ (a_{21}T_{2\_0n}) + (a_{22}T_{10\_0n}) \\ (a_{21}T_{3\_0n}) + (a_{22}T_{11\_0n}) \\ (a_{21}T_{4\_0n}) + (a_{22}T_{12\_0n}) \\ (a_{21}T_{5\_0n}) + (a_{22}T_{13\_0n}) \\ (a_{21}T_{6\_0n}) + (a_{22}T_{14\_0n}) \\ (a_{21}T_{7\_0n}) + (a_{22}T_{15\_0n}) \\ (a_{21}T_{8\_0n}) + (a_{22}T_{16\_0n}) \end{Bmatrix} \tag{G.37}$$

$$\{L_n\} = \left\{ \begin{array}{l} l_1 \\ l_2 \\ l_3 \\ l_4 \\ l_5 \\ l_6 \\ l_7 \\ l_8 \\ l_9 \\ l_{10} \\ l_{11} \\ l_{12} \\ l_{13} \\ l_{14} \\ l_{15} \\ l_{16} \end{array} \right\} = h \left\{ \begin{array}{l} a_{11} \left( T_{1_{-0n}} + \frac{1}{2} k_1 \right) + a_{12} \left( T_{9_{-0n}} + \frac{1}{2} k_9 \right) \\ a_{11} \left( T_{2_{-0n}} + \frac{1}{2} k_2 \right) + a_{12} \left( T_{10_{-0n}} + \frac{1}{2} k_{10} \right) \\ a_{11} \left( T_{3_{-0n}} + \frac{1}{2} k_3 \right) + a_{12} \left( T_{11_{-0n}} + \frac{1}{2} k_{11} \right) \\ a_{11} \left( T_{4_{-0n}} + \frac{1}{2} k_4 \right) + a_{12} \left( T_{12_{-0n}} + \frac{1}{2} k_{12} \right) \\ a_{11} \left( T_{5_{-0n}} + \frac{1}{2} k_5 \right) + a_{12} \left( T_{13_{-0n}} + \frac{1}{2} k_{13} \right) \\ a_{11} \left( T_{6_{-0n}} + \frac{1}{2} k_6 \right) + a_{12} \left( T_{14_{-0n}} + \frac{1}{2} k_{14} \right) \\ a_{11} \left( T_{7_{-0n}} + \frac{1}{2} k_7 \right) + a_{12} \left( T_{15_{-0n}} + \frac{1}{2} k_{15} \right) \\ a_{11} \left( T_{8_{-0n}} + \frac{1}{2} k_8 \right) + a_{12} \left( T_{16_{-0n}} + \frac{1}{2} k_{16} \right) \\ a_{21} \left( T_{1_{-0n}} + \frac{1}{2} k_1 \right) + a_{22} \left( T_{9_{-0n}} + \frac{1}{2} k_9 \right) \\ a_{21} \left( T_{2_{-0n}} + \frac{1}{2} k_2 \right) + a_{22} \left( T_{10_{-0n}} + \frac{1}{2} k_{10} \right) \\ a_{21} \left( T_{3_{-0n}} + \frac{1}{2} k_3 \right) + a_{22} \left( T_{11_{-0n}} + \frac{1}{2} k_{11} \right) \\ a_{21} \left( T_{4_{-0n}} + \frac{1}{2} k_4 \right) + a_{22} \left( T_{12_{-0n}} + \frac{1}{2} k_{12} \right) \\ a_{21} \left( T_{5_{-0n}} + \frac{1}{2} k_5 \right) + a_{22} \left( T_{13_{-0n}} + \frac{1}{2} k_{13} \right) \\ a_{21} \left( T_{6_{-0n}} + \frac{1}{2} k_6 \right) + a_{22} \left( T_{14_{-0n}} + \frac{1}{2} k_{14} \right) \\ a_{21} \left( T_{7_{-0n}} + \frac{1}{2} k_7 \right) + a_{22} \left( T_{15_{-0n}} + \frac{1}{2} k_{15} \right) \\ a_{21} \left( T_{8_{-0n}} + \frac{1}{2} k_8 \right) + a_{22} \left( T_{16_{-0n}} + \frac{1}{2} k_{16} \right) \end{array} \right\} \quad (\text{G.38})$$

$$\{M_n\} = \begin{cases} m_1 \\ m_2 \\ m_3 \\ m_4 \\ m_5 \\ m_6 \\ m_7 \\ m_8 \\ m_9 \\ m_{10} \\ m_{11} \\ m_{12} \\ m_{13} \\ m_{14} \\ m_{15} \\ m_{16} \end{cases} = h \left\{ \begin{array}{l} a_{11} \left( T_{1_{-0n}} + \frac{1}{2} l_1 \right) + a_{12} \left( T_{9_{-0n}} + \frac{1}{2} l_9 \right) \\ a_{11} \left( T_{2_{-0n}} + \frac{1}{2} l_2 \right) + a_{12} \left( T_{10_{-0n}} + \frac{1}{2} l_{10} \right) \\ a_{11} \left( T_{3_{-0n}} + \frac{1}{2} l_3 \right) + a_{12} \left( T_{11_{-0n}} + \frac{1}{2} l_{11} \right) \\ a_{11} \left( T_{4_{-0n}} + \frac{1}{2} l_4 \right) + a_{12} \left( T_{12_{-0n}} + \frac{1}{2} l_{12} \right) \\ a_{11} \left( T_{5_{-0n}} + \frac{1}{2} l_5 \right) + a_{12} \left( T_{13_{-0n}} + \frac{1}{2} l_{13} \right) \\ a_{11} \left( T_{6_{-0n}} + \frac{1}{2} l_6 \right) + a_{12} \left( T_{14_{-0n}} + \frac{1}{2} l_{14} \right) \\ a_{11} \left( T_{7_{-0n}} + \frac{1}{2} l_7 \right) + a_{12} \left( T_{15_{-0n}} + \frac{1}{2} l_{15} \right) \\ a_{11} \left( T_{8_{-0n}} + \frac{1}{2} l_8 \right) + a_{12} \left( T_{16_{-0n}} + \frac{1}{2} l_{16} \right) \\ a_{21} \left( T_{1_{-0n}} + \frac{1}{2} l_1 \right) + a_{22} \left( T_{9_{-0n}} + \frac{1}{2} l_9 \right) \\ a_{21} \left( T_{2_{-0n}} + \frac{1}{2} l_2 \right) + a_{22} \left( T_{10_{-0n}} + \frac{1}{2} l_{10} \right) \\ a_{21} \left( T_{3_{-0n}} + \frac{1}{2} l_3 \right) + a_{22} \left( T_{11_{-0n}} + \frac{1}{2} l_{11} \right) \\ a_{21} \left( T_{4_{-0n}} + \frac{1}{2} l_4 \right) + a_{22} \left( T_{12_{-0n}} + \frac{1}{2} l_{12} \right) \\ a_{21} \left( T_{5_{-0n}} + \frac{1}{2} l_5 \right) + a_{22} \left( T_{13_{-0n}} + \frac{1}{2} l_{13} \right) \\ a_{21} \left( T_{6_{-0n}} + \frac{1}{2} l_6 \right) + a_{22} \left( T_{14_{-0n}} + \frac{1}{2} l_{14} \right) \\ a_{21} \left( T_{7_{-0n}} + \frac{1}{2} l_7 \right) + a_{22} \left( T_{15_{-0n}} + \frac{1}{2} l_{15} \right) \\ a_{21} \left( T_{8_{-0n}} + \frac{1}{2} l_8 \right) + a_{22} \left( T_{16_{-0n}} + \frac{1}{2} l_{16} \right) \end{array} \right\} \quad (G.39)$$

$$\{N_n\} = \left\{ \begin{array}{l} n_1 \\ n_2 \\ n_3 \\ n_4 \\ n_5 \\ n_6 \\ n_7 \\ n_8 \\ n_9 \\ n_{10} \\ n_{11} \\ n_{12} \\ n_{13} \\ n_{14} \\ n_{15} \\ n_{16} \end{array} \right\} = h \left\{ \begin{array}{l} a_{11} \left( T_{1_{-0n}} + \frac{1}{2} m_1 \right) + a_{12} \left( T_{9_{-0n}} + \frac{1}{2} m_9 \right) \\ a_{11} \left( T_{2_{-0n}} + \frac{1}{2} m_2 \right) + a_{12} \left( T_{10_{-0n}} + \frac{1}{2} m_{10} \right) \\ a_{11} \left( T_{3_{-0n}} + \frac{1}{2} m_3 \right) + a_{12} \left( T_{11_{-0n}} + \frac{1}{2} m_{11} \right) \\ a_{11} \left( T_{4_{-0n}} + \frac{1}{2} m_4 \right) + a_{12} \left( T_{12_{-0n}} + \frac{1}{2} m_{12} \right) \\ a_{11} \left( T_{5_{-0n}} + \frac{1}{2} m_5 \right) + a_{12} \left( T_{13_{-0n}} + \frac{1}{2} m_{13} \right) \\ a_{11} \left( T_{6_{-0n}} + \frac{1}{2} m_6 \right) + a_{12} \left( T_{14_{-0n}} + \frac{1}{2} m_{14} \right) \\ a_{11} \left( T_{7_{-0n}} + \frac{1}{2} m_7 \right) + a_{12} \left( T_{15_{-0n}} + \frac{1}{2} m_{15} \right) \\ a_{11} \left( T_{8_{-0n}} + \frac{1}{2} m_8 \right) + a_{12} \left( T_{16_{-0n}} + \frac{1}{2} m_{16} \right) \\ a_{21} \left( T_{1_{-0n}} + \frac{1}{2} m_1 \right) + a_{22} \left( T_{9_{-0n}} + \frac{1}{2} m_9 \right) \\ a_{21} \left( T_{2_{-0n}} + \frac{1}{2} m_2 \right) + a_{22} \left( T_{10_{-0n}} + \frac{1}{2} m_{10} \right) \\ a_{21} \left( T_{3_{-0n}} + \frac{1}{2} m_3 \right) + a_{22} \left( T_{11_{-0n}} + \frac{1}{2} m_{11} \right) \\ a_{21} \left( T_{4_{-0n}} + \frac{1}{2} m_4 \right) + a_{22} \left( T_{12_{-0n}} + \frac{1}{2} m_{12} \right) \\ a_{21} \left( T_{5_{-0n}} + \frac{1}{2} m_5 \right) + a_{22} \left( T_{13_{-0n}} + \frac{1}{2} m_{13} \right) \\ a_{21} \left( T_{6_{-0n}} + \frac{1}{2} m_6 \right) + a_{22} \left( T_{14_{-0n}} + \frac{1}{2} m_{14} \right) \\ a_{21} \left( T_{7_{-0n}} + \frac{1}{2} m_7 \right) + a_{22} \left( T_{15_{-0n}} + \frac{1}{2} m_{15} \right) \\ a_{21} \left( T_{8_{-0n}} + \frac{1}{2} m_8 \right) + a_{22} \left( T_{16_{-0n}} + \frac{1}{2} m_{16} \right) \end{array} \right\} \quad (G.40)$$

Nonzero elements of  $\{T_n(\phi_1)\}$  computed by using Matlab Symbolic Toolbox are listed as follows:

$T_{1_{ln}}$ :

$$\begin{aligned}
 & 1 + 1/6 h a_{11} + 1/3 \xi_1 + 1/3 \\
 & \quad h (a_{11} (1 + 1/2 \xi_1) + 1/2 a_{12} h (a_{21} (1 + 1/2 h a_{11}) + 1/2 a_{22} h a_{21})) \\
 & \quad + 1/6 h (a_{11} (1 + 1/2 \\
 & \quad h (a_{11} (1 + 1/2 \xi_1) + 1/2 a_{12} h (a_{21} (1 + 1/2 h a_{11}) + 1/2 a_{22} h a_{21})) \\
 & \quad ) + 1/2 a_{12} h \\
 & \quad (a_{21} (1 + 1/2 \xi_1) + 1/2 a_{22} h (a_{21} (1 + 1/2 h a_{11}) + 1/2 a_{22} h a_{21}))) \\
 & \xi_1 := h (a_{11} (1 + 1/2 h a_{11}) + 1/2 a_{12} h a_{21})
 \end{aligned} \tag{G.41}$$

$T_{3_{ln}}$ :

$$\begin{aligned}
 & 1/6 h a_{12} + 1/3 h \xi_2 + 1/3 h (1/2 a_{11} h \xi_2 + a_{12} \xi_1) + 1/6 h ( \\
 & \quad 1/2 a_{11} h (1/2 a_{11} h \xi_2 + a_{12} \xi_1) \\
 & \quad + a_{12} (1 + 1/2 h (1/2 a_{21} h \xi_2 + a_{22} \xi_1))) \\
 & \xi_1 := 1 + 1/2 h (1/2 a_{12} h a_{21} + a_{22} (1 + 1/2 h a_{22})) \\
 & \xi_2 := 1/2 a_{11} h a_{12} + a_{12} (1 + 1/2 h a_{22})
 \end{aligned} \tag{G.42}$$

$T_{6_{ln}}$ :

$$\begin{aligned}
 & 1 + 1/6 h a_{11} + 1/3 \xi_1 + 1/3 \\
 & \quad h (a_{11} (1 + 1/2 \xi_1) + 1/2 a_{12} h (a_{21} (1 + 1/2 h a_{11}) + 1/2 a_{22} h a_{21})) \\
 & \quad + 1/6 h (a_{11} (1 + 1/2 \\
 & \quad h (a_{11} (1 + 1/2 \xi_1) + 1/2 a_{12} h (a_{21} (1 + 1/2 h a_{11}) + 1/2 a_{22} h a_{21})) \\
 & \quad ) + 1/2 a_{12} h \\
 & \quad (a_{21} (1 + 1/2 \xi_1) + 1/2 a_{22} h (a_{21} (1 + 1/2 h a_{11}) + 1/2 a_{22} h a_{21}))) \\
 & \xi_1 := h (a_{11} (1 + 1/2 h a_{11}) + 1/2 a_{12} h a_{21})
 \end{aligned} \tag{G.43}$$

$T_{8\_ln}$ :

$$\begin{aligned}
 & 1/6 h a_{12} + 1/3 h \%2 + 1/3 h (1/2 a_{11} h \%2 + a_{12} \%1) + 1/6 h ( \\
 & \quad 1/2 a_{11} h (1/2 a_{11} h \%2 + a_{12} \%1) \\
 & \quad + a_{12} (1 + 1/2 h (1/2 a_{21} h \%2 + a_{22} \%1))) \\
 & \%1 := 1 + 1/2 h (1/2 a_{12} h a_{21} + a_{22} (1 + 1/2 h a_{22})) \\
 & \%2 := 1/2 a_{11} h a_{12} + a_{12} (1 + 1/2 h a_{22})
 \end{aligned} \tag{G.44}$$

$T_{9\_ln}$ :

$$\begin{aligned}
 & 1/6 h a_{21} + 1/3 h \%1 + 1/3 h (a_{21} \%2 + 1/2 a_{22} h \%1) + 1/6 h ( \\
 & \quad a_{21} (1 + 1/2 h (a_{11} \%2 + 1/2 a_{12} h \%1)) \\
 & \quad + 1/2 a_{22} h (a_{21} \%2 + 1/2 a_{22} h \%1)) \\
 & \%1 := a_{21} (1 + 1/2 h a_{11}) + 1/2 a_{22} h a_{21} \\
 & \%2 := 1 + 1/2 h (a_{11} (1 + 1/2 h a_{11}) + 1/2 a_{12} h a_{21})
 \end{aligned} \tag{G.45}$$

$T_{11\_ln}$ :

$$\begin{aligned}
 & 1 + 1/6 h a_{22} + 1/3 \%1 + 1/3 \\
 & \quad h (1/2 a_{21} h (1/2 a_{11} h a_{12} + a_{12} (1 + 1/2 h a_{22})) + a_{22} (1 + 1/2 \%1)) \\
 & \quad + 1/6 h (1/2 a_{21} h \\
 & \quad (1/2 a_{11} h (1/2 a_{11} h a_{12} + a_{12} (1 + 1/2 h a_{22})) + a_{12} (1 + 1/2 \%1)) \\
 & \quad + a_{22} (1 + 1/2 \\
 & \quad h (1/2 a_{21} h (1/2 a_{11} h a_{12} + a_{12} (1 + 1/2 h a_{22})) + a_{22} (1 + 1/2 \%1)) \\
 & \quad )) \\
 & \%1 := h (1/2 a_{12} h a_{21} + a_{22} (1 + 1/2 h a_{22}))
 \end{aligned} \tag{G.46}$$

$T_{14\_1n}$ :

$$\begin{aligned}
& 1/6 h a_{21} + 1/3 h \xi_1 + 1/3 h (a_{21} \xi_2 + 1/2 a_{22} h \xi_1) + 1/6 h ( \\
& \quad a_{21} (1 + 1/2 h (a_{11} \xi_2 + 1/2 a_{12} h \xi_1)) \\
& \quad + 1/2 a_{22} h (a_{21} \xi_2 + 1/2 a_{22} h \xi_1)) \\
& \xi_1 := a_{21} (1 + 1/2 h a_{11}) + 1/2 a_{22} h a_{21} \\
& \xi_2 := 1 + 1/2 h (a_{11} (1 + 1/2 h a_{11}) + 1/2 a_{12} h a_{21})
\end{aligned} \tag{G.47}$$

$T_{16\_1n}$ :

$$\begin{aligned}
& 1 + 1/6 h a_{22} + 1/3 \xi_1 + 1/3 \\
& h (1/2 a_{21} h (1/2 a_{11} h a_{12} + a_{12} (1 + 1/2 h a_{22})) + a_{22} (1 + 1/2 \xi_1)) \\
& + 1/6 h (1/2 a_{21} h \\
& (1/2 a_{11} h (1/2 a_{11} h a_{12} + a_{12} (1 + 1/2 h a_{22})) + a_{12} (1 + 1/2 \xi_1)) \\
& + a_{22} (1 + 1/2 \\
& h (1/2 a_{21} h (1/2 a_{11} h a_{12} + a_{12} (1 + 1/2 h a_{22})) + a_{22} (1 + 1/2 \xi_1)) \\
& )) \\
& \xi_1 := h (1/2 a_{12} h a_{21} + a_{22} (1 + 1/2 h a_{22}))
\end{aligned} \tag{G.48}$$

If  $[y_1(\phi_1)]_{nc}$ ,  $[y_1(\phi_1)]_{ns}$ ,  $[y_1(\phi_0)]_{nc}$ , and  $[y_1(\phi_0)]_{ns}$  assumed to be prescribed, then (G.28) results in

$$\begin{bmatrix} T_{3\_1n} & T_{4\_1n} \\ T_{7\_1n} & T_{8\_1n} \end{bmatrix} \begin{Bmatrix} [y_2(\phi_0)]_{nc} \\ [y_2(\phi_0)]_{ns} \end{Bmatrix} = 0 \tag{G.49}$$

The pertaining characteristic equation is obtained by finding the nontrivial solution of (G.49).

$$\left| (T_{3\_1n} T_{8\_1n}) - (T_{4\_1n} T_{7\_1n}) \right| = 0 \tag{G.50}$$

In (G.50), both  $T_{4\_1n}$  and  $T_{7\_1n}$  equals to zero, and  $T_{3\_1n}$  and  $T_{8\_1n}$  are both equal to the following (rewriting (G.42) and (G.44)):

$$\begin{aligned}
& \frac{1}{6} h a_{12} + \frac{1}{3} h \xi_2 + \frac{1}{3} h \left( \frac{1}{2} a_{11} h \xi_2 + a_{12} \xi_1 \right) + \frac{1}{6} h \left( \right. \\
& \quad \left. \frac{1}{2} \epsilon_{11} h \left( \frac{1}{2} a_{11} h \xi_2 + a_{12} \xi_1 \right) \right. \\
& \quad \left. + a_{12} \left( 1 + \frac{1}{2} h \left( \frac{1}{2} a_{21} h \xi_2 + a_{22} \xi_1 \right) \right) \right) \tag{G.51} \\
& \xi_1 := 1 + \frac{1}{2} h \left( \frac{1}{2} a_{12} h a_{21} + a_{22} \left( 1 + \frac{1}{2} h a_{22} \right) \right) \\
& \xi_2 := \frac{1}{2} \epsilon_{11} h a_{12} + a_{12} \left( 1 + \frac{1}{2} h a_{22} \right)
\end{aligned}$$

where (G.51) is same as  $T_{2\_1}$  in (G.24). As a result, it can be concluded that the determinant obtained by the finite exponential Fourier transform method is the square power of the determinant obtained by the traditional Fourier decomposition method for a generic two point boundary problem having two fundamental variables.

## APPENDIX H

### MODE SHAPES OF SYMMETRIC, ANTISYMMETRIC and UNSYMMETRIC LAYUPS for N=0, 1, and 2 CASES

i) SYMMETRIC LAYUP

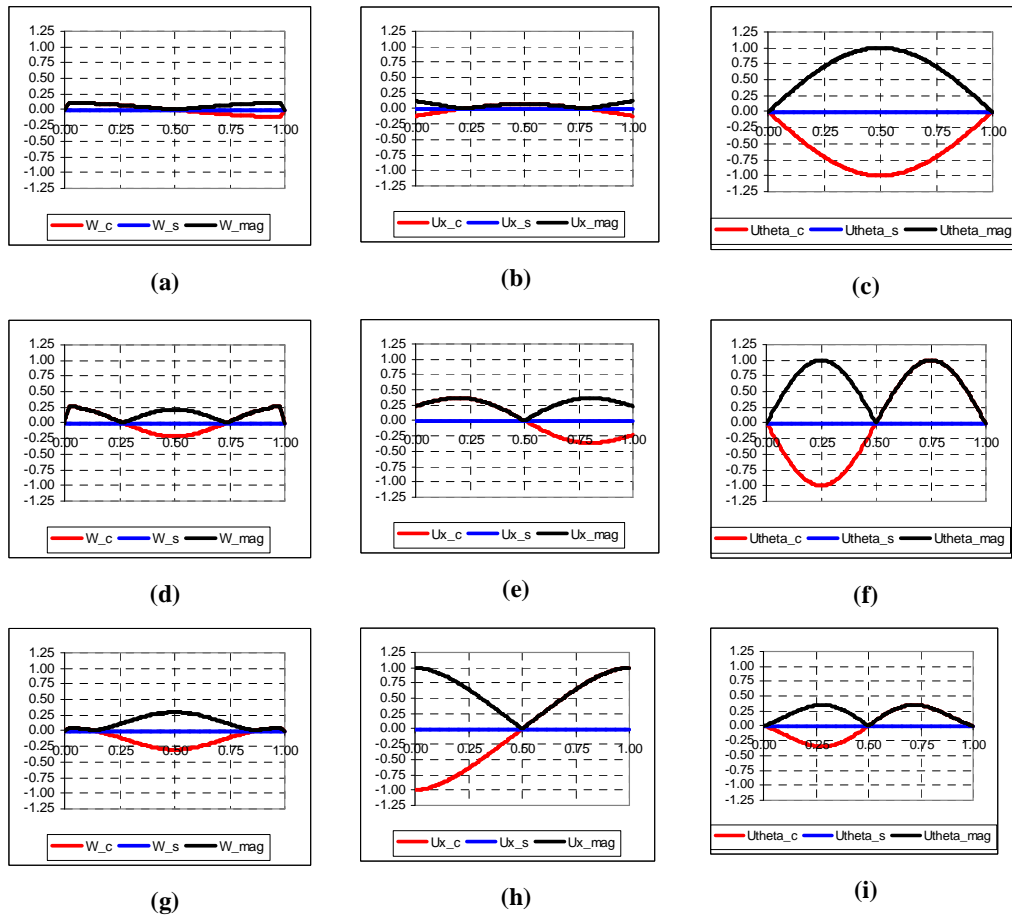


**Figure H.1** Mode Shapes in displacements of (a)  $w$  (b)  $u_\phi$  (c)  $u_\theta$  for (n=0) and (m=1); (d)  $w$  (e)  $u_\phi$  (f)  $u_\theta$  for (n=0) and (m=2); and (g)  $w$  (h)  $u_\phi$  (i)  $u_\theta$  for (n=0) and (m=3)

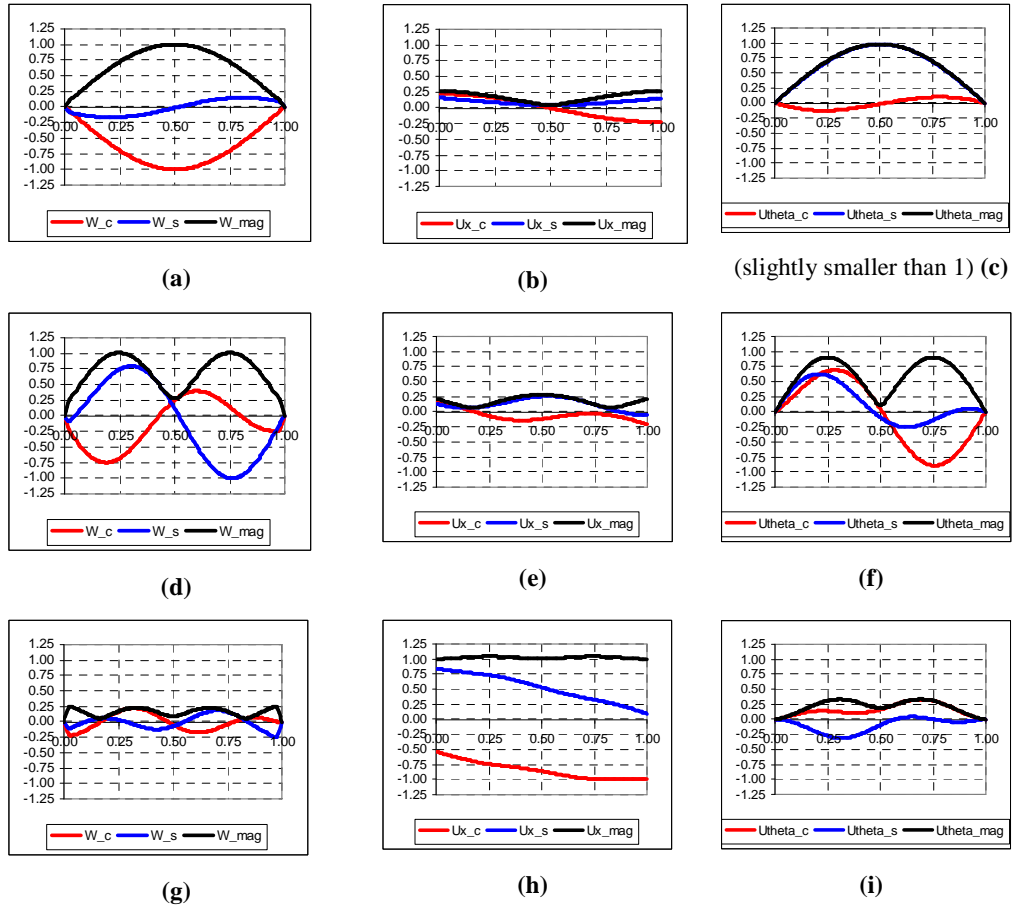


**Figure H.2** Mode Shapes in displacements of (a)  $w$  (b)  $u_\phi$  (c)  $u_\theta$  for  $(n=1)$  and  $(m=1)$ ;  
 (d)  $w$  (e)  $u_\phi$  (f)  $u_\theta$  for  $(n=1)$  and  $(m=2)$ ; and (g)  $w$  (h)  $u_\phi$  (i)  $u_\theta$  for  $(n=1)$  and  $(m=3)$

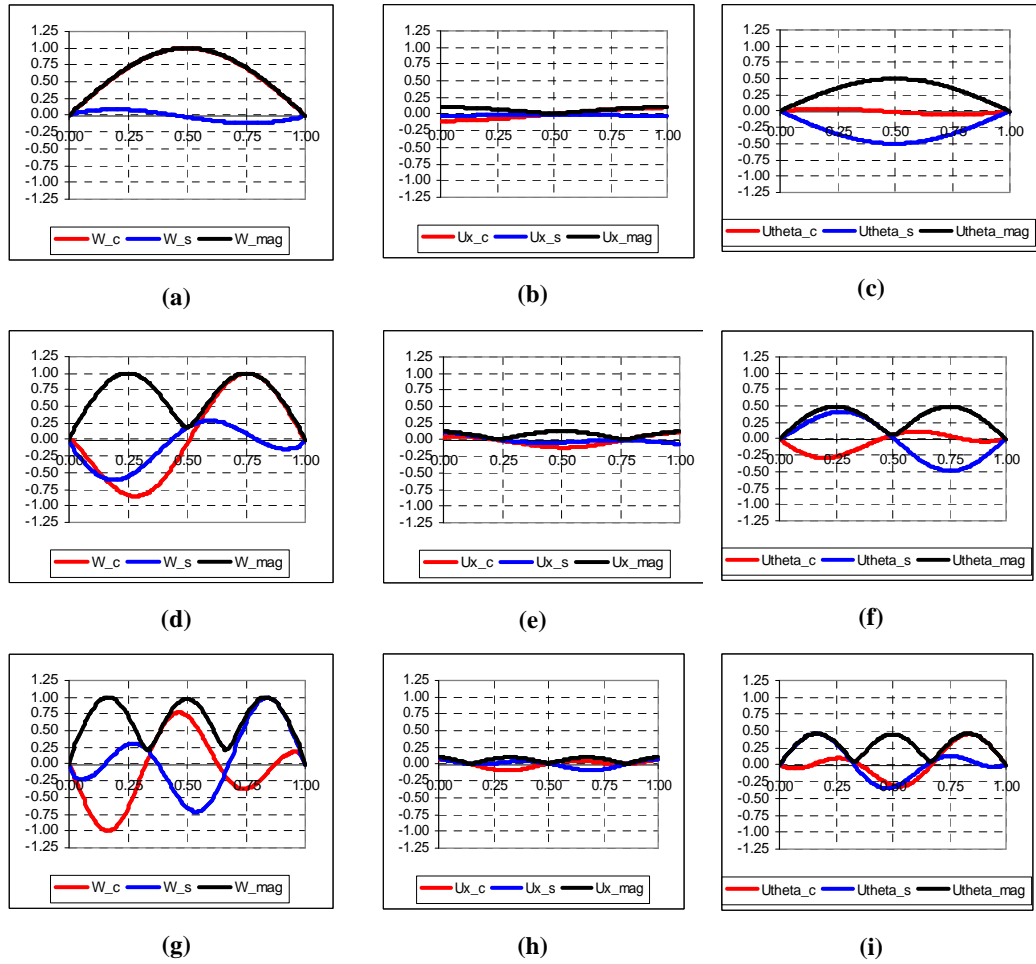


**Figure H.3** Mode Shapes in displacements of (a)  $w$  (b)  $u_\phi$  (c)  $u_\theta$  for  $(n=2)$  and  $(m=1)$ ;  
 (d)  $w$  (e)  $u_\phi$  (f)  $u_\theta$  for  $(n=2)$  and  $(m=2)$ ; and (g)  $w$  (h)  $u_\phi$  (i)  $u_\theta$  for  $(n=2)$  and  $(m=3)$

ii) ANTISYMMETRIC LAYUP

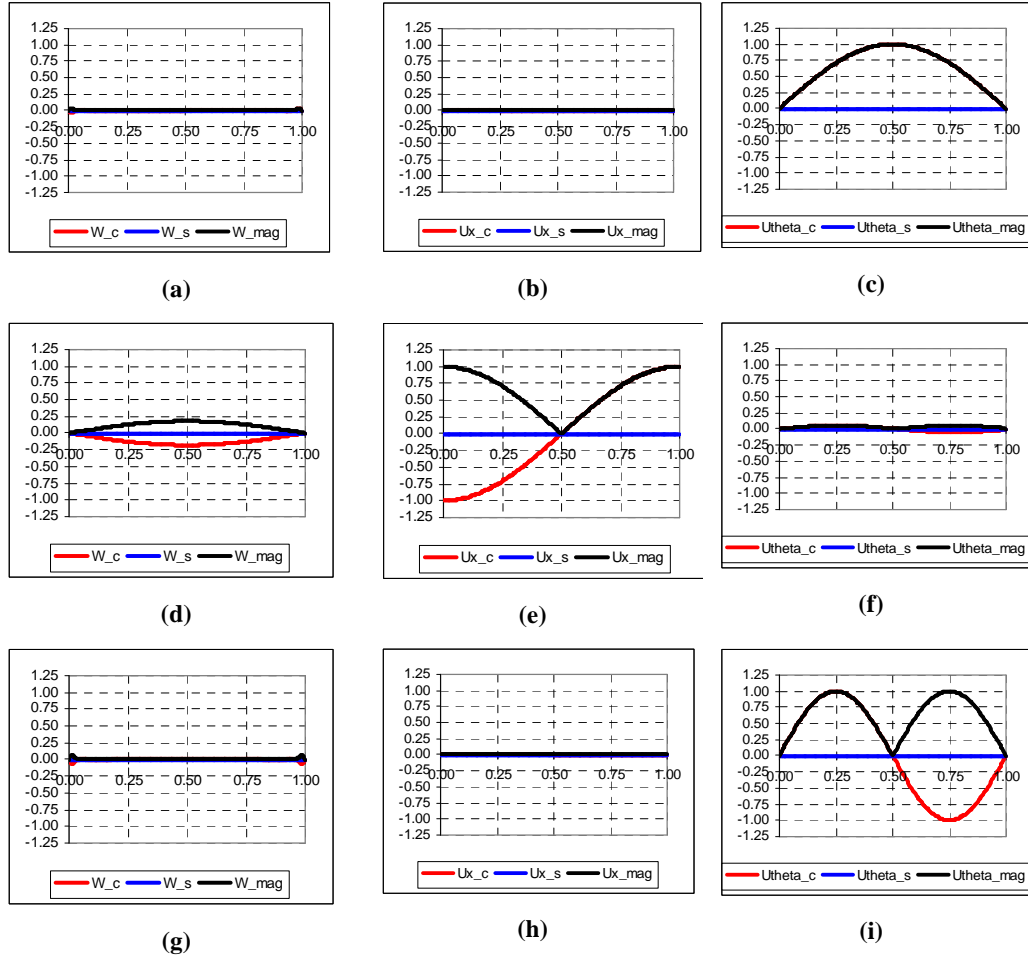
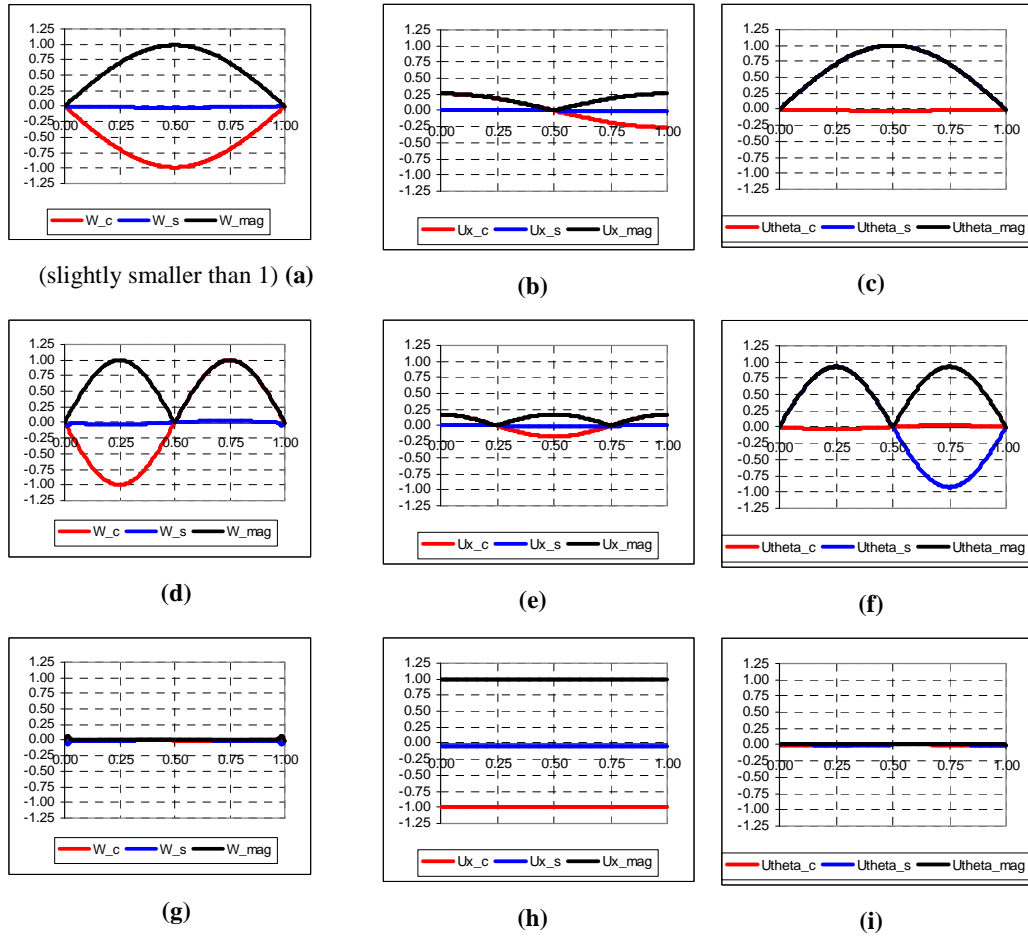
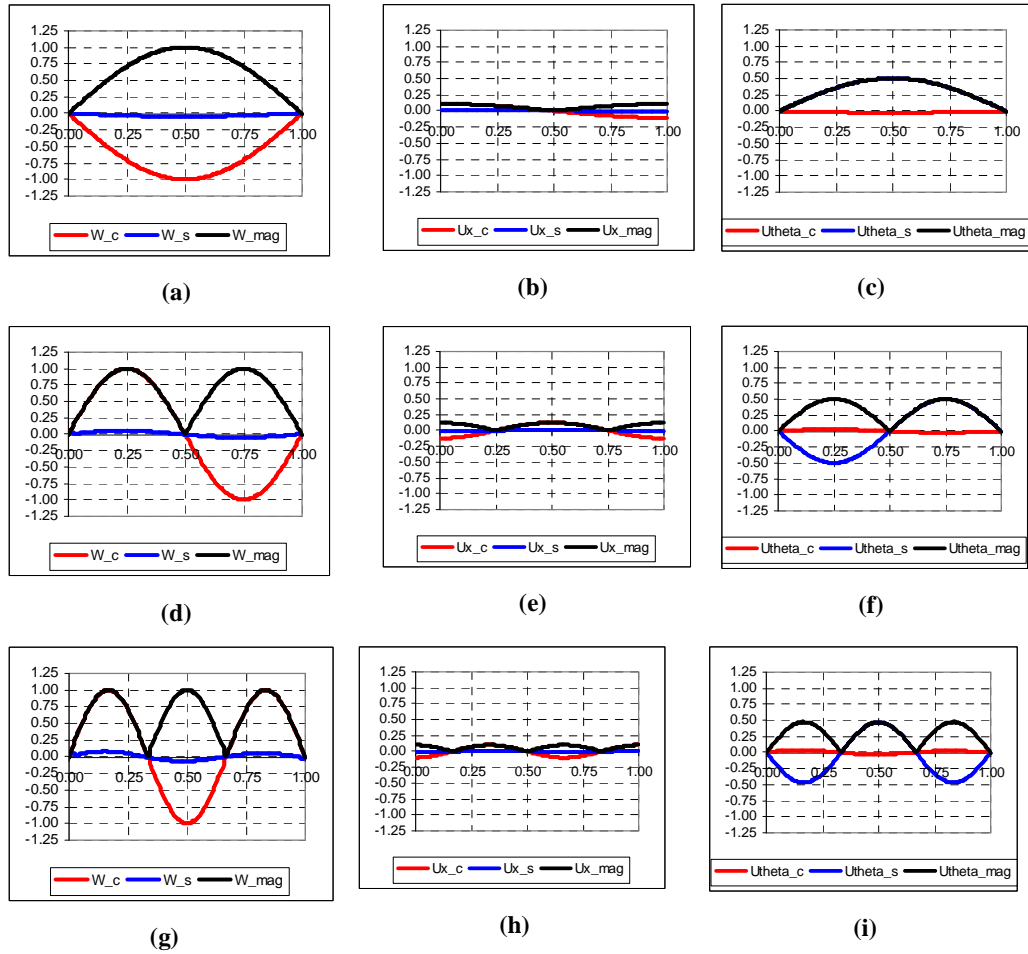


Figure H.4 Mode Shapes in displacements of (a)  $w$  (b)  $u_\phi$  (c)  $u_\theta$  for (n=0) and (m=1); (d)  $w$  (e)  $u_\phi$  (f)  $u_\theta$  for (n=0) and (m=2); and (g)  $w$  (h)  $u_\phi$  (i)  $u_\theta$  for (n=0) and (m=3)



**Figure H.5** Mode Shapes in displacements of (a)  $w$  (b)  $u_\phi$  (c)  $u_\theta$  for ( $n=1$ ) and ( $m=1$ ); (d)  $w$  (e)  $u_\phi$  (f)  $u_\theta$  for ( $n=1$ ) and ( $m=2$ ); and (g)  $w$  (h)  $u_\phi$  (i)  $u_\theta$  for ( $n=1$ ) and ( $m=3$ )



**Figure H.6** Mode Shapes in displacements of (a)  $w$  (b)  $u_\phi$  (c)  $u_\theta$  for  $(n=2)$  and  $(m=1)$ ; (d)  $w$  (e)  $u_\phi$  (f)  $u_\theta$  for  $(n=2)$  and  $(m=2)$ ; and (g)  $w$  (h)  $u_\phi$  (i)  $u_\theta$  for  $(n=2)$  and  $(m=3)$

iii) UNSYMMETRIC LAYUP

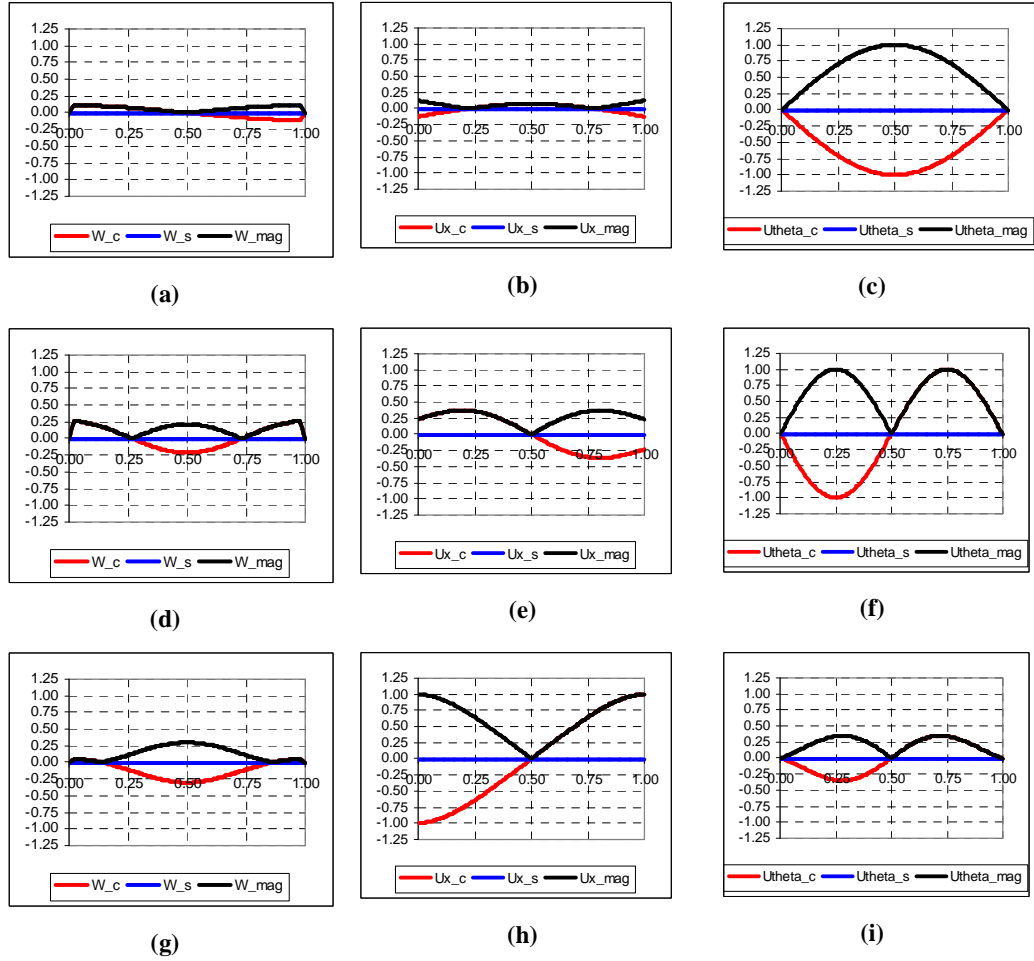


**Figure H.7** Mode Shapes in displacements of (a)  $w$  (b)  $u_\phi$  (c)  $u_\theta$  for (n=0) and (m=1);

(d)  $w$  (e)  $u_\phi$  (f)  $u_\theta$  for (n=0) and (m=2); and (g)  $w$  (h)  $u_\phi$  (i)  $u_\theta$  for (n=0) and (m=3)

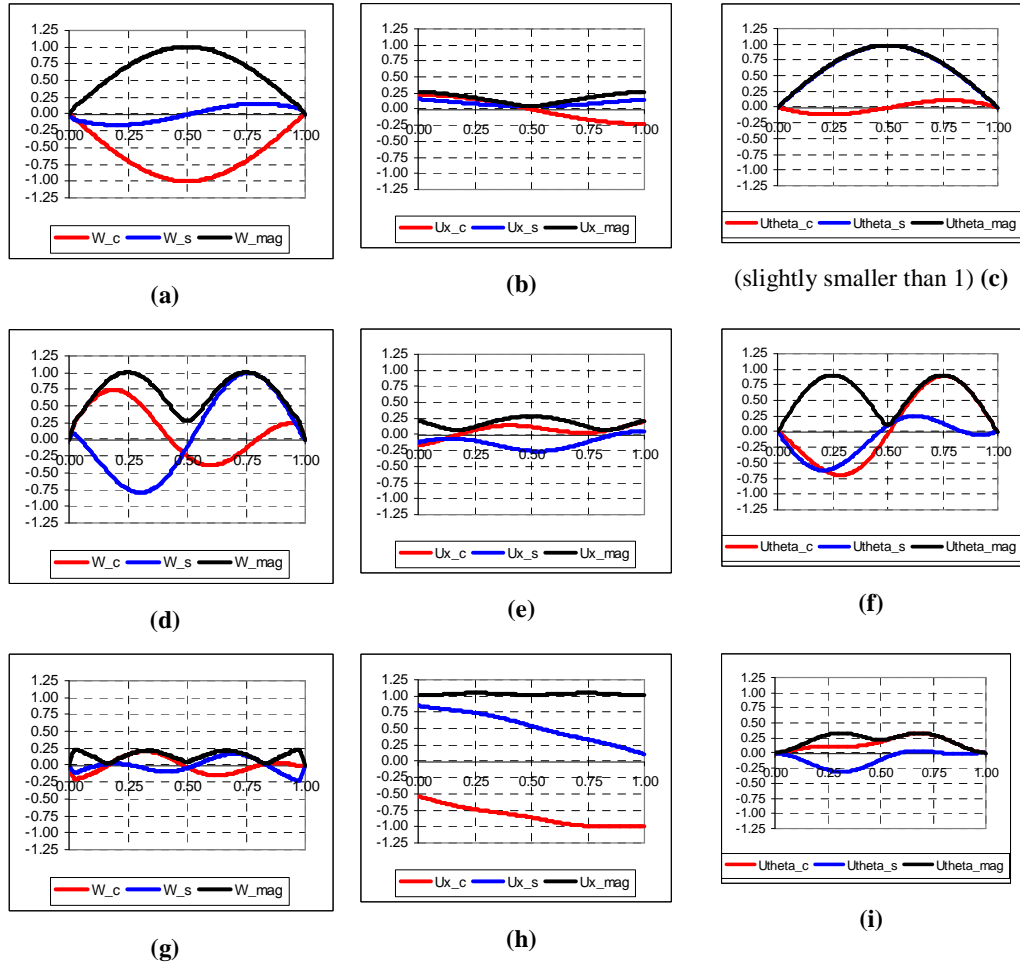


**Figure H.8** Mode Shapes in displacements of (a)  $w$  (b)  $u_\phi$  (c)  $u_\theta$  for  $(n=1)$  and  $(m=1)$ ; (d)  $w$  (e)  $u_\phi$  (f)  $u_\theta$  for  $(n=1)$  and  $(m=2)$ ; and (g)  $w$  (h)  $u_\phi$  (i)  $u_\theta$  for  $(n=1)$  and  $(m=3)$

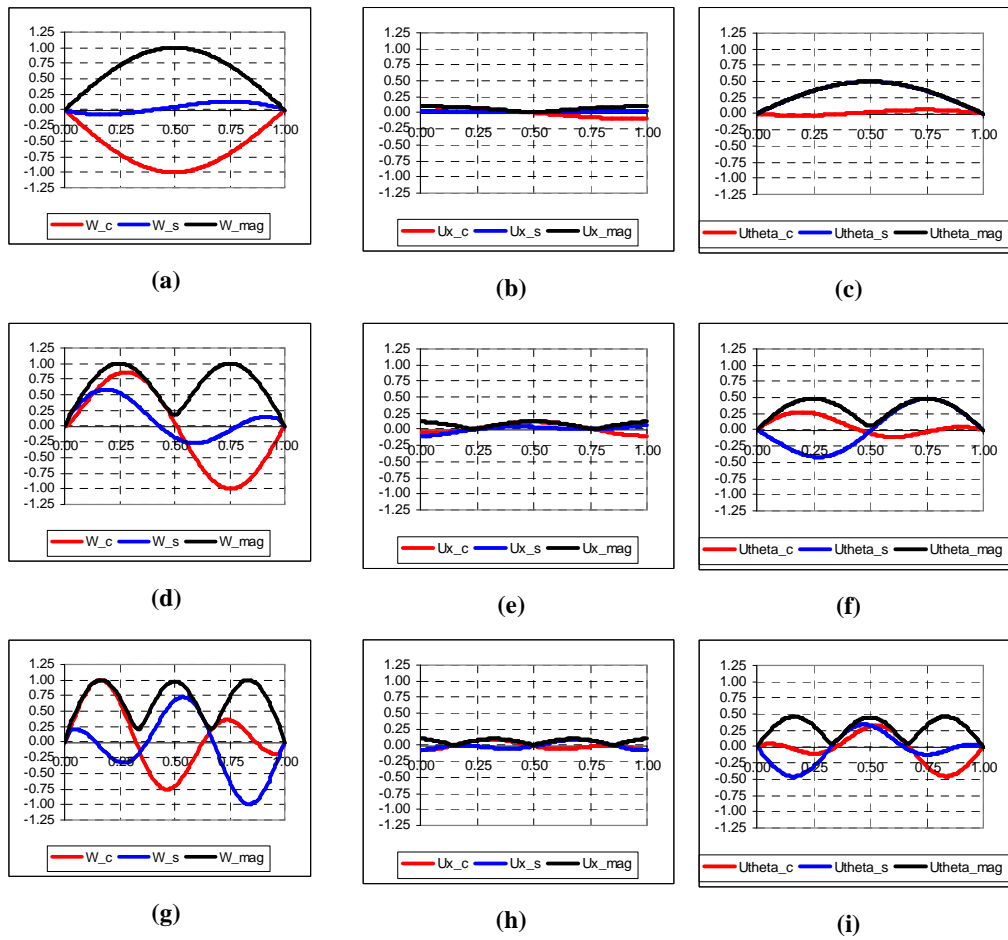


**Figure H.9** Mode Shapes in displacements of (a)  $w$  (b)  $u_\phi$  (c)  $u_\theta$  for ( $n=2$ ) and ( $m=1$ );  
 (d)  $w$  (e)  $u_\phi$  (f)  $u_\theta$  for ( $n=2$ ) and ( $m=2$ ); and (g)  $w$  (h)  $u_\phi$  (i)  $u_\theta$  for ( $n=2$ ) and ( $m=3$ )